(NASA-CR-180869) FULL SCALE TECHNOLOGY N90-10049
DEMONSTRATION OF A MODERN COUNTERROTATING
UNDUCTED FAN ENGINE CONCEPT. ENGINE TEST
(GE) 340 p CSCL 21E Unclas
G3/07 0237153

CR-180869

National Aeronautics and
Space Administration

FULL SCALE TECHNOLOGY DEMONSTRATION OF A MODERN COUNTERROTATING UNDUCTED FAN ENGINE CONCEPT

ENGINE TEST

i

FOREWORD

This report presents the results of engine tests and a discussion thereof, as conducted by GE Aircraft Engines, Cincinnati, Ohio. These engine tests were performed on behalf of the NASA Lewis Research Center, Cleveland, Ohio, under Contract NAS3-24210. The program was carried out under the technical cognizance of Mr. R.D. Hager of the Advanced Turboprop Project Office. The contract effort was conducted at the Evendale Plant of GE Aircraft Engines by the GE36 Project Department.

PRECEDING PAGE BLANK NOT FILMED

PAGE ii INTENTIONALLY BLANK

TABLE OF CONTENTS

Section | Page
1.0 ENGINE TEST SUMMARY 1
1.1 SIGNIFICANT HARDWARE CHANGES AND MODIFICATIONS 6
1.2 OVERALL HISTORY OF UDF™ ENGINE TESTING 7

2.0 INTRODUCTION 11
2.1 ENGINE DESCRIPTION 11
2.2 INSTRUMENTATION 18

3.0 REVIEW OF UDF™ TESTING 19
3.1 FORWARD STATIONARY CARBON SEAL FAILURE 20
3.2 FORWARD TELEMETRY ANTENNA REPAIR 20
3.3 TELEMETRY SYSTEM TEMPERATURE PROBLEMS 20
3.4 STAGE 1 TURBINE BLADE FAILURE AND STALL EVENT 32
3.5 TURBINE BLADE DAMPER EFFECTIVENESS 37
3.6 SUBIDLE OIL LEAK PROBLEM 51
3.7 STATIONARY EXHAUST NOZZLE (CENTERBODY) REPLACEMENT 52
3.8 FAN BYPASS BLEED VALVE CALIBRATION 52
3.9 FAN BYPASS BLEED VALVE DIFFUSER FAILURE/REPLACEMENT 52
3.10 PROPULSOR FAN-BLADE-LOSS EVENT 57
3.11 PROPULSOR FAN BLADE HISTORY AND TEST DATA 60
3.11.1 Fan Blade Test History 60
3.11.2 Fan Blade Test Data 60
3.12 POWER TURBINE FRAME STRESS 73
3.13 EFFECT OF VORTEX DESTROYER ON STRESS 73
3.14 EFFECT OF TEST SITE CHANGE ON STRESS 80
3.15 ROTOR LOCKUP AFTER SHUTDOWN RESULTING FROM FUEL LEAK 85
3.16 LOW/HIGH CYCLE FATIGUE TESTING 85
3.17 ROTOR-TO-ROTOR LOCKUP/PROPULSOR DISASSEMBLY AND REBUILD 85
3.18 MISCELLANEOUS HARDWARE STRESS DATA 99
3.19 OIL LEAK/GULPING PROBLEM 101

4.0 HEAT TRANSFER AND SECONDARY FLOW SYSTEM 110
4.1 MIXER FRAME HEAT TRANSFER 110
4.2 POWER TURBINE SECONDARY FLOW SYSTEM 117

PRECEDING PAGE BLANK NOT FILMED

PAGE iv INTENTIONALLY BLANK

TABLE OF CONTENTS (Continued)

Section Page

4.3 POWER TURBINE HEAT TRANSFER 121

4.4 NACELLE VENTILATION 121

4.5 CENTER CAVITY VENTILATION 127

5.0 ENGINE SYSTEM DYNAMICS 129

6.0 BEARINGS AND SEALS 143

6.1 HARDWARE CONDITION 143

6.1.1 Rotor Support Main Bearings 143
6.1.2 Inner Actuation Bearings 147
6.1.3 Actuation Tapered Roller Bearings 147
6.1.4 Fan Retention Bearings and Seals 147

6.2 MEASURED TEMPERATURES 151

6.2.1 Rotor Support Main Bearings 151
6.2.2 Fan Retention Thrust Bearings 151

7.0 PERFORMANCE 156

7.1 DATA SUMMARY 156

7.2 DATA REDUCTION METHODOLOGY 156

7.3 COMPARISON OF PRETEST PREDICTIONS AND REDUCED TEST DATA 160

7.4 LCF CYCLIC TESTING AND RESULTANT DETERIORATION 174

7.5 DEFINITION OF PREFLIGHT TEST CYCLE 181

7.6 COMPARISON BETWEEN GROUND PRETEST CYCLES AND REDUCED TEST DATA 181

7.7 PERFORMANCE SUMMARY 185

7.8 KEY RESULTS 185

8.0 ENGINE OPERABILITY 192

8.1 IPC STALL MARGIN 192

8.1.1 IPC Bleed Control System 197
8.1.2 Control Threshold for Throttle Retard Rate 197
8.1.3 Maximum Allowable IPC Pressure Ratio Schedule 199
8.1.4 Final IPC Bleed Control Status 199

8.2 TRANSIENT TESTING EXPERIENCE 202

8.3 ENGINE TRANSIENT PERFORMANCE ANALYSIS AND PREDICTIONS 202

9.0 ENGINE CONTROL 208

TABLE OF CONTENTS (Concluded)

Section Page

9.1 BUILD 1 - ENGINE CONTROL TESTING 208
  9.1.1 Speed Sensing Anomaly 208
  9.1.2 Pitch Control 208
  9.1.3 Gas Generator Control 208
  9.1.4 Throttle System 211
  9.1.5 Engine Starting 211
  9.1.6 Off-Engine Harnesses 211
  9.1.7 Lube Oil Bypass 211

9.2 BUILD 2 - ENGINE CONTROL TESTING 211
  9.2.1 Speed Control 212
  9.2.2 Duct Bleed 212
  9.2.3 Transient Testing 212
  9.2.4 Control Parameters 219
  9.2.5 Vibration System 219
  9.2.6 Overspeed System 219
  9.2.7 Reverse Testing 219
  9.2.8 Control System Modifications 219

9.3 BUILD 3 - ENGINE CONTROL TESTING 224
  9.3.1 Endurance Testing 224
  9.3.2 Core Response Modifications 224
  9.3.3 Reverse Thrust Testing 224
  9.3.4 UPS (Uninterruptable Power Supply) Systems 224
  9.3.5 Transient Testing 226

9.4 SUMMARY 226

10.0 NACELLE STRUCTURES 231
  10.1 FAN BLADE AIRFOIL LOSS 231
  10.2 STRAIN EVALUATION OF THE STRUT 235
  10.3 ACOUSTIC FATIGUE 235

11.0 RESULTS 239

12.0 CONCLUSIONS 241

13.0 SYMBOLS/ABBREVIATIONS 243

14.0 REFERENCES 246

APPENDIX A - STEADY-STATE TEST DATA - BUILD 3 247

APPENDIX B - STRAIN DATA FOR THE STRUT 279

LIST OF ILLUSTRATIONS

Figure		Page
1-1.	Total Run Time at Various XN48, Times as of July 8, 1986.	2
1-2.	Total Run Times at Various XN49, Times as of July 8, 1986.	3
1-3.	Total Run Time at Various T46, Time as of July 8, 1986.	4
1-4.	Run Time at Various Thrust Levels, Build 082-001/03 Only.	5
2-1.	Cross Section of Unducted Fan Engine.	12
2-2.	Cross Section of UDF™ Engine (Enlarged View).	13
2-3.	UDF™ Engine at Peebles Test Site 4A.	14
2-4.	UDF™ Engine at Peebles Test Site 4A.	15
2-5.	UDF™ Engine at Peebles Test Site 3D.	16
3-1.	Carbon Seal Assembly Fix.	21
3-2.	Forward Telemetry System Support.	22
3-3.	GE36 Telemetry System.	24
3-4.	Telemetry System Scoop Designs.	25
3-5.	Forward Telemetry Temperatures - Raw Data.	26
3-6.	Forward Telemetry Temperatures - Normalized with T_{AMB}.	27
3-7.	Aft Telemetry Temperatures - Raw Data.	28
3-8.	Aft Telemetry Temperatures - Normalized with T_{AMB}.	29
3-9.	Forward Telemetry Temperatures - Reverse Testing.	30
3-10.	Aft Telemetry Temperatures - Reverse Testing.	31
3-11.	Summary of Hardware Damage.	33
3-12.	Turbine Blade 1F Stress Trend.	34
3-13.	History of Turbine Blade Response, Run to Thrust and Stall.	35
3-14.	Turbine Blade Fix.	38
3-15.	Power Turbine Blade Vibratory Response, Damper Effectiveness - Stage 1.	39
3-16.	Power Turbine Blade Vibratory Response, Build 1 (Undamped) Versus Build 2 (Damped).	40
3-17.	Stage 1 Turbine Blade Response, Accel to 25,000 lbf Thrust: February 4, 1986.	41
3-18.	Stage 2 Turbine Blade Response, Accel to 25,000 lbf Thrust: February 4, 1986.	42
3-19.	Stage 3 Turbine Blade Response, Accel to 25,000 lbf Thrust: February 4, 1986.	43

LIST OF ILLUSTRATIONS (Continued)

Figure		Page
3-20.	Stage 4 Turbine Blade Response, Accel to 25,000 lbf Thrust: February 4, 1986.	44
3-21.	Stage 6 Turbine Blade Response, Accel to 25,000 lbf Thrust: February 4, 1986.	45
3-22.	Stage 7 Turbine Blade Response, Accel to 25,000 lbf Thrust: February 4, 1986.	46
3-23.	Stage 8 Turbine Blade Response, Accel to 25,000 lbf Thrust: February 4, 1986.	47
3-24.	Stage 9 Turbine Blade Response, Accel to 25,000 lbf Thrust: February 4, 1986.	48
3-25.	Stage 10 Turbine Blade Response, Accel to 25,000 lbf Thrust: February 4, 1986.	49
3-26.	Stage 11 Turbine Blade Response, Accel to 22,000 lbf Thrust: January 11, 1986.	50
3-27.	UDF™ Engine Centerbody Separation Parameter, Cruise Condition $M = 0.72$; 35,000; $PT8/P_0 = 1.4$.	53
3-28.	UDF™ Engine - Redesigned Centerbody.	54
3-29.	Bypass Bleed Valve Diffuser.	55
3-30.	Redesigned Bypass Bleed Valve Diffuser.	56
3-31.	Spar Schematic.	58
3-32.	Total Run Until Fan Failure.	61
3-33.	Original Fan Blade Airfoil Mechanical Design.	62
3-34.	Improved Fan Blade Mechanical Design.	63
3-35.	Stage 2 Fan Blades Engine Test History.	64
3-36.	Fan Blade Structural Improvement.	65
3-37.	Fan Blade Response Summary - ksi pp.	66
3-38.	Stage 1 Fan Blade Response Summary.	67
3-39.	Stage 2 Fan Blade Response Summary.	68
3-40.	Fan Blade Response Summary - February 4, 1986 Maximum Power Run (25,000 lbf Corrected Thrust).	69
3-41.	Stage 1 Fan Blade Response, Accel to 24,000 lbf: June 24, 1986.	70
3-42.	Stage 2 Fan Blade Response, Accel to 24,000 lbf: June 24, 1986.	71
3-43.	Fan Blade Strain Gage Locations.	72

LIST OF ILLUSTRATIONS (Continued)

Figure Page

3-44. Fan Blade Response with Facility Fans Turned On. 74

3-45. Power Turbine Frames Vibratory Response Summary. 75

3-46. Power Turbine Frames Vibratory Response, Updated Scope Limits Versus Site 4A Response. 76

3-47. Power Turbine Frames Vibratory Response, Stage 12 Component Strain Distribution Test Results. 77

3-48. Power Turbine Frames Vibratory Response, Material HCF Test Results. 78

3-49. Power Frame Vibratory Response, Build 3. 79

3-50. Fan Blades Vibratory Response, Effect of Vortex Destroyer. 81

3-51. Power Turbine Frames Vibratory Response, Effect of Vortex Destroyer. 82

3-52. Fan Blade Response Comparison, Site 3D Versus Site 4A. 83

3-53. Power Turbine Frames Vibratory Response, Effect of Site Change. 84

3-54. Suspected IGV/Spool Rub. 86

3-55. Low Cycle Fatigue Cycle. 87

3-56. IGV and 1-4 Inner Spool. 90

3-57. IGV Crack/Tear at Braze Joint (ALF). 91

3-58. Suspected Stage 1 Rub. 92

3-59. Stage One Blade Cracks at Leading Edge Root. 93

3-60. Aft Outer Flowpath Seals. 95

3-61. Midsump Seals. 97

3-62. Suspected Stage 11 Rub. 98

3-63. IGV and 1-4 Inner Spool. 100

3-64. Power Turbine OGV - Engine Test Data. 102

3-65. Power Turbine IGV - Engine Test Data. 103

3-66. Forward Outer Rotating Seal Response, Decel from 25,000 lbf Thrust: February 4, 1986. 104

3-67. Aft Outer Rotating Seal Response, Accel to [illegible],000 lbf Thrust: February 4, 1986. 105

3-68. Outer Turbine Spool Response (1-4), Accel to 25,000 lbf Thrust: February 4, 1986. 106

3-69. Outer Turbine Spool Response (7-11), Acceleration to 35,000 lbf Thrust: February 4, 1986. 107

LIST OF ILLUSTRATIONS (Continued)

Figure		Page
3-70.	Inner Turbine Spool (6-11) Response, Accel to 25,000 lbf Thrust: February 4, 1986.	108
4-1.	Mixer Frame Flows at Takeoff Power, Test Versus Predicted.	111
4-2.	Mixer Frame Pressure Losses Comparison of Measured and Predicted Pressures.	112
4-3.	Mixer Frame Flowpath Static Pressure Distribution Takeoff Power.	113
4-4.	Mixer Frame Backflow Margin - Build 01 Engine.	114
4-5.	Mixer Frame Backflow Margin - Build 02 Engine.	115
4-6.	Mixer Frame Temperatures.	116
4-7.	Power Turbine Secondary Flow Circuit.	118
4-8.	Potential Forward Seal Problem.	120
4-9.	Rotor Cavity Temperatures at Takeoff Power.	122
4-10.	Power Turbine Temperatures Based on Analysis.	123
4-11.	Spool Temperatures, Hot Day Takeoff.	124
4-12.	Nacelle Temperatures Based on Test Data at Takeoff Power.	125
4-13.	Forward Fan Blade Hub Temperatures; Hot Day Takeoff, Mach = 0.0, Full Thrust.	126
4-14.	Center Cavity Ventilation at Takeoff Power.	128
5-1.	IPC One-Per-Rev Signature Comparison.	130
5-2.	HPC One-Per-Rev Signature Comparison.	130
5-3.	IPC One-Per-Rev Signature Comparison.	132
5-4.	HPC One-Per-Rev Signature Comparison.	132
5-5.	Subidle UDF™ One-Per-Rev Vibration Signature Comparison.	133
5-6.	Subidle UDF™ One-Per-Rev Vibration Signature Comparison.	133
5-7.	UDF™ One-Per-Rev Vibration Signature on 2-Minute Accel to 24,000 lb Thrust, Housing Vertical.	135
5-8.	UDF™ One-Per-Rev Vibration Signature on 2-Minute Accel to 24,000 lb Thrust, Housing Horizontal.	135
5-9.	Maximum Static Deflection.	137
5-10.	Unbalance Forces Lineup in Vertical Plane.	139
5-11.	Unbalance Forces Lineup in Horizontal Plane.	140
5-12.	GE36 Demonstrator Engine 082-001/3 T/D 7-1-86 Time History Plots at Ground Idle Power.	141

LIST OF ILLUSTRATIONS (Continued)

Figure		Page
6-1.	Seal Cavity Closure.	145
6-2.	Possible Running Condition with 1R Spanner Nut Loose.	145
6-3.	Disassembly Problem and Roller Corner Damage.	146
6-4.	Problem Solution - Positive Nut Locking.	146
6-5.	Gearbox Stackup Problem Causing Incorrect Loading of Ball Bearing and Cap Looseness.	148
6-6.	Bearing Housing Deflection.	150
6-7.	Irregular Wear Pattern of Roller "Path."	150
6-8.	Main Propulsor Bearings.	152
6-9.	Main Propulsor Bearings, 2-Minute Accel to 24,000 lb Thrust.	153
6-10.	Main Propulsor Bearings, 4-Minute Accel/Decel to 1200 rpm.	153
6-11.	Forward and Aft Fan Hub Temperatures.	155
6-12.	Forward and Aft Fan Hub Temperatures, Accel to Full Power.	155
7-1.	Instrumentation for UDF™/F404 Demo.	158
7-2.	Core Engine Temperature Ratio Versus Pressure Ratio.	161
7-3.	IPC Stall Margin Versus IPC Corrected Flow.	162
7-4.	Power Turbine Flow Function Versus Energy Function.	163
7-5.	Power Turbine Efficiency Versus Energy Function.	164
7-6.	UDF™ Thrust Coefficient Versus Power Coefficient.	166
7-7.	Front Rotor Blade Angle Versus Core Engine Pressure Ratio.	167
7-8.	Rear Rotor Blade Angle Versus Core Engine Pressure Ratio.	168
7-9.	Corrected SFC Versus Corrected Thrust.	169
7-10.	UDF™ Engine - Redesigned Centerbody.	170
7-11.	UDF™ Engine Centerbody Separation Parameter.	171
7-12.	UDF™ Engine - Core Plug Static Pressures.	172
7-13.	Nozzle Flow Coefficient Versus Core Engine Pressure Ratio.	173
7-14.	Corrected SFC Versus Corrected EPR Power Hook Evaluation.	175
7-15.	Corrected SFC Versus Corrected EPR Power Hook Evaluation.	176
7-16.	Wind Velocity Versus Wind Angle.	177
7-17.	Corrected SFC Versus Corrected Thrust.	178
7-18.	Corrected Thrust Versus Corrected Pressure Ratio.	179
7-19.	Core Temperature Ratio Versus Control Pressure Ratio.	180

LIST OF ILLUSTRATIONS (Continued)

Figure		Page
7-20.	IPC Efficiency Versus Control Pressure Ratio.	182
7-21.	IPC Flow Versus Control Pressure Ratio.	183
7-22.	IPC Flow Versus IPC Corrected Speed.	184
7-23.	Compare Pretest Cycle Versus Posttest Cycle Versus Test Data.	186
7-24.	Compare Pretest Cycle Versus Posttest Cycle Versus Test Data.	187
7-25.	Compare Pretest Cycle Versus Posttest Cycle Versus Test Data.	188
7-26.	Compare Pretest Cycle Versus Posttest Cycle Versus Test Data.	189
7-27.	Compare Pretest Cycle Versus Posttest Cycle Versus Test Data.	190
8-1.	IPC Operating and Stall Line Sea Level Static.	193
8-2.	Steady-State IPC Operating Lines; 2,750 ft.	194
8-3.	Steady-State IPC Operating Lines; 38,000 ft.	195
8-4.	IPC Stator Schedule.	196
8-5.	Predicted IPC ΔPRS Usage During Throttle Decels; 2,750 ft.	198
8-6.	Predicted IPC ΔPRS Usage During Throttle Decels; 38,000 ft.	200
8-7.	Maximum Allowable IPC Pressure Ratio.	201
8-8.	Predicted IPC ΔPRS Usage During Throttle Decels; 2,750 ft.	203
8-9.	Predicted IPC ΔPRS Usage During Throttle Decels; 38,000 ft.	204
8-10.	Transient Testing Analytical Comparison with Updated Transient Cycle Deck T/C from 97% Takeoff Thrust.	206
8-11.	Transient Testing Analytical Comparison with Updated Transient Cycle Deck Burst to 20,000 lb Thrust.	207
9-1.	Fan Speed Sensor Segments.	209
9-2.	Fan Speed Sensor Segments.	210
9-3.	Duct Bleed System.	213
9-4.	Throttle Chop Decels.	214
9-5.	Throttle Chop.	215
9-6.	Throttle Chop.	216
9-7.	Throttle Chop.	217
9-8.	Throttle Chop.	218
9-9.	Reverse Thrust.	220
9-10.	Reverse Thrust.	221
9-11.	Reverse Thrust.	222

LIST OF ILLUSTRATIONS (Concluded)

Figure		Page
9-12.	Reverse Thrust.	223
9-13.	P_{S3} Accumulator Configuration.	225
9-14.	Throttle Burst.	227
9-15.	Throttle Burst.	228
9-16.	Throttle Burst.	229
9-17.	Throttle Burst.	230
10-1.	UDF™ Engine 082-001 Accelerometer Definition.	232

LIST OF TABLES

Table		Page
1-1.	GE36 Test History - Engine 082-001, Build 1/1A.	8
1-2.	GE36 Test History - Engine 082-001, Build 2.	9
1-3.	GE36 Test History - Engine 082-001, Build 3.	10
3-1.	Power Turbine Vibratory Response Resolution.	80
3-2.	GE36 HCF Cycle Count.	88
3-3.	Turbine Blade Inspection Summary.	96
4-1.	Power Turbine Secondary Flow (%W25), Takeoff Power.	119
7-1.	Data Summary.	157
7-2.	Chronology of the Acquired Data.	157
8-1.	Significant Transients - GE36 Proof-of-Concept.	205
10-1.	Vibration Response.	233
10-2.	UDF™ Engine Mount Loads Due to Airfoil Loss.	234
10-3.	UDF™ Engine Comparison of Mount Loads for Airfoil-Out Event.	236
10-4.	UDF™ Engine Airfoil-Out Event Comparison of Deflections.	236
10-5.	Stress Data - Strut.	237

1.0 ENGINE TEST SUMMARY

This Engine Test Report covers the UDF™ (unducted fan) Engine 082-001 ground testing at the GE Aircraft Engines Peebles Test Facility and includes Builds 1 through 3 of Engine 082-001. Note: A new build number indicates a significant change in engine hardware.

The UDF™ engine successfully completed a ground-test program exceeding 100-hours duration. The basic concepts of the engine have been successfully demonstrated. Some of the accomplishments are as follows:

- Full thrust (25,000 pounds corrected) demonstrated
- Full propulsor rotor speed demonstrated (1393+ rpm)
- Specific fuel consumption (sfc) was better than predicted; sfc of < 0.24 lb/hr/lb was demonstrated
- Flawless operation of the F404 gas generator
- Counterrotation of structures, turbines, and fan blades
- Actuation system operation successfully demonstrated
- Control system operation successfully demonstrated
- New fan blade design successfully demonstrated
- Reverse thrust successfully demonstrated.

The UDF™ was ground tested at Peebles for a total run time of 100:51 hours. This was split between Builds 1 through 3 as follows.

Build	Run Time per Build	Total Run Time
1	5:24	5:24
2	29:20	43:44
3	66:07	100:51

In Figures 1-1 through 1-4, the engine run time is a function of Stage 1 propulsor fan speed (XN48), Stage 2 propulsor fan speed (XN49), exhaust gas temperature (T46), and thrust, respectively. Thrust data were available for Build 3 only. Note that on the plots of run time as a function of propulsor

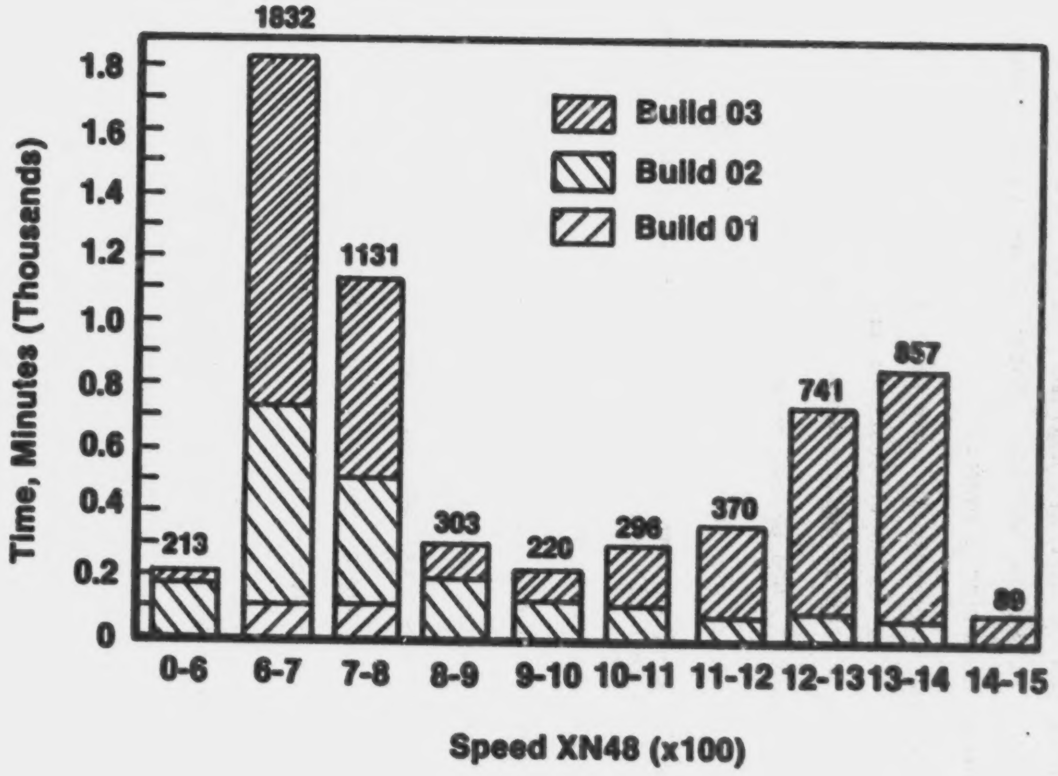

Figure 1-1. Total Run Time at Various XN48, Times as of July 8, 1986.

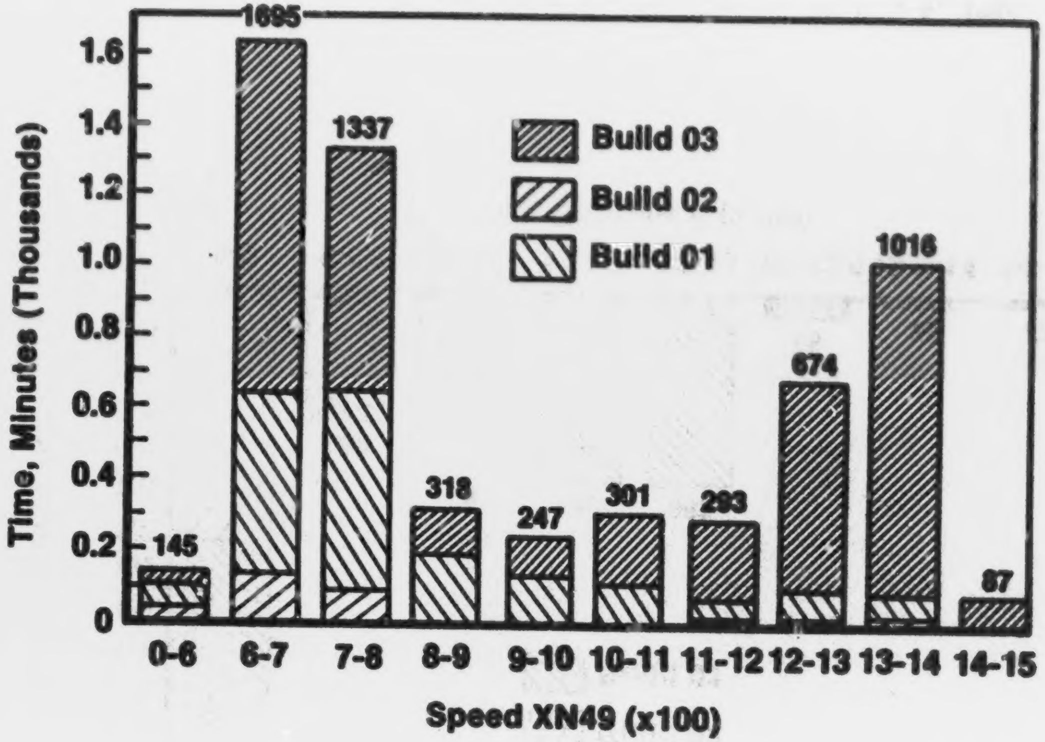

Figure 1-2. Total Run Times at Various XN49, Times as of July 8, 1986.

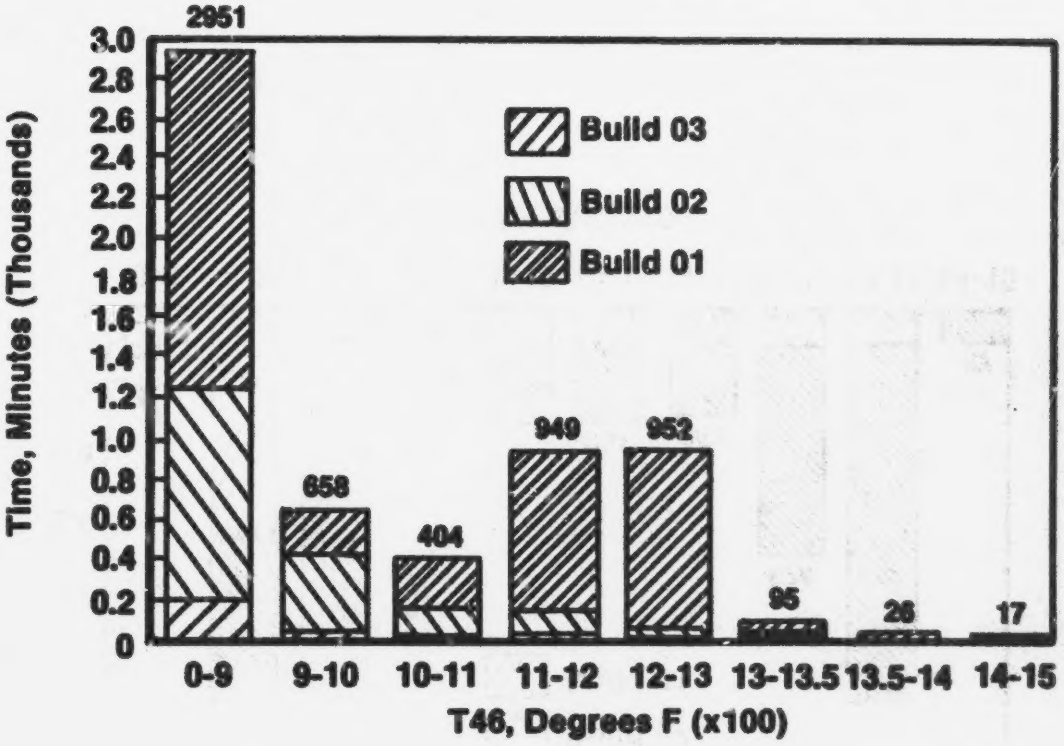

Figure 1-3. Total Run Time at Various T46, Time as of July 8, 1986.

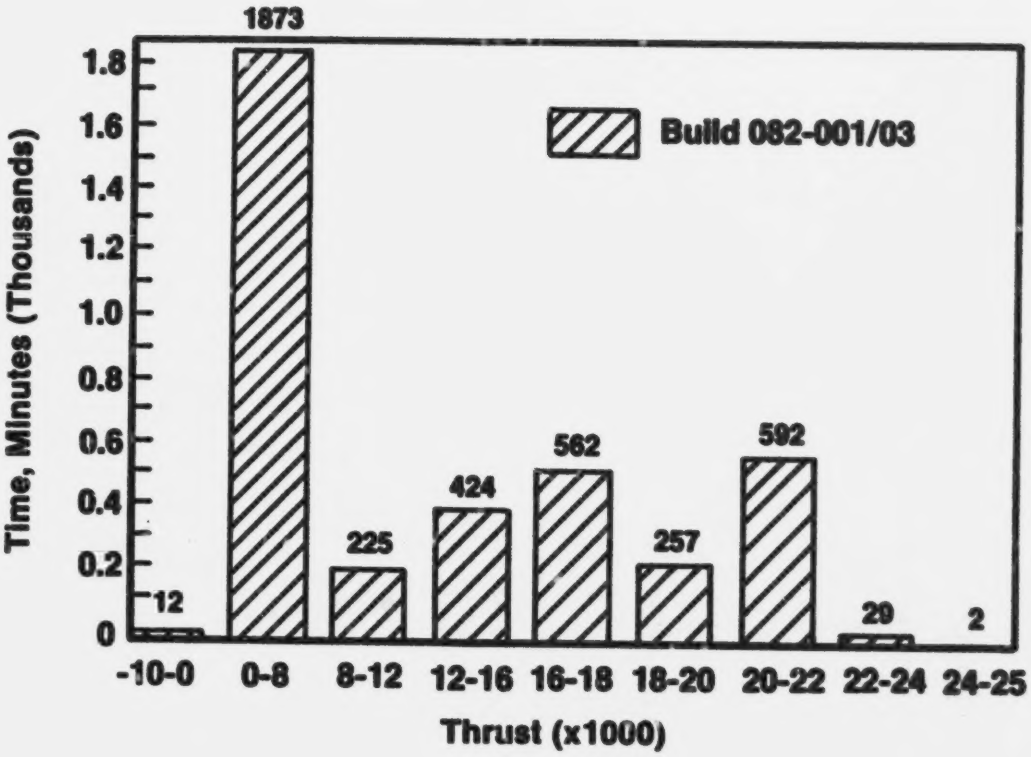

Figure 1-4. Run Time at Various Thrust Levels, Build 082-001/03 Only.

speed, there is a large amount of time spent in the ranges of 600 to 700 rpm and 700 to 800 rpm. Most of this time was spent in the immediate vicinity of 700 rpm, which is idle for this engine. Also note that the vast majority of time spent in the 1400 to 1500 rpm range was actually spent near 1400 rpm.

1.1 SIGNIFICANT HARDWARE CHANGES AND MODIFICATIONS

Significant hardware changes and modifications which occurred during the UDF™ ground test are listed below. A more detailed discussion is provided in the sections enumerated.

	Section
Build 1 to 1A	
Forward stationary carbon seal and 2R bearing replaced	3.1
Build 1A	
Forward telemetry system antenna modified	3.2
Added pipe-elbow air scoops to exhaust nozzle to aid aft telemetry system cooling	3.3
Build 1A to Build 2	
All propulsor turbine blades replaced (Stages 1-4 and 6-11)	3.4
Propulsor turbine blade tip clearances increased	3.4
Damper pins added between all propulsor turbine blades	3.4, 3.5
Spool distress repaired	3.4
Pipe-elbow scoops were replaced with aerodynamic air scoops	3.3
Leading edge plugs were installed in propulsor fan blades	3.11
Installed redesigned stationary exhaust nozzle (centerbody)	3.7, 7.3
Installed hardware to solve subidle oil leak problem	3.6
Build 2	
Propulsor Stage 2, No. 7 fan blade replaced after blade-out	3.10
Added additional holes to telemetry system air scoops	3.3
Installed compressor discharge pressure (PS3) accumulator system	6.0
Installed redesigned fan bypass bleed valve diffuser	3.9

	Section
Build 2 to Build 3	
Installed redesigned propulsor Stages 1 and 2 fan blades	3.11
Installed improved PS3 accumulator system	6.0
Build 3	
No significant changes	
Postbuild 3	
Replaced all propulsor Stage 1 turbine blades	3.17
Replaced three propulsor Stage 11 turbine blades	3.17
Added positive mechanical retention feature to 1R bearing nut	3.17
Replaced 1R and 2R bearings	3.17
Repaired IGV (inlet guide vane) - lip replaced with honeycomb	3.17
Drilled oil drain holes in propulsor	3.17
Borescope ports added to mixer frame to gain better access to Stage 1 turbine blades	3.17
Replaced actuator control rods	3.17
Installed additional air scoops for cooling aft telemetry system	3.3

1.2 OVERALL HISTORY OF UDF™ ENGINE TESTING

Tables 1-1 through 1-3 present an overall history of UDF™ testing.

Table 1-1. GE36 Test History - Engine 082-001, Build 1/1A.

Date (1985)		TRT
Aug. 29	First Run to Idle; Broken Carbon Seal Caused Internal Oil Leak Resulting in a Rotor Unbalance; Caused a Turbine Rub Which Cracked Some Stage 11 Turbine Blades	0:02
Aug. 30-Sept. 11	Engine Removed from Site; Carbon Seal and 2R Bearing Replaced	
	Build 1A	
Sept. 14	Engine Returned to Test; Idle Achieved	0:11
Sept. 15-17	Worked Instrumentation Faults	
Sept. 18	Mechanical Check-Out	0:14
Sept. 19	Mechanical Check-Out Reached Full Propulsor Speed	1:10
Sept. 20-26	Modified Forward Telemetry Antenna	
Sept. 27	Reached 22,000 lbf; Shutdown Due to High Aft Telemetry Temperatures	3:43
Sept. 28-Oct. 1	Added Air Scoops to Exhaust Nozzle to Cool Aft Telemetry System	
Oct. 2	Reached 24,000 lbf; Engine S/D Following Stall (Stage 1 Turbine Blade Failure)	5:24
Oct. 3	Engine Removed for Repair	

Table 1-2. GE36 Test History - Engine 082-001, Build 2.

Date (1986)		Build 2 Run Time	TRT
Jan. 30-31	Resumed Testing; Mechanical Check-Out; Reached 22,000 Thrust	3:38	9:02
Feb. 2-3	Testing With Facility Fans On; Fan Bypass Bleed Valve Calibration; Bleed Valve Diffuser Can Failure; Engine Trim Balance (20,000 Maximum Thrust)	9:49	15:13
Feb. 5-8	Repaired Instrumentation and Aft Telemetry System	13:28	18:52
Feb. 9	Telemetry System Check-Out (to 1200 rpm Fan Speed); Started Down Power Calibration Ran Twice to 24,000 Thrust; on 2nd 24,000 Pt. Lost Stage 2, No. 7 Fan Blade Shell	15:16	20:40
Feb. 17-18	Engine Health Check - With New Blade Reached 1200 rpm Fan Speed; 16,000 Thrust; Tested with Vortex Destroyer	16:30	21:54
Feb. 28	Turbine Frame Stress Investigation; 1000 rpm Maximum Fan Speed	20:36	26:00
March 5	Stress Survey; 1029 rpm Maximum Fan Speed	22:55	28:19
March 6-30	Moved Engine from Site 4A to 3D		
April 1-2	Stress Survey; 1150 rpm Maximum Fan Speed	25:44	30:68
April 3-7	Added Additional Holes to Aft Telemetry System Cooling Scoops		
April 8	Reverse Testing/Cooling Scoop Testing	26:22	31:46
April 18	Control Verification; Control Fault Caused Stage 2 Overspeed; Engine Shutdown	28:30	33:54
April 19-23	Installed PS3 Accumulator to Slow Propulsor Accel Rate		
April 24	Engine Test With PS3 Accumulator; 1150 rpm Maximum Fan Speed	29:20	34:44

Table 1-3. GE36 Test History - Engine 082-001, Build 3.

Date (1986)		Build 3 Run Time	TRT
June 20	Returned to Test; Achieved Idle	0:16	35:02
June 23	Reverse Testing; Mechanical Check-Out; 1270 rpm Maximum Fan Speed	0:45 2:07	35:29 36:51
June 24	Mechanical Check-Out/Trim Balance Reached 24,000 Maximum Thrust	4:33	39:17
June 25	Trim Balance/Bleed Valve Calibration Reached 18,000 Thrust	8:18	43:02
June 26	Bleed Valve Calibration/Trim Balance Reached 23,000 Thrust	10:00	44:44
June 29	Bleed Valve Calibration; Reached 19,000 Thrust	12:17	47:01
June 30	Down Power Calibration; Shutdown from 19,000 Thrust Due to Fuel Leak; Aft Propulsor Rotor Locked up Until Engine Cooled	12:51	47:35
July 1	Down Power Calibration; Reached 24,000 Thrust; Performance Optimization Testing	17:36 20:18	52:20 55:02
July 3	Performance Optimization/Vibration Survey/Trim Balance; Reached 21,000 Thrust Control Tests; Reached 24,000 lbf	25:38 29:53	60:22 64:37
July 4	Reverse Testing (to 850 rpm Fan Speed)	30:34	65:28
July 4-7	LCF Cycles (100)	59:45	94:29
July 8	Bodes; Reached 21,000 Thrust; Trim Balance; Reached 22,000 Thrust; Propulsor Rotors Locked Together after a Normal Shutdown	62:31 66:07	97:15 100:51
	End of Ground Testing at Peebles		

2.0 INTRODUCTION

2.1 ENGINE DESCRIPTION

The UDF™ engine is a new aircraft engine concept that is based on an ungeared, counterrotating, unducted ultra-high-bypass turbofan configuration. This engine is being developed by General Electric to provide a high thrust-to-weight ratio power plant with exceptional fuel efficiency for subsonic aircraft application.

The engine encompasses the operational flexibility and fuel efficiency of a two-spool core gas generator with the propulsive efficiency of a propeller (moderate diameter and tip speed). The engine is based on an aft-mounted, counterrotating power turbine that aerodynamically couples with a basic gas generator engine and provides for direct conversion of the gas generator engine power into propulsive thrust without requiring a gearbox or additional shafting. The concept of counterrotating fan blades is being utilized to capitalize on the full propulsive efficiency of this configuration; that is, the exit swirl from the first blade row is recovered by the second row and converted into propulsive thrust. The turbine transmits its power through two counterrotating power turbine frames which, in turn, transmit power to the UDF™ blades through the polygonal support rings which act as the primary-load carrying support structure for the fan blades. This isolates the turbine flowpath from out-of-round distortions from the fan blade loads.

The counterrotating turbine rotors, power turbine frames, fan blades, and static structures are components which comprise the "propulsor" for the UDF™ engine. Mounted in front of the propulsor is a gas generator engine which provides the required gas horsepower. The gas generator is a modified production F404 turbofan engine.

Figure 2-1 shows a cross-sectional view of the UDF™ engine. An enlarged cross section of the propulsor is presented in Figure 2-2. Figures 2-3 and 2-4 are UDF™ photos at Peebles Test Site 4A, and Figure 2-5 depicts a UDF™ at Test Site 3D.

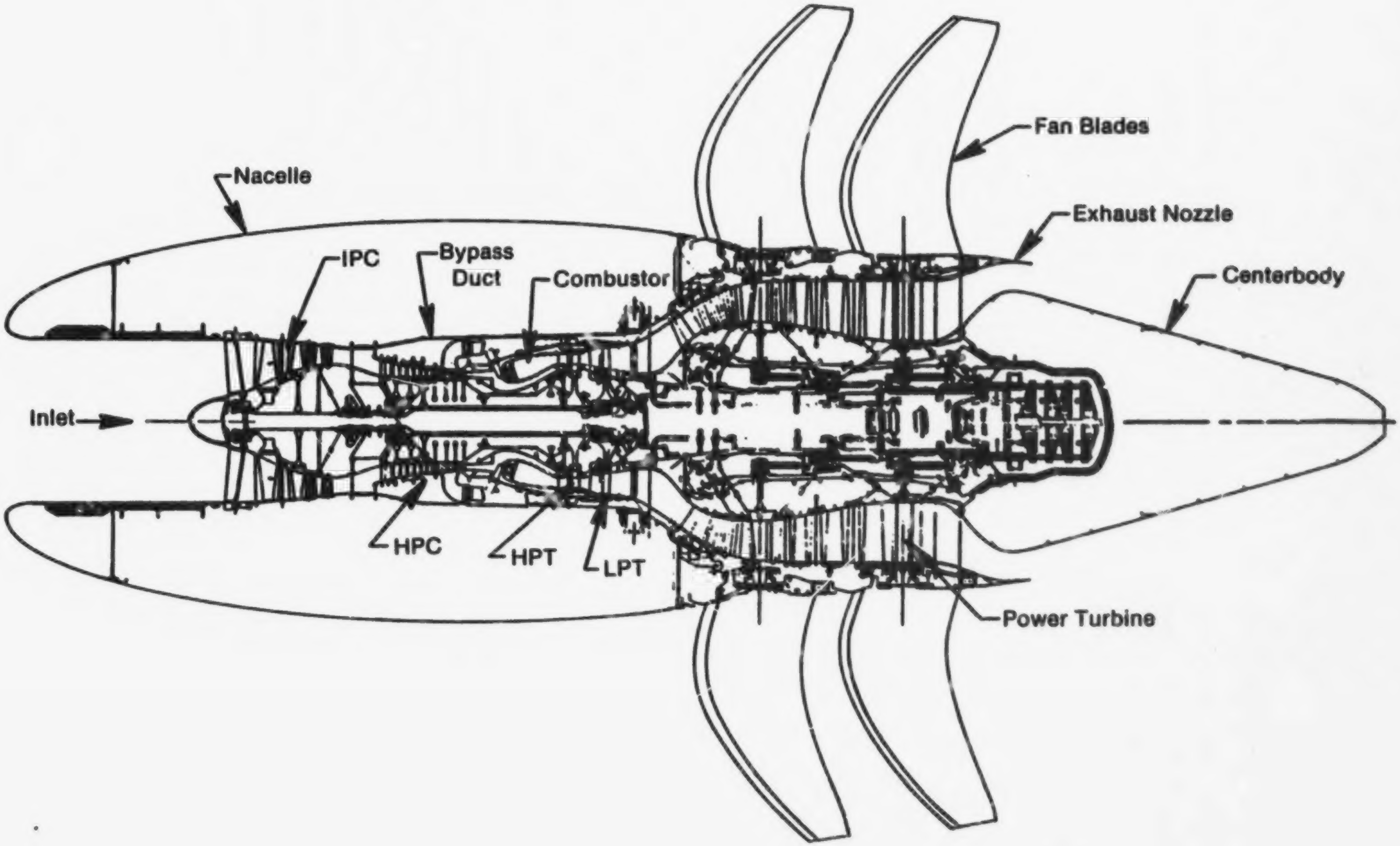
Nacelle
IPC
Bypass Duct
Combustor
Fan Blades
Exhaust Nozzle
Centerbody
Inlet
HPC
HPT
LPT
Power Turbine

Figure 2-1. Cross Section of Unducted Fan Engine.

ORIGINAL PAGE IS
OF POOR QUALITY

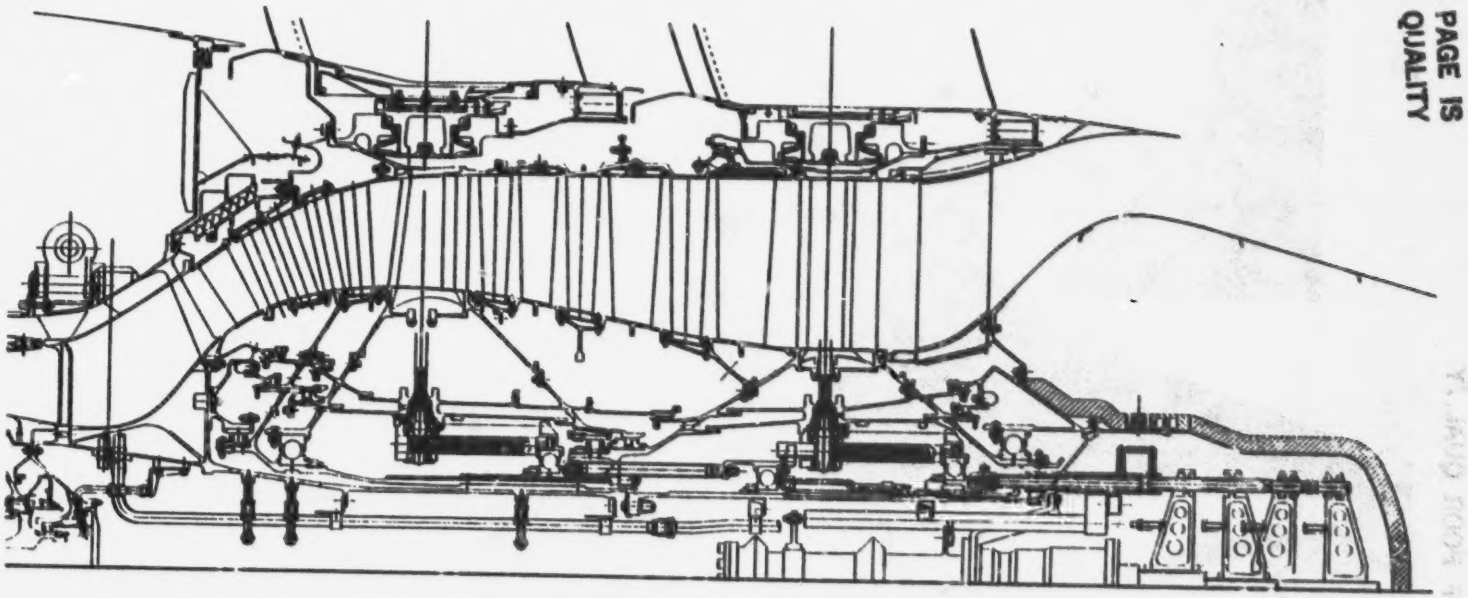

Figure 2-2. Cross Section of UDF™ Engine (Enlarged View).

~~ORIGINAL PAGE IS~~
~~OF POOR QUALITY~~

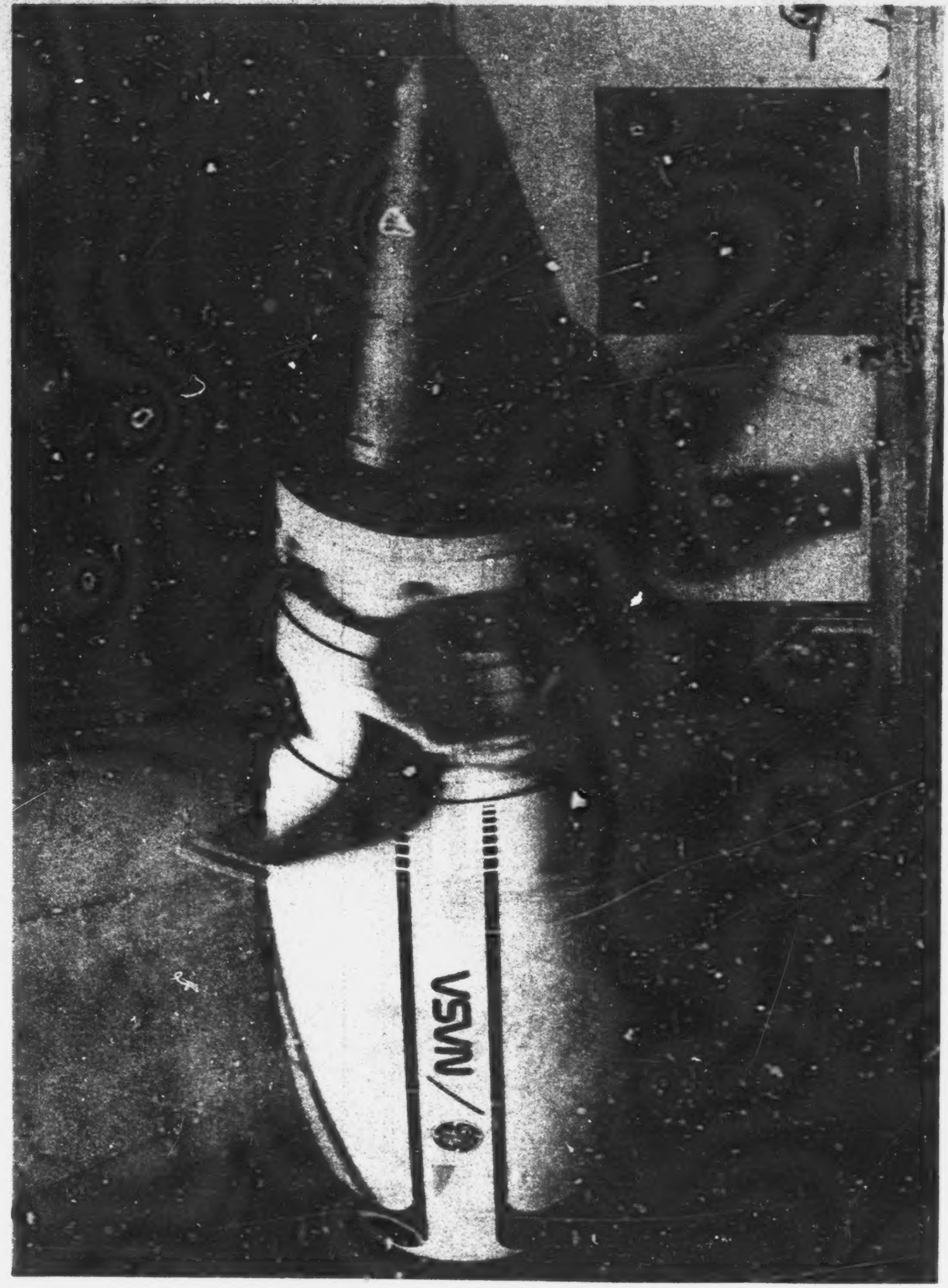

Figure 2-3. UDF™ Engine at Peebles Test Site 4A.

ORIGINAL PAGE
BLACK AND WHITE PHOTOGRAPH

~~ORIGINAL PAGE IS
OF POOR QUALITY~~

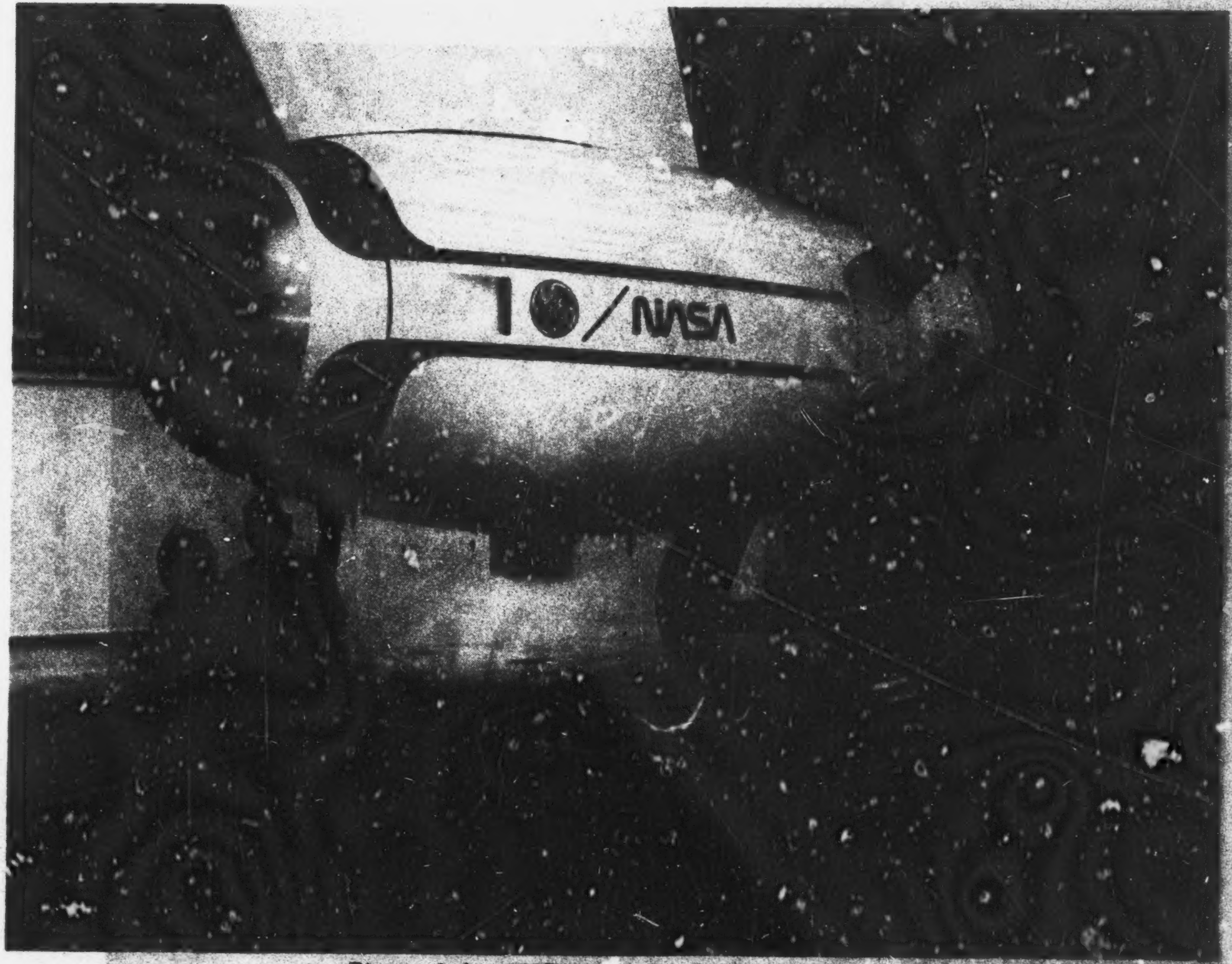

Figure 2-4. UDF™ Engine at Peebles Test Site 4A.

ORIGINAL PAGE
BLACK AND WHITE PHOTOGRAPH

ORIGINAL PAGE
BLACK AND WHITE PHOTOGRAPH

Figure 2-5. UDF™ Engine at Peebles Test Site 3D.

ORIGINAL PAGE IS
OF POOR QUALITY

The major design characteristics of the UDF™ engine are as follows:

Gas Generator

Model	F404-GE-400
Type	Low bypass turbofan
Fan	3-stage axial flow
Compressor	7-stage axial flow
Turbines	
Low pressure	One stage
High pressure	One stage
Rotor speeds	
Fan	13,270 rpm (100%)
Compressor	16,810 rpm (100%)
Maximum airflow	Approximately 140 lbm/s
Thrust	16,000 lbf class
Thrust-to-weight ratio	8:1 class
Overall compression ratio (maximum climb)	26:1

UDF™ Engine Propulsor

Maximum nacelle diameter	76.4 inches
Fan blade tip diameter	11.67 feet
Fan design point tip speed, physical (maximum cruise; 35,000 ft; 0.80 Mach; ISA)	780 feet/second
Fan rotor speed	1393 rpm (100%)
Fan disk loading, class SHP/A (maximum cruise; 35,000 ft; 0.80 Mach; ISA)	87 HP/ft^2
Fan blade radius ratio	0.415
Power turbine inlet temperature (SL, T/O, ISA +27° F).	1310° F

The gas generator/propulsor combination produces an engine with a net thrust of 25,000 pounds. Other significant design features which have been incorporated into this engine are:

- Advanced unducted fan aerodynamics that incorporate custom-tailored composite fan blades over an inner titanium spar that serves as the attachment mechanism to the engine for the fan blades.

- Fully developed and available gas generator to provide the necessary power for the engine.
- DEC (digital electronic control) that provides overall engine control by monitoring gas generator power and speed and propulsor speeds and pitch angles. The engine uses the existing gas generator control and a separate propulsor control to minimize development costs without sacrificing control flexibility.
- Hydraulic/mechanical actuation system enabling setting the fan blade pitch angle of the two fan blade rotors either together or differentially; this system is driven by the control system.
- Modular assembly of the gas generator and propulsor.
- Individually replaceable propulsor fan blades with the engine installed on the aircraft or test stand.

2.2 INSTRUMENTATION

The UDF™ instrumentation consists both of static and rotating instrumentation, with the rotating instrumentation being read out by telemetry on the rotors. Static instrumentation includes temperature, pressure, kulite, strain gage, and accelerometer instrumentation on the engine, pylon, and nacelle. Rotating instrumentation includes temperature, pressure, and strain gage instrumentation on the counterrotating rotors. Detailed information on UDF™ instrumentation is contained in the Instrumentation Plan (Statement of Work Paragraph 4.2 of Contract No. NAS-24210). Included in this is Drawing No. 4013341-034, which shows the engine cross section with the location of engine instrumentation and the corresponding parameter names. Reference GE36 Second Ground Test TPS No. MA-0004 for a detailed description of the instrumentation system and for a list and description of all parameters.

3.0 REVIEW OF UDF™ TESTING

The following significant events, data points, and problem areas from UDF™ testing will be expanded upon in the indicated sections:

	Builds Involved	Section
Forward stationary carbon seal failure	1	3.1
Forward telemetry antenna repair	1	3.2
Telemetry system temperature problem (includes reverse thrust test data)	1,2,3	3.3
Stage 1 turbine blade failure and stall event	1	3.4
Turbine blade damper effectiveness	1,2,3	3.5
Subidle oil leak problem	1,2	3.6
Stationary exhaust nozzle (centerbody) replacement	1,2	3.7,7.3
Fan bypass bleed valve calibration	2,3	3.8
Fan bypass bleed valve diffuser failure/replacement	2	3.9
Propulsor fan-blade-loss event	2	3.10
Propulsor fan blade history and test data	1,2,3	3.11
Power turbine frame stress investigation	2	3.12
Effect of "vortex destroyer" on stress	2,3	3.13
Effect of test site change on stress	2,3	3.14
Rotor lockup after shutdown resulting from fuel leak	3	3.15
LCF/HCF (low cycle fatigue/high cycle fatigue) testing	1,2,3	3.16
Rotor-to-rotor lockup/propulsor disassembly and rebuild	3	3.17
Miscellaneous hardware: stress data	1,2,3	3.18
Oil leak/oil gulping problem	2,3	3.19
Heat transfer and secondary flow system	1,2,3	4.0
Engine systems dynamics	1,2,3	5.0
Bearings and seals	1,2,3	6.0
Performance	1,2,3	7.0
Engine operability	1,2,3	8.0
Engine control	1,2,3	9.0
Nacelle structures	1,2,3	10.0

3.1 FORWARD STATIONARY CARBON SEAL FAILURE

After the first engine start, the engine was shut down due to a low oil level warning. Carbon seal pieces were found in the propulsor scavenge screens. The engine was removed from the test site, and the propulsor was separated from the gas generator. After separation, it was found that the forward stationary carbon seal was damaged. It was determined that the seal was damaged during assembly. The 2R bearing was also found damaged, this due to carbon seal debris. New hardware was added to the engine to help guide the propulsor rotors together to avoid any damage to the seal (Figure 3-1), which was completely replaced with new hardware, along with the 2R bearing. The propulsor was remated with the gas generator with no problems, and the engine was put back on test. There were no oil leaks when the engine tests resumed.

While running the engine with the damaged carbon seal, the resulting internal oil leak caused an unbalance in the rotors. This unbalance caused the Stages 7, 9, and 11 propulsor turbine blades to rub hard against the inner 6-11 spool. Twenty-two Stage 11 blades were found to have cracks in the root. It was decided to not replace these blades but to closely monitor their stress levels.

3.2 FORWARD TELEMETRY ANTENNA REPAIR

Operational problems with the forward telemetry system were caused by insufficient clearance between the static and rotating forward telemetry antenna components. These components were modified to increase the cold running clearance from 0.135 to 0.250 inch, as diagrammed in Figure 3-2.

3.3 TELEMETRY SYSTEM TEMPERATURE PROBLEMS

Problems with the telemetry system, due to high temperatures, resulted in design changes to increase cooling. Cooling scoops were added to the rotating exhaust nozzle to bring in additional ambient air to cool the telemetry system (especially that of Stage 2). Prior to the addition of cooling scoops, there were flush vent holes in the exhaust nozzle. The following summarizes the design changes:

- **Added New Engine Hardware To Guide Rotor**

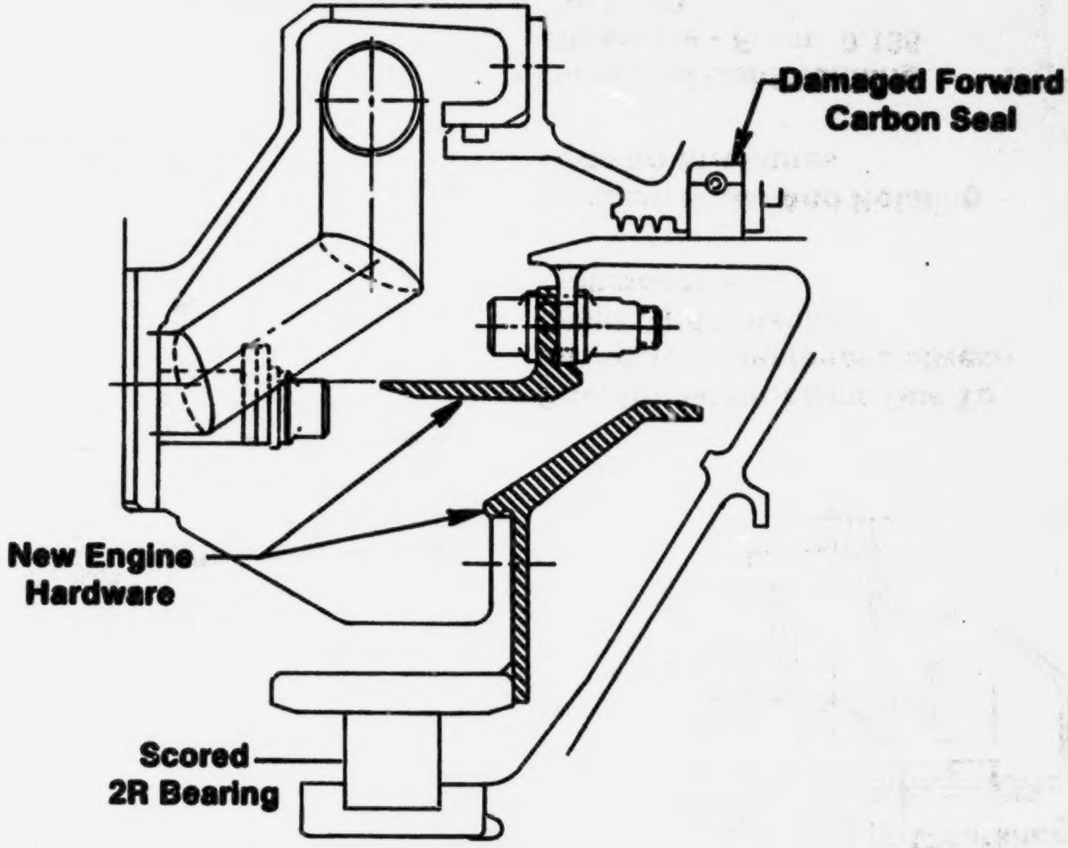
Damaged Forward Carbon Seal
New Engine Hardware
Scored 2R Bearing

Figure 3-1. Carbon Seal Assembly Fix.

ORIGINAL PAGE IS
OF POOR QUALITY

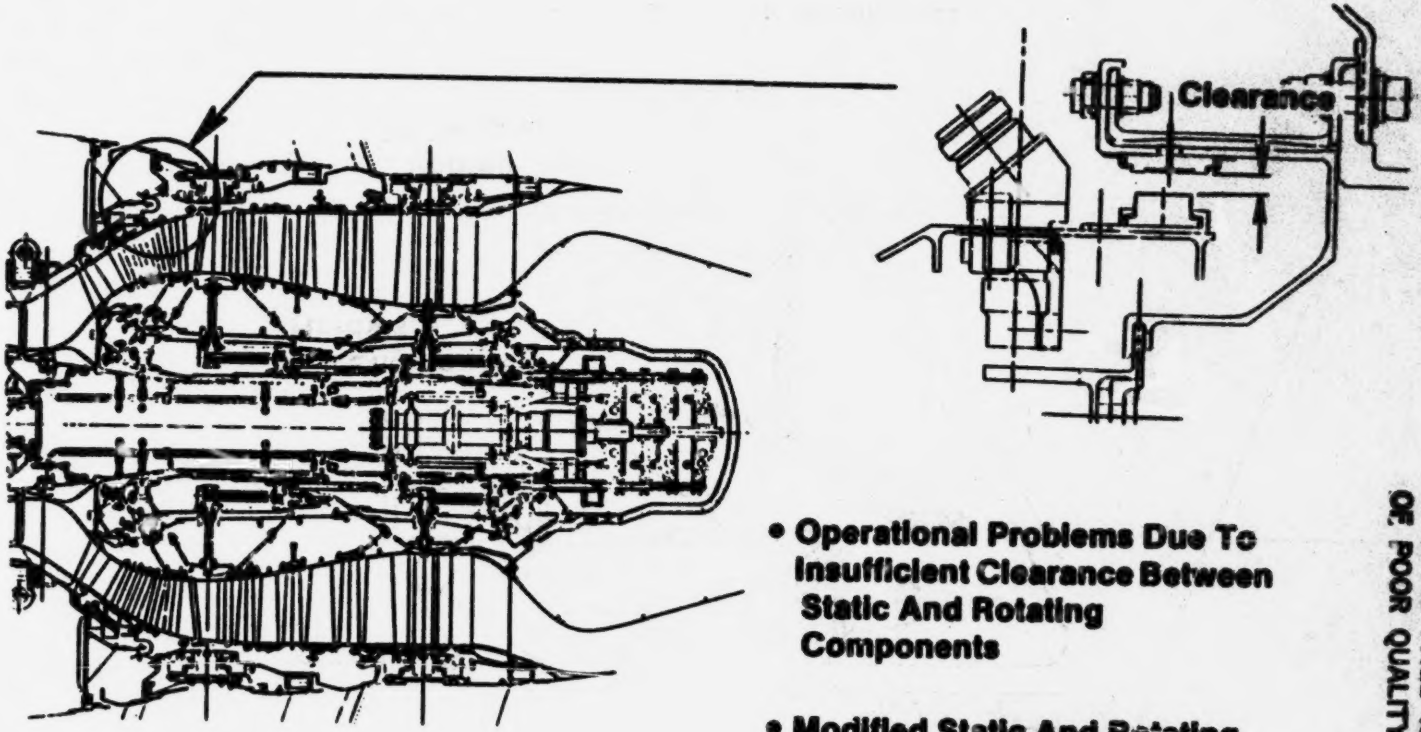

- Operational Problems Due To Insufficient Clearance Between Static And Rotating Components
- Modified Static And Rotating Support Structures
- Increased Cold Running Clearance - From: 0.135 To: 0.250

Figure 3-2. Forward Telemetry System Support.

Configuration	**Run Time With Configuration**
No Scoops - flush holes (0.468-inch diameter) in exhaust nozzle, 60 total. Build 1; August 29 to September 27, 1985 Data Symbol: None	3:43 hr
Pipe Elbow Scoops - with 0.375-inch diameter openings, 30 total. Build 1; October 2, 1985 Data Symbol: Pipe	1:41 hr
Aerodynamic Scoops - with 0.500-inch diameter openings, 30 total. Build 2; January 30 to April 2, 1986 Data Symbol: Aero	25:44 hr
Modified Aerodynamic Scoops - four 0.188-inch diameter holes added to side of scoops, 30 total. Build 2; April 8 to 24, 1986. Build 3; June 20 to July 8, 1986 Data Symbol: Mod Aero	69:43 hr

The addition of four holes to the side of the scoops were an attempt to increase flow to the telemetry system during static ground testing. Sixty of the modified aerodynamic scoops will be used for flight test. Figures 3-3 and 3-4 illustrate the telemetry system and cooling scoop designs.

Figures 3-5 through 3-8 show both raw telemetry temperature data and data normalized with the ambient temperature (T_{AMB}). The data was normalized due to the large variation in ambient temperature which has a direct effect on the telemetry temperatures. Note that temperatures recorded during Configuration 3 were cooler than those of Configuration 4. This shows the effect of ambient temperature on the telemetry temperatures. Also during Configuration 4, there was more test time and more time at power which would tend to increase temperatures. Also note that there is no data for the first two configurations for Stage 1; the thermocouple was not reading at those times. The telemetry temperature limit set during ground testing, after the first configuration, was 300° F.

During reverse thrust testing, Stage 2 telemetry temperatures increased throughout the time the engine was in reverse. Figures 3-9 and 3-10 show the telemetry temperatures during a reverse thrust cycle. This was the fifth of a series of consecutively run reverse cycles.

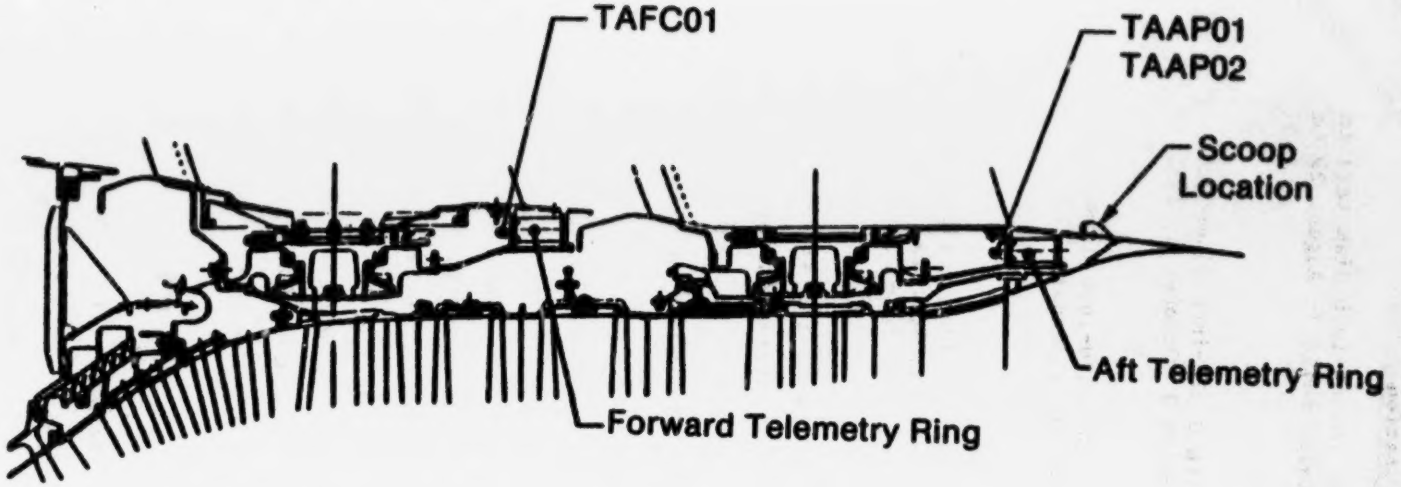
TAFC01
TAAP01
TAAP02
Scoop
Location
Forward Telemetry Ring
Aft Telemetry Ring

Figure 3-3. GE36 Telemetry System.

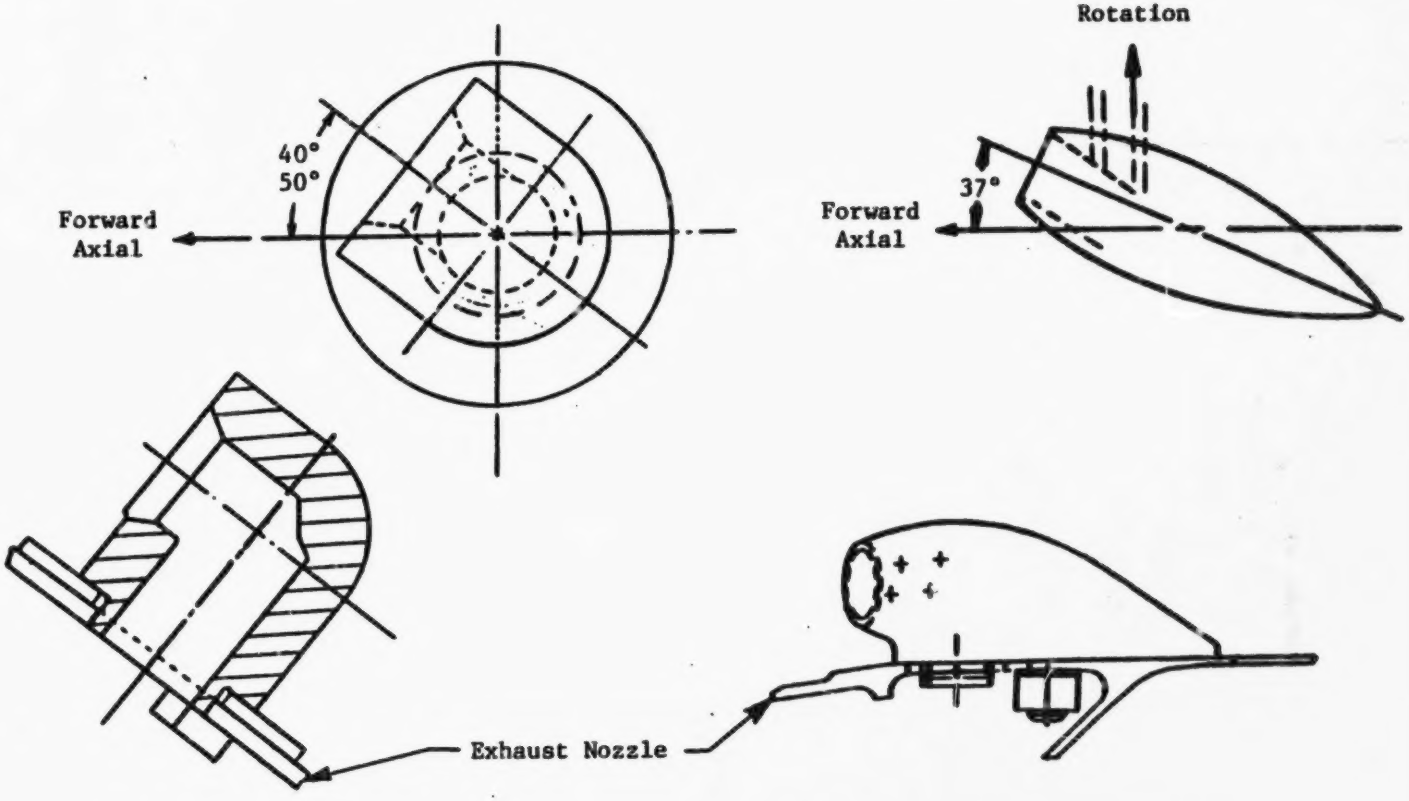
Rotation
40°
50°
Forward
Axial
37°
Forward
Axial
Exhaust Nozzle

Pipe Elbow
Scoops

Aerodynamic Scoops Shown
with Hole Locations

Figure 3-4. Telemetry System Scoop Designs.

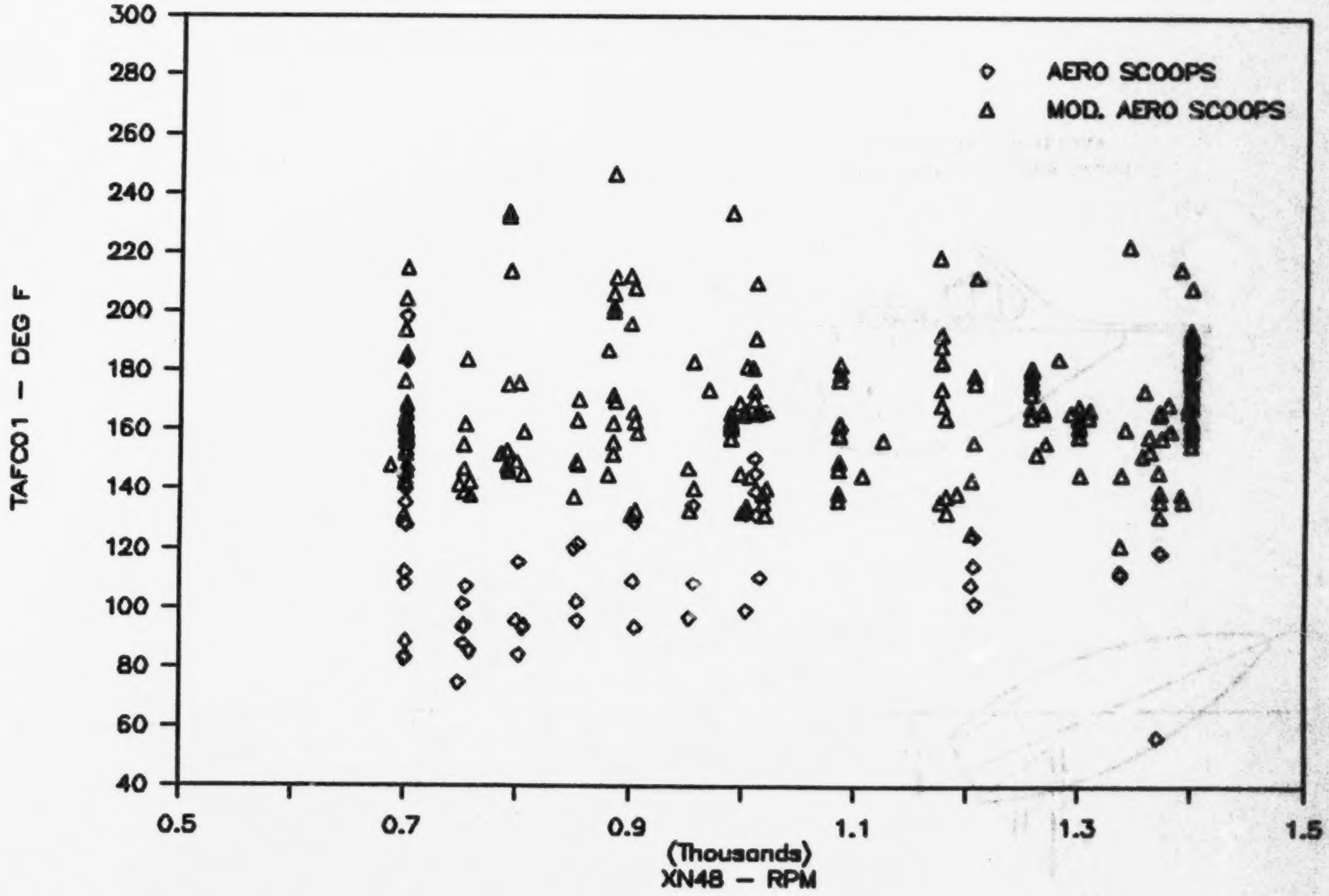

Figure 3-5. Forward Telemetry Temperatures - Raw Data.

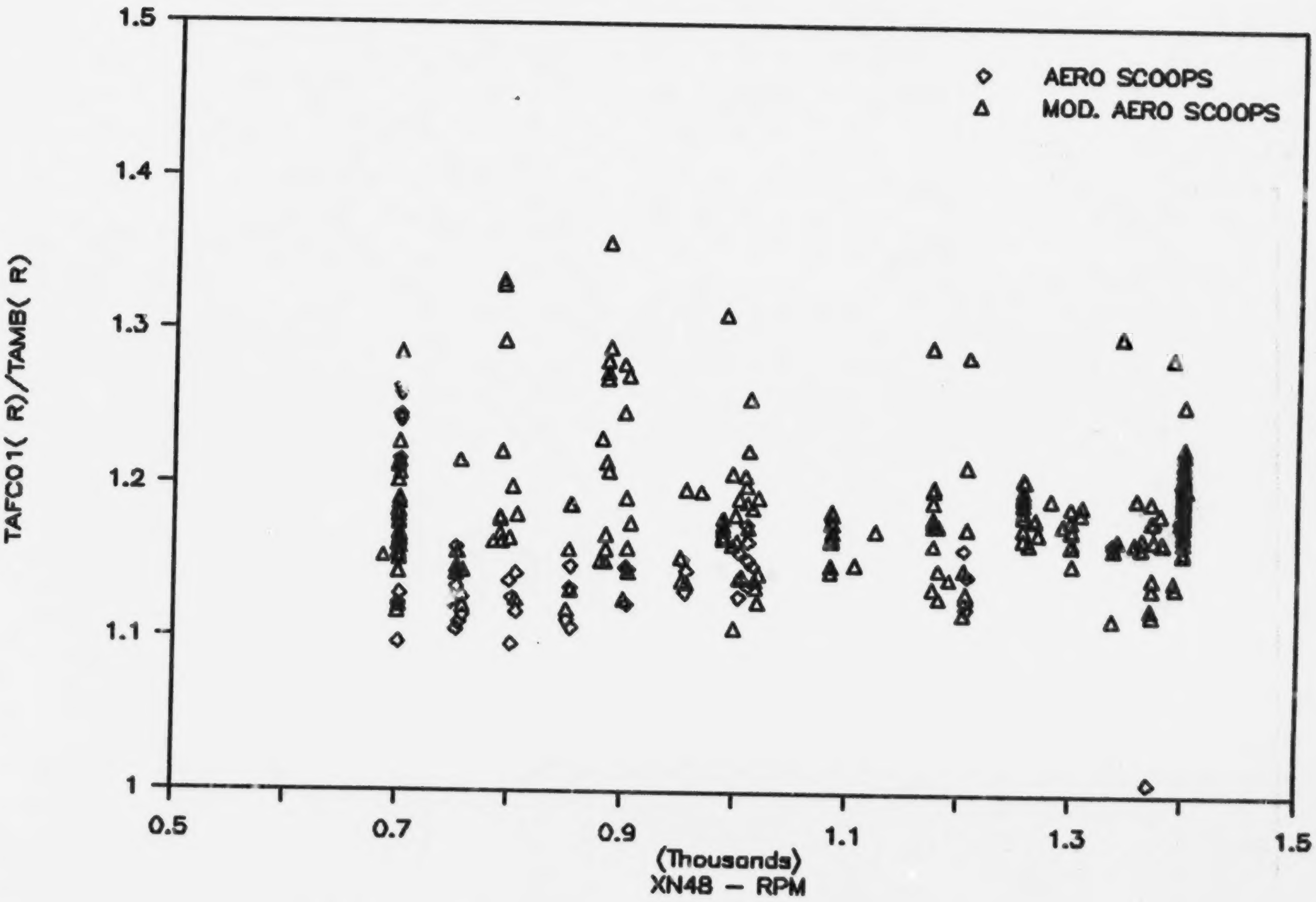

Figure 3-6. Forward Telemetry Temperatures - Normalized with T_{AMB}.

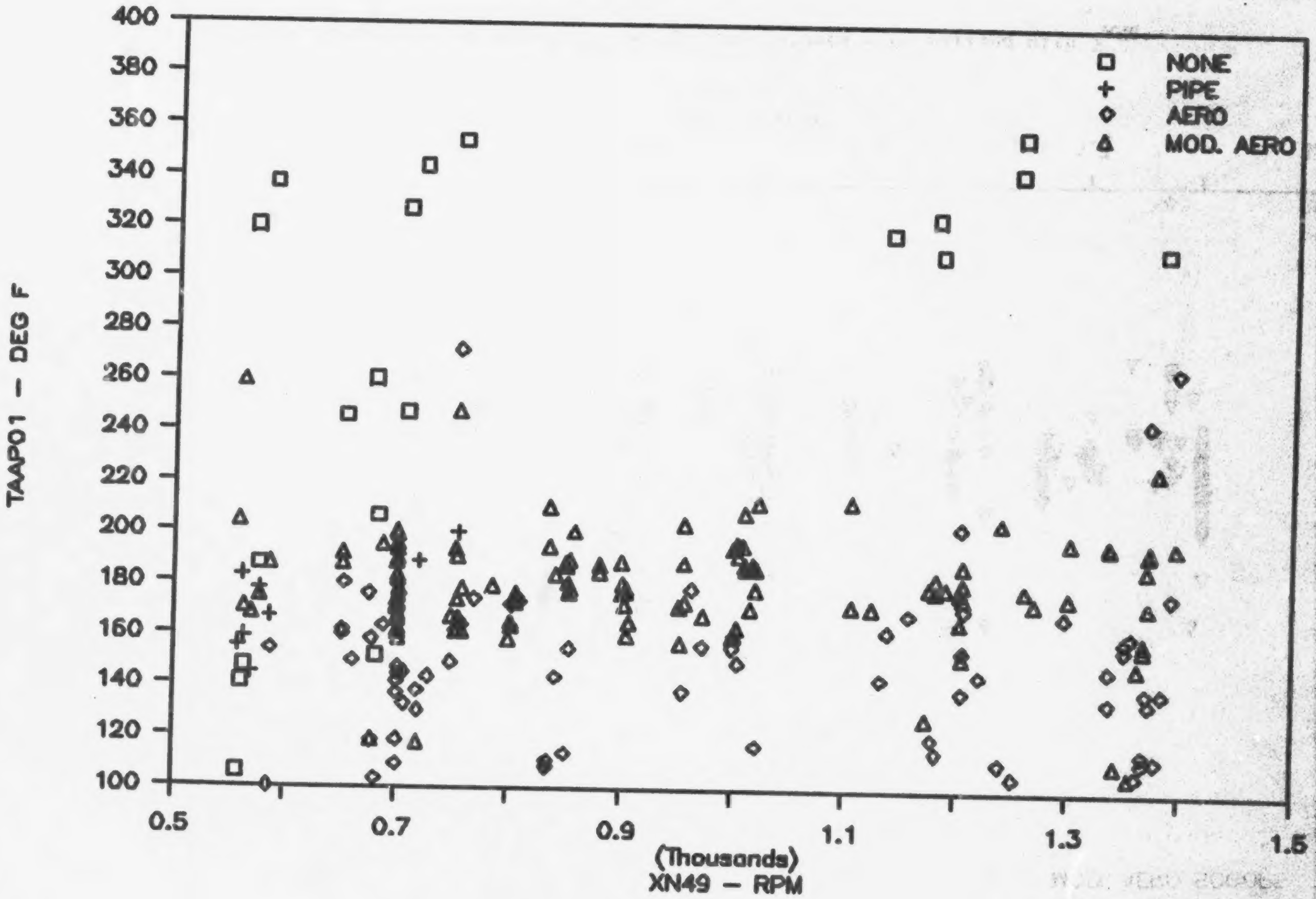

Figure 3-7. Aft Telemetry Temperatures - Raw Data.

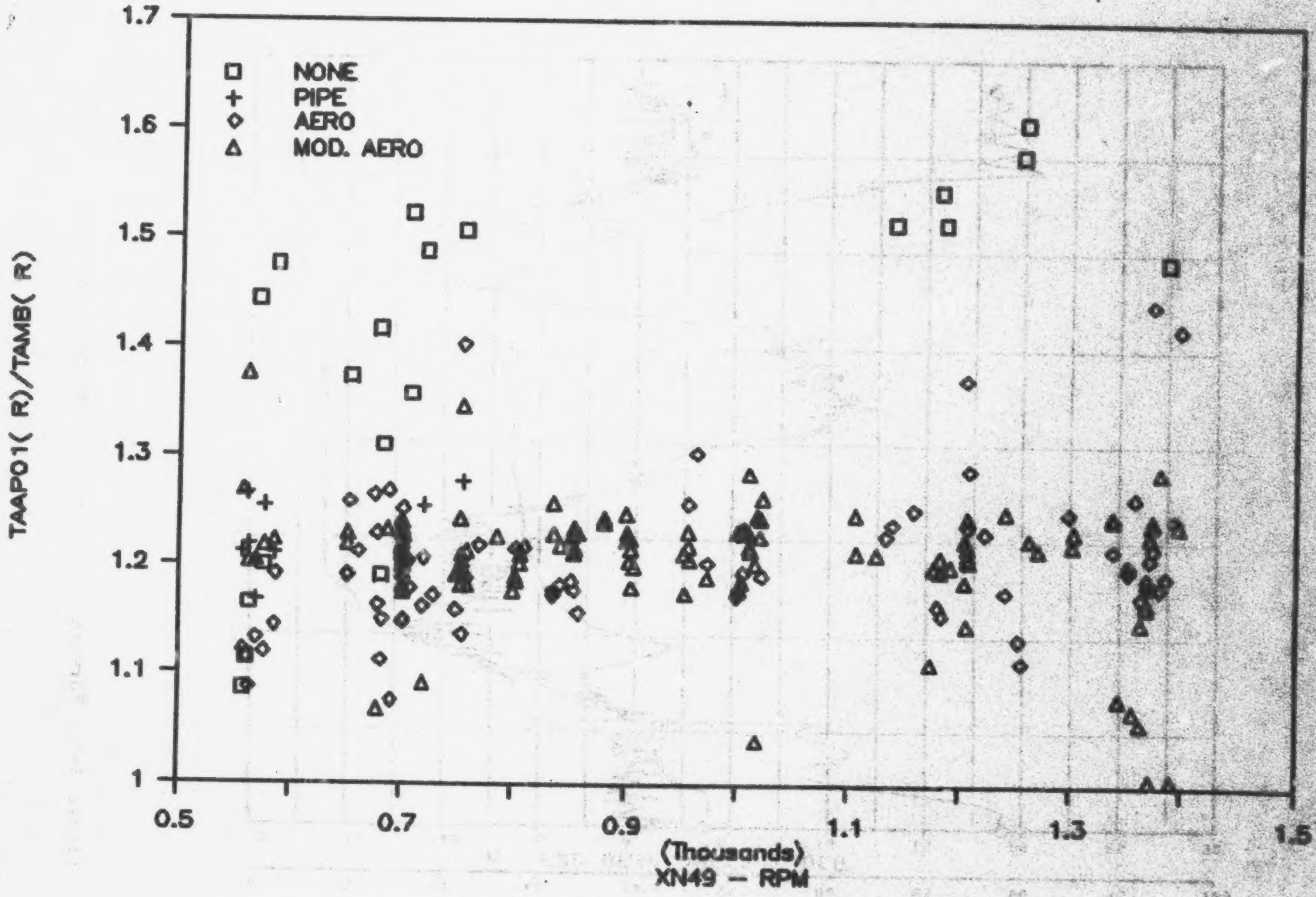

Figure 3-8. Aft Telemetry Temperatures - Normalized with T_{AMB}.

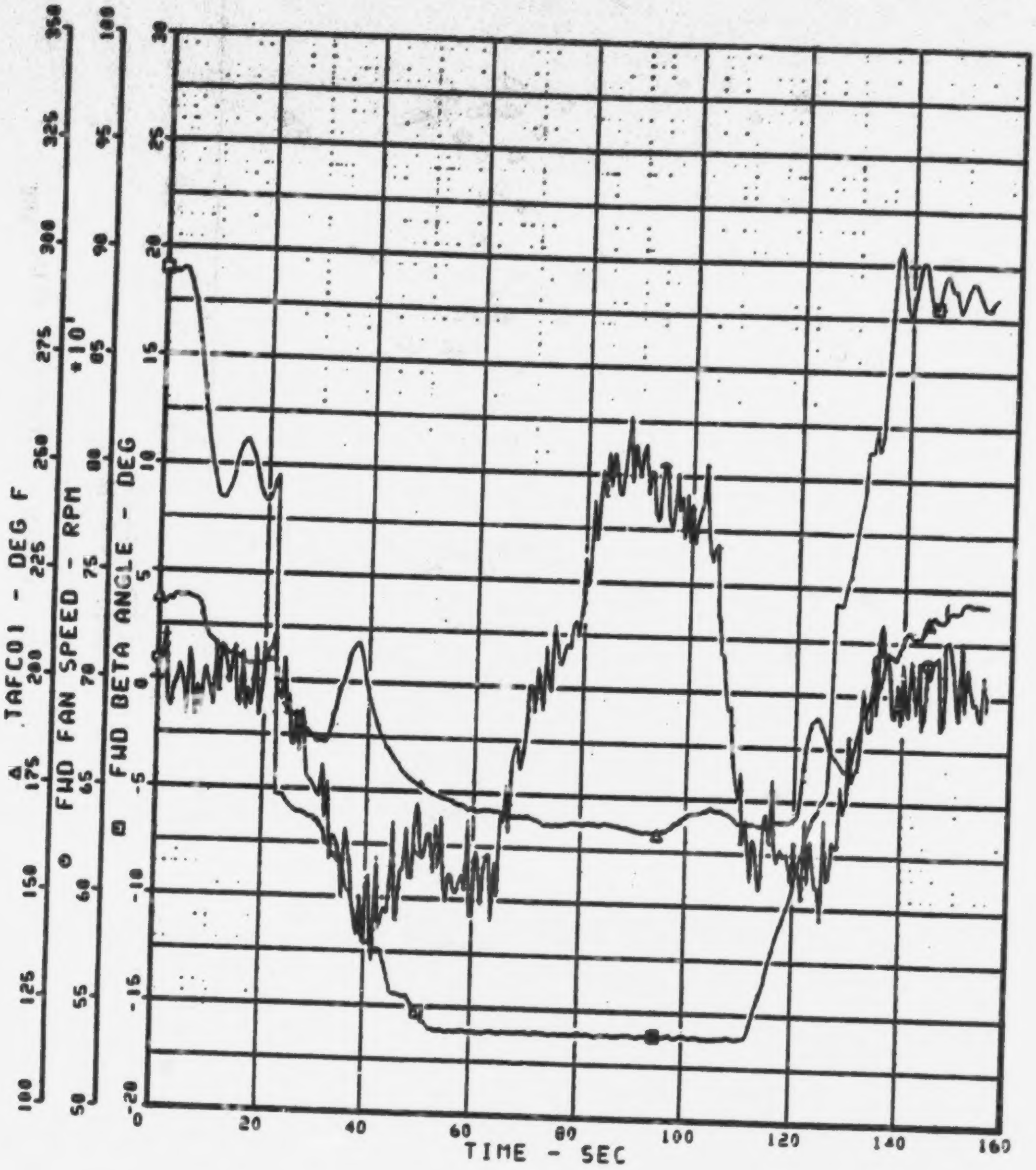

Figure 3-9. Forward Telemetry Temperatures - Reverse Testing.

ORIGINAL PAGE IS
OF POOR QUALITY

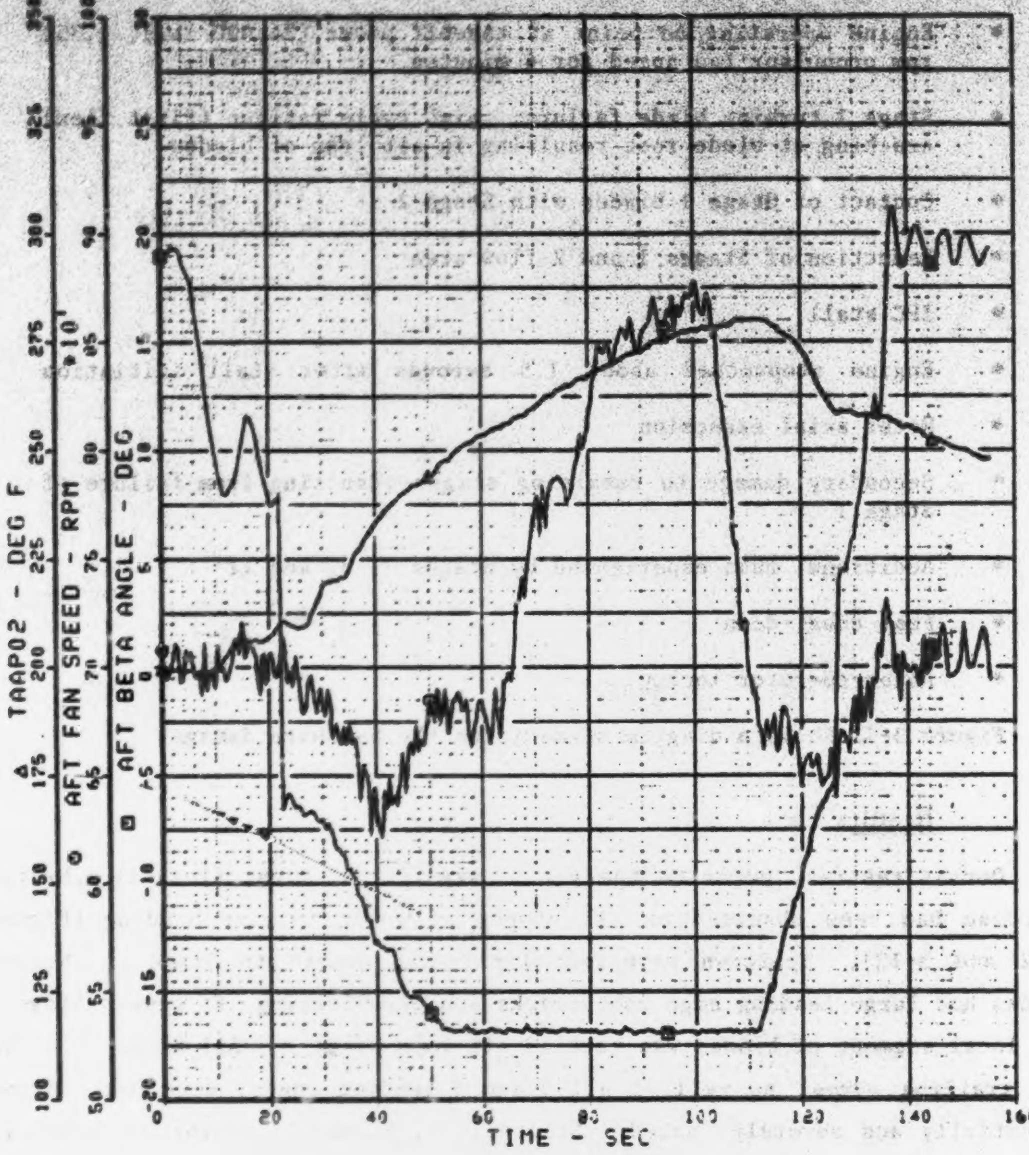

Figure 3-10. Aft Telemetry Temperatures - Reverse Testing.

ORIGINAL PAGE IS
OF POOR QUALITY

3.4 STAGE 1 TURBINE BLADE FAILURE AND STALL EVENT

Sequence of Events

- Engine operating on point at takeoff power (24,000 lbf), 1,350 rpm propulsor fan speed for 4 minutes
- Stage 1 turbine blade failure: high cycle fatigue (first flex) cracking at blade root resulting in aft lean of blades
- Contact of Stage 1 blades with Stage 2
- Reduction of Stages 1 and 2 flow area
- IPC stall
- Engine stopcocked about 1.5 seconds after stall initiation
- Rotor axial excursion
- Secondary damage to remaining stages resulting from failure of Stage 1
- Additional rubs experienced by Stages 7, 9, and 11
- Fast coast-down
- Rotor-to-rotor lockup.

Figure 3-11 shows a diagram summarizing the hardware damage.

Results

During testing, prior to the stall, significant first flexural vibratory response had been observed on all stages of power turbine blading (Figures 3-12 and 3-13). Teardown revealed significant damage to Stage 1. Several blades had large leading edge root cracks and were leaning aft toward Stage 2. One local segment of blades was buckled aft into Stage 2. All Stage 2 leading and trailing edges, as well as all Stage 3 leading edges, were bent circumferentially and severely rubbed. Stages 1, 7, 9, and 11 exhibited severe tip rub. While Stages 7, 9, and 11 had rubbed previously during Build No. 1 due to oil leakage past a broken carbon seal, the poststall rubs were more severe. Stage 4 had very light tip rub only at the trailing edge. Stages 2, 3, 6, and 8 exhibited no tip rub. Stage 10 rubbed only one blade, which was bent at the platform. Stages 7, 9, and 11 had several bent airfoils. The rotor inner

ORIGINAL PAGE IS
OF POOR QUALITY

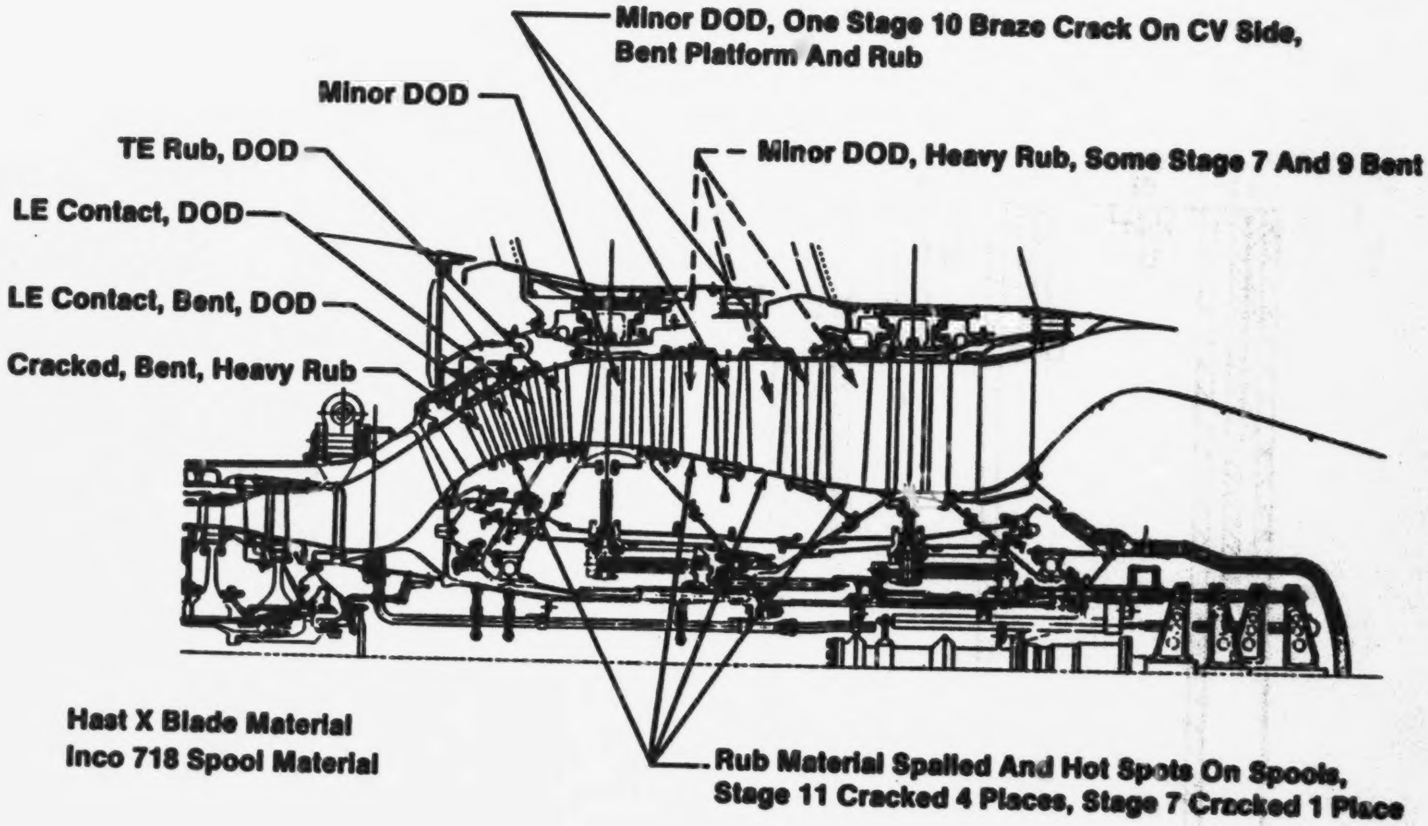
Minor DOD, One Stage 10 Braze Crack On CV Side, Bent Platform And Rub
Minor DOD
TE Rub, DOD
Minor DOD, Heavy Rub, Some Stage 7 And 9 Bent
LE Contact, DOD
LE Contact, Bent, DOD
Cracked, Bent, Heavy Rub
Hast X Blade Material
Inco 718 Spool Material
Rub Material Spalled And Hot Spots On Spools, Stage 11 Cracked 4 Places, Stage 7 Cracked 1 Place

Figure 3-11. Summary of Hardware Damage.

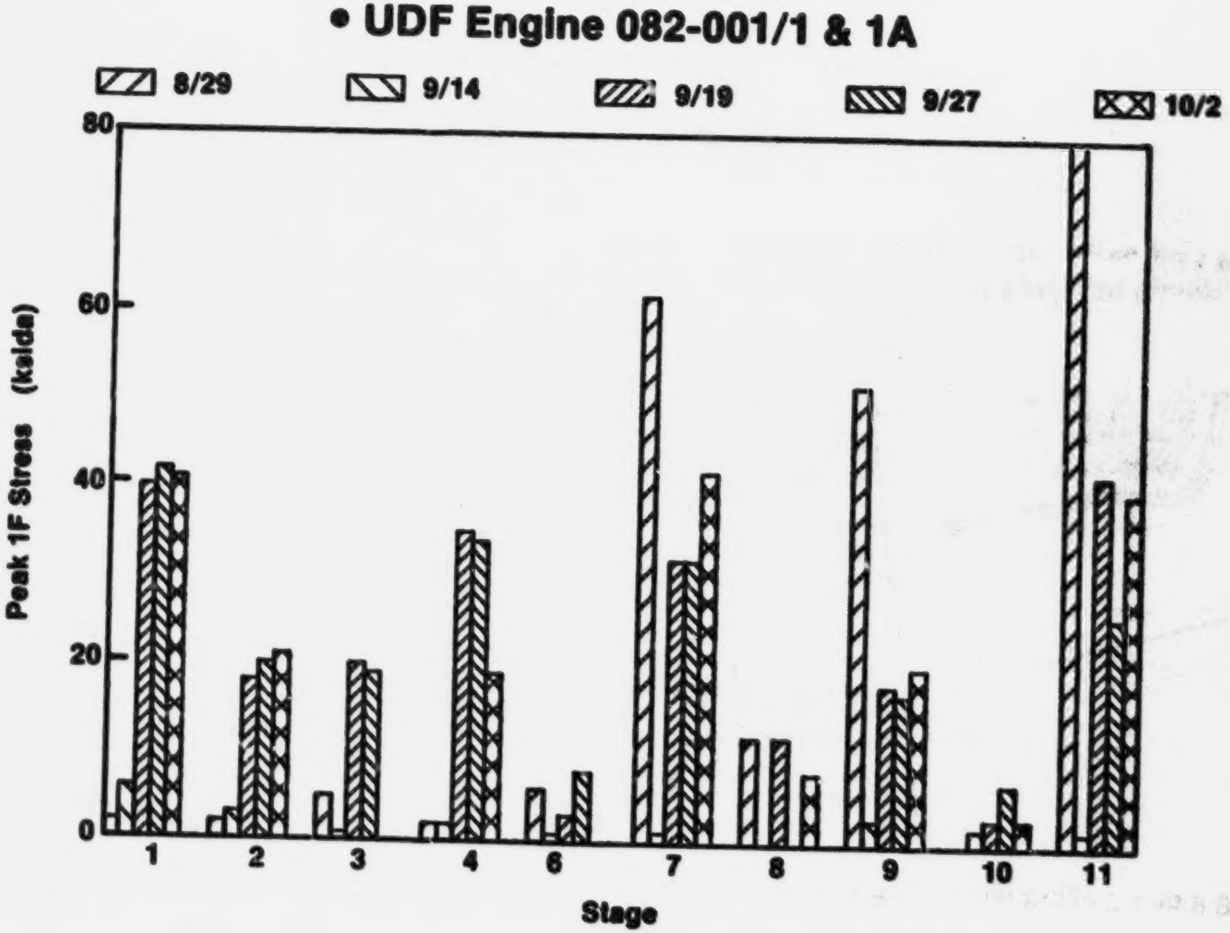

Figure 3-12. Turbine Blade 1F Stress Trend.

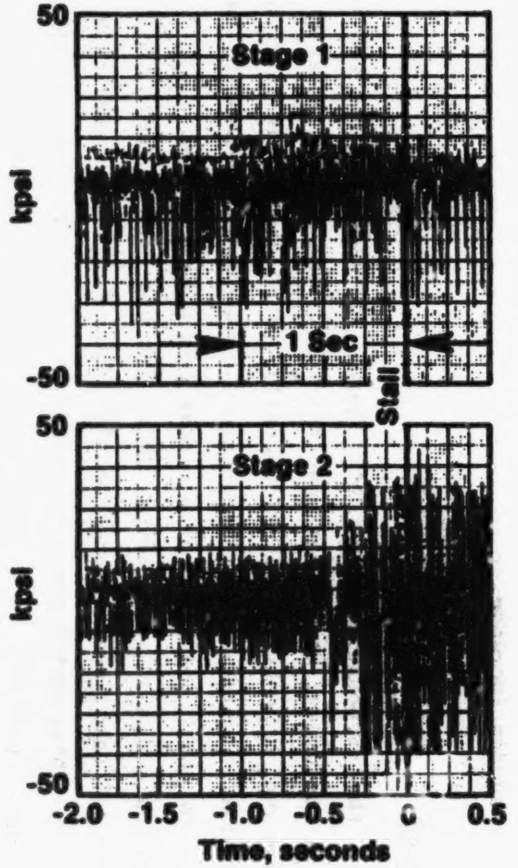

- Morning Run Similar To 9-19-85 And 9-27-85 Runs
- Accel To 1200 - Back Off For Stage 1 20 Per Rev/1F
- Accel To 1300 - Back Off For Stage 7 8 Per Rev/1F
- Accel To Thrust - Back Off For T46
- Accel To Thrust And Stabilize
- Stress Stable Until 0.5 - 1 Second Before Stall

Figure 3-13. History of Turbine Blade Response, Run to Thrust and Stall.

ORIGINAL PAGE IS
OF POOR QUALITY

spools exhibited local burn spots at Stages 1, 7, 9, and 11 rub locations, with cracking evident at Stages 7 and 11. Domestic object debris damage was confined to the power turbine flowpath. Nicks and dents were significant only on the forward turbine blade stages. The power frame and OGV (outlet guide vanes) airfoils exhibited only minor debris damage.

Metallurgical evaluation of the Stage 1 blades found root leading edge cracks on 117 of 124 airfoils. However, none of the airfoils were completely separated. Crack lengths varied from approximately 0.02 to 1.2 inch. SEM (scanning electron microscopy) revealed evidence of high cycle fatigue along the entire fracture surface. Evidence of root fatigue cracking was also found on Stages 2, 4, 6, and 11. Stages 7 and 9, and the one bent Stage 10 blade, were found to have tensile cracks at the root braze joints and tensile tears in some of the platform braze joints. Local burn spots on the spools showed evidence of severe overtemperature of the Inco 718 substrate. Four locations at Stage 11 and one at Stage 7 were confirmed cracked.

Posttest review of recorded data indicated stable engine operation while sitting on point until approximately 0.5 to 1 second prior to the stall. At that time, propulsor speed started dropping slowly while the control increased fuel flow to compensate, and vibratory response on the forward turbine blade stages showed a sudden increase.

Conclusions

Based on the responsiveness of all stages of power turbine blading at first flexural frequency, it is concluded that the blade and spool design configuration did not provide effective dovetail Coulomb damping as anticipated. Hardware condition indicates that the Stage 1 blades were cracked to varying degrees prior to stall and that these cracks propagated in high cycle fatigue while sitting on point on October 2, 1985. As the cracks grew, the blades leaned further aft until one or more contacted Stage 2, causing the slow drop-off in propulsor rotor speed prior to the stall. Contact with Stage 2 rolled the leading edge, resulting in a sudden reduction in power turbine flow function. The reduction in flow function caused the F404 gas generator to stall. The remainder of the damage was secondary during the rapid shutdown.

Corrective Action

All power turbine blades were replaced for Build 2. Spanning across adjacent blades, coulomb dampers (in the form of René 41 pins) were designed for all stages of blading as illustrated in Figure 3-14. Effectiveness of the damper design has been substantiated by component rig spin ("whirligig") and bench wear tests. Although no evidence of fatigue was indicated for the power frames, dampers were also added to Stage 12 as a precaution due to a predicted first flexural response with the outlet guide vane passing frequency. Strain gages have also been added to the Stages 5 and 12 power frame airfoils for Build 2.

Low cycle fatigue and crack growth analyses of the spools indicate that they have sufficient life capability for the remainder of planned testing. The spools have been weld repaired and the rub coats stripped and reapplied to provide additional margin.

Because of the severity of rub during Build 1 when oil leaked past the forward intershaft carbon seal and during the Build 1A stall, power turbine blade tip clearances have been increased an additional 0.050-inch on the outer attached blades and 0.030-inch on the inner attached blades, and all tips have been tapered to 0.005 to 0.015-inch thickness as a precautionary measure.

3.5 TURBINE BLADE DAMPER EFFECTIVENESS

Coulomb damper pins were added to all turbine blade stages (1-4, 6-11) and to Stage 12 power turbine frame airfoils (Section 3.4 and Figure 3-14). Figure 3-15 demonstrates the Stage 1 turbine blade vibratory-stress reduction resulting from the addition of the damper pins. Figure 3-16 shows the Stage 1 vibratory stress in relation to the scope limits before and after addition of the dampers. Figures 3-17 through 3-26 illustrate the vibratory stress for all turbine blade stages after installation of the dampers. Data are from an accel to 25,000 lbf, except for Stage 11 blades data (bad telemetry signal) which is from an accel to 22,000 lbf. Section 3.11 contains stress data for the turbine frame blades.

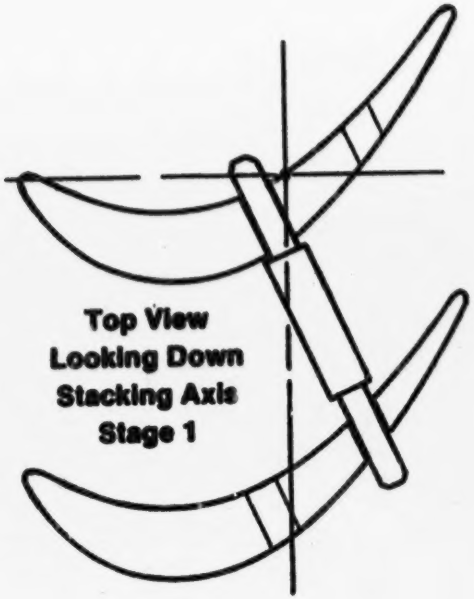
Top View
Looking Down
Stacking Axis
Stage 1

- Blade-To-Blade Damper Pins
- Increased Tip Clearance
  + 0.050 Inch Stages 1, 3, 7, 9, 11
  + 0.030 Inch Stages 2, 4, 6, 8, 10
- Reduced Tip Thickness
  (0.030 → 0.015)

Figure 3-14. Turbine Blade Fix.

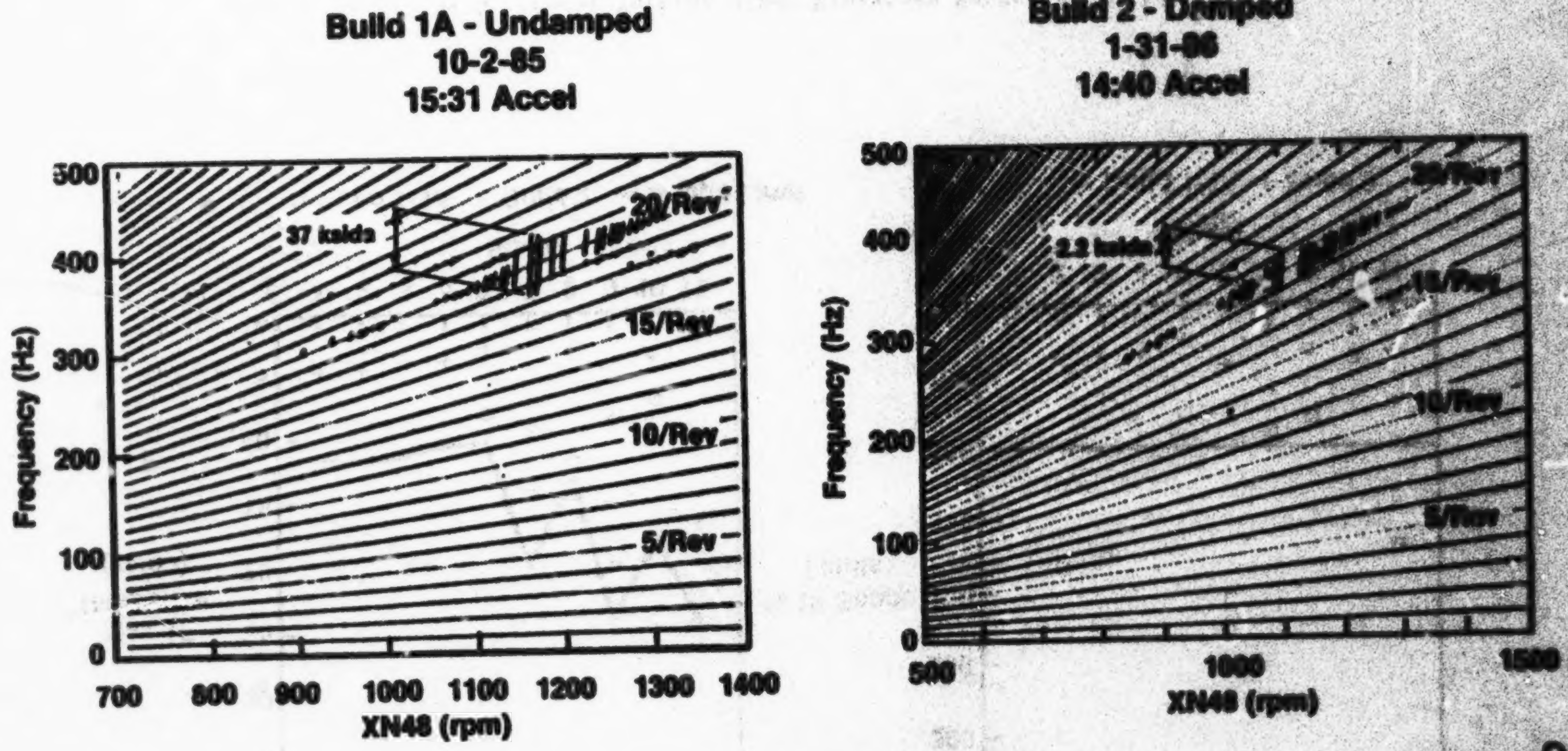

Dampers Highly Effective

Figure 3-15. Power Turbine Blade Vibratory Response, Damper Effectiveness - Stage 1.

ORIGINAL PAGE IS
OF POOR QUALITY

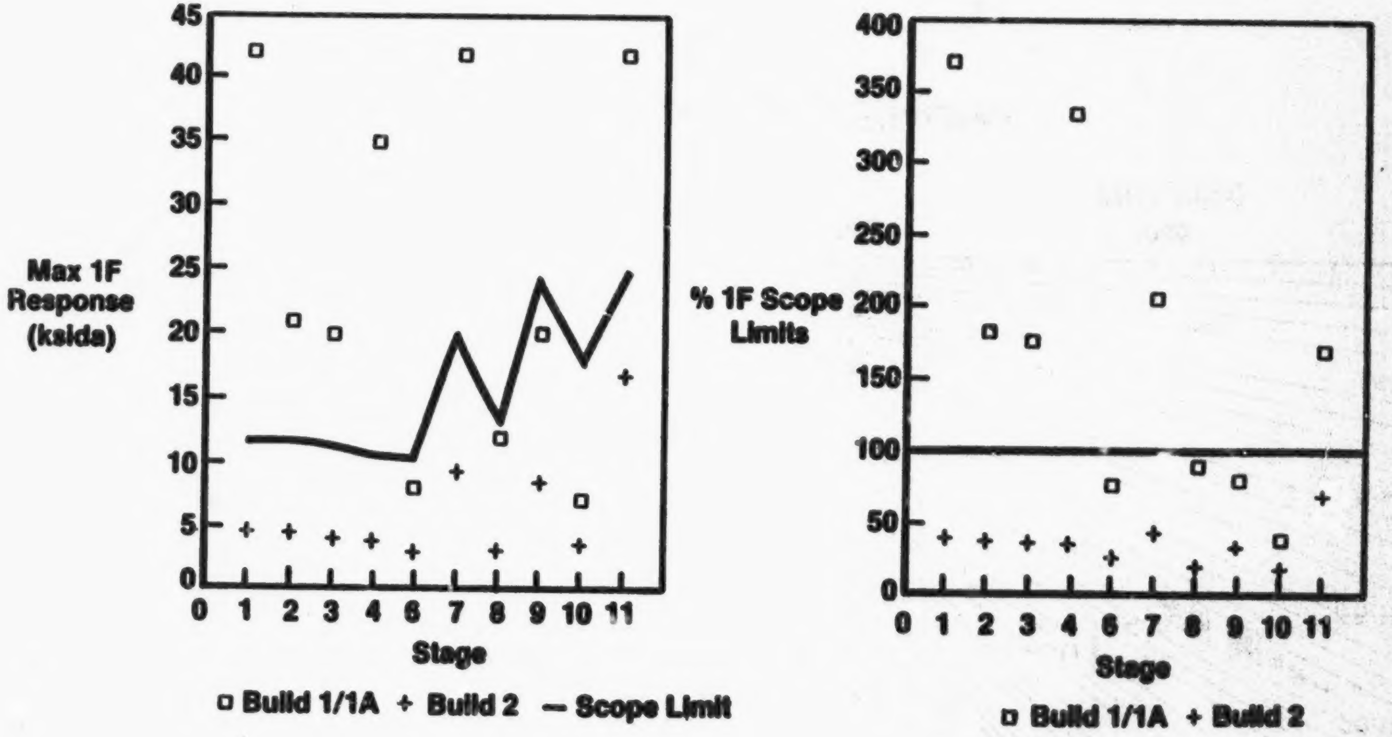

Figure 3-16. Power Turbine Blade Vibratory Response, Build 1 (Undamped) versus Build 2 (Damped).

ORIGINAL PAGE IS
OF POOR QUALITY

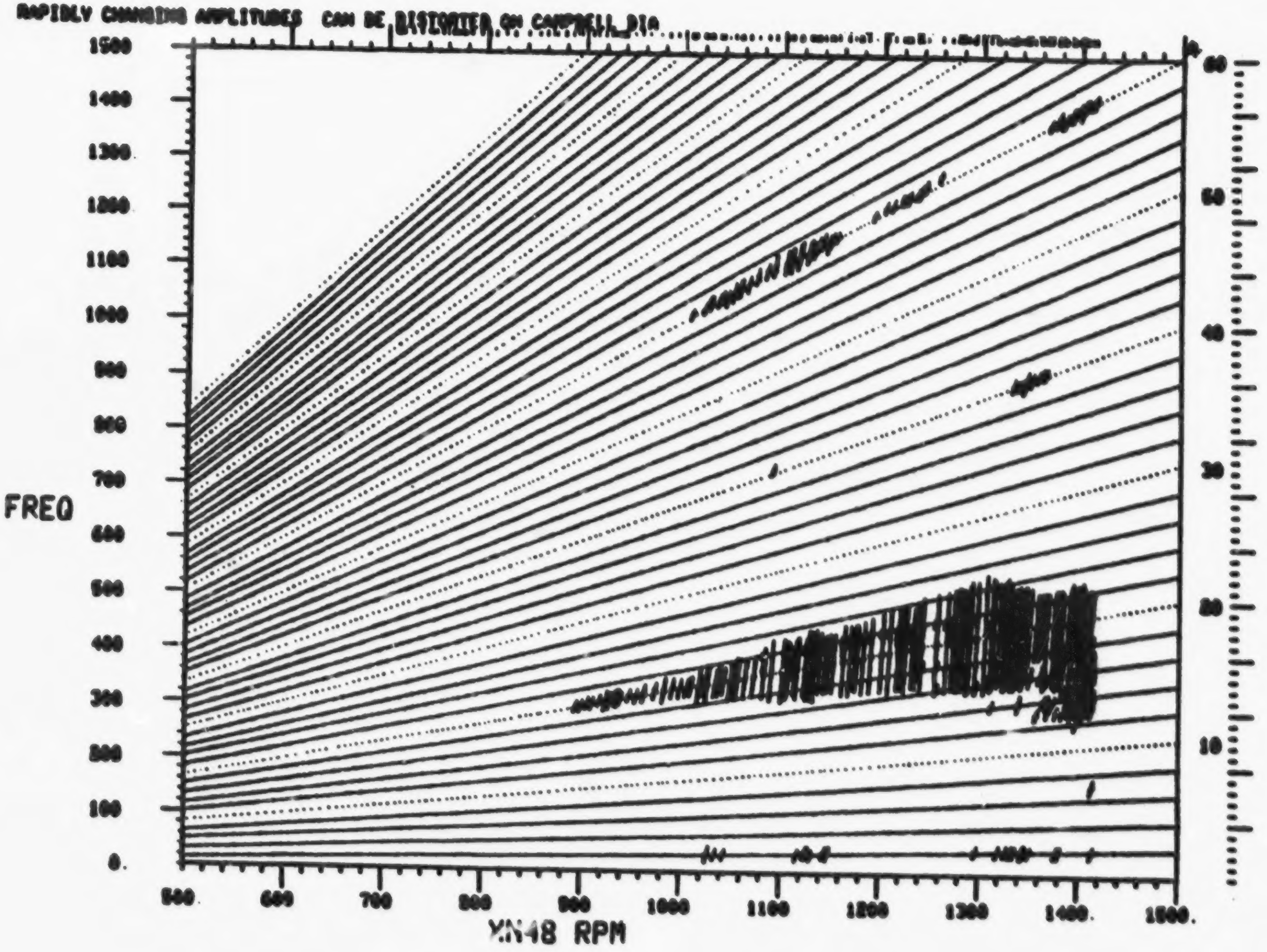

Figure 3-17. Stage 1 Turbine Blade Response, Accel to 25,000 lbf Thrust: February 4, 1986.

ORIGINAL PAGE IS
OF POOR QUALITY

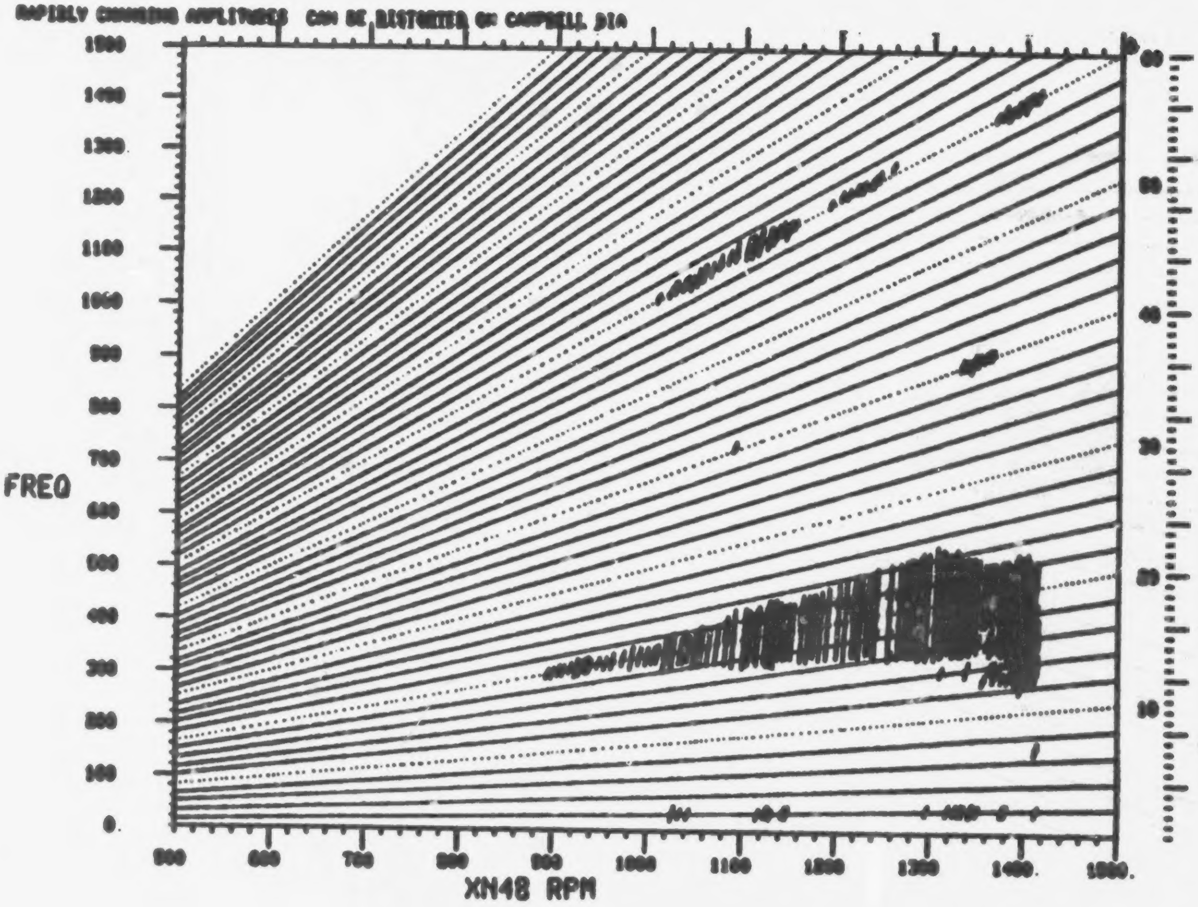

Figure 3-18. Stage 2 Turbine Blade Response, Accel to 25,000 lbf Thrust: February 4, 1986.

ORIGINAL PAGE IS OF POOR QUALITY

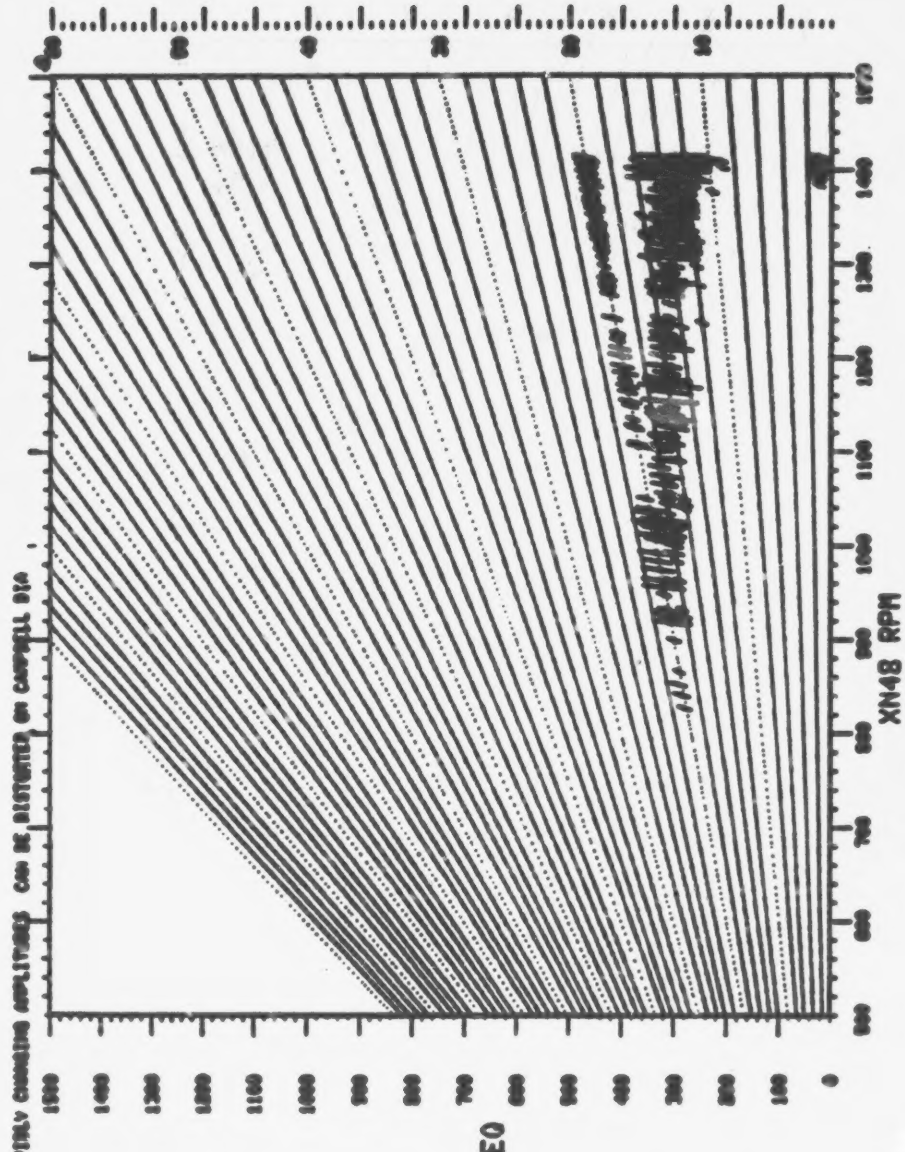

Figure 3-19. Stage 3 Turbine Blade Response, Accel to 25,000 lbf Thrust: February 4, 1986.

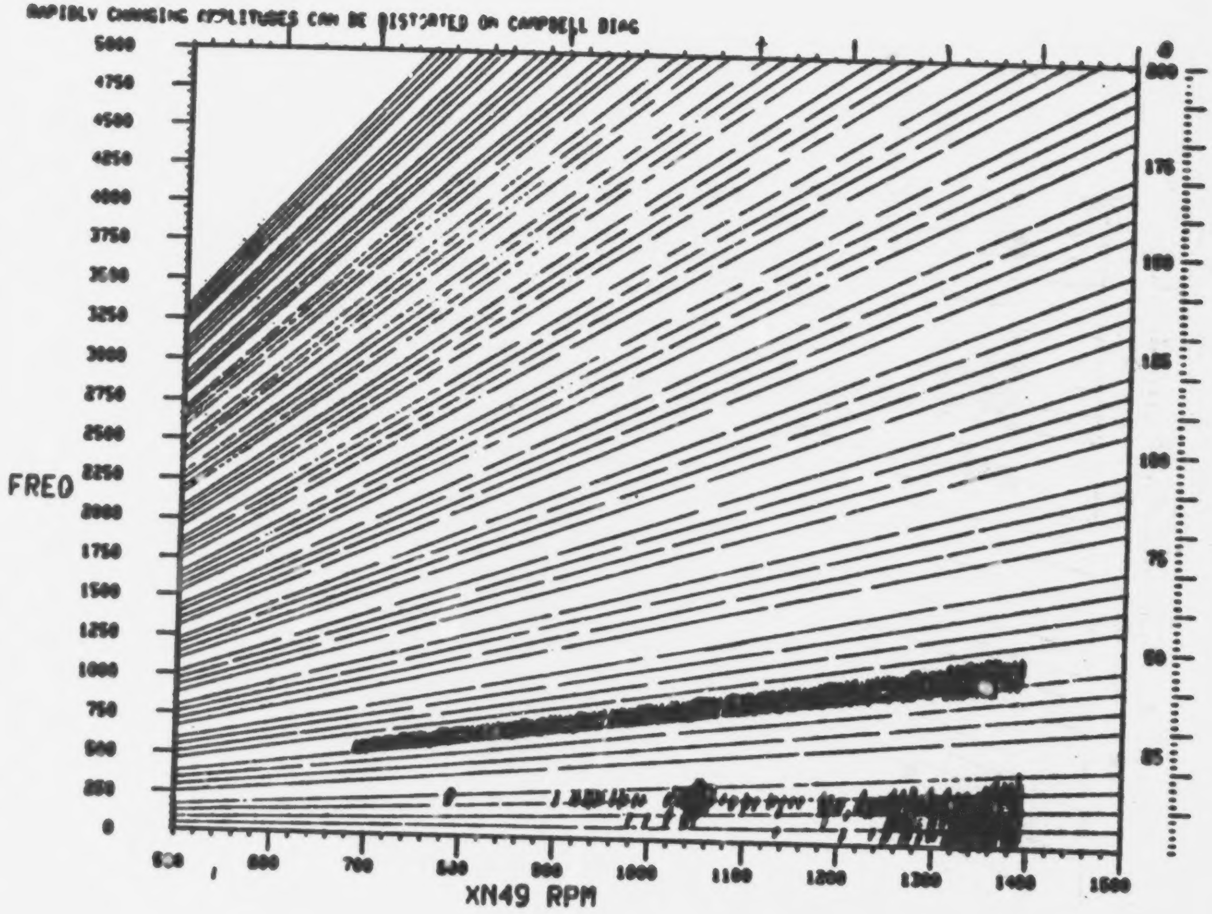

Figure 3-20. Stage 4 Turbine Blade Response, Accel to 25,000 lbf Thrust: February 4, 1986.

ORIGINAL PAGE IS
OF POOR QUALITY

ORIGINAL PAGE IS
OF POOR QUALITY

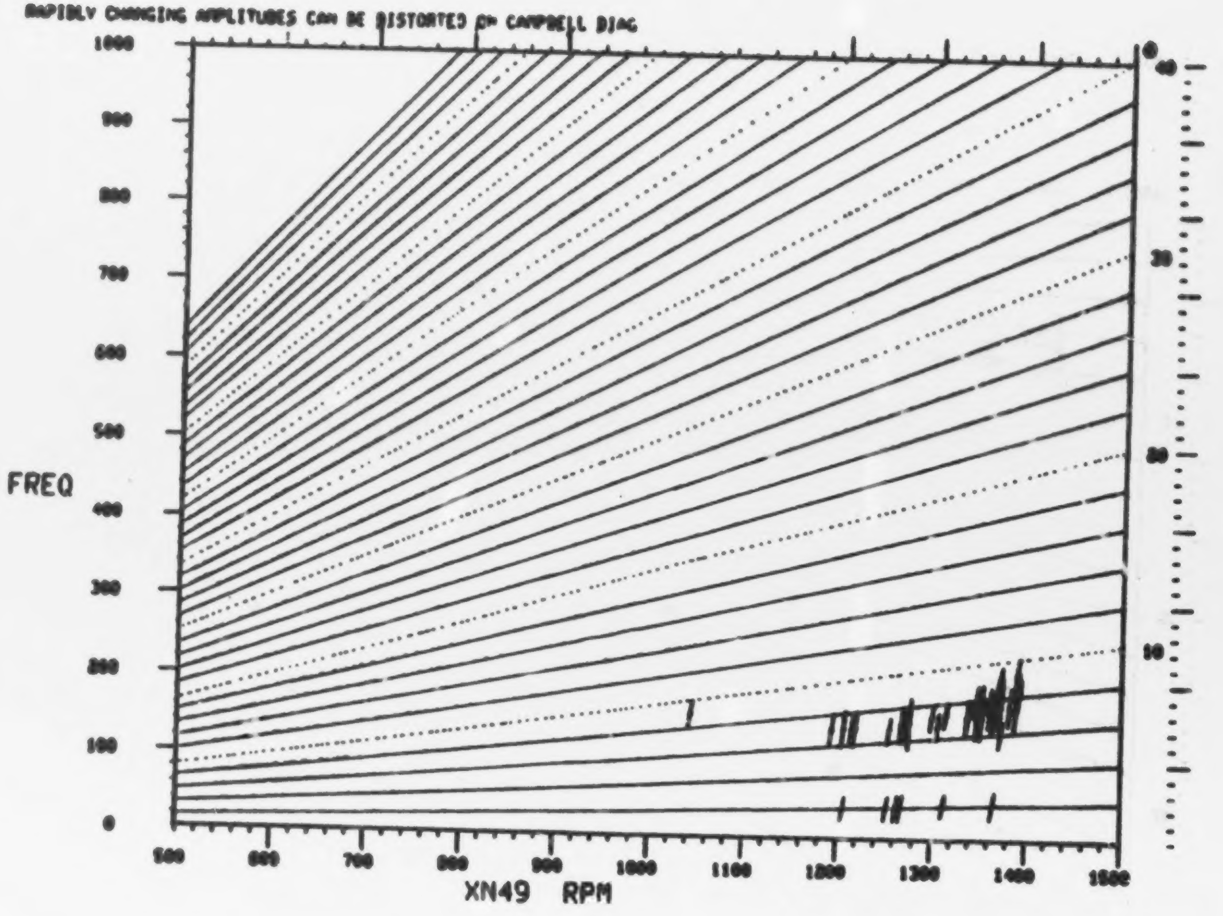

Figure 3-21. Stage 6 Turbine Blade Response, Accel to 25,000 lbf Thrust: February 4, 1986.

ORIGINAL PAGE IS
OF POOR QUALITY

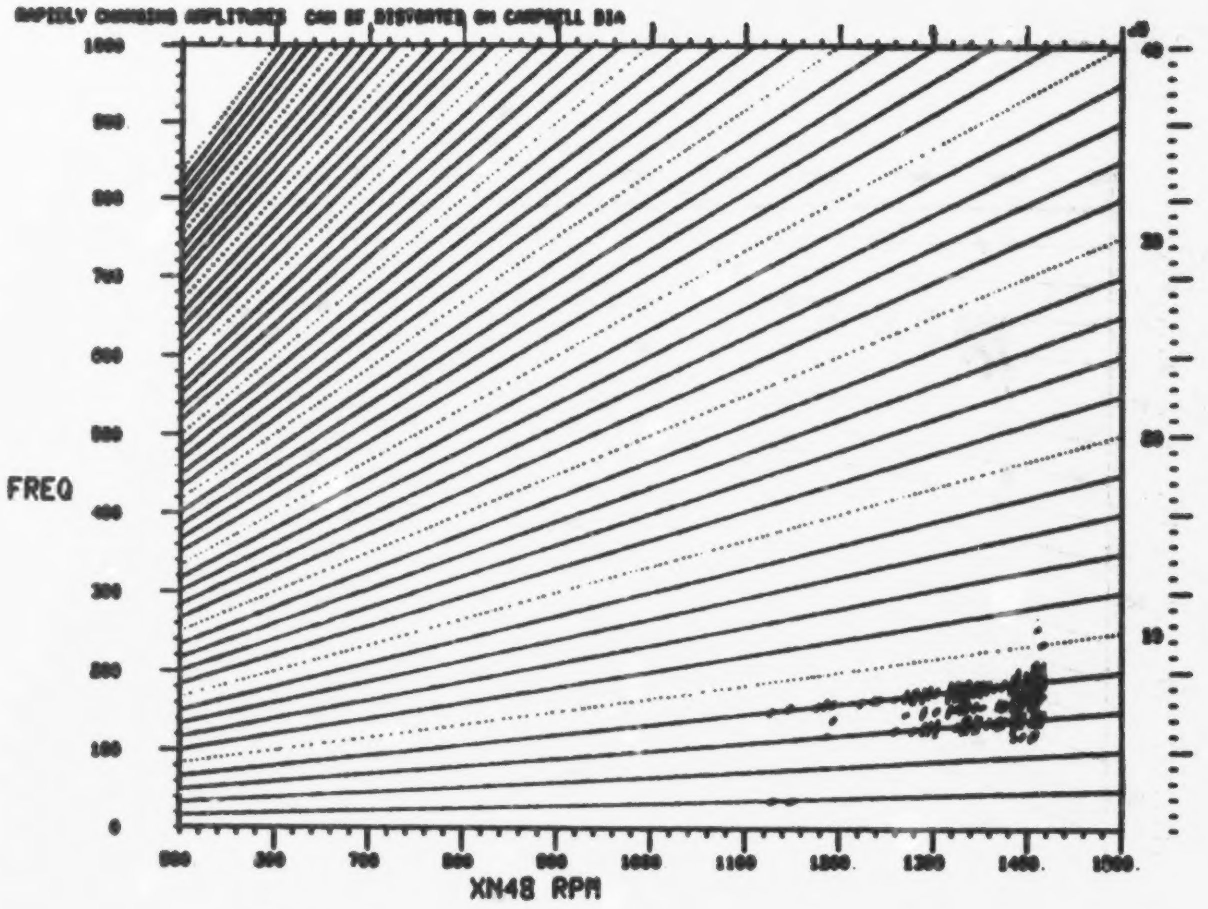

Figure 3-22. Stage 7 Turbine Blade Response, Accel to 25,000 lbf Thrust: February 4, 1986.

ORIGINAL PAGE IS
OF POOR QUALITY

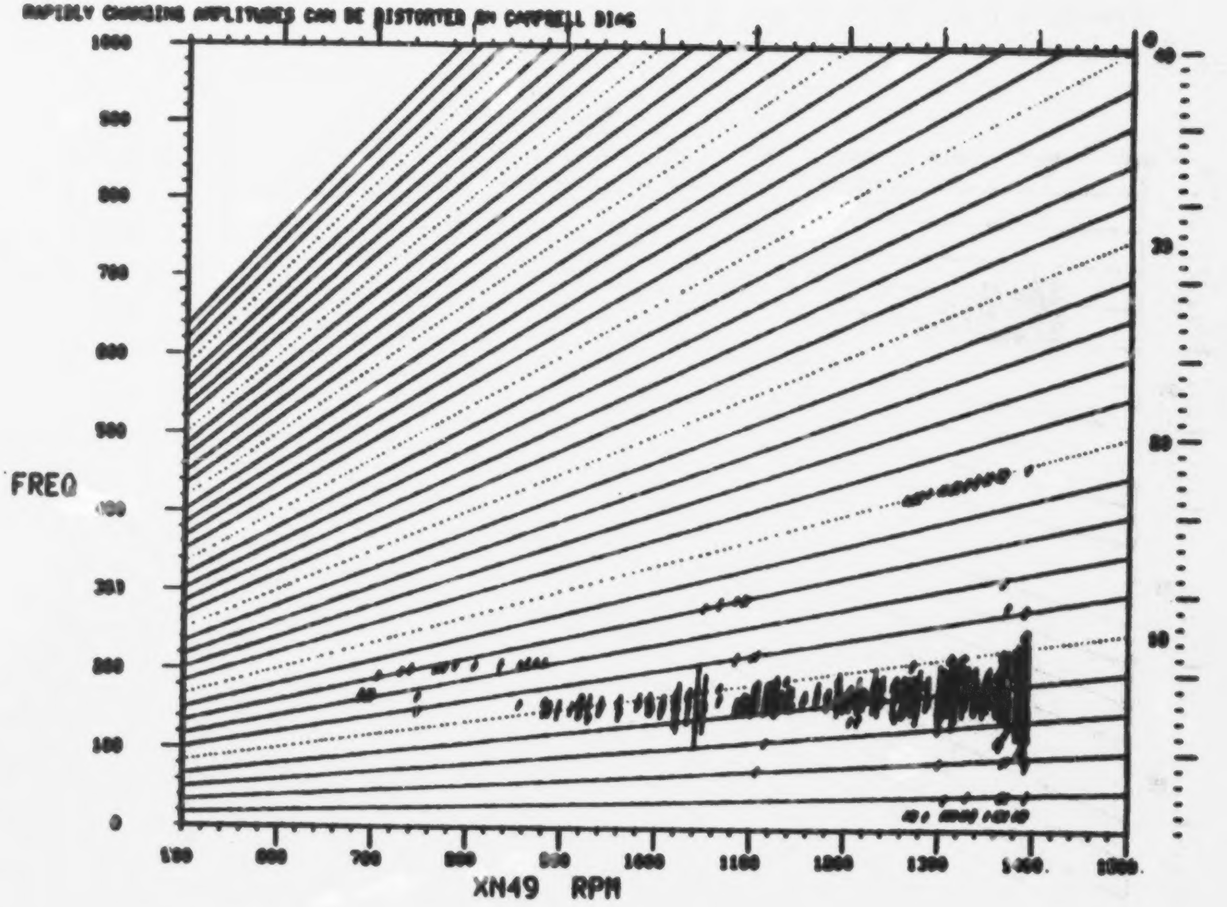

Figure 3-23. Stage 8 Turbine Blade Response, Accel to 25,000 lbf Thrust: February 4, 1986.

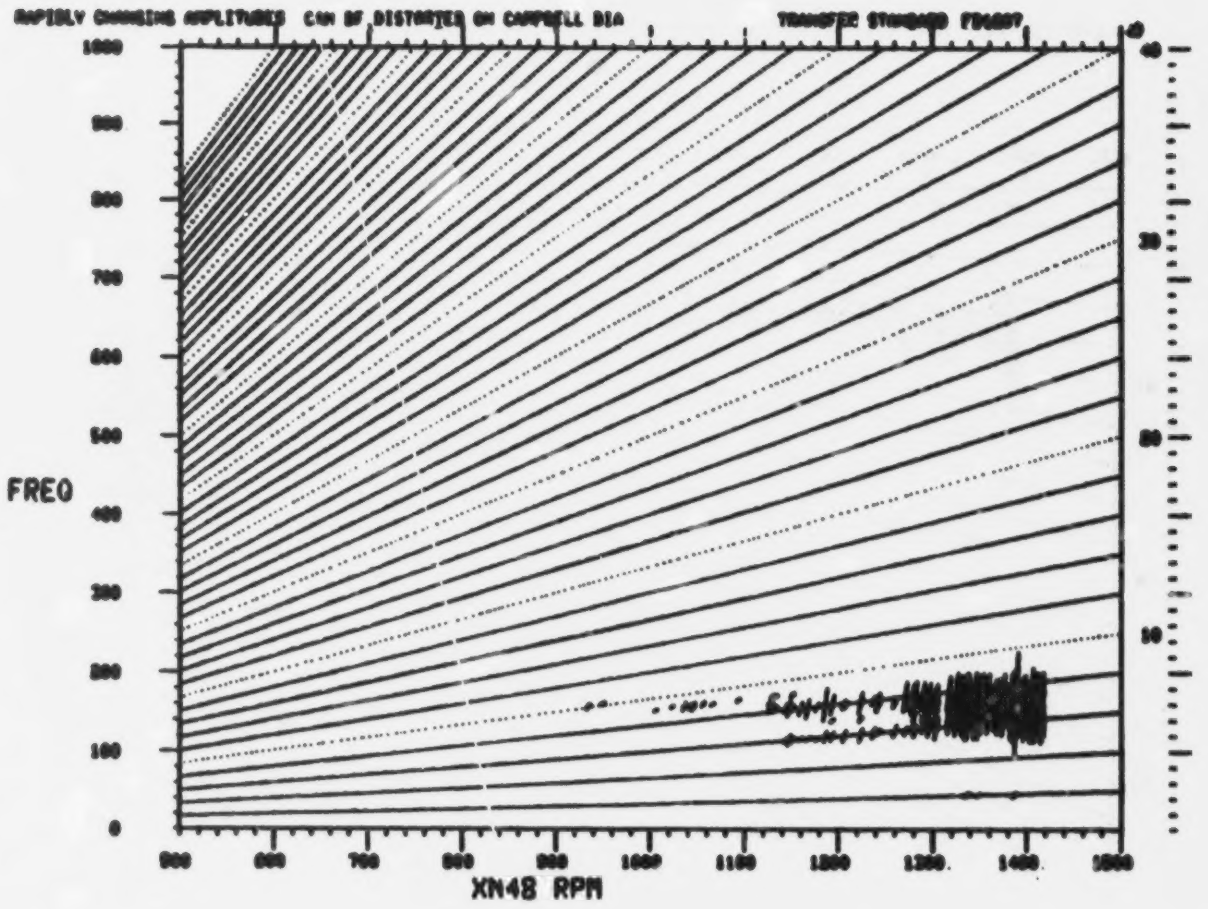

Figure 3-24. Stage 9 Turbine Blade Response, Accel to 25,000 lbf Thrust: February 4, 1986.

ORIGINAL PAGE IS
OF POOR QUALITY

ORIGINAL PAGE IS
OF POOR QUALITY

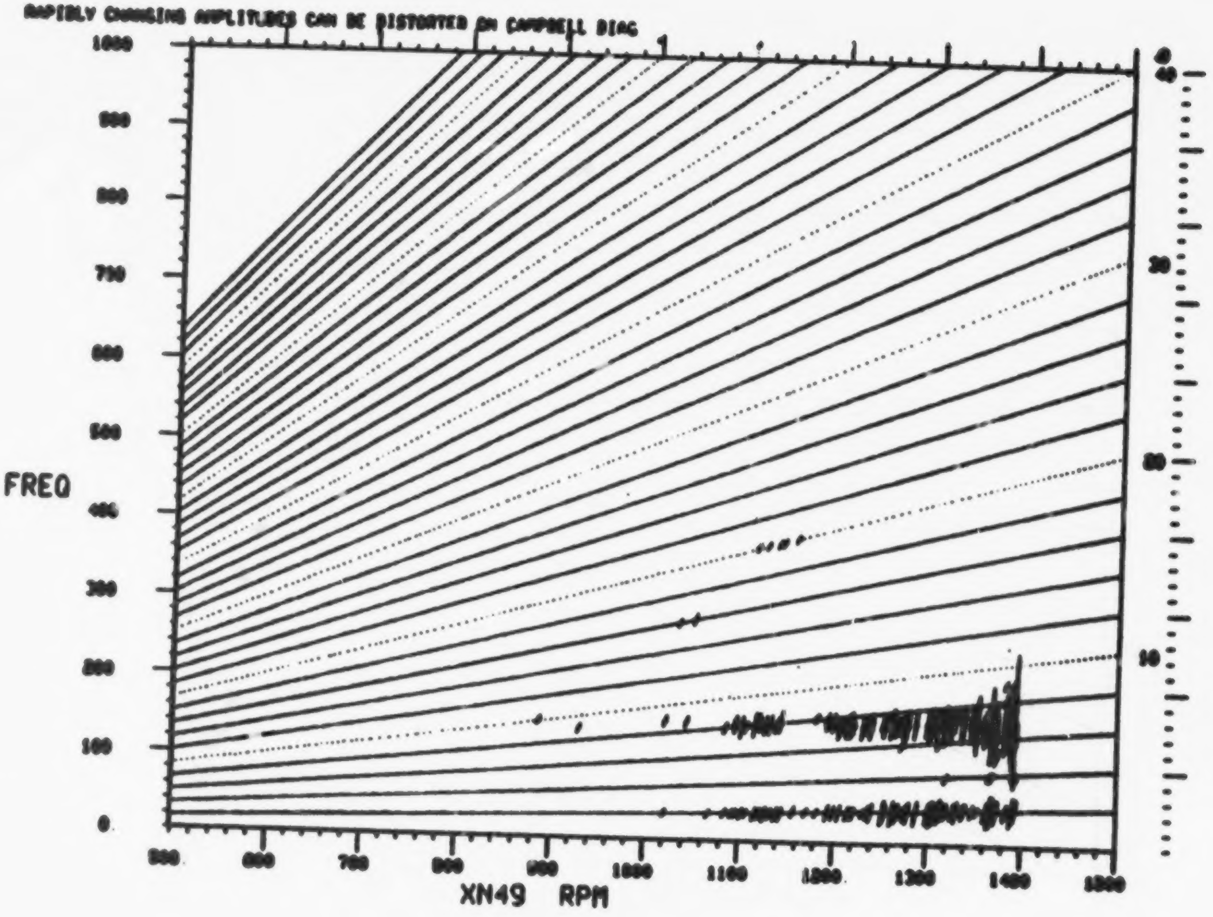

Figure 3-25. Stage 10 Turbine Blade Response, Accel to 25,000 lbf Thrust: February 4, 1986.

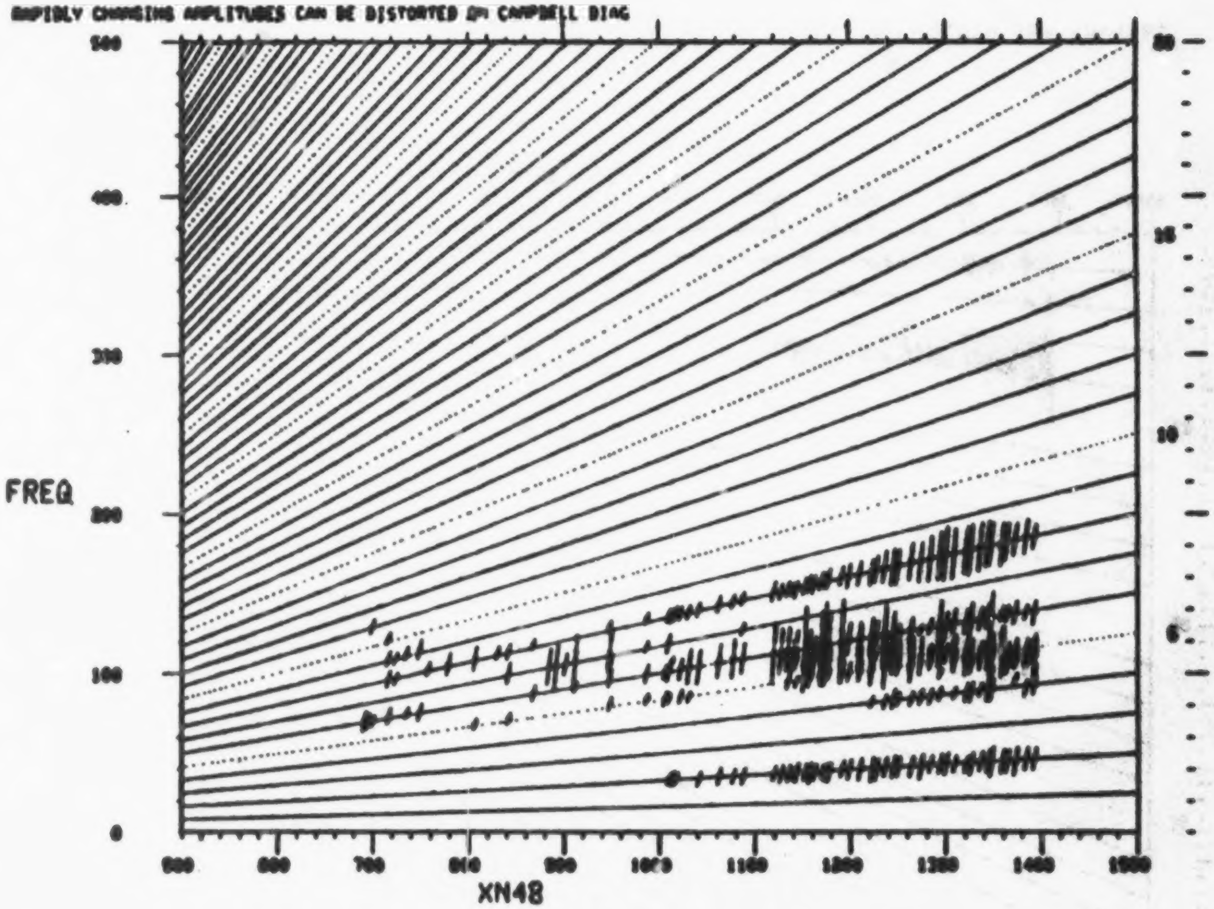

Figure 3-26. Stage 11 Turbine Blade Response, Accel to 22,000 lbf Thrust: January 11, 1986.

ORIGINAL PAGE IS
OF POOR QUALITY

3.6 SUBIDLE OIL LEAK PROBLEM

After the carbon seal failure from assembly damage was repaired, the propulsor still leaked oil into the rotors, flowpath, and nacelles. Oil loss was visible, both during operation and on shutdown, in the form of smoke and oil drips. The oil was leaking through the carbon seals during low speed operation. Although the amount of oil lost was not large, it was decided that it was desirable to reduce the amount of smoke after shutdown.

During early operation, much of the engine testing was at subidle speeds and below, as control and starting problems were worked out. The design idle speed was 650 rpm. Initial testing proved that idle speed had to be increased to 700 rpm for several reasons: the 650-rpm idle speed was too close to the subidle rotor critical; the vibration level was unacceptable; the telemetry cooling system was not effective at the lower speed; and propulsor stresses were lower at the higher idle speed.

Test data showed that the pressure drop on the aft carbon seal approached zero using the 650-rpm idle speed. The carbon seal leaked without a positive pressure drop. At 700 rpm, the seal pressure drop is increased enough to limit the oil loss out of the aft carbon seal. At higher power settings, the pressure drop across the seal is well above that which is required for oil sealing.

At low speeds (subidle), for very short runs, and during starts until the elevated idle speed is reached, the propulsor sump is not scavenged properly. At low speeds, the oil is not pumped to the ends of the rotating sumps where it can be scavenged. Due to the frame design, scavenge lines at each end of the sump run uphill initially; this forms a trap that requires some small sump pressure to overcome prior to flowing to the scavenge element. The scavenge pump used (from a CF6-50 engine) has a reputation as one that is difficult to get primed and establish full scavenge flow. For these reasons, a subidle lube bypass valve was designed and installed on the propulsor lube system.

The initial bypass system was a facility design - air actuated and controlled by the engine stopcock. In order to preclude complete loss of oil to the engine in a control or valve failure, the system was designed to divert most, but not all, of the supply oil to the propulsor. At subidle, supply oil was diverted to the scavenge circuit just at the exit of the air oil cooler. Hoses and hardware used were made on site and were not flight quality. The system, combined with the new higher idle speed, reduced or eliminated the low speed leak/smoke problem.

For flight-test, the system had to be replaced with a digital electronic-controlled solenoid valve. The facility system as configured above did not function as desired on engine shutdown. The scavenge pressure decay lagged the supply pressure decay, so that the propulsor supply was actually diverted to a higher pressure circuit, and briefly, oil flow was increased to the propulsor. This condition was somewhat alleviated by removing the air oil cooler from the scavenge circuit (which was not required) and by lowering line losses in the bypass circuit with flight quality hardware. These changes ended the leak and smoke problems.

3.7 STATIONARY EXHAUST NOZZLE (CENTERBODY) REPLACEMENT

Between Builds 1 and 2, a redesigned centerbody was installed on the engine. This redesign was necessary, because analysis and wind tunnel testing indicated that at some flight conditions there would be an undesirable flow separation from the centerbody. The predicted flow separation data for both centerbodies is shown in Figure 3-27. No flow separation was detected or predicted for ground testing. Figure 3-28 compares the two centerbody designs. Further information is provided in Section 7.3, Performance.

3.8 FAN BYPASS BLEED VALVE CALIBRATION

During Builds 1 and 2, tests were performed to calibrate the fan bypass air (from the gas generator) bleed valve. This was done to provide necessary information about the amount of fan bleed air required to maintain stall margin in the UDF™. These data are extrapolated for use in finding the amount of bleed air required in flight.

3.9 FAN BYPASS BLEED VALVE DIFFUSER FAILURE/REPLACEMENT

During Build 2, the fan bypass bleed valve diffuser failed in high cycle fatigue (Figure 3-29). Until a redesigned diffuser (Figure 3-30) could be

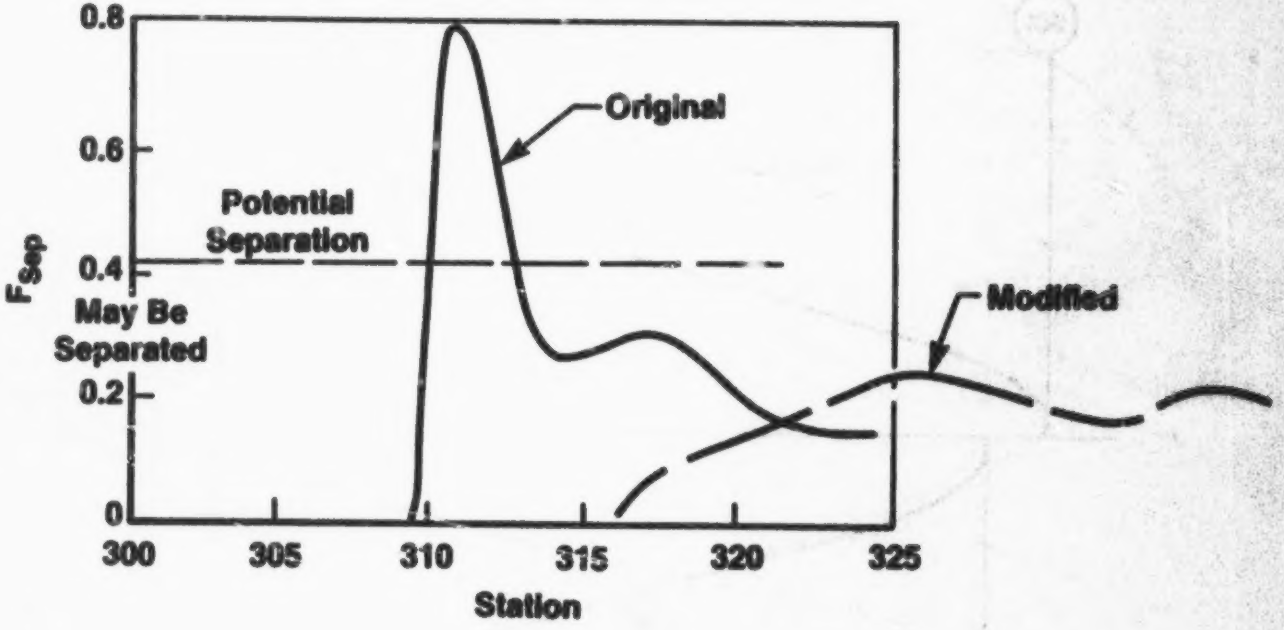

Figure 3-27. UDF™ Engine Centerbody Separation Parameter, Cruise Condition M = 0.72; 35,000; $PT8/P_0$ = 1.4.

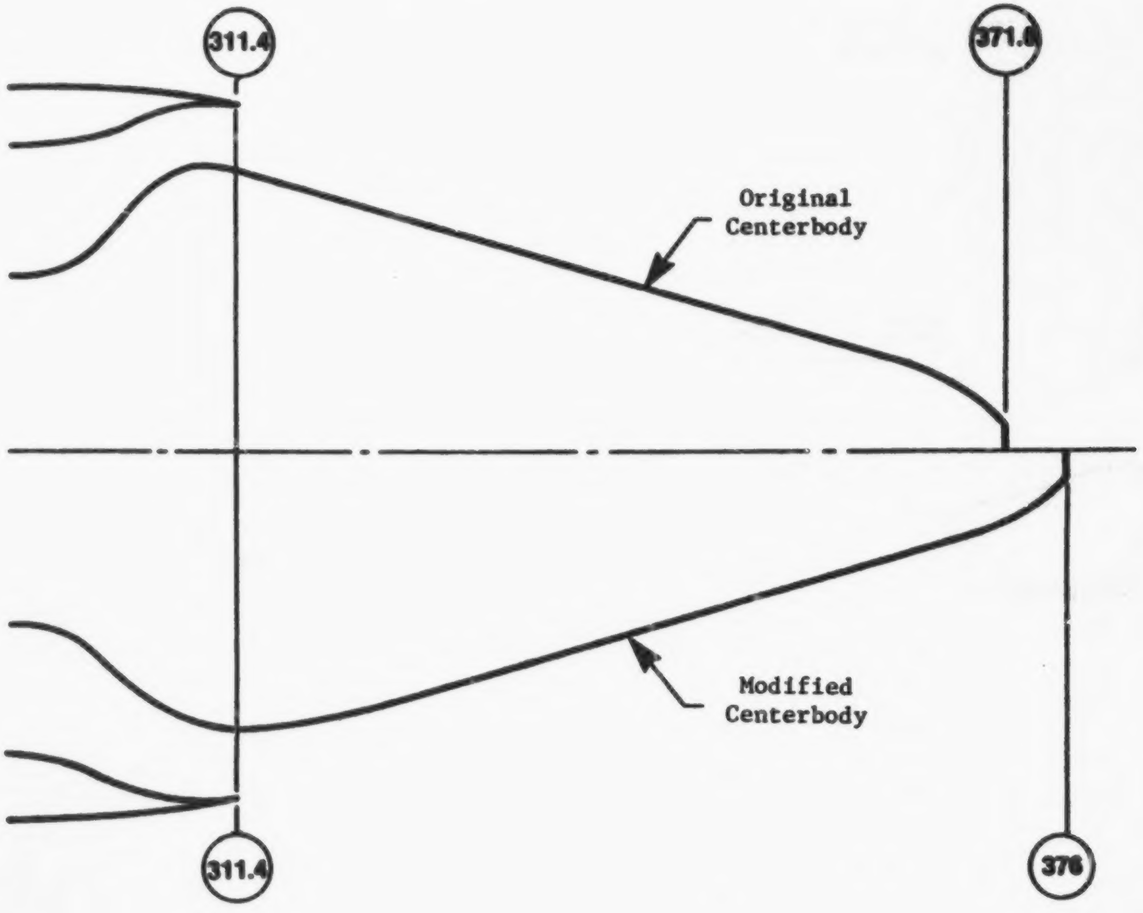
311.4
371.6
Original Centerbody
Modified Centerbody
311.4
376

Figure 3-28. UDF™ Engine - Redesigned Centerbody.

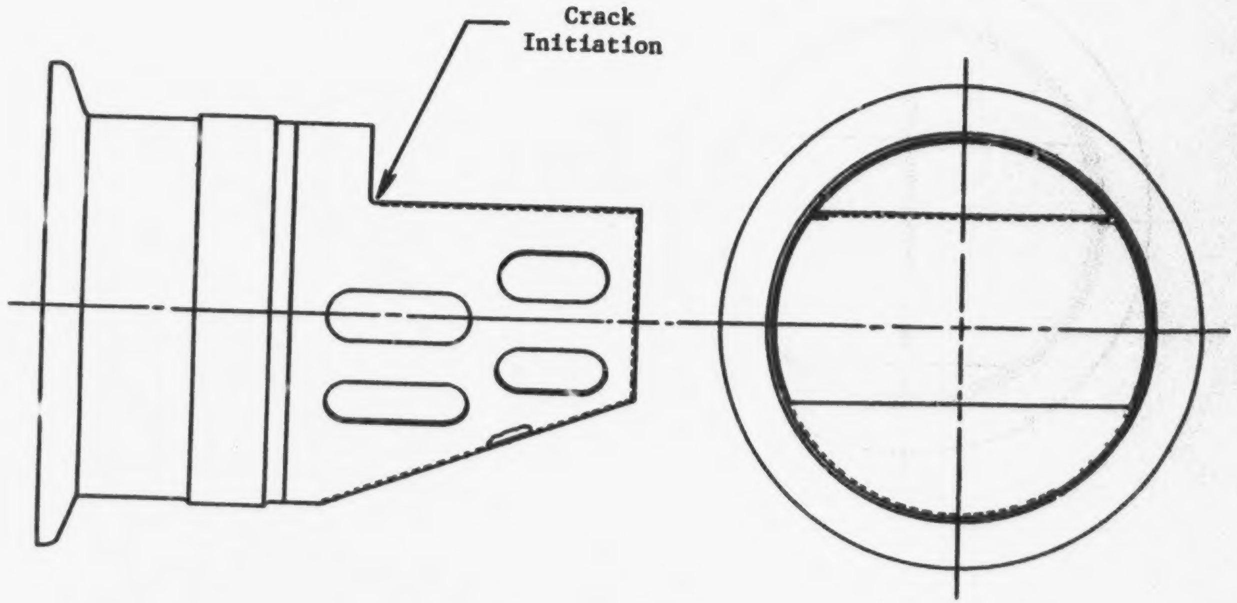
Crack
Initiation

Figure 3-29. Bypass Bleed Valve Diffuser.

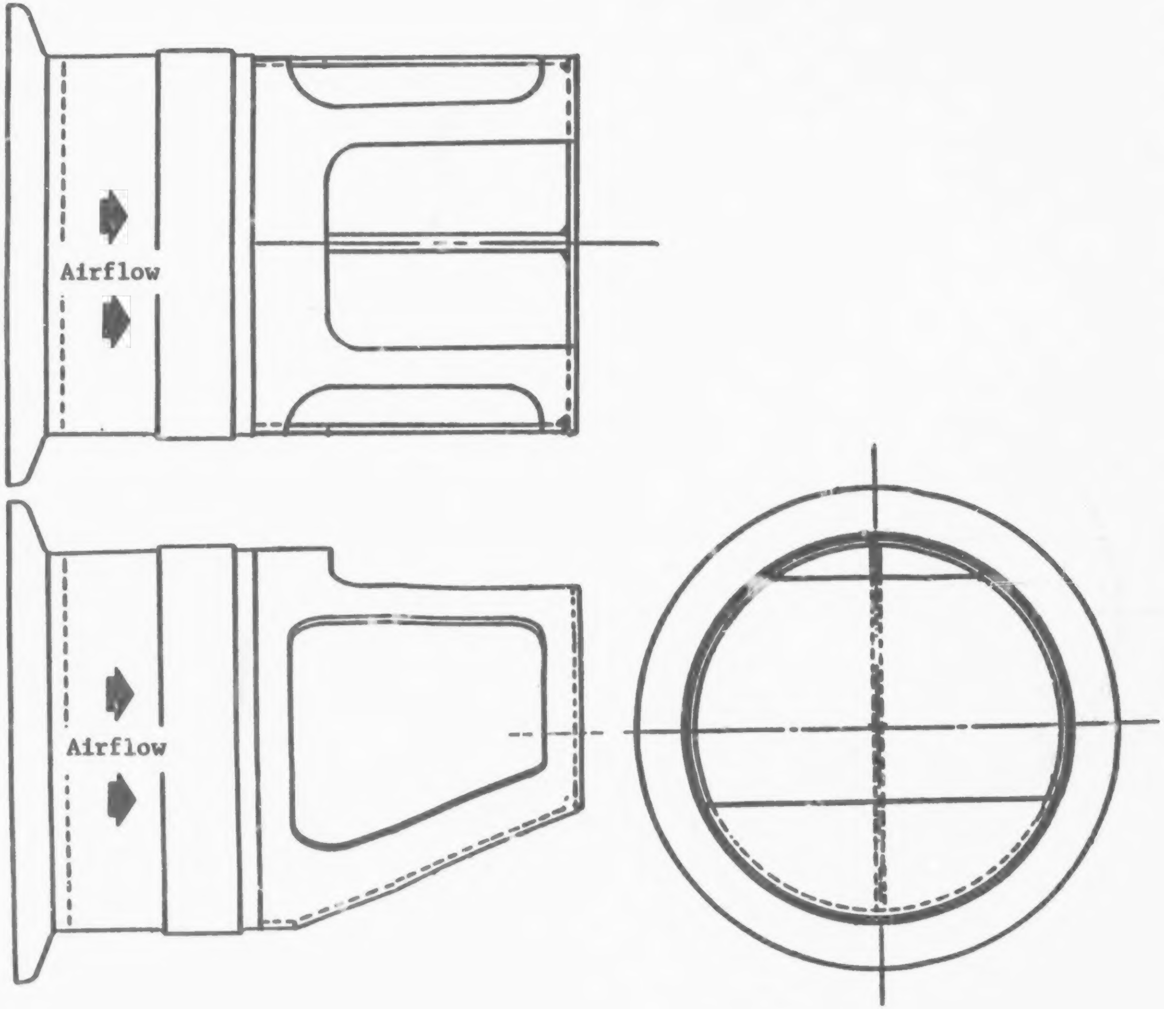
Airflow
Airflow

Figure 3-30. Redesigned Bypass Bleed Valve Diffuser.

designed and manufactured, the damaged portion of the diffuser was cut off and used "as is." When the redesigned diffuser was available, it was installed on the engine.

3.10 PROPULSOR FAN-BLADE-LOSS EVENT

Summary of Event

- The engine reached test point: 24,000 lbf, 1371 rpm propulsor fan speed.
- Stage 2, No. 7 composite fan blade shell separated from titanium spar and was released; however, the spar remained attached to the trunnion.
- No high fan stress or other anomalies prior to blade loss.
- Shutdown initiated at blade loss - 1 second chop to idle and stopcock within 9 seconds.
- No gas generator stall.
- Propulsor spool-down was normal.
- Due to a large imbalance (approximately 260,000 gm/inch) caused by the missing composite, a noticeable amount of engine vibration was experienced.
- Control/actuation system functioned normally after blade loss.

Spar Damage

Inspection of the spar following shutdown indicated the titanium had cracked at the EB (electron beam) weld line the entire width of the spar. The EB weld crack was clearly visible over the midspan of the blade (Figure 3-31).

Secondary Damage

Blade No. 6, which was next to the released blade, had a slight nick in the polyurethane coating where the composite material from Blade 7 hit Blade 6 before striking the ground. The nick was an indication that only light contact occurred.

The isolators contain an absorption material which is intended to yield under high unbalance conditions such as blade loss. Deformation of the aft

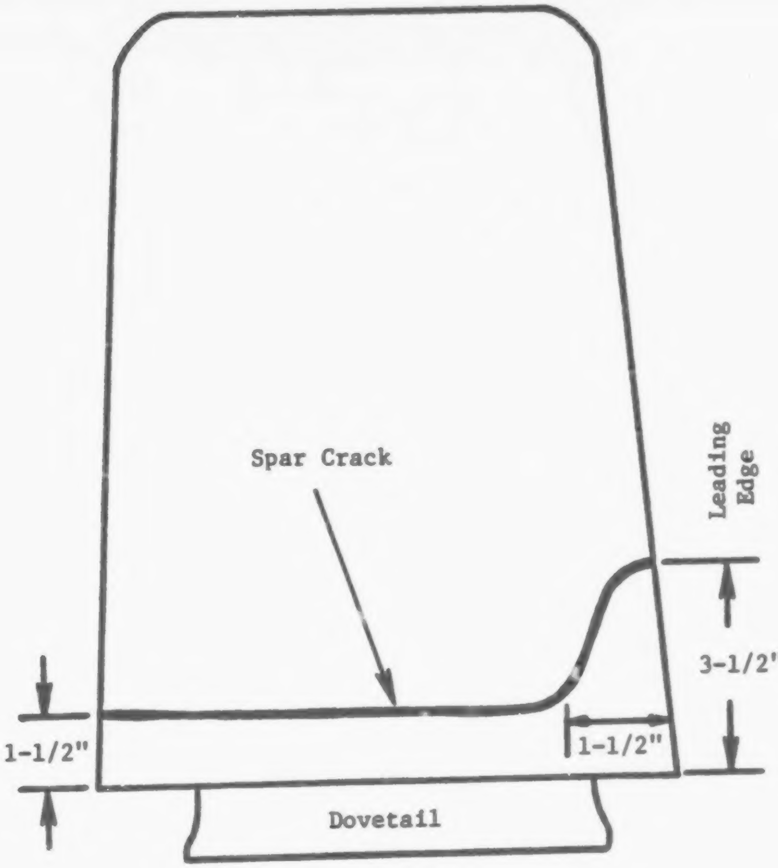
Spar Crack
Leading Edge
3-1/2"
1-1/2"
1-1/2"
Dovetail

Figure 3-31. Spar Schematic.

isolator pads was observed, and the isolators were returned to the vendor for inspection. The aft isolators had their original values of spring rate and damping coefficient. Since there was deformation of the aft isolator pads, they were refurbished as a precautionary measure and returned to engine test. No damage to the forward isolator was observed.

There was also concern that the transfer gearbox attached to released blade trunnion No. 7 may have suffered some damage. The gearbox was torn down and both the MPI (magnetic particle inspection) and FPI (fluorescent penetrant inspection) of the gears and pinnions indicated no abnormal wear.

Bolts attaching the Stage 12 power frame to the rotating exhaust nozzle showed interference with the OGV assembly, with the heaviest wear at blade Location 7. The OGV assembly is designed to clear the bolt circle by 0.100 to 0.160 inch. The OGV assembly showed light wear all the way around, with a 1-inch section indicating a harder rub. No repair was required. The OGV assembly had no other distress.

The Stage 11 turbine blades rubbed the inner spool at some time during the event, leaving a 4-inch x 3/8-inch rub mark on the inner rotor. The rub coincided with Stage 2 fan blade Location 4. The indication was a surface discoloration with no measurable depth. The Stage 11 blade trailing edge tip did not have any discoloration or tip curl that would suggest a heavy rub.

Both Stages 1 and 2 fan blades were returned to Evendale for inspection. No debonding was found in the Stage 1 set, but one Stage 2 blade was found to have a section of composite separating from the spar.

Fan Blade Corrective Action

Corrective action included the addition of a portable ultrasonic scan of all fan blades following each hour of engine run time. Ultrasonic scanning at Evendale proved to give accurate results when trying to determine if debonding has occurred. The ultrasonic scan used when the blades were returned to Evendale indicated a Stage 2 blade had started to debond. Portable scan equipment also verified debonding of the composite. Because the previous test method, ping checking, indicated the debonded blade was acceptable, the ping test was discarded as a debonding check.

Test History of Failed Fan Blade

The blade that failed had been run 20:40 hours prior to the failure. A breakdown of run time versus propulsor fan speed is provided in Figure 3-32.

3.11 PROPULSOR FAN BLADE HISTORY AND TEST DATA

3.11.1 Fan Blade Test History

None of the original design Stage 1 fan blades had to be replaced due to failure or debonding. After Build 2, the blades were replaced with redesigned blades with mechanical retention features. Figures 3-33 and 3-34 compare the original and redesigned fan blades. All of the redesigned Stage 1 fan blades ran through Build 3 without problems.

Some of the original design Stage 2 fan blades failed inspection during Builds 1 and 2 due to debonding. These were replaced once any discrepancy was found. Figure 3-35 depicts the history of the Stage 2 blades during Builds 1 and 2. Investigation into the two debonded blades found after Build 1 determined that the probable cause of debonding was from propagation from cracks in the foam inside the blades. This foam filled the cavity between the composite shell and the titanium spar. Cracks in the foam during manufacturing propagated into the shell/spar bond. A design change was made (Figure 3-36) to try to prevent this from happening.

Section 3.10 discusses the Stage 2 fan blade failure in Build 2. After this fan blade failure, the engine was limited to 1000-rpm fan speed until the redesigned fan blades were available (Build 3 testing).

3.11.2 Fan Blade Test Data

Figure 3-37 summarizes fan blade vibratory stresses for Builds 1, 2, and 3. Figures 3-38 through 3-42 present specific examples of stress data. Note there are differences in fan blade stress levels with seemingly equivalent test points. This difference is caused to a large degree by differing wind conditions (that is, wind direction, velocity, gusting). Figure 3-43 depicts the strain gage locations. Location No. 4, which gives the highest first flex vibratory stress, is the strain gage used for the given data.

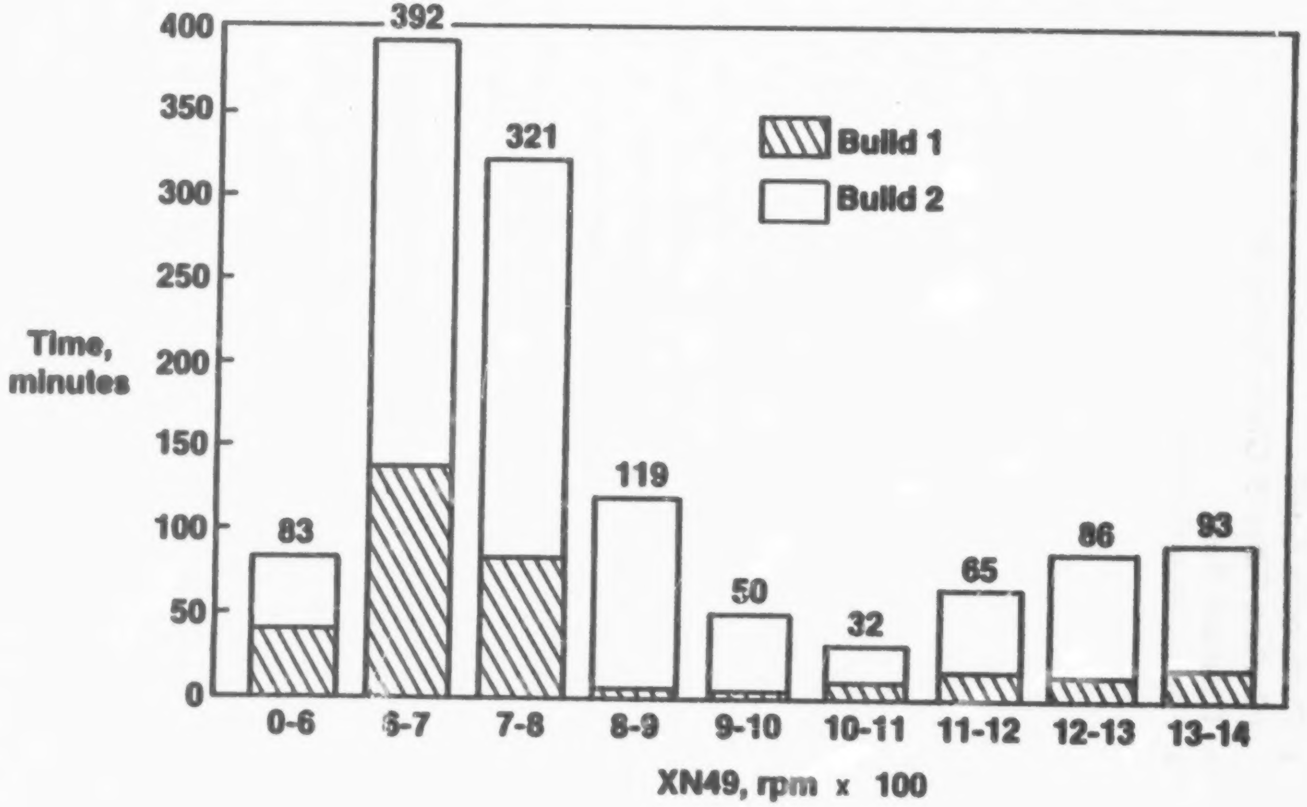

Figure 3-32. Total Run Until Fan Failure.

- **Composite Shell (Carbon Fiber-S-Glass Epoxy Matrix)**
- **Titanium Spar**
- **Foam Filled Cavities**

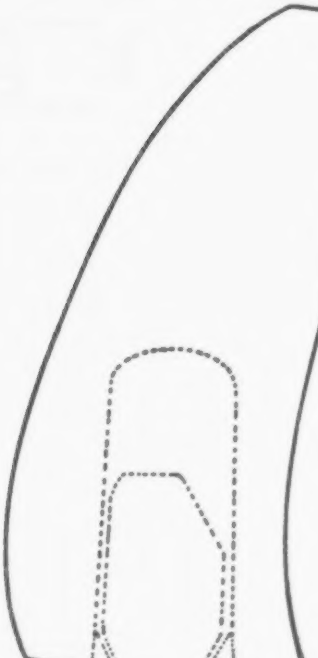

Figure 3-33. Original Fan Blade Airfoil Mechanical Design.

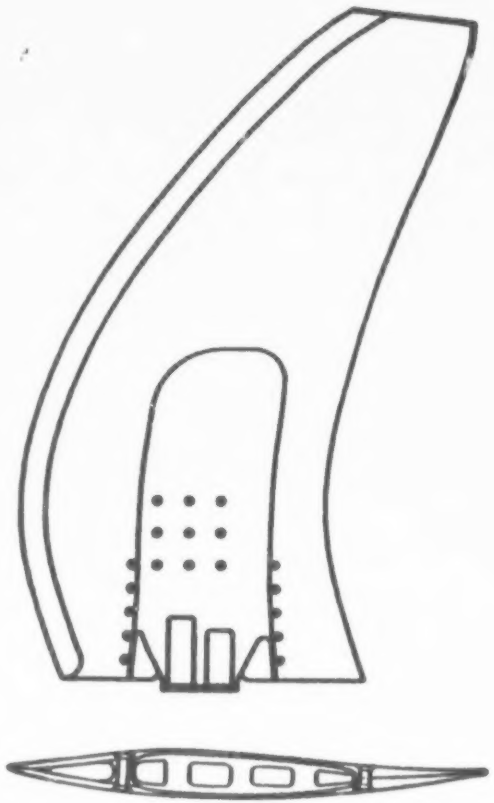

- **Solid Spar with EDM Pockets (2 Plugs)**
- **Same Ply Lay-Up Pattern**
- **Add One 0.005" Adhesive Layer on Spar Surface**
- **Positive Shell Retention**
- **New Foam Material, Rohacell, Replaces Syntactic Foam**
- **Composite Channel Sections at Spar LE to Reinforce Spar/Shell Bond Joints**
- **Composite Close Out at Airfoil Base**
- **Wider LE Lap Joints**
- **Solid Composite in TE Cavity**
- **Improved Shell Taper Pattern at Root**
  - **Full Ply Length on the Spar Surface**

Figure 3-34. Improved Fan Blade Mechanical Design.

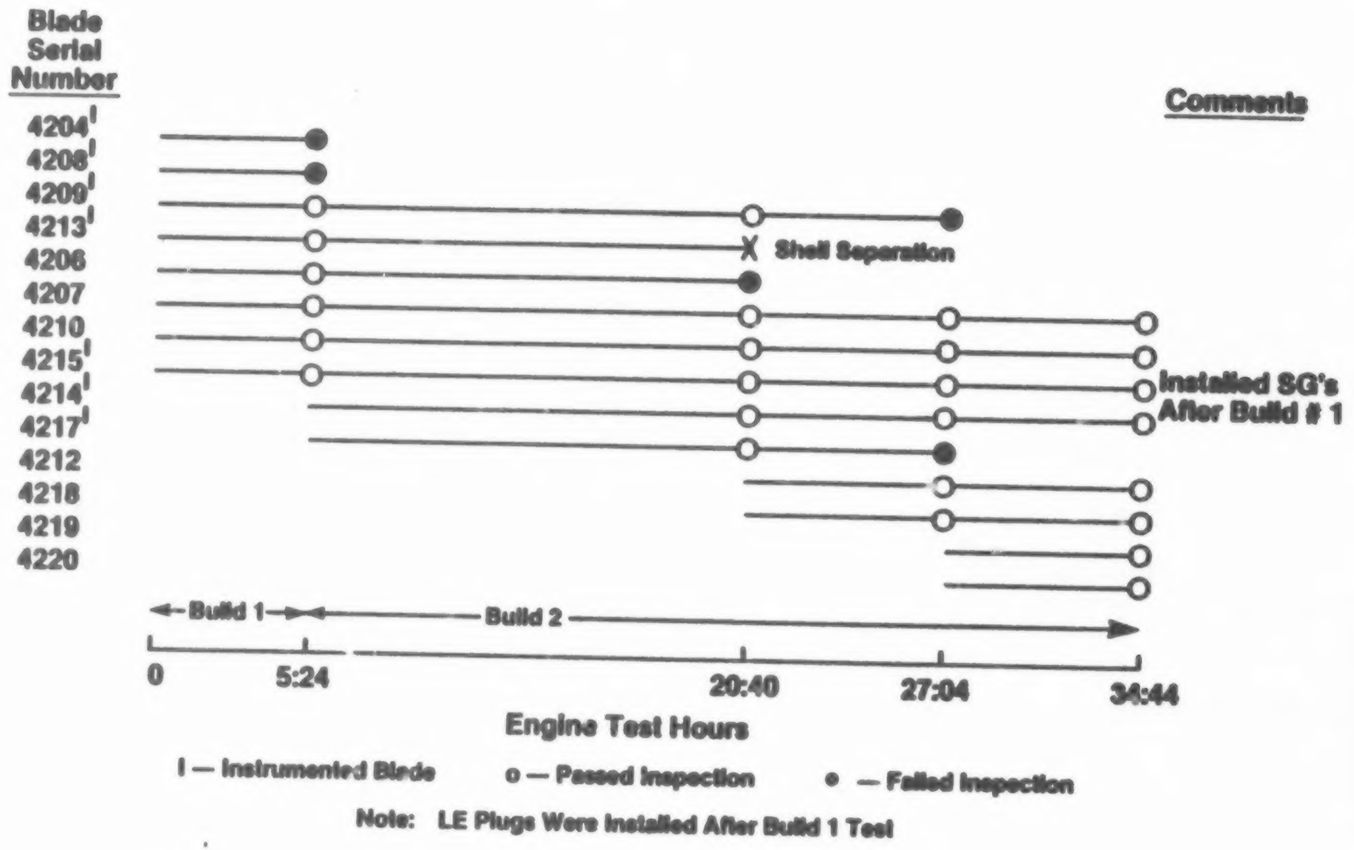

Figure 3-35. Stage 2 Fan Blades Engine Test History.

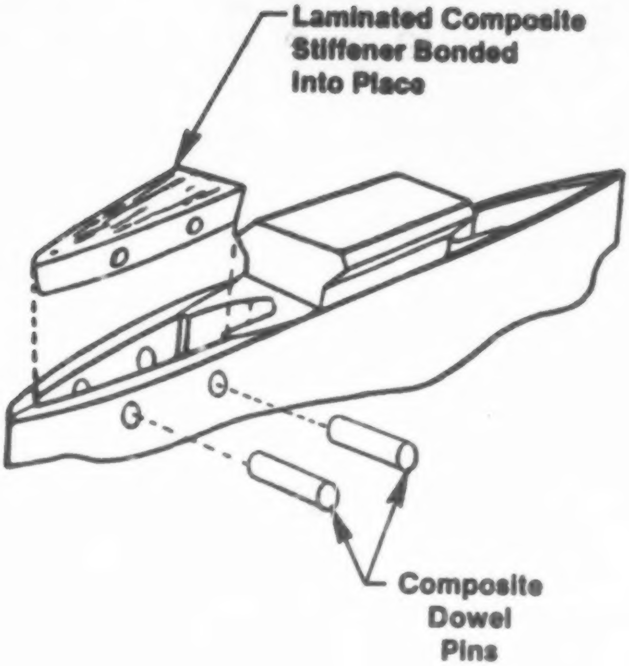
Laminated Composite Stiffener Bonded Into Place
Composite Dowel Pins

- **Plug Retrofit Creates Stiff 'Closed-Box' To Preclude Crack Propagation And Increase Tolerance To Thermal Cycling**

Figure 3-36. Fan Blade Structural Improvement.

	Stage 1		Stage 2	
	1/Rev	2/Rev	1/Rev	2/Rev
● Build 1				
- Part Power	0	6-8	0	4-6
- 24K Run	1.0	7-8	1.0	5-6
● Build 2				
- Mechanical Check	1.0	6-8	1.0	10-12
- Mismatched Speed	1.0	3-5	1.0	7-10
- 25K Run	1.0	4-6	1.0	8-10
- Health Verification Run	1.0	3-4	1.0	7-8
● Build 3				
- Mech. Checkout - 24K	1.5	5.1	1.5	8.7
- LCF Cycles	0.8	1.3	1.0	4.6

Figure 3-37. Fan Blade Response Summary - ksi pp.

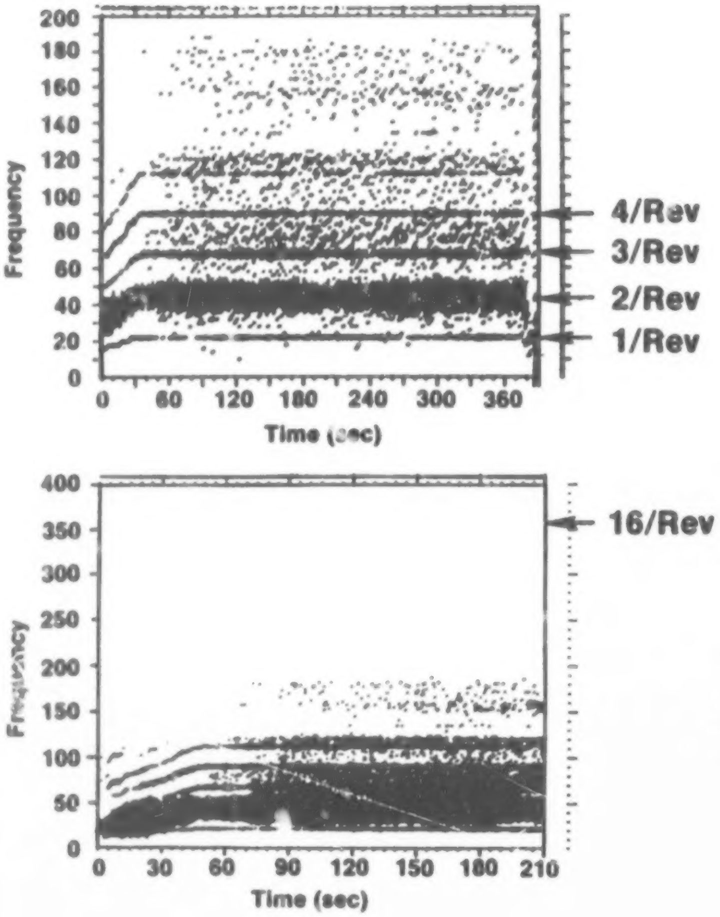

- Blade Stable
- No Flow Separation Induced Vibration
- Low/Rev Responses
  - Less Than 35% Scope Limit
    - 10 ksi Overall
    - 8 ksi at 2/Rev
    - 2 ksi at 3/Rev
    - 1 ksi at 4/Rev
    - Nondiscernable at 16/Rev

24,000 lbf Thrust Run: October 2, 1986
5 ksida = ƒ

Figure 3-38. Stage 1 Fan Blade Response Summary.

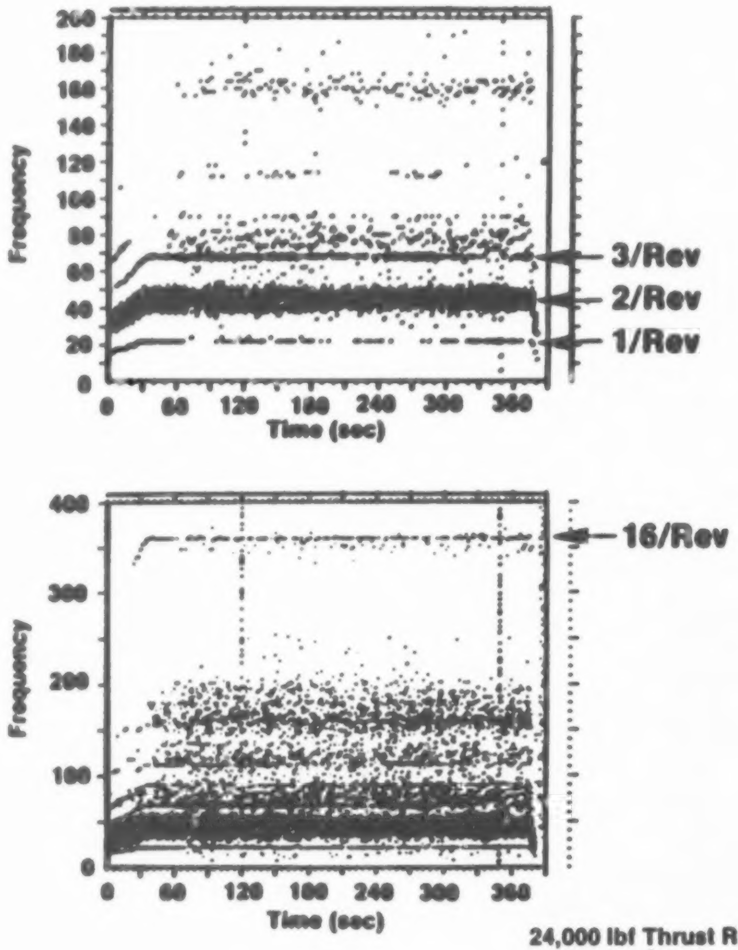

- Blade Stable
- No Flow Separation Induced Vibration
- Low/Rev Responses
  - Less Than 35% Scope Limit
    - 8 ksi overall
    - 7 ksi at 2/Rev
    - 1 ksi at 3/Rev
    - Nondiscernable at 16/Rev

24,000 lbf Thrust Run: October 2, 1986
5 ksipp = /

Figure 3-39. Stage 2 Fan Blade Response Summary.

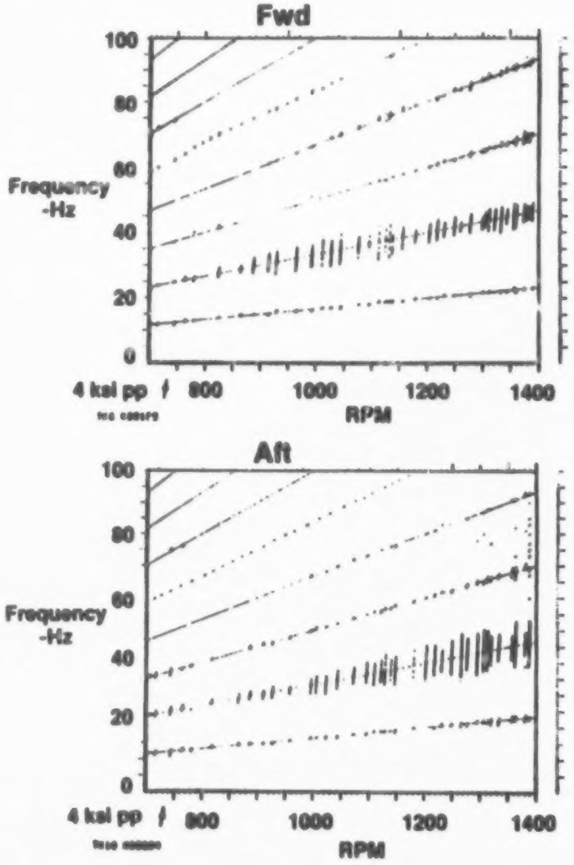

- No Flutter
- No Separated Flow Vibration
- Per Rev Responses — ksi pp

	1/Rev	2/Rev	3/Rev
Stage 1	(0.5/1.0)*	4.0/8.0	3.0/5.0
Stage 2	1.0/2.0	9.0/15.0	1.5/3.0

* (Steady/Peak**)

** Due to 6-18 mph Unsteady Crosswind

Figure 3-40. Fan Blade Response Summary - February 4, 1986 Maximum Power Run (25,000 lbf Corrected Thrust).

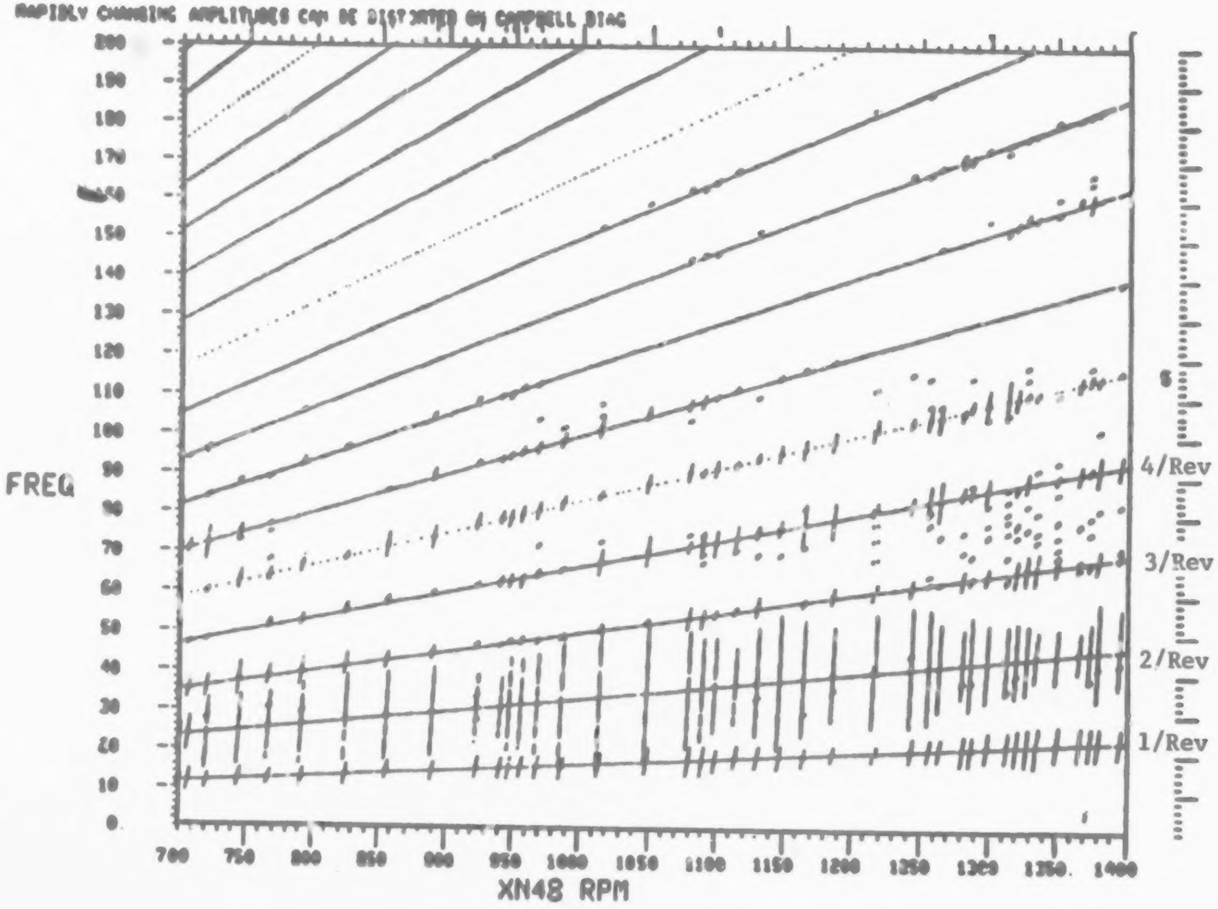

Figure 3-41. Stage 1 Fan Blade Response, Accel to 24,000 lbf: June 24, 1986.

ORIGINAL PAGE IS
OF POOR QUALITY

ORIGINAL PAGE IS
OF POOR QUALITY

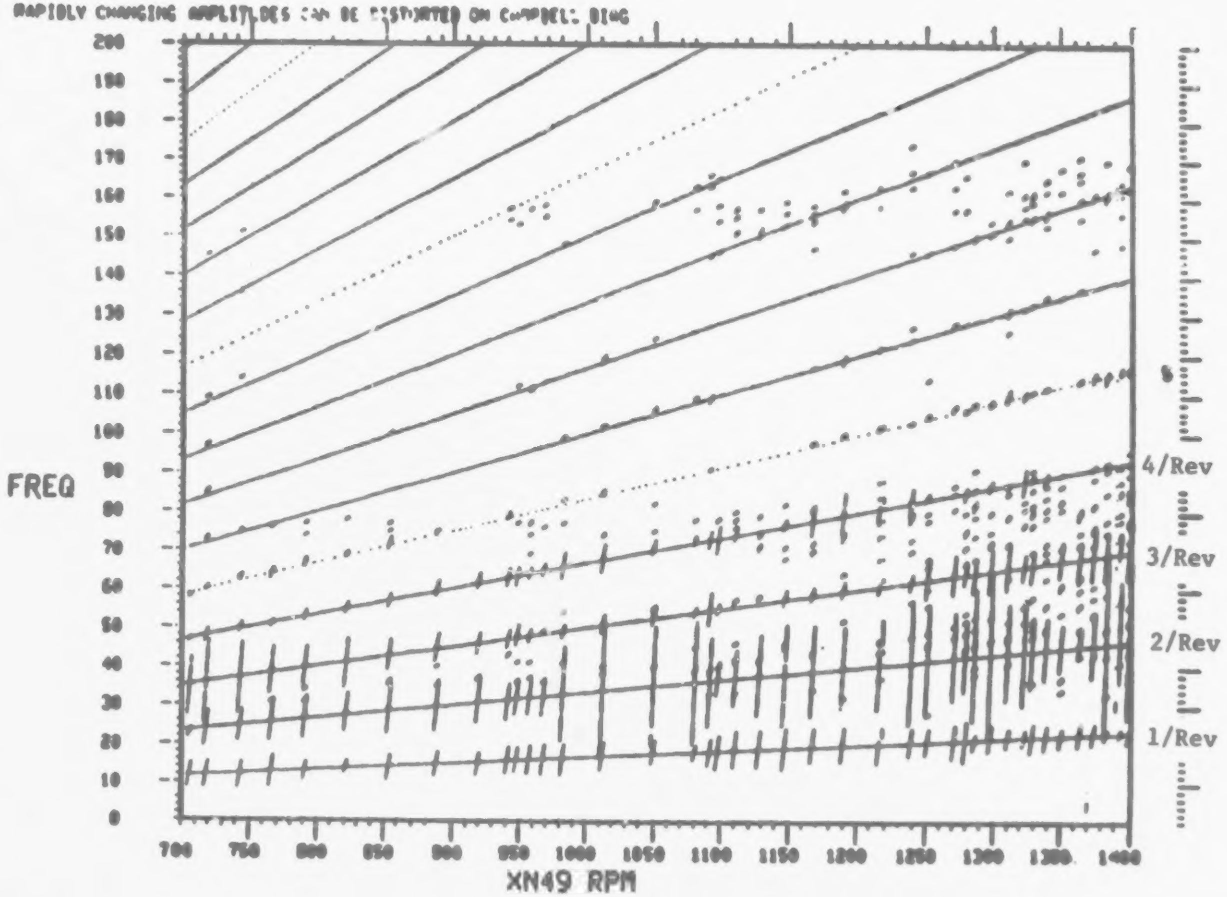

Figure 3-42. Stage 2 Fan Blade Response, Accel to 24,000 lbf: June 24, 1986.

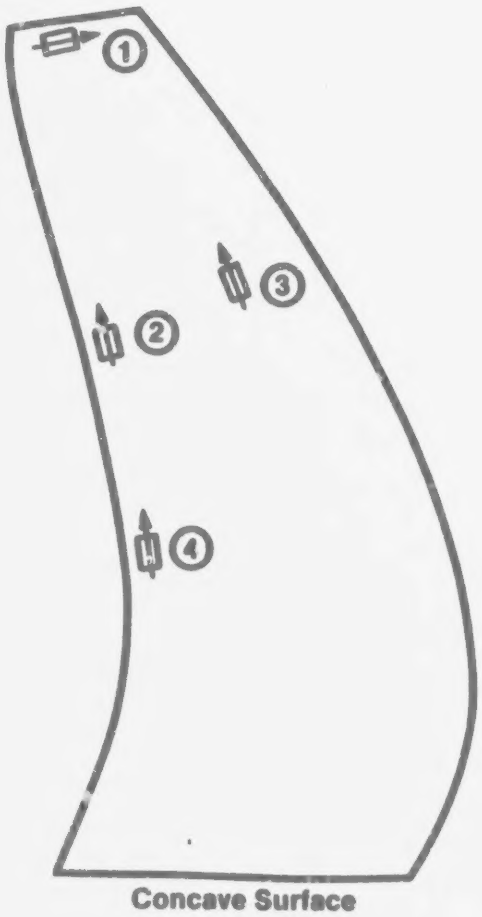

- Total Of 16 Gages Per Stage
  4 Gages/Blade And 4 Blades/Stage

① - Gage - Sensitive To 1 Torsion And High Order Modes

② - Gage - Sensitive To 2 Flex And I/P Forced Response

③ - Gage - Sensitive To Axial Mode And High Order Flex Modes

④ - Gage - Location of Highest SS Stress And 1 Flex Vibratory Stress

Figure 3-43. Fan Blade Strain Gage Locations.

Fan Blade Response with Facility Fans

At the first test site (4A) a set of 12 facility fans were arranged in front of the UDF™ inlet. Figure 3-44 shows a schematic of the facility fan configuration. These fans attempt to simulate forward velocity of an engine and try to smooth out airflow through and around the engine. It was desired to see if some combination of these fans would lower fan blade stress. The results can be seen in Figure 3-44; the first data point (no fans on) gave a lower vibratory stress level than with any number of fans on. Stress levels varied widely, depending on the number of fans that were on, but all levels were higher than those without any fans. Since the engine centerline and the facility fan centerline were not in line, it was believed that the fans created additional disturbances in the flow field instead of smoothing the airflow.

3.12 POWER TURBINE FRAME STRESS

During Build 2, power turbine frame vibratory stresses were higher than predicted. The stresses were found to be predominantly 2/rev forced response. This was caused from the fan Rotor 2 nodal, first flex mode (note that the turbine frame and the fan blade rotor are mechanically linked). This causes the frame stress to track the fan blade stress. Figure 3-45 provides a stress comparison.

A detailed investigation into the frame stress allowed the vibratory stress limits to be increased for the forced response mode (Figure 3-46). A summary of this investigation and its results is in Table 3-1; supporting data is shown in Figures 3-47 and 3-48. Build 3 data is presented in Figure 3-49.

3.13 EFFECT OF VORTEX DESTROYER ON STRESS

Vortices were seen between the ground and the fan blades at the bottom of the engine. Visualization of these vortices was aided by having moisture on the ground or by releasing smoke bombs. To see if the placement of a vortex destroyer (a large metal grating) under the fan blades would reduce the fan blade and power turbine frame vibratory stress levels, a vortex destroyer was placed under the fan blades approximately 6 inches off the ground. Fan blade

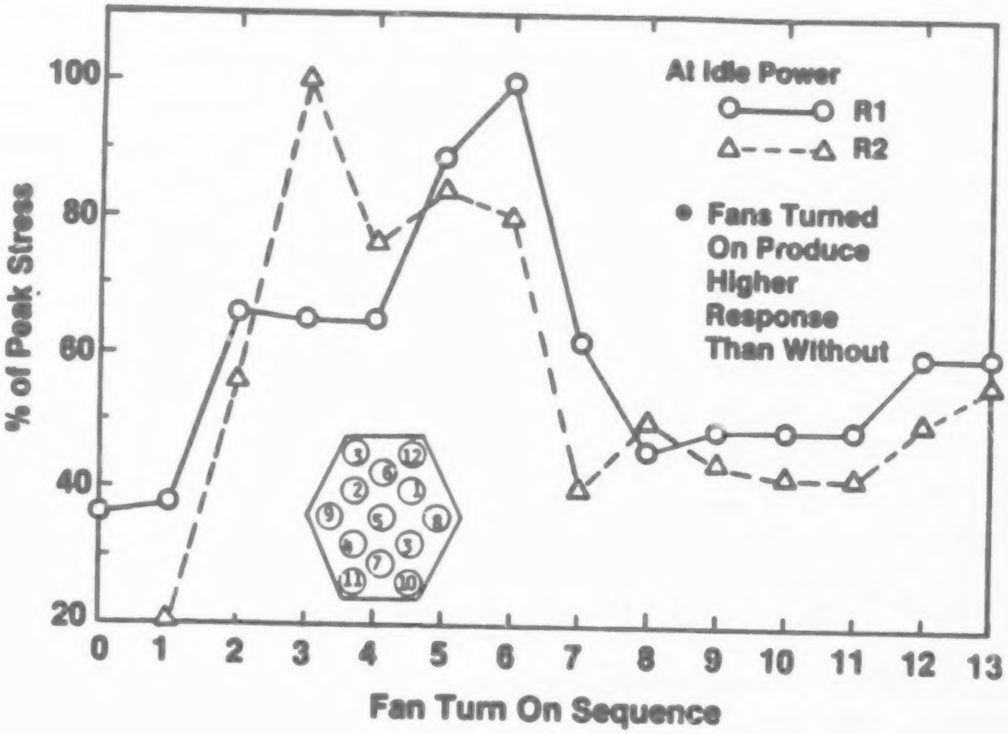

Figure 3-44. Fan Blade Response with Facility Fans Turned On.

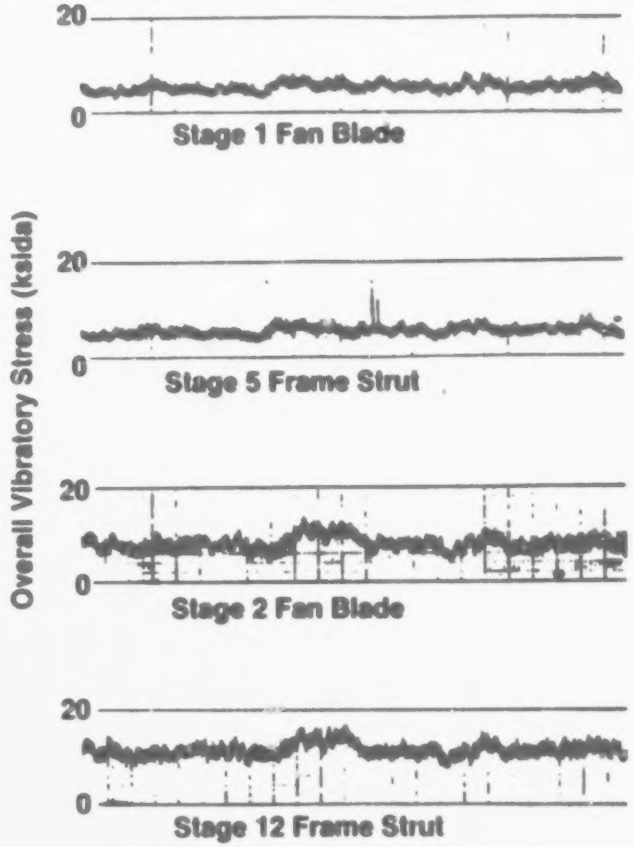

- Build 2 Observations
  - Higher Than Expected Vibratory Stress
  - Predominantly 2/Rev Forced Response
  - Frames Track Fan Blades
- Diagnosis
  - Fan Rotor 2 Nodal — 1st Flexible System Mode
  - Limits Not Well Defined for This Mode

Figure 3-45. Power Turbine Frames Vibratory Response Summary.

Results:

- Updated Scope Limits Versus Site 4A Response
- HCF Testing

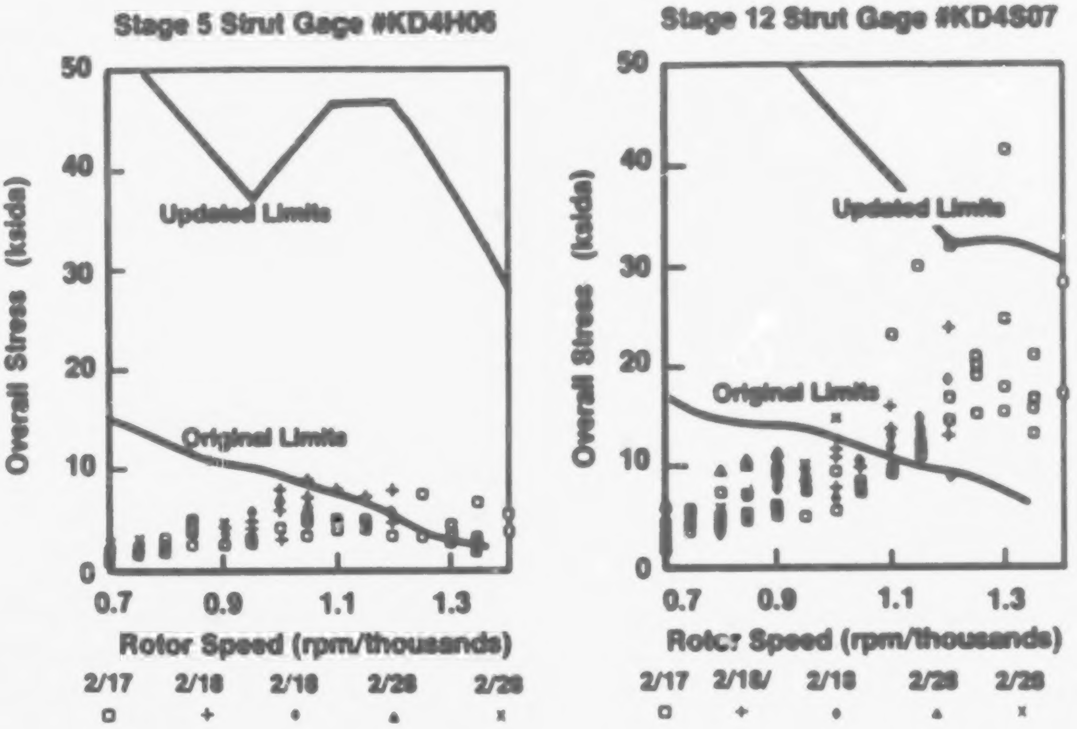

Figure 3-46. Power Turbine Frames Vibratory Response, Updated Scope Limits Versus Site 4A Response.

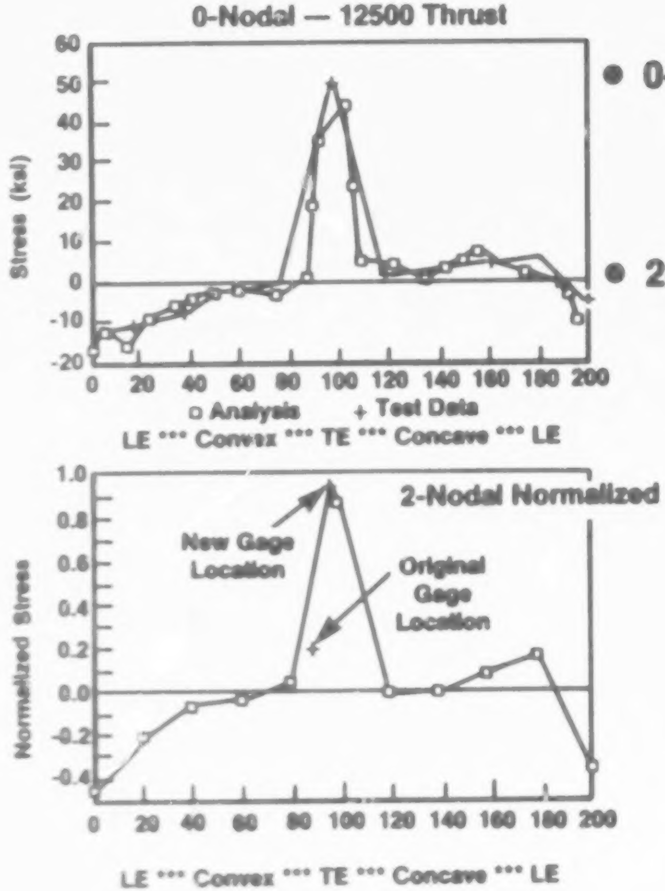

- 0-Nodal Load
  - Mean Stress Analysis Correlated
  - High Local Root TE Stress Confirmed
- 2-Nodal Load
  - High Local Stress/Deflection Controlled Loading Confirmed
  - Original Gage Location
    - Selected for Airfoil Modes
    - Poor for 2N Mode
  - New Gages Applied
    - Higher Response Location
    - Used to Correlate Original Gages

Figure 3-47. Power Turbine Frames Vibratory Response, Stage 12 Component Strain Distribution Test Results.

- **Frame Properties Better Than Material Handbook Average**

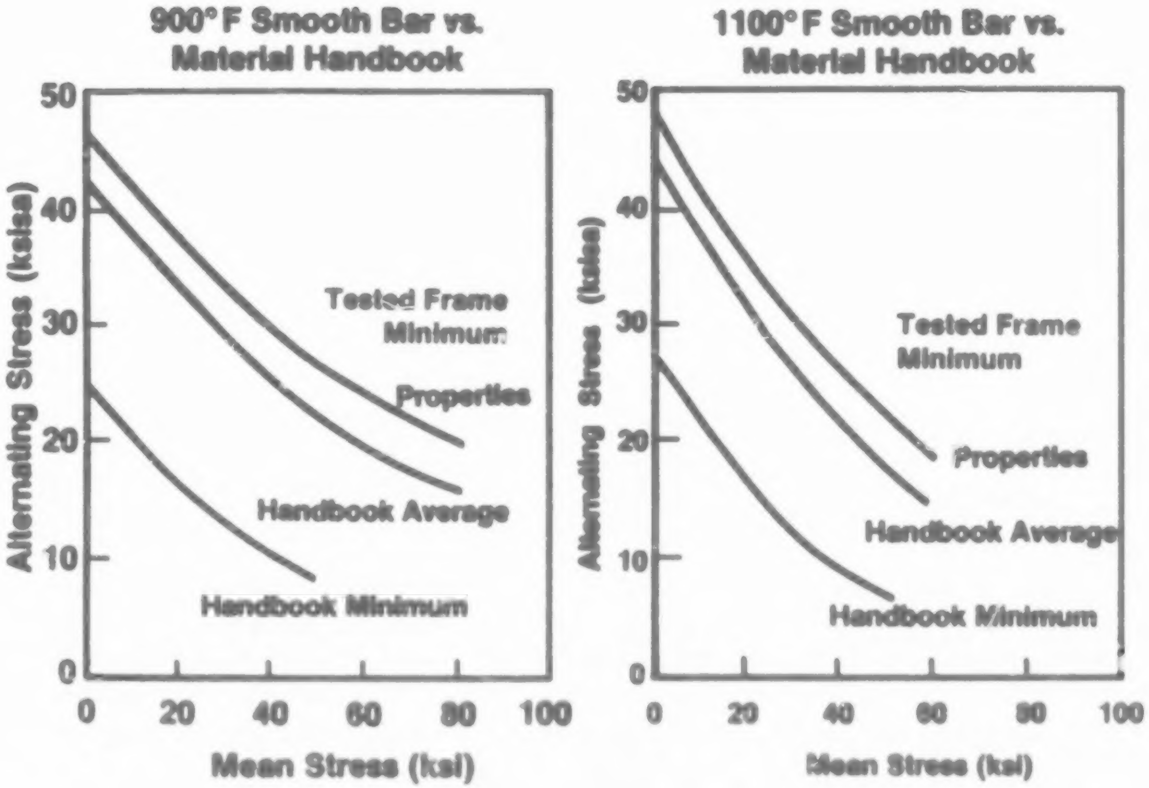

Figure 3-48. Power Turbine Frames Vibratory Response, Material HCF Test Results.

- **Peak Levels**
  - Consistent with Build 2
  - Below Scope Limits

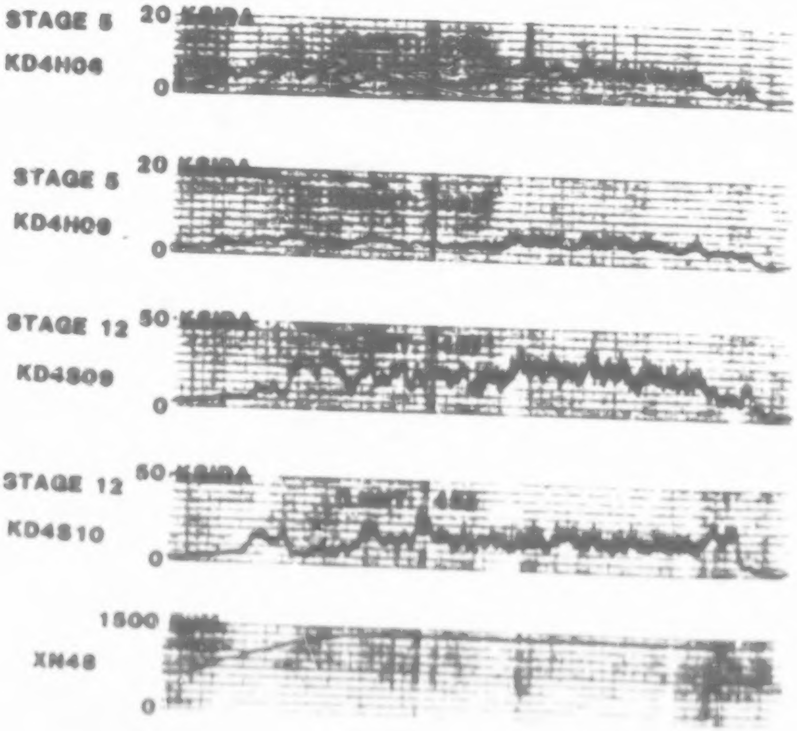

Figure 3-49. Power Frame Vibratory Response, Build 3

ORIGINAL PAGE IS
OF POOR QUALITY

stress data both with and without the vortex destroyer is contained in Figure 3-50. The same type of data are shown for the turbine frames in Figure 3-51. Since this testing was performed after the Stage 2 fan blade loss, and before installation of the redesigned fan blades, the engine was limited to 1000-rpm fan speed, thus limiting available analytical data for comparison. The vortex destroyer seemed to have a small positive or negligible effect on stresses; however, it was decided to complete all remaining engine testing with the destroyer in place. Wind conditions and the limited data (due to the 1000-rpm fan speed limit) did make comparisons difficult.

Table 3-1. Power Turbine Vibratory Response Resolution.

Vortex Destroyer	No Significant Effect (Section 3.13)
Change Test Sites	Slight Improvement (Section 3.14)
Component Strain Distribution Test	Mean Stress Analysis Verified
	Stage 12 Engine Gage Poorly Located for 2N Mode
	New Stage 12 Gage Applied Which Read Maximum Stress
Material HCF Testing	Significant Property Improvement Over Handbook Average
Updated Scope Limits	Stage 5 Frame Okay
	Stage 12 Frame Marginally Okay

3.14 EFFECT OF TEST SITE CHANGE ON STRESS

To try to reduce vibratory stress levels in the fan blades and the forced vibration of the power turbine frames, the engine was moved from Site 4A to 3D. The site change increased the clearance between the ground and fan blades from 28 inches to 64 inches as well as eliminated the frontal blockage area at Site 4A caused by the permanent facility fan system that was in front of the UDF™ inlet. Stress data are shown from both sites for the fan blades (Figure 3-52) and the turbine frames (Figure 3-53). There was no significant decrease in either fan blade or turbine frame stresses. Fan blade stress data, after the site change, was prior to the installation of the redesigned fan blades

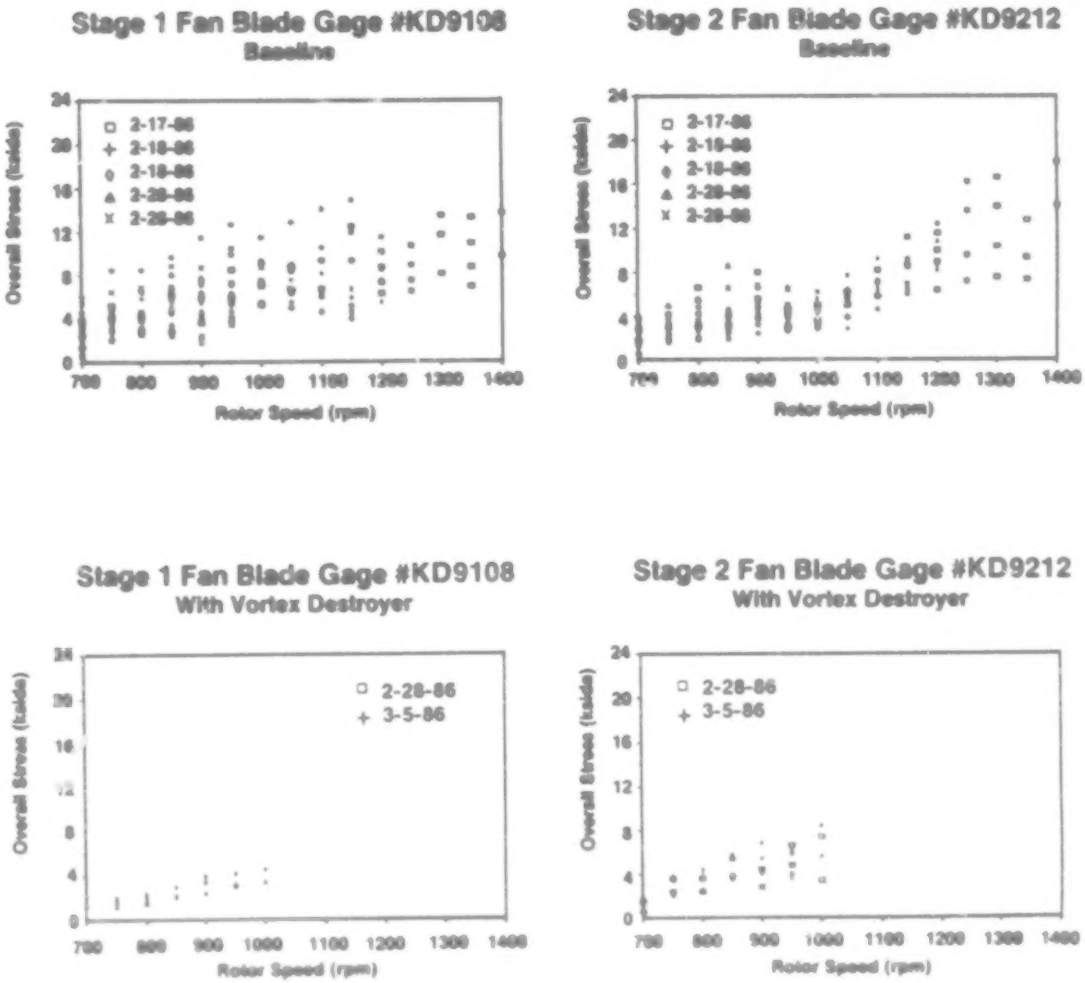

Figure 3-50. Fan Blades Vibratory Response, Effect of Vortex Destroyer.

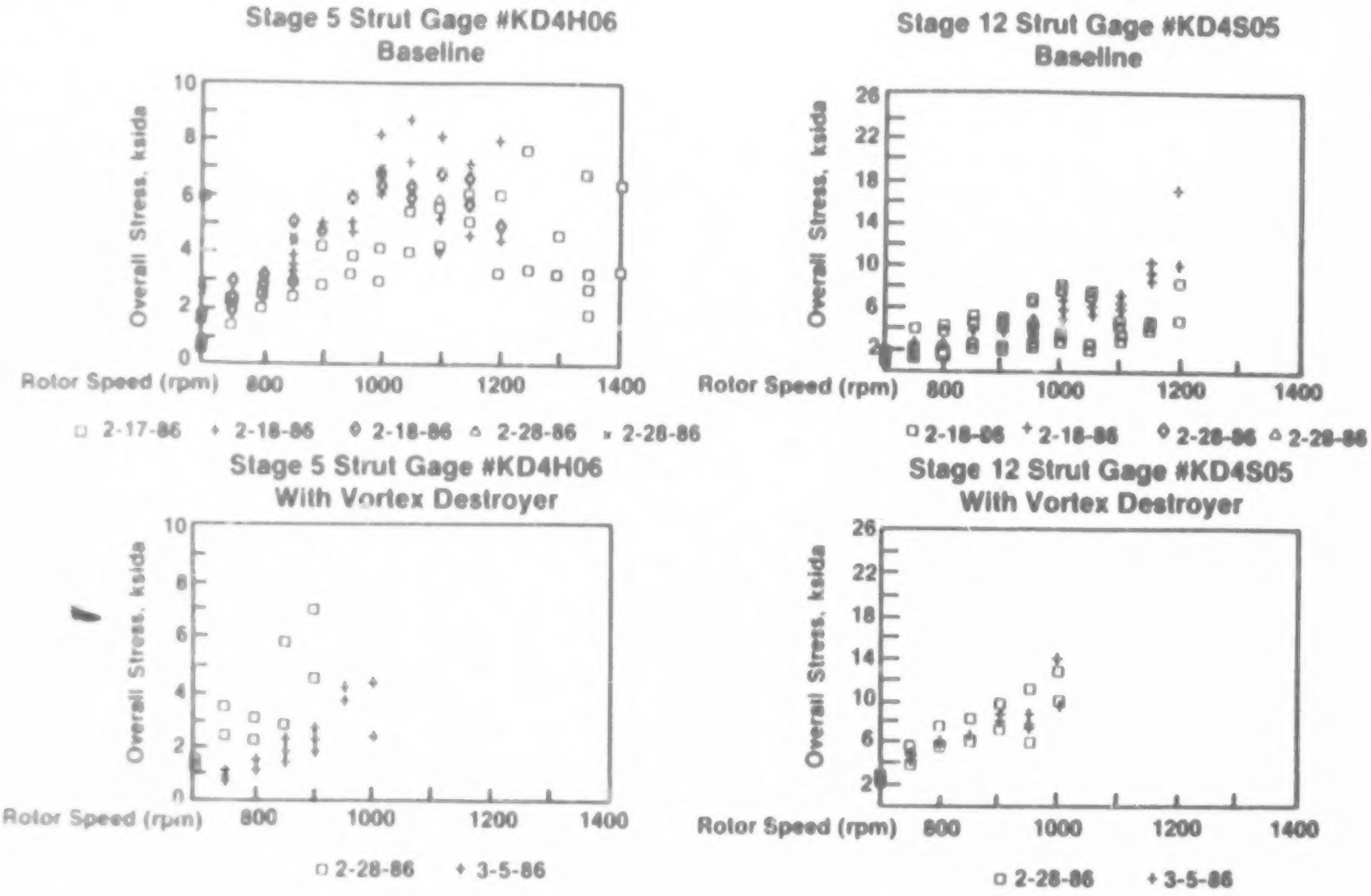

Figure 3-51. Power Turbine Frames Vibratory Response, Effect of Vortex Destroyer.

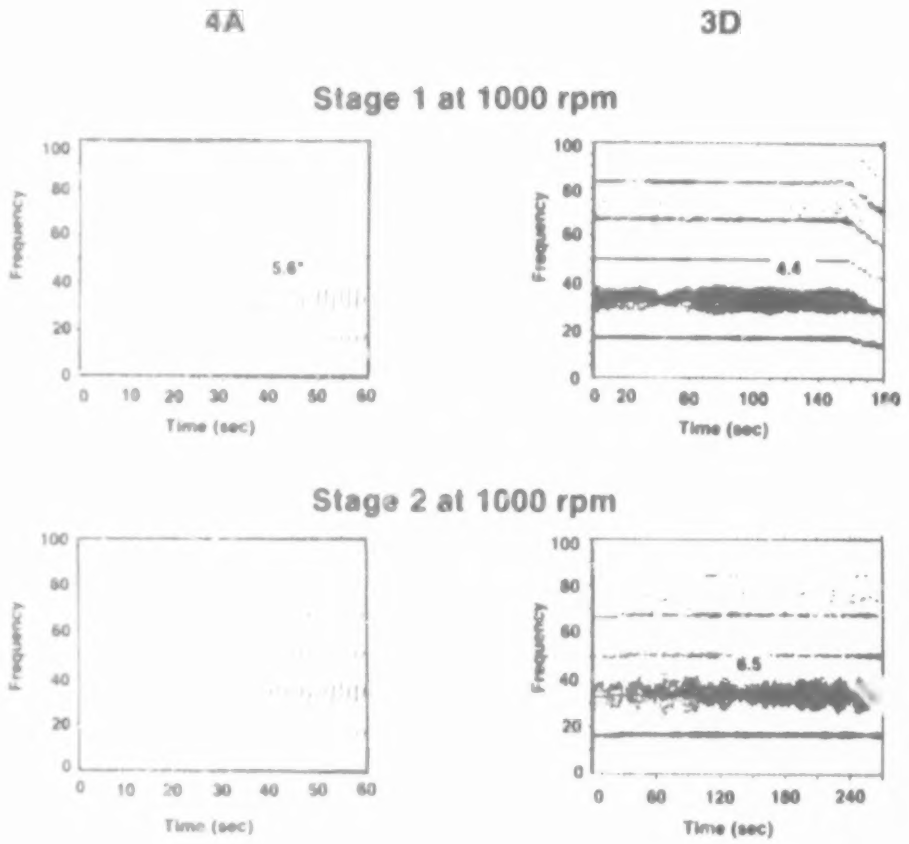

4A

3D

Stage 1 at 1000 rpm

Stage 2 at 1000 rpm

- Site Differences
  - Ground Clearance Increased from 28" on 4A to 64" on 3D
  - Reduced Frontal Blockage at 3D
- Results
  - No Apparent Differences In Low Speed Response Level or Content
  - Maximum Steady State Speed Obtained on 3D is 1000 rpm, No Maximum Power Runs
  - Low Ambient Winds During 3D Testing

*Peak Stress in KSIDA

Figure 3-52. Fan Blade Response Comparison, Site 3D Versus Site 4A.

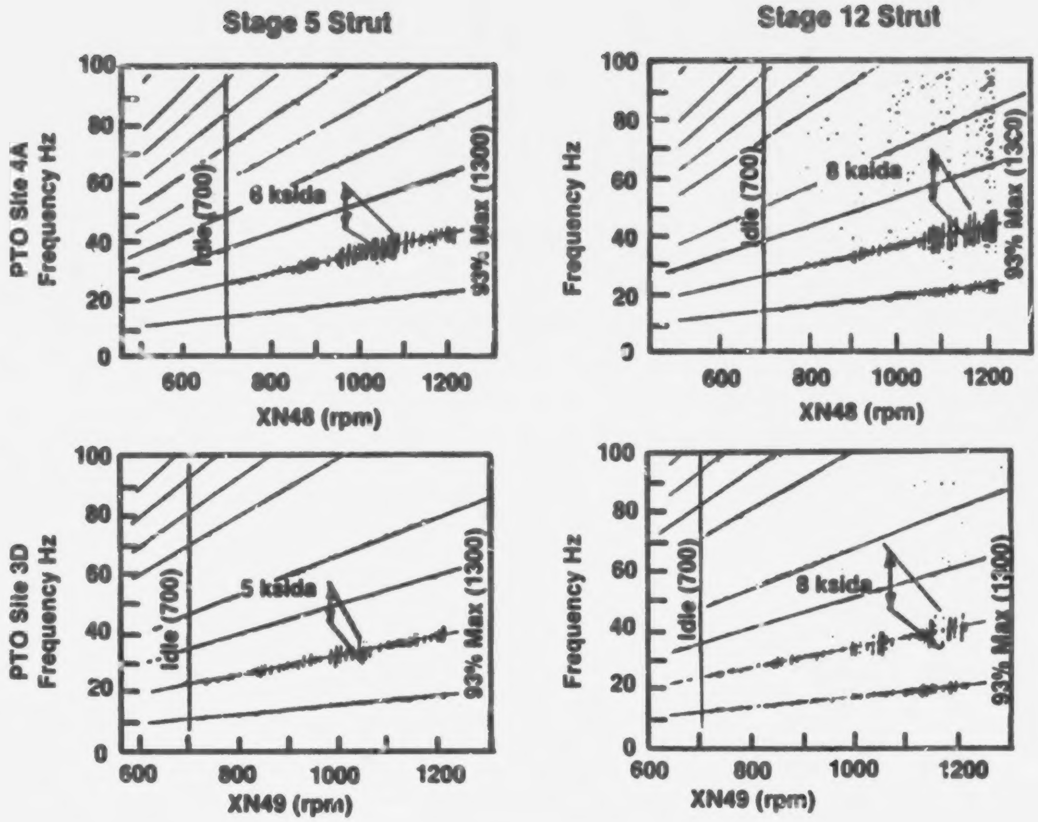

Figure 3-53. Power Turbine Frames Vibratory Response, Effect of Site Change.

C-2

so that a direct comparison of fan blade stress could be made. Fan speed was limited to 1000 rpm until the redesigned fan blades were installed. Turbine frame stress data, after the site change, is from Build 3 (after installation of the redesigned fan blades).

3.15 ROTOR LOCKUP AFTER SHUTDOWN RESULTING FROM FUEL LEAK

While running a power-down calibration at 19,000 lbf on June 30, 1986, a fuel leak was observed, and the engine was quickly shut down. After propulsor spool down, the Stage 2 rotor would not rotate until the engine had cooled for several hours. At that time, the exact cause was not known; however, based on a later teardown, it is believed that the IGV lip seal had deflected thermally and bound to the 1-4 inner spool. When the engine had cooled sufficiently, the IGV and the spool separated enough to allow rotation of the Stage 2 rotor. From looking at strain gage data for Stages 1 and 2 turbine blades, it appears (Figure 3-54) that the IGV and spool had started to rub as early as June 24. Heat generated from this interference eventually closed the Stage 1 turbine blade clearance causing severe turbine blade tip rubs; Section 3.17 discusses this further.

3.16 LOW/HIGH CYCLE FATIGUE TESTING

During Build 3, 100 low cycle fatigue cycles were run for endurance testing. The cycle that was run is shown in Figure 3-55.

No dedicated high cycle fatigue testing was necessary because cycles in excess of 1×10^6 were accumulated through the course of normal testing. The number of cycles accumulated on each component was calculated using the component first flex natural frequency and the engine run time versus propulsor rpm relationship.

Table 3-2 shows the number of high- and low-cycle fatigue cycles that the turbine blades, fan blades, and power frame airfoils experienced.

3.17 ROTOR-TO-ROTOR LOCKUP/PROPULSOR DISASSEMBLY AND REBUILD

During an attempt to make a normal start, it was noticed that the forward and aft rotors although locked together could be turned with force. During

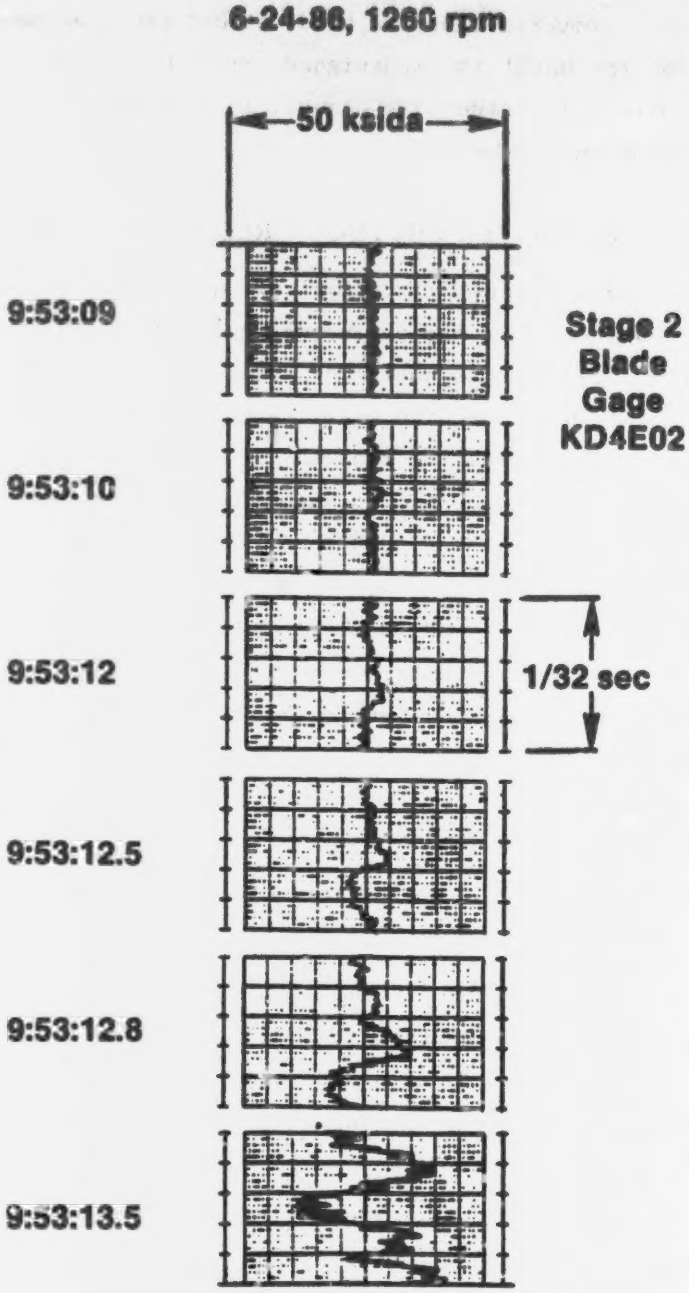

Figure 3-54. Suspected IGV/Spool Rub.

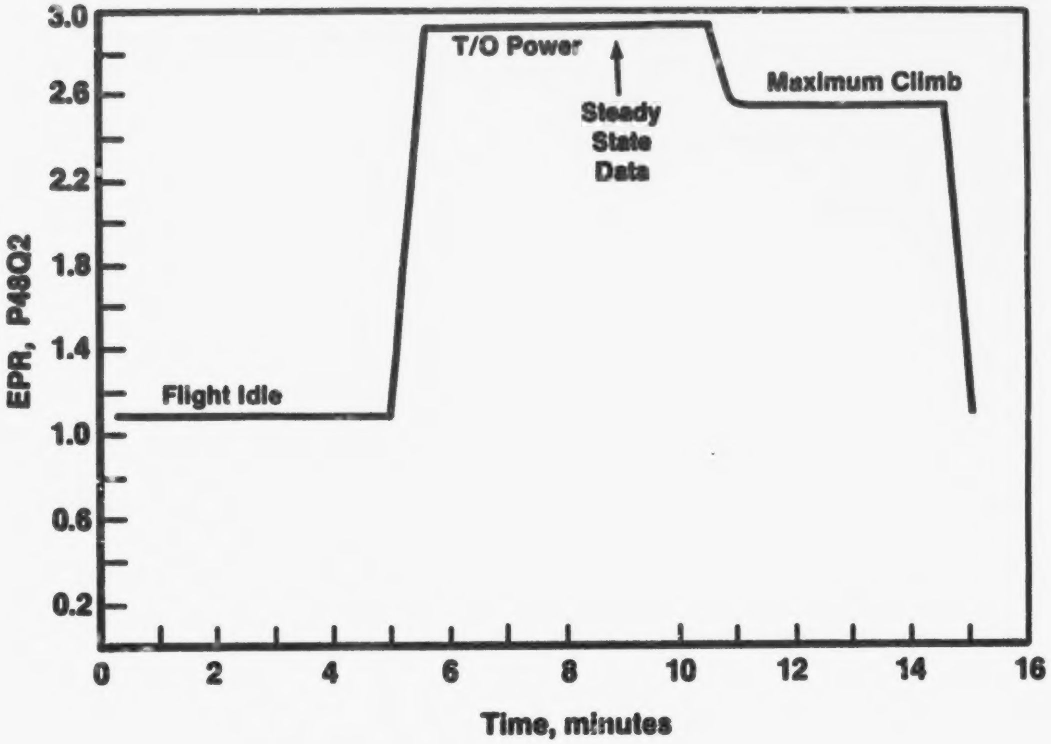

Figure 3-55. Low Cycle Fatigue Cycle.

trim balancing, previously, the engine had run up to 22,000 lbf. No problems occurred before the rotors locked. The force required to turn the rotors increased when the blade actuation system was commanded to full reverse. It was found that the forward actuator would not move to full reverse (-20°), but only went to -12°. The rotors did not free up as the engine cooled, and the decision was made to remove it from the test site to investigate the problem.

Table 3-2. GE36 HCF Cycle Count.

Turbine Blades	HCF Cycles	LCF Cycles	Remarks
Stage 1	6.23×10^6	100	53 Cracked Blades
Stage 2	4.09×10^6	100	No Discrepancies
Stage 3	5.00×10^6	100	No Discrepancies
Stage 4	18.18×10^6	100	No Discrepancies
Stage 6	14.10×10^6	100	No Discrepancies
Stage 7	7.5×10^6	100	No Discrepancies
Stage 8	15.15×10^6	100	No Discrepancies
Stage 9	1.2×10^6	100	No Discrepancies
Stage 10	2.5×10^6	100	No Discrepancies
Stage 11	1.3×10^6	100	3 Cracked Blade
Fan Blades Stages 1/2	3.69×10^6/ 3.78×10^6	100 100	No Discrepancies
Power Frames Stage 5/12	4.04×10^6/ 4.2×10^6	100 100	No Discrepancies

When the engine was returned to the vertical build stand, it was noted that the rotors rotated freely. The actuation system was exercised and found that the forward system still would not travel to the full reverse extension. With the actuation system in the stopped reverse position, the rotors became bound in the same manner as seen on the test stand. A scale was utilized to measure the force required to rotate the forward rotor holding the aft rotor stationary. With the engine vertical and the actuator fully forward (feather or 90°), the force to turn the Stage 1 rotor was 4 lb. When the actuator was driven fully aft (full reverse or -20°), the rotors bound, and the force which was required to turn the forward rotor increased to 40 lb.

	Full Forward	Full Reverse
Forward Rotor	4 pounds	40 pounds
Aft Rotor	5 pounds	10 pounds

The above tabulation provides a comparison of the forces required to turn the rotors independently, with the other held stationary. It was also found that the lack of full travel in the actuator could easily be seen when watching the actuator. The forward system lacked 0.5 inch of its full travel. As the pressure in the hydraulic system was increased (actuator in reverse), the force required to turn the forward rotor increased to 40 lb at 600 psi. The decision was made to pull the propulsor from the gas generator and begin the teardown to investigate the rotor binding.

Removal of the propulsor revealed problems unrelated to the rotor binding. Inlet guide vanes to the propulsor had cracks at the trailing edge ID (inner diameter) braze. The ID was very irregular, and evidence of contact with the Stage 1-4 inner spool was noted. The area between the IGV and the inner seal was black from oil coking, and the Stage 1-4 inner spool was discolored from varnishing. Figure 3-56 diagrams the IGV seal area as-designed, and after test. Figure 3-57 shows the ALF (aft looking forward) view of the tear/crack.

The IGV had worn a 0.010-inch groove in the Stage 1-4 inner spool around the entire circumference. The heat generated by the continual interference between the IGV and spool resulted in a spool growth that closed the Stage 1 blade tip clearance. The spool had heavy rub indications where the Stage 1 blade tips rubbed. The Stage 1 blade rub appears to have begun as early as June 24, after 3 hours of Build 3 testing (Figure 3-58). Examination of the strain gage data for Stages 1 and 2 of the power turbine indicates the IGV-to-inner spool rub occurred prior to the Stage 1 blade rub (Section 3.15).

The Stage 1 blades were found to have HCF cracks that initiated at the leading edge root. The blades with the most visible cracks are illustrated in Figure 3-59. There is a total of 124 Stage 1 blades; of these, 19 blades had

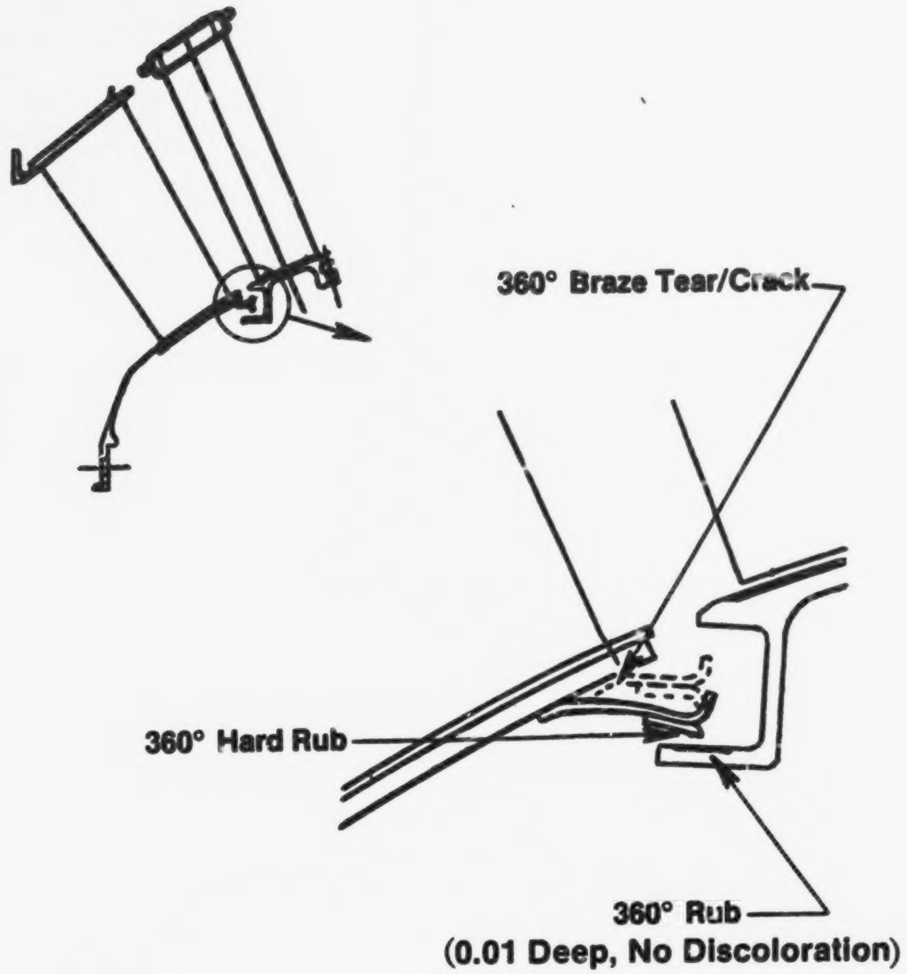
360° Braze Tear/Crack
360° Hard Rub
360° Rub
(0.01 Deep, No Discoloration)

Figure 3-56. IGV and 1-4 Inner Spool.

ORIGINAL PAGE IS
OF POOR QUALITY

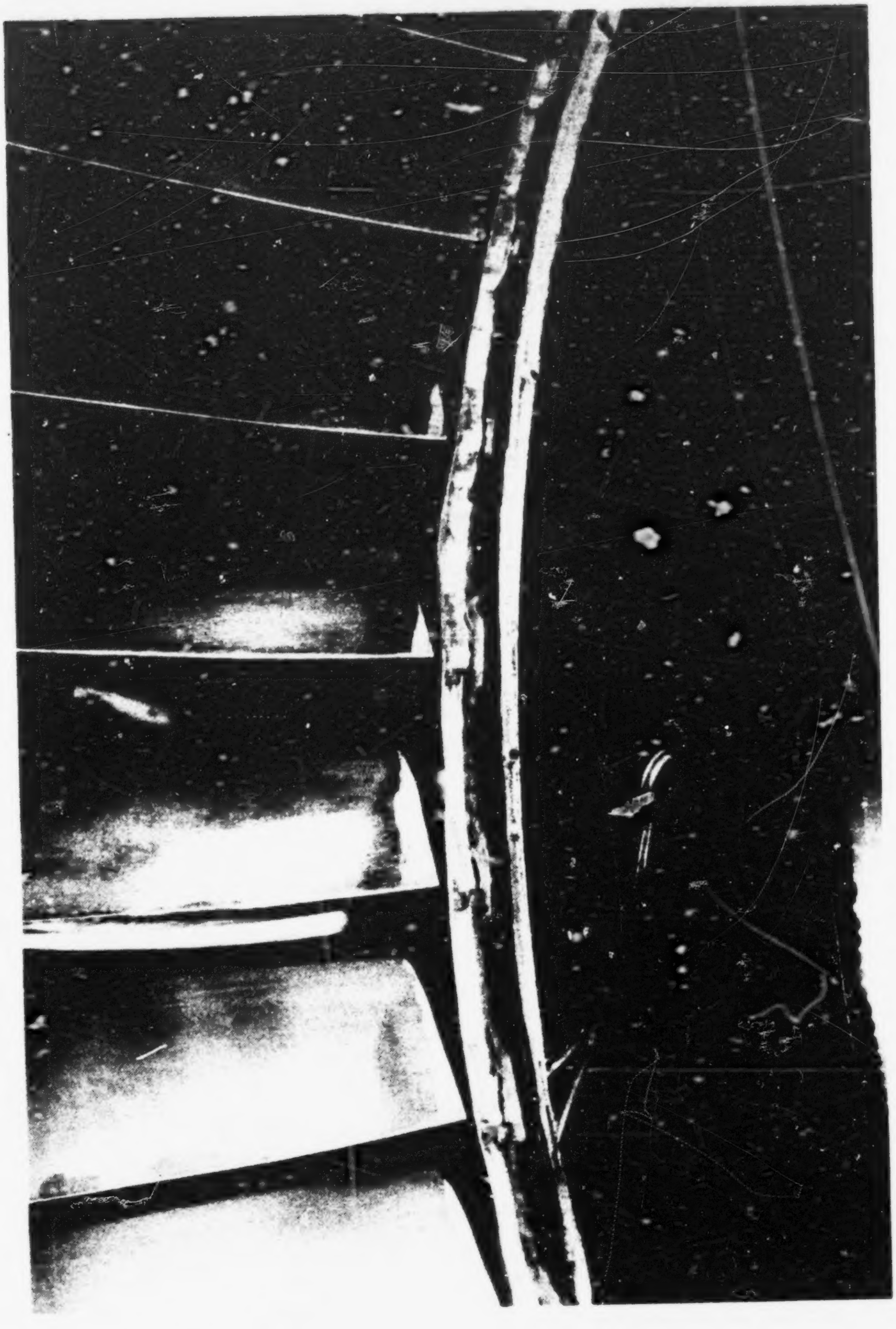

Figure 3-57. IGV Crack/Tear at Braze Joint (ALF).

ORIGINAL PAGE
BLACK AND WHITE PHOTOGRAPH

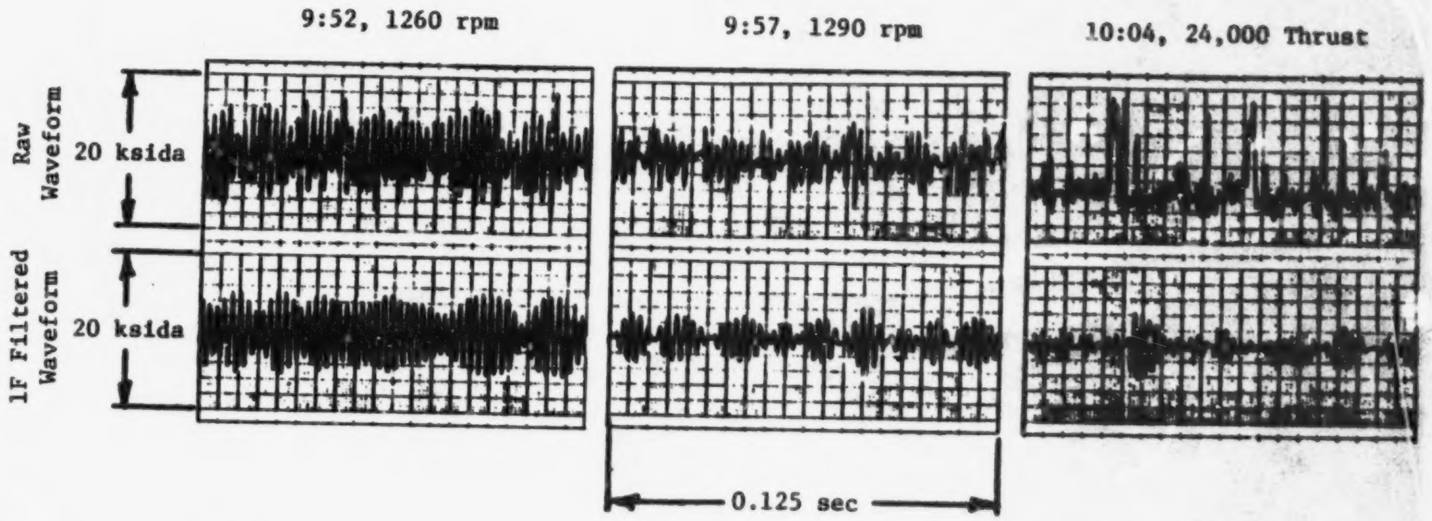

Figure 3-58. Suspected Stage 1 Rub.

ORIGINAL PAGE IS
OF POOR QUALITY

~~ORIGINAL PAGE IS~~
~~OF POOR QUALITY~~

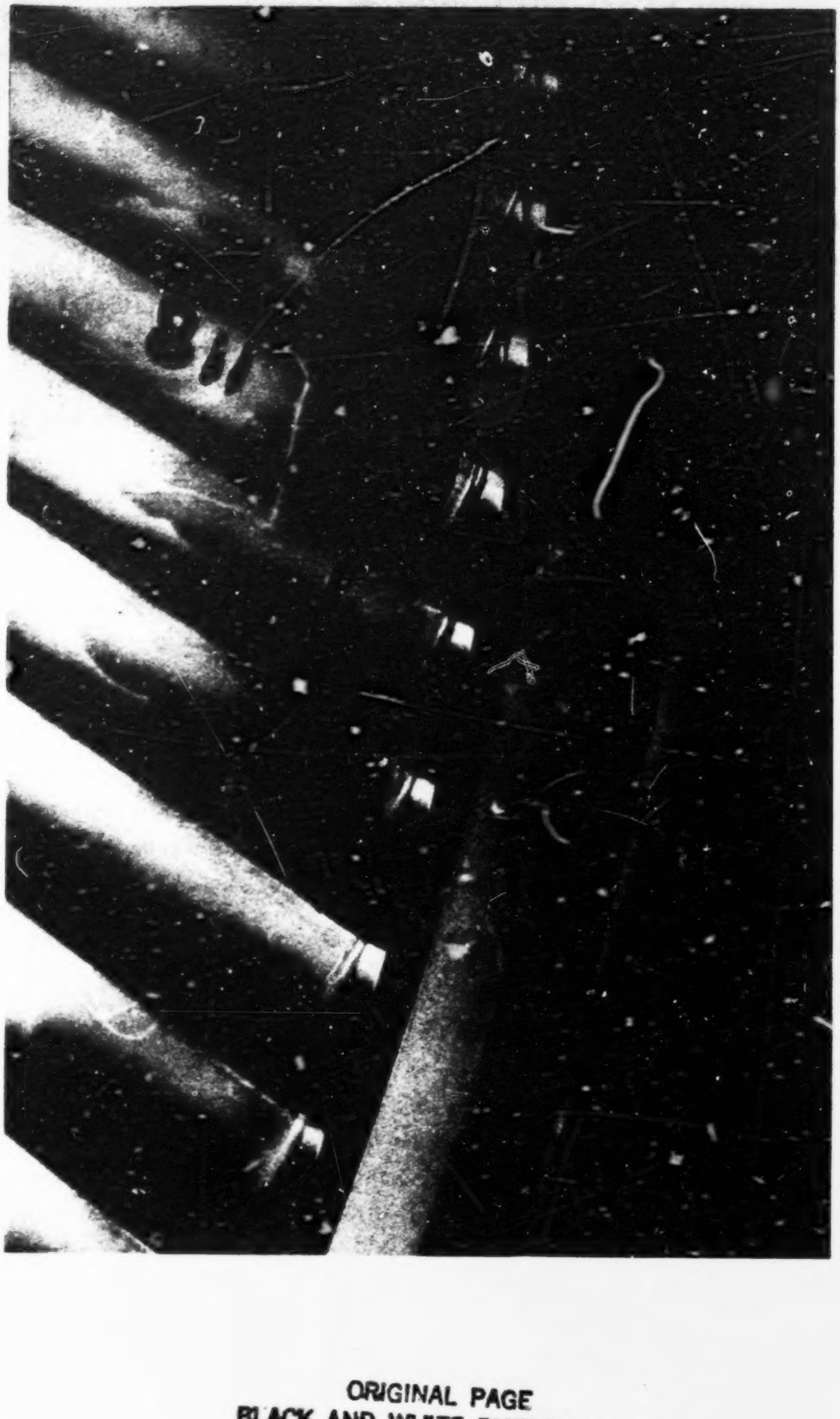

Figure 3-59. Stage One Blade Cracks at Leading Edge Root.

ORIGINAL PAGE
BLACK AND WHITE PHOTOGRAPH

cracks visible to the naked eye, and an additional 34 were found cracked when examined at 40×. The entire set was removed, and new blades were installed. Tip clearance was increased an additional 0.037 inch at the blade leading edge and 0.016 inch at the trailing edge for the new set of blades.

The Stage 2 polygonal ring was removed, followed by the outer seal. The seal teeth had no damage, and coating wear was normal for the engine run time. A cross-sectional view of the seal is shown in Figure 3-60.

Following removal of the Stage 1 polygonal ring, the aft stationary hardware was removed. The eight actuator control rods which penetrate the No. 2 bearing static housing were all observed to have varying degrees of wear. The heaviest wear was on the rods at 12 and 6 o'clock. The aft support had heavy scoring on the forward OD (outer diameter) where the aft actuator travels over it. Wear marks were in the same position as the sting tube support brackets. Blocks providing support were reduced to lightweight springs during rebuild. The scored area was cleaned and covered with a Teflon coating (Emralon 333) to reduce friction between the actuator and support. The coating when scratched will not flake but will lubricate to protect the material below.

The aft actuation subassembly was lifted out followed by a borescope of the forward sumps. Entering the sump through the mid-driveshaft actuator rod cutouts revealed the source of the binding rotors. The No. 1 roller bearing (1R) outer race nut had come completely off (Reference Figures 6-2 and 6-3, Section 1.1). The actuator could not travel the full distance because the nut was interfering with the last 0.5 inch of actuator travel.

The 6-12 assembly, less the midshaft, was removed for further inspection and set in the teardown tooling.

Upon removal of the forward actuator, the 1R bearing housing was removed so that access to the 1R bearing could be made. The outer race nut was laying inside the actuator assembly, and the outer race was found almost completely off. The rollers were pushed inward and the two shafts were easily separated. The rollers sustained disassembly damage, making the bearing not serviceable but repairable. The outer race had no visible grooves. The outer race nut backed off as a result of Stage 1-5 rotor aft shaft growth caused by thermal expansion.

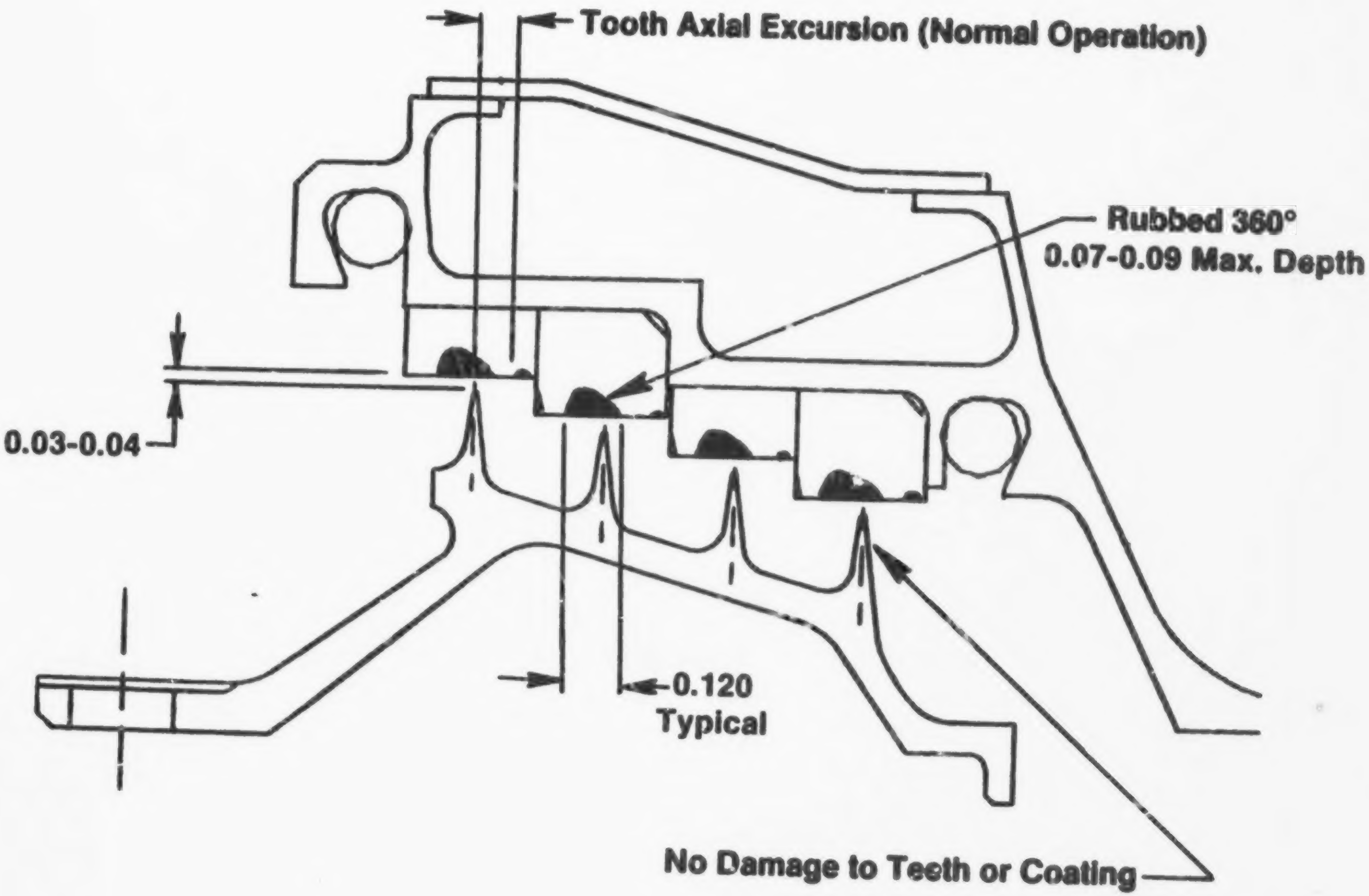
Tooth Axial Excursion (Normal Operation)
Rubbed 360°
0.07-0.09 Max. Depth
0.03-0.04
0.120
Typical
No Damage to Teeth or Coating

Figure 3-60. Aft Outer Flowpath Seals.

Because the carbon seal aft of the 1R bearing, sealing the cavity, was in remarkably good condition and repairable, the seal was removed for inspection, the carbon segments were replaced, and the seal assembly installed. The mid-sump seal aft of the carbon seal had rubbed grooves about 0.14-inch long × 0.04-inch deep in the honeycomb. As shown in Figure 3-61, the honeycomb and seal teeth were all serviceable and reused.

All Stage 11 blades were heavily rubbed, and Stage 10 was lightly rubbed (Figure 3-62); 3 Stage 11 blades were discovered with cracks in the leading edge root, and the inner spool had evidence of a hard rub. The outer spool (odd rotor) aft stages are cantilevered from the Stage 5 power frame. If the 1R bearing were not providing adequate radial support, it would account for a rub at the aft stages of the outer spool. The 3 cracked Stage 11 blades were replaced prior to rebuild. Table 3-3 summarizes the results of the turbine blade inspection.

Table 3-3. Turbine Blade Inspection Summary.

Stage	1	2	3	4	6	7	8	9	10	11
No. of Blades	124	118	120	94	90	72	84	54	82	56
No. Cracked (1× Visual)	19	0	0	0	0	-	-	-	-	0
Additional No. Cracked (Borescope)	0	0	0	0	-	0*	0*	0*	0	3
Additional No. Cracked (10× Visual)	0	0	-	-	-	-	-	-	-	-
Additional No. Cracked (40× Visual)	34	-	-	-	-	-	-	-	-	-
Total Cracked	53 (42.7%)	0	0	0	0	0	0	0	0	3 (5.4%)

* Approximately 25% Sample; Others Inspected 100%

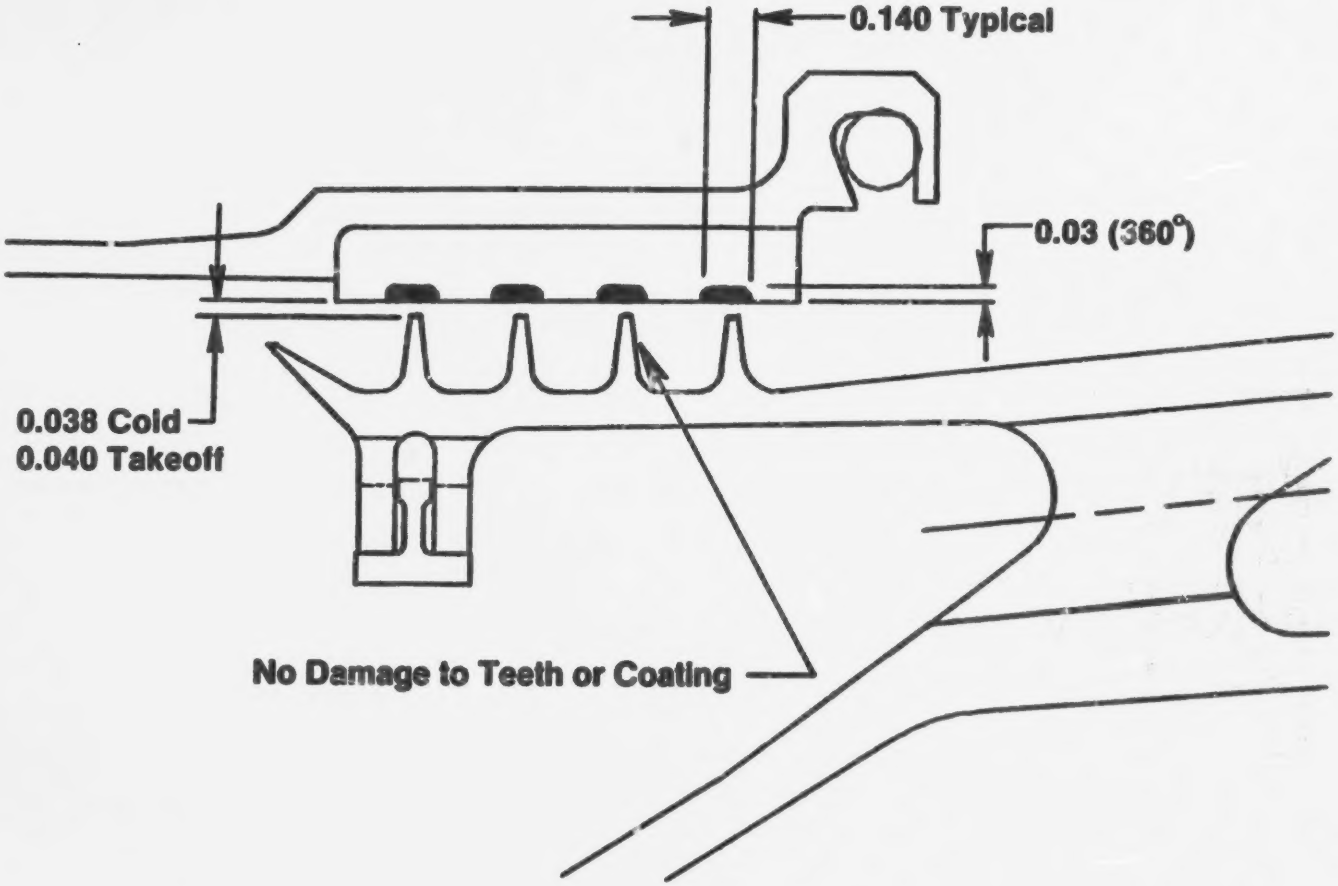
0.140 Typical
0.03 (360°)
0.038 Cold
0.040 Takeoff
No Damage to Teeth or Coating

Figure 3-61. Midsump Seals.

7-8-86, 10:45, 22,300 Thrust

Gage KD4N03

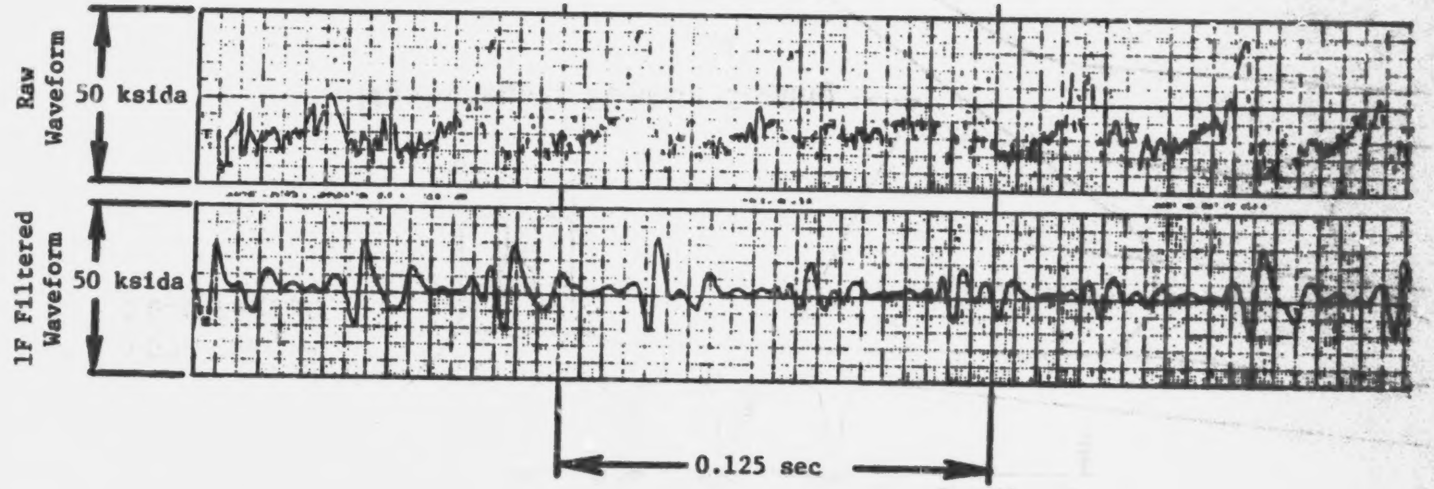

Figure 3-62. Suspected Stage 11 Rub.

ORIGINAL PAGE IS
OF POOR QUALITY

The 2R bearing was removed for a detailed examination at Evendale. One roller had a rounded micro dent which would not affect the design intent of the part. The 2R bearing was serviceable and was stored for later use, if required.

Corrective action for the binding rotors included an improved locking feature for the 1R outer race nut and other spanner nuts in the propulsor assembly. Upon installation of a new No. 1 roller bearing, the spanner nut was installed with a small amount of Loctite applied axially in four places across the threads of the nut. Both threaded surfaces were cleaned and dried prior to nut installation. An additional locking feature was added with two pins installed between the shaft and nut, which were also tack welded in place (Reference Figure 6-4). The inner race nut was installed only with Loctite. A new carbon seal was also installed to replace the one damaged from the 1R bearing problem. In addition, the 1B inner race nut had Loctite applied; all others were untouched and remained as they were.

The IGV was repaired and modified to include a honeycomb seal to prevent spool damage if a reoccurrence of the rub persists in later engine operation. Figure 3-63 is a view of the IGV/spool seal area. During assembly of the propulsor to the gas generator, the gap between the IGV and spool was checked and measured at 0.125 to 0.188 inch, with a minimum of 0.125 inch per the drawing.

Oil drain holes were drilled into the 1-4 inner, 1-2 outer, and 3-4 outer turbine spools to drain any accumulated oil.

Borescope ports were added through the mixer frame flange for better visibility to the IGV and Stage 1 blades. The inspection interval was set at 10 hours to keep better records of Stage 1 blade activity and IGV spool gap.

3.18 MISCELLANEOUS HARDWARE STRESS DATA

This section presents data on hardware that had no indication of high stress (vibratory stress was always under limits) during testing and has not been previously presented in other sections.

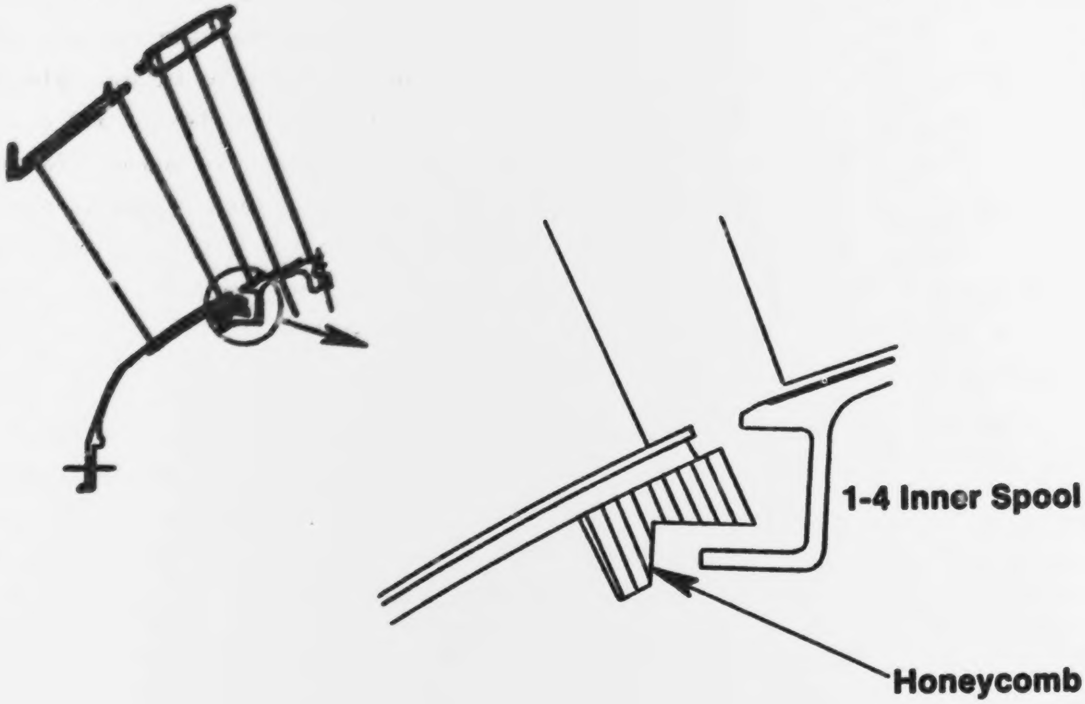
1-4 Inner Spool
Honeycomb

Figure 3-63. IGV and 1-4 Inner Spool.

Nomenclature	Limits (ksida)	Figure
Outer Guide Vanes (OGV)	20.0	3-64
Inner Guide Vanes (IGV)	3.4	3-65
Forward Outer Rotating Seal	74.0 (2/rev) 11.0 (3,4/rev) 8.0 (5/rev)	3-66
Aft Outer Rotating Seal	15.0	3-67
Turbine Spools	30.0*	
1-4 Outer		3-68
7-11 Outer		3-69
6-11 Inner		3-70

* 10.0 for Turbine Blade Rubs

3.19 OIL LEAK/GULPING PROBLEM

During the latter portion of Build 2 and, more markedly, during Build 3, the propulsor oil consumption limited the UDF™ test time (oil consumption increased from 0.35 to 1.58 quarts/hour from Build 2 to Build 3). The engine was limited to about 2.5 hours of testing to allow for reservicing of the propulsor oil tank. By this stage of testing, the test site facility remote oil fill system had been removed since it would not be available for flight-test.

Two major leaks contributed to the high oil consumption. The carbon seal in the starter gearbox was leaking into the core nacelle and then back into the fan, and oil leaked through worn actuation rods and seals in the aft sump wall into the sting tube area in the center of the propulsor (aft stationary support). Oil lost into the sting tube could be pumped out after engine shutdown. A total of 39 quarts was recovered during Build 3 testing (66 hours). The fan nacelle and propulsor rotors remained dry, indicating the oil loss was not through the main propulsor carbon seals. Oil was also found leaking from an instrumentation fitting in the aft sump wall. The propulsor lube oil leak limited the engine test time in two ways.

First, as previously stated, the low lube level inside the sting tube required careful monitoring to ensure that enough oil did not collect to flow out of the mixer frame. The cavity was pumped approximately every 2.5 hours, and about 2.5 quarts were removed each time (toward the end of Build 3).

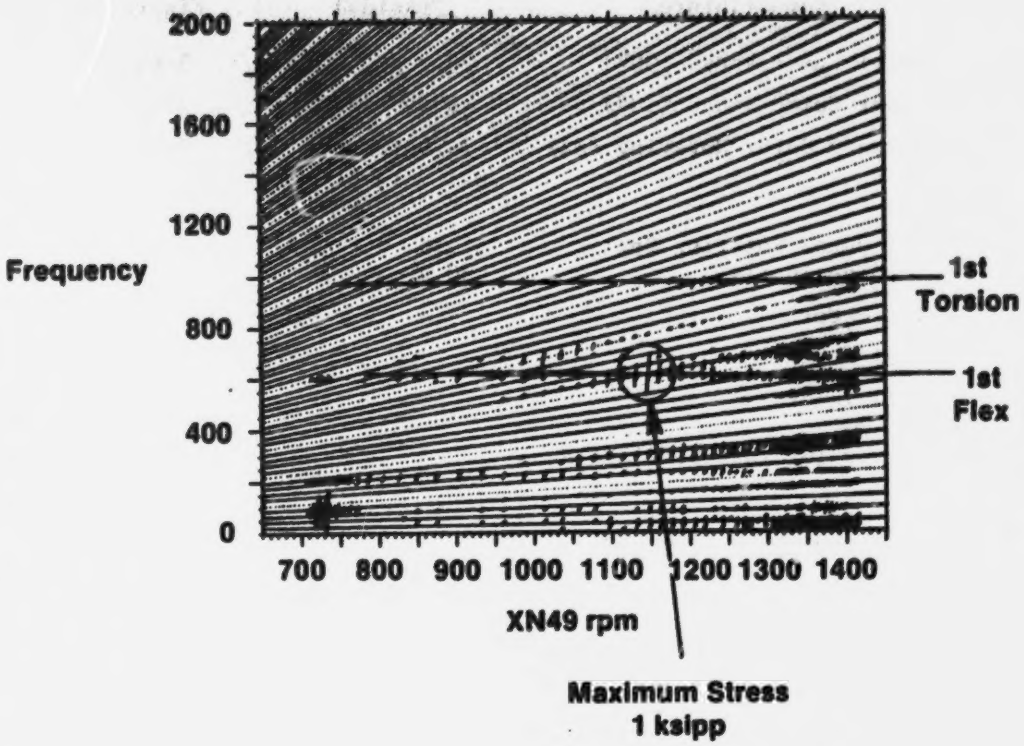

- 1F And 1T Responses
- Low Amplitude
- Maximum Allowable 20 ksipp
- Predicted Values
  - 1F 600 Hz
  - 1T 970 Hz
- Data Typical For Engine Testing To Date

Figure 3-64. Power Turbine OGV - Engine Test Data.

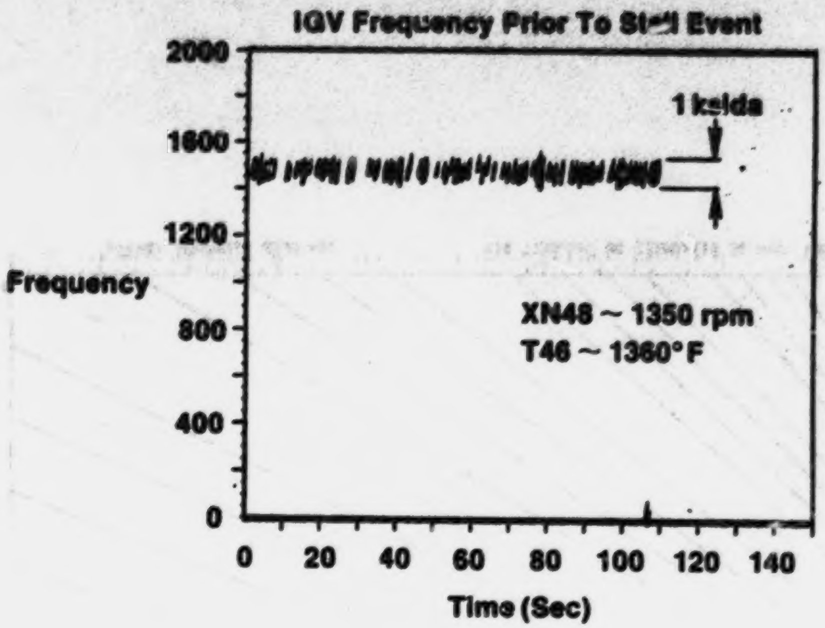

- **Engine Test Dynamic Strain Gage Frequency = 1475 Hz (1 Flex)**
- **Predicted 1st Flex Frequency Is 1425 Hz**
- **Allowable Stress Level Is 3.4 ksida**
- **Trace Is Typical Of Vane Data Seen During Engine Test**

Figure 3-65. Power Turbine IGV - Engine Test Data.

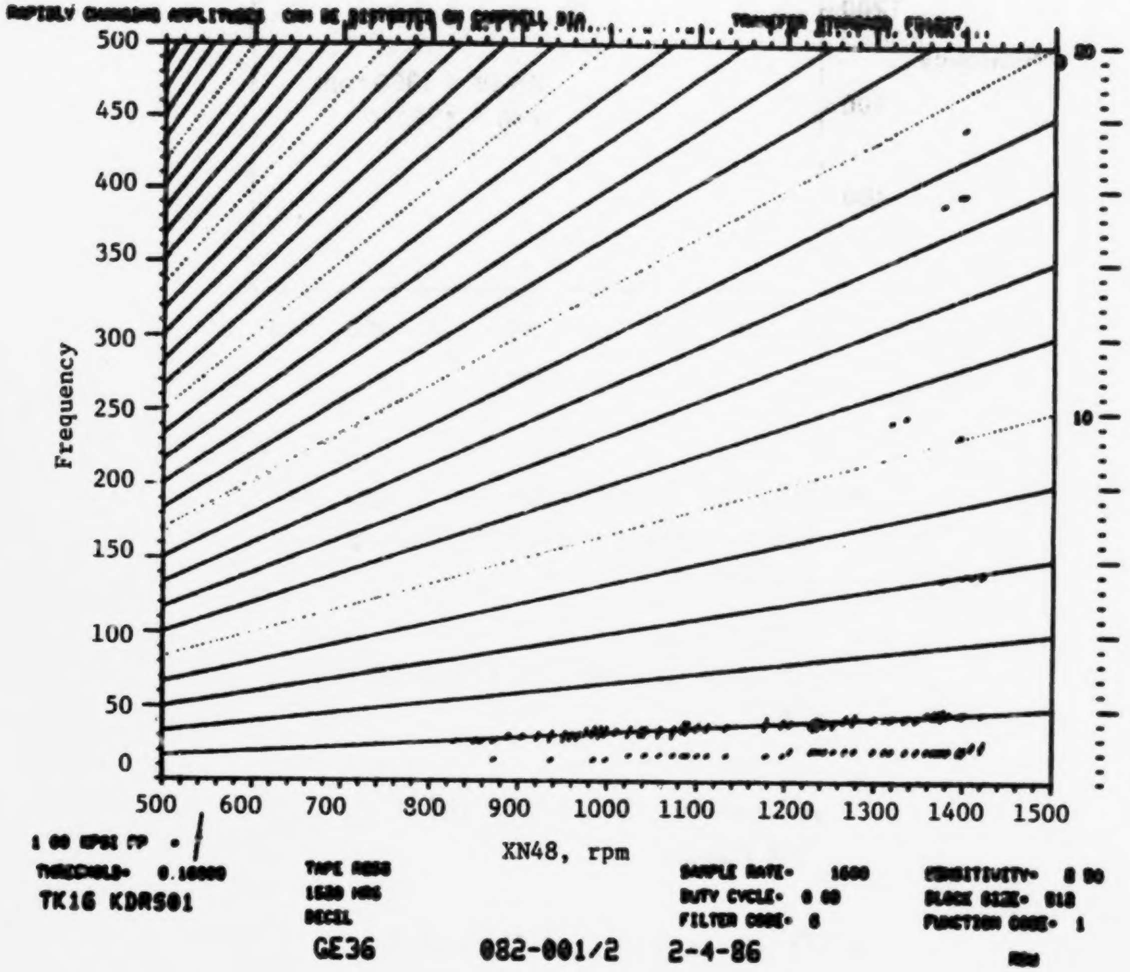

Figure 3-66. Forward Outer Rotating Seal Response, Decel from 25,000 lbf Thrust: February 4, 1986.

ORIGINAL PAGE IS
OF POOR QUALITY

ORIGINAL PAGE IS
OF POOR QUALITY

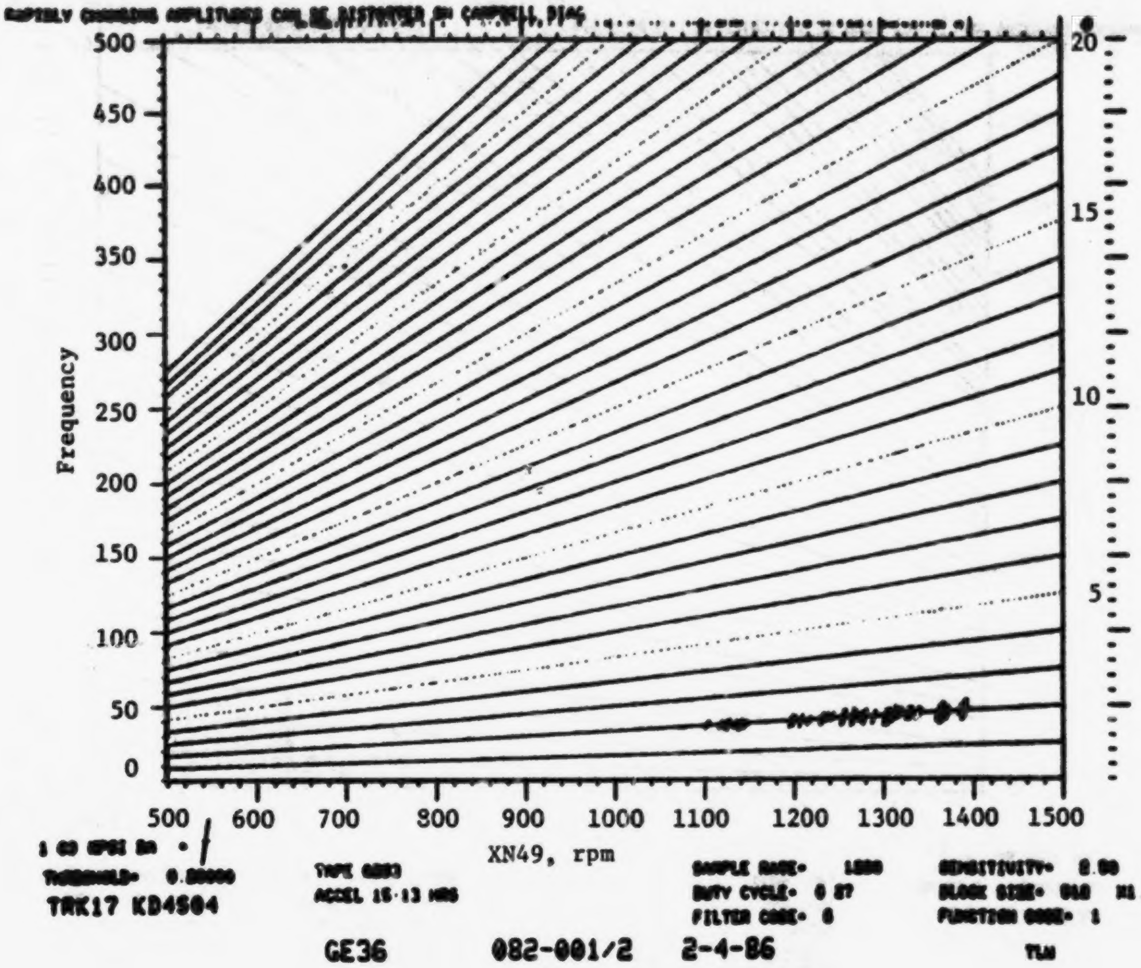

Figure 3-67. Aft Outer Rotating Seal Response, Accel to 25,000 lbf Thrust: February 4, 1986.

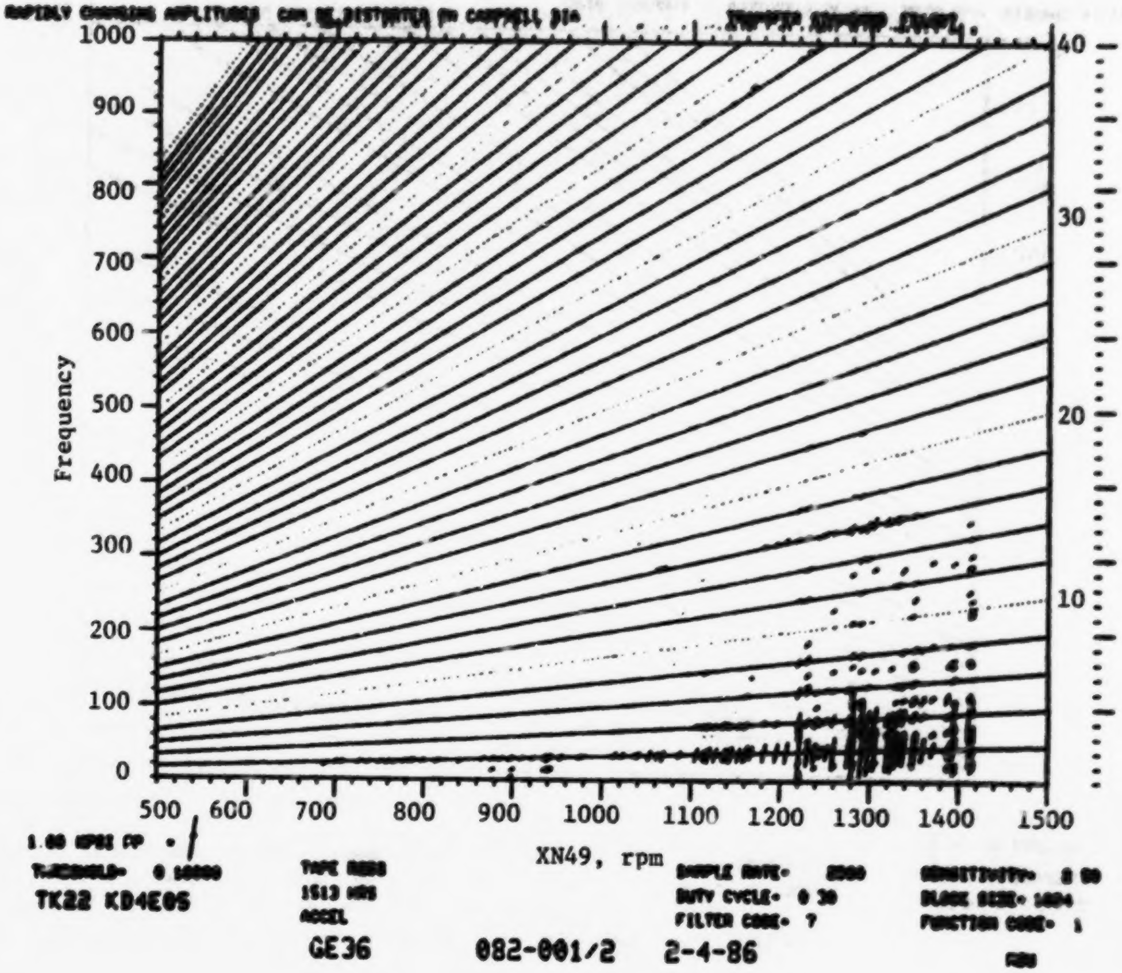

Figure 3-68. Outer Turbine Spool Response (1-4), Accel to 25,000 lbf Thrust: February 4, 1986.

ORIGINAL PAGE IS
OF POOR QUALITY

ORIGINAL PAGE IS
OF POOR QUALITY

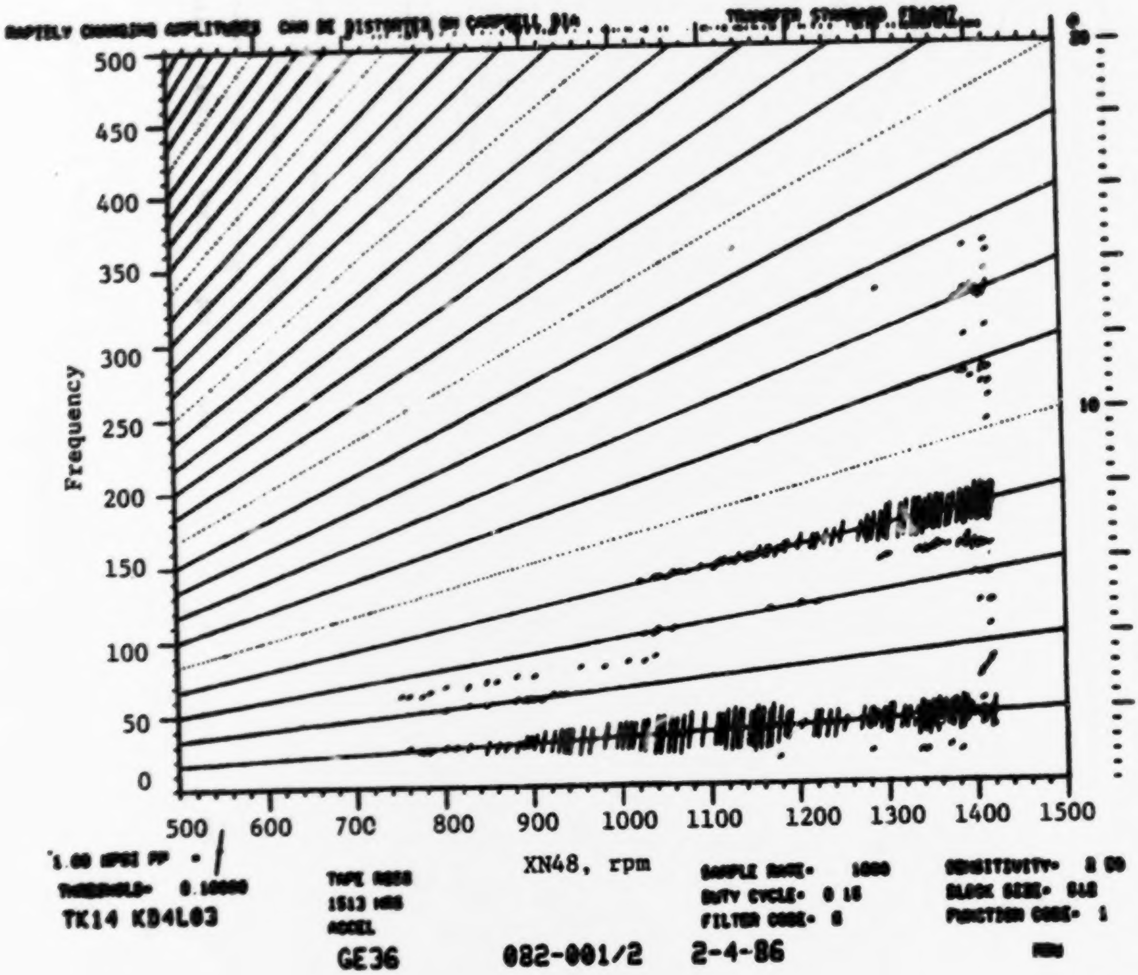

Figure 3-69. Outer Turbine Spool Response (7-11), Acceleration to 35,000 lbf Thrust: February 4, 1986.

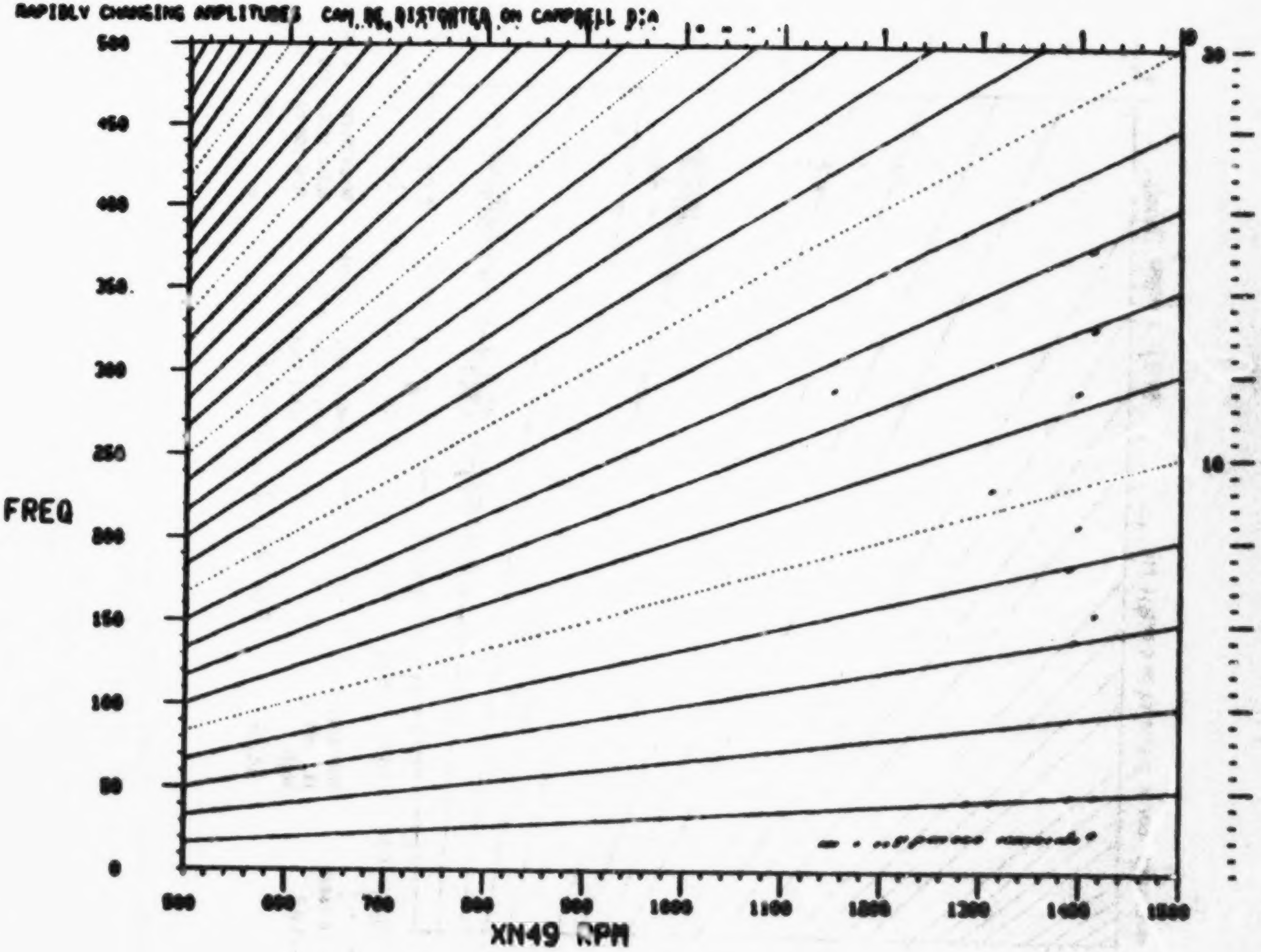

ORIGINAL PAGE IS
OF POOR QUALITY

Figure 3-70. Inner Turbine Spool (6-11) Response, Accel to 25,000 lbf Thrust: February 4, 1986.

Second, combined with the excessive leakage, the gulp limited testing duration. The propulsor gulps about 2.5 quarts of oil with increasing power from idle to maximum. This is consistent over all engine testing. As speed is reduced, the oil level will return. That is, it will return if the propulsor is not losing oil from leaks in the sump wall or gearbox carbon seal. With a normal oil consumption rate, oil gulping is not a problem with the 11 quart tank.

Following Build 3, the leaks were fixed; new actuation rods and seals were installed in the actuation system, a new starter adapter gearbox was installed, and the instrumentation fittings were replaced. A larger scavenge port was installed in the new starter adapter gearbox to improve scavenging and to keep oil away from the aft carbon seal that leaked on Build 3. A new flight-type static vent air demister was installed, and oil drain holes were added to the turbine spools.

4.0 HEAT TRANSFER AND SECONDARY FLOW SYSTEM

4.1 MIXER FRAME HEAT TRANSFER

The mixer frame flow circuit is shown in Figure 4-1. At takeoff power, film-hole flow is 15% less than predicted, outer flowpath secondary flow is 10% less than predicted, and total sump flow is 6% higher than predicted. The outer flowpath flow and sump flow are determined through use of pressure tap readings, and film-hole flow is determined by subtracting these flows from the total fan bypass flow.

Figure 4-2 provides a comparison of mixer frame predicted and measured internal pressures at takeoff power; whereas, a comparison of predicted and measured flowpath static pressures at takeoff power is depicted in Figure 4-3. Although very few pressure readings are available, test data indicates that the pressure drop across the film holes is close to that predicted. The low film-hole flow appears, therefore, to be due to undersized film flow area.

The total pressure drop available to the frame film holes is very low, making BFM (backflow margin) a concern. The regions of minimum BFM are the inner flowpath fairing upstream of the strut leading edge and strut leading edge cavity at the root. A comparison of predicted and measured pressures for engine Build 1 is shown in Figure 4-4. While the BFM across the inner flowpath fairing film holes is slightly less than predicted, the BFM across the strut leading edge cavity film holes is much higher than predicted.

Installation of power turbine blade dampers for engine Build 2 resulted in a lower level BFM. The inner flowpath fairing pressures for engine Build 2 are shown in Figure 4-5 for takeoff and maximum cruise, the minimum backflow condition. Takeoff pressures are taken from test data, and the maximum cruise pressures are predictions based on test results. The 0.79% BFM at maximum cruise condition is low, but it is in a very localized region. The BFM in all other regions is significantly higher.

Figure 4-6 illustrates mixer frame metal temperatures, both predicted and actual, for hot day takeoff power. All thermocouple data have been scaled up to hot day conditions by multiplying the raw data by the ratio of the hot day

ORIGINAL PAGE IS
OF POOR QUALITY

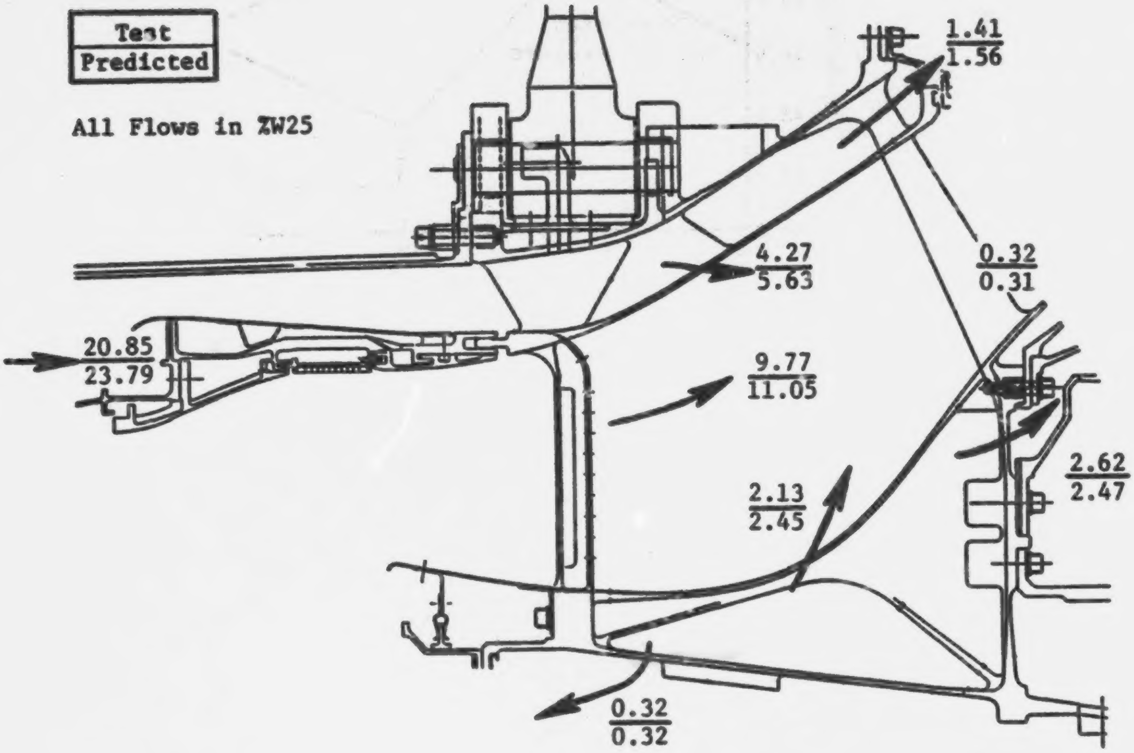
Test
Predicted
All Flows in %W25
1.41
1.56
4.27
5.63
0.32
0.31
20.85
23.79
9.77
11.05
2.62
2.47
2.13
2.45
0.32
0.32

Figure 4-1. Mixer Frame Flows at Takeoff Power, Test Versus Predicted.

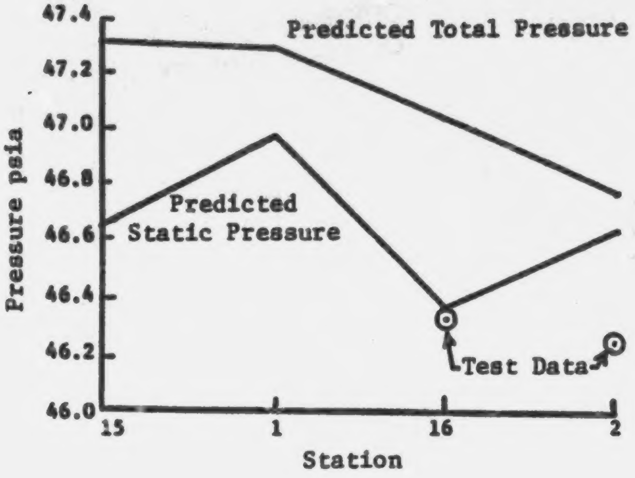

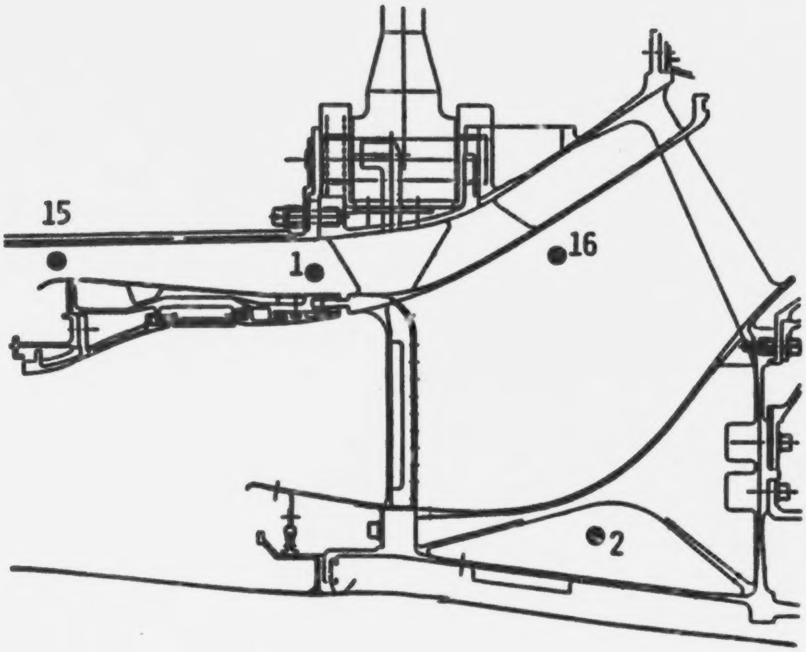

Figure 4-2. Mixer Frame Pressure Losses Comparison of Measured and Predicted Pressures.

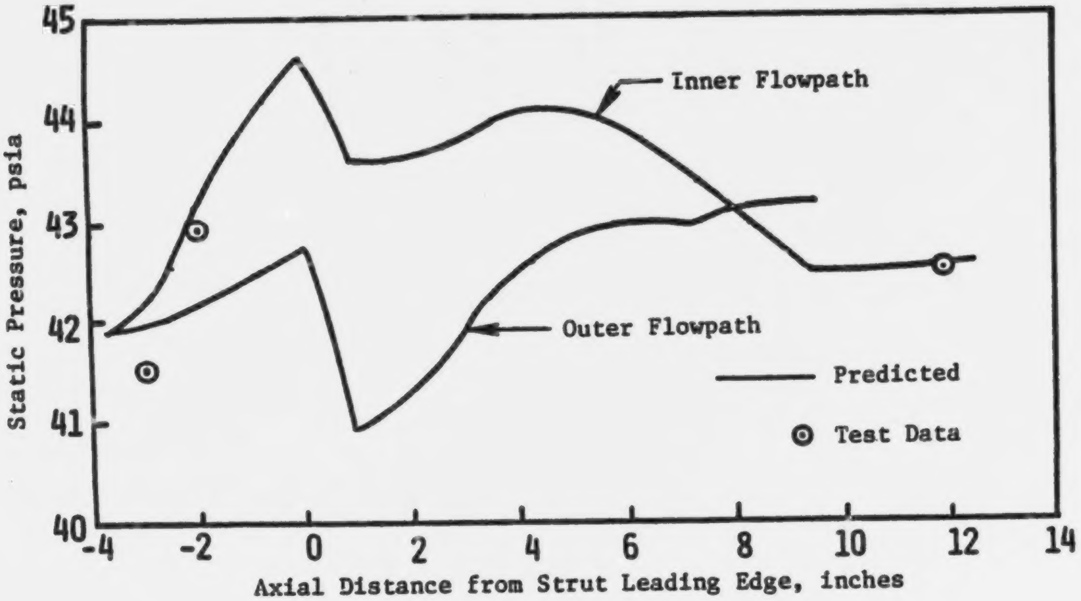

Figure 4-3. Mixer Frame Flowpath Static Pressure Distribution Takeoff Power.

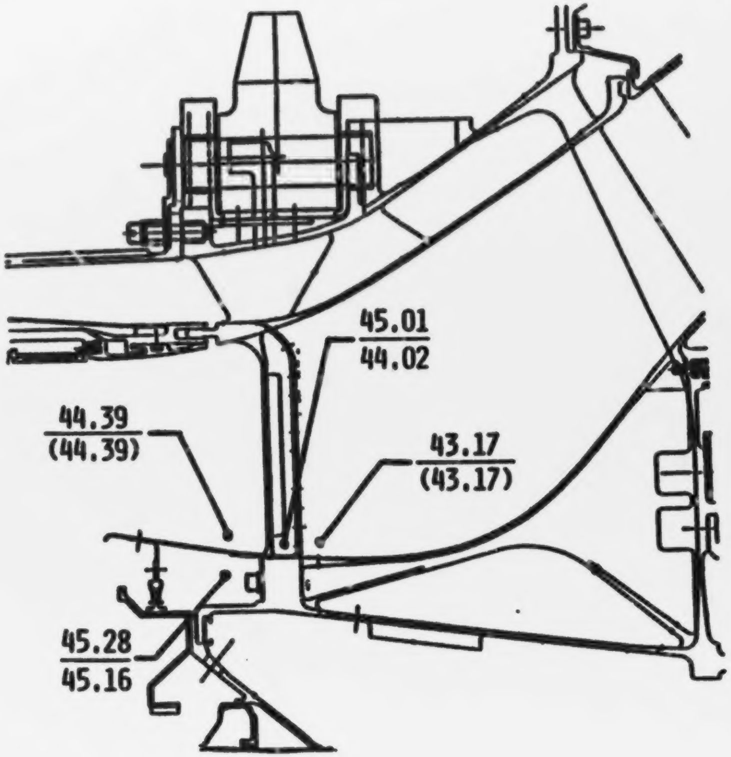
45.01
44.02
44.39
(44.39)
43.17
(43.17)
45.28
45.16

TEST DATA / PREDICTED : TEST DATA / (INPUT)

- INNER BAND BACKFLOW MARGIN IS 2.0% VS 1.7% PREDICTED.
- STRUT LEADING EDGE BACKFLOW MARGIN IS 4.3% VS 2.0% PREDICTED.
- BACKFLOW MARGIN IS HIGHER IN ALL OTHER REGIONS.
- MIXER FRAME ANALYTICAL FLOW MODEL HAS BEEN MODIFIED TO REFLECT TEST RESULTS.

Figure 4-4. Mixer Frame Backflow Margin - Build 01 Engine.

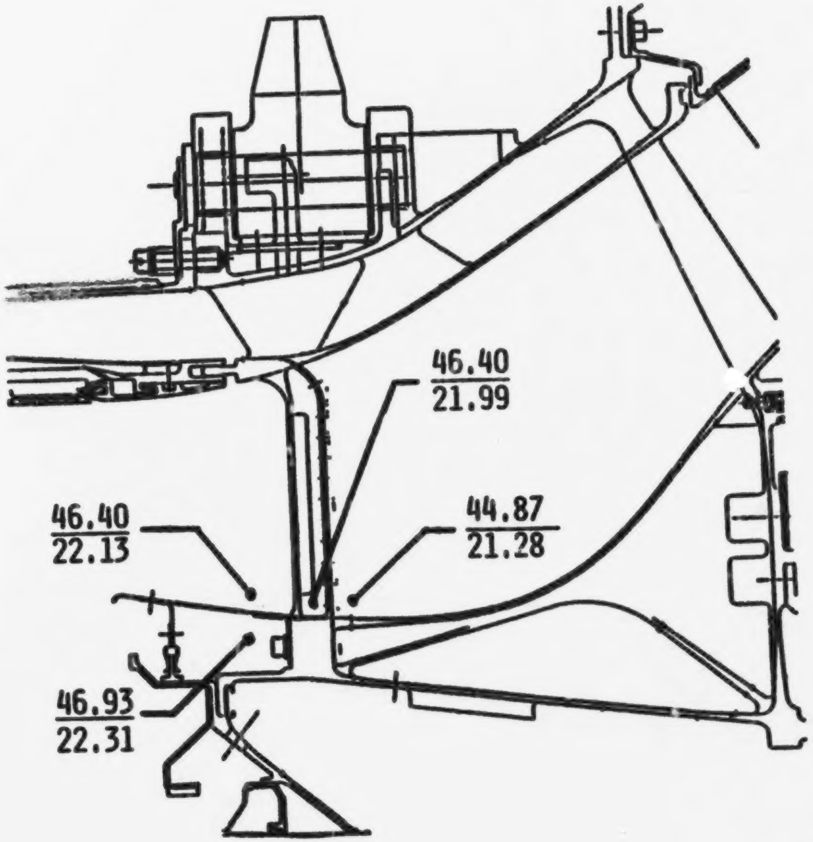
46.40
21.99
46.40
22.13
44.87
21.28
46.93
22.31

TAKEOFF
MAX CRUISE

- BFM = 1.1% AT TAKEOFF.
- BFM = .79% AT MAXIMUM CRUISE CONDITION.
- LOWER BUILD 02 BACKFLOW MARGIN IS RESULT OF LOWER POWER TURBINE FLOW FUNCTION.
  - INSTALLATION OF POWER TURBINE BLADE DAMPERS.

Figure 4-5. Mixer Frame Backflow Margin - Build 02 Engine.

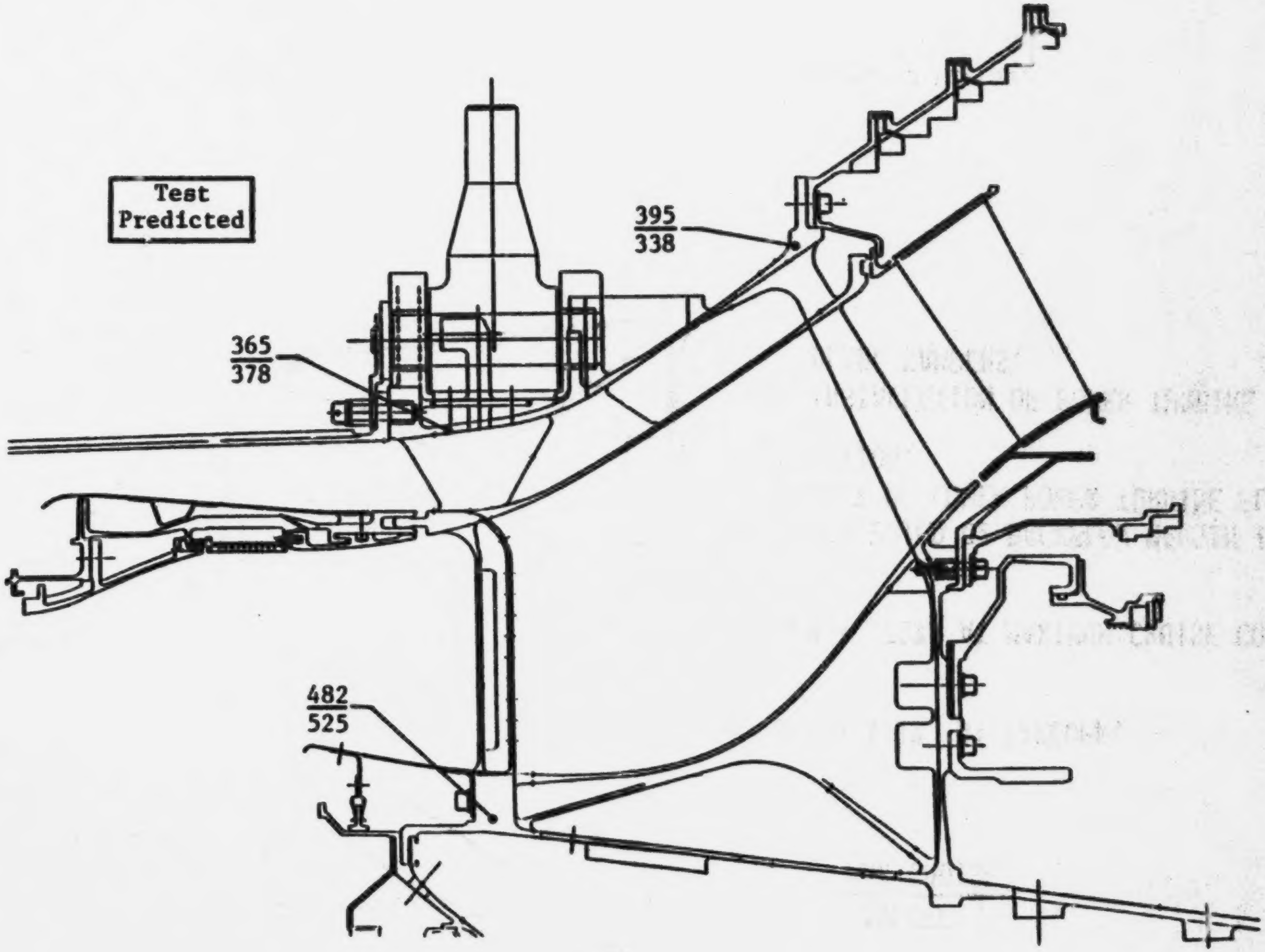
Test
Predicted
395/338
365/378
482/525

Figure 4-6. Mixer Frame Temperatures.

ambient temperature over the test day ambient temperature. No thermocouples are available along flowpath portions of the frame, but the existing thermocouple readings indicate that the frame is adequately cooled. Also, there are no visible signs of overtemperature.

4.2 POWER TURBINE SECONDARY FLOW SYSTEM

Figure 4-7 illustrates the power turbine secondary flow system. The flow rates, predicted and actual, are tabulated in Table 4-1. Although the total secondary flow for engine Build 1 neared prediction, the Stage 1 inner flowpath purge flow was significantly lower than predicted. This redistribution of flow is a result of a mixer frame supply hole flow coefficient that is lower than predicted and shafting hole flow coefficients that are greater than predicted. The increased pressure drop across the mixer frame supply holes, combined with reduced pressure drop through the shafting annular holes, serves to lower the supply pressure to the forward seal. Also, the sump vent flow was higher than predicted due to large carbon seal leakage areas. This additional vent flow results in a further decrease in Stage 1 purge flow.

During Build 1 testing, Stage 1 cavity temperature was 830° F at takeoff power, as compared to 795° F predicted. Although there was no evidence of gas ingestion, it was observed that the forward seal ΔP decreases with increase in power setting. Figure 4-8 plots ΔP versus P46Q2.

Extrapolation of the test data indicates that for Build 1 testing, backflow could occur at maximum power. To maintain positive flow in all cases, the mixer frame supply hole area was increased from 5.4 in^2 to 5.84 in^2. The resulting increase in forward seal ΔP from Build 1 testing to Build 2 testing is significant (Figure 4-8); however, the impact of this area increase on the remaining purge flows is negligible. The aft labyrinth seal flow increased significantly from Build 1 to Build 2 testing, presumably due to an increased seal clearance, indicated by a reduction in pressure drop across the seal.

During Build 3 engine testing, rubs occurred on two middle inner flowpath seals (G and H). There is an increase in the flows of these two seals, but because the system is metered for the most part by the supply hole and the shafting holes, the total secondary flow increases only slightly (Figure 4-7).

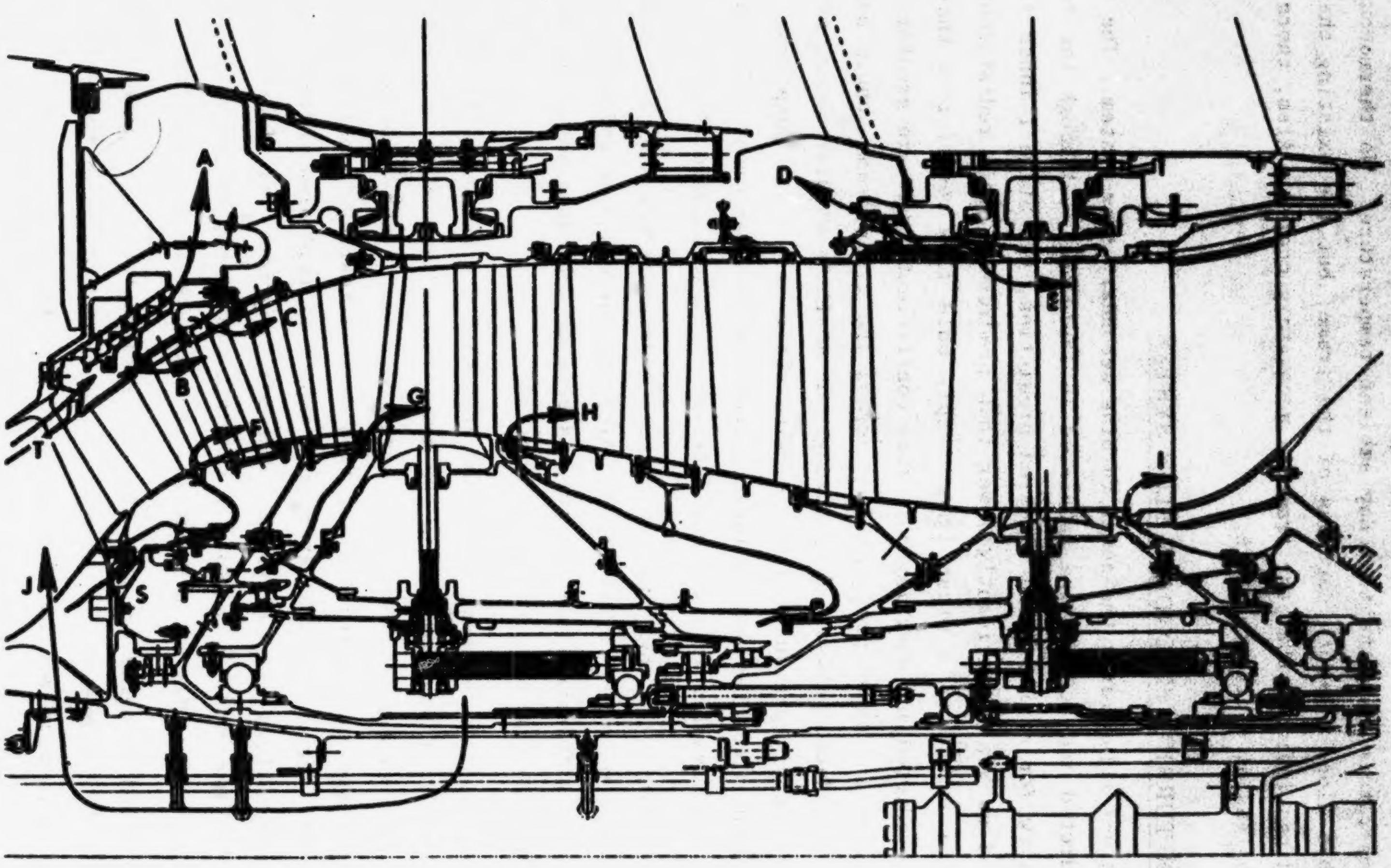
A
B
C
D
E
F
G
H
I
J
S
T

Figure 4-7. Power Turbine Secondary Flow Circuit.

ORIGINAL PAGE IS
OF POOR QUALITY

Table 4-1. Power Turbine Secondary Flow (%W25), Takeoff Power.

	Flowpath Seals											
	A	B	C	T	D	E	F	G	H	I	J	S
Predicted	0.573	0.868	0.122	1.563	0.296	0.682	0.382	0.444	0.340	0.373	0.025	2.543
Build 1	0.638	0.659	0.107	1.404	0.297	0.719	0.114	0.444	0.385	0.385	0.303	2.621
Build 2	0.568	0.702	0.100	1.370	0.293	0.687	0.231	0.411	0.375	0.516	0.185	2.697
Build 3	0.568	0.702	0.100	1.370	0.292	0.634	0.186	0.458	0.486	0.492	0.182	2.729

- PROBLEM: EXTRAPOLATION OF TEST DATA INDICATES THAT FORWARD SEAL COULD BACKFLOW AT MAX POWER.
- CAUSE: UNDERSIZED SUPPLY HOLE AND OVERSIZED ANNULUS HOLES REDUCE THE SEAL SUPPLY PRESSURE.
- SOLUTION: INCREASE SUPPLY HOLE AREA.

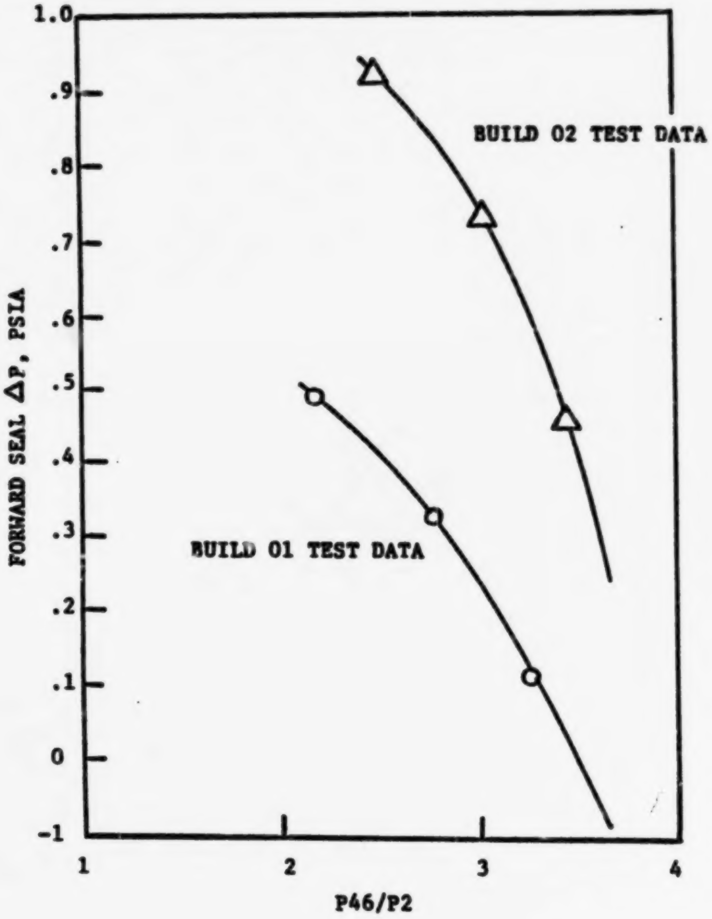

Figure 4-8. Potential Forward Seal Problem.

It should be noted that the very limited amount of instrumentation makes direct measurement of most of the individual flows impossible. The available pressure and temperature readings were used to rebalance the analytical flow network model which yields the best estimate of the flow distribution. The two flows leaving the mixer frame (S and T) are directly measured.

According to thermocouple data, all cavities are adequately purged. A comparison of predicted and actual temperatures is presented in Figure 4-9.

4.3 POWER TURBINE HEAT TRANSFER

The power turbine spool and frame temperatures, predicted and actual, are shown on Figures 4-10 and 4-11 for hot day takeoff power. The original predictions (Figure 4-10) were determined using a finite difference heat transfer program. The actual temperatures (Figure 4-11) have been scaled up to hot day conditions, as described in the mixer frame section. Because the fan bypass air temperature is lower than predicted, most of the cavity temperatures are also lower. The cavity temperatures have a direct impact on the inner spool temperatures. Unfortunately, there was too little instrumentation to be able to draw any firm conclusions about inner spool temperatures, as compared to predictions.

4.4 NACELLE VENTILATION

The nacelle ventilation system is depicted on Figure 4-12, with component temperatures at takeoff condition. All thermocouple data have been scaled up to hot day conditions, as described in the mixer frame section. Although some components are higher in temperature than predicted, all of the hardware is adequately cooled.

During initial engine Build 1 testing, ambient air was to be brought in to the nacelle cavity aft of the Stage 2 telemetry through radial holes in the cowling. However, poor ventilation in that region led to an overheating of the aft telemetry, probably due to a low level of static pressure at the inner flowpath. A total of 30 air scoops were then mounted to the holes. The additional ventilation air resulted in the temperatures presented in Figure 4-13.

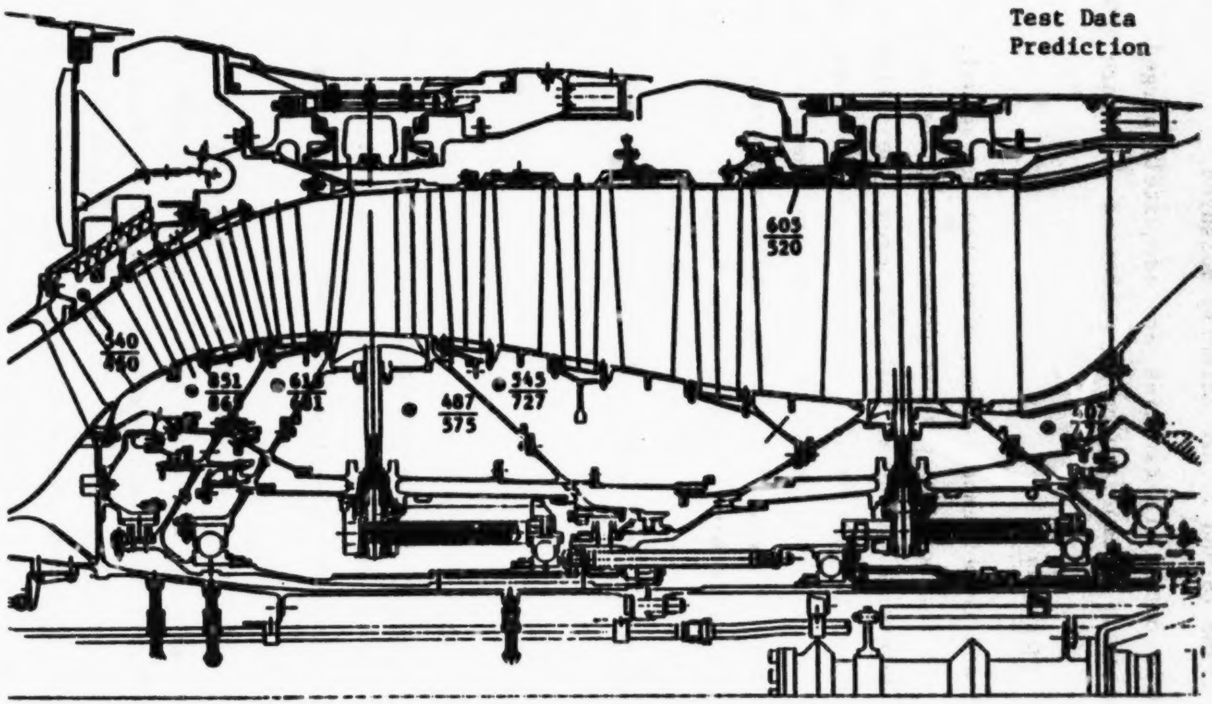

Test Data
Prediction
603
520
540
440
851
545
727
487
575
407

- Test Data Corrected to Hot Day Takeoff
- Inner Cavity Temperatures Are Below Prediction
- Outer Flowpath Seal Packing Air Temperature Is Above Predicted
- No Evidence of Gas Ingestion.

Figure 4-9. Rotor Cavity Temperatures at Takeoff Power.

ORIGINAL PAGE IS
OF POOR QUALITY

ORIGINAL PAGE IS
OF POOR QUALITY

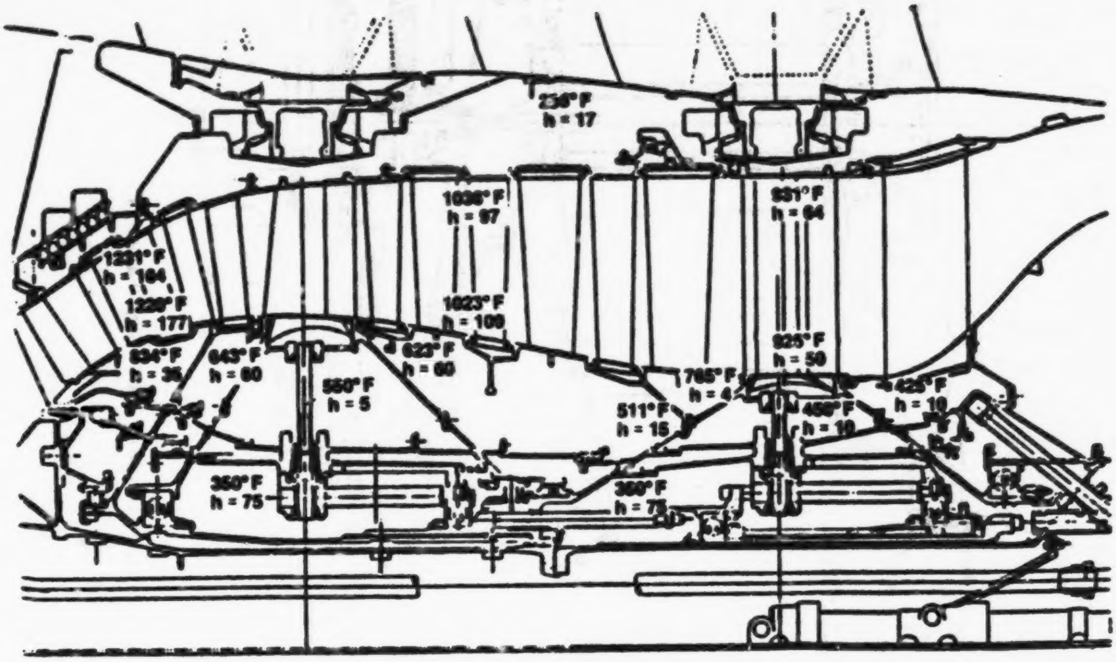
256° F
h = 17
1036° F
h = 97
931° F
h = 64
1231° F
h = 164
1228° F
h = 177
1023° F
h = 109
925° F
h = 50
834° F
h = 36
643° F
h = 60
623° F
h = 60
550° F
h = 5
765° F
h = 4
425° F
h = 10
511° F
h = 15
450° F
h = 10
350° F
h = 75
360° F
h = 75

Hot Day (+27° F) Rated Take-Off
Steady-State Conditions
h = [BTU/hr. ft.^{2} °F]

Figure 4-10. Power Turbine Temperatures Based on Analysis.

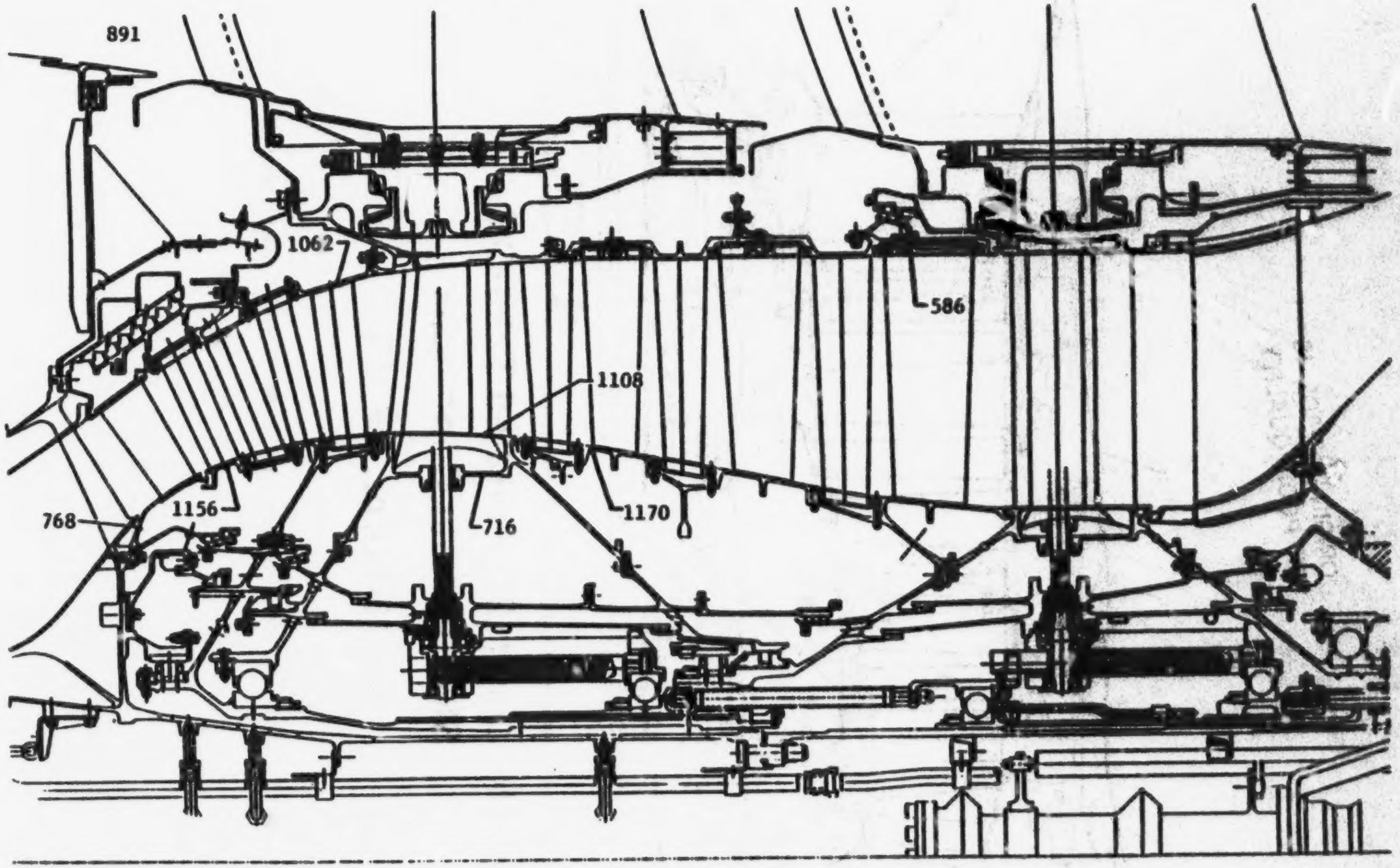
891
1062
586
1108
768
1156
716
1170

Figure 4-11. Spool Temperatures, Hot Day Takeoff.

ORIGINAL PAGE IS
OF POOR QUALITY

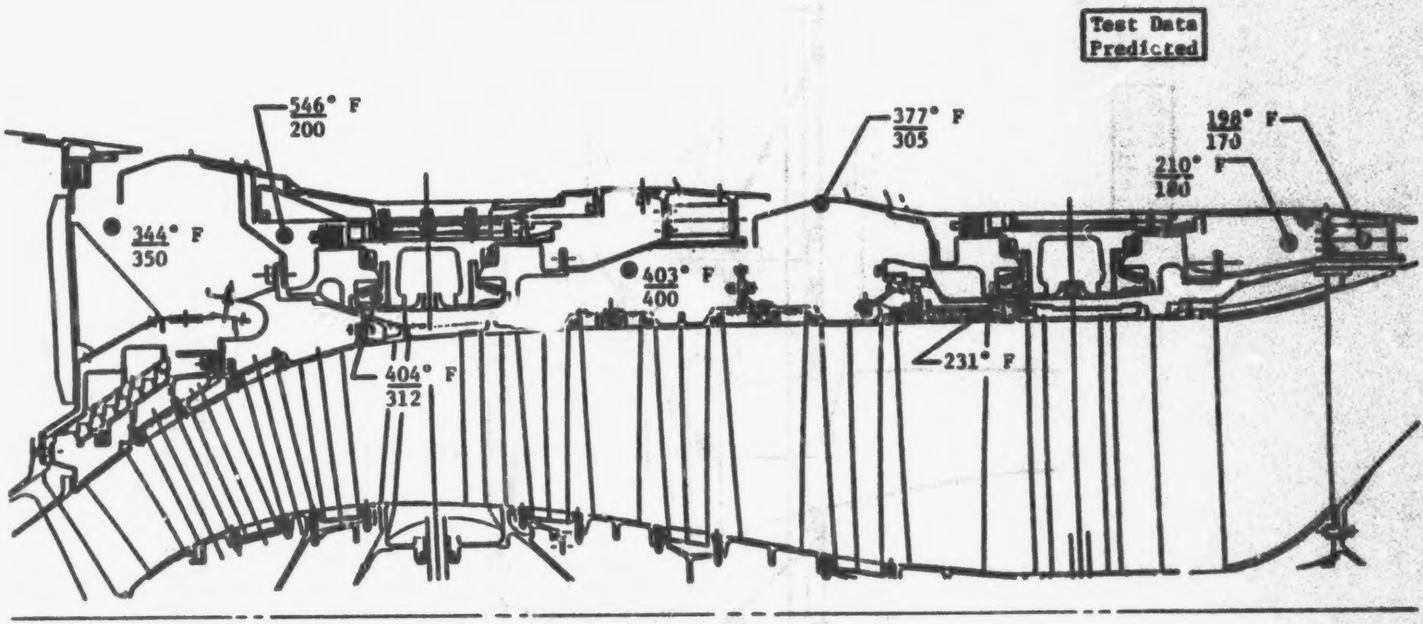
Test Data
Predicted
546° F
200
344° F
350
404° F
312
403° F
400
377° F
305
231° F
198° F
170
210° F
180

ORIGINAL PAGE IS
OF POOR QUALITY

Figure 4-12. Nacelle Temperatures Based on Test Data at Takeoff Power.

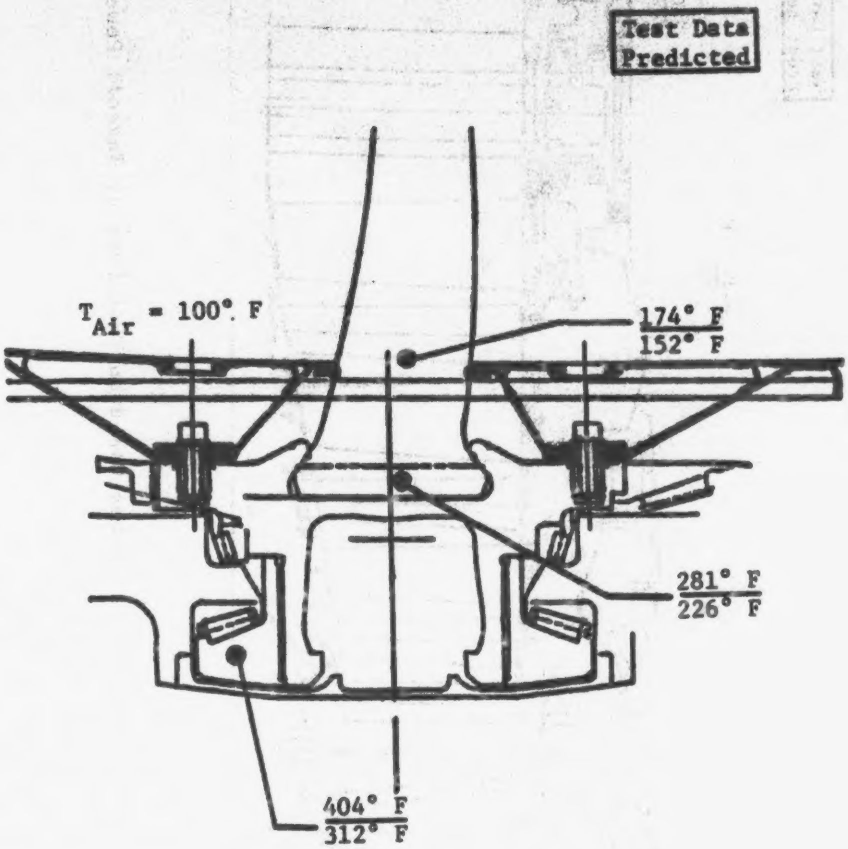
Test Data
Predicted
T_{Air} = 100° F
174° F
152° F
281° F
226° F
404° F
312° F

Figure 4-13. Forward Fan Blade Hub Temperatures; Hot Day Takeoff, Mach = 0.0, Full Thrust.

It was determined during initial Build 1 testing that, although the aft telemetry modules were adequately cooled, the solder which fixes the thermocouple leads to the aft telemetry circuit board, was overtemperatured. Even though the solder temperature is not measured directly, it was found that the solder melts when the nearby air thermocouple reaches a temperature of just over 300° F.

The solder, although adequately cooled during high power, is marginally cool at idle conditions. Set to match the prop flow at takeoff, the scoop direction is misaligned with the flow direction at idle. For +27 DTAMB conditions, the solder temperature is 219° F at takeoff, 235° F at flight idle, and 283° F at ground idle.

Figure 4-13 gives a breakdown of the forward fan blade hub temperatures for hot day takeoff. The 404° F trunnion temperature is taken from thermocouple data. All other temperatures are determined by rebalancing the heat transfer model on the basis of the trunnion temperature. All temperatures are higher than predicted, but are still within allowable limits.

4.5 CENTER CAVITY VENTILATION

The center cavity is portrayed (Figure 4-14) with temperatures at takeoff power; normal operating temperatures are as listed. The actuator axial position sensor (LVDT) temperature of 312° F is well below the normal operating temperature of 360° F (the maximum temperature limit is 400° F). The speed sensor temperature was not measured directly, but it is probably less than the LVDT temperature since it sees less radiation from the cavity wall than does the LVDT. In addition, the sump oil may provide a sink to the speed sensor. There is no indication of speed sensor or LVDT overtemperature problems.

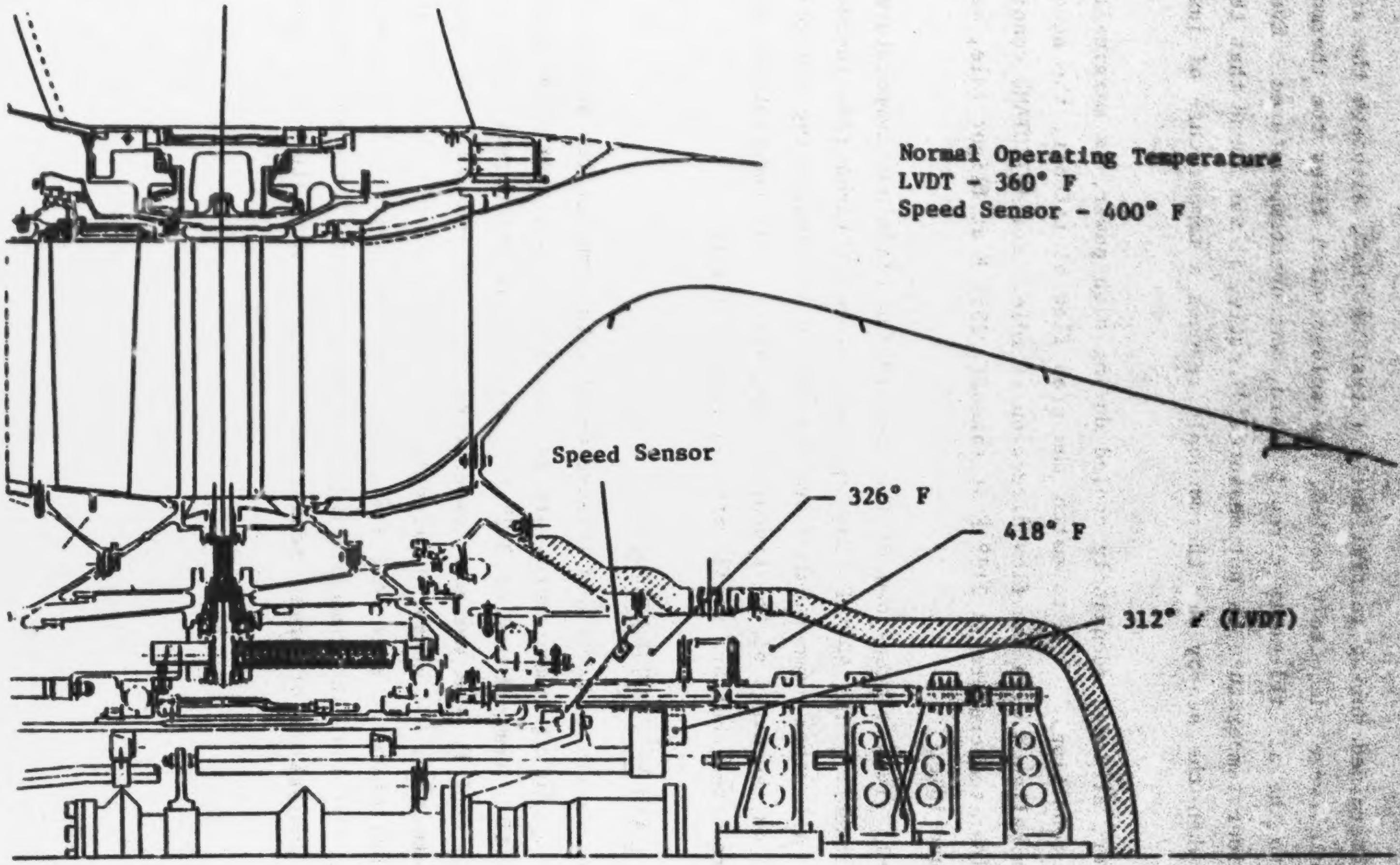
Normal Operating Temperature
LVDT - 360° F
Speed Sensor - 400° F
Speed Sensor
326° F
418° F
312° F (LVDT)

Figure 4-14. Center Cavity Ventilation at Takeoff Power.

ORIGINAL PAGE IS
OF POOR QUALITY

5.0 ENGINE SYSTEM DYNAMICS

Valuable engine dynamics experience was obtained during ground testing of the UDF™ Demonstrator Engine (GE36 S/N 082-001). This ground testing, along with a series of mechanical impedance tests conducted on the support system and Peebles test facility, was used to modify and verify the analytical model of the engine. Topics that are discussed in a later section regarding this subject include such gas generator vibration signatures as: synchronous 1/rev IPC and HPC responses, linear subidle UDF™ 1/rev signature and its depeadency on support structure/test facility stiffness, linear UDF™ 1/rev response recorded in the operational speed range, and nonlinear UDF™ 1/rev response observed during the Stage 2 propulsor airfoil separation event.

The UDF™, with its counterrotating propulsion system, also demonstrated that more sophisticated methods and hardware are required beyond turbofan engine experience with regards to propulsor trim balancing and vibration measuring techniques.

Gas Generator Vibration Signature

The gas generator used to power the GE36 Demonstrator is an F404 engine. Its rear frame is replaced by the mixer frame, and the gas generator is mated to the UDF™. Gas generator synchronous IPC (intermediate pressure compressor) and HPC (high pressure compressor) vibration levels were well within the prescribed F404 limits throughout ground testing. Both the maximum IPC and HPC 1/rev levels observed in the operational speed range during testing occurred at the F404 fan case vertical location. The maximum IPC 1/rev response was 0.24-inch/second (average velocity) at 11,700 rpm and was observed during Build 3 testing.

Figure 5-1 presents IPC signatures for Builds 1A, 2, and 3, demonstrating that the IPC 1/rev levels remained similar and low throughout ground testing. The maximum HPC 1/rev response was 0.28-inch/second at 13,700 rpm as observed on Build 2. Figure 5-2 compares HPC 1/rev vibration signatures for Builds 1A, 2, and 3 (F404 fan case vertical location). Like the IPC vibration signature, the HPC synchronous response remained similar and low throughout testing.

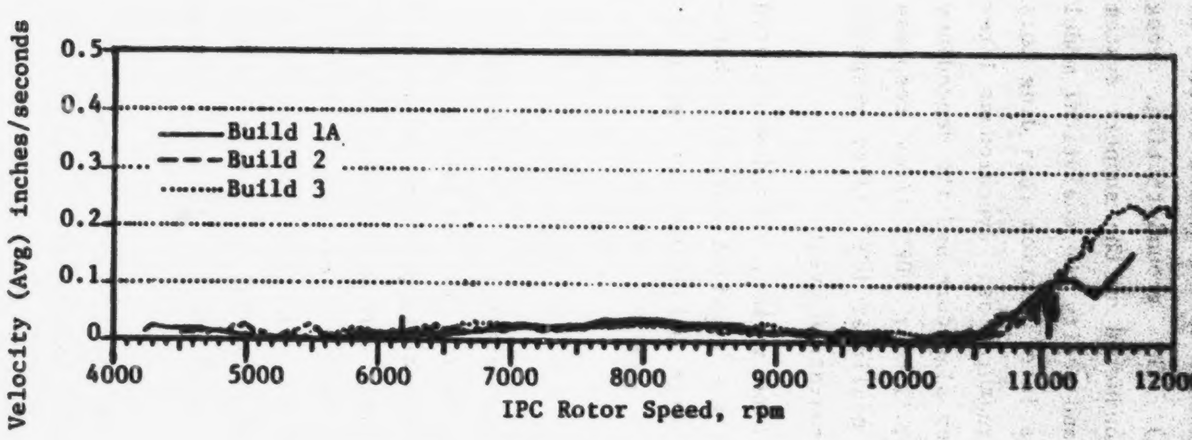

Figure 5-1. IPC One-Per-Rev Signature Comparison.

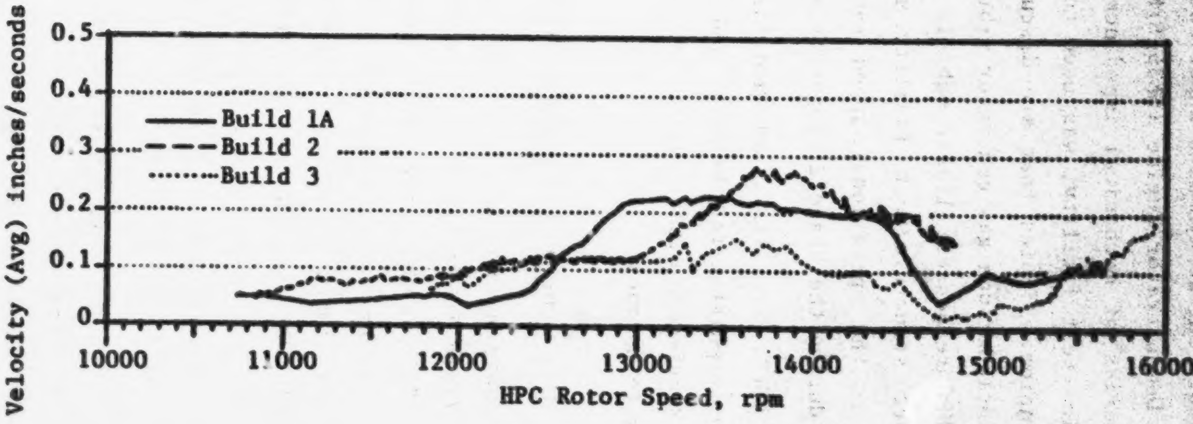

Figure 5-2. HPC One-Per-Rev Signature Comparison.

ORIGINAL PAGE IS
OF POOR QUALITY

The F404 predicted engine dynamics show little change between the turbofan engine and the GE36 gas generator application. These predictions were verified by comparing the vibration data from the check-out (at GE-Lynn) of the turbofan configuration with the results observed during the GE36 ground test. Demonstrating little change between both configurations, the results are shown in Figures 5-3 and 5-4; readings were taken at the F404 midframe horizontal location (only common accelerometer location between the two configurations) for the IPC and HPC 1/rev vibration signatures, respectively.

UDF™ Vibration Signature

The test facility and aircraft structure play a major role in the overall support structure stiffness of the engine and resulting rigid body mode definition of the entire system. Mechanical impedance tests were conducted during January 1986 (between Builds 1A and 2) to obtain the support structure stiffness. The pylon/isolators system was tested with the pylon attached to ground to obtain pylon and isolator stiffnesses and also mounted at Peebles Site 4A facility to obtain the entire support system stiffness. These results were incorporated in both updated linear and nonlinear (propulsor blade-out) analytical dynamic models and will be referenced in subsequent discussion of UDF™ vibration results.

The rigid-body modes occur primarily in the subidle speed range. Since the demo engine was tested at both Sites 4A and 3D, subidle resonances were subject to change due to the differences in facility stiffness properties. To demonstrate these differences, a comparison of Build 2 UDF™ 1/rev vibration signature obtained during engine starts at both sites are shown in Figures 5-5 and 5-6. Figure 5-5 compares the subidle vibration signatures at the F404 fan case vertical location (vertical direction for Peebles test is in line with the strut). The signatures indicate that the overall support system stiffness was softer at Site 3D in this direction. Figure 5-6 compares the two subidle signatures at the same location in the horizontal (normal-to-strut) direction. Overall system stiffness effects at Site 3D acted to decouple the predominant rigid-body modes observed at Site 4A.

The UDF™ 1/rev operational speed range vibration signature at the No. 2 ball bearing housing location is illustrated in Figure 5-7 for the vertical

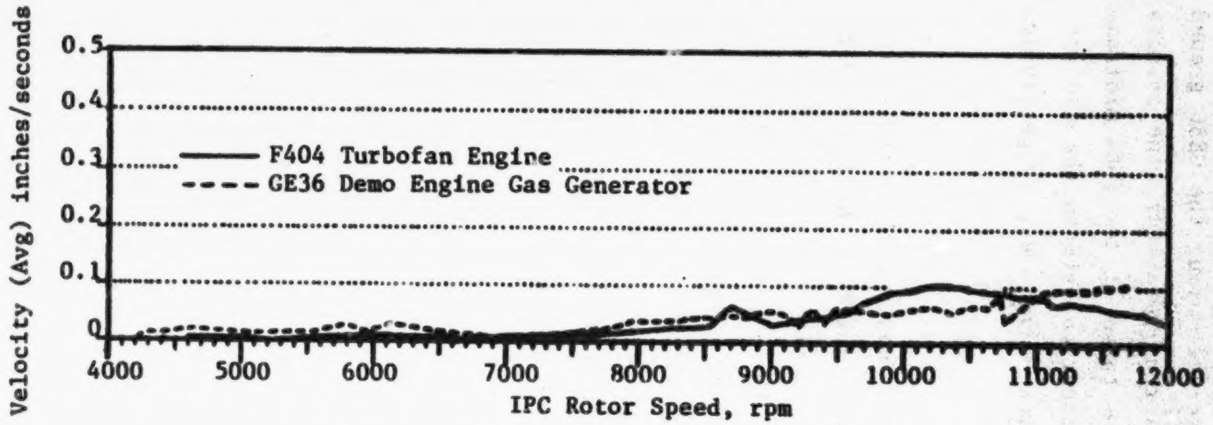

Figure 5-3. IPC One-Per-Rev Signature Comparison.

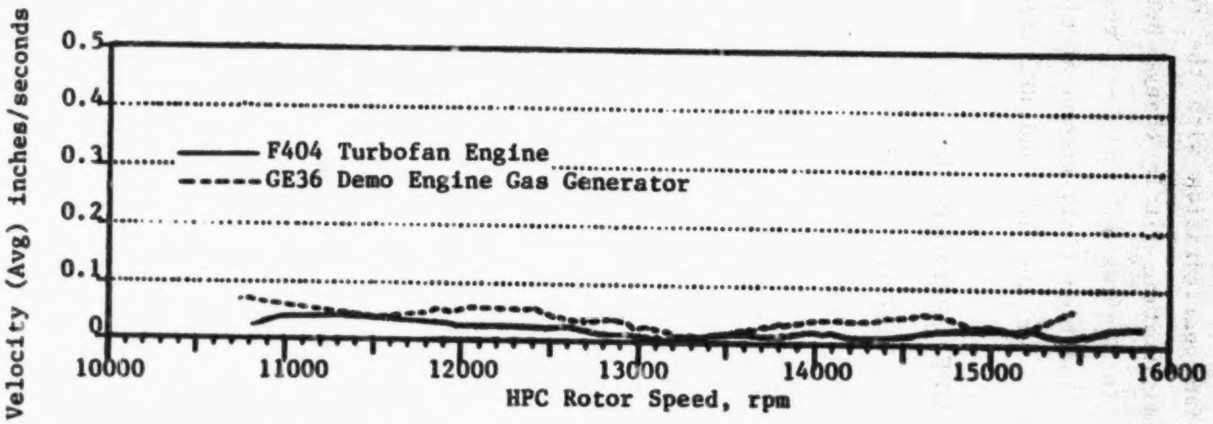

Figure 5-4. HPC One-Per-Rev Signature Comparison.

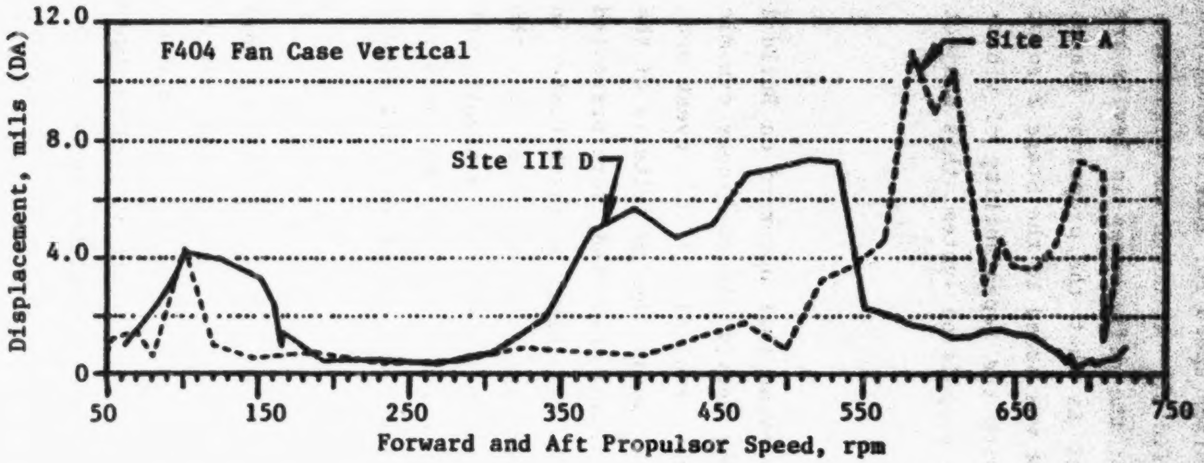

Figure 5-5. Subidle UDF^{TM} One-Per-Rev Vibration Signature Comparison.

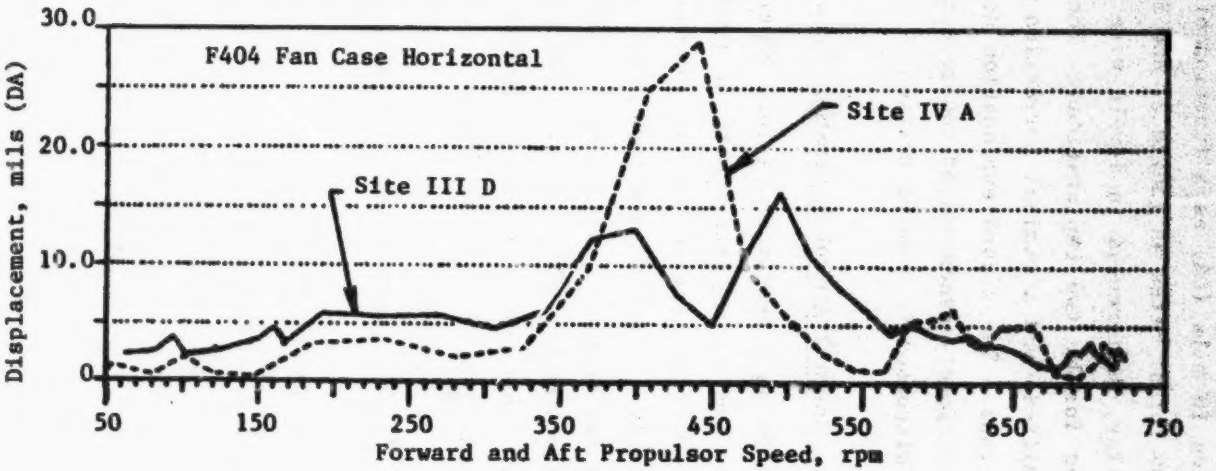

Figure 5-6. Subidle UDF^{TM} One-Per-Rev Vibration Signature Comparison.

direction and in Figure 5-8 for the horizontal direction; each indicates the deflection in mils (DA) as a function of propulsor speed for accels conducted to 24,000 lbf at Sites 4A (Build 2) and 3D (Build 3). Although the signatures are similar, differences in levels were noted; the differences in levels are accounted for by two explanations. The first is that the propulsor blades were modified, and a nominal correction weight was added to the Stage 2 rotor between runs. The second explanation deals with the repeatability of vibration on a closely synchronized counterrotating propulsion system; this subject will be discussed in a later section.

Stage 2 Airfoil Separation Event

The Stage 2 propulsor airfoil separation event that occurred on Build 2 (Site 4A) led to an opportunity to modify and verify the nonlinear dynamic model predictions (by mechanical impedance test results) for this event and, subsequently, to apply this knowledge to the blade-out design criteria of the aircraft application. The dynamics, both actual and predicted, were presented during the May 13, 1986 Quarterly Review at the Nasa-Lewis Research Center in Cleveland, Ohio. A major benefit resulting from this event was proof that the pylon isolators function as designed. This was demonstrated by a significant reduction of motion through the isolators, and the fact that the isolators soften with the increased loading and, thus, lower the system resonant speed.

Trim Balance Experience

The initial efforts to trim balance the propulsors during Build 2 were hampered by the hardware used. The basic trim balance test sequence was to separate propulsor speeds by 100 rpm (1.67 Hz) and take amplitude and phase readings from the existing SD119C Trim Balance Analyzer unit at predetermined steady-state speed conditions. Making the initial trim balance unsuccessful, the built-in 3 Hz (%1.5 Hz) bandwidth tracking filter of the SD119C unit did not adequately separate the vibration response of the two rotors and, thus, did not give correct amplitude and phase information.

A modified SD119C unit was purchased with a 1.0 Hz (%0.5 Hz) bandwidth tracking filter and was evaluated during Build 3 testing. Improvements were achieved in the balance of each rotor utilizing this new unit and applying

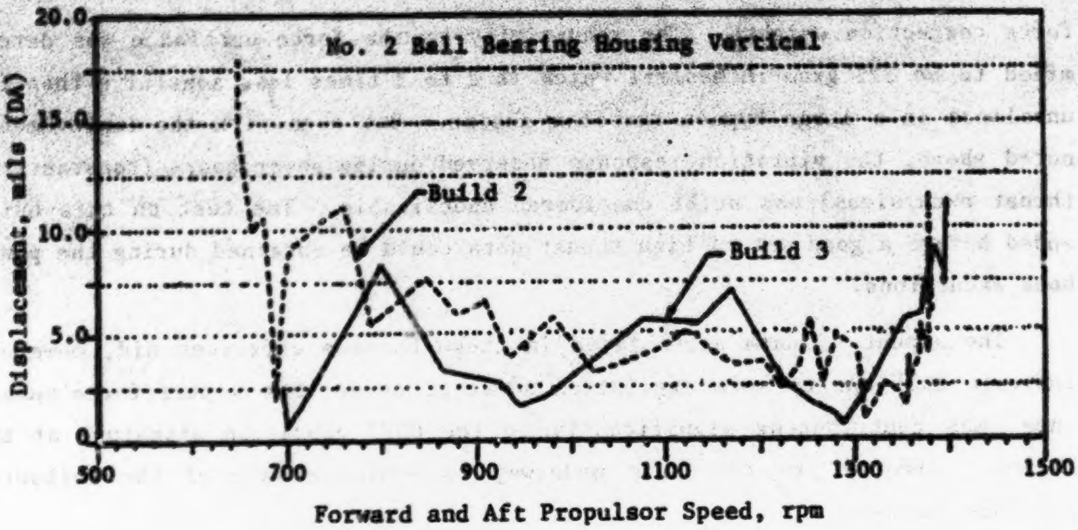

Figure 5-7. UDF™ One-Per-Rev Vibration Signature on 2 Minute Accel to 24,000 lb Thrust, Housing Vertical.

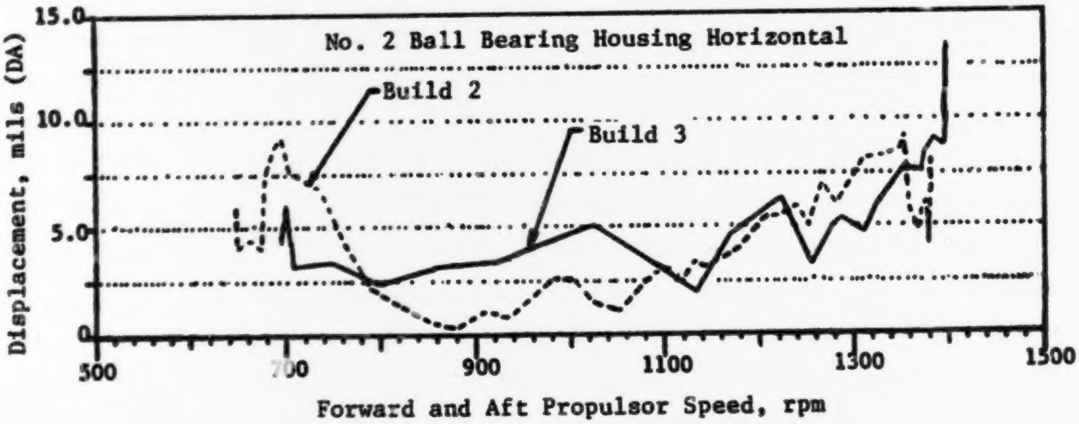

Figure 5-8. UDF™ One-Per-Rev Vibration Signature on 2 Minute Accel to 24,000 lb Thrust, Housing Horizontal.

force correction weights. The sensitivity to the force unbalance was determined to be 325 gram-inches/mil which is 2 to 3 times less sensitive than fan unbalance in a large bypass turbofan engine. But even with the improvements noted above, the vibration response observed during power hooks (constant rpm thrust excursions) was still considered undesirable. The test on this build ended before a good set of high thrust data could be obtained during the power hook excursions.

The amount of data accumulated in these balance exercises did, however, indicate that one or more excitation sources, other than a pure force unbalance, was contributing significantly to the UDF™ vibration signature of the engine. Efforts are currently underway to evaluate each of the following possible sources:

- Changes in either force or mechanical moment unbalance due to the blade actuation system (from low- to high-power condition)
- Aerodynamic moment unbalance being introduced by any propulsor-blade tracking problem.

Measuring Techniques

For a simple one degree of freedom system, the maximum sensed deflection would lag the forcing function (rotor unbalance) by 90° at its first natural frequency. The deflection level is a function of the unbalance force magnitude, the damping, and the mode shape at this given frequency. For a single rotor application, such as a high bypass turbofan engine, the maximum static deflection at any circumferential location, even though not necessarily equal, would occur in one revolution of the rotor and would be repeatable from one revolution to another, provided the unbalance or rpm were unchanged. Using this simple one degree of freedom system and assuming that the mode shapes in the vertical and horizontal directions are identical, Figure 5-9 demonstrates this point.

The UDF™ engine, on the other hand, may not sense the maximum deflection at a given circumferential location during a revolution of its counterrotating propulsor rotors. For example, assume that both the forward and aft rotors are exactly synchronized, that the forcing functions are equal at each rotor, and the mode shapes are identical in both the vertical and horizontal planes.

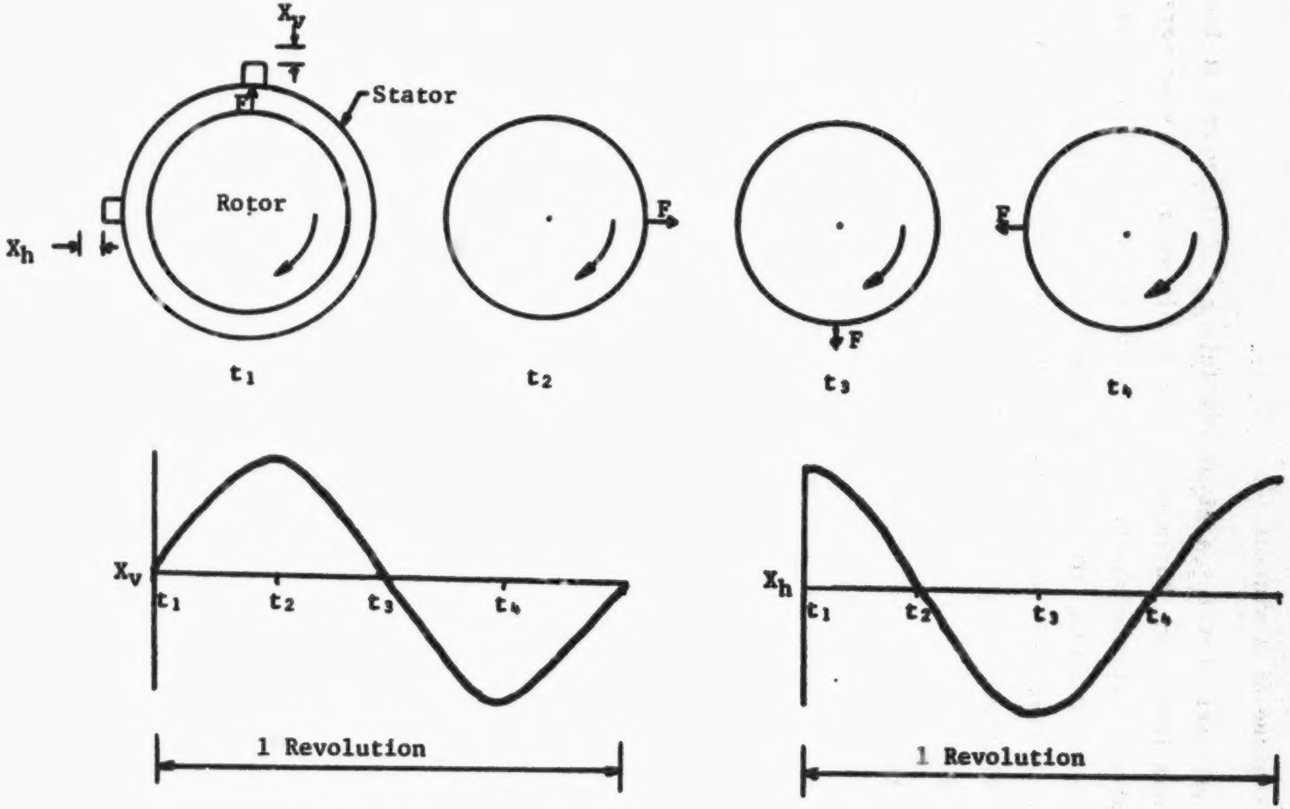
X_v
Stator
F
Rotor
X_h
t_1
F
t_2
F
t_3
F
t_4
X_v
t_1
t_2
t_3
t_4
1 Revolution
X_h
t_1
t_2
t_3
t_4
1 Revolution

Figure 5-9. Maximum Static Deflection.

Now, using the single rotor example above, we have two cases (Figures 5-10 and 5-11) which show either the vertical or the horizontal deflection at a maximum level, and the other plane at a minimum.

This example indicates that for a given revolution, if the vertical location is at the maximum level, the horizontal response is zero, and vice versa. This example also shows that the maximum deflections in each plane are equal, and that the minimum deflections are not only equal but are, in fact, zero. Expanding this example into real-world application, we find that the maximum response in a given plane will always result in the minimum response occurring in its orthogonal plane.

First, let the force unbalance of each rotor be different. In this case, maximum deflection for both the vertical and horizontal planes will still be equal, as will the minimum levels, but these minimum values will no longer be zero. Second, let the mode shape definition and force unbalance be different. At this point, neither maximum nor minimum deflections between the two planes would be expected to be equal. The final step in approaching the real world is to leave the one degree of freedom system and enter the actual multidegree freedom system situation. This step does nothing more than to vary the phase-angle lag between the lined up forces, and the resultant maximum deflection circumferential location, as a function of the engine dynamics.

Test data is provided in Figure 5-12 demonstrating the above discussion and illustrating the UDF™ 1/rev response at ground idle power for the approximately orthogonally mounted accelerometers at the No. 2 ball bearing housing location. Also shown is the phase-angle lag between the forward and aft propulsor 1/rev indicators. The phase data indicates that the rotors are close but not totally synchronized. The vibration data shows the 1/rev levels are modulating at the same frequency as the propulsor rotors difference frequency. These data demonstrate, as earlier stated in the discussion, that the maximum response in one plane occurs at the minimum response of the other plane, and vice versa. The two rotors unbalance line up at a phase-angle lag of 240° to yield the maximum vertical response and at a phase-angle lag of 60° to yield the maximum horizontal response.

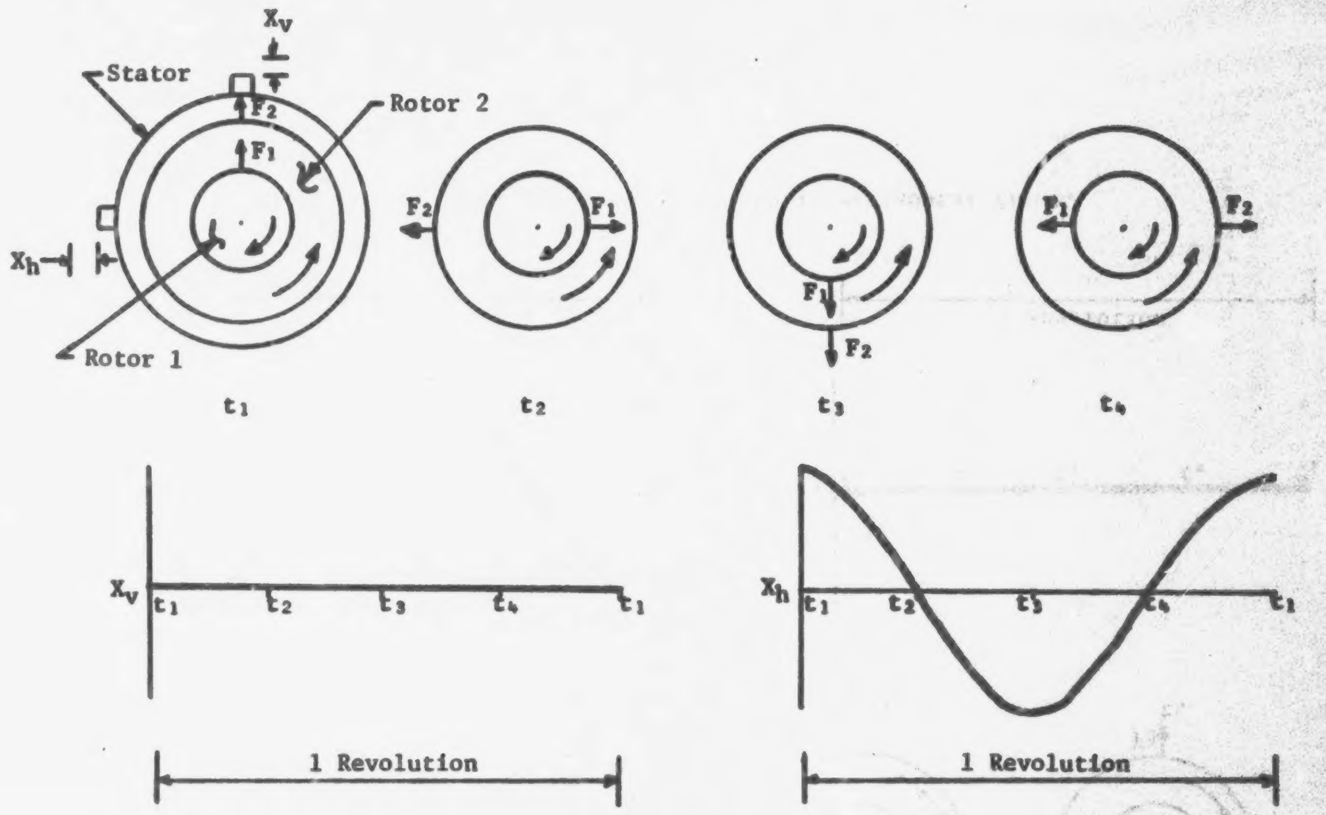
X_v
Stator
Rotor 2
F_2
F_1
X_h
Rotor 1
t_1
F_2
F_1
t_2
F_1
F_2
t_3
F_1
F_2
t_4
X_v
t_1
t_2
t_3
t_4
t_1
X_h
t_1
t_2
t_3
t_4
t_1
1 Revolution
1 Revolution

Figure 5-10. Unbalance Forces Lineup in Vertical Plane.

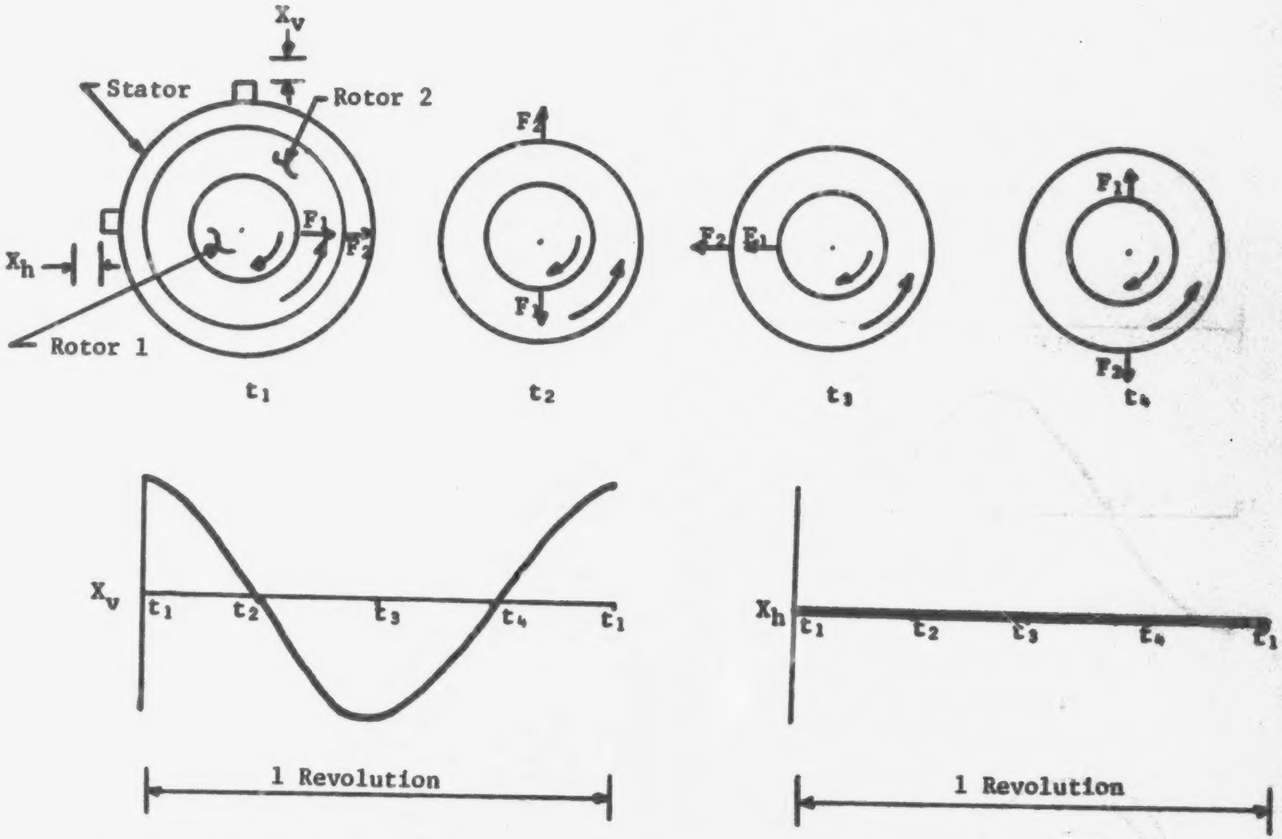
Stator
Rotor 2
Rotor 1
X_v
X_h
F_1
F_2
t_1
t_2
t_3
t_4
1 Revolution
1 Revolution

Figure 5-11. Unbalance Forces Lineup in Horizontal Plane.

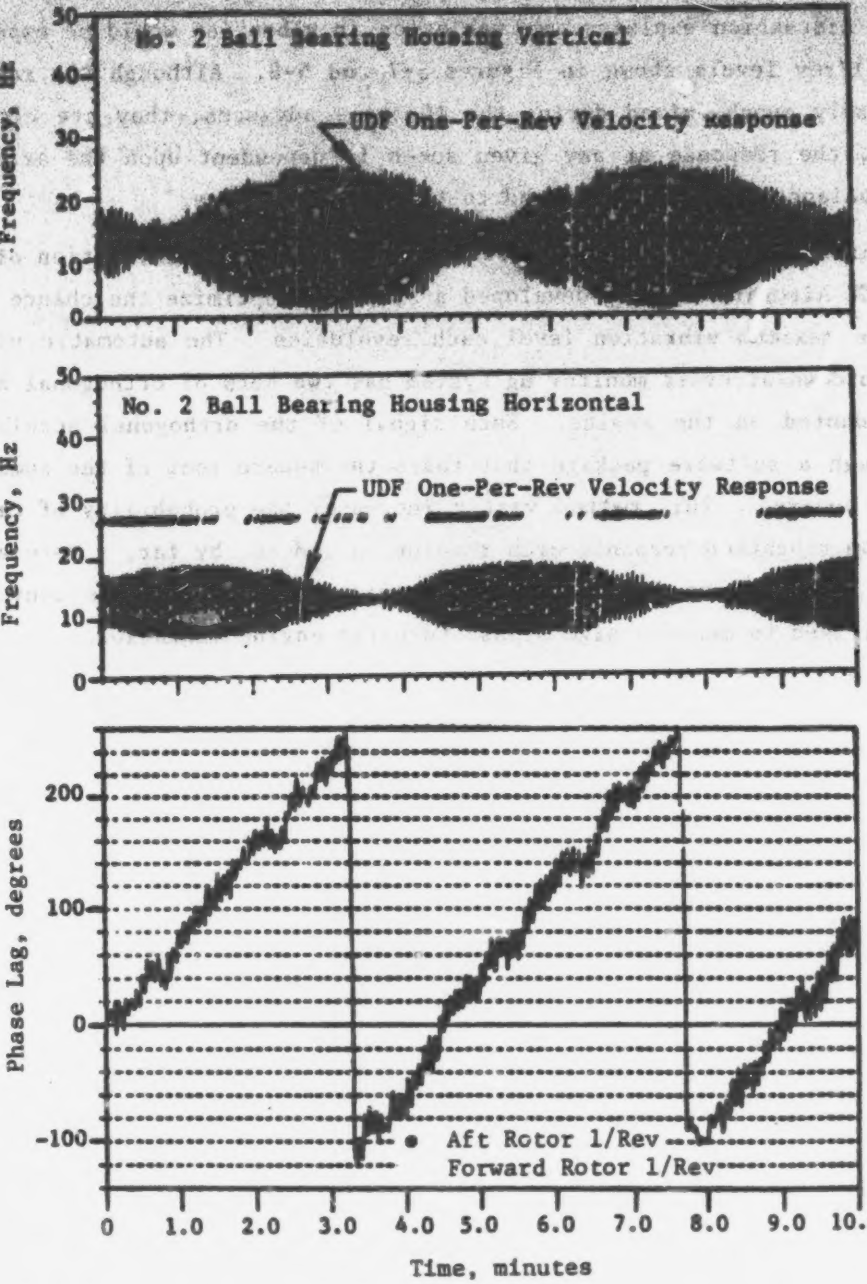

Figure 5-12. GE36 Demonstrator Engine 082-001/3 T/D 7-1-86 Time History Plots at Ground Idle Power.

This discussion explains why variation in vibration would be expected in the UDF™ 1/rev levels shown in Figures 5-7 and 5-8. Although the rotors are not precisely synchronized during the throttle advances, they are close, and therefore, the response at any given speed is dependent upon the orientation of the unbalances to each other and to the sensing device.

Realizing that this characteristic existed prior to initiation of ground testing, GE Aircraft Engines developed a system to optimize the chance of capturing the maximum vibration level each revolution. The automatic vibration engine shutdown/aircraft monitoring system has two sets of orthogonal accelerometers mounted on the engine. Each signal of the orthogonal accelerometer goes through a software package that takes the square root of the sums of the responses squared. This method vastly increases the probability of capturing the maximum vibration response each revolution and is, by far, a more accurate measuring tool for synchronized counterrotating rotors than the conventional method utilized to measure high bypass turbofan engine vibration.

6.0 BEARINGS AND SEALS

This section covers the main propulsor bearings and all actuation system support bearings. All of the bearings performed well during ground testing, from a design standpoint. Some problems arose as a result of debris produced during manufacture of other engine parts; however, engine operability was not compromised. Seals in the fan blade retention system performed well during testing except for a few torn fan blade thrust bearing seals resulting from insufficient lubrication.

6.1 HARDWARE CONDITION

6.1.1 Rotor Support Main Bearings

Debris Ingestion

The main bearings operated well, which was to be expected, as they had ample capacity.

The two roller bearings were replaced twice during ground testing when they were exposed at disassembly. They were replaced because debris damage had scored some of the rollers. The debris was comprised almost exclusively of 0.007-inch-diameter steel shot particles, with some other manufacturing and wear debris present in very small quantities. Prior to engine teardown, oil sample analysis had identified the possibility of a debris problem.

A blind cavity in the forward intershaft carbon seal land, designed to prevent possible thermal coning, had trapped a quantity of steel shot during the peening process. The shot did not wash out during manufacture but was sluiced out by the hot lube oil during engine running.

Causing extensive scoring of the rollers, the shot became imbedded in the soft silver plate of the rolling element retainer of the bearing. This would cause both a breakdown of the hydrodynamic lube film because of the high loads and low rotational speeds and a diminished fatigue life. However, no surface distress due to rubbing was observed.

Bearings were returned to the manufacturer for refurbishment, although only inner rings and cages were usable. The rings were rehoned and the cages stripped and replated. The design of the roller retention features permitted roller removal without damage to the cage.

To prevent further debris damage, the blind cavity was ultrasonically cleaned and sealed closed with a nichrome strip (Figure 6-1). This was fairly successful, although one or two pieces of shot were still found in subsequent oil samples.

Retention Nut Loosening

The outer ring retention nut of the 1R intershaft bearing came loose and completely disengaged during the final stage of ground testing; this permitted axial movement of the outer ring.

The nut is believed to have jammed the actuation system preventing blade-angle adjustment. On teardown, forward and aft rotors could not be separated in the normal disassembly sequence. This was caused by the rollers no longer being in contact with the outer raceway. Borescope inspection prior to disassembly had shown the rollers still engaged, so running in this disengaged condition had not occurred. When the rotors were separated, the bearing was found to be in remarkably good condition, except for the damage to the roller corners caused when the rollers dropped into the region of the outer shaft, from which the ring had moved, and hung up on the shaft shoulder (Figures 6-2 and 6-3).

Examination of the spanner nut indicated no obvious thread damage, and the Vespel insert retention feature appeared undamaged. The appearance of the raceway did not indicate any running off the normal roller path; however, some coning was indicated. The shaft coning was in the direction to move the shaft radially away from the nut, and the wedge effect would exert an axial force on the nut in the direction to promote untorquing. There was no damage from ring spinning on either the outer ring OD or the shaft bore.

For subsequent engine testing, a hole was line-drilled axially in the thread, and a roll-pin was mechanically locked in the thread to prevent the nut becoming untorqued (Figure 6-4).

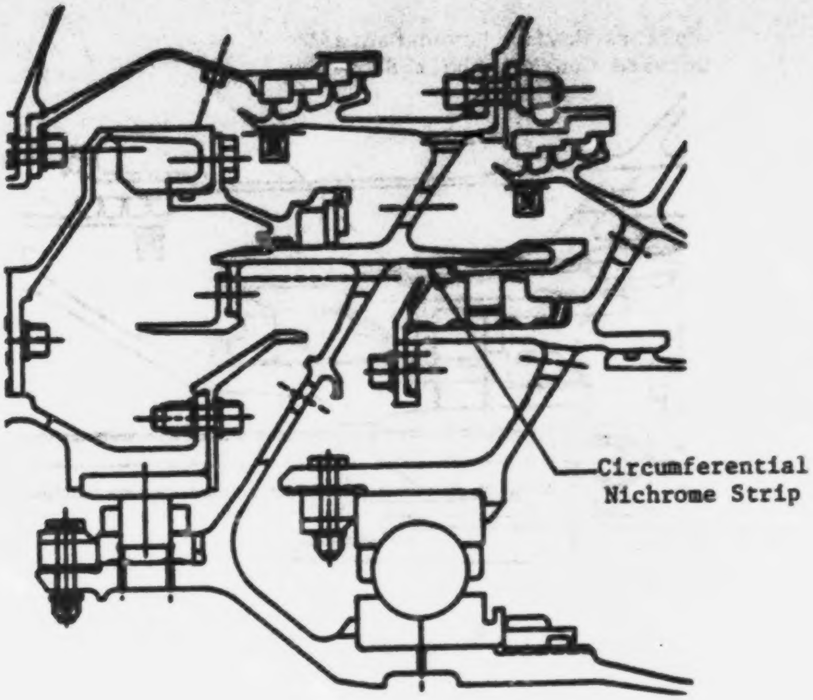
Circumferential
Nichrome Strip

Figure 6-1. Seal Cavity Closure.

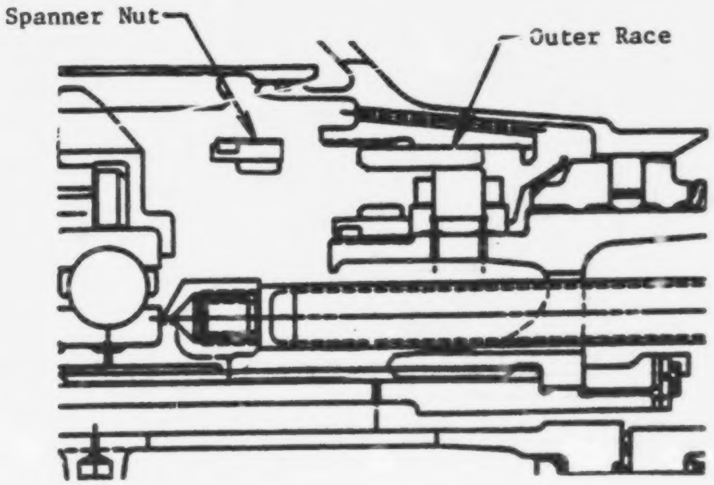
Spanner Nut
Outer Race

Figure 6-2. Possible Running Condition with 1R Spanner Nut Loose.

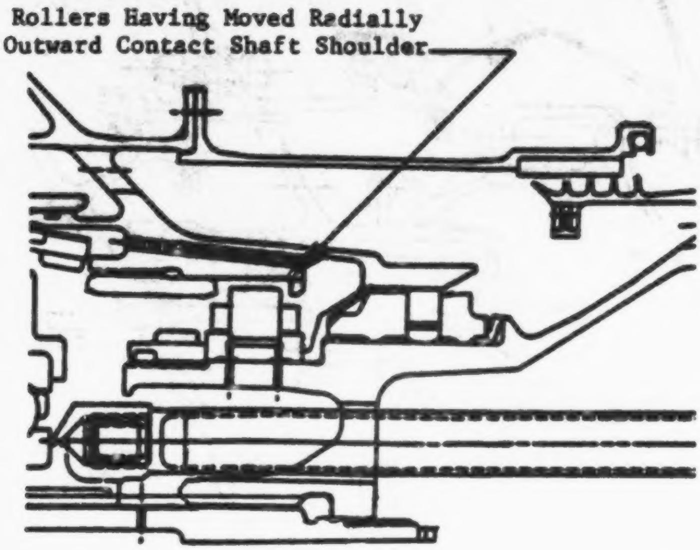
Rollers Having Moved Radially
Outward Contact Shaft Shoulder

Figure 6-3. Disassembly Problem and Roller Corner Damage.

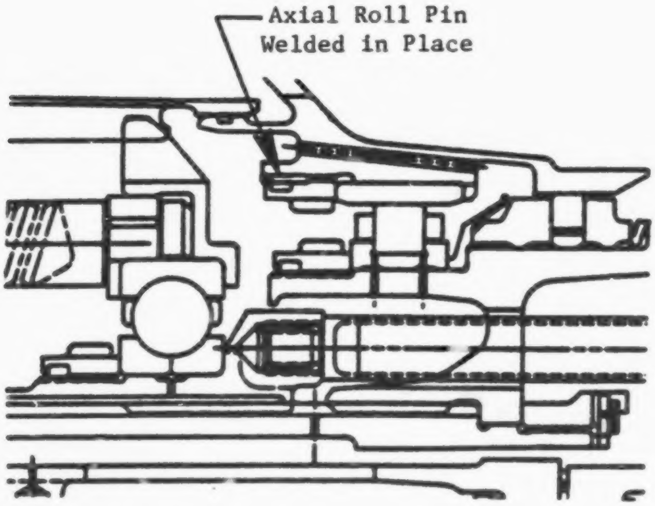
Axial Roll Pin
Welded in Place

Figure 6-4. Problem Solution - Positive Nut Locking.

6.1.2 Inner Actuation Bearings

Actuation Ball Bearings

No problems were encountered with the large mainshaft actuation ball bearings. These bearings were examined at the last teardown for any evidence of irregular wear or cage impact that might occur due to the calculated axial distortion of the outer ring from the four gear rack loads, but no indication of abnormalities was seen.

Radial Quill Shaft Gearbox Bearings

The inner bearings supporting the radial shafts could not be seen without teardown of the gearboxes; however, since no problem existed and they operated flawlessly, no teardown was performed.

The outer gearboxes were examined because of the loosening of the outer housing nut. The nut butts against and clamps the outer ball bearing, which locates the pinion gear. The cause of the loosening was found to be a stackup problem incurred by a change in a washer thickness (Figure 6-5), and the problem was corrected. Although the bearings are grease lubricated, most of the grease had been expelled, and some bearings showed wear.

6.1.3 Actuation Tapered Roller Bearings

The tapered roller bearings supporting the counterbalance torque tubes and bevel gears were examined and showed no deleterious effect except for some slight corrosion. This problem was manifest because the grease lubricating these bearings is centrifuged outwards, and the bearings are not adequately protected from the high humidity experienced during testing, some of which occurred during moderate rain.

6.1.4 Fan Retention Bearings and Seals

Setup Bearing

The setup bearing is incorporated to react the blade overturning moment and carry most of that load. However, at speed, the centrifugal load is sufficiently high that a very large moment would be required to unseat the main

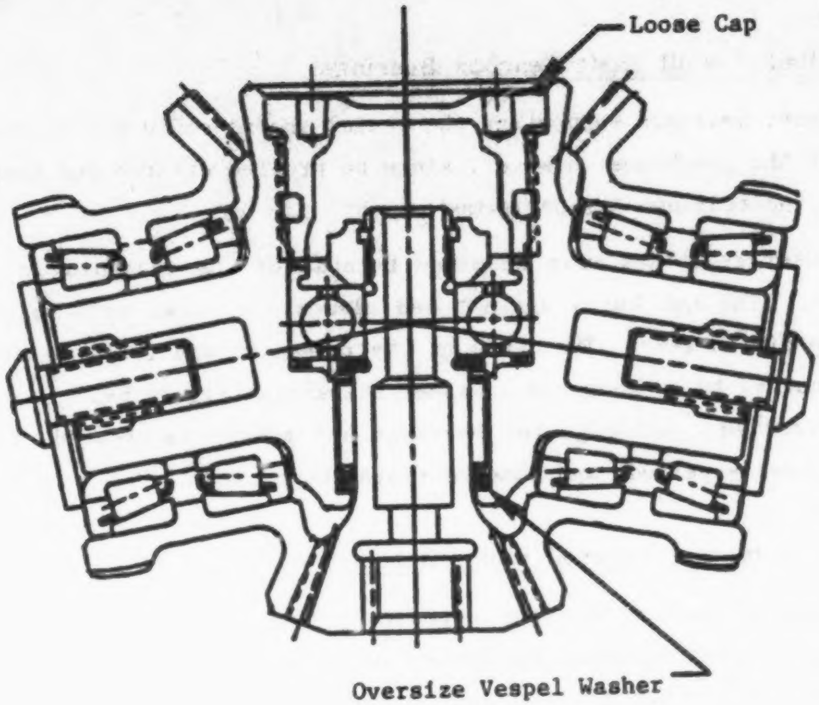
Loose Cap
Oversize Vespel Washer

Figure 6-5. Gearbox Stackup Problem Causing Incorrect Loading of Ball Bearing and Cap Looseness.

thrust bearing. Therefore, the setup bearing has a relatively easy life. The only problem associated with these bearings was, again, corrosion. Although protected by a silicone seal and lubricated by grease, because the grease is permeable, some corrosion was seen, but not severe and none on the active surfaces of the bearing.

Fan Thrust Bearing

Bearing Condition and Seal Condition - The main fan thrust bearing reacts the considerable centrifugal load of the blade and is subjected to dither from blade vibrations and actuation system load fluctuations. Therefore, false brinelling and fretting were the major concerns.

Most noticeable about the condition of the bearings was the disparity in appearance between forward and aft rotor parts. The front rotor was in a much hotter environment, sometimes as much as 100° F hotter. Bearings from this rotor were slightly blued, but the aft rotor bearings were not discolored. Some fretting corrosion was present on both rotor bearings; however, this had not progressed to the point were the bearings were unserviceable.

The lubricant in the forward rotor was dry and discolored; whereas, the aft rotor grease looked like new. Grease seals in some of the forward rotor parts had been torn due to lack of lubrication.

The roller wear paths on the raceway of the cup and cone showed evidence of bearing distortion due to the unsymmetrical loads caused by the housings deflecting, as was predicted by finite element analysis. The bearing cone had been made more flexible to compensate; however, even the cone bending was not enough to provide an even loading. Deflection analysis was performed using a lighter blade weight than we currently have (Figures 6-6 and 6-7).

Thread Clamp Condition - During ground check-out for flight, play in the trunnion support bearings was discovered which caused blade tip movement. The clamp load was measured using a unique eddy-current technique for determining the stretch in the trunnion threads. The technique had been calibrated during ground testing at Peebles to substantiate the torques used at assembly. The results revealed a loss of clamp load, and the rings were returned to Evendale for retorquing the trunnions. This gave us the opportunity to examine all the

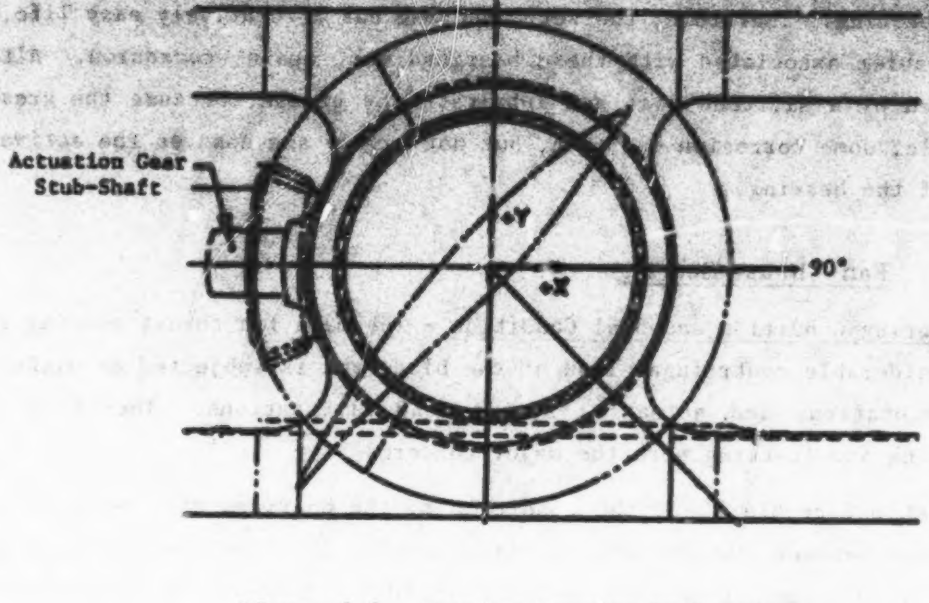
Actuation Gear
Stub-Shaft
Y
X
90°

Figure 6-6. Bearing Housing Deflection.

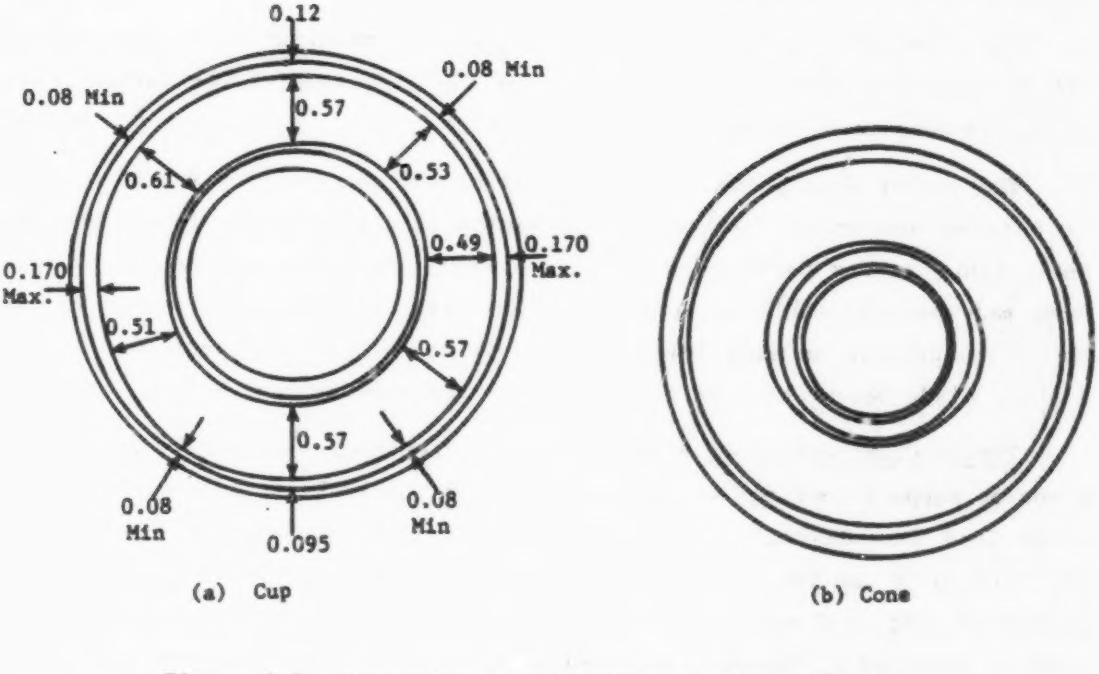
0.12
0.08 Min
0.57
0.08 Min
0.61
0.53
0.170 Max.
0.49
0.170 Max.
0.51
0.57
0.57
0.08 Min
0.08 Min
0.095

(a) Cup

(b) Cone

Figure 6-7. Irregular Wear Pattern of Roller "Path".

trunnion bearings. Thus, the condition of all of the retention bearings was known. Due to minor surface distress, coupled with increased trunnion/bearing thread torque, two bearings were replaced; however, all other bearings were acceptable for flight testing as is. The consumable parts (seals, shims, and grease) were also replaced where necessary.

6.2 MEASURED TEMPERATURES

6.2.1 Rotor Support Main Bearings

The main bearings were instrumented initially with three thermocouples at each bearing location. The thermocouples were at 120° circumferential locations; however, loss of signal and lack of available recording channels left only one gage at each position providing good data.

Steady-State Temperatures

The bearing temperatures were influenced by environment (oil, metal, and cavity temperatures) and by engine speed. The intershaft bearings ran hotter than the Stage 2 rotor supports, as would be expected due to the higher relative speed (Figure 6-8).

The Stage 1 rotor bearing temperatures increased from 240° F at 700 rpm (idle) to 340° F at 1393 rpm (maximum thrust). The Stage 2 rotor bearing temperatures were lower, with that of the 2B bearing rising 50° F, to 250° F at maximum thrust. Oil supply temperature rose 100° F over the same ranges.

Transient Temperatures

The bearings did not pick up temperature very rapidly during fast accels. A 40° F rise in intershaft bearing temperatures is attributable to increased centrifugal loads. The Stage 2 rotor support bearings changed little during a 2-minute accel to full power. However, a 4-minute accel/decel demonstrated a similar 40° to 50° F rise in all bearings (Figures 6-9 and 6-10).

6.2.2 Fan Retention Thrust Bearings

The fan retention tapered roller bearings were not instrumented; however, thermocouples were placed inside the trunnion adjacent to the bearing. Since

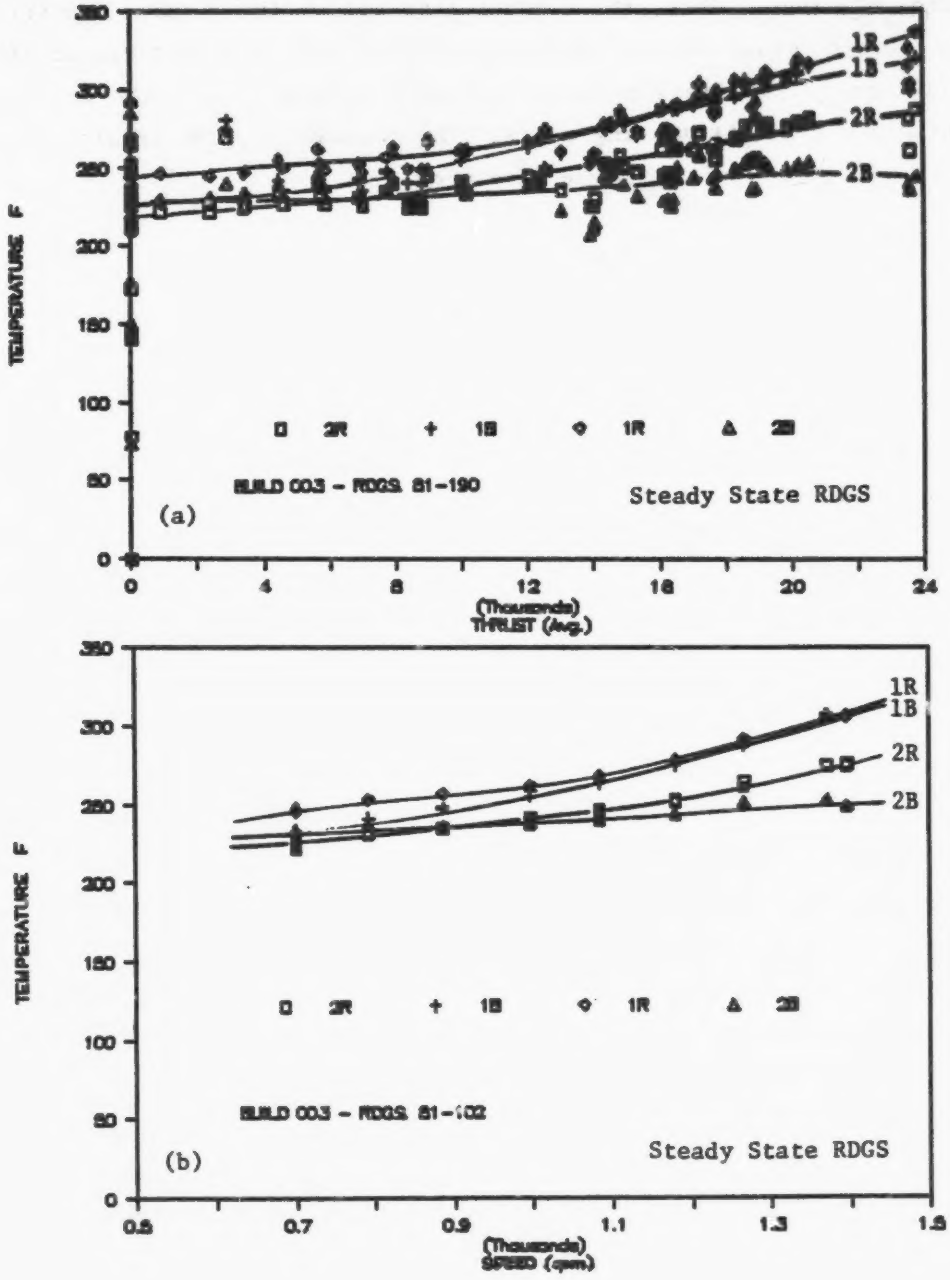

Figure 6-8. Main Propulsor Bearings.

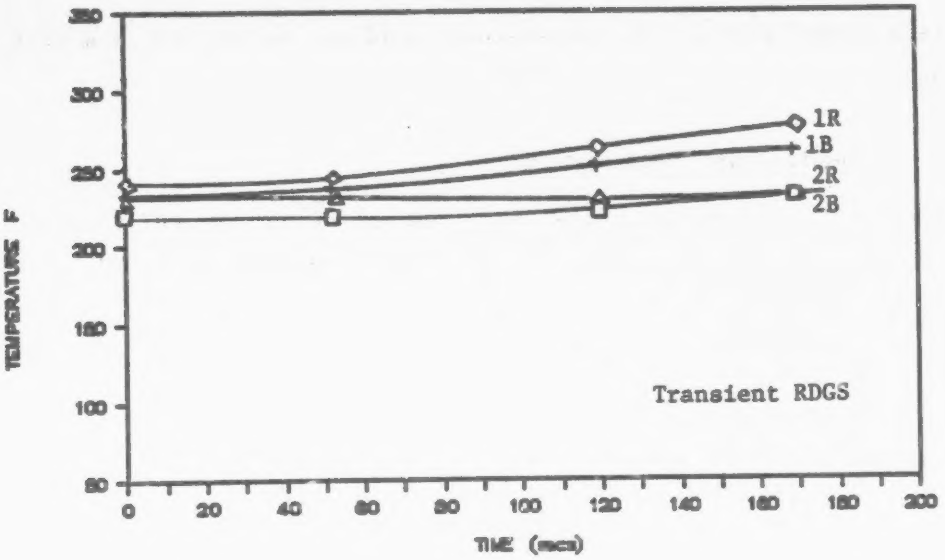

Figure 6-9. Main Propulsor Bearings, 2 Minute Accel to 24,000 lbs Thrust.

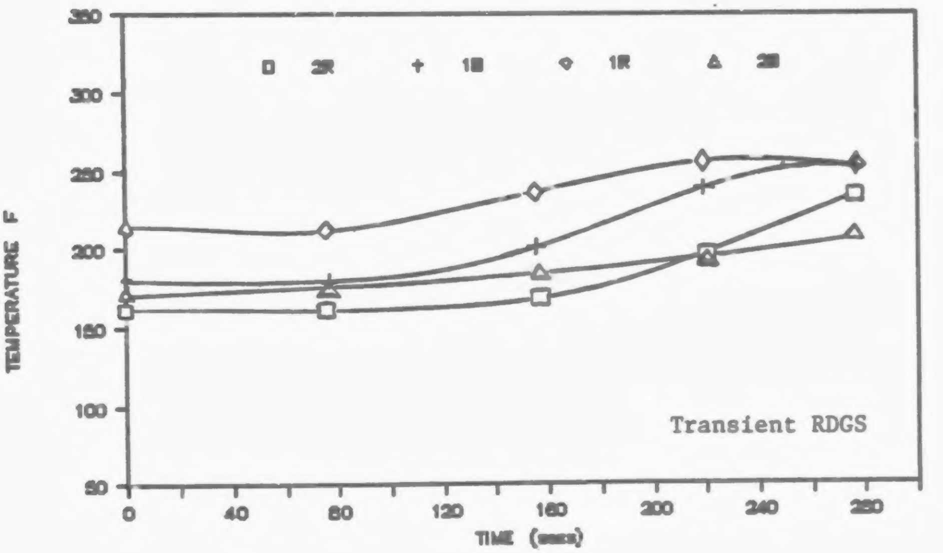

Figure 6-10. Main Propulsor Bearings, 4 Minute Accel/Decel to 1200 rpm.

this is a closed cavity, the temperature would not be too far from that of the bearing.

Steady-State Temperatures

The forward hub temperatures rose from approximately 340° F at 700 rpm to about 390° F at 1393 rpm. The aft hub went from 190° to 250° F in the same range (Figure 6-11).

Transient Temperatures

There was little difference between a 2-minute accel and a 4-minute decel, in that the temperatures of both forward and aft hubs rose about 20° to 40° F. This is due to the fact that the thermocouples were in a closed cavity and, although influenced by turbine air gas temperatures, they are shielded from the immediate effect by the fan ring bulkhead plate (Figure 6-12).

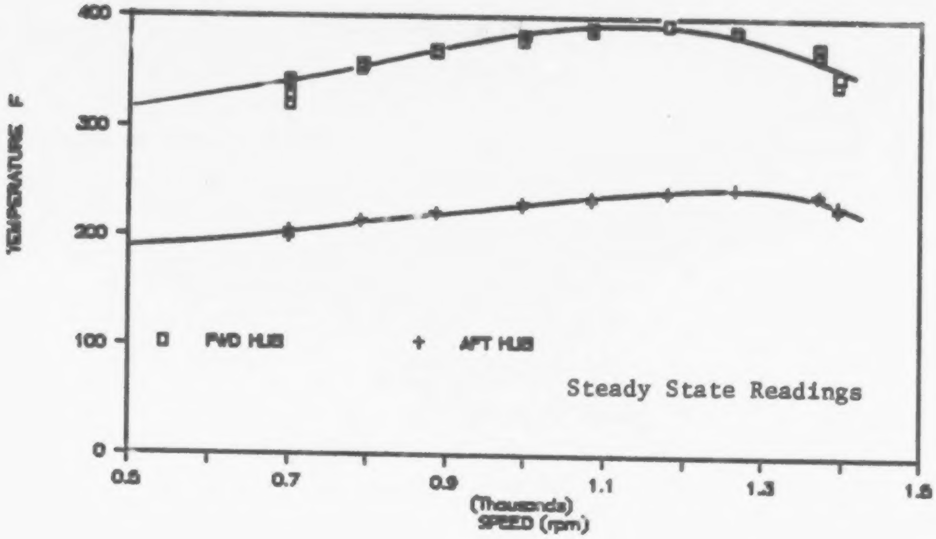

Figure 6-11. Forward and Aft Fan Hub Temperatures.

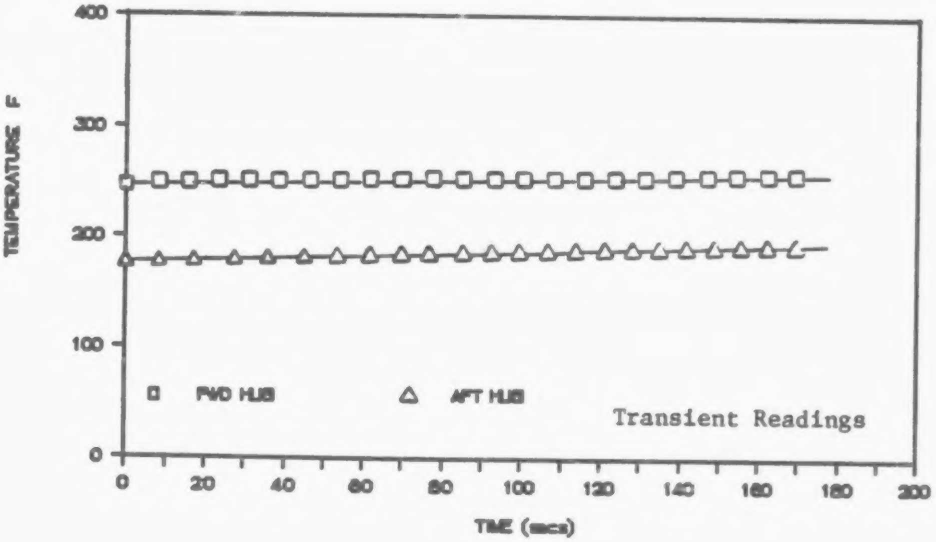

Figure 6-12. Forward and Aft Fan Hub Temperatures, Accel to Full Power.

7.0 PERFORMANCE

This section describes the steady-state data acquired during Build 3 testing at Peebles Site 3D and the various analyses employed to support the test effort. The major items covered are as follows:

- Data summary
- Data reduction methodology
- Comparison between pretest predictions and reduced test data
- LCF cyclic testing and resultant deterioration
- Comparison between ground and flight pretest cycles and reduced test data
- Overall summary
- Key results
- Conclusions.

7.1 DATA SUMMARY

During Build 1 testing at Site 4A, a total of 46 steady-state DMS (data management system readings were taken, none of which were usable for performance analysis since all the points were recorded mainly for mechanical checkout and were not stable.

During Build 2 testing, 104 steady-state DMS readings were taken at Site 4A, and an additional 31 at Site 3D. Some of the data points were usable for analysis.

Table 7-1 shows the breakdown of steady-state DMS readings for Build 3. Note that of the total of 358 data points recorded, 27 readings were expressly taken to define the baseline performance, with an additional 48 data points recorded to map the UDF™ performance at off-schedule conditions. Table 7-2 shows the chronology of the acquired data.

Appendix A presents a listing of the Build 3 steady-state data points.

7.2 DATA REDUCTION METHODOLOGY

Figure 7-1 shows the schematic of the engine and the positioning of the performance-related instrumentation.

Table 7-1. Data Summary.

Breakdown of Steady-State DMS Readings for Build -03.	
	Points
Zero Readings	86
Ground Idle Readings	2
Flight Idle Readings	16
Trim Balance Data Readings	36
Bleed Evaluation Readings	28
EPR Power Hooks	48
Down Power Calibration	27
LCF Cycles	102
Miscellaneous Data Points	15
Total	358

Table 7-2. Chronology of the Acquired Data.

Breakdown of Steady-State DMS Readings for Build -03		
Readings	Date	Points
1 to 5	6/20/86	5
6 to 15	6/23/86	10
16 to 31	6/24/86	16
32 to 47	6/25/86	16
48 to 56	6/26/86	9
57 to 70	6/29/86	14
71 to 77	6/30/86	7
78 to 149	7/1/86	72
150 to 197	7/3/86	48
198 to 209	7/4/86	12
210 to 251	7/5/86	42
252 to 304	7/6/86	53
305 to 330	7/7/86	26
331 to 358	7/8/86	28
Total		358

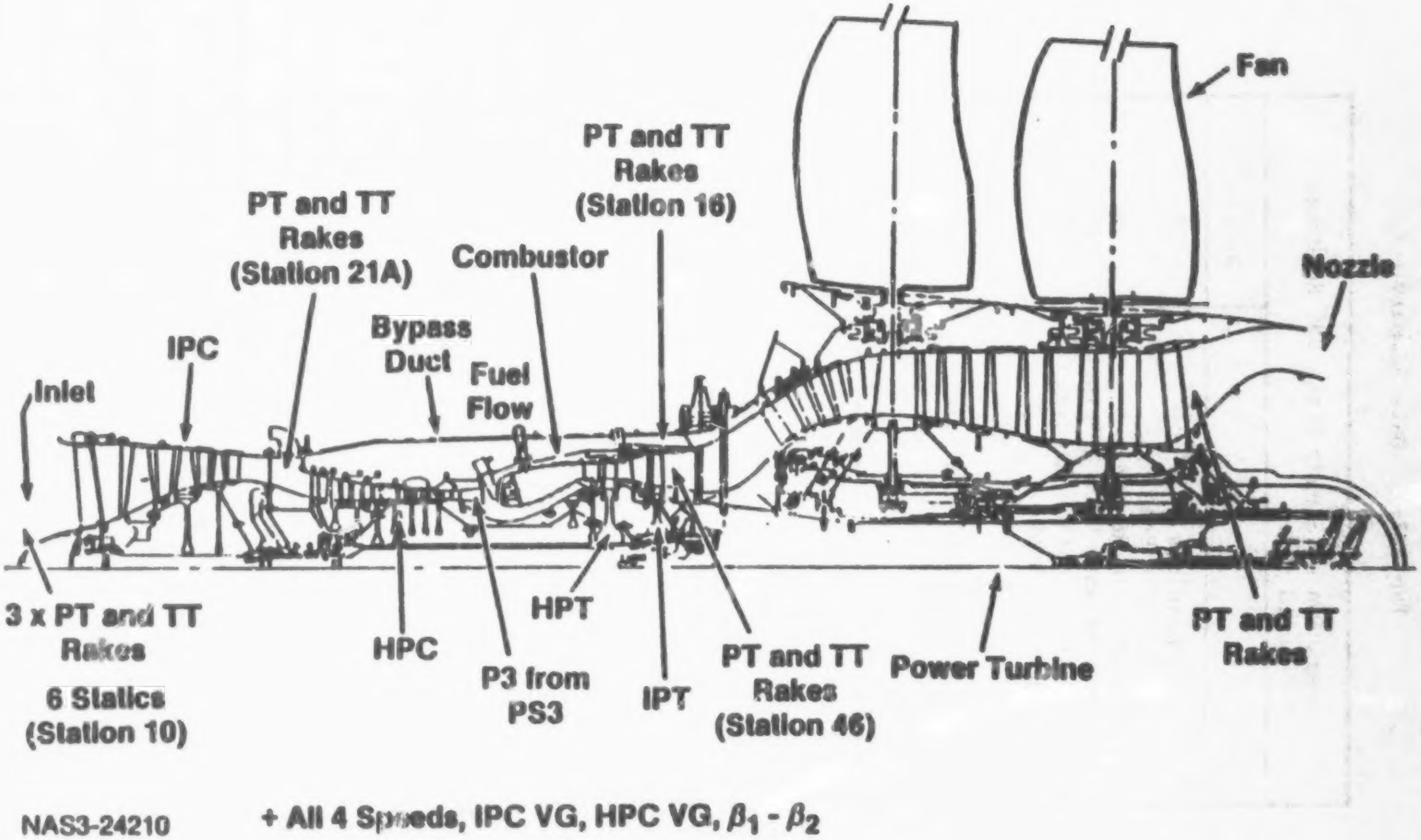
Fan
Nozzle
PT and TT
Rakes
(Station 16)
PT and TT
Rakes
(Station 21A)
Combustor
IPC
Bypass
Duct
Fuel
Flow
Inlet
3 x PT and TT
Rakes
6 Statics
(Station 10)
HPC
HPT
P3 from
PS3
IPT
PT and TT
Rakes
(Station 46)
Power Turbine
PT and TT
Rakes
NAS3-24210
+ All 4 Speeds, IPC VG, HPC VG, β1 - β2

Figure 7-1. Instrumentation for UDF™/F404 Demo.

IPC

Inlet flow - From inlet total rakes, circumferential pressure statics, physical area, flow coefficient

Pressure ratio - From inlet and exit total pressure rakes

Efficiency - From inlet and exit total pressure and temperature rakes.

HPC

Flow - From HPT flow function (iteration)

Pressure ratio - From IPC exit conditions and stratification logic to define inlet pressure, PS3 correlation to define P3

Efficiency - From matching core overall performance.

Bypass Duct

Flow - From IPC exit conditions and stratification logic

Pressure drops - Measurements at IPC exit and duct exit

Temperatures - Measurements at IPC exit and duct exit.

Combustor

Efficiency - Assumed (map value)

Pressure drops - Assumed (map value)

Fuel flow - Measured (including all parameters for corrections).

HPT

All parameters assumed (map).

IPT

Efficiency - Energy balance with IPC

Exit from IPT - (T46) - From fuel flow and inlet airflow, together with assumed secondary flows

- (P46) - Measured.

Mixer Frame

Assumed losses, mixing characteristics.

Secondary Flows

Assumed level and distribution (based on model test and some measurements).

Power Turbine

Inlet - Mixer frame exit conditions, secondary flows

Exit - From total pressure and temperature rakes

Power - From airflow, delta temperature

Efficiency - From delta temperature and delta pressure.

Core Nozzle

Inlet - PT (power turbine) exit conditions

Exit - Ambient conditions.

Thrust

Installed - Measured

Core component - From PT exit conditions, nozzle coefficients

Uninstalled - From installed thrust, assumed drags

UDF™ component - From uninstalled thrust and core thrust.

7.3 COMPARISON OF PRETEST PREDICTIONS AND REDUCED TEST DATA

The steady-state data points used for the performance evaluation were restricted to the down power calibration and maximum power points recorded on July 1 and July 3, 1986. Data points taken for UDF™ mapping EPR (engine pressure ratio) power hooks were recorded on July 1, 1986. The pretest prediction used to compare the test data is the Status D5C cycle. The Status D5C cycle was expressly defined for Build 3, and it includes the following major items:

- PT derates on efficiency due to open clearances and the blade damper pins
- PT flow function adjustments for open clearances and the blade damper pins
- Revised exhaust nozzle characteristics as a result of new nozzle hardware.

Core Performance - Figure 7-2 shows the overall core (F404) temperature ratio versus pressure ratio. Note that the core performance is approximately as predicted at takeoff power conditions and is better than predicted at lower powers (70% takeoff and below). Figure 7-3 presents IPC stall margin versus corrected flow, illustrating that the IPC operating line was approximately as predicted.

Power Turbine Performance - Figure 7-4 shows the PT flow function versus the PT energy function. The PT flow function was within 0.5% of the predicted value at higher powers (80% takeoff and above). Figure 7-5 illustrates the PT

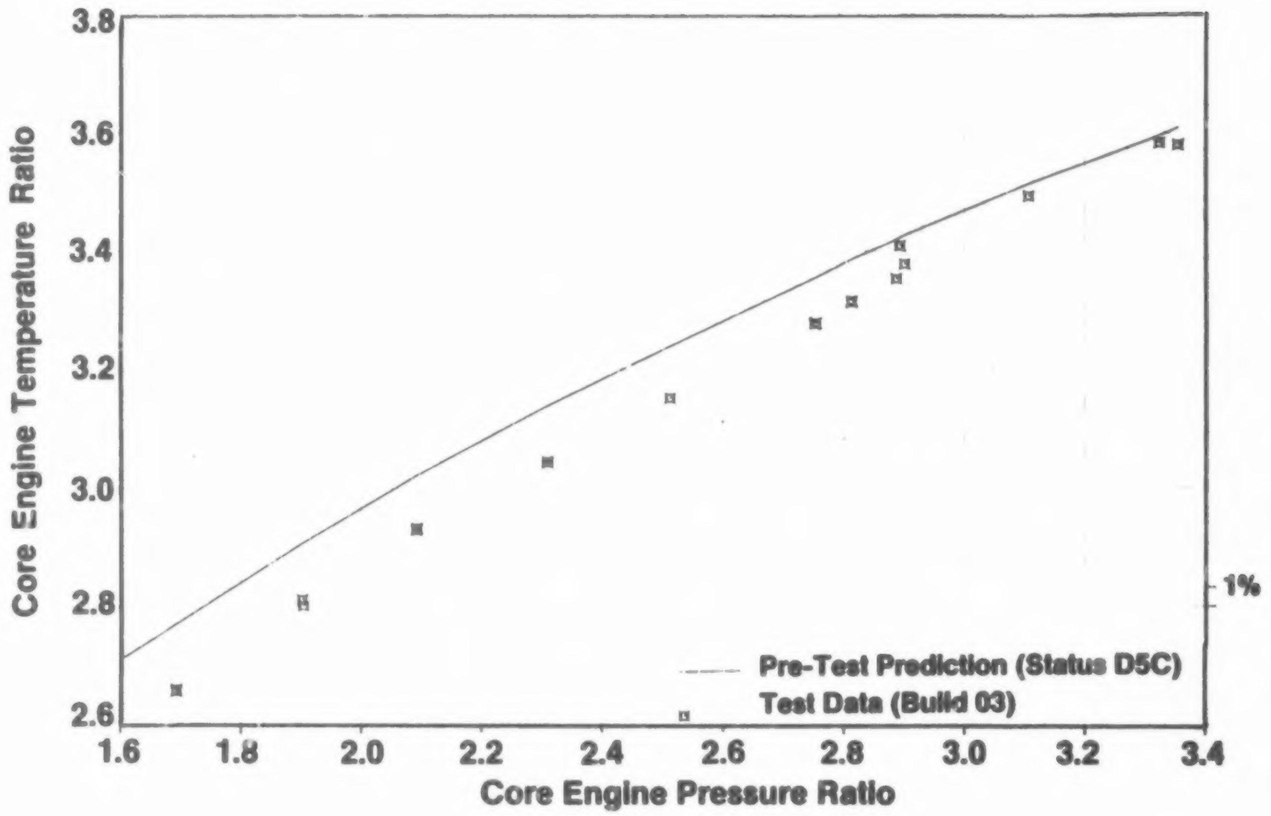

Figure 7-2. Core Engine Temperature Ratio Versus Pressure Ratio.

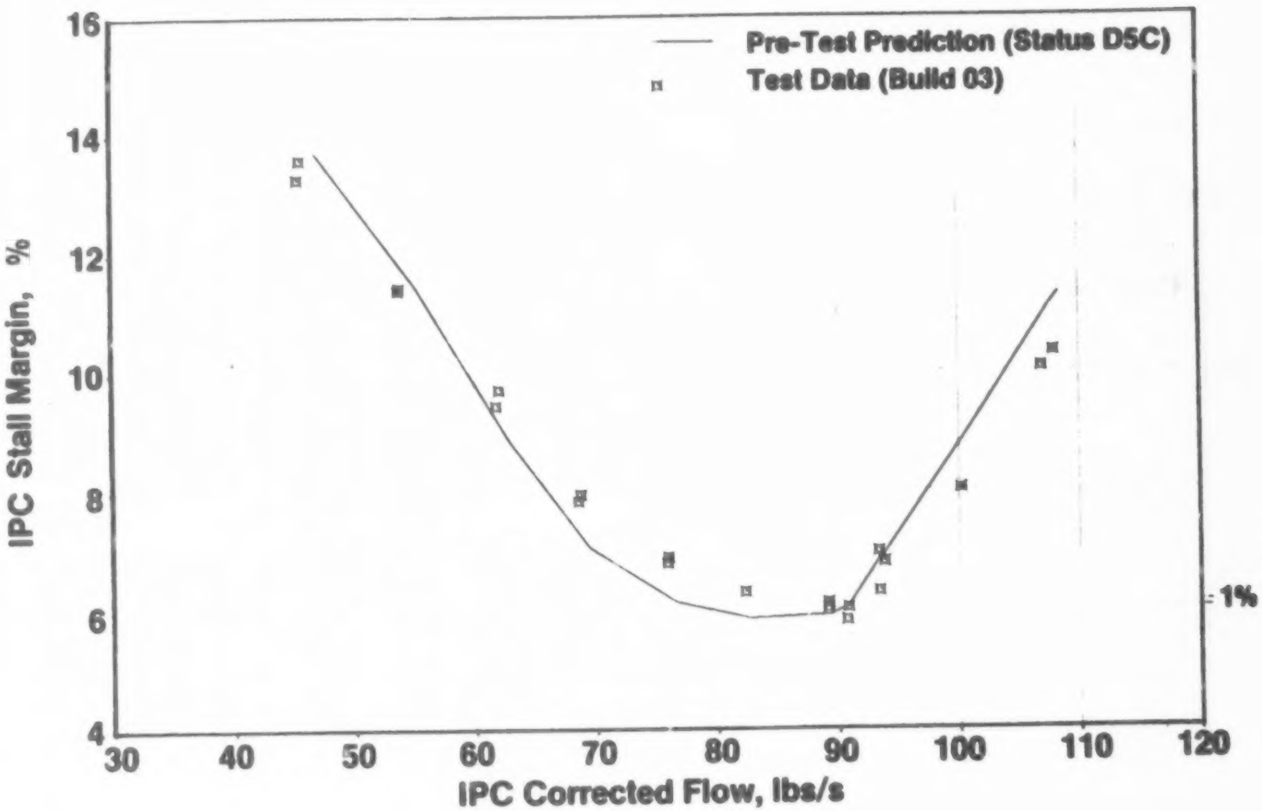

Figure 7-3. IPC Stall Margin Versus IPC Corrected Flow.

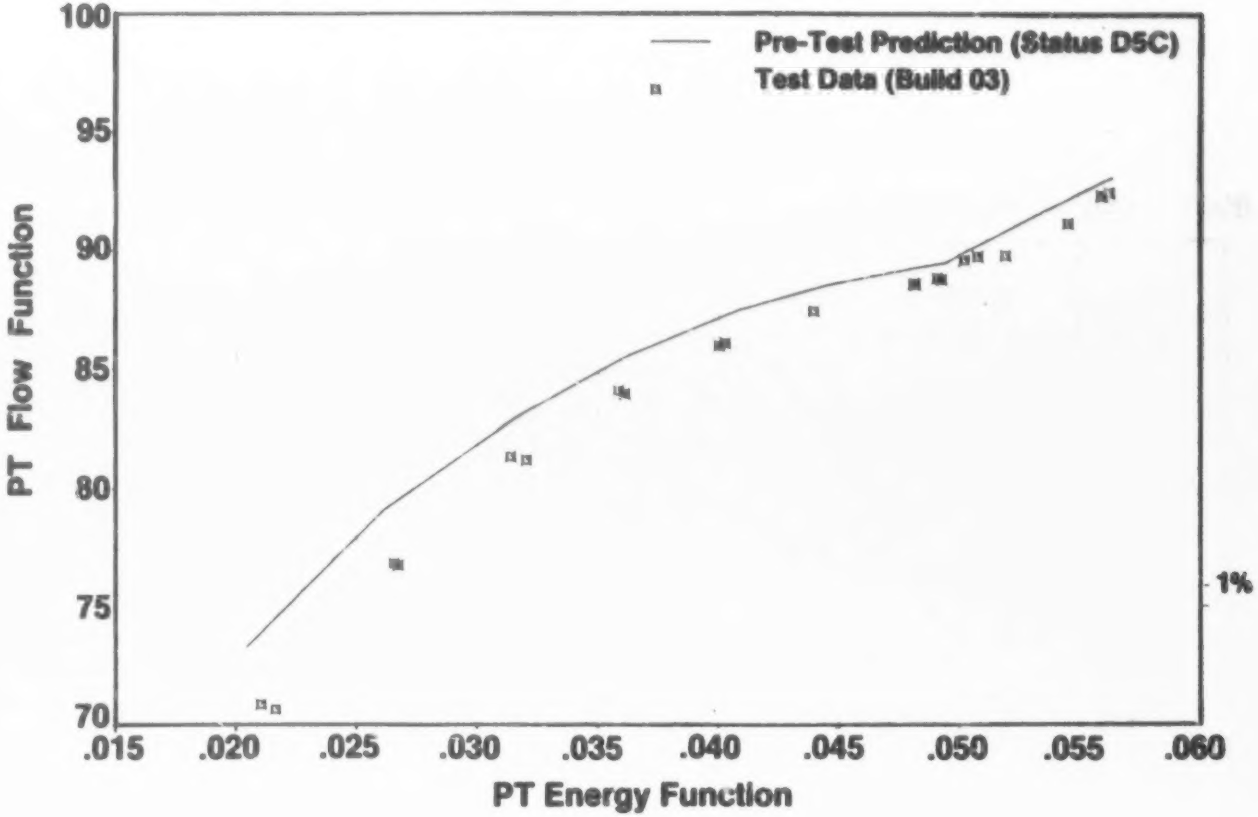

Figure 7-4. Power Turbine Flow Function Versus Energy Function.

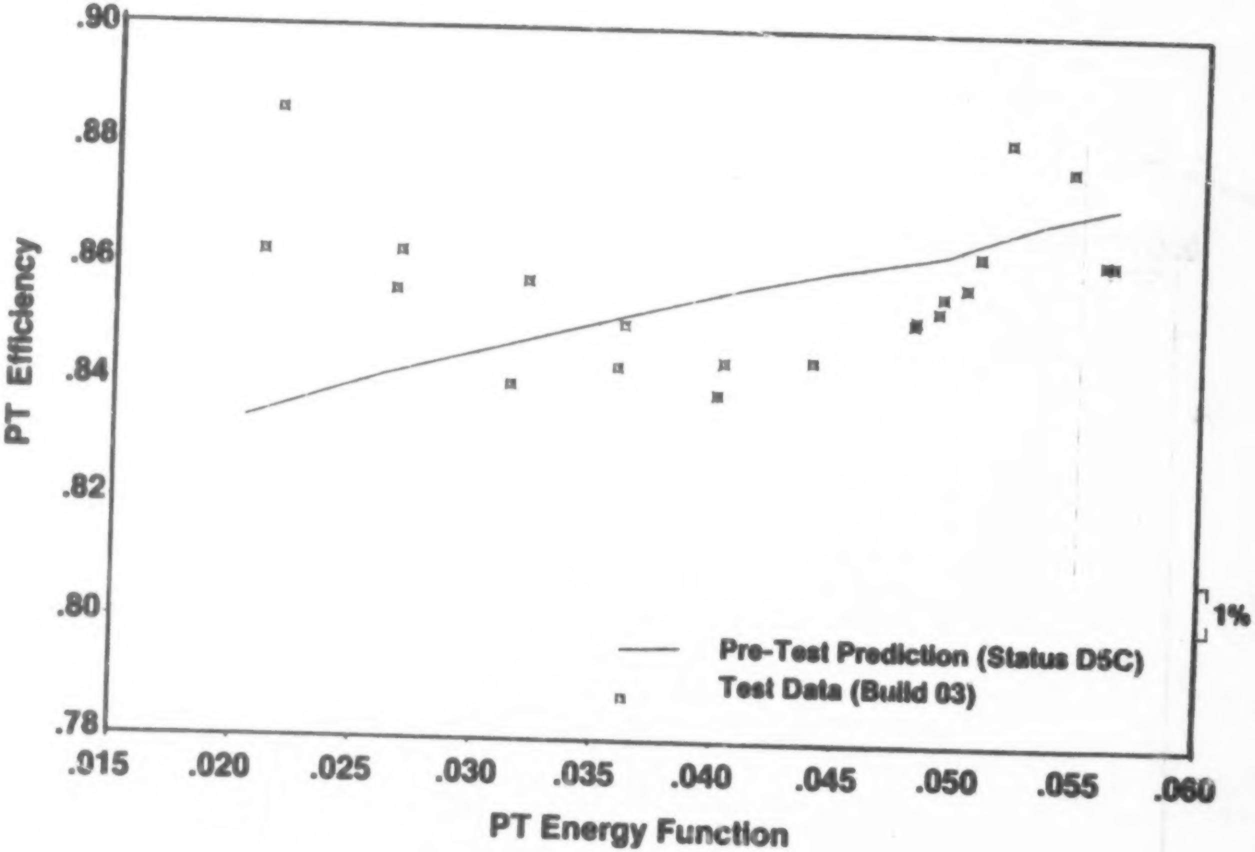

Figure 7-5. Power Turbine Efficiency Versus Energy Function.

efficiency versus PT energy function. The efficiency was within +1.5% of the predicted value and within the scatter range observed in LP turbines of large turbofan engines.

UDF™ Performance - Figure 7-6 depicts the UDF™ thrust coefficient versus power coefficient. Note that the test data describe a shallower slope than predicted. Thrust coefficient is approximately 4% worse than predicted at a power coefficient of 1.95 (takeoff condition), nearly as predicted at power coefficient of 1.70 (92% takeoff), and approximately 4% better than predicted at power coefficient of around 1.32, which covers a range of power from 30% to 80% takeoff thrust. Figures 7-7 and 7-8 compare predicted versus actual UDF™ rotor blade pitch angles for front and rear rotors, respectively.

Overall Performance - Figure 7-9 shows corrected installed specific fuel consumption (SFCI1R) versus corrected installed thrust (FNI1QA). The SFCI1R can be seen to be approximately 4% poorer than predicted at takeoff power. At 92% takeoff thrust the SFCI1R is about as predicted; whereas, at 80% takeoff thrust and below, SFCI1R is 4% to 6% better than predicted. Most of the discrepancy between actual and predicted performance is due to the characteristic exhibited by the UDF™, as discussed above under "UDF™ Performance." Magnitude of overall improvement in excess of that expected from the UDF™ performance at 70% takeoff thrust and below is due to the core engine performance being better than predicted, as discussed in "Core Performance."

Nozzle Performance - Between Builds 1 and 2, a redesigned stationary exhaust nozzle (centerbody) was installed on the engine. The original plug was analytically predicted to have flow separation at cruise conditions. The plug was redesigned so that no flow separation would occur at any flight condition. Figure 7-10 compares the original and redesigned plug lines. Scale models were made of both the original and redesigned plugs, and then tested. Figure 7-11 makes a comparison of the separation parameter (F_{sep}) for the two plugs at cruise conditions, illustrating that the new plug lines would keep F_{sep} below potential separation conditions. Figure 7-12 shows a comparison between predicted and actual engine test data for both plugs to demonstrate good match between prediction and data. Figure 7-13 presents a comparison between predicted and engine test nozzle flow coefficient versus core engine pressure ratio (P46Q2). Note that at P46Q2 of 2.9 and below (approximately

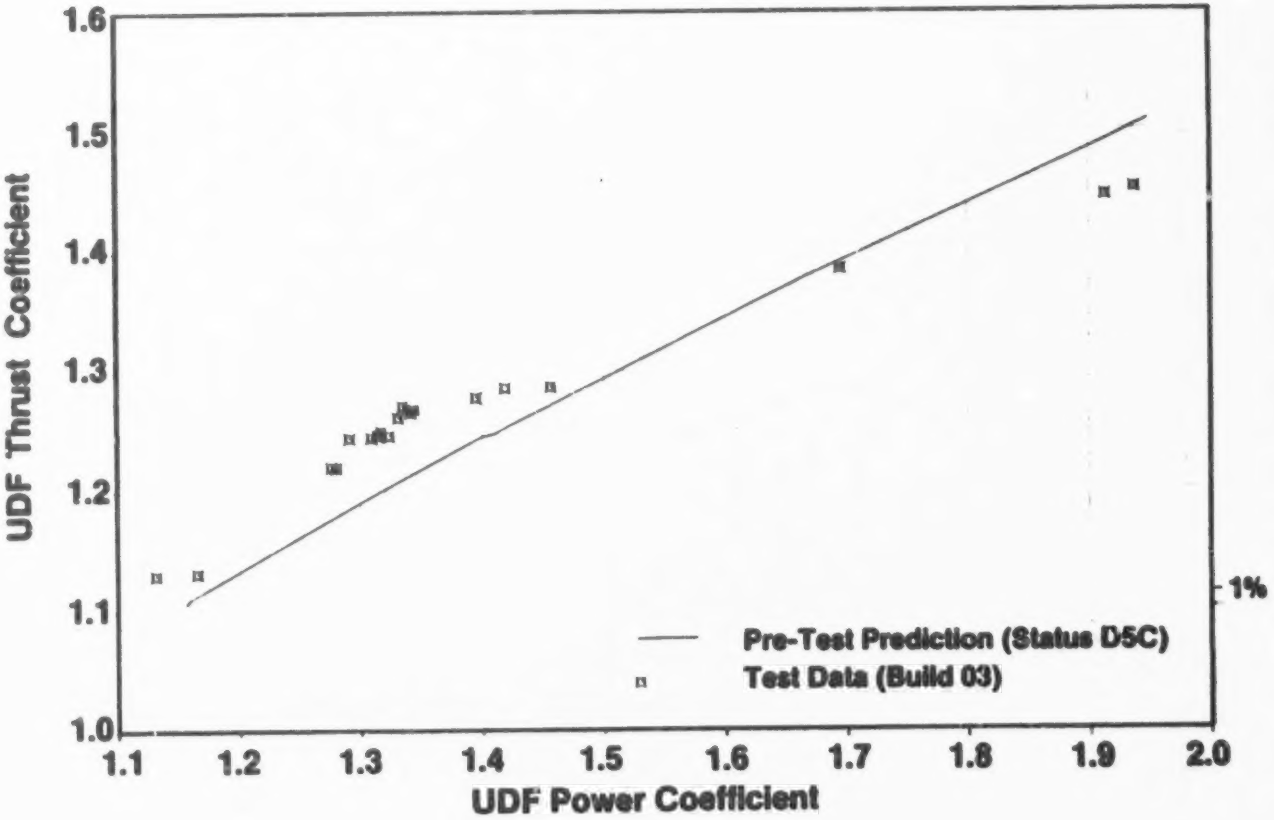

Figure 7-6. UDF™ Thrust Coefficient Versus Power Coefficient.

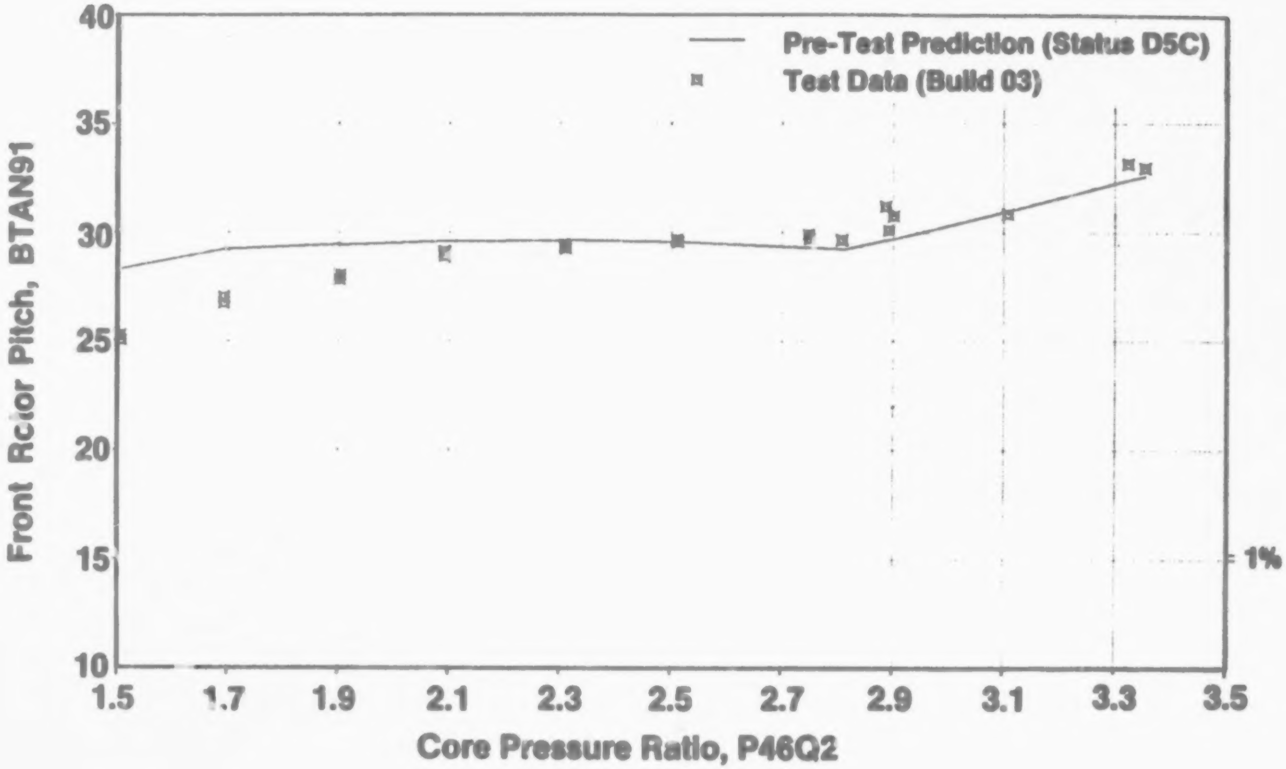

Figure 7-7. Front Rotor Blade Angle Versus Core Engine Pressure Ratio.

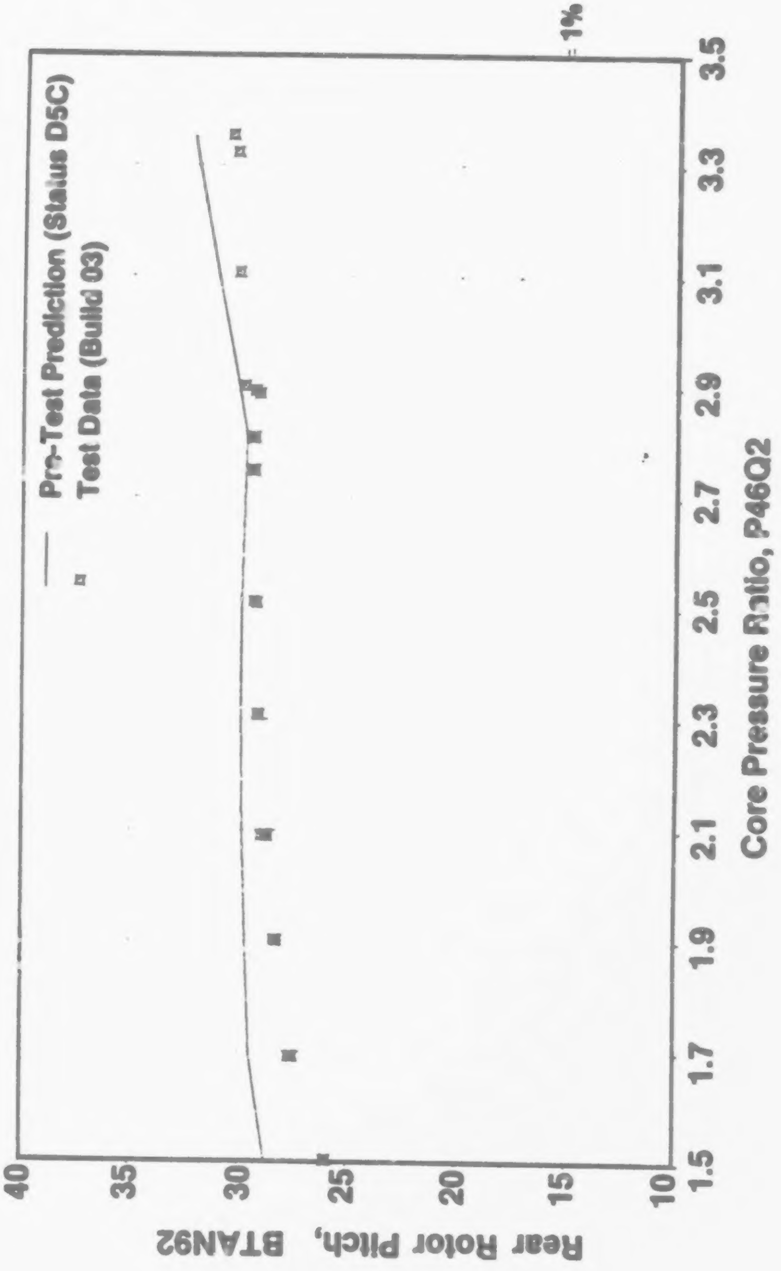

Figure 7-8. Rear Rotor Blade Angle Versus Core Engine Pressure Ratio.

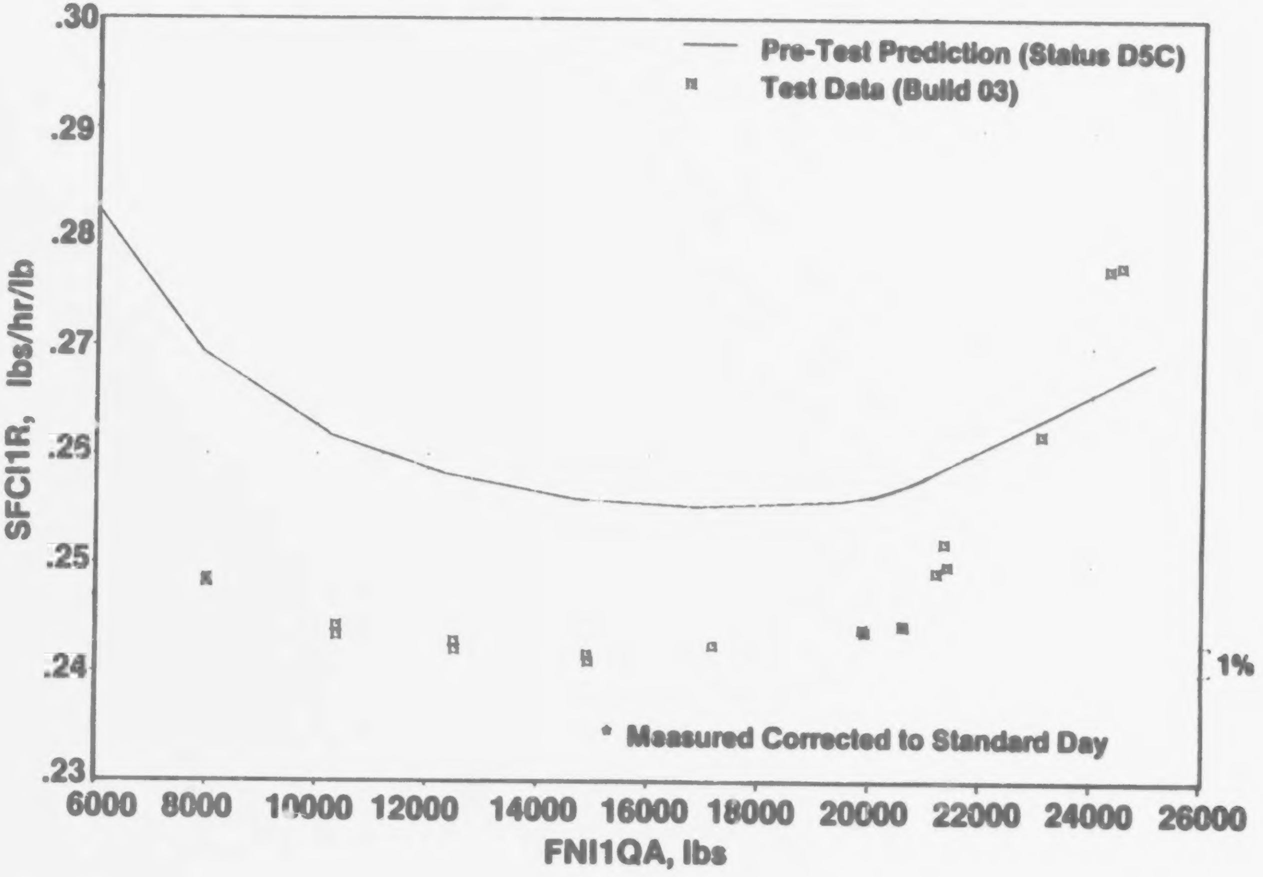

Figure 7-9. Corrected SFC Versus Corrected Thrust.

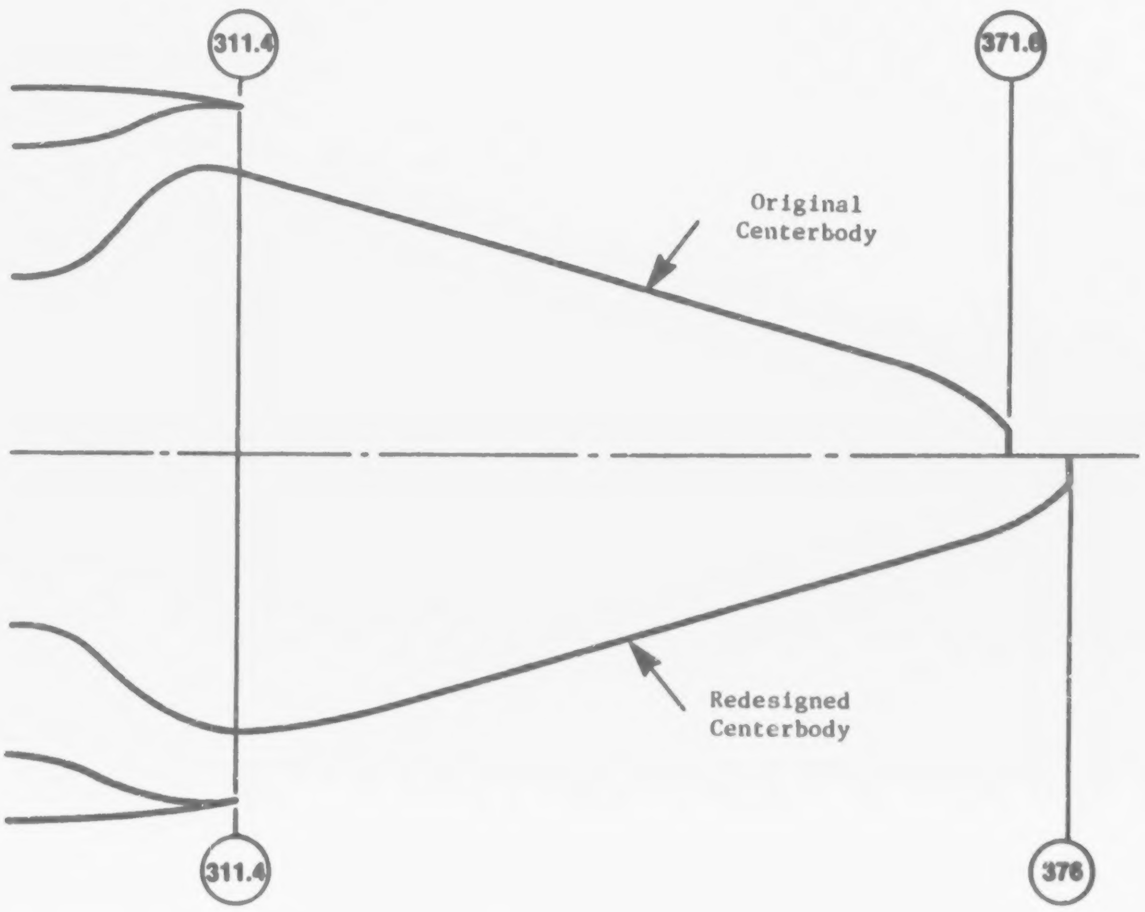
311.4
371.6
Original
Centerbody
Redesigned
Centerbody
311.4
378

Figure 7-10. UDF^{TM} Engine - Redesigned Centerbody.

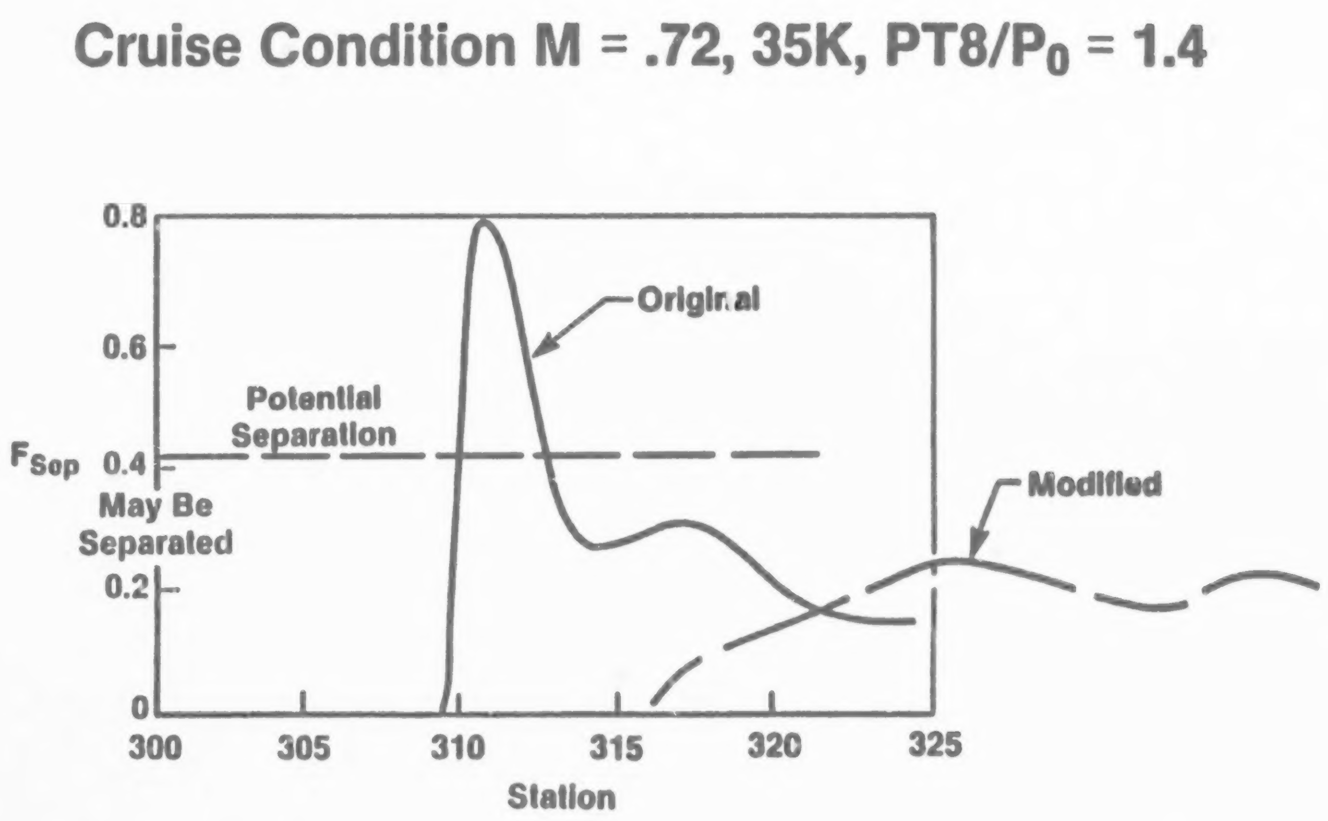

Figure 7-11. UDF™ Engine Centerbody Separation Parameter.

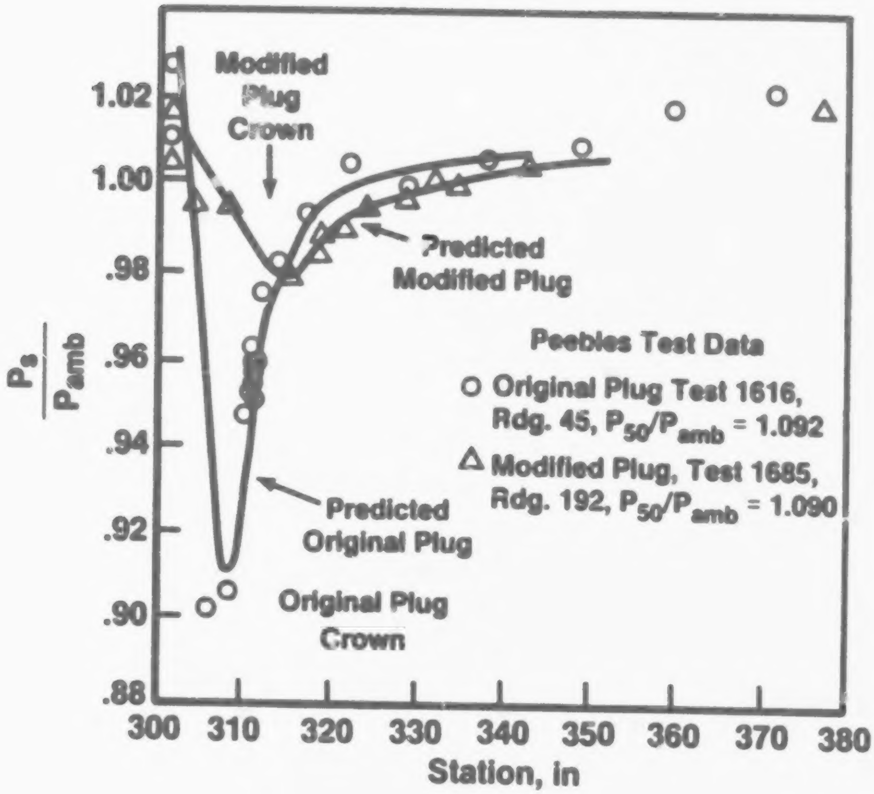

Figure 7-12. UDF™ Engine - Core Plug Static Pressures.

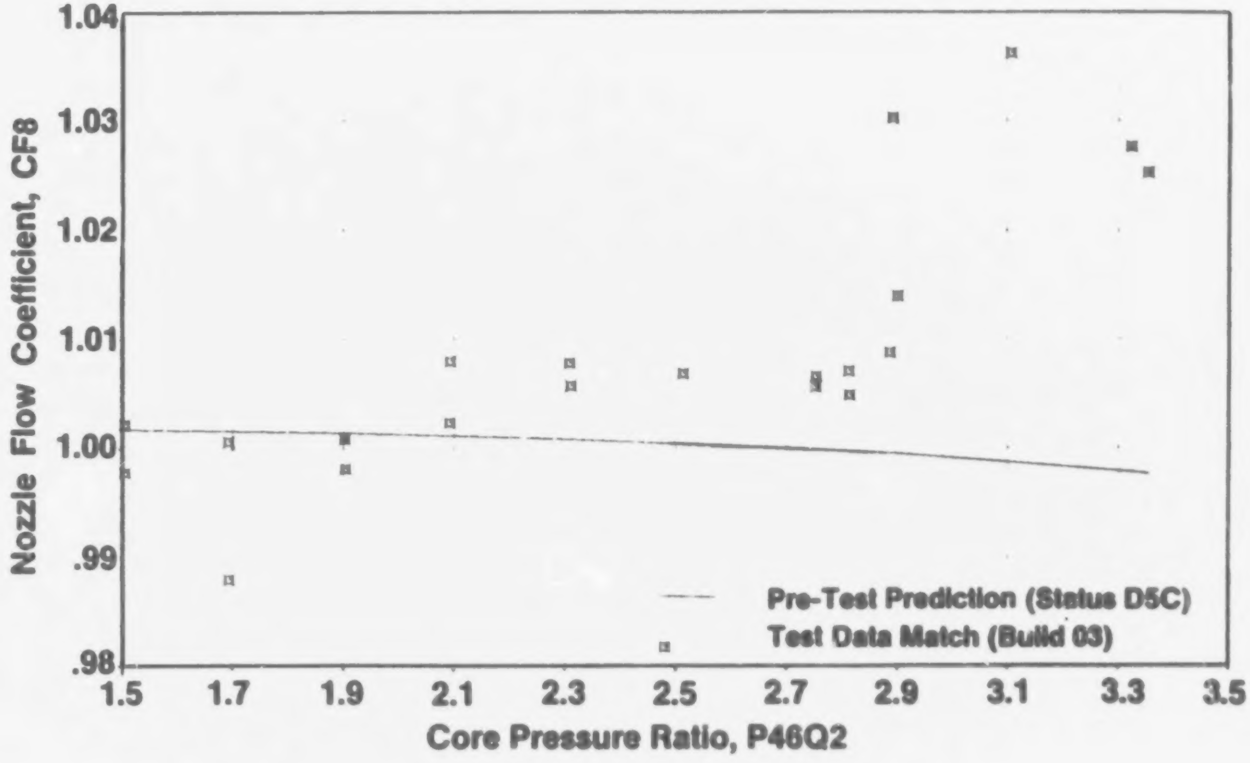

Figure 7-13. Nozzle Flow Coefficient Versus Core Engine Pressure Ratio.

80% takeoff thrust and below) the calculated flow coefficient is within +1% of the prediction. However, at takeoff power there is a discrepancy of about 3%. This is probably due to the fact that the flow coefficient is sensitive to the UDF™ exit pressure which was not a measured parameter, but rather, the value being assumed from the performance maps. This discrepancy is not a concern, since 3% change in flow coefficient changes sfc at thrust by only 0.005%.

EPR Hooks - These test points were run to map UDF™ performance at off-schedule speeds. The test was conducted at six different propulsor rotational speeds where the propulsor speed would be held constant, and core power level would be varied by demanding various EPR levels; hence, EPR hooks.

Figure 7-14 shows installed corrected specific fuel consumption (SFCI1R) versus installed corrected thrust (FNI1QA) for on-speed schedule and constant propulsor speed pretest prediction, with Figure 7-15 showing the equivalent reduced test data. Note that the on-speed schedule lines on both figures are the same as those found in Figure 7-9. The test further proved that the UDF™ characteristics were different than predicted, with significantly higher speed sensitivity than prediction.

7.4 LCF CYCLIC TESTING AND RESULTANT DETERIORATION

The LCF testing involved running the engine through a power cycle as is illustrated in Figure 3-54; a total of 100 complete cycles were run. In the following comparisons, a sample of early data is compared with a sample of late data in order to quantify the magnitude of scatter as well as the magnitude and source of deterioration. Figure 7-16 shows that the wind conditions were relatively consistent, and all data points, except one, were within the prescribed performance testing wind envelope.

Figure 7-17 shows that at corrected installed thrust, corrected installed specific fuel consumption deteriorated by approximately 0.040%.

Figure 7-18 demonstrates that at EPR, corrected installed thrust followed the predicted trends and showed no signs of degradation. This indicates that the power extraction at EPR by the LP turbine and the thrust produced by the UDF™ for LP turbine power remained unchanged during the tests. Figure 7-19

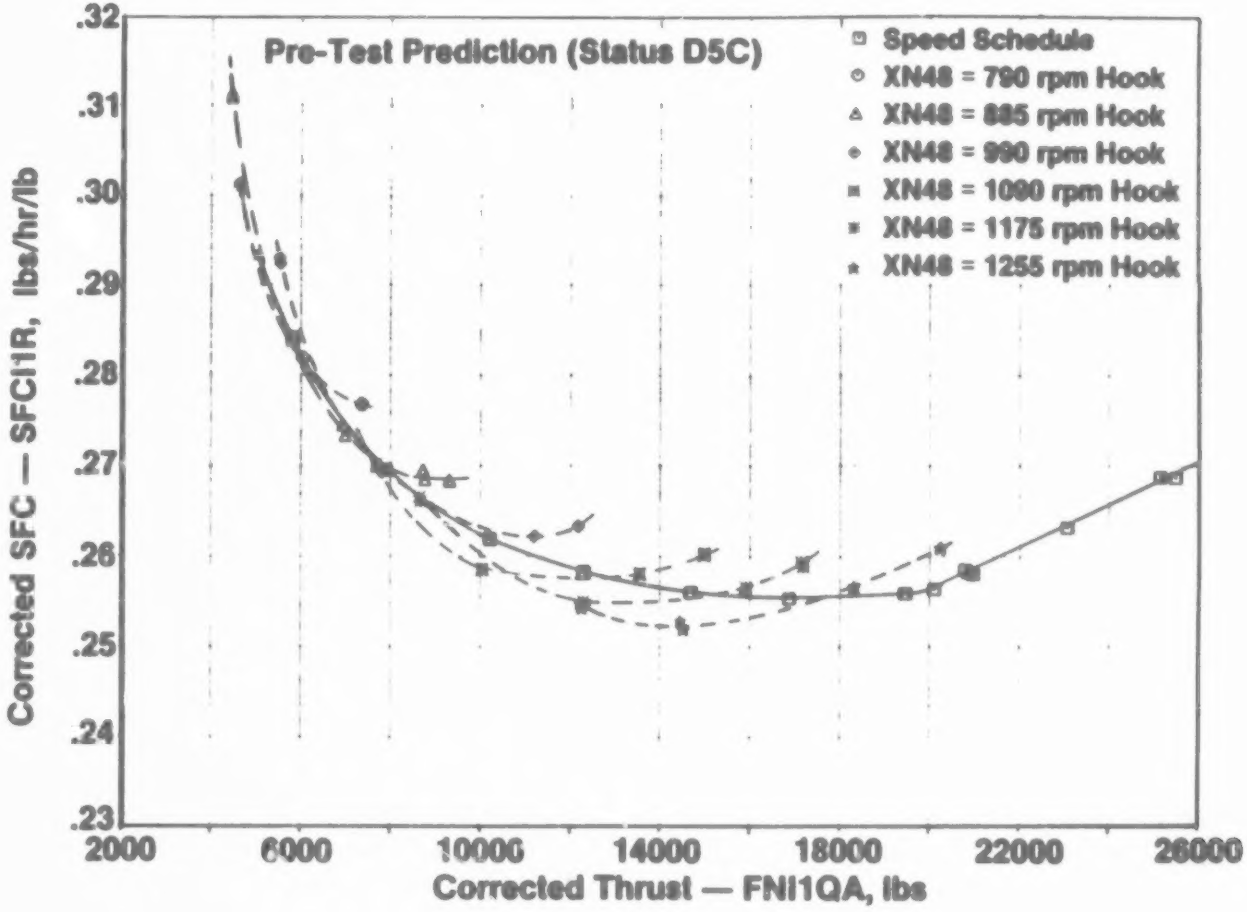

Figure 7-14. Corrected SFC Versus Corrected EPR Power Hook Evaluation.

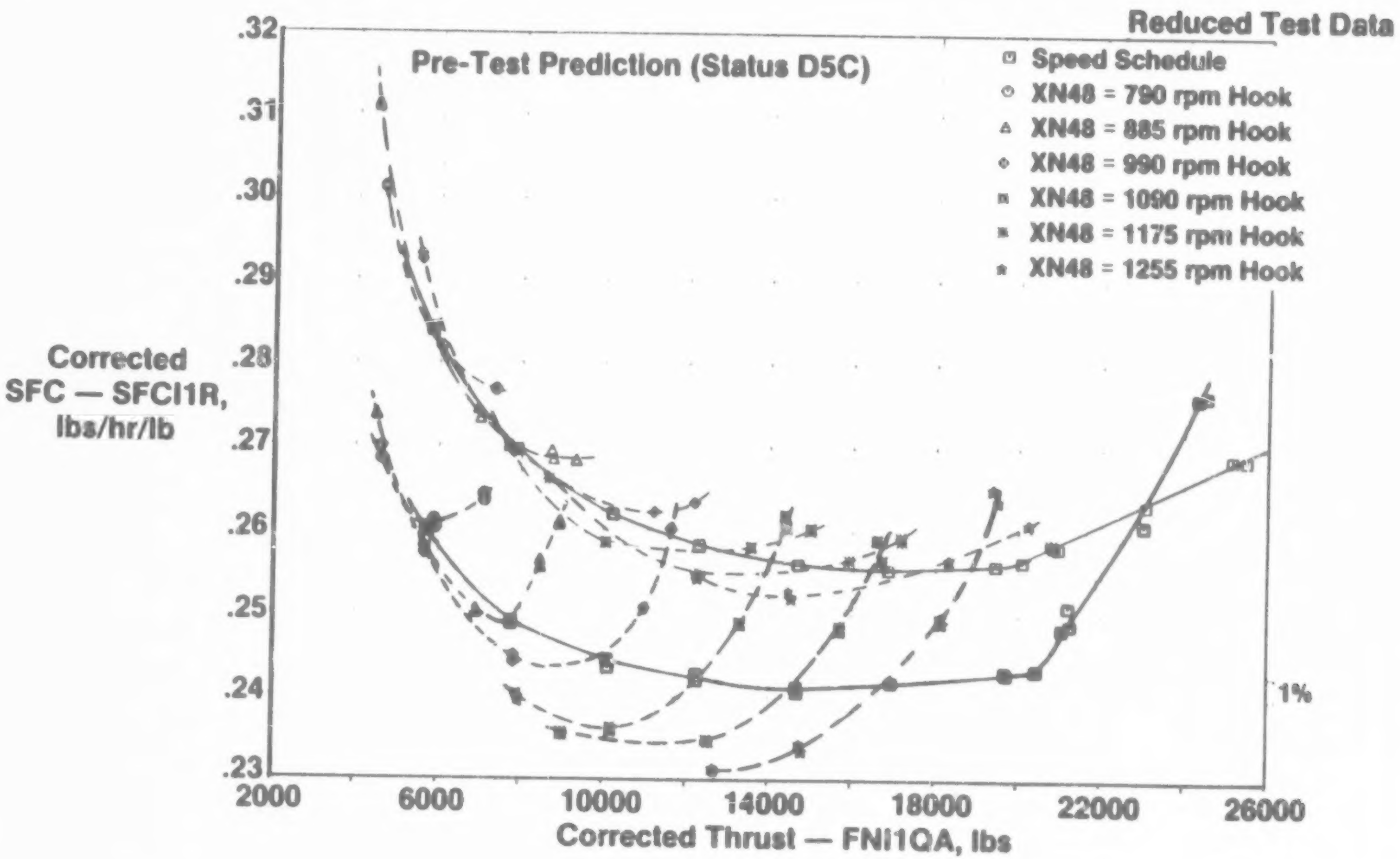

Figure 7-15. Corrected SFC Versus Corrected EPR Power Hook Evaluation.

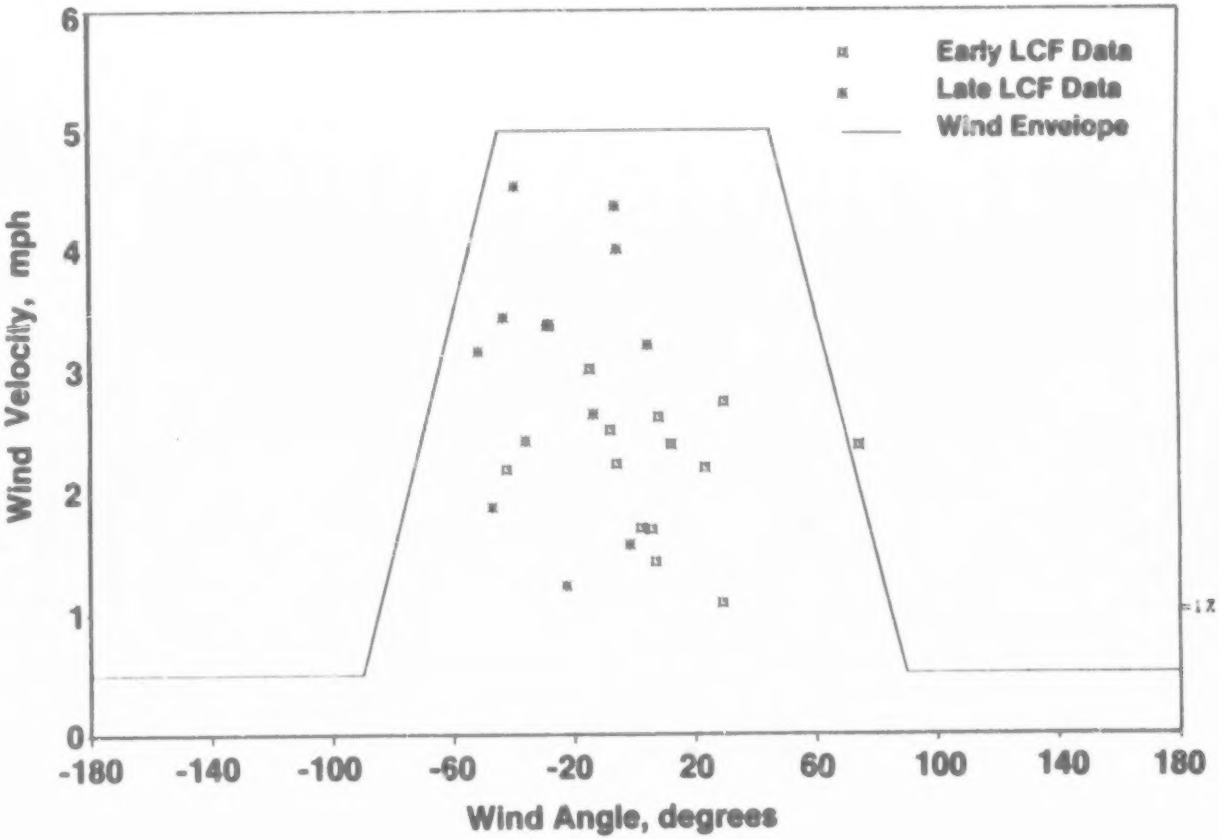

Figure 7-16. Wind Velocity Versus Wind Angle.

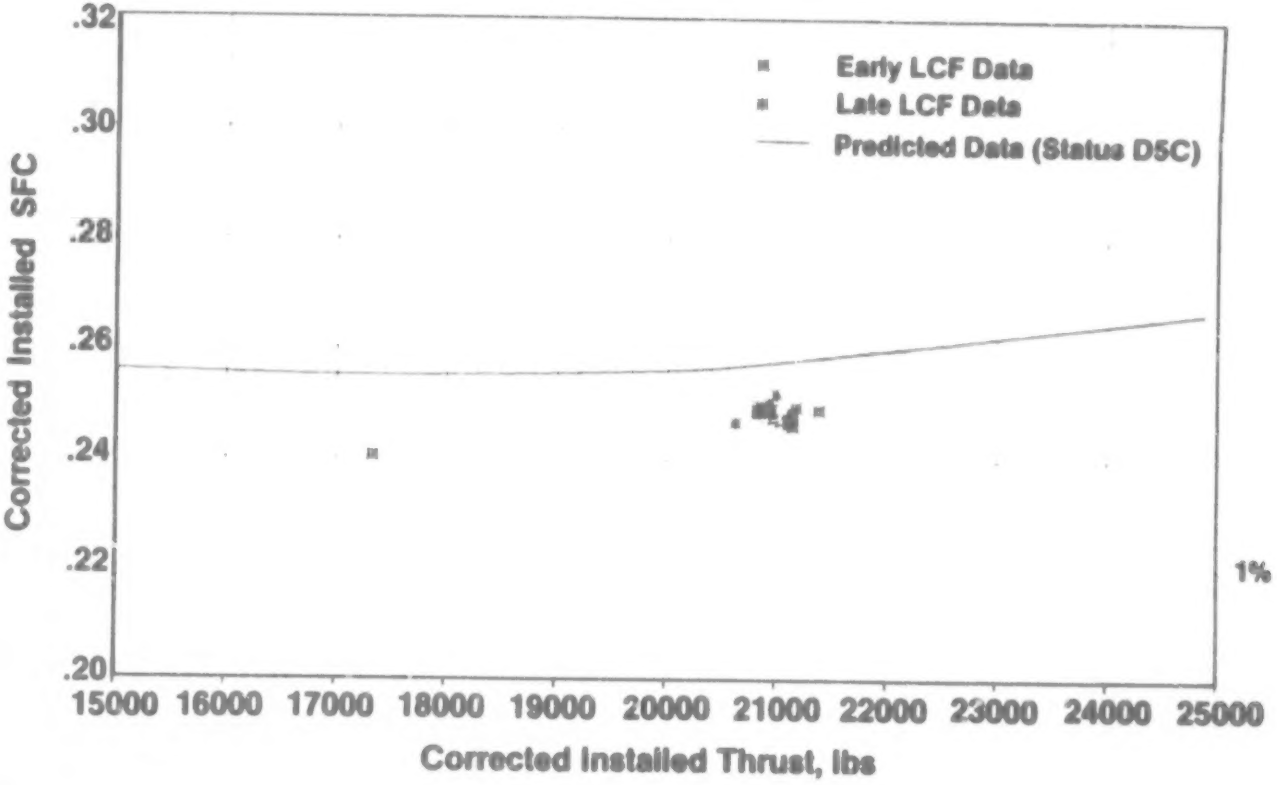

Figure 7-17. Corrected SFC Versus Corrected Thrust.

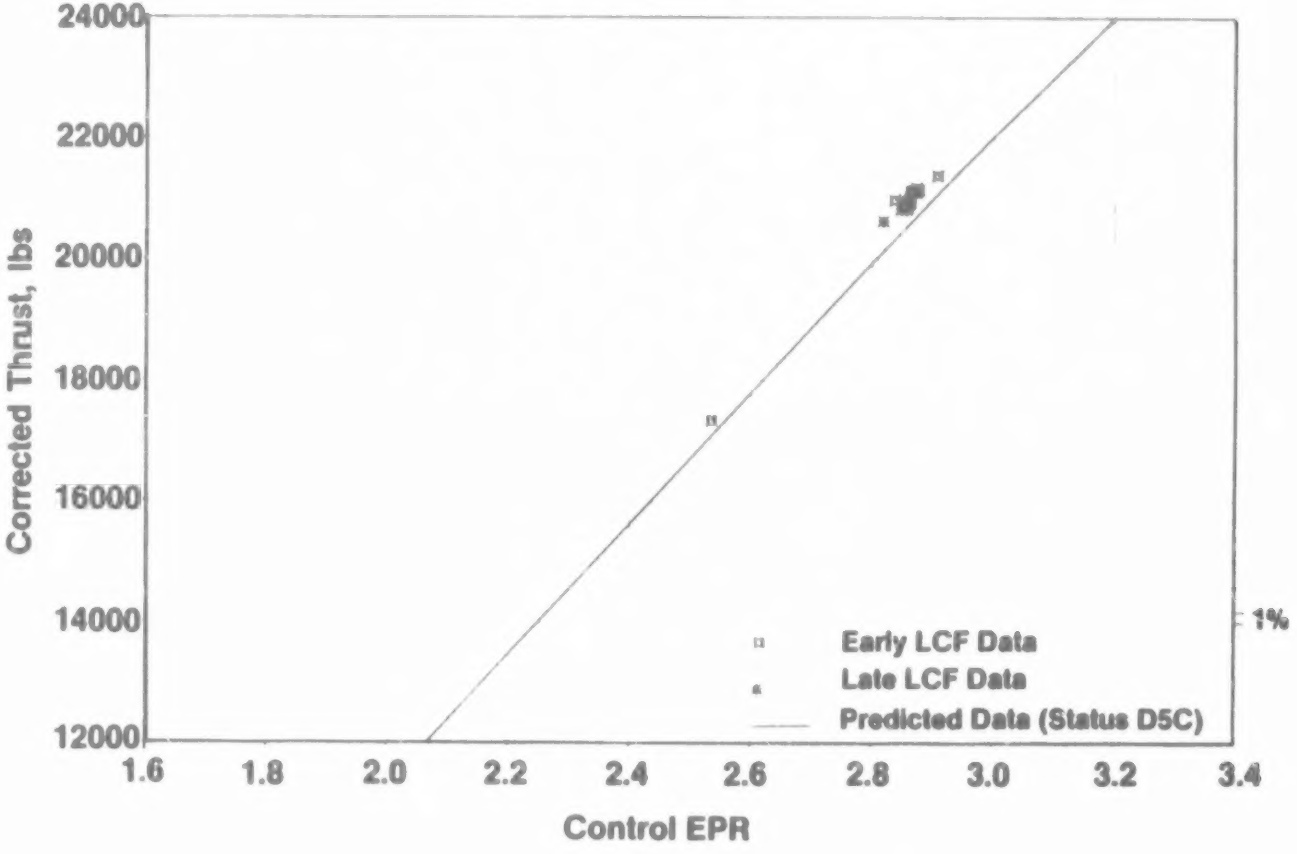

Figure 7-18. Corrected Thrust Versus Corrected Pressure Ratio.

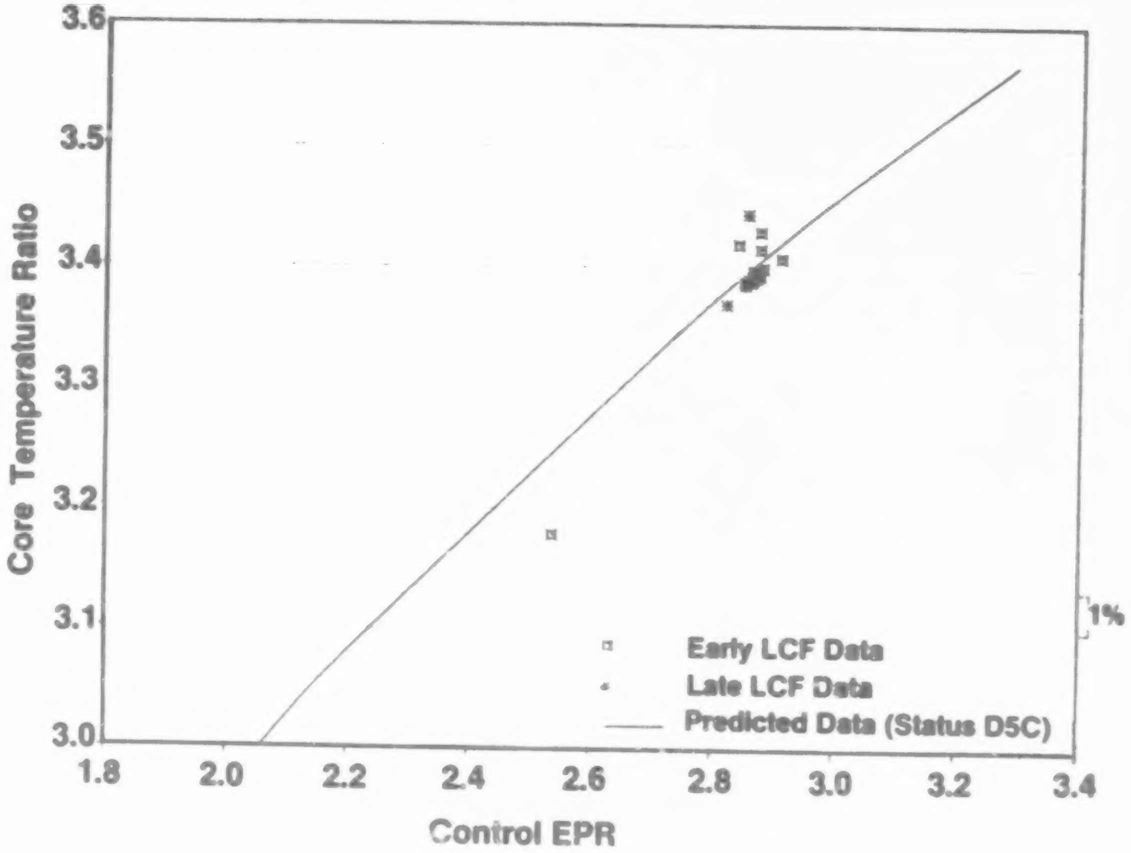

Figure 7-19. Core Temperature Ratio Versus Control Pressure Ratio.

reveals that at EPR, core engine temperature ratio was essentially unchanged, and the core showed little or no signs of deterioration.

Figure 7-20 illustrates that at EPR, intermediate power compressor (IPC) efficiency was down 0.60 points during the latter part of the test compared to the early part of the test. However, Figure 7-21 shows that at EPR, IPC flow follows the predicted trends, confirming that inlet flow and core engine power output remained consistent. This implies a dirty IPC, which is further substantiated by Figure 7-22 indicating that the flow versus speed characteristic of the IPC deteriorated, with approximately 0.50% drop in corrected IPC flow at corrected IPC speed.

In general, there was no evidence of mechanical deterioration, with performance degradation due mainly to a dirty intermediate power compressor.

7.5 DEFINITION OF PREFLIGHT TEST CYCLE

The base cycle used for Build 3 pretest predictions was the Status D5C cycle. Listed below are the changes made to the Status D5C cycle to define the preflight test cycle; this being the Status D8B cycle:

- Modify IPC flow-speed characteristics
- Modify IPC efficiency characteristics
- Modify HPC flow-speed characteristics
- Modify HPC efficiency characteristics
- Revise bypass duct losses and effective area
- Scale IPT efficiency
- Modify LPT efficiency characteristics
- Modify LPT flow function characteristics
- Modify UDF™ thrust coefficient characteristics at Mach No. = 0.00, no change at Mach No. ≧ 0.20
- Use NASA MPS test-derived UDF™ maps for Mach number ≧ 0.67
- Extra cooling air scoops for telemetry system modeled.

7.6 COMPARISON BETWEEN GROUND PRETEST CYCLES AND REDUCED TEST DATA

The following comparisons between the ground pretest cycle (Status D5C), flight pretest cycle (Status D8B), and reduced test data are made to compare

C-3

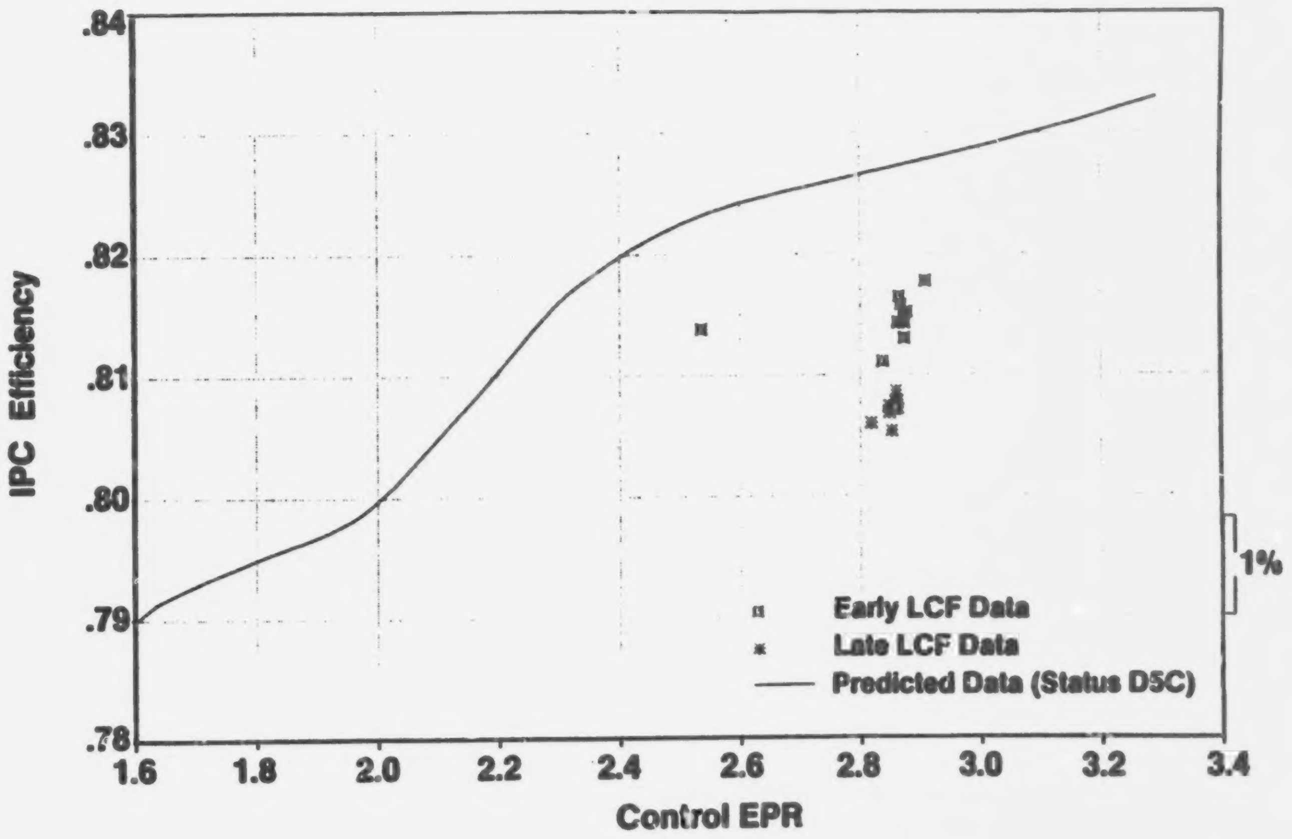

Figure 7-20. IPC Efficiency Versus Control Pressure Ratio.

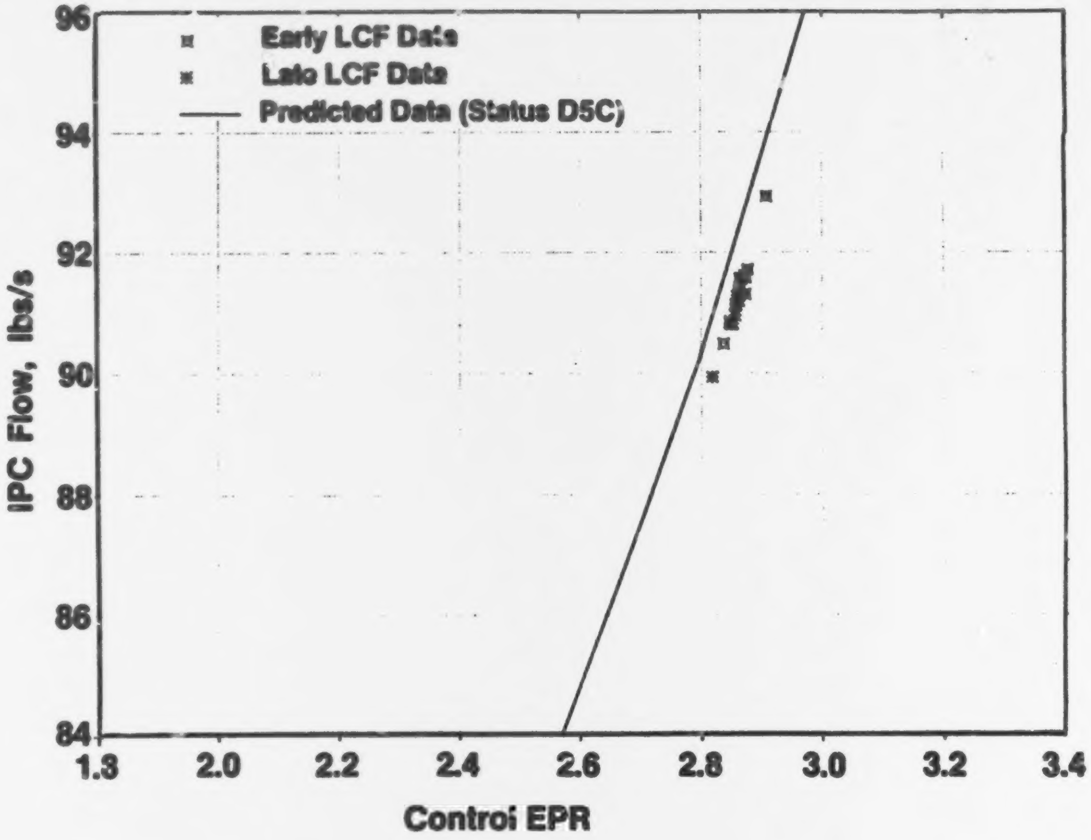

Figure 7-21. IPC Flow Versus Control Pressure Ratio.

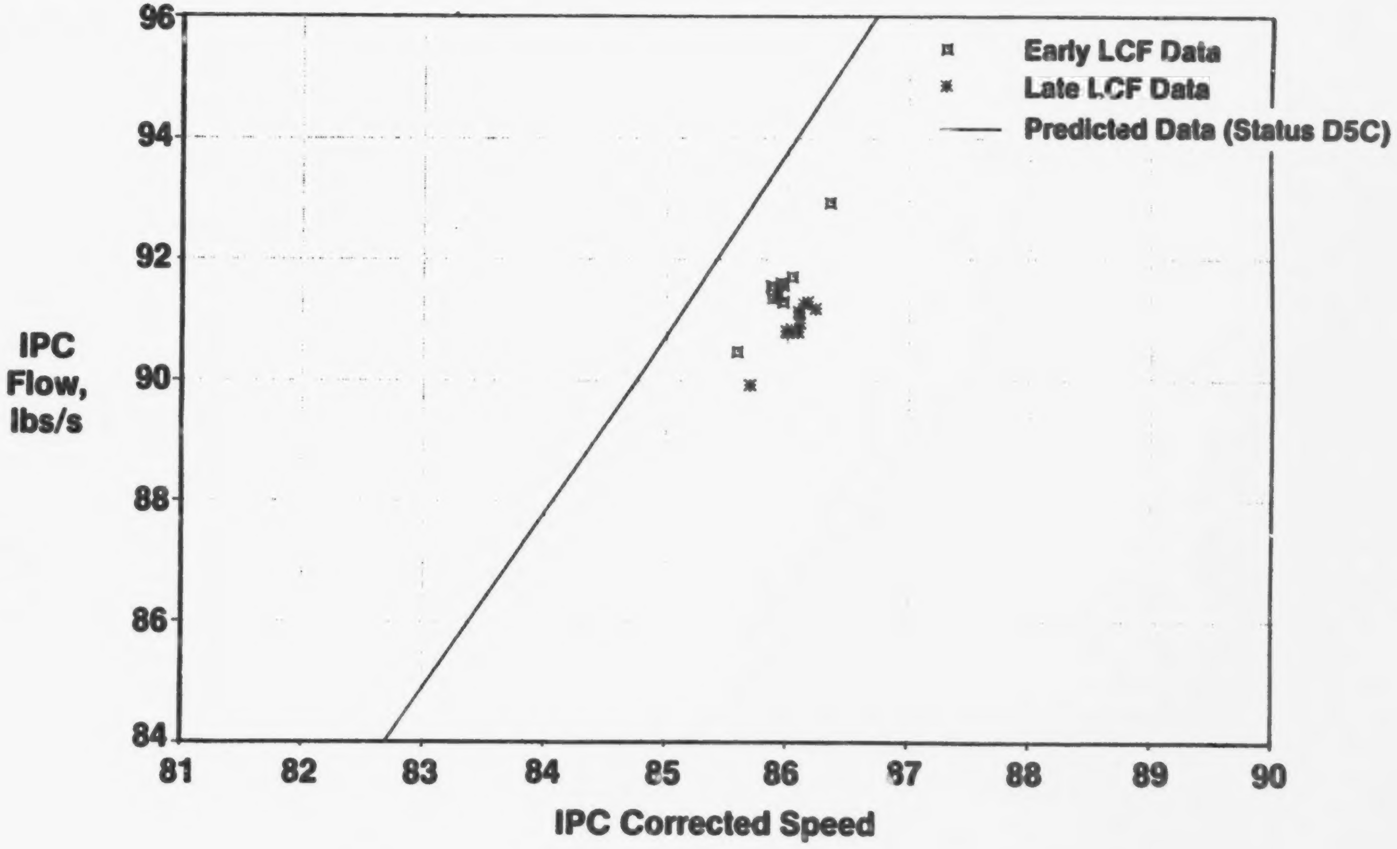

Figure 7-22. IPC Flow Versus IPC Corrected Speed.

the starting status, ending status, and data used to define the ending status against each other.

Figure 7-23 shows the core temperature ratio versus core pressure ratio. Figure 7-24 illustrates LPT flow function versus LPT energy function. Figure 7-25 demonstrates IPC stall margin versus IPC corrected flow. Figure 7-26 is a comparison of UDF™ thrust coefficient versus UDF™ power coefficient. Figure 7-27 depicts the overall performance, corrected installed sfc versus corrected installed thrust. Note that in all of the above comparisons, the Status D8B cycle more closely matches the test data than did the Status D5C cycle.

7.7 PERFORMANCE SUMMARY

In the testing of the UDF™ engine at Peebles, the following performance and capabilities were demonstrated:

Performance

- 25,000 lbf installed corrected thrust
- 0.232 lb/hr/lbf installed corrected specific fuel consumption
- 15,000+ physical total shaft horsepower.

Capabilities

- Running at full power statically
- Data was repeatable statically
- Prediction of low speed, low pressure, counterrotating turbine performance with an accuracy comparable to that of high speed, conventional, low pressure turbines.

Comparing data recorded early and late in the LCF testing, performance deterioration was confined to a dirty IPC; there was no evidence of mechanical deterioration.

7.8 KEY RESULTS

The F404 gas generator provided repeatable and predictable performance and was better than predicted at lower powers (below 70% takeoff power).

UDF™ blade performance sensitivity to rotational speed was much greater than predicted.

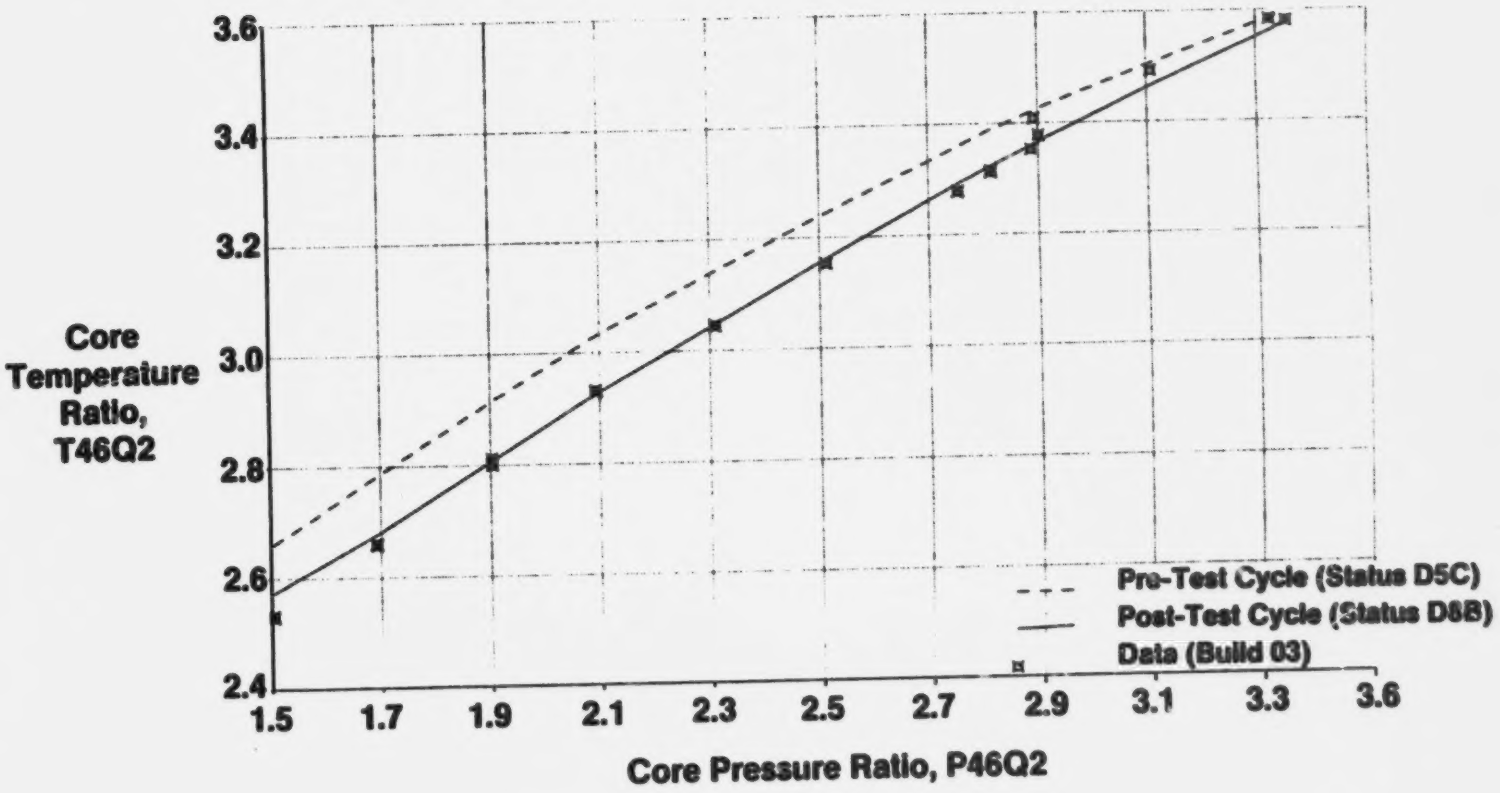

Figure 7-23. Compare Pretest Cycle Versus Posttest Cycle Versus Test Data.

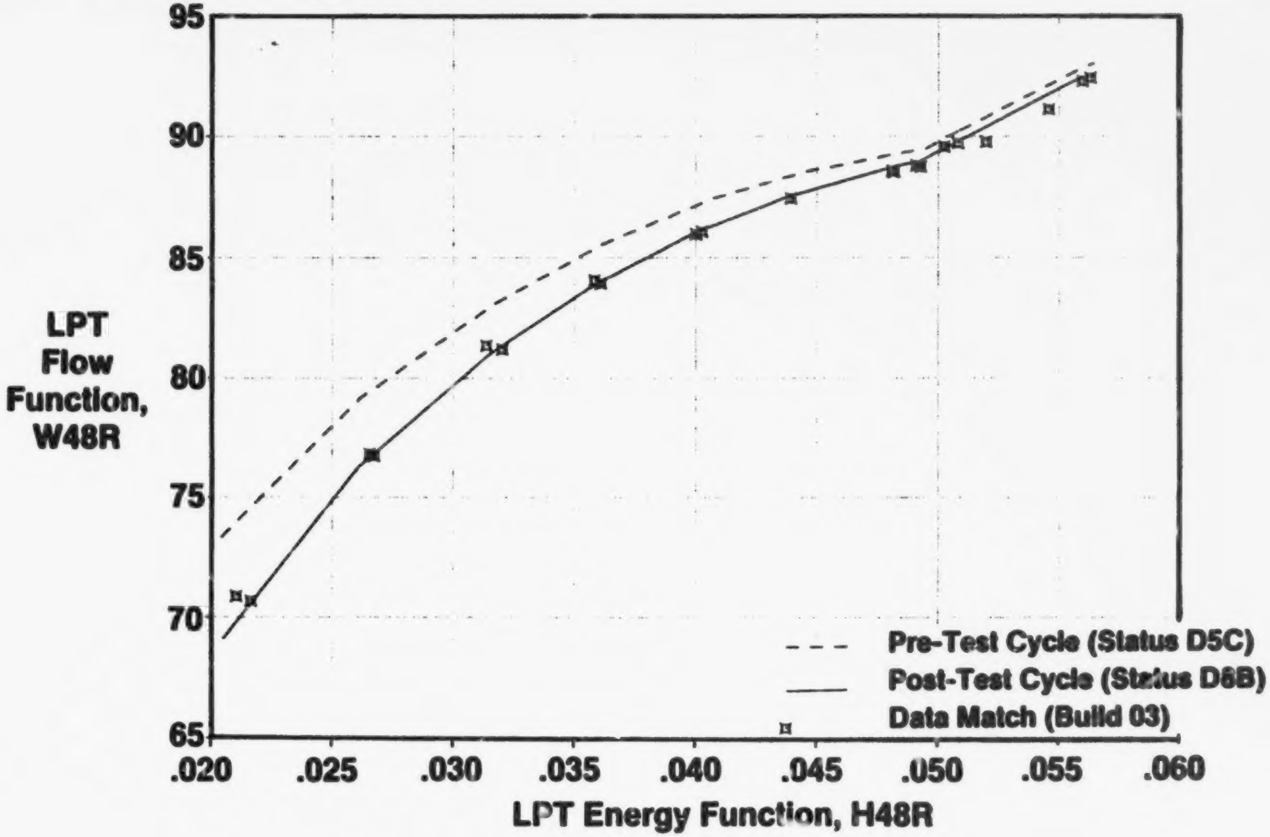

Figure 7-24. Compare Pretest Cycle Versus Posttest Cycle Versus Test Data.

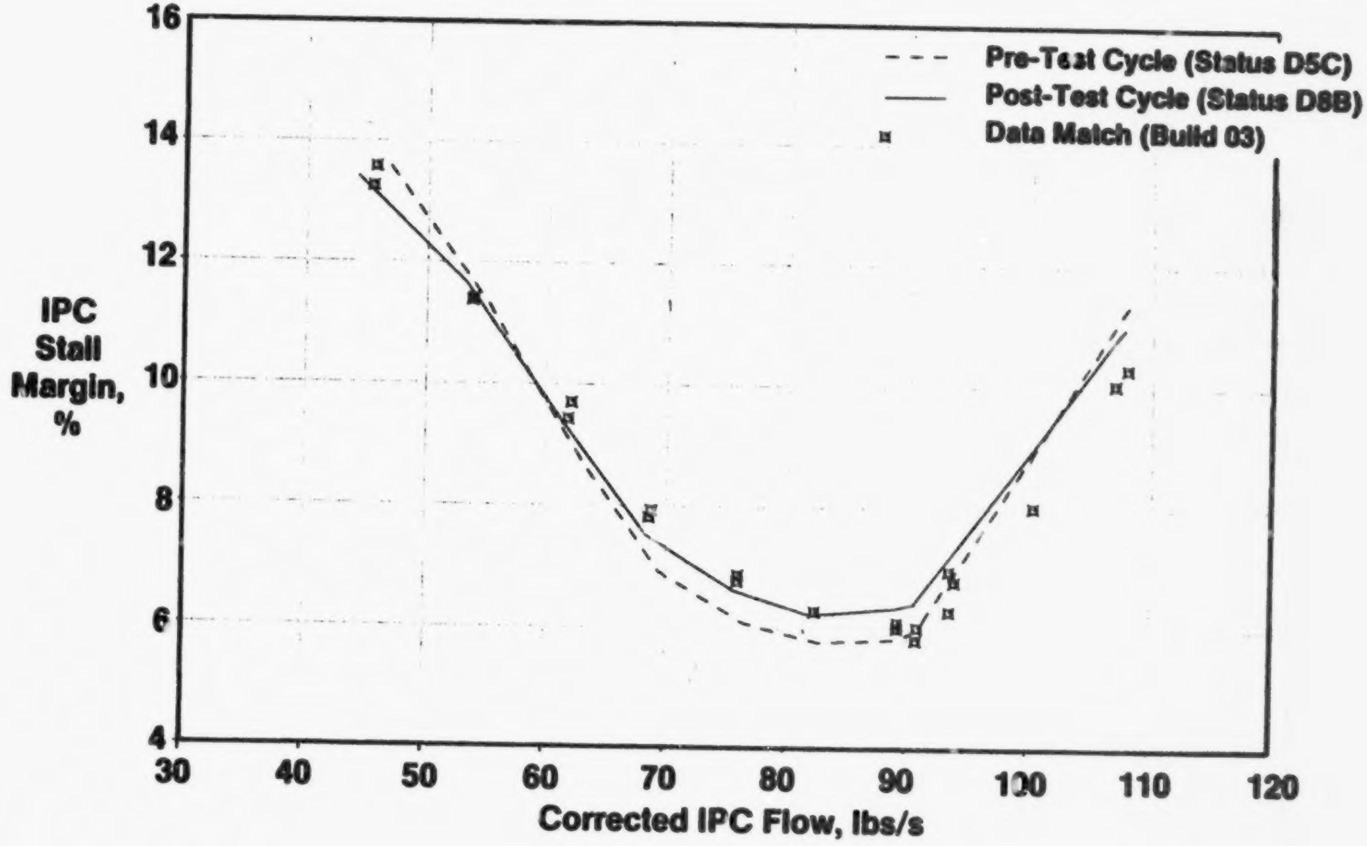

Figure 7-25. Compare Pretest Cycle Versus Posttest Cycle Versus Test Data.

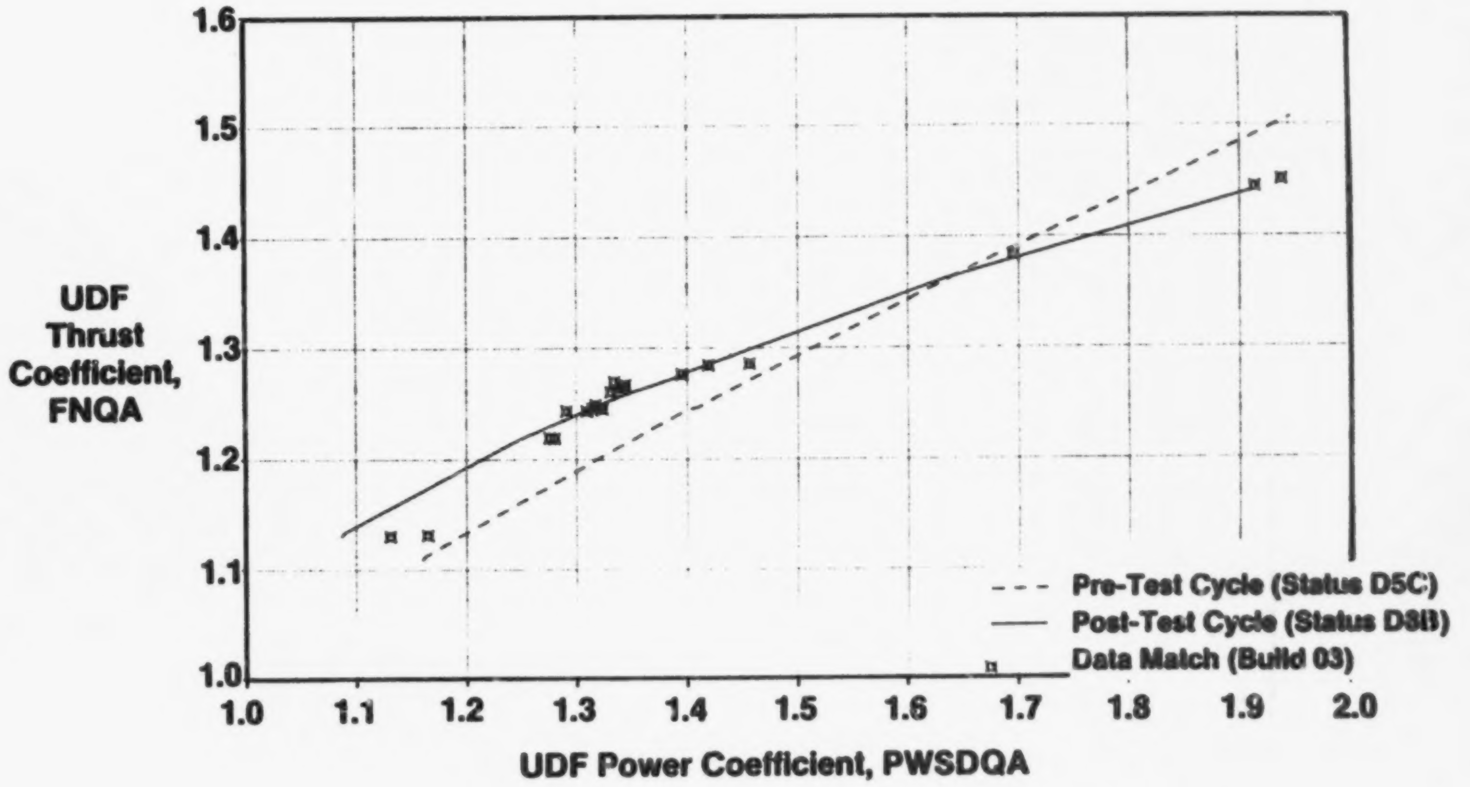

Figure 7-26. Compare Pretest Cycle Versus Posttest Cycle Versus Test Data.

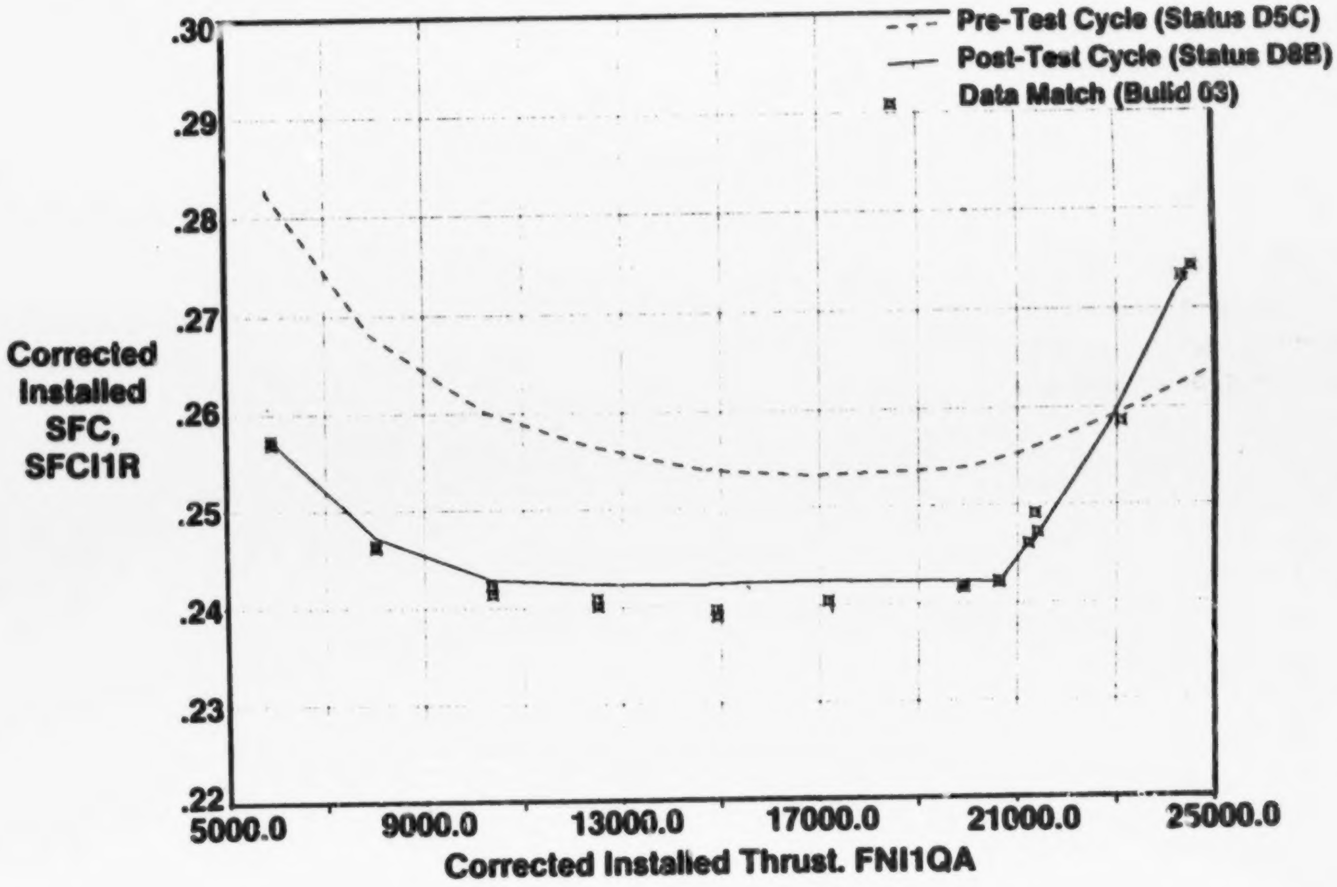

Figure 7-27. Compare Pretest Cycle Versus Posttest Cycle Versus Test Data.

At power coefficient = 1.32, thrust coefficient was 4% better than predicted (approximately 60% takeoff power). At power coefficient = 1.95, thrust coefficient was 4% worse than predicted (approximately 100% takeoff power).

Power turbine efficiency was approximately as predicted, being within +1.5 points over the major portion of the operating range. The flow function was within +0.5% of prediction at high powers (above 80% takeoff thrust).

Overall performance was better than predicted up to 92% takeoff power (23,000 lbf corrected installed thrust), but was poorer than predicted beyond 92% takeoff power (23,000 lbf corrected installed thrust) due to UDF™ speed sensitivity as noted above.

At 60% takeoff thrust (15,000 lbf), sfc was approximately 5.50% better than predicted. At 92% takeoff thrust (23,000 lbf), sfc was approximately as predicted. At 100% takeoff thrust (25,000 lbf), sfc was approximately 4.00% worse than predicted.

8.0 ENGINE OPERABILITY

The most important operability concern with the GE36 proof-of-concept engine is the stability of the IPC (F404 compressor). Replacing the F404 variable area exhaust nozzle with the GE36 UDF™ propulsor assembly reduced the Station 48 (F404 nozzle/UDF™ power turbine inlet) flow function by about 15%. This raises the IPC operating line (Figure 8-1) and reduces the stall margin. To help increase IPC stall margin and ensure stall-free operation of the IPC, two design modifications were incorporated:

- Variable Stator 1 and more closed IGV schedule (raises the IPC stall line)
- IPC bleed system (lowers the IPC operating line).

The GE36 proof-of-concept HPC has an adequate stability margin since the stall and operating lines are similar to those for the F404. Due to the more limited operating range and flight envelope encountered during GE36 ground and flight test, the stall margin requirements are lower.

8.1 IPC STALL MARGIN

Steady-state IPC operating lines at 2,750 ft/0Mn/+31° F and at 38,000 ft/0.80Mn/ISA, as predicted by the Status D6C cycle model, are shown in Figures 8-2 and 8-3. Also shown is the nominal IPC stall line and the, statistically, worst-case IPC stall line which includes analytical estimate of effects due to deterioration, inlet pressure distortion, and IPC tracking error. The nominal stall line shown in these figures is from the F404 green run results with the GE36 variable geometry schedule (Figures 8-1 and 8-4).

Transient cycle model predictions of IPC operating line migration during decel transients from maximum power with no IPC bleed and with maximum IPC bleed are included in Figures 8-2 and 8-3. These predictions demonstrate the need for, and potential of, the IPC bleed system to prevent IPC stalls during rapid decel transients.

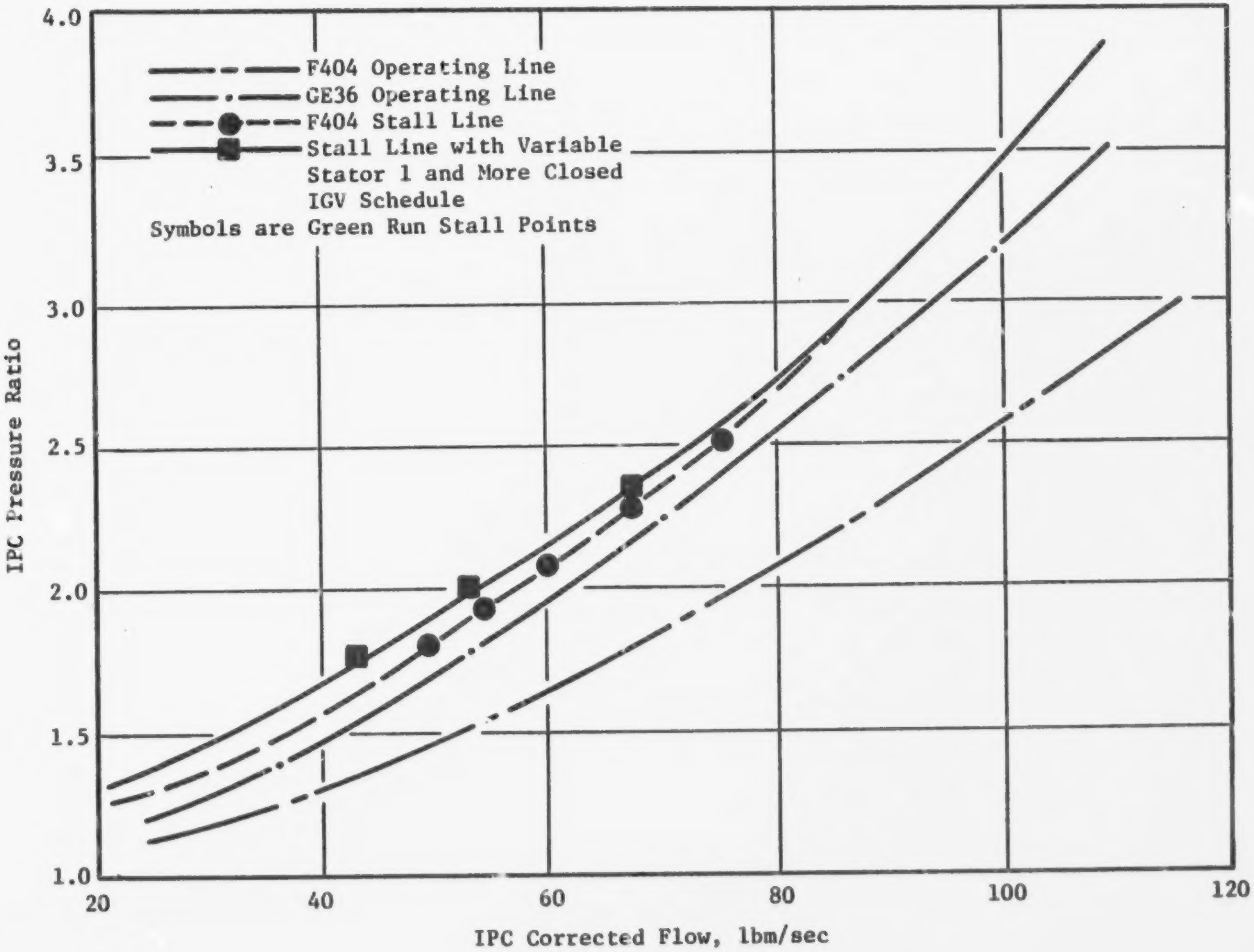

Figure 8-1. IPC Operating and Stall Line Sea Level Static.

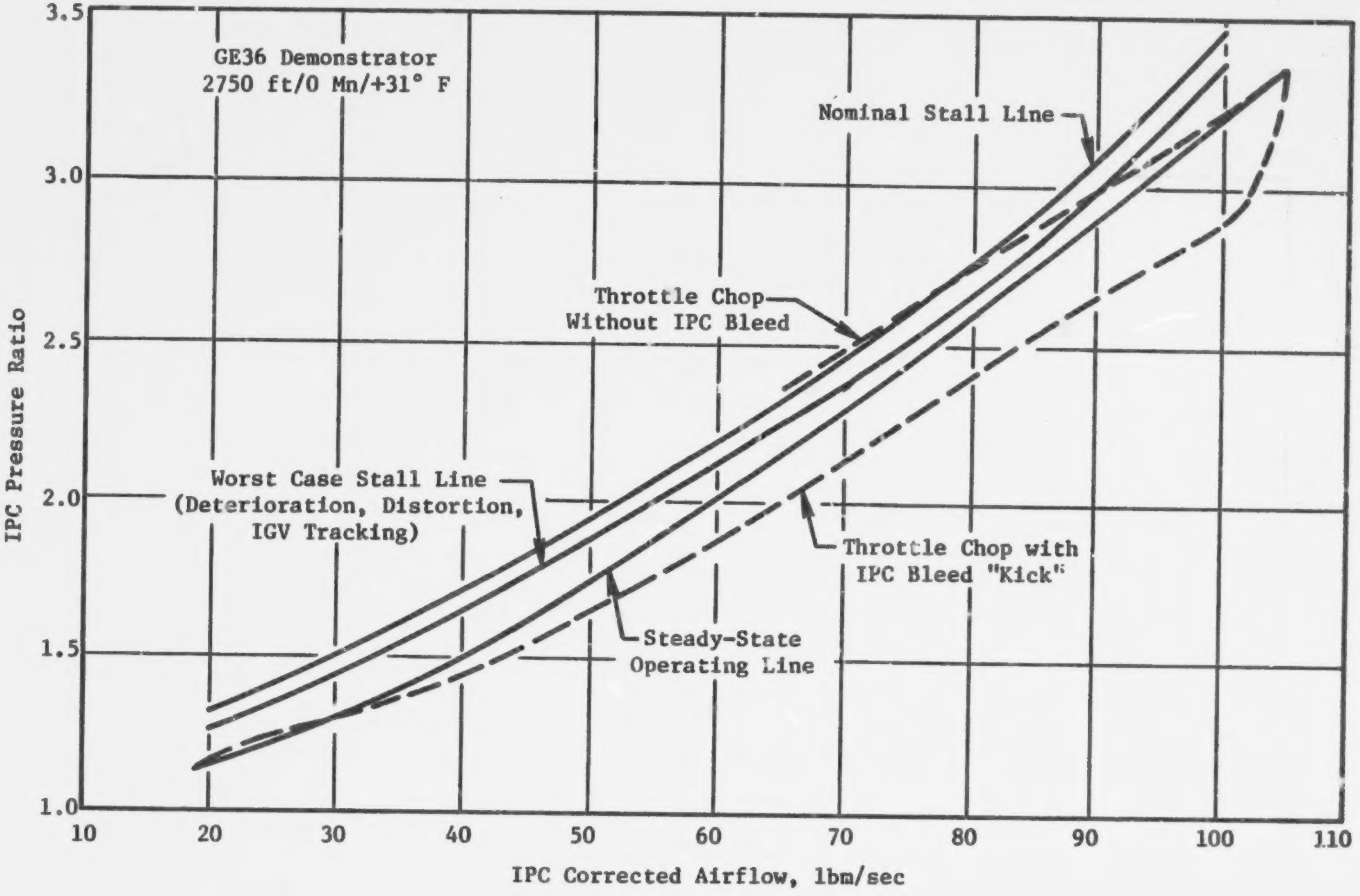

Figure 8-2. Steady-State IPC Operating Lines; 2750 ft.

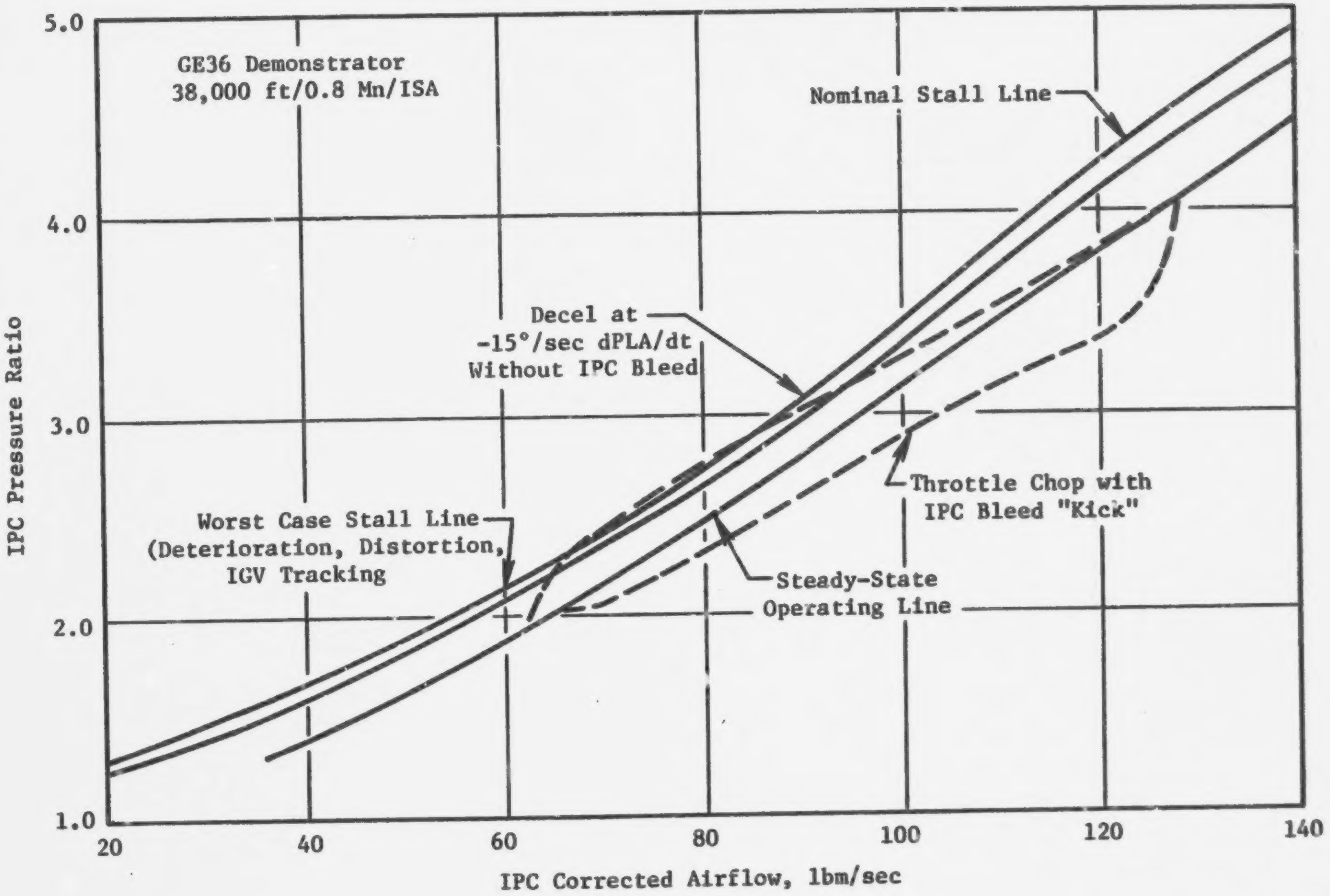

Figure 8-3. Steady-State IPC Operating Lines; 38,000 ft.

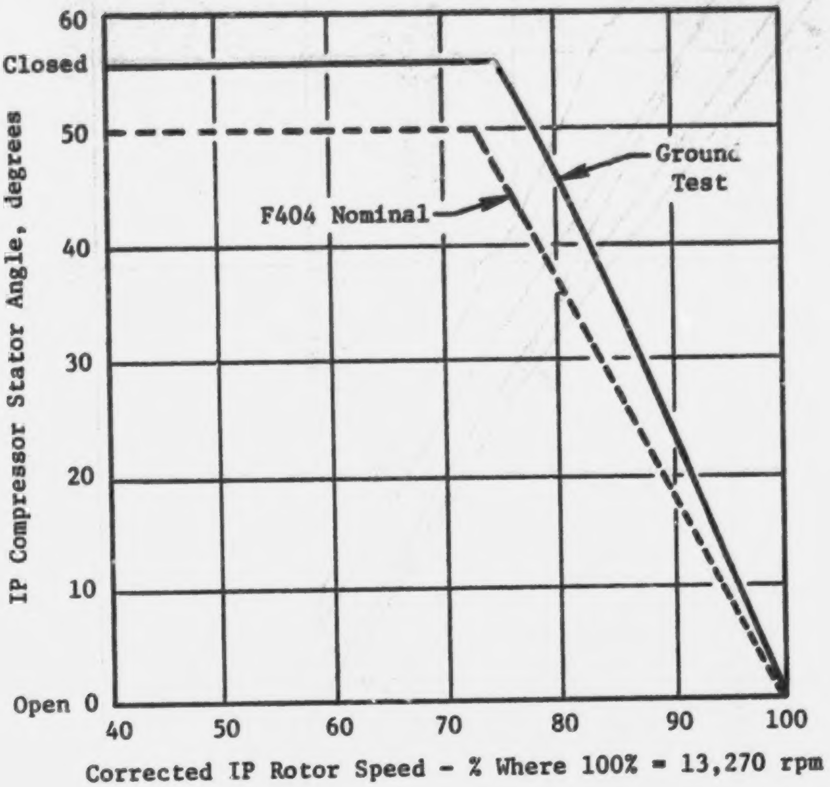

Figure 8-4. IPC Stator Schedule.

8.1.1 IPC Bleed Control System

The IPC bleed valve position is controlled by the DEC. The control logic opens the bleed valve in response to any one of the following inputs:

a. d(PLA)/dt - throttle retard rate > threshold
b. PLA - throttle step > threshold
c. d(P)/dt - IPC exit pressure decay rate > threshold
d. IPC P/P - scheduled maximum allowable P/P (f[XN2R]).

Thresholds "a" and "b" indicate a decel transient condition to the control, in which case additional IPC stall margin could be required. Threshold "c" would be exceeded in the event of engine surge. Schedule "d" is designed to maintain a minimum level of IPC stall margin under all normal operating conditions.

If thresholds a, b, or c are exceeded, the control logic is designed to "kick" the valve full open, hold for 5 seconds after the last demand for full open, and then ramp close in 5 seconds. The slow closing will avoid transient pressure pulses. In addition, for Input c, the control downtrims fuel flow to maximum authority, further decreasing engine system pressures. If scheduled Value d is exceeded, the control modulates the bleed valve to maintain the scheduled maximum allowable IPC pressure ratio. In the event multiple inputs are received, the valve kicking logic takes precedent.

8.1.2 Control Threshold for Throttle Retard Rate

Figures 8-2 and 8-3 show the PRS usage (stall pressure ratio normalized to stall line), as predicted by the transient cycle model, during decel transients from maximum power without IPC bleed. Shown are decels at various PLA rates at 2,750 ft/0Mn/+31° F and at 38,000 ft/0.8Mn/ISA. Also indicated in these figures is the current status available PRS and the minimum available PRS as a worst-case estimate. Figure 8-5 shows that with the current level of available margin at SLS (sea level static) conditions, an IPC stall would be predicted during a throttle chop from maximum power without IPC bleed, yet a decel transient at -10°/second d(PLA)/dt would not consume all of the current available margin. A decel transient from high power at -10°/second d(PLA)/dt, without IPC bleed, was successfully accomplished without stall during ground

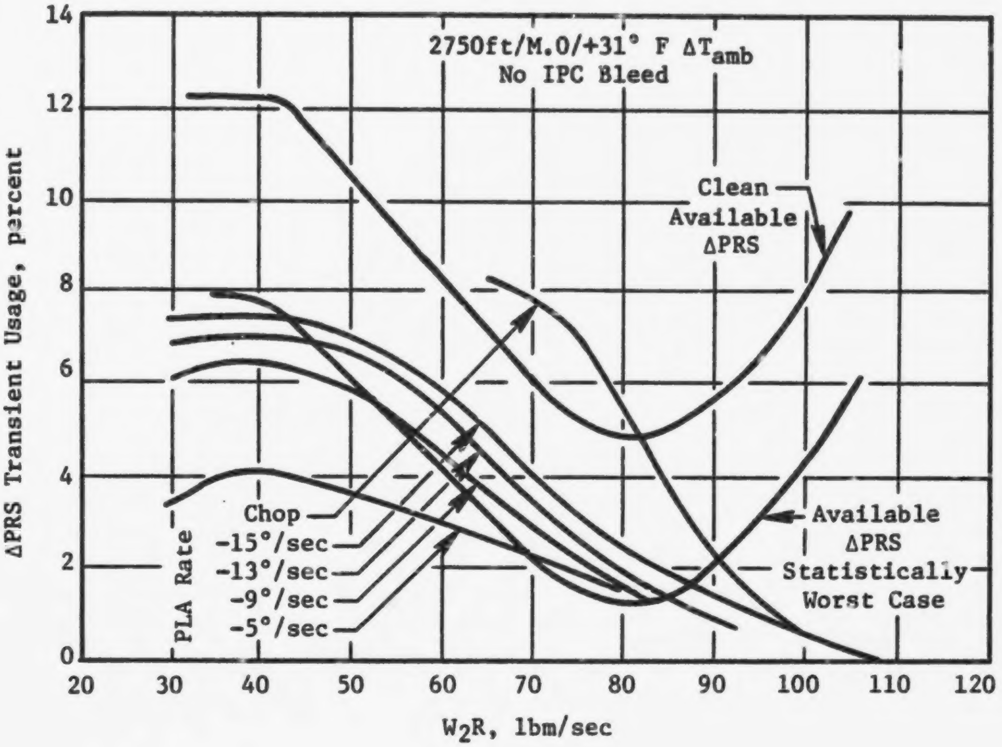

Figure 8-5. Predicted IPC ΔPRS Usage During Throttle Decels; 2750 ft.

testing; thus, confirming the analytical prediction. At altitude, however, the operating line migration during a decel exceeding -9°/second d(PLA)/dt is expected to consume all of the available margin, even at the current quality of the engine (Figure 8-6).

Considering the statistically worst-case IPC stability condition, Figures 8-5 and 8-6 show that even an IPC bleed kick threshold of -5°/second d(PLA)/dt is not sufficient to assure stall-free operation. This illustrates the necessity of the maximum allowable P/P schedule (bleed valve modulation).

8.1.3 Maximum Allowable IPC Pressure Ratio Schedule

The maximum allowable IPC pressure ratio (P15/P2 versus XN2R) was set at approximately 1% above the engine ground test operating level (Figure 8-7). This was accomplished at the end of ground testing, after analysis of control measurement data. The effect of the expected control measurement variation on this maximum allowable P/P schedule was determined to be equivalent to approximately +0.015 PRS (pressure ratio schedule).

This bleed modulation function will be effective during steady-state operation if the IPC operating line migrates upward due to the altitude/Mach effects (not predicted) or deterioration effects. It will also be effective during decel transients which do not exceed IPC bleed kick threshold levels.

8.1.4 Final IPC Bleed Control Status

During the engine ground testing, the IPC bleed system was successfully demonstrated; proper mechanical function and pressure relief capability were verified. Each of the control inputs (a through d) were individually checked and verified. By the end of the ground test, threshold levels were adjusted to appropriate levels, as follows:

a. d(PLA)/dt (throttle rate threshold = -5°/second)
b. PLA (throttle step threshold = -2°/0.25 second)
c. d(P15)/dt (IPC exit pressure decay rate threshold = -20%/second
d. P15/P2 versus XN2R (scheduled maximum allowable IPC pressure ratio set at approximately 1% above engine ground test operating level).

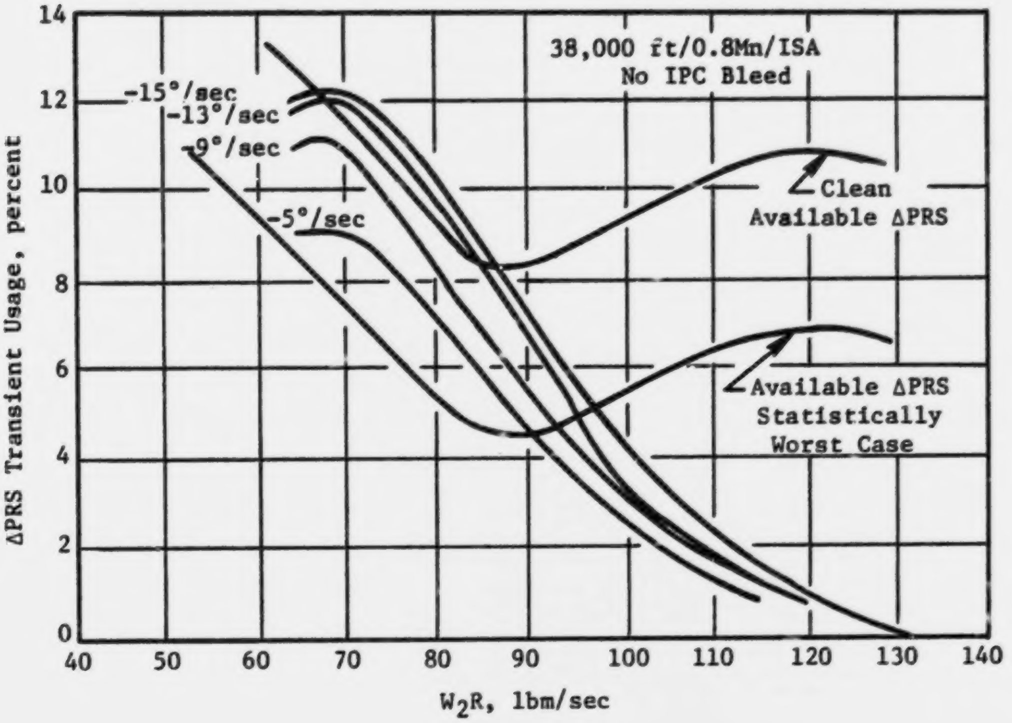

Figure 8-6. Predicted IPC ΔPRS Usage During Throttle Decels; 38,000 ft.

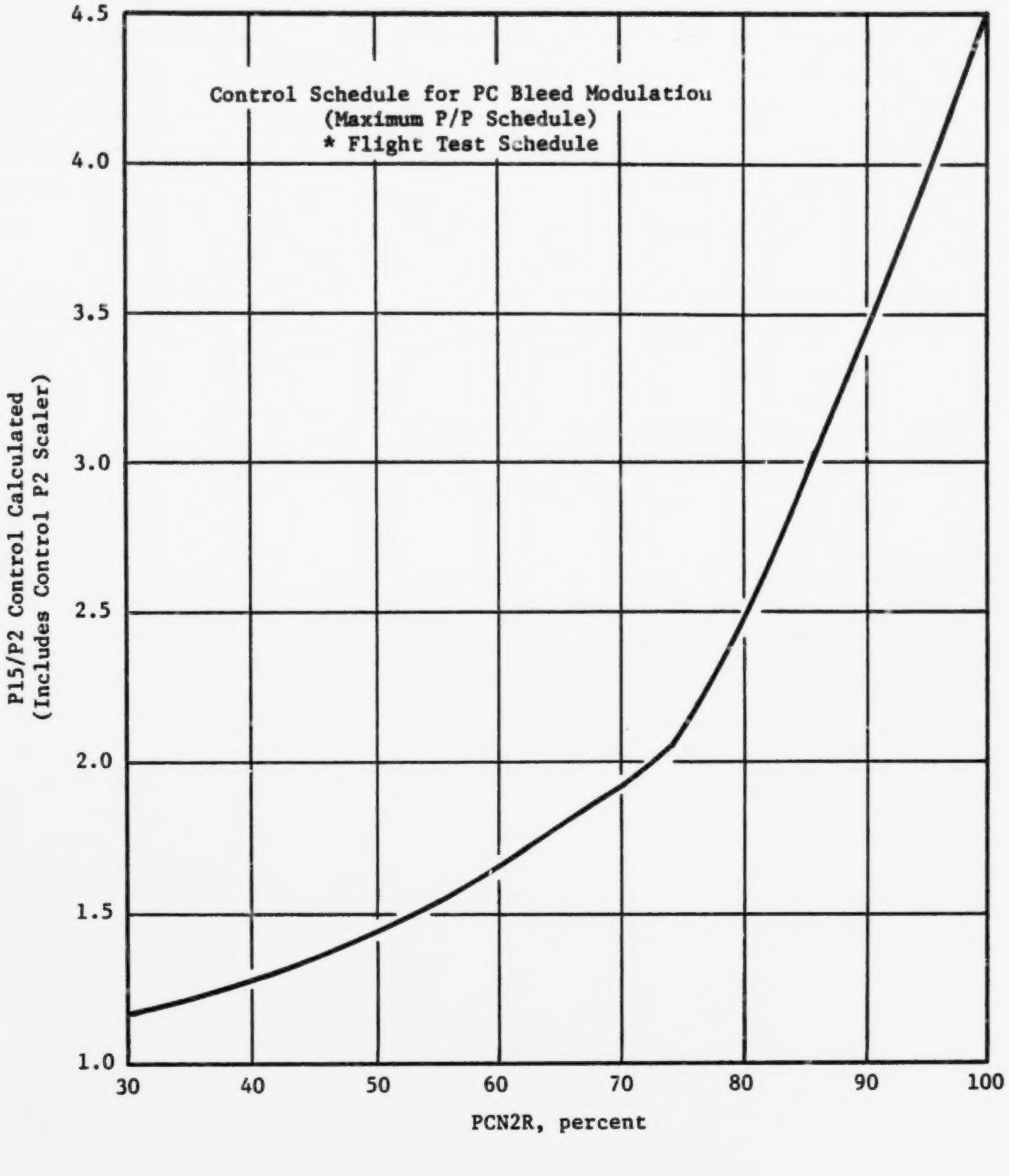

Figure 8-7. Maximum Allowable IPC Pressure Ratio.

Figures 8-8 and 8-9 show the predicted PRS usage during decel transients at 2,750 ft/0Mn/+31°F and at 38,000 ft/0.8Mn/ISA, with bleed system control thresholds set as defined previously. For decel transients which exceed -5°/second d(PLA)/dt, the kick function is effective, and the PRS transient usage is zero. This was demonstrated during a throttle chop from high power in which the bleed valve kicked open, and the transient data indicated that the IPC operating line during decel was lower than the steady-state level. For decel transients which do not exceed -5°/second d(PLA)/dt, the bleed modulation function is effective. If the operating line migrates above the steady-state ground test level, the control will modulate the bleed to maintain the maximum allowable P/P during the decel.

Figures 8-8 and 8-9 show that the IPC bleed control system should prevent the IPC operating line from migrating to even the worst-case stall line, thus, assuring stall-free operation.

8.2 TRANSIENT TESTING EXPERIENCE

Table 8-1 summarizes the significant transient tests conducted. Small PLA accels and decels were conducted to verify control functions and to adjust control gains to appropriate levels to ensure control stability; control fault trips were checked, resulting in throttle chops and stopcocks.

Several unintentional decel transients were encountered, both operator and control initiated, due to instrumentation faults and operating limits. For cycle operability evaluation, large PLA accels, decels, and bodes were conducted. All transient testing of the demonstrator engine during ground testing was accomplished without adverse results.

8.3 ENGINE TRANSIENT PERFORMANCE ANALYSIS AND PREDICTIONS

The transient cycle model is used to predict the operating line migration of the compression components during engine transients. In order to foresee any stall or operational problems prior to transient testing, good agreement between the cycle model predictions and test data is necessary. Two engine transients conducted during the ground test were simulated by the transient cycle model with good results; a throttle chop from 97% thrust and a throttle

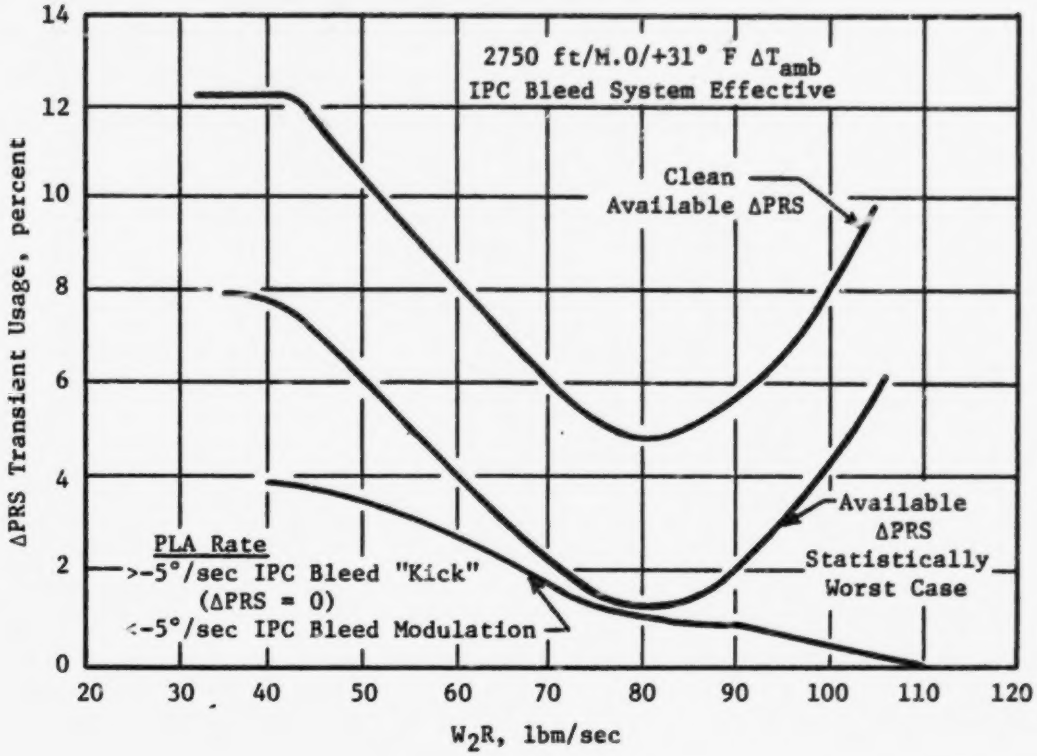

Figure 8-8. Predicted IPC ΔPRS Usage During Throttle Decels; 2750 ft.

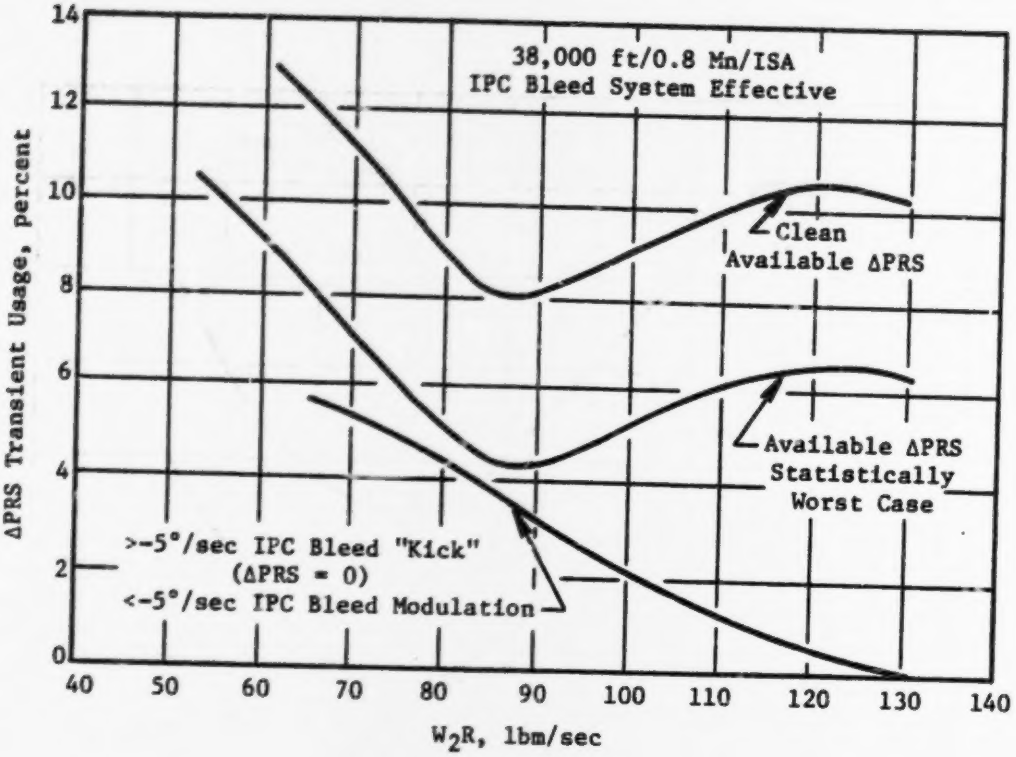

Figure 8-9. Predicted IPC ΔPRS Usage During Throttle Decels; 38,000 ft.

burst to 20,000 thrust. Figures 8-10 and 8-11 show the transient cycle model simulations, as compared to the test data, for selected parameters.

The results of these comparisons provide confidence in transient cycle model predictions of IPC operating line migration during decel transients which were used in designing and optimizing the IPC bleed control system.

Table 8-1. Significant Transients - GE36 Proof-of-Concept.

Date	Maneuver	Reason
2-09-86	Throttle Chop from 24,000 Fn	No. 7 Aft Blade Debonded
4-18-86	Stopcock at 11,000 Fn	XN49 O/S Trip
7-8-86	10 Throttle Bursts to 18,000 Fn	Planned
7-8-86	2 Throttle Bursts to 20,000 Fn	Planned
7-8-86	Throttle Burst to 21,000 Fn, Chop to Idle	Planned/Overspeed
7-8-86	2 Bodes (Chop from 20,000 Fn to Idle, Burst to 20,000 Fn)	Planned

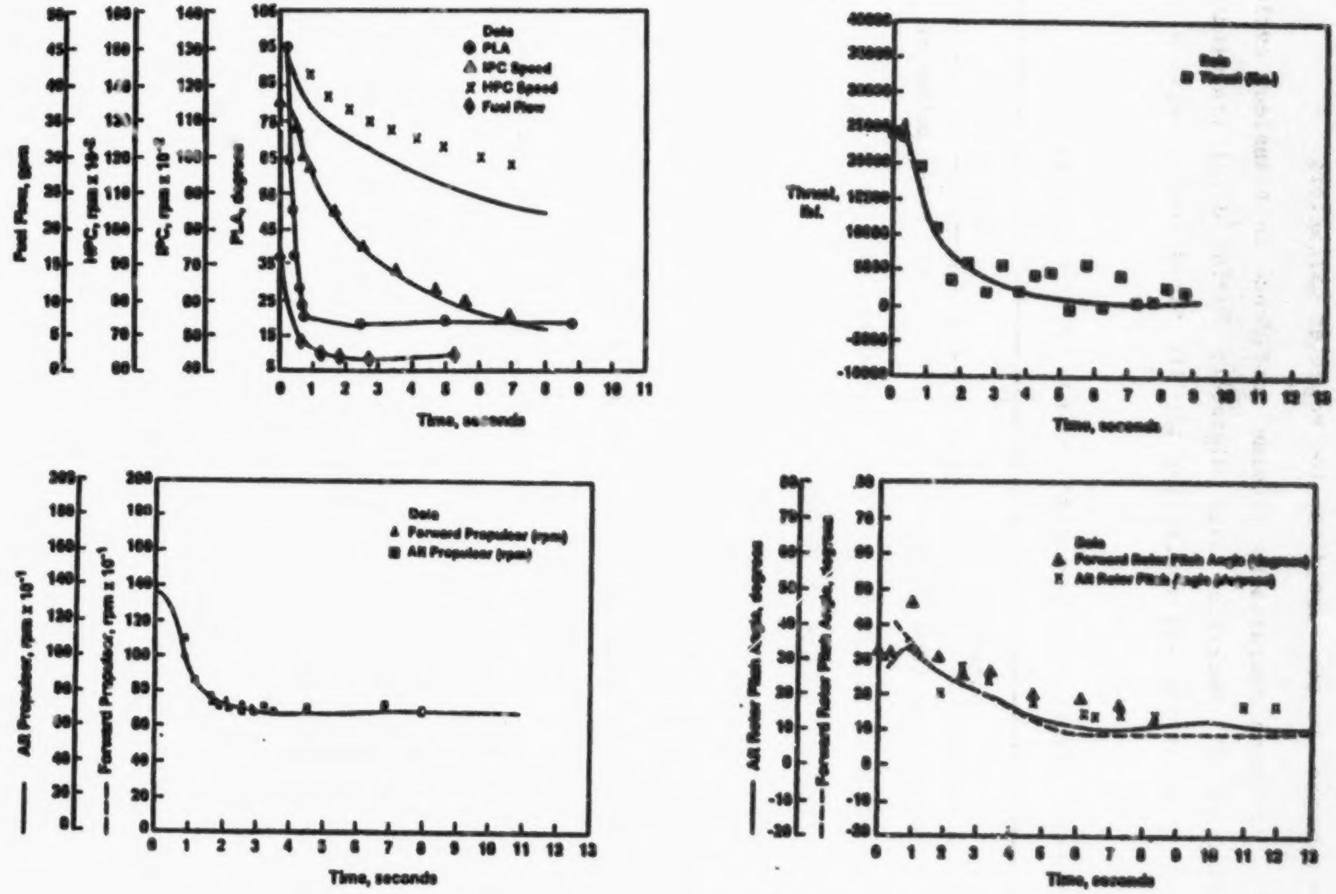

Figure 8-10. Transient Testing Analytical Comparison with Updated Transient Cycle Deck T/C from 97% Takeoff Thrust.

ORIGINAL PAGE IS
OF POOR QUALITY

ORIGINAL PAGE IS
OF POOR QUALITY

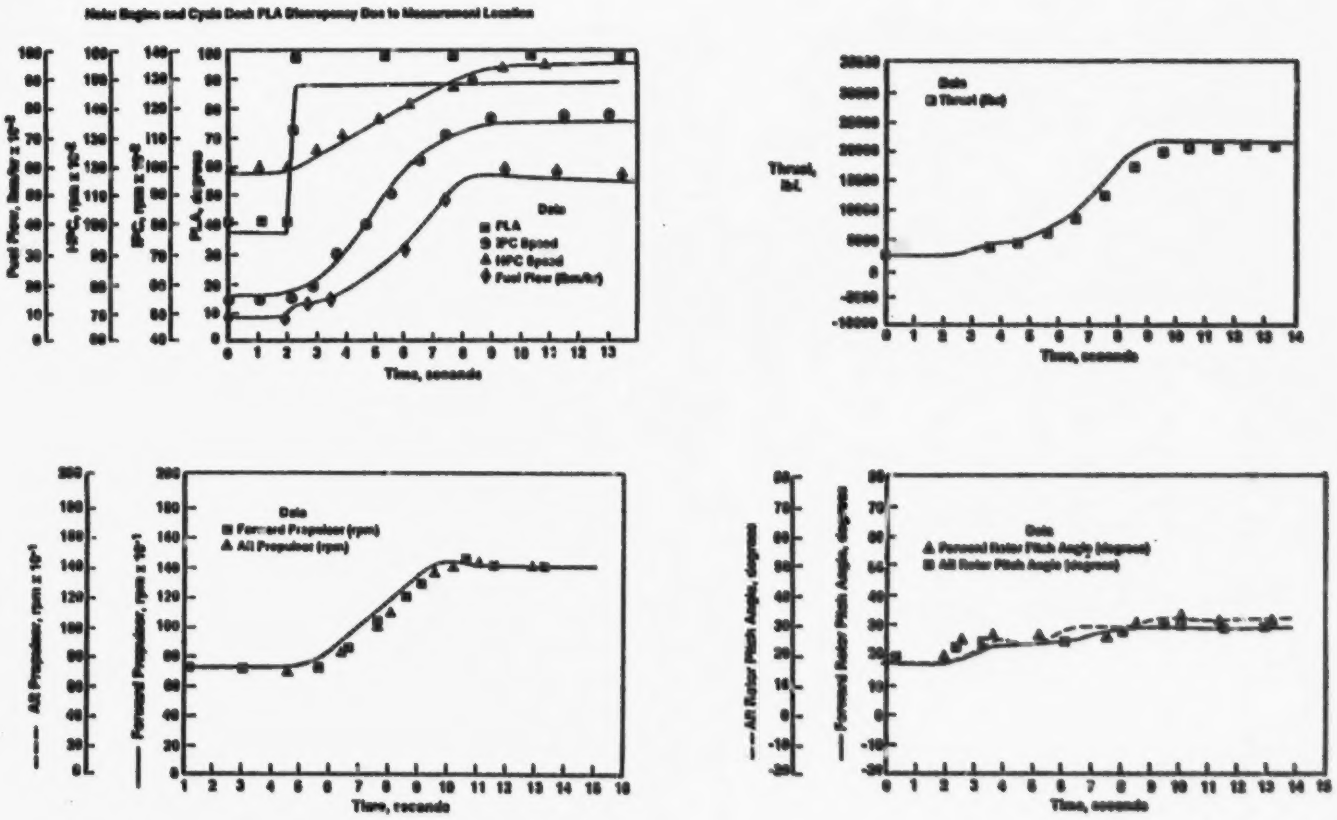

Figure 8-11. Transient Testing Analytical Comparison with Updated Transient Cycle Deck Burst to 20,000 lb Thrust.

9.0 ENGINE CONTROL

This section provides a summary of the GE36 control system performance during the ground test program performed at GE's engine test facility near Peebles, Ohio. This summary is divided into three parts; each portion covers the milestones associated with each of the three engine builds.

9.1 BUILD 1 - ENGINE CONTROL TESTING

The control system performance for Build 1 was successful. A limited amount of testing was performed due to the propulsor turbine failure.

9.1.1 Speed Sensing Anomaly

During Build 1 testing, it was discovered that the speed being sensed by the control for the forward propulsor rotor (XN48) was incorrect. A further study as to the cause showed that the gaps in the target wheel, which was divided into eight segments, were inducing a superfluous signal onto the magnetic speed-sensing pickups (Figure 9-1). This caused a higher sensed speed, up to two times actual. The situation was initially corrected by a change in speed signal processing. A more elegant solution was identified for implementation on Build 2. This solution consisted of locating the teeth on the target wheel directly at the segment gaps (Figure 9-2).

9.1.2 Pitch Control

For Build 1, the engine was controlled to pitch angle, rather than to propulsor speed.

9.1.3 Gas Generator Control

The gas generator control performed as expected. The EPR (engine pressure ratio), HP (high pressure) and IP (intermediate pressure) stator control, and the control of the duct bleed system all exhibited stable operation during this engine build testing. A new control strategy for stall avoidance and recovery for the duct bleed system was identified during this build and was incorporated into the control system during Build 2.

- Original Design
- 6 Segments Total
- 1 Tooth Centered In Each Segment

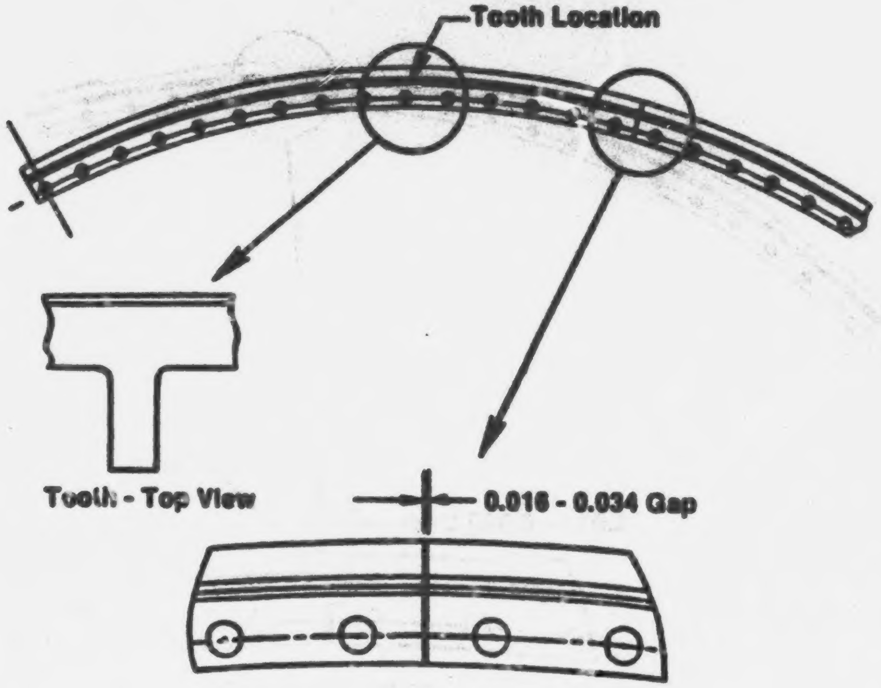
Tooth Location
Tooth - Top View
0.016 - 0.034 Gap

Figure 9-1. Fan Speed Sensor Segments.

- Redesign
  - 8 Interlocking Segments
  - 1 Tooth Per Segment
  - Tooth Positioned On End
  - Gap Width Reduced

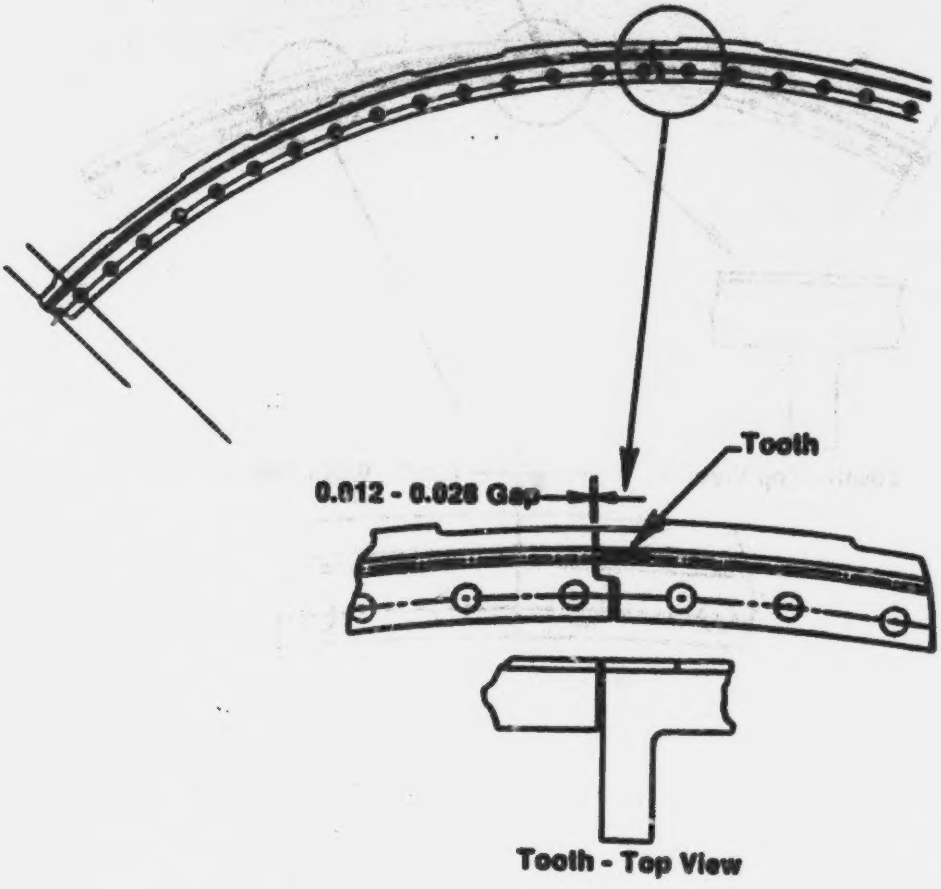
Tooth
0.012 - 0.028 Gap
Tooth - Top View

Figure 9-2. Fan Speed Sensor Segments.

9.1.4 Throttle System

The throttle system was redesigned to minimize hysteresis. The resolver was relocated to the HMU (hydromechanical unit) fuel lever to provide a more accurate indication of fuel lever angle. A rotary potentiometer was added to the system at the throttle converter to provide an input for PLA which would provide for a reverse indication and redundancy for the resolver.

9.1.5 Engine Starting

Starting tests during this build achieved expected results. The engine was first dry motored to check instrumentation and control signals. After successful dry motoring, the engine was wet motored (engine motoring with fuel on), also without incident. After wet motoring, the engine was fired to idle power. The control performed as expected, successfully controlling HP rotor speed to the HP rotor starting speed schedule. Due to the aforementioned speed sensing anomaly, limited propulsor speed control testing was performed.

9.1.6 Off-Engine Harnesses

Crosstalk was observed on multiconductor off-engine cables during testing as well as inaccuracies on alternating current type sensors. This situation was corrected by placing twisted pairs for each circuit inside the same shield and removing unused pairs.

9.1.7 Lube Oil Bypass

Scavenge capability of the propulsor lube oil system was marginal during Build 1 testing. A solution was identified for use on Build 2. This solution involved installing in the propulsor lube system a bypass valve which allowed lube oil into the propulsor only after a light-off had been detected by the control. This prevented excess lube oil from entering the propulsor during start operations, thus minimizing the effects.

9.2 BUILD 2 - ENGINE CONTROL TESTING

Due to lessons learned during Build 1 testing, Build 2 testing involved further testing of the engine in the realms of transient testing, verification of control schedules, and modifications to the control. This testing further demonstrated the stability of the control system. Full control was maintained under a blade-out condition.

9.2.1 Speed Control

Closed-loop speed control (modulation of fan pitch to maintain scheduled fan speed) was used by the control successfully for all power settings, with the exception of reverse and windmill testing. The propulsor speed was demonstrated to be stable from 550 rpm to 1400 rpm and from idle to 25,000 lbs, corrected thrust. This modulation of pitch to control fan speed also was demonstrated for Mach numbers up to 0.1 using facility fans.

9.2.2 Duct Bleed

Modifications to the duct (fan bypass) bleed control logic were verified for P15Q2, PLA chop, and simulated stall. A throttle chop from 97% takeoff thrust was performed without IPC stall; also, unrestricted throttle chops from all power settings were performed. Figure 9-3 is a schematic of the engine bleed system.

9.2.3 Transient Testing

A limited number of small, part, and full power throttle chops and small part power accelerations were performed. During a throttle burst from idle to 1150 rpm, an overspeed incident occurred. It was determined to have been caused by the fan pitch actuator becoming force-limited due to a too rapid response time of the gas generator. A fix was identified to slow down the accel rate of the core by putting an accumulator on the CDP (compressor discharge pressure) sensing line to the HMU. A preliminary fix was installed on the engine which adequately slowed the core accel rate. A more polished design was used on Build 3.

As a result of the blade-out incident, the engine was chopped from 24,000 corrected thrust to idle, then stopcocked approximately 10 seconds later. As illustrated in Figures 9-4 through 9-8, the control system maintained complete control during the blade-out, chop to idle, and subsequent stopcock.

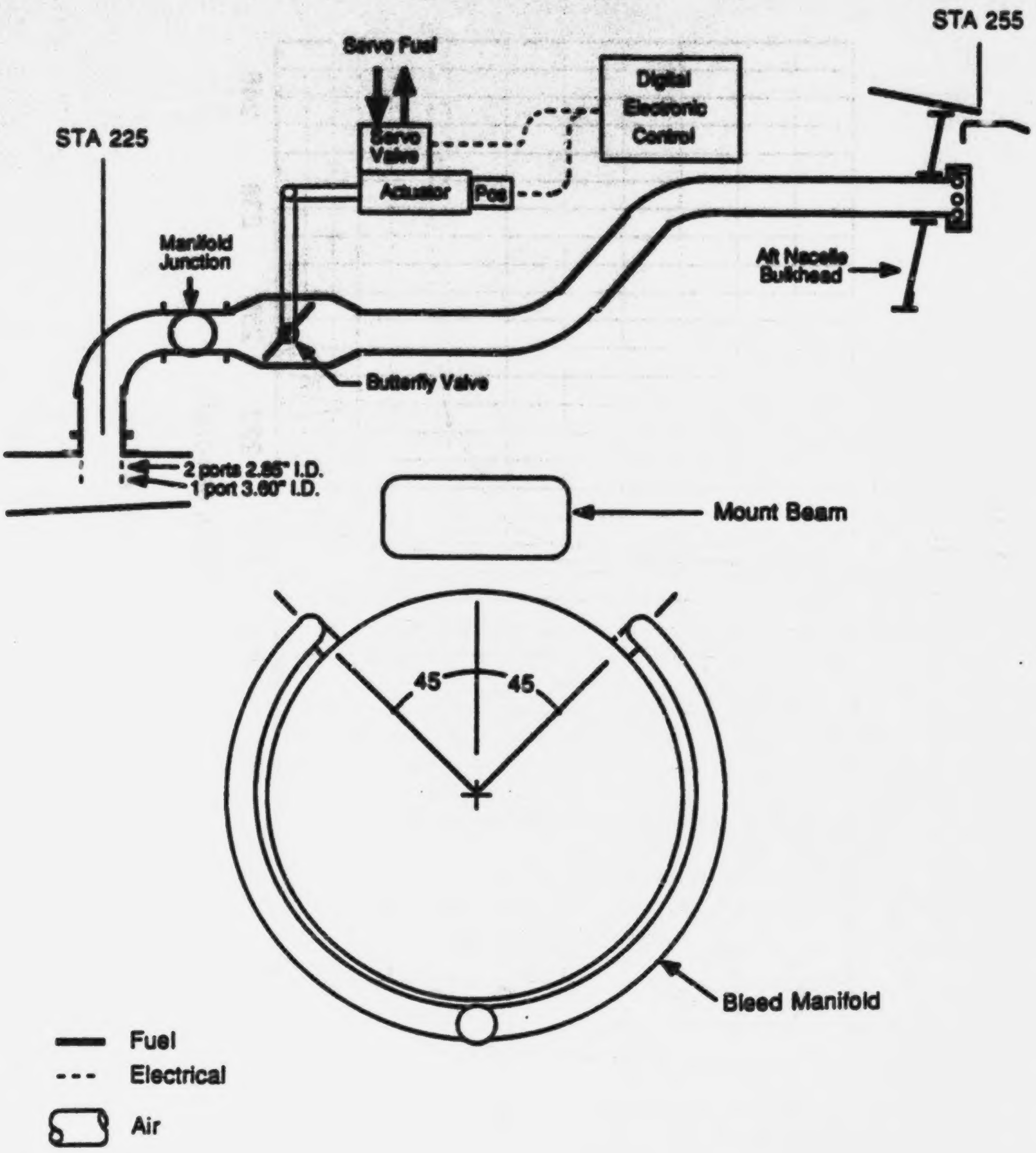
STA 255
Servo Fuel
Digital Electronic Control
STA 225
Servo Valve
Actuator
Pos
Manifold Junction
Aft Nacelle Bulkhead
Butterfly Valve
2 ports 2.85" I.D.
1 port 3.60" I.D.
Mount Beam
45
45
Bleed Manifold
Fuel
Electrical
Air

Figure 9-3. Duct Bleed System.

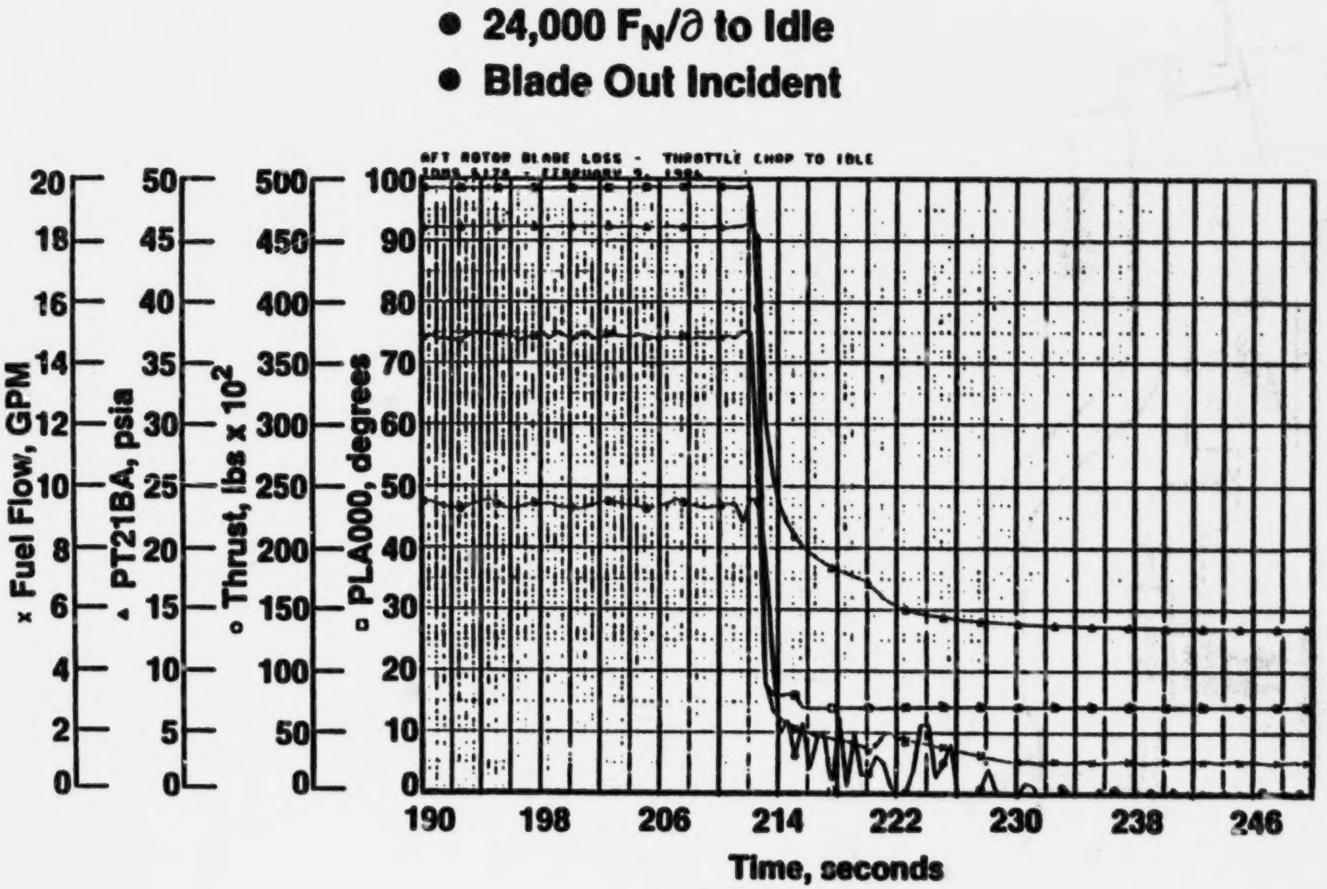

Figure 9-4. Throttle Chop Decels.

- 24,000 F_N/∂ to Idle
- P46Q2 Control Prior to Chop
- Blade Out Incident

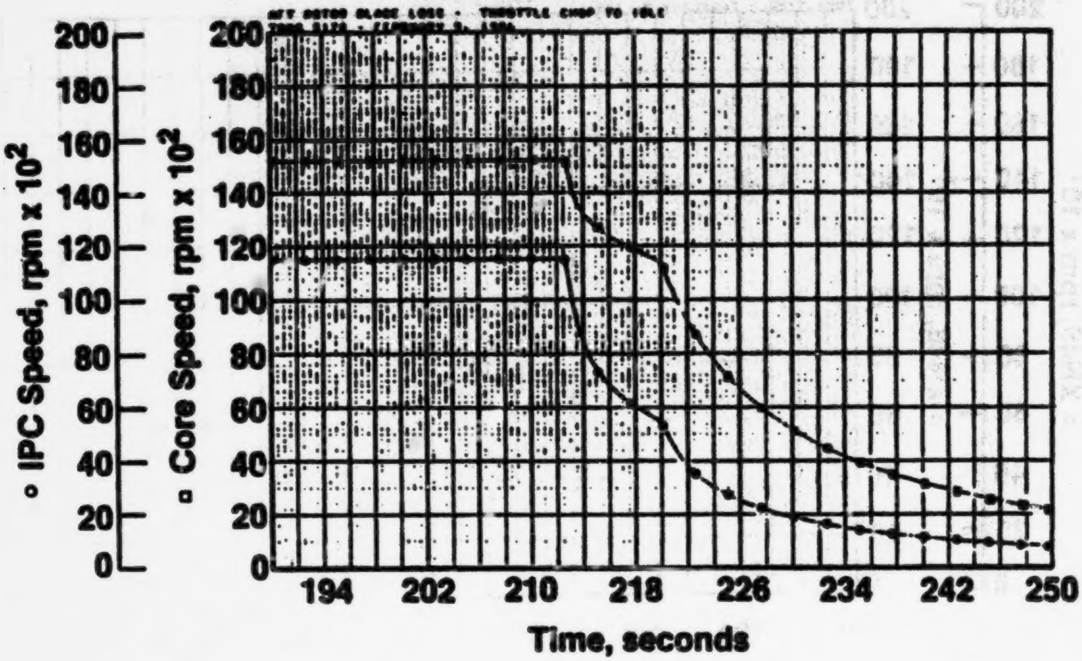

Figure 9-5. Throttle Chop.

ORIGINAL PAGE IS
OF POOR QUALITY

- 24,000 F_N/∂ to Idle
- P46Q2 Control Prior to Chop
- Blade Out Incident

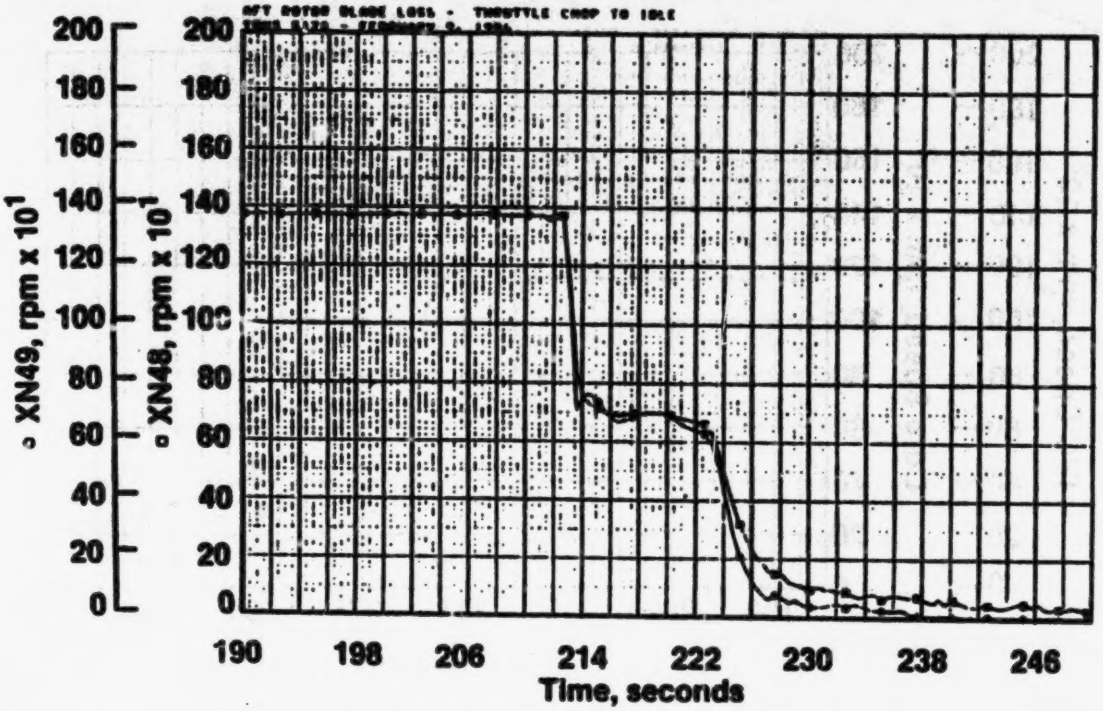

Figure 9-6. Throttle Chop.

ORIGINAL PAGE IS
OF POOR QUALITY

ORIGINAL PAGE IS
OF POOR QUALITY

- **24,000 F_N/∂ to Idle**
- **P46Q2 Control Prior to Chop**
- **Blade Out Incident**

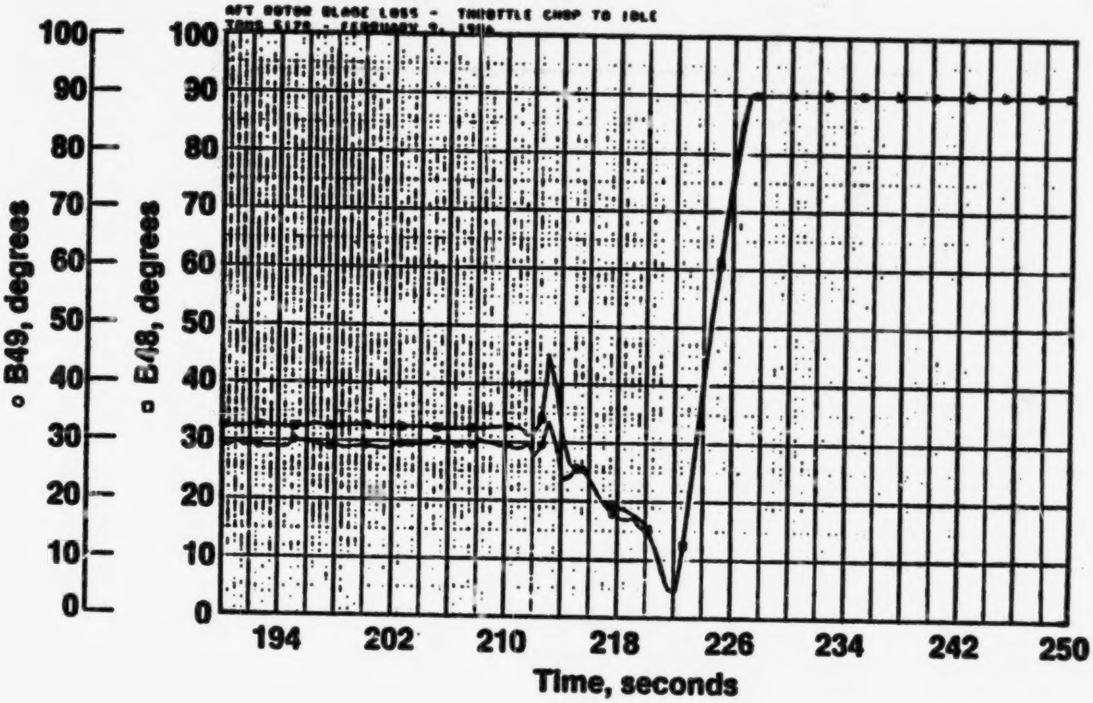

Figure 9-7. Throttle Chop.

- 24,000 F_N/∂ to Idle
- P46Q2 Control Prior to Chop
- Blade Out Incident

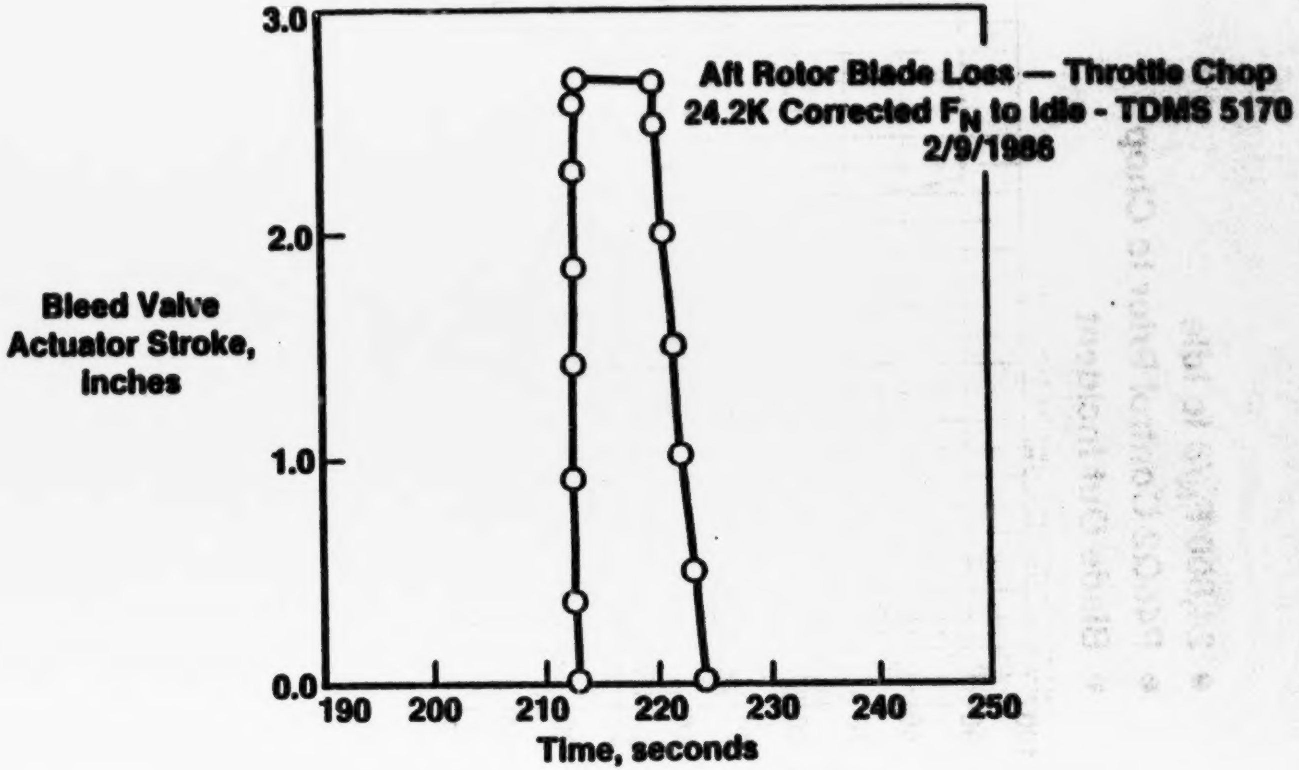

Figure 9-8. Throttle Chop.

9.2.4 Control Parameters

All control parameters were stable.

9.2.5 Vibration System

The vibration monitoring system proved to be functional; however, it was discovered that there was not enough gain in the amplifier for small vibration signals. As a result of the blade-out incident, readings were gathered that allowed for the scaling of the vibration signal. To increase its gain by a factor of four, the amplifier was reworked; this change was implemented during Build 3 testing.

9.2.6 Overspeed System

The capability of the overspeed system was demonstrated during an overspeed incident. During a throttle burst from 550 to 1150 rpm, the fan pitch actuator became force-limited and was unable to modulate fan pitch to control rear rotor speed. An overspeed condition resulted, which was quickly sensed by the overspeed system which immediately shut down the engine in a controlled manner.

9.2.7 Reverse Testing

Limited by the telemetry system, this due to high temperatures, reverse testing for Build 2 consisted of a throttle push from idle to 1000 rpm (3000 lb reverse thrust at static conditions). Figures 9-9 through 9-12 illustrate a transient from forward idle, to reverse idle; then throttle is pushed until a maximum propulsor speed of 1000 rpm is obtained, followed by a decel and return to forward idle. The fan speed is controlled by modulating pitch in forward thrust, and PLA is used to schedule pitch directly in reverse thrust, hence, the difference in propulsor speeds in reverse thrust.

9.2.8 Control System Modifications

Two areas of the control system hardware were modified during this build to improve performance. The hardware modified was the pitch actuation system transfer valves and the watchdog monitor circuit of the control computer.

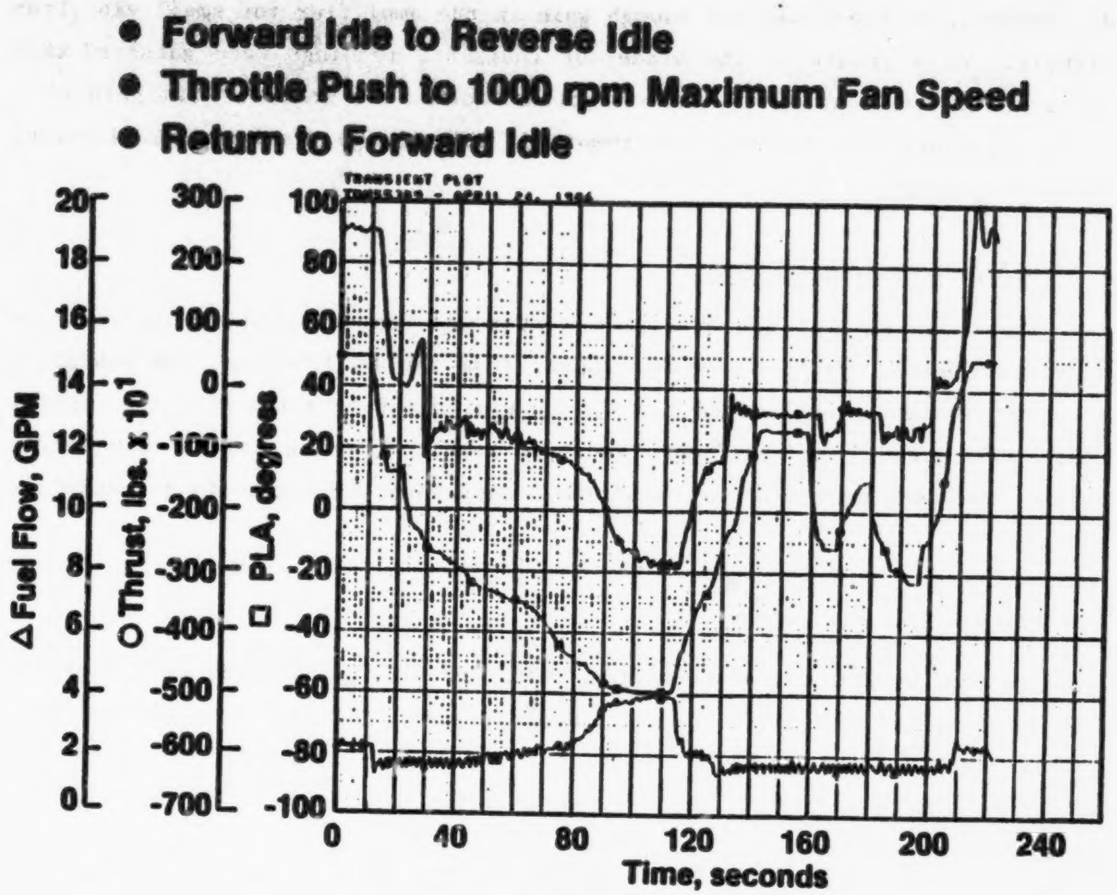

Figure 9-9. Reverse Thrust.

- **Forward Idle to Reverse Idle**
- **Throttle Push to 1000 rpm Maximum Fan Speed**
- **Return to Forward Idle**

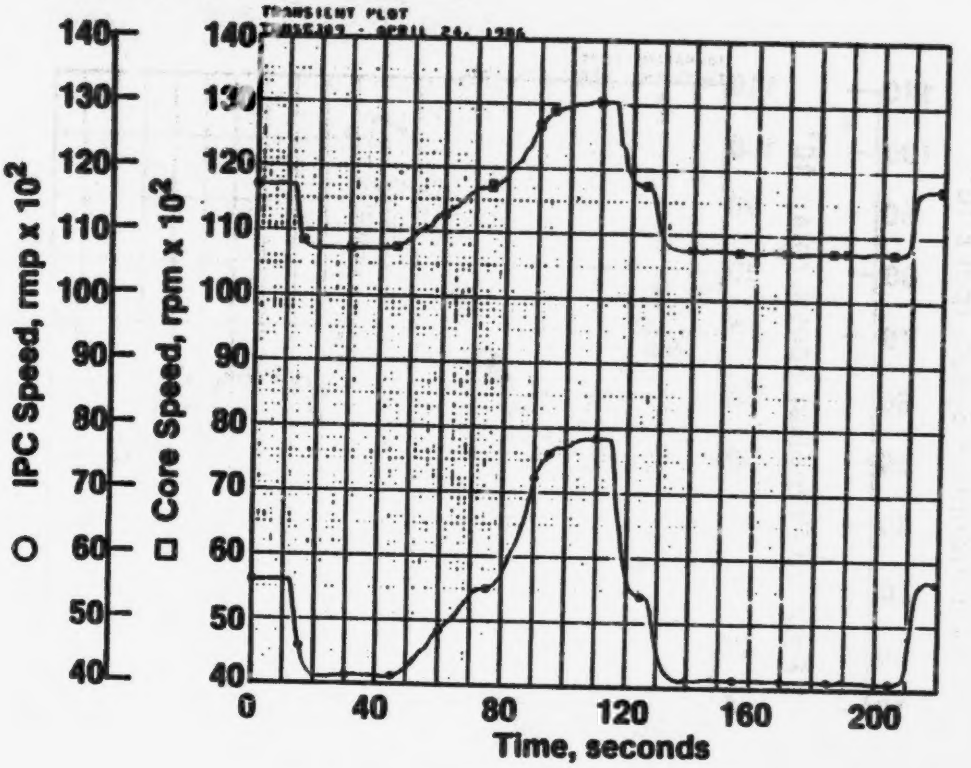

Figure 9-10. Reverse Thrust.

- Forward idle to Reverse idle
- Throttle Push to 1000 rpm Maximum Fan Speed
- Return to Forward Idle

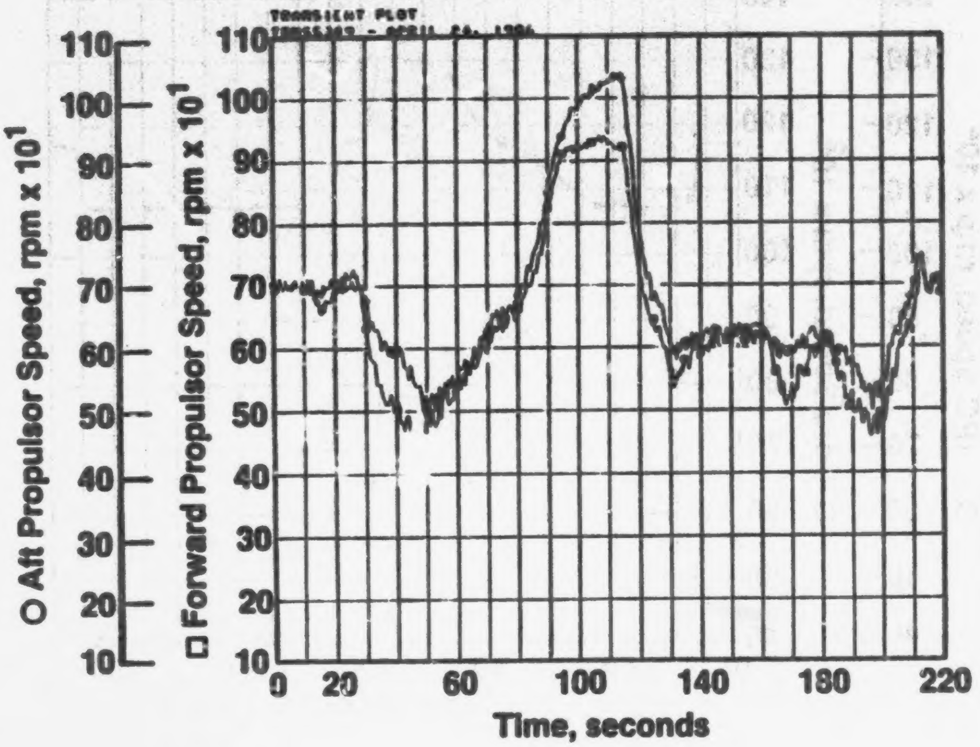

Figure 9-11. Reverse Thrust.

ORIGINAL PAGE IS
OF POOR QUALITY

ORIGINAL PAGE IS
OF POOR QUALITY

- **Forward Idle to Reverse Idle**
- **Throttle Push to 1000 rpm Maximum Fan Speed**
- **Return to Forward Idle**

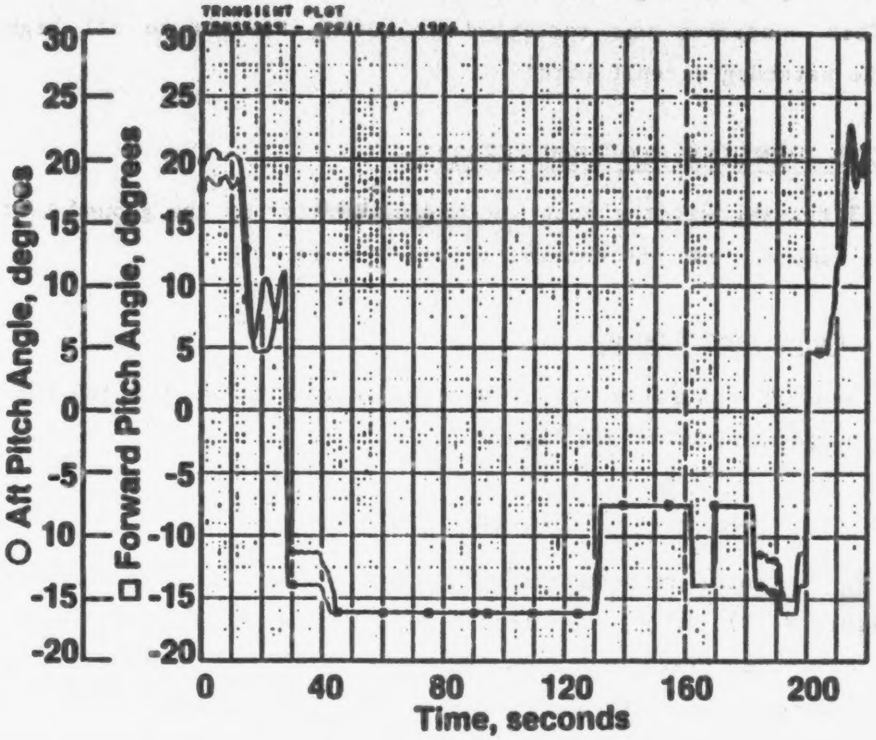

Figure 9-12. Reverse Thrust.

The transfer valves exhibited erratic performance during the beginning of this build. It was determined that the filtering of the hydraulic oil was inadequate. To correct this problem, the filters for the hydraulic system were changed from 5 micron to 3 micron.

The watchdog monitor circuit on the control initiated several inadvertent automatic shutdowns, later discovered to be caused by noise on the backplane of the control propagating into the watchdog circuit and inducing erroneous pulses. This condition was corrected by adding filters to all high speed lines on the watchdog circuit card.

9.3 BUILD 3 - ENGINE CONTROL TESTING

Build 3 testing was the most successful portion of the ground test, both in terms of time on test and control system testing.

9.3.1 Endurance Testing

Pitch and EPR controller gains were optimized during the 100 LCF cycles which were performed (Reference Figure 3-54).

9.3.2 Core Response Modifications

The gas generator response time was reduced with an orifice/accumulator system (Figure 9-13) in the CDP (compressor discharge pressure) line to the HMU (hydromechanical unit) and a control rate control. This modification was due to an overspeed incident caused by a force-limited actuator. The orifice/accumulator was sized to give an 8-second idle-to-rated-thrust response.

9.3.3 Reverse Thrust Testing

Reverse testing during Build 3 achieved maximum speeds of 850 rpm limited by high telemetry temperatures.

9.3.4 UPS (Uninterruptable Power Supply) Systems

The UPS systems for the control were successfully demonstrated during this build. The UPS powered the control computer, the overspeed unit, and the peripheral computer. The UPS systems were tested, by removing/reconnecting

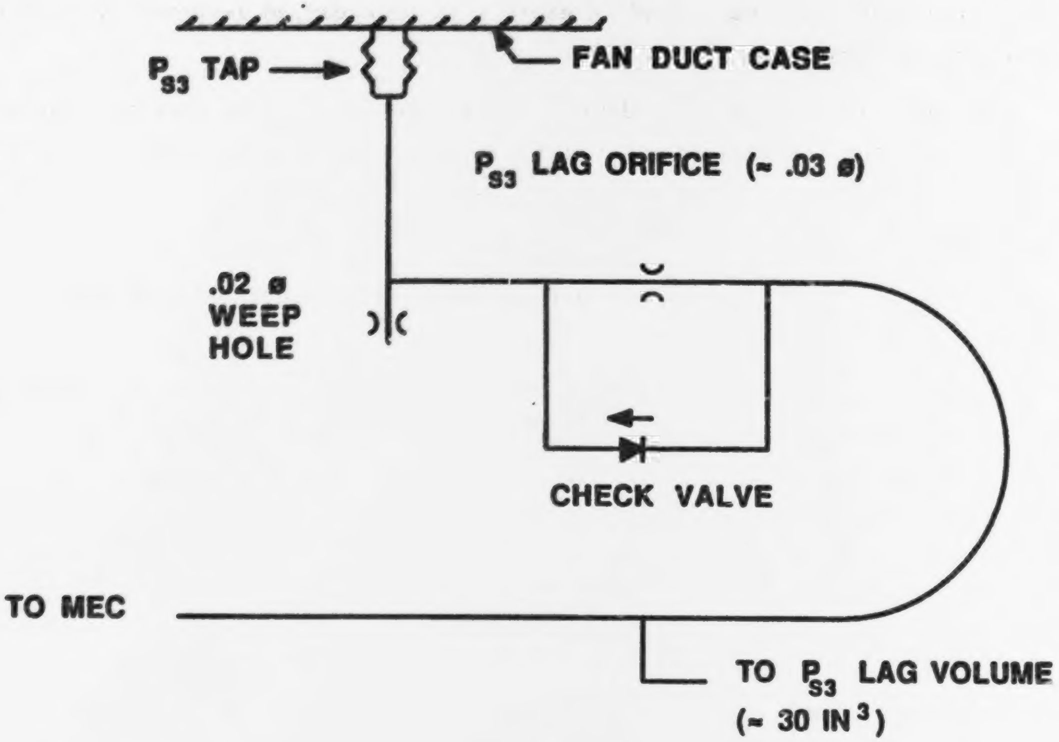
FAN DUCT CASE
P_{S3} TAP
P_{S3} LAG ORIFICE (≈ .03 ø)
.02 ø WEEP HOLE
CHECK VALVE
TO MEC
TO P_{S3} LAG VOLUME (≈ 30 IN^3)

Figure 9-13. P_{S3} Accumulator Configuration.

input power, both statically and with the engine running without affecting control performance in any way.

9.3.5 Transient Testing

Transient testing consisted of accelerations, decelerations, and throttle bodes. The controller was found to exhibit an underdamped response above 2.85 engine pressure ratio.

Figures 9-14 through 9-17 depict a throttle burst from idle to approximately 18,500 lbf. Satisfactory control response was demonstrated.

9.4 SUMMARY

Testing of the UDF™ provided valuable data and demonstrated the viability of the unducted fan concept and its control system.

Further, test results verified that the control system concepts of using EPR as the thrust parameter and utilizing EPR to schedule propulsor speed are sound. The modulation of pitch to maintain scheduled propulsor speed has been demonstrated statically and for Mach numbers up to 0.1.

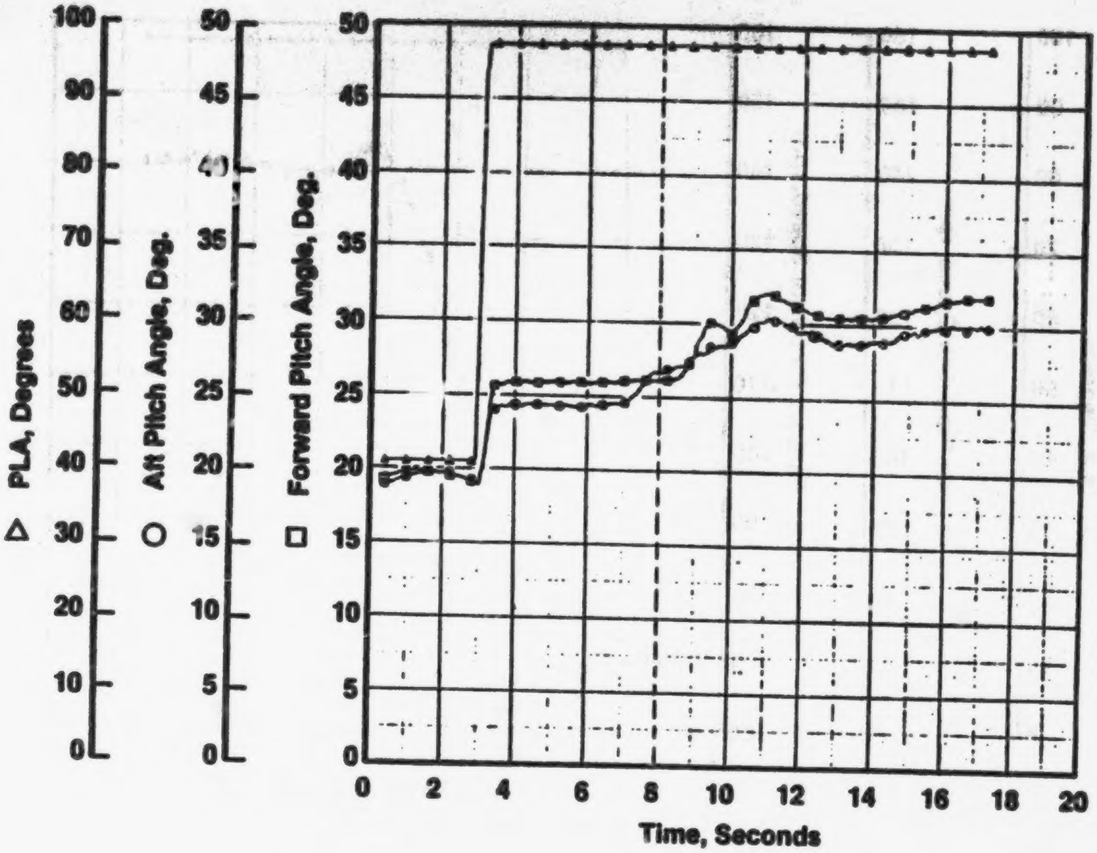

Figure 9-14. Throttle Burst.

[illegible]

ORIGINAL PAGE IS
OF POOR QUALITY

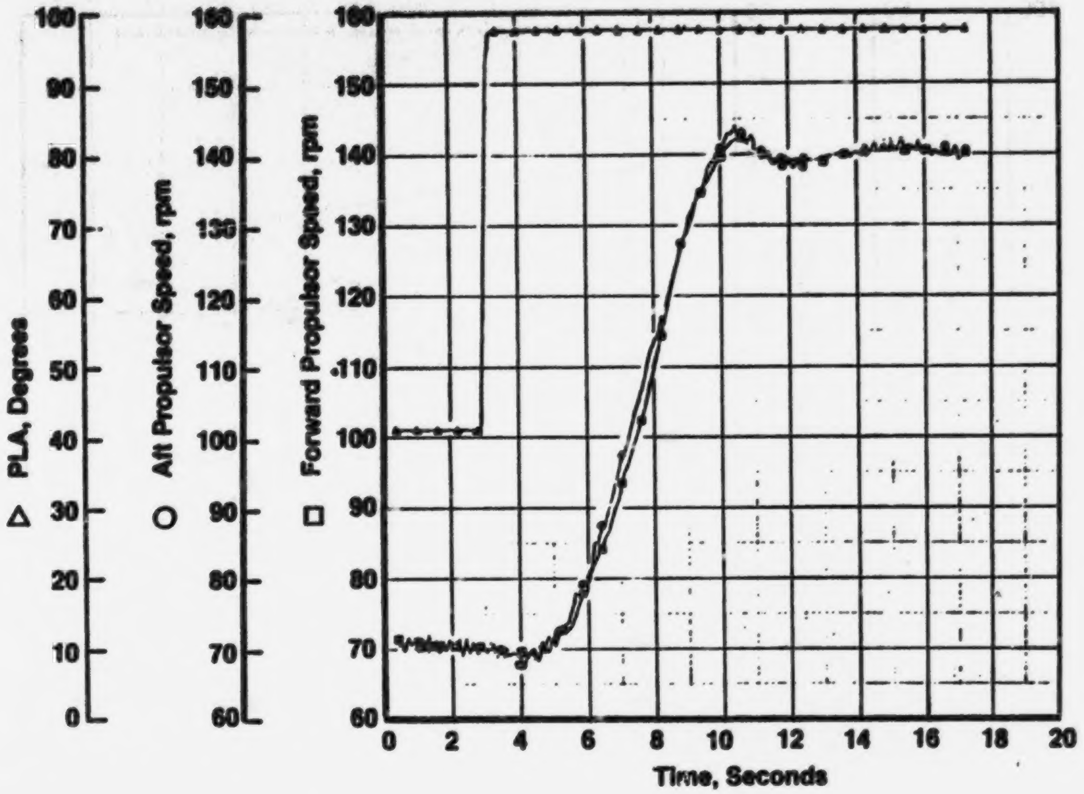

Figure 9-15. Throttle Burst.

ORIGINAL PAGE IS
OF POOR QUALITY

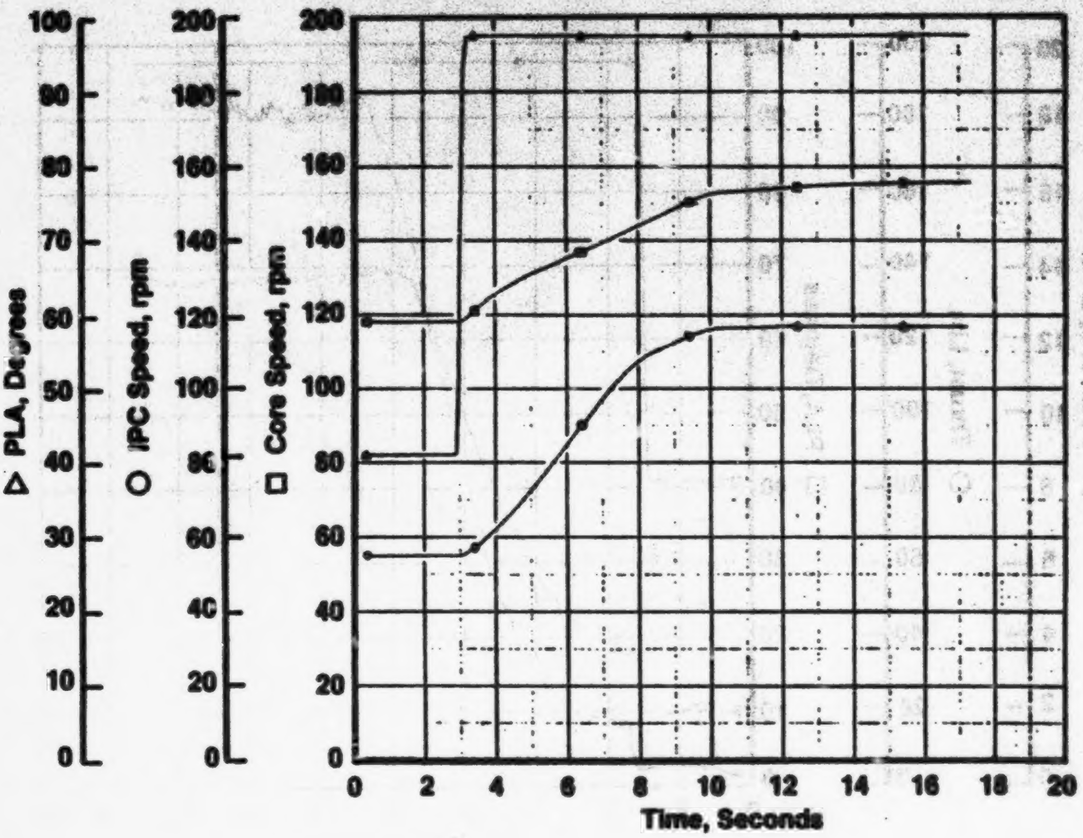

Figure 9-16. Throttle Burst.

[illegible]

ORIGINAL PAGE IS
OF POOR QUALITY

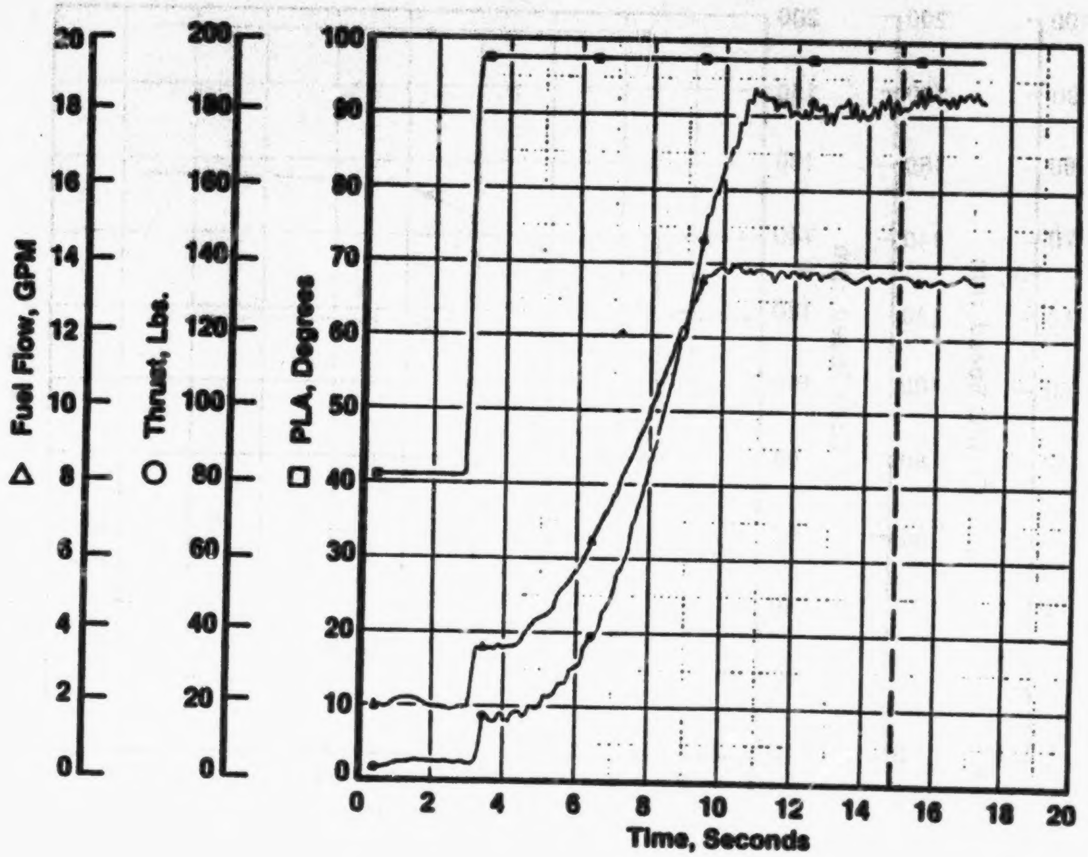

Figure 9-17. Throttle Burst.

10.0 NACELLE STRUCTURES

No problems occurred for any of the nacelle structures components during ground testing conducted at Peebles, Ohio.

The fan blade airfoil loss provided valuable data pertaining to the nacelle structural and dynamic integrity. No structural damage occurred, and the isolators absorbed the unbalance as expected. Based on data taken during the airfoil loss, the isolator/mount structure provided a minimum margin of safety of 0.47 and an average margin of safety of 2.54 for all components.

Strain measurements taken on the strut during ground testing revealed extremely low stress levels. The maximum stress level recorded, 1.4 kpsi peak to peak, corresponds to a margin of safety of 80.4 based on shear strengths of the strut material. The minimum margin of safety was found in the composite mid-fairing. Based on the interlaminar shear strength, this margin was 2.7, which is an acceptable figure. Based on the strain measurements, the acoustic fatigue of the strut and fairings was deemed to be of little concern.

10.1 FAN BLADE AIRFOIL LOSS

The fan blade airfoil loss incurred on February 9, 1986 caused a 262,000 gm-inch (577 lb-inch) unbalance load. This failure occurred at a fan speed of 1371 rpm and a thrust level of 24,000 pounds. Engine, isolator, mount beam, and strut accelerometers were located as shown in Figure 10-1.

At blade-out, the rear-mount horizontal vibration level reached 200 mils double amplitude, while its normal level is 10 mils. The front mount along the horizontal axis reached 95 mils, while its normal level is 15 mils. The engine was then chopped to idle (680 rpm) in 1.23 seconds, where it remained for 9.0 seconds before being shut down. Vibration levels of the vertical axes of the front and rear mounts reached 200 mils DA (double amplitude) from their normal levels of 2 mils each. As attested in Table 10-1, the maximum vibration levels occurred in the rigid body modes during coast down.

Mount loads were estimated based on relative motion across the isolators and on the isolator dynamic spring rates (from the Barry Qualification Test

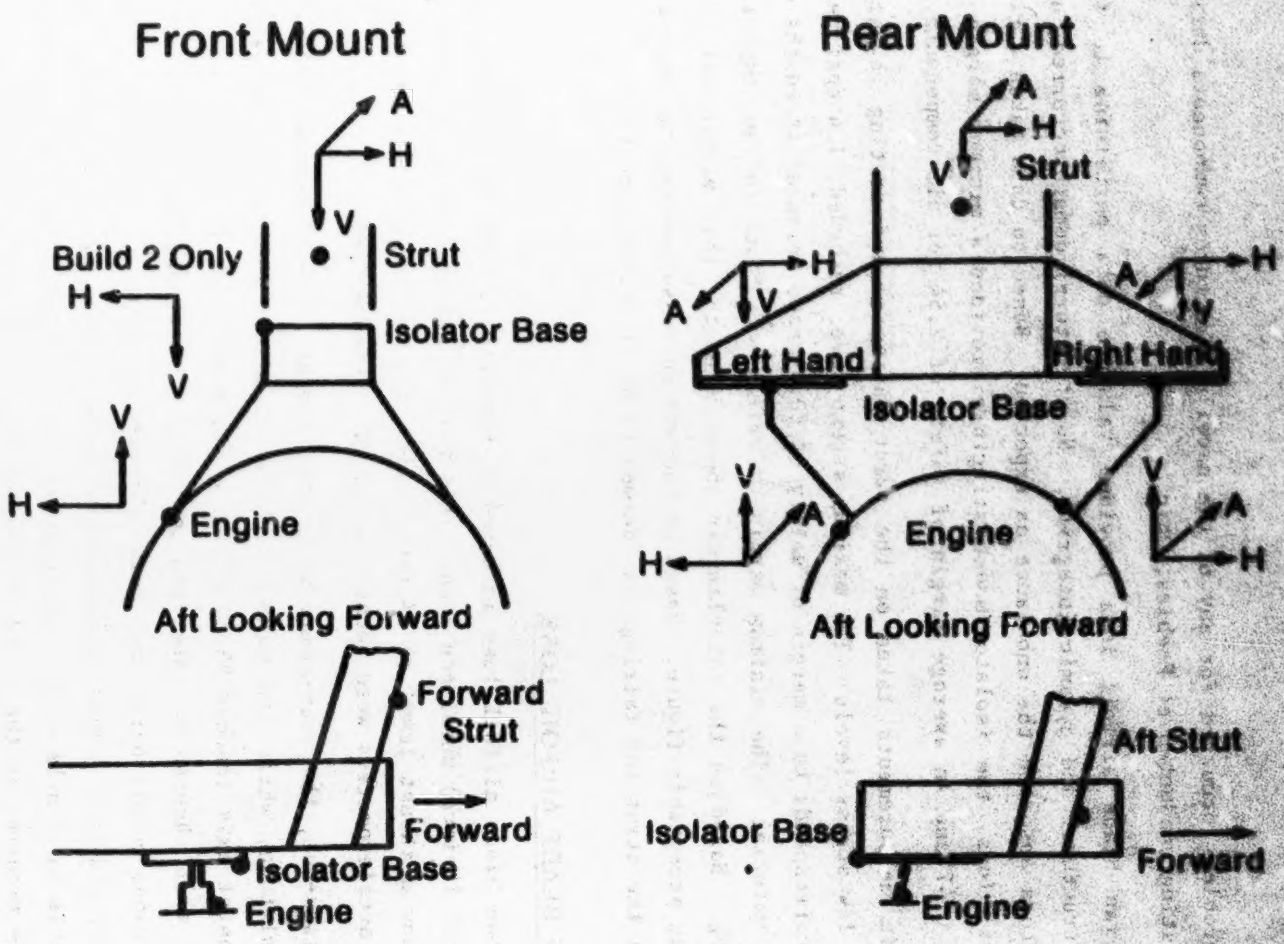
Front Mount
A
H
V
Build 2 Only
Strut
H
V
Isolator Base
V
H
Engine
Aft Looking Forward
Forward Strut
Forward
Isolator Base
Engine
Rear Mount
A
H
V
Strut
H
V
A
A
H
V
Left Hand
Right Hand
Isolator Base
V
A
H
Engine
V
A
H
Aft Looking Forward
Aft Strut
Isolator Base
Forward
Engine

Figure 10-1. UDF™ Engine 082-001 Accelerometer Definition.

Report). Table 10-2 shows that these loads were well below the design loads. The minimum margin of safety turned out to be 0.47, which was for the rear mount along the axial axis at 460 rpm; the load it carried (40.9 kips) was the maximum load for the system. The average margin of safety for the isolators was 2.54.

Table 10-1. Vibration Response.

Sensor	Displacement, mils DA		
	1370 rpm	Idle (680 rpm)	Coast Down (rpm)
Front Mount Vertical	80	200	560 (460)
Front Mount Horizontal	95	50	385 (280)
Right Rear Vertical	170	200	450 (200)
Right Rear Horizontal	200	105	165 (200)
Right Rear Axial	95	330	980 (460)
Left Rear Vertical*	---	---	---
Left Rear Horizontal	120	130	430 (200)
Left Rear Axial*	---	---	---

* Sensor Inoperable Before Event

The overall response of the isolators indicated that they functioned as designed, significantly reducing the motion at the pylon/mount interface and softening with increased loading. The resonant speeds of the system decreased for the airfoil loss event. Further, the isolators reduced mount loads on the engine and pylon. These loads were well within design limits.

Physically, the isolators performed as designed during the airfoil loss. No wear or deformation of the isolator structure was incurred (or in any other structure). The Met-L-Flex wire mesh showed some minor deformation in the aft isolators. The mesh in the front isolator was undamaged. All isolators were sent to the manufacturer, Barry Controls, for inspection and testing. Despite the fact that all the load-deflection data for the isolators indicated little

Table 10-2. UDF™ Engine Mount Loads Due to Airfoil Loss.

Mount	Direction	rpm	Relative Motion*	Dynamic Spring Rate, K	Resulting Load**, lb	Design Loads, lb	Margin of Safety
Front	Horizontal	280	0.100	133	13,330	60,000	3.50
Front	Vertical	460	0.145	165	24,000	80,000	2.33
Rear	Radial	200	0.202	81.3	16,400	50,000	2.05
Rear	Radial	460	0.108	107	11,600	50,000	3.31
Rear	Axial	200	0.075	175	13,100	60,000	3.58
Rear	Axial	460	0.292	140	40,900	60,000	0.47

* Relative Motion Assumes Vibration in Phase Across Isolator

** Stiffness Data from Barry Qualification Test Report for Applied Loads and Deflections change and were still within limits, the wire mesh in the aft isolators was replaced. The front isolators were used "as is."

Predictions that maximum loads would occur in subidle modes were verified. However, modes were not matched for the front mount (Tables 10-3 and 10-4). Also, as predicted, the highest load occurs on the aft mount in the axial direction. Both magnitude and speed were in good agreement with prediction; however, the front mount loads measured were higher than predicted.

10.2 STRAIN EVALUATION OF THE STRUT

Extensive strain tests were performed on various strut components during ground testing. Corresponding stress levels were calculated and recorded. As illustrated in Table 10-5, the greatest stress level recorded was in the upper middle portion of the mount beam at a high pressure compressor speed of 7800 rpm. This stress level, 1.4 kpsi peak-to-peak, is well within the acceptable levels and corresponds to a margin of safety of 80.4 (compared with the ultimate shear strength of the material of which it is made - AMS 5528 stainless steel). The minimum margin of safety occurs in the mid-fairing in the axial direction at an intermediate pressure compressor. The recorded stress level is 0.96 kpsi, peak-to-peak. This corresponds to a margin of safety of 2.7 with respect to the interlaminar shear strength.

Appendix B shows the range of data tested in terms of calculated stress versus frequencies and speeds; figures contained therein (Figures B-1 through and B-40) illustrate the positioning of the strain gages used. Note that some are arranged in rosettes; while others are uniaxial.

10.3 ACOUSTIC FATIGUE

A preliminary acoustic fatigue analysis of the strut fairing calculated a response frequency of 174 Hz (the fundamental blade passing frequency range for the engine operating range, 600 to 1400 rpm, is 80 to 187 Hz); however, this figure is questionable due to the numerous assumptions and uncertainties involved in the calculation. The operating conditions assumed were those of cruise. Further, the panel was assumed flat; whereas, a slight panel curvature or irregularity would increase the response frequency; finally, the damping ratio was estimated rather than known.

Table 10-3. UDF™ Engine Comparison of Mount Loads for Airfoil-Out Event.

	Maximum Load			
	Modified Nastran Model		Test Results*	
Location	Load, lb	rpm	Load, lb	rpm
FMV	8,800	228	24,000	460
FMH	7,500	528	13,300	280
RRMR	10,500	228	16,400	260
RRMA	44,000	444	40,900	460
LRMR	12,000	228	---	---
LRMA	31,000	420	---	---

* Using Barry Mount Data and Relative Deflection, Unbalance = 262,000 gm-inch

Table 10-4. UDF™ Engine Airfoil-Out Event Comparison of Deflections (Absolute).

	Maximum Displacement, mils DA			
	Modified Nastran Model		Measured Test Results	
Location	Deflection, mils	rpm	Deflection, mils	rpm
FMV	440	228	560	460
FMH	1120	540	385	280
RRMR	600	450	350	200
RRMA	1100	420	988	460
LRMR	750	228	---	---
LRMA	1100	420	---	---

Note: Unbalance = 262,000 gm-inch

ORIGINAL PAGE IS
OF POOR QUALITY

Table 10-5. Stress Data - Strut.

GAGE	[illegible]	[illegible]	[illegible]
FAIRING, VERT	2 (0.37)	3 (0.13)	1 (0.13)
FAIRING, DIAG	3 (0.056)	3 (0.091)	1 (0.54)
FAIRING, AXIAL	2 (0.96)	2 (0.20)	2 (0.19)
FWD ISO	3 (0.72)	3 (0.74)	1 (0.91)
BR OF SPAR, VERT	0	0	4 (0.059)*
BR OF SPAR, DIAG	0	0	4 (0.015)*
BR OF SPAR, HORIZ	0	0	4 (0)*
SIDE OF SPAR, VERT	0	0	4 (0.29)*
SIDE OF SPAR, HORZ	0	0	4 (0.22)*
SIDE OF SPAR, DIAG	0	0	4 (0.12)*
LT AFT ISO CLEVIS	2 (0.53)	2 (0.5)*	4 (0.39)
RT BM,TOP AFT,VERT	3 (0.12)	3 (0.10)	3 (0.65)
RT BM,TOP AFT,DIAG	0	0	4 (0.12)
RT BM,TOP AFT,HORZ	3 (0.20)	3 (0.18)	3 (0.20)
RT BM,BTM AFT,HORZ	3 (0.22)	2 (0.17)	3 (0.23)
RT BM,TOP MID,HORZ	3 (0.01)	2 (1.4)	2 (0.20)
RT BM,TOP MID, VERT	3 (0.44)	3 (0.42)	2 (0.21)
RT BM,BTM FWD,VERT	3 (0.14)	3 (0.02)	2 or 4 (0)
AFT RT BM SUPT FTG,HOR	2 (1.08)	2 (0.21)	2 (0.10)
RT AFT ISO CLEVIS	2 (0.08)	3 (0.94)	3 (0.92)
RT BR MT, TANG	0	0	4 (0.66)*
BR OF SPAR,LWR AFT,VER	3 (0.36)	3 (0.41)	3 (0.36)
SAME, HORIZ	3 (0.18)	3 (0.15)	2 (0.17)
BR OF SPAR,UPR AFT,VER	0	0	4 (3)*
SAME, DIAG	0	0	4 (0.50)*
SAME, HORIZ	0	0	4 (0.12)*

CODES:

0: NO DATA AVAILABLE
1: START/ACCELERATE
2: START/ACCELERATE TO 700
3: ACCELERATE TO 24,400 LBS.
4: ACCELERATE TO 24K FL
*: ONLY ONE DATA POINT AVAILABLE

FORMAT IS: CODE # (MAXIMUM STRESS IN KPSI PP)

For instance, if the curvature of the panel was as slight as 99 inches, this frequency would then become 383 Hz. What is known is that strain gage data discussed in Section 10.2 and displayed in Appendix B, show that stresses are relatively low. Thus, there appears to be no resonant vibration within the operating range of the engine and that acoustic fatigue is not a problem.

11.0 RESULTS

The 100+ hour ground test program of the UDF™ engine demonstrated the following:

- 25,000 lbf installed corrected thrust
- High fuel efficiency: 0.232 lb/hr/lbf installed corrected sfc (specific fuel consumption)
- 15,000+ physical total shaft horsepower
- Full propulsor speed (1393+ rpm)
- Advanced UDF™ aerodynamics that incorporates custom-tailored composite fan blades over an inner titanium spar that serves as the attachment mechanism to the engine for the fan blades
- Individually replaceable propulsor fan blades with the engine installed on the aircraft or test stand
- DEC (digital electronic control) provides overall engine control by monitoring gas generator power and speed and propulsor speeds and pitch angles; the engine utilizes the existing gas generator control and a separate propulsor control to minimize development costs without sacrificing control flexibility; this control system drives a hydraulic/mechanical actuation system that permits setting the fan blade pitch angle of the two fan blade rotors either together or differentially
- Flawless operation of the F404 gas generator
- Counterrotation of structures, turbines, and fan blades
- Reverse thrust capability
- Capability to withstand a fan blade airfoil loss with no structural or secondary damage
- Failure of Stage 1 turbine blades and the subsequent damage to following turbine blade rows; turbine structures withstood the failures with little or no damage.

Also demonstrated were the following capabilities:

- Running at full power statically
- Data was repeatable statically

- Prediction of low speed, low pressure, counterrotating turbine performance with accuracy comparable to that of the high speed, conventional, low pressure turbines

- Comparing data recorded early and late in the LCF testing, performance deterioration was confined to a dirty IPC; there was no evidence of mechanical deterioration

- F404 gas generator provided repeatable and predictable performance and was better than predicted at lower powers (below 70% takeoff power)

- UDF™ blade performance sensitivity to rotational speed was much greater than predicted

- At power coefficient = 1.32, thrust coefficient was 4% better than predicted (approximately 60% takeoff power)

- At power coefficient = 1.95, thrust coefficient was 4% worse than predicted (approximately 100% takeoff power)

- Power turbine efficiency was approximately as predicted, being within +1.5 points over the major portion of the operating range; the flow function was within +0.5% of prediction at high powers (above 80% takeoff thrust)

- Overall performance was better than predicted up to 92% takeoff power (23,000 lbf corrected installed thrust), and was poorer than predicted beyond 92% takeoff power (23,000 lbf corrected installed thrust) due to UDF™ speed sensitivity as noted above

- At 60% takeoff thrust (15,000 lbf), sfc was approximately 5.50% better than predicted

- At 92% takeoff thrust (23,000 lbf), sfc was approximately as predicted

- At 100% takeoff thrust (25,000 lbf), sfc was nearly 4.00% worse than predicted.

12.0 CONCLUSIONS

As a result of the 100+ hour UDF™ test program, it can be concluded that all of the major objectives of this engine can be and have been met. Some of these objectives are as follows:

- The demonstrated feasibility of an unducted, ungeared, counterrotating ultra-high-bypass turbofan
- Capability to produce at least 25,000 lbf and at least 15,000 shaft horsepower with an engine of this configuration
- Exceptional fuel efficiency as compared to other turbofan or turbojet engines
- The capability to produce thrust with a new fan blade design of composite materials over a titanium spar
- The capability to control the engine and actuate the fan blades with a digital electronic control
- Capability to produce reverse thrust with the fan blades without the use of a thrust reverser
- UDF™ propulsor capable of producing thrust as predicted
- Current computer model cycle deck techniques can adequately model a counterrotating turbofan
- Propulsor deterioration (large seals, turbine, etc.) was not encountered over the duration of testing, which exceeded 100 hours
- Operation of the engine, and its performance, is stable at takeoff power statically.

As expected in an engine program utilizing such new technologies and concepts as the UDF™, numerous problems have been discovered. However, it is believed that none of these problems will present a major stumbling block to future flight test of this engine or to the development of this concept into an important new entry into the arena of subsonic commercial and military transport aircraft. Every problem that has occurred during ground testing has been addressed and adequately solved. Fine tuning may be necessary, and more problems may be discovered of course, as the testing of this engine continues. No significant fundamental aerodynamic or control problems were uncovered, and only two mechanical problems created significant setbacks to the test program. Both of these problems were solved by rather simple, but successful means:

1. Fan Blade Airfoil Loss - Although static component tests verified the integrity of the airfoil bonding to the titanium spar, actual engine testing brought into effect additional factors leading to the loss of one airfoil. At that time, only the adhesive qualities of the composite to titanium bonding agent held the airfoil to the spar. By adding positive retention features to the design (by adding fasteners), airfoil retention proved to be of no problem for the duration of testing and is not expected to present a problem in the future.

2. Turbine Blade Failure - Stage 1 turbine blade dynamic response was excessive due to insufficient damping, which eventually led to their failure. Damping, in the form of friction, was introduced to all blade rows by placing simple damper pins between each blade; this satisfactorily reduced the dynamic response.

13.0 SYMBOLS/ABBREVIATIONS

ALF	Aft, Looking Forward
Beta Angle	Fan Blade Pitch Angle, degrees
BFM	Backflow Margin, %
BTAN91	Front Rotor Pitch, degrees
BTAN92	Rear Rotor Pitch, degrees
BTWT	Boeing Transonic Wind Tunnel
CV	Convex
DA	Double Amplitude
DEC	Digital Electronic Control
dia.	Diameter
DMS	Data Management System
DOD	Domestic Object Damage
DTAMB	ΔT from Standard Day/ISA Conditions
EB	Electron Beam
EDM	Electrical Discharge Machining
EPR	Engine Pressure Ratio
F404 Fan	Bypass Pressure Ratio
F404-GE-400	Low Bypass Turbofan Gas Generator
FHV	Fuel Heating Valve
FMH	Front Mount, Horizontal
FMV	Front Mount, Vertical
FNI1QA	Installed Thrust, lb
FPI	Fluorescent Particle Inspection
F_{sep}	Flow Separation Parameter
h	Coefficient of Heat Transfer (Btu/hr ft^2, ° F)
HCF	High Cycle Fatigue
Hz	Hertz, cycles/second
ID	Inner Diameter
1F	First-Flexural Frequency, cycles/second
IGV	Inlet Guide Vanes
IPC	Intermediate Pressure Compressor
1T	First-Torsional Frequency, cycles/second
LCF	Low Cycle Fatigue

LE	Leading Edge
LPT	Low Pressure Turbine
LRMA	Left Rear Mount, Axial
LRMR	Left Rear Mount, Radial
LRMV	Left Rear Mount, Vertical
LVDT	Linear Variable Differential Transducer
Max	Maximum
Min	Minimum
Mn	Mach Number
MPI	Magnetic Particle Inspection
OGV	Outlet Guide-Vanes
ON	O-Nodal
P15/Pz	F404 Fan Bypass Pressure Ratio
P46Q2	Gas Generator Pressure Ratio
P48Q2	Engine Pressure Ratio
PLA	Power Lever Angle, degrees
P_o	Ambient Pressure, psi
PRS	Stall Pressure Ratio
P_s	Static Pressure, psi
PS3	Gas Generator Compressor Discharge Pressure, psi
PT	Total Pressure, psi ... (also Power Turbine)
PT_8	Power Turbine Exhaust Pressure, psi
PTO	Peebles Test Operation
P_z	Compressor Inlet Pressure, psi
RDGS	Readings
RRMA	Right Rear Mount, Axial
RRMR	Right Rear Mount, Radial
S/D	Shutdown
sfc	Specific Fuel Consumption, lb/hr/lb
SFCI1R	Installed Specific Fuel Consumption, lb/lb
SG	Strain Gage
S/N	Serial Number
T46	Propulsor Exhaust Gas Temperature, ° F
T46Q2	Gas Generator Temperature Ratio
T_{Amb}	Ambient Temperature, ° F

TAAP01	Stage 1 Fan Telemetry Ring Cavity Thermocouple, ° F
TAAP02	Stage 2 Fan Telemetry Ring Cavity Thermocouple, ° F
TAFC01	Stage 1 Fan Telemetry Ring Cavity Thermocouple, ° F
TE	Trailing Edge
TT	Total Temperature, ° F
2R	No. 2 Roller
UDF™	GE36 Unducted Fan Engine
W_{25}	HPC Inlet Flow, lb/second
W48R	Power Turbine Flow Function, Corrected
X_h	Horizontal Displacement, inch
X_v	Vertical Displacement, inch
XN48	Stage 1 Propulsor Fan Speed, rpm
XN49	Stage 2 Propulsor Fan Speed, rpm
ZN	Z-Nodal

14.0 References

1. Carlson, S.L., "Engine Damage Report," No. GE36-003, March 18, 1986.

2. Carlson, S.L., "Engine Damage Report," No. GE36-004, August 14, 1986.

3. Cote, M.J., "GE36 Nacelle Fairing Sonic Fatigue Analysis," Memo of July 24, 1986.

4. Gaffney, E., Review of Airfoil Loss, "In The Unducted Fan Engine; GE Quarterly Review No. 8," May 13, 1986.

5. General Electric, "Full-Scale Technology Demonstration of a Modern Counterrotating Unducted Fan Engine Concept - Component Test," NASA Contract No. NAS3-24210, CR-180868, December 1987.

6. General Electric, "Full-Scale Technology Demonstration of a Modern Counterrotating Unducted Fan Engine Concept - Design," NASA Contract No. NAS3-24210, CR-180867, December 1987.

7. General Electric, "The Unducted Fan Engine - Quarterly Review No. 6, "NASA Contract No. NAS3-24210, August 16, 1985.

8. General Electric, "The Unducted Fan Engine - Quarterly Review No. 7," NASA Contract No. NAS3-24210, November 18, 1986.

9. General Electric, "The Unducted Fan Engine - Quarterly Review No. 8," NASA Contract No. NAS3-24210, May 13, 1987.

10. General Electric, "UDF$^{\text{TM}}$ Airworthiness Executive Review," NASA Contract No. NAS3-24210, July 1986.

11. Kirkpatrick, R.A., "Failure Report: Engine S/N 082-001/A: High Power Stall of October 2, 1985," December 13, 1985.

12. Kroger, J.P., "GE36 Second Ground Test," Test Project Sheet No. MA-004, January 13, 1986.

13. Nelson, E. (Barry Controls), "Qualification Test Report for 94624 Engine Isolators: GE-36 Demonstrator Engine Program," Document No. WD04624-1-005, Revision A, May 14, 1986.

14. Smith, R.E., "Engine Damage Report," No. GE36-002, Revision A, January 6, 1986.

APPENDIX A

STEADY-STATE TEST DATA - BUILD 3

DATA LEGEND

XN2	IPC Physical Speed (rpm)
XN2R	IPC Corrected Speed (rpm)
PCN2R	Percent IPC Corrected Speed (%)
XN25	HPC Physical Speed (rpm)
XN25R	HPC Corrected Speed (rpm)
PCN25R	Percent HPC Corrected Speed (%)
XN48	Stage 1 Physical Speed (rpm)
XN49	Stage 2 Physical Speed (rpm)
UT91R2	Corrected Stage 1 Tip Speed (feet/second)
UT92R2	Corrected Stage 2 Tip Speed (feet/second)
BTAN91	Stage 1 Pitch Angle (degree)
BTAN92	Stage 2 Pitch Angle (degree)
W13	Bypass Duct Inlet Flow (lb/second)
W15	Bypass Duct Exit Flow (lb/second)
WF36	Fuel Flow (lb/hr)
WF36R2	Corrected Fuel Flow (lb/hr)
FNI1QA	Corrected Installed Net Thrust (lb)
SFC184	Corrected Installed Net Specific Fuel Consumption, FHV = 18,400 (lb_{fuel}/lb_{thrust} hr)
TAMB	Ambient Temperature (° R)
T10	Inlet Total Temperature (° R)
PAMB	Ambient Pressure (psia)
P10M	Inlet Total Pressure (psia)
HUMSER	Specific Humidity (grains/lb dry air)
RELHUM	Relative Humidity (%)
WINVAV	Average Wind Velocity (knots)
WINAAV	Average Wind Angle (degree)
XM0	Mach Number
P46Q2	Engine Pressure Ratio
CT46	Calculated T46 (° R)
T46X	Measured T46 (° R)

PRECEDING PAGE BLANK NOT FILMED

PAGE 248 INTENTIONALLY BLANK

GE36/UDF-1 ENGINE 082001-03 TEST READINGS - SITE IIID
RDGS. 1 - 5 ON 06.20.86 RDGS. 6 - 15 ON 06.23.86
RDGS. 16 - 31 ON 06.24.86 RDGS. 32 - 47 ON 06.25.86
RDGS. 48 - 57 ON 06.26.86

RDG.	1	2	3	4	5	6	7	8	9	10	11	12	13
XN2	0.	724.28	538.03	4106.5	463.39	0.	5592.4	5437.6	419.28	0.	5470.1	678.21	678.21
XN2R	0.	715.61	531.53	4072.5	457.43	0.	5494.1	5337.1	410.45	0.	5352.8	660.62	659.56
PCN2R	0.	5.3927	4.0055	30.689	3.4471	0.	41.402	40.219	3.0931	0.	40.338	4.9783	4.9703
XN25	0.	85.38	118.9	10619.	136.19	0.	11776.	11682.	164.48	0.	11717.	143.52	143.52
XN25R	0.	83.918	116.82	10258.	129.41	0.	11060.	10988.	158.22	0.	10986.	136.45	137.85
PCN25R	0.	.62532	.8705	76.439	.96428	0.	82.416	81.881	1.179	0.	81.863	1.0168	1.0272
XN48	0.	467.89	96.579	699.9	415.38	0.	700.16	700.03	558.84	0.	700.16	164.09	164.09
XN49	0.	0.	10.314	687.04	699.49	0.	700.43	700.3	700.43	0.	700.43	699.49	699.49
UT91R2	0.	283.89	58.591	426.24	251.8	0.	422.41	421.93	335.95	0.	420.75	98.153	97.995
UT92R2	0.	0.	6.0822	406.7	412.16	0.	410.74	410.28	409.28	0.	409.12	406.7	406.04
BTAN91	80.59	86.6	86.734	9.8483	86.65	80.343	18.191	17.743	86.664	86.96	17.788	86.939	86.959
BTAN92	80.306	86.093	86.22	10.089	86.082	80.266	19.719	19.041	86.52	86.764	19.118	86.701	86.731
W13	-.5	-4.7497	-5.4954	3.7509	-5.497	-.5	5.7381	5.4167	-6.1277	-.5	5.823	-5.0419	-5.1496
W15	0.	-4.7497	-5.4954	3.7509	-5.497	0.	5.7381	5.4167	-6.1277	0.	5.3897	-5.0419	-5.1496
WF36	168.08	169.44	177.48	663.98	179.74	140.34	880.3	830.57	149.38	130.13	845.05	139.24	141.05
WF36R2	169.66	172.06	180.04	677.01	182.03	140.96	889.74	838.42	150.21	129.07	850.25	139.21	140.8
FNI1QA	0.	0.	0.	690.66	0.	10.518	2568.2	2289.3	0.	-2.7313	2321.9	0.	-.79557
SFC184	.5	.5	.5	.9909	.5	13.547	.35022	.37021	.5	-47.77	.37016	.5	-178.9
TAMB	533.63	531.26	528.48	528.52	527.4	540.77	540.58	541.32	541.48	544.74	544.7	542.62	542.5
T10	536.3	531.32	531.44	527.37	532.27	541.85	537.4	538.4	541.24	552.43	541.65	546.66	548.43
PAMB	14.24	14.247	14.258	14.263	14.266	14.204	14.204	14.203	14.203	14.198	14.19	14.188	14.179
P10M	14.24	14.247	14.258	14.263	14.267	14.209	14.204	14.204	14.205	14.199	14.192	14.189	14.18
HUMSER	67.567	64.473	59.714	57.572	58.289	113.7	107.7	112.01	110.48	93.645	96.205	91.979	94.29
RELHUM	52.566	54.392	55.479	53.464	56.263	68.958	65.825	66.756	65.532	50.176	51.546	52.73	54.202
WINVAV	7.3229	1.049	3.2623	2.6296	7.8227	2.4738	1.3076	5.6358	7.6706	4.0519	6.0543	4.6921	3.7711
WINAAV	161.53	117.66	149.43	-139.57	-165.66	-128.1	-152.9	-12.692	-9.4649	-20.213	16.952	-9.6835	-17.435
XMO	0.	0.	0.	0.	0.	0.	0.	0.	0.	0.	0.	0.	0.
P46Q2	9.99+10	1.0011	1.0009	1.1009	1.0015	9.99+10	1.1953	1.1829	1.0013	9.99+10	1.1846	1.0012	1.0012
CT46	9.99+10	846.28	870.65	1380.1	946.53	9.99+10	1347.7	1316.4	844.7	9.99+10	1341.4	830.16	814.5
T46X	537.98	685.03	568.15	1399.2	735.01	538.85	1326.	1280.8	720.45	630.92	1311.6	703.99	629.3
Comments	Zero	Zero	Zero	GI Speeds Mis-matched	Zero	Zero	F.I.	F.I.	Zero	Zero	F.I.	Zero	Zero

GE36/UDF1 Pembles Tests
082001-03
Test Log - Site IIID
Sheet 001 of 029

GE36/UDF-1 ENGINE 082001-03 ...ST READINGS - SITE IIID
RDGS. 1 - 5 ON 06.20.86 RDGS. 6 - 15 ON 06.23.86
RDGS. 16 - 31 ON 06.24.86 RDGS. 32 - 47 ON 06.25.86
RDGS. 48 - 57 ON 06.26.86

RDG.	14	15	16	17	18	19	20	21	22	23	24	25	26
XN2	5464.4	9157.2	10594.	11096.	0.	5640.4	11030.	102.86	0.	5565.5	7339.5	8563.4	9888.7
XN2R	5355.1	8982.9	10391.	10887.	0.	5573.1	10889.	100.61	0.	5481.9	7231.8	8436.6	9741.6
PCN2R	40.355	67.693	78.305	82.039	0.	41.998	82.061	.75816	0.	41.31	54.497	63.577	73.411
XN25	11705.	13776.	14647.	15125.	0.	11770.	15027.	130.95	0.	11757.	12778.	13462.	14145.
XN25R	10990.	12134.	12466.	12615.	0.	11104.	12582.	123.74	0.	11073.	11697.	12038.	12307.
PCN25R	81.891	90.42	92.889	94.001	0.	82.739	93.757	.92206	0.	82.512	87.159	89.703	91.707
XN48	700.16	906.58	1124.3	1269.2	0.	699.9	1260.9	156.59	0.	653.68	752.	850.99	1006.5
XN49	700.3	906.98	1124.8	1269.6	0.	101.27	1261.3	126.58	0.	784.82	852.33	951.46	1106.7
UT91R2	421.37	546.13	677.17	764.69	0.	424.68	764.46	94.058	0.	395.39	455.02	514.85	608.9
UT92R2	409.65	531.08	658.53	743.52	0.	59.726	743.29	73.907	0.	461.42	501.29	559.52	650.77
BTAN91	17.724	28.578	29.471	29.782	86.903	18.901	30.295	86.876	87.148	19.486	24.846	27.131	28.71
BTAN92	18.905	27.823	29.082	29.48	86.343	19.646	29.328	86.675	86.833	17.808	22.558	24.972	26.231
W13	5.4412	10.14	12.192	12.982	-.5	5.6613	13.867	-7.1572	-.5	5.1598	7.6467	9.3194	10.825
W15	5.4412	10.14	12.192	12.982	0.	5.6613	13.867	-7.1572	0.	5.1598	7.6467	9.3194	10.825
WF36	837.38	2055.5	3174.	4082.5	151.5	885.12	4239.2	168.65	155.66	851.31	1304.5	1767.7	2331.2
WF36R2	845.25	2079.1	3210.5	4131.7	154.48	902.04	4318.3	169.43	152.97	862.89	1322.7	1792.4	2566.6
FN11QA	2356.6	8283.	13222.	16953.	24.588	2657.8	17329.	28.652	0.	2541.3	4972.7	7220.3	10661.
SFC184	.36258	.25373	.24545	.24636	6.3511	.34309	.25191	5.9776	.5	.34324	.26888	.25094	.24337
TAMB	542.03	540.8	540.39	540.05	531.95	534.21	534.67	534.29	537.82	538.13	537.39	537.62	537.94
T10	540.04	538.99	539.12	538.81	531.03	531.27	532.11	542.11	558.92	534.62	534.24	534.38	534.45
PAMB	14.174	14.168	14.168	14.168	14.192	14.199	14.199	14.2	14.215	14.216	14.217	14.217	14.218
P10M	14.175	14.169	14.169	14.169	14.192	14.199	14.199	14.201	14.215	14.215	14.218	14.218	14.217
HUMSER	100.3	93.586	92.396	93.213	78.5	72.215	74.879	73.064	69.305	63.729	61.38	60.926	59.919
RELHUM	58.446	56.828	56.857	57.994	64.243	54.882	56.003	55.365	46.801	42.659	42.117	41.503	40.402
WINVAV	2.4232	4.4413	2.3847	4.2043	1.5986	1.5115	2.5894	7.6595	3.5378	2.942	2.4333	3.019	2.2477
WINAAV	11.632	-35.053	26.309	7.1803	-26.477	55.17	-83.301	163.33	134.12	127.02	-125.73	107.3	146.92
XMO	0.	0.	0.	0.	0.	0.	0.	0.	0.	0.	0.	0.	0.
P46Q2	1.1847	1.7205	2.1604	2.4895	9.99+10	1.2022	2.4854	1.0023	9.99+10	1.1955	1.3712	1.5572	1.9082
CT46	1327.5	1476.2	1624.	1722.5	9.99+10	1329.4	1771.3	942.82	9.99+10	1306.5	1352.9	1416.4	1538.4
T46X	1285.9	1472.8	1620.9	1707.5	544.7	1303.5	1738.4	740.19	619.62	1266.3	1333.6	1411.	1536.6
Comments	F.I.	Part Power	Part Power	Part Power	Zero	F.I. Bad XN49	Part Power Unstable Data Acq. Incomplete	Zero	Zero	F.I. Field Balance Run---------------→ Mismatched Speeds: (XN48-XN49)→ -130	Part -100	Part -100	Part -100

GE36/UDF1 Peebles Tests
082001-03
Test Log - Site IIID
Sheet 002 of 029

ORIGINAL PAGE IS
OF POOR QUALITY

GE36/UDF-1 ENGINE 082001-03 .ST READINGS - SITE IIID
RDGS. 1 - 5 ON 06.20.86 RDGS. 6 - 15 ON 06.23.86
RDGS. 16 - 31 ON 06.24.86 RDGS. 32 - 47 ON 06.25.86
RDGS. 48 - 57 ON 06.26.86

RDG.	27	28	29	30	31	32	33	34	35	36	37	38	39
XN2	10459.	10799.	86.428	86.428	0.	1428.9	10355.	9021.2	9050.5	9039.1	9038.7	9987.	9991.3
XN2R	10301.	10636.	84.374	82.518	0.	1421.2	10379.	9020.6	9052.9	9029.8	9033.	9975.	9983.3
PCN2R	77.626	80.147	.63583	.62184	0.	10.71	78.216	67.978	68.221	68.047	68.07	75.169	75.232
XN25	14513.	14844.	87.999	87.999	0.	4192.	14370.	13571.	13576.	13561.	13557.	14070.	14074.
XN25R	12437.	12553.	83.484	79.618	0.	4061.2	12488.	12172.	12174.	12168.	12171.	12356.	12366.
PCN25R	92.674	93.541	.62209	.59328	0.	30.262	93.058	90.704	90.718	90.669	90.694	92.072	92.143
XN48	1103.1	1199.	642.3	642.3	0.	7503.2	1105.1	899.22	903.37	900.15	900.69	1020.3	1020.2
XN49	1203.6	1299.9	880.46	880.46	0.	7503.2	1205.4	899.62	903.64	900.15	900.69	1020.2	1020.7
UT91R2	667.17	725.18	385.06	376.59	0.	4582.8	680.23	552.17	554.9	552.21	552.76	625.01	625.98
UT92R2	707.55	764.17	513.06	501.77	0.	4454.5	721.21	536.95	539.52	536.75	537.28	608.21	608.78
BTAN91	29.606	29.612	87.178	87.148	87.293	87.041	28.448	27.449	27.41	27.83	27.327	28.63	28.163
BTAN92	26.429	27.133	86.911	86.862	86.81	86.664	27.61	28.784	28.681	28.276	28.796	28.907	29.346
W13	11.639	12.499	-7.3808	-7.3892	-.5	-1.029	12.349	10.64	10.607	11.284	11.549	11.734	11.687
W15	11.639	12.499	-7.3808	-7.3892	0.	-1.029	12.349	10.64	10.607	11.078	11.014	11.734	11.687
WF36	3039.1	3587.3	157.31	157.21	183.17	198.39	3131.1	2033.4	2045.6	2029.2	2028.2	2629.1	2623.5
WF36R2	3080.8	3636.7	157.44	152.6	185.99	202.51	3232.2	2091.4	2104.8	2084.2	2084.3	2699.8	2695.5
FN11QA	12914.	15388.	-18.641	0.	0.	0.	13639.	8553.6	8673.7	8490.5	8518.6	0.	11201.
SFC184	.24115	.2389	-8.5379	.5	.5	.5	.23956	.24717	.2453	.24814	.24731	.5	.24327
TAMB	538.65	538.	538.63	535.62	526.33	516.58	518.34	521.	521.69	522.59	522.05	522.47	522.06
T10	534.71	534.7	544.23	568.99	531.55	524.32	516.24	518.74	518.4	519.74	519.33	539.92	519.3
PAMB	14.218	14.218	14.217	14.216	14.243	14.303	14.305	14.306	14.307	14.308	14.308	14.307	14.308
P10M	14.218	14.219	14.217	14.217	14.243	14.303	14.305	14.307	14.308	14.308	14.308	14.308	14.309
HUMSER	63.709	58.369	58.647	62.419	54.582	54.975	55.327	53.95	55.151	57.086	54.901	54.97	54.782
RELHUM	41.92	39.282	38.662	45.404	54.616	77.959	73.638	65.351	65.172	65.345	64.063	63.215	63.905
WINVAV	2.6083	4.0917	2.8129	4.172	1.3197	3.3211	7.5184	8.0547	8.1916	2.9925	7.4772	2.0767	6.5725
WINAAV	152.35	126.	115.17	170.07	117.78	-112.9	158.21	161.3	166.22	-121.28	167.49	-105.78	-155.82
XMO	0.	0.	0.	0.	0.	0.	0.	0.	0.	0.	0.	0.	0.
P46Q2	2.1108	2.333	1.0018	1.0009	9.99+10	1.0016	2.156	1.723	1.7323	1.7243	1.7179	1.947	1.9494
CT46	1598.1	1654.7	910.17	902.39	9.99+10	917.27	1563.1	1414.9	1412.8	1411.4	1409.5	1506.6	1500.7
T46X	1596.4	1649.9	738.79	629.72	573.68	549.73	1562.7	1414.2	1414.3	1412.2	1409.9	1506.5	1506.4
Comments	Part Power	Part Power	Zero	Zero	Zero	Zero	Part Power	Part Power	Part Power	Part Power	Part Power	Part Power	Part Power

Field Balance Run (cont'd)
Mismatched Speeds
-100 -100

Field Bal Bleed Evaluation-------------------------------→
Mismatched Stroke =
Speed 0% 0% 35% 80% 0% 0%
-100
No FM

GE36/UDF1 Peebles Tests
082001-03
Test Log - Site IIID
Sheet 003 of 029

ORIGINAL PAGE IS
OF POOR QUALITY

GE36/UDF-1 ENGINE 082001-03 .ST READINGS - SITE IIID
RDGS. 1 - 5 ON 06.20.86 RDGS. 6 - 15 ON 06.23.86
RDGS. 16 - 31 ON 06.24.86 RDGS. 32 - 47 ON 06.25.86
RDGS. 48 - 57 ON 06.26.86

RDG.	40	41	42	43	44	45	46	47	48	49	50	51	52
XN2	10012.	10016.	9991.5	10705.	10690.	10700.	10705.	587.5	0.	6032.6	11321.	11315.	11325.
XN2R	9999.2	9995.8	9963.3	10668.	10658.	10670.	10657.	583.94	0.	6016.1	11251.	11246.	11246.
PCN2R	75.352	75.327	75.081	80.388	80.318	80.404	80.307	4.4004	0.	45.336	84.783	84.747	84.747
XN25	14056.	14080.	14049.	14703.	14641.	14655.	14651.	126.24	0.	11888.	15291.	15283.	15284.
XN25R	12370.	12369.	12372.	12560.	12555.	12575.	12573.	122.95	0.	11246.	12714.	12754.	12783.
PCN25R	92.178	92.169	92.188	93.593	93.558	93.702	93.687	.9162	0.	83.798	94.736	95.039	95.256
XN48	1017.2	1019.8	1009.9	1190.8	1180.8	1180.6	1174.2	106.89	0.	699.76	1370.5	1360.5	1354.2
XN49	1017.8	1020.	1010.1	1191.	1181.3	1181.5	1175.3	1128.	0.	0.	1371.5	1362.2	1355.5
UT91R2	623.86	624.97	618.4	728.71	722.94	722.97	717.83	65.244	0.	428.54	836.35	830.37	825.86
UT92R2	606.72	607.63	601.25	708.39	703.02	703.21	698.37	669.23	0.	0.	813.57	808.07	803.46
BTAN91	28.142	28.461	28.727	29.785	28.954	28.744	28.98	87.206	82.055	20.581	30.604	30.178	29.942
BTAN92	29.239	29.05	28.634	29.303	29.92	29.543	29.279	86.946	81.855	21.878	29.611	29.694	29.412
W13	12.811	12.367	13.19	13.065	14.133	14.606	15.284	-5.1923	-.5	6.4506	14.011	14.624	15.68
W15	12.206	12.367	12.052	13.065	13.843	13.863	14.003	-5.1923	0.	6.4506	14.011	14.161	13.781
WF36	2605.	2616.3	2564.5	3618.1	3537.5	3539.3	3501.9	166.64	164.08	977.7	4877.9	4717.1	4621.4
WF36R2	2674.4	2683.4	2627.3	3704.	3624.5	3626.9	3579.6	169.84	168.25	1002.2	4979.4	4815.7	4712.4
FN11QA	11101.	11111.	10808.	15329.	15094.	15101.	14816.	0.	0.	3226.4	20240.	19824.	19449.
SFC184	.24354	.24414	.24574	.24426	.24274	.24279	.24422	.5	.5	.31401	.24869	.24557	.24493
TAMB	523.06	523.59	524.94	524.9	524.77	524.92	525.34	526.04	523.73	524.08	527.92	528.25	529.24
T10	520.02	520.78	521.61	522.33	521.79	521.62	523.38	525.02	521.13	521.52-	525.19	525.11	525.95
PAMB	14.309	14.309	14.309	14.308	14.308	14.308	14.31	14.31	14.297	14.298	14.299	14.299	14.299
P10M	14.31	14.309	14.31	14.31	14.308	14.309	14.312	14.311	14.298	14.299	14.299	14.3	14.301
HUMSER	52.958	55.032	55.72	56.095	55.553	53.906	54.961	56.379	57.334	60.477	63.666	65.996	62.201
RELHUM	59.674	60.855	58.763	59.234	58.926	56.904	57.168	57.232	63.001	65.599	60.421	61.895	56.436
WINVAV	3.2132	2.5168	3.7491	8.1252	4.2212	2.3243	2.262	4.9036	1.1172	1.3106	2.624	3.5259	1.7794
WINAAV	119.	151.17	-61.304	-43.078	146.41	111.06	33.033	-36.545	-90.63	-147.83	-51.425	-63.637	-36.56
XHO	0.	0.	0.	0.	0.	0.	0.	0.	0.	0.	0.	0.	0.
P46Q2	1.9388	1.944	1.9163	2.3244	2.3014	2.3001	2.2798	1.0018	9.99+10	1.2714	2.7705	2.7445	2.7072
CT46	1494.	1499.1	1486.8	1625.6	1605.5	1604.	1601.5	874.1	9.99+10	1308.1	1774.7	1730.	1716.9
T46X	1500.4	1504.6	1498.3	1619.4	1601.2	1598.1	1596.9	710.96	528.63	1277.4	1736.1	1708.6	1695.
Comments	Part Power	Part Power	Part Power	Part Power	Part Power	Part Power	Part Power	Zero	Zero	F.I. Bad XN49	Part Power	Part Power	Part Power
	Bleed Evaluation--→										Bleed Evaluation--------→		
	Stroke =										Stroke =		
	35%	0%	100%	0%	35%	80%	100%				0%	35%	80%

GE36/UDF1 Peebles Tests
082001-03
Test Log - Site IIID
Sheet 004 of 029

GE36/UDF-1 ENGINE 082001-03-TEST READINGS - SITE II[illegible]
RDGS. 1 - 5 ON 06.20.86 RDGS. 6 - 15 ON 06.23.86
RDGS. 16 - 31 ON 06.24.86 RDGS. 32 - 47 ON 06.25.86
RDGS. 48 - 57 ON 06.26.86

RDG.	53	54	55	56	57
XN2	11329.	10751.	10072.	326.61	0.
XN2R	11246.	10668.	9984.4	321.67	0.
PCN2R	84.75	80.394	75.24	2.424	0.
XN25	15254.	14699.	14151.	113.14	0.
XN25R	12795.	12611.	12421.	108.58	0.
PCN25R	95.344	93.975	92.559	.80912	0.
XN48	1341.8	1172.6	1016.8	446.33	0.
XN49	1342.7	1173.9	1018.6	481.02	0.
UT91R2	817.98	714.53	619.02	269.94	0.
UT92R2	795.64	695.32	602.72	282.76	0.
BTAN91	30.452	29.135	27.94	87.284	86.683
BTAN92	29.261	29.379	28.564	86.959	86.384
W13	16.6	15.637	13.911	-6.4314	-.5
W15	13.206	12.097	10.646	-6.4314	0.
WF36	4543.4	3432.1	2531.5	155.06	157.07
WF36R2	4630.8	3495.	2574.1	156.2	159.22
FN11QA	19009.	14559.	10726.	0.	0.
SFC184	.24626	.24266	.2426	.5	.5
TAMB	529.64	530.39	530.98	534.99	536.16
T10	526.31	526.78	527.77	534.71	536.23
PAMB	14.3	14.3	14.301	14.297	14.18
P10M	14.301	14.302	14.302	14.298	14.181
HUMSER	64.567	61.929	67.066	61.219	100.29
RELHUM	57.754	54.042	57.285	45.745	70.88
WINVAV	1.3753	.35346	.60236	4.4641	4.7464
WINAAV	-81.896	-67.648	4.581	-6.8343	-159.02
XMO	0.	0.	0.	0.	0.
P46Q2	2.6699	2.2727	1.9257	1.0014	9.99+10
CT46	1707.5	1592.6	1483.	876.21	9.99+10
T46X	1690.1	1585.9	1491.1	714.71	536.24
Comments:	Part Power	Part Power	Part Power	Zero	Zero
	Bleed Evaluation-------→				
	Stroke = 100%	100%	100%		

GE36/UDF-1 ENGINE 082001-03 EST READINGS - SITE IIID
RDGS. 57 - 70 ON 06.29.86 RDGS. 71 - 77 ON 06.30.86
RDGS. 78 - 149 ON 07.01.86 RDGS. 150 - 197 ON 07.03.86
RDGS. 198 - 209 ON 07.04.86 RDGS. 210 - 251 ON 07.05.86

RDG.	57	58	59	60	61	62	63	64	65	66	67	68	69
XN2	0.	11448.	11415.	11450.	11444.	761.61	0.	5283.8	11442.	5664.4	5739.7	11350.	11409.
XN2R	0.	11276.	11243.	11260.	11265.	745.05	0.	5210.5	11272.	5593.	5670.7	11208.	11243.
PCN2R	0.	84.971	84.723	84.855	84.891	5.6146	0.	39.266	84.943	42.147	42.733	84.465	84.726
XN25	0.	15489.	15423.	15502.	15423.	127.81	0.	11519.	15502.	11839.	11811.	15131.	15295.
XN25R	0.	12778.	12778.	12790.	12792.	122.63	0.	10903.	12777.	11206.	11180.	12719.	12750.
PCN25R	0.	95.214	95.216	95.306	95.324	.91379	0.	81.243	95.211	83.502	83.308	94.774	95.009
XN48	0.	1391.4	1370.3	1389.1	1368.8	513.84	0.	699.9	1387.7	700.03	700.03	1290.5	1338.7
XN49	0.	1392.	1371.5	1390.4	1370.2	137.84	0.	700.83	1388.9	701.1	701.37	1291.4	1340.3
UT91R2	0.	841.57	828.78	838.91	827.49	308.69	0.	423.84	839.51	424.46	424.72	782.62	810.16
UT92R2	0.	818.4	806.29	816.21	805.11	80.486	0.	412.53	816.72	413.21	413.62	761.26	788.42
BTAN91	86.683	30.425	30.527	30.205	29.74	87.257	86.736	17.007	30.314	18.95	19.024	30.458	29.975
BTAN92	86.384	28.877	28.801	28.808	29.084	87.278	86.902	17.753	29.099	18.788	19.076	29.005	29.043
W13	-.5	13.514	14.649	13.695	15.249	-4.4668	-.5	5.6675	13.511	7.4598	7.9167	19.504	16.873
W15	0.	13.514	14.1	13.695	13.866	-4.4668	0.	5.4647	13.511	5.1858	5.3447	12.533	12.873
WF36	157.07	4862.6	4687.3	4774.6	4670.8	156.92	161.47	813.71	4861.6	816.25	853.28	4420.9	4533.5
WF36R2	159.22	4945.7	4766.6	4845.9	4746.4	157.94	163.79	829.33	4950.5	832.89	871.41	4514.3	4616.7
FN11QA	0.	20234.	19561.	19956.	19528.	0.	0.	2180.2	20391.	0.	2573.	17783.	18765.
SFC184	.5	.24708	.24633	.24546	.2457	.5	.5	.38453	.24542	.5	.34236	.25662	.2487
TAMB	536.16	537.6	537.12	538.7	538.78	540.18	534.77	534.26	533.58	532.9	532.65	532.64	532.39
T10	536.23	534.64	534.72	536.27	535.24	541.97	536.81	533.35	534.47	532.01	531.36	531.83	534.07
PAMB	14.18	14.175	14.175	14.175	14.176	14.177	14.16	14.158	14.161	14.165	14.166	14.167	14.168
P10M	14.181	14.176	14.177	14.177	14.178	14.178	14.161	14.16	14.163	14.168	14.168	14.172	14.17
HUMSER	100.29	100.09	98.079	96.328	97.522	96.421	93.172	95.111	95.478	95.907	95.61	97.146	96.181
RELHUM	70.88	67.429	67.16	62.625	63.223	59.739	68.964	71.581	73.521	75.579	75.973	77.194	77.11
WINVAV	4.7464	4.4568	5.2019	4.5996	3.7526	2.7214	.14307	.25299	2.076	1.1041	1.1273	1.3079	1.9541
WINAAV	-159.02	16.301	-29.165	37.359	-22.668	-128.2	-18.701	61.84	-32.613	-4.4225	1.8491	4.972	-5.0498
XMO	0.	0.	0.	0.	0.	0.	0.	0.	0.	0.	0.	0.	0.
P46Q2	9.99+10	2.7869	2.7313	2.7694	2.7209	1.0013	9.99+10	1.1989	2.7926	1.2397	1.2279	2.5523	2.6504
CT46	-9.99+10	1779.1	1748.1	1763.	1743.5	868.85	9.99+10	1320.5	1772.4	1210.4	1251.9	1741.2	1734.8
T46X	536.24	1743.4	1725.	1732.7	1719.	736.83	562.39	1299.1	1740.1	1228.	1241.6	1707.	1710.7
Comments:	Zero	Part Power Bleed Evaluation → Stroke - 0%	Part Power 35%	Part Power 80%	Part Power 100%	Zero	Zero	F.I.	Part Power Bleed Evaluation Stroke - 0%	F.I. 0% No FN	Part Power 100%	Part Power 100%	Part Power 80%

GE36/UDF1 Peebles Tests
082001-03
Test Log - Site IIID
Sheet 006 of 029

NOTE:
Manual Control T2 →

ORIGINAL PAGE IS
OF POOR QUALITY

GE36/UDF-1 ENGINE 082001-03 ST READINGS - SITE IIID
RDGS. 57 - 70 ON 06.29.86 RDGS. 71 - 77 ON 06.30.86
RDGS. 78 - 149 ON 07.01.86 RDGS. 150 - 197 ON 07.03.86
RDGS. 198 - 209 ON 07.04.86 RDGS. 210 - 251 ON 07.05.86

RDG.	70	71	72	73	74	75	76	77	78	79	80	81	82
XN2	11393.	81.428	11318.	0.	5622.2	5612.2	5615.8	5620.3	116.79	11364.	11354.	11391.	11389.
XN2R	11263.	79.943	11186.	0.	5571.4	5561.2	5565.	5570.	114.54	11284.	11278.	11316.	11314.
PCN2R	84.877	.60244	84.297	0.	41.985	41.908	41.937	41.974	.86315	85.034	84.99	85.274	85.26
XN25	15303.	130.95	15313.	0.	11725.	11736.	11740.	11742.	137.76	15350.	15353.	15403.	15404.
XN25R	12754.	122.98	12716.	0.	11097.	11109.	11116.	11117.	129.5	12740.	12755.	12786.	12789.
PCN25R	95.034	.91641	94.753	0.	82.69	82.777	82.828	82.836	.96496	94.932	95.042	95.277	95.296
XN48	1379.6	109.71	1361.3	0.	700.16	700.03	700.3	700.03	309.43	1378.5	1378.	1395.2	1395.4
XN49	1380.9	129.4	1361.6	0.	701.37	701.1	701.1	701.1	101.27	1379.7	1378.6	1395.8	1396.6
UT91R2	837.5	66.141	826.29	0.	426.08	425.98	426.16	426.03	186.36	840.54	840.53	851.19	851.25
UT92R2	814.85	75.829	803.32	0.	414.87	414.69	414.7	414.74	59.284	817.73	817.39	827.68	828.13
BTAN91	30.335	87.146	30.725	76.706	18.937	19.064	18.962	18.803	86.764	29.95	29.889	29.638	29.618
BTAN92	28.761	87.257	28.717	81.62	18.988	18.969	19.366	19.357	86.729	29.608	29.467	29.364	29.44
W13	13.749	-7.4455	14.318	-.5	5.9546	5.6503	5.8283	5.7034	-7.1141	13.594	13.584	13.214	13.325
W15	13.749	-7.4455	14.318	0.	5.9546	5.6503	5.8283	5.7034	-7.1141	13.594	13.584	13.214	13.325
WF36	4711.	171.33	4769.5	176.23	887.71	880.28	877.46	875.26	179.79	4895.9	4843.6	4855.1	4848.3
WF36R2	4818.1	173.36	4874.2	179.78	908.92	901.36	898.55	896.49	181.64	5037.3	4985.9	4998.2	4991.2
FN11QA	19848.	0.	19378.	0.	2685.2	2638.3	2632.6	2653.5	0.	20427.	20346.	20630.	20611.
SFC184	.24539	.5	.25427	.5	.34217	.34536	.34503	.34152	.5	.24928	.24772	.24491	.24479
TAMB	531.63	531.39	529.67	529.46	529.26	529.36	529.33	529.31	527.98	527.3	526.9	526.84	526.8
T10	530.73	538.12	530.93	531.13	528.17	528.22	528.18	528.09	539.21	526.08	525.69	525.54	525.57
PAMB	14.168	14.172	14.173	14.183	14.188	14.187	14.186	14.185	14.173	14.17	14.17	14.172	14.171
P10M	14.169	14.173	14.177	14.184	14.19	14.189	14.188	14.187	14.175	14.171	14.171	14.173	14.172
HUMSER	95.405	93.624	92.822	101.94	101.48	101.92	101.41	102.3	100.09	98.114	95.181	96.457	95.504
RELHUM	78.481	77.694	81.689	90.247	90.488	90.568	90.215	91.022	93.192	93.511	92.064	93.452	92.684
WINVAV	2.7495	.0001	1.7592	2.5319	1.1485	2.148	1.8073	1.9152	2.4646	3.3228	2.5153	4.5126	4.9621
WINAAV	-10.889	-71.231	-45.818	-172.01	159.77	-108.03	-158.7	-143.18	169.71	-149.76	-165.61	-122.38	-161.17
XMO	0.	0.	0.	0.	0.	0.	0.	0.	0.	0.	0.	0.	0.
P46Q2	2.7472	1.0009	2.7166	9.99+10	1.2304	1.2295	1.2291	1.2293	1.0009	2.7773	2.7744	2.8081	2.8074
CT46	1744.7	888.33	1795.7	9.99+10	1324.7	1317.9	1310.7	1306.8	930.87	1785.7	1770.2	1750.7	1749.2
T46X	1717.7	641.58	1729.	541.42	1288.7	1284.3	1279.7	1268.7	661.24	1742.5	1729.6	1718.6	1717.5
Comments:	Part Power Bleed Eval. Stroke = 35%	Zero	Part Power	Zero	F.I.	F.I.	F.I.	F.I.	Zero	Part Power	Part Power	Down Pt. 1a	Power Cal. Pt. 1b

High Rel. Humidity (Rain?)

Manual Control T2 ⟶

GE36/UDF1 Peebles Tests
082001-03
Test Log - Site IIID
Sheet 007 of 029

GE36/UDF-1 ENGINE 082001-03 TEST READINGS - SITE IIID

RDGS. 57 - 70 ON 06.29.86 RDGS. 71 - 77 ON 06.30.86
RDGS. 78 - 149 ON 07.01.86 RDGS. 150 - 197 ON 07.02.86
RDGS. 198 - 209 ON 07.04.86 RDGS. 210 - 251 ON 07.05.86

RDG.	83	84	85	86	87	88	89	90	91	92	93	94	95
XN2	11308.	11310.	10983.	10978.	10685.	10686.	10327.	10328.	10329.	9781.8	9776.3	8885.5	8885.8
XN2R	11235.	11237.	10913.	10908.	10619.	10620.	10265.	10266.	10267.	9724.5	9717.8	8832.6	8832.6
PCN2R	84.665	84.683	82.24	82.203	80.025	80.031	77.355	77.36	77.371	73.282	73.231	66.561	65.561
XN25	15327.	15328.	15015.	15010.	14721.	14721.	14386.	14384.	14383.	14044.	14037.	13580.	13578.
XN25R	12767.	12767.	12671.	12667.	12580.	12580.	12468.	12466.	12466.	12350.	12342.	12164.	12162.
PCN25R	95.135	95.137	94.42	94.388	93.74	93.741	92.908	92.893	92.89	92.028	91.971	90.643	90.624
XN48	1369.3	1369.7	1265.8	1265.4	1179.4	1179.3	1083.3	1083.5	1084.2	996.46	994.99	886.09	885.42
XN49	1370.3	1371.	1266.9	1266.1	1180.4	1180.8	1084.5	1085.	1085.1	997.67	996.73	887.03	887.03
UT91R2	835.41	835.67	772.42	772.17	719.81	719.77	661.22	661.37	661.83	608.34	607.36	540.9	540.48
UT92R2	812.66	813.07	751.43	750.95	700.21	700.5	643.42	643.73	643.86	592.03	591.39	526.31	526.3
BTAN91	29.885	29.653	29.537	29.648	29.31	29.219	29.07	28.875	29.071	27.998	27.809	26.985	26.698
BTAN92	29.375	29.476	29.353	29.23	29.125	29.186	28.69	28.941	28.767	28.362	28.243	27.472	27.65
W13	13.238	13.251	12.975	13.005	12.618	12.609	11.931	11.842	12.011	11.067	10.963	9.7849	9.9043
W15	13.238	13.251	12.975	13.005	12.618	12.609	11.931	11.842	12.011	11.067	10.963	9.7849	9.9043
WF36	4671.	4675.	4009.3	4007.5	3465.6	3461.1	2909.2	2912.3	2916.9	2428.9	2433.9	1913.4	1915.6
WF36R2	4809.	4813.6	4128.4	4126.4	3568.8	3564.8	2995.9	2999.2	3004.1	2501.6	2506.3	1970.8	1972.9
FN11QA	19884.	19922.	0.	17176.	14909.	14928.	0.	12505.	12489.	10374.	10358.	8012.3	8010.1
SFC184	.24449	.24425	.5	.24285	.24196	.2414	.5	.24244	.24316	.24376	.24459	.24865	.24898
TAMB	526.69	526.71	526.63	526.56	526.45	526.44	526.43	526.38	526.29	526.2	526.25	526.17	526.22
T10	525.45	525.43	525.31	525.31	525.14	525.07	524.97	524.99	524.92	524.79	524.94	524.91	524.93
PAMB	14.171	14.171	14.17	14.171	14.171	14.171	14.172	14.172	14.172	14.172	14.173	14.169	14.169
P10M	14.173	14.172	14.172	14.173	14.173	14.172	14.174	14.173	14.174	14.174	14.174	14.17	14.17
HUMSER	96.437	96.526	96.481	95.93	94.879	95.395	95.793	94.947	95.705	95.273	95.73	94.864	95.253
RELHUM	93.94	93.962	94.151	93.861	93.21	93.731	94.154	93.522	94.523	94.402	94.688	94.101	94.324
WINVAV	5.1581	3.3497	3.1338	2.4933	4.3682	1.7148	4.0479	1.4784	2.3773	1.1536	4.3176	2.2481	4.8718
WINAAV	-155.83	-162.4	-142.09	131.71	166.44	-143.54	-139.88	133.66	155.19	-132.07	144.19	-110.49	168.
XMO	0.	0.	0.	0.	0.	0.	0.	0.	0.	0.	0.	0.	0.
P46Q2	2.7479	2.7487	2.5124	2.5104	2.3078	2.3095	2.0895	2.0906	2.0917	1.9025	1.901	1.6924	1.6922
CT46	1730.7	1730.9	1663.3	1664.9	1608.5	1607.4	1546.4	1547.9	1548.9	1480.4	1485.8	1405.9	1407.4
T46X	1705.3	1700.4	1642.	1642.8	1597.3	1598.6	1541.1	1542.7	1543.4	1480.9	1483.9	1403.1	1404.3

Comments:

Down Power Calibration →
Manual Control T2 →
High Relative Humidity (Rain?) →

Pt.2a	Pt.2b	Pt.3a	Pt.3b	Pt.4a	Pt.4b	Pt.5a	Pt.5b	Pt.5c	Pt.6a	Pt.6b	Pt.7a	Pt.7b
		No FN				No FN						

GE36/UDF1 Peebles Tests
082001-03
Test Log - Site IIID
Sheet 008 of 029

GE36/UDF-1 ENGINE 082001-0[illegible] TEST READINGS - SITE IIID
RDGS. 57 - 70 ON 06.29.86 RDGS. 71 - 77 ON 06.30.86
RDGS. 78 - 149 ON 07.01.86 RDGS. 150 - 197 ON 07.03.86
RDGS. 198 - 209 ON 07.04.86 RDGS. 210 - 251 ON 07.05.86

RDG.	96	97	98	99	100	101	102	103	104	105	106	107	108
XN2	7870.1	7871.6	6314.7	6313.3	5429.7	5431.2	4169.2	8756.5	8755.4	8008.8	8008.6	7130.3	7131.3
XN2R	7824.7	7826.3	6278.1	6277.5	5397.9	5400.2	4144.2	8709.9	8708.8	7967.4	7966.3	7093.3	7094.6
PCN2R	58.965	58.978	47.311	47.306	40.678	40.695	31.23	65.636	65.627	60.041	60.033	53.454	53.463
XN25	13035.	13034.	12153.	12151.	11616.	11614.	10728.	13463.	13463.	13074.	13074.	12605.	12605.
XN25R	11912.	11910.	11414.	11414.	11055.	11054.	10366.	12099.	12101.	11922.	11920.	11679.	11679.
PCN25R	88.762	88.75	85.053	85.051	82.38	82.372	77.246	90.159	90.169	88.836	88.825	87.028	87.03
XN48	791.38	790.85	699.49	700.43	700.16	700.16	700.16	789.91	789.91	789.78	789.38	789.91	789.64
XN49	792.59	792.32	700.83	701.37	701.24	701.24	701.1	790.85	790.98	790.98	790.98	791.12	791.12
UT91R2	483.18	482.86	427.06	427.69	427.45	427.51	427.38	482.5	482.49	482.49	482.2	482.56	482.42
UT92R2	470.37	470.22	415.9	416.27	416.12	416.18	415.98	469.55	469.62	469.7	469.65	469.77	469.79
BTAN91	25.271	25.015	21.321	21.639	17.658	17.594	10.516	29.949	29.962	26.973	26.243	23.235	22.582
BTAN92	26.	25.922	22.799	22.674	18.687	18.795	11.076	29.361	29.508	26.773	26.536	23.267	23.822
W13	8.6834	8.5114	6.261	6.3375	5.7189	5.7571	3.838	10.103	10.287	8.6711	8.7659	7.332	7.4253
W15	8.6834	8.5114	6.261	6.3375	5.6233	5.5881	3.838	10.103	10.287	8.6711	8.7659	7.332	7.4253
WF36	1470.2	1472.2	1002.5	1004.8	827.29	828.84	653.57	1842.8	1839.1	1523.	1524.1	1227.7	1229.5
WF36R2	1514.5	1516.7	1032.4	1034.9	851.86	853.7	672.9	1899.6	1895.7	1569.6	1570.5	1265.1	1267.1
FN11QA	5900.6	5898.2	3575.6	3531.6	2462.2	2464.	919.47	7267.8	7275.2	6077.2	6105.9	4743.9	4776.9
SFC184	.25945	.25994	.29187	.29623	.34974	.35024	.73979	.26421	.26341	.26108	.26001	.26958	.26814
TAMB	526.14	526.06	525.91	526.08	525.89	525.78	525.85	525.5	525.58	525.42	525.42	525.37	525.3
T10	524.71	524.69	524.74	524.61	524.8	524.64	524.95	524.24	524.24	524.07	524.18	524.09	524.05
PAMB	14.169	14.169	14.171	14.171	14.171	14.17	14.169	14.17	14.17	14.175	14.175	14.175	14.175
P10M	14.171	14.17	14.173	14.172	14.173	14.172	14.171	14.171	14.172	14.176	14.176	14.177	14.176
HUMSER	94.687	94.807	94.235	94.371	94.321	92.696	93.67	92.817	92.352	92.374	92.44	91.673	93.67
RELHUM	94.027	94.379	94.346	93.906	94.484	93.254	93.96	94.271	93.546	94.119	94.2[illegible]6	93.581	95.809
WINVAV	1.3367	2.2079	4.6007	2.2312	1.1312	3.1201	1.5844	1.647	1.2155	2.6304	1.64[illegible]	2.4408	2.3434
WINAAV	-65.167	-101.96	153.11	-105.64	-151.98	-161.49	-157.23	148.19	99.952	-116.19	99.564	82.246	-153.69
XMO	0.	0.	0.	0.	0.	0.	0.	0.	0.	0.	0.	0.	0.
P46Q2	1.5053	1.5055	1.301	1.3006	1.2156	1.2158	1.1204	1.6476	1.6467	1.5244	1.5244	1.4027	1.4027
CT46	1337.4	1339.7	1274.5	1276.5	1269.1	1270.8	1328.8	1400.1	1397.1	1348.1	1348.4	1306.4	1306.8
T46X	1331.4	1332.8	1246.	1247.	1220.9	1246.1	1343.	1390.1	1388.7	1340.2	1341.1	1290.7	1291.5

Comments: Down Power Calibration → "EPR POWER BOOK" 1 →
Manual Control T2 → →
High Relative Humidity (Rain) → →

Pt.8a	Pt.8b	Pt.9a	Pt.9b	Pt.10a F.I.	Pt.10b F.I.	Pt.11 C.I.	Pt.1a	Pt.1b	Pt.2a	Pt.2b	Pt.3a	Pt.3b

GE36/UDF1 Peebles Tests
082001-03
Test Log - Site IIID
Sheet 009 of 029

GE36/UDF-1 ENGINE 082001-03 TEST READINGS - SITE IIID
RDGS. 57 - 70 ON 06.29.86 RDGS. 71 - 77 ON 06.30.86
RDGS. 78 - 149 ON 07.01.86 RDGS. 150 - 197 ON 07.03.86
RDGS. 198 - 209 ON 07.04.86 RDGS. 210 - 251 ON 07.05.86

RDG.	109	110	111	112	113	114	115	116	117	118	119	120	121
XN2	7741.8	9558.9	9559.8	9306.	9308.5	8468.1	8455.1	7055.5	7056.7	10372.	10379.	10179.	10181.
XN2R	7702.	9510.3	9511.5	9257.9	9261.8	8425.9	8411.8	7019.1	7019.5	10321.	10327.	10130.	10132.
PCN2R	58.041	71.668	71.677	69.766	69.795	63.495	63.39	52.895	52.898	77.774	77.825	76.336	76.355
XN25	12914.	13885.	13888.	13751.	13751.	13336.	13335.	12577.	12573.	14383.	14388.	14212.	14213.
XN25R	11810.	12276.	12279.	12220.	12221.	12054.	12053.	11669.	11664.	12464.	12465.	12401.	12402.
PCN25R	88.004	91.475	91.5	91.061	91.068	89.818	89.81	86.95	86.915	92.873	92.883	92.41	92.414
XN48	790.45	883.68	884.08	883.68	883.54	884.08	883.14	883.41	883.41	988.02	988.43	987.89	987.36
XN49	791.38	885.02	884.88	885.02	884.88	885.15	884.88	834.88	885.02	988.69	988.96	989.1	989.23
UT91R2	482.91	539.9	540.17	539.86	539.86	540.2	539.56	539.7	539.64	603.75	603.99	603.73	603.44
UT92R2	469.95	525.58	525.52	525.54	525.54	525.71	525.49	525.46	525.49	587.25	587.4	587.54	587.66
BTAN91	25.796	30.514	31.19	29.567	29.681	25.592	25.425	20.22	20.28	31.2	31.212	29.799	29.379
BTAN92	26.274	29.19	29.101	28.516	28.427	26.035	25.797	21.091	21.014	29.85	30.124	29.854	29.963
W13	5.9692	11.496	11.275	10.843	10.853	9.4526	9.5407	7.0128	6.8518	12.684	12.811	11.856	11.776
W15	5.9692	11.496	11.275	10.843	10.853	9.4526	9.5407	7.0128	6.8518	12.684	12.811	11.856	11.776
WF36	1474.6	2287.3	2283.8	2134.1	2137.	1721.9	1718.2	1209.2	1212.3	2950.1	2953.3	2697.4	2698.6
WF36R2	1519.3	2356.4	2352.9	2198.1	2201.5	1774.	1770.	1245.7	1248.9	3042.9	3046.	2782.9	2784.6
FN11QA	0.	9114.7	9110.6	8688.2	8668.7	7156.3	7151.1	4602.2	4617.7	11792.	11811.	11194.	11200.
SFC184	.5	.26133	.26106	.25575	.25672	.25059	.25021	.27363	.27341	.26085	.2607	.2513	.25134
TAMB	525.28	525.32	525.28	525.34	525.54	525.22	525.3	525.36	525.34	524.99	525.02	524.91	524.97
T10	524.04	523.98	523.95	524.06	523.91	523.89	524.02	524.06	524.18	523.82	523.83	523.72	523.64
PAMB	14.18	14.183	14.184	14.185	14.185	14.183	14.181	14.179	14.177	14.171	14.17	14.168	14.169
P10M	14.18	14.185	14.185	14.187	14.187	14.186	14.184	14.181	14.178	14.173	14.174	14.171	14.17
HUMSER	90.893	91.576	91.308	92.01	92.452	91.348	89.662	93.168	92.011	91.553	91.959	90.732	91.011
RELHUM	93.147	93.716	93.591	94.108	93.865	93.8	91.854	95.146	94.048	94.676	94.985	94.085	94.187
WINVAV	3.8504	2.1101	.97881	1.2416	3.2066	1.59	2.6592	2.3706	2.6219	2.5572	2.3114	3.4157	2.0326
WINAAV	152.85	-155.02	-151.76	-59.463	-29.707	-58.405	-27.854	-62.716	-56.198	121.92	157.02	167.08	-123.53
XMO	0.	0.	0.	0.	0.	0.	0.	0.	0.	0.	0.	0.	0.
P46Q2	1.4234	1.8253	1.8253	1.7731	1.773	1.6118	1.6098	1.4007	1.4007	2.0872	2.0895	1.994	1.9949
CT46	1355.4	1466.2	1464.1	1439.	1439.3	1376.7	1377.5	1303.1	1306.2	1553.3	1551.	1519.9	1520.
T46X	1334.1	1462.9	1461.3	1436.7	1436.1	1372.9	1373.5	1293.5	1295.1	1545.6	1544.3	1517.9	1517.9

Comments:	109	110 – 117	118 – 121
	Aborted Point No FN	"EPR Power Hook" 2 → Manual Control T2 → High Relative Humidity (Rain?) →	"EPR Power Hook" 3 → → →

110	111	112	113	114	115	116	117	118	119	120	121
Pt.1a	Pt.1b	Pt.2a	Pt.2b	Pt.3a	Pt.3b	Pt.4a	Pt.4b	Pt.1a	Pt.1b	Pt.2a	Pt.2b

GE36/UDF1 Peebles Tests
082001-03
Test Log - Site IIID
Sheet 010 of 029

ORIGINAL PAGE IS
OF POOR QUALITY

GE36/UDF-1 ENGINE 082001-03 TEST READINGS - SITE IIID
RDGS. 57 - 70 ON 06.29.86 RDGS. 71 - 77 ON 06.30.86
RDGS. 78 - 149 ON 07.01.86 RDGS. 150 - 197 ON 07.03.86
RDGS. 198 - 209 ON 07.04.86 RDGS. 210 - 251 ON 07.05.86

RDG.	122	123	124	125	126	127	128	129	130	131	132	133	134
XN2	8822.2	8806.7	7744.7	7739.3	300.54	0.	0.	409.46	0.	10833.	10831.	11163.	11167.
XN2R	8780.6	8763.1	7707.4	7700.9	298.17	0.	0.	403.95	0.	10709.	10701.	11030.	11036.
PCN2R	66.169	66.037	58.082	58.032	2.2469	0.	0.	3.0441	0.	80.698	80.643	83.12	83.164
XN25	13537.	13532.	12973.	12969.	90.095	0.	0.	115.76	0.	14893.	14907.	15191.	15198.
XN25R	12143.	12141.	11882.	11878.	87.378	0.	0.	110.29	0.	12625.	12634.	12710.	12717.
PCN25R	90.487	90.466	88.537	88.51	.65111	0.	0.	.82182	0.	94.073	94.146	94.71	94.765
XN48	987.76	987.49	976.1	977.17	460.39	0.	0.	514.77	0.	1206.5	1207.4	1197.9	1197.8
XN49	989.1	989.5	989.23	989.5	479.14	0.	0.	539.15	0.	1307.2	1308.4	1298.9	1299.5
UT91R2	603.71	603.41	596.54	597.1	280.5	0.	0.	311.86	0.	732.39	732.63	726.87	726.94
UT92R2	587.61	587.71	587.64	587.7	283.75	0.	0.	317.49	0.	771.32	771.69	766.09	766.56
BTAN91	24.114	23.891	20.682	20.688	87.118	86.948	86.89	86.834	87.004	29.723	29.8	31.441	31.383
BTAN92	24.54	24.912	21.545	21.503	87.087	86.976	86.867	86.92	86.999	27.102	26.916	28.026	28.327
W13	9.6551	9.3895	7.9772	7.7816	-6.1845	-.5	-.5	-5.7185	-.5	12.273	11.978	13.169	13.198
W15	9.6551	9.3895	7.9772	7.7816	-6.1845	0.	0.	-5.7185	0.	12.273	11.978	13.169	13.198
WF36	1907.5	1900.5	1448.2	1448.3	183.28	171.87	170.83	171.46	170.88	3631.5	3604.7	4199.8	4200.4
WF36R2	1967.8	1960.2	1493.5	1493.2	188.13	175.2	173.98	174.83	174.06	3723.	3693.1	4304.1	4306.4
FN11QA	8110.4	8109.8	5870.5	5852.2	0.	0.	0.	0.	0.	15538.	15442.	17130.	1721.
SFC184	.24526	.24434	.25717	.25792	.5	.5	.5	.5	.5	.24222	.24177	.25399	.25291
TAMB	524.89	524.95	524.91	524.95	525.04	531.99	532.14	532.6	532.18	532.31	532.32	532.25	532.33
T10	523.6	523.85	523.69	523.86	526.94	532.18	533.6	532.93	534.8	530.8	531.28	531.25	531.04
PAMB	14.169	14.169	14.172	14.173	14.173	14.176	14.162	14.157	14.137	14.129	14.128	14.127	14.125
P10M	14.172	14.17	14.174	14.175	14.175	14.176	14.163	14.158	14.139	14.131	14.132	14.13	14.128
HUMSER	91.779	91.473	91.117	92.322	91.687	108.31	113.42	115.87	115.91	115.97	113.59	113.48	114.58
RELHUM	95.222	94.739	94.515	95.616	94.666	87.814	91.313	91.741	92.955	92.545	90.67	90.799	91.398
WINVAV	5.566	4.0384	2.9572	1.7913	2.4753	1.804	2.6792	2.5888	6.7578	5.4003	6.6822	7.4165	7.0775
WINAAV	-45.912	-38.488	-41.98	-54.588	-176.18	165.89	162.14	-36.515	-47.08	-32.524	-14.119	-33.064	-21.301
XMO	0.	0.	0.	0.	0.	0.	0.	0.	0.	0.	0.	0.	0.
P46Q2	1.6938	1.6911	1.5058	1.505	1.0012	9.99+10	9.99+10	1.0014	9.99+10	2.3602	2.3583	2.5633	2.566
CT46	1408.	1409.	1339.1	1340.3	942.25	9.99+10	9.99+10	937.39	9.99+10	1646.	1638.8	1699.5	1695.6
T46X	1406.9	1406.6	1335.	1336.1	717.32	553.66	551.26	729.56	608.03	1639.9	1633.6	1679.1	1677.6

Comments: "EPR Power Hook" 3 ⟶ Zero Zero Zero Zero Zero Trim Balance Rpm ⟶
Manual Control T2 ⟶ Mismatched speeds, (XN48-XN49 = -100)
High Relative Humidity (Rain?) ⟶ ⟶
Pt.3a Pt.3b Pt.4a Pt.4b

GE36/UDF1 Problem Tests
082001-03
Test Log - Site IIID
Sheet 011 of 029

ORIGINAL PAGE IS
OF POOR QUALITY

GE36/UDF-1 ENGINE 082001-03 TEST READINGS - SITE IIID
RDGS. 57 - 70 ON 06.29.86 RDGS. 71 - 77 ON 06.30.86
RDGS. 78 - 149 ON 07.01.86 RDGS. 150 - 197 ON 07.03.86
RDGS. 198 - 209 ON 07.04.86 RDGS. 210 - 251 ON 07.05.86

RDG.	135	136	137	138	139	140	141	142	143	144	145	146	147
XN2	11271.	11277.	11440.	11440.	11583.	11585.	11132.	11132.	11378.	11380.	11512.	11512.	11684.
XN2R	11139.	11144.	11308.	11309.	11451.	11454.	11007.	11007.	11252.	11253.	11386.	11384.	11553.
PCN2R	83.938	83.977	85.218	85.219	86.295	86.313	82.948	82.95	84.791	84.797	85.799	85.785	87.058
XN25	15288.	15295.	15428.	15430.	15543.	15545.	15186.	15186.	15405.	15408.	15515.	15517.	15652.
XN25R	12745.	12748.	12785.	12787.	12817.	12819.	12715.	12716.	12785.	12786.	12814.	12815.	12849.
PCN25R	94.968	94.991	95.27	95.28	95.503	95.52	94.749	94.753	95.266	95.276	95.484	95.489	95.746
XN48	1197.5	1198.1	1197.5	1198.1	1197.9	1198.2	1297.7	1297.6	1298.	1297.9	1297.7	1298.1	1297.9
XN49	1299.2	1299.2	1299.5	1298.9	1298.9	1298.7	1398.7	1399.3	1399.	1398.7	1398.7	1398.6	1399.
UT91R2	726.73	727.06	726.95	727.23	727.25	727.49	788.	787.9	788.21	788.05	788.17	788.27	788.04
UT92R2	766.36	766.36	766.74	766.39	766.5	766.42	825.56	825.85	825.76	825.51	825.73	825.51	825.67
BTAN91	31.75	31.687	32.851	33.085	34.403	34.396	29.967	29.89	30.64	30.717	31.341	31.376	31.909
BTAN92	28.639	28.706	29.182	29.078	29.438	29.435	27.486	27.65	28.304	28.407	28.506	28.315	29.114
W13	13.456	13.519	13.635	13.896	14.061	14.02	12.485	12.548	13.177	13.145	13.593	13.47	13.716
W15	13.456	13.519	13.635	13.896	14.061	14.02	12.485	12.548	13.177	13.145	13.593	13.47	13.716
WF36	4397.3	4402.	4715.8	4712.3	5002.7	5002.4	4188.6	4188.4	4652.5	4652.5	4920.3	4915.4	5270.7
WF36R2	4508.5	4512.9	4837.7	4833.8	5133.3	5134.	4299.6	4298.9	4776.	4775.6	5052.1	5046.1	5410.6
FN11QA	17747.	17753.	18493.	18474.	19092.	19099.	17928.	17952.	19377.	19390.	20067.	20053.	21015.
SFC184	.2568	.25697	.26444	.2645	.2718	.27173	.24244	.24207	.24916	.24897	.2545	.25437	.26026
TAMB	532.21	532.36	532.14	532.09	531.91	531.83	531.52	531.46	531.32	531.28	531.23	531.19	531.18
T10	531.1	531.1	530.79	530.85	530.7	530.59	530.48	530.5	530.42	530.53	530.25	530.44	530.54
PAMB	14.125	14.125	14.123	14.123	14.122	14.121	14.119	14.119	14.12	14.119	14.119	14.12	14.12
P10M	14.127	14.128	14.125	14.126	14.125	14.124	14.121	14.122	14.123	14.122	14.123	14.122	14.122
HUMSER	113.34	113.02	112.16	111.86	111.82	111.87	110.68	111.41	109.98	110.28	111.23	109.04	109.67
RELHUM	90.783	90.092	90.075	89.991	90.506	90.778	90.777	91.531	90.821	91.193	92.108	90.475	91.204
WINVAV	5.6517	5.4682	6.2839	7.3706	7.5661	6.5787	5.8379	7.2179	6.2727	8.2222	7.4408	6.7403	10.205
WINAAV	-8.0927	-14.537	-15.674	-20.098	-20.514	-23.497	-17.647	-21.818	-15.04	-17.285	-21.006	-17.588	-23.897
XMO	0.	0.	0.	0.	0.	0.	0.	0.	0.	0.	0.	0.	0.
P46Q2	2.633	2.6349	2.7431	2.7427	2.8388	2.8401	2.5768	2.5763	2.7356	2.7366	2.8258	2.8247	2.943
CT46	1715.5	1715.3	1743.	1741.6	1766.3	1764.9	1698.4	1698.4	1740.7	1740.	1762.2	1762.4	1792.9
T46X	1694.5	1694.5	1713.5	1712.8	1737.3	1736.9	1680.2	1680.2	1720.5	1720.6	1735.4	1735.4	1764.9

Comments: Trim Balance Run →
Mismatched Speeds (XN48 - XN49 = -100) →
High Relative Humidity (Rain?) →

GE36/UDF1 Peebles Tests
082001-03
Test Log - Site IIID
Sheet 012 of 029

GE36/UDF-1 ENGINE 082001-03 TEST READINGS - SITE IIID
RDGS. 57 - 70 ON 06.29.86 RDGS. 71 - 77 ON 06.30.86
RDGS. 78 - 149 ON 07.01.86 RDGS. 150 - 197 ON 07.03.86
RDGS. 198 - 209 ON 07.04.86 RDGS. 210 - 251 ON 07.05.86

RDG.	148	149	150	151	152	153	154	155	156	157	158	159	160
XN2	11688.	602.68	0.	10737.	183.93	10766.	10770.	10526.	10528.	9660.6	9654.	8767.4	8764.2
XN2R	11565.	595.32	0.	10717.	183.39	10749.	10754.	10510.	10513.	9647.2	9640.4	8750.	8751.5
PCN2R	87.149	4.4862	0.	80.759	1.382	81.005	81.036	79.203	79.224	72.699	72.648	65.976	65.949
XN25	15655.	129.9	0.	14713.	92.19	14717.	14727.	14521.	14522.	13952.	13949.	13500.	13495.
XN25R	12856.	126.03	0.	12583.	90.101	12572.	12581.	12527.	12528.	12337.	12336.	12157.	12152.
PCN25R	95.8	.93911	0.	93.762	.6714	93.679	93.745	93.343	93.352	91.933	91.926	90.586	[illegible].551
XN48	1297.9	672.3	0.	1084.7	377.88	1084.9	1084.6	1084.6	1084.9	1085.	1084.9	1084.9	1084.9
XN49	1398.7	661.05	0.	1085.5	413.51	1085.7	1085.9	1085.9	1086.2	1085.8	1086.1	1086.1	1086.2
UT91R2	788.56	407.81	0.	664.84	231.37	665.2	665.02	665.06	665.29	665.37	665.28	665.27	665.25
UT92R2	826.05	389.76	0.	646.71	246.1	647.06	647.2	647.24	647.46	647.22	647.37	647.36	647.42
BTAN91	31.979	87.203	86.602	31.923	86.712	32.185	32.023	30.694	30.359	26.584	26.222	23.076	22.88
BTAN92	29.203	87.217	84.768	29.426	86.732	29.477	29.66	28.651	28.749	25.39	25.567	22.75	23.074
W13	13.782	-4.9219	-.5	13.653	-6.7314	13.901	13.732	13.052	12.725	10.541	11.039	8.8799	9.1387
W15	13.782	-4.9219	0.	13.653	-6.7314	13.901	13.732	13.052	12.725	10.541	11.039	8.8799	9.1387
WF36	5282.3	175.39	190.91	3594.6	187.92	3668.4	3655.8	3239.6	3241.	2387.7	2387.7	1896.	1896.2
WF36R2	5427.5	179.62	197.12	3719.1	194.01	3796.3	3783.3	3351.5	3354.3	2470.7	2470.	1961.7	1961.6
FN11QA	21062.	0.	-.22841	14389.	0.	14531.	14558.	13495.	13512.	10490.	10507.	8200.2	8227.9
SFC184	.26049	.5	-872.36	.26127	.5	.26409	.26271	.25106	.25095	.23809	.23764	.24183	.241
TAMB	531.24	531.05	522.41	521.82	521.59	521.26	521.2	521.25	521.18	521.	520.94	520.83	520.87
T10	529.84	531.58	521.84	520.68	521.72	520.25	520.27	520.21	520.11	520.12	520.13	520.14	520.18
PAMB	14.12	14.12	14.185	14.188	14.189	14.193	14.193	14.194	14.194	14.194	14.195	14.195	14.196
P10M	14.122	14.121	14.186	14.19	14.19	14.195	14.194	14.199	14.195	14.195	14.199	14.195	14.197
HUMSER	110.94	108.34	75.88	74.874	74.336	73.235	73.235	72.812	72.764	72.961	72.543	72.194	71.94
RELHUM	91.861	90.337	86.279	86.953	87.055	86.826	87.004	86.377	86.536	87.306	87.013	86.922	86.383
WINVAV	7.3455	6.8006	2.652	2.3281	1.0232	3.0268	3.2939	2.4016	2.9972	1.3622	.83494	1.3939	1.846
WINAAV	-22.608	-24.642	-22.79	17.23	-16.239	-53.574	-44.912	15.338	12.472	25.349	28.983	-5.7549	11.328
XMO	0.	0.	0.	0.	0.	0.	0.	0.	0.	0.	0.	0.	0.
P46Q2	2.9475	1.0031	9.99+10	2.3279	1.0017	2.3517	2.3544	2.2161	2.217	1.894	1.8929	1.6976	1.6969
CT46	1790.3	907.71	9.99+10	1623.2	947.76	1635.1	1627.7	1574.9	1574.7	1471.	1470.	1403.	1404.5
T46X	1763.5	725.26	531.92	1607.6	715.26	1615.1	1601.6	1568.	1567.7	1474.5	1475.8	1404.7	1405.7

Comments:	Trim. Bal. Run. Mis-matched Speeds High Humidity	Zero	Zero	Part Power	Zero	"EPR POWER HOOK" 4 →							
						Pt.1a	Pt.1b	Pt.2a	Pt.2b	Pt.3a	Pt.3b	Pt.4a	Pt.4b

GE36/UDF1 Pembles Tests
082001-03
Test Log - Site IIID
Sheet 013 of 029

GE36/UDF-1 ENGINE 082001-03 TEST READINGS - SITE IIID
RDGS. 57 - 70 ON 06.29.86 RDGS. 71 - 77 ON 06.30.86
RDGS. 78 - 149 ON 07.01.86 RDGS. 150 - 197 ON 07.03.86
RDGS. 198 - 209 ON 07.04.86 RDGS. 210 - 251 ON 07.05.86

ORIGINAL PAGE IS
OF POOR QUALITY

RDG.	161	162	163	164	165	166	167	168	169	170	171	172	173
XN2	11055.	11054.	10848.	10848.	10270.	10275.	9154.3	9155.8	11444.	11449.	11156.	11158.	10592.
XN2R	11034.	11036.	10833.	10835.	10257.	10265.	9146.4	9147.8	11438.	11445.	11147.	11151.	10584.
PCN2R	83.146	83.166	81.634	81.647	77.295	77.356	68.925	68.936	86.196	86.25	84.	84.032	79.761
XN25	15031.	15033.	14844.	14844.	14335.	14333.	13716.	13713.	15372.	15376.	15139.	15137.	14634.
XN25R	12688.	12692.	12635.	12636.	12482.	12481.	12257.	12252.	12799.	12802.	12735.	12735.	12585.
PCN25R	94.543	94.577	94.154	94.16	93.01	93.003	91.335	91.297	95.372	95.398	94.896	94.896	93.776
XN48	1174.6	1174.8	1174.5	1175.2	1174.8	1174.6	1174.8	1175.2	1254.9	1254.9	1255.3	1254.6	1254.5
XN49	1176.1	1176.2	1175.7	1176.	1176.	1176.2	1176.1	1176.2	1255.9	1256.2	1255.9	1256.3	1255.9
UT91R2	719.9	720.22	720.22	720.79	720.5	720.61	720.79	721.02	770.24	770.36	770.2	769.99	769.76
UT92R2	700.63	700.94	700.78	701.09	701.04	701.39	701.41	701.48	749.32	749.59	749.04	749.47	749.09
BTAN91	32.017	31.486	30.864	30.792	27.375	27.173	22.929	23.061	33.04	32.532	30.793	31.366	28.026
BTAN92	29.284	29.749	29.104	28.909	26.2	26.503	22.974	22.889	29.565	29.878	29.37	29.046	26.834
W13	13.655	13.456	12.241	12.752	10.981	10.999	9.1915	8.7562	13.908	13.947	16.107	13.489	11.806
W15	13.655	13.456	12.241	12.752	10.981	10.999	9.1915	8.7562	13.908	13.947	15.808	13.489	11.806
WF36	4185.1	4181.1	3807.4	3811.3	2899.4	2911.5	2112.2	2112.7	4996.4	4999.	4418.9	4421.6	3405.1
WF36R2	4327.7	4326.4	3940.7	3945.8	3000.2	3013.9	2186.4	2186.8	5178.	5181.5	4575.7	4579.9	3524.4
FN11QA	16737.	16867.	15895.	15881.	12791.	12857.	9312.6	9303.	19472.	19590.	18334.	18297.	15021.
SFC184	.26138	.25929	.25061	.25116	.2371	.23696	.23733	.23762	.2688	.26737	.25229	.25302	.23719
TAMB	521.28	521.34	521.24	521.11	520.78	520.64	520.48	520.44	520.18	520.13	520.07	520.1	520.06
T10	520.72	520.38	520.14	519.92	519.98	519.71	519.57	519.58	519.15	518.99	519.54	519.27	519.47
PAMB	14.198	14.199	14.2	14.2	14.202	14.202	14.202	14.202	14.204	14.205	14.207	14.207	14.208
P10M	14.198	14.196	14.195	14.195	14.199	14.199	14.2	14.2	14.199	14.2	14.202	14.203	14.206
HUMSER	70.186	70.156	69.791	70.175	69.769	70.012	69.805	69.959	69.657	70.187	69.073	69.451	69.151
RELHUM	83.245	83.026	82.899	83.725	84.237	84.971	85.178	85.506	85.935	86.727	85.565	85.962	85.723
WINVAV	3.3679	2.4447	2.964	3.209	2.1319	1.6139	2.1175	1.174	2.2912	2.0476	4.0252	3.2148	2.3576
WINAAV	-7.4529	26.522	18.307	17.188	-22.659	-4.2657	71.84	129.42	-33.508	28.718	-45.19	13.269	-13.38
XMO	0.	0.	0.	0.	0.	0.	0.	0.	0.	0.	0.	0.	0.
P46Q2	2.5551	2.556	2.4329	2.4343	2.1003	2.1028	1.7921	1.793	2.8434	2.8475	2.6588	2.6603	2.2981
CT46	1678.2	1674.6	1636.3	1634.2	1539.9	1542.2	1435.5	1437.8	1748.9	1746.2	1684.6	1692.1	1594.4
T46X	1647.3	1645.5	1612.	1611.7	1538.6	1540.3	1438.4	1439.8	1715.4	1713.2	1663.6	1664.2	1587.6

Comments: "EPR POWER HOOK" 5 ⟶ "EPR POWER HOOK" 6 ⟶

	161	162	163	164	165	166	167	168	169	170	171	172	173
Comments:	Pt.1a	Pt.1b	Pt.2a	Pt.2b	Pt.3a	Pt.3b	Pt.4a	Pt.4b	Pt.1a	Pt.1b	Pt.2a	Pt.2b	Pt.3a

GE36/UDF-1 ENGINE 082001-0: ST READINGS - SITE IIID
RDGS. 57 - 70 ON 06.29.86 RDGS. 71 - 77 ON 06.30.86
RDGS. 78 - 149 ON 07.01.86 RDGS. 150 - 197 ON 07.03.86
RDGS. 198 - 209 ON 07.04.86 RDGS. 210 - 251 ON 07.05.86

RDG.	174	175	176	177	178	179	180	181	182	183	184	185	186
XN2	10592.	10244.	10239.	10241.	5784.1	422.86	0.	10979.	10986.	11121.	11712.	10936.	135.71
XN2R	10588.	10242.	10237.	10239.	5781.	420.37	0.	10874.	10884.	10999.	11578.	10815.	133.36
PCN2R	79.79	77.181	77.142	77.158	43.565	3.1678	0.	81.945	82.018	82.889	87.246	81.498	1.0049
XN25	14631.	14316.	14312.	14311.	11887.	167.62	0.	14996.	15005.	15168.	15671.	14993.	114.71
XN25R	12586.	12480.	12476.	12475.	11335.	162.78	0.	12620.	12629.	12679.	12827.	12636.	110.31
PCN25R	93.786	92.995	92.969	92.956	84.465	1.2129	0.	94.038	94.105	94.481	95.585	94.16	.82202
XN48	1254.7	1255.	1254.7	1255.3	700.3	573.85	0.	1254.2	1256.6	1301.5	1299.9	1230.7	227.85
XN49	1256.2	1255.9	1256.1	1256.2	701.1	122.83	0.	1255.7	1257.4	1399.3	1398.9	1357.5	268.17
UT91R2	770.23	770.56	770.37	770.68	429.82	350.32	0.	762.86	764.47	790.48	789.1	747.41	137.49
UT92R2	749.55	749.54	749.6	749.66	418.27	72.888	0.	742.38	743.55	826.08	825.42	801.28	157.29
BTAN91	27.878	25.748	25.903	25.91	20.23	87.248	77.765	29.383	29.463	29.925	32.511	29.665	87.286
BTAN92	27.055	25.458	25.412	25.348	20.319	87.188	77.559	29.666	29.505	27.249	28.605	26.647	87.238
W13	11.604	10.664	10.629	10.676	6.3215	-5.6218	-.5	12.875	12.974	12.598	13.852	12.469	-7.1869
W15	11.604	10.664	10.629	10.676	5.593	-5.6218	0.	12.875	12.974	12.598	13.852	12.469	-7.1869
WF36	3407.5	2903.3	2898.2	2903.3	848.42	186.94	168.22	4019.3	4010.9	4271.1	5415.2	3868.6	161.11
WF36R2	3529.1	3006.9	3001.6	3006.6	877.64	191.88	167.11	4101.	4093.1	4348.9	5512.2	3938.8	162.46
FNI1QA	15090.	13009.	12964.	12981.	2965.9	0.	0.	16889.	16958.	18199.	21213.	16638.	0.
SFC184	.23641	.23366	.23406	.23413	.29913	.5	.5	.24547	.244	.24156	.26267	.2393	.5
TAMB	520.02	519.85	519.82	519.85	520.3	520.53	531.47	532.16	531.85	533.04	533.56	534.07	533.94
T10	519.06	518.84	518.87	518.89	519.22	524.83	548.52	520.68	528.48	530.22	530.75	530.38	537.18
PAMB	14.209	14.21	14.21	14.21	14.213	14.213	14.244	14.242	14.241	14.243	14.241	14.238	14.237
P10M	14.205	14.208	14.208	14.208	14.213	14.214	14.246	14.239	14.24	14.241	14.238	14.238	14.239
HUMSER	69.057	69.244	69.007	68.857	64.324	67.137	62.86	53.117	59.604	58.552	57.614	60.032	52.517
RELHUM	85.736	86.48	86.296	85.998	79.155	81.916	52.649	43.567	49.32	46.566	45.027	46.089	40.558
WINVAV	1.3263	1.4311	1.5607	1.8261	2.5259	1.702	2.0863	8.7989	7.4522	.87259	3.3704	2.9745	7.3289
WINAAV	72.559	56.546	-14.545	11.273	60.439	-164.73	111.96	-158.36	162.5	82.663	-111.01	149.86	171.44
XMO	0.	0.	0.	0.	0.	0.	0.	0.	0.	0.	0.	0.	0.
P46Q2	2.3004	2.1048	2.1038	2.1045	1.3657	1.0022	9.99+10	2.4772	2.4817	2.583	2.9754	2.4477	1.0026
CT46	1594.5	1542.7	1542.5	1544.2	1164.4	947.22	9.99+10	1699.9	1689.8	1721.7	1811.2	1669.8	899.81
T46X	1588.5	1541.2	1542.1	1543.	1220.4	721.84	559.36	1666.6	1660.7	1689.9	1775.3	1644.4	735.05

Comments:	"EPR POWER HOOK" 6 ——→				F.I. Bad Reading	Zero	Zero	Part Power	Part Power	Part Power	Part Power	Part Power	Zero
	Pt.3b	Pt.4a	Pt.4b	Pt.4c				Pt.1a	Pt.1b				

GE36/UDF-1 ENGINE 082001-03 TEST READINGS - SITE IIID
RDGS. 57 - 70 ON 06.29.86 RDGS. 71 - 77 ON 06.30.86
RDGS. 78 - 149 ON 07.01.86 RDGS. 150 - 197 ON 07.03.86
RDGS. 198 - 209 ON 07.04.86 RDGS. 210 - 251 ON 07.05.86

RDG.	187	188	189	190	191	192	193	194	195	196	197	198	199
XN2	0.	12115.	12121.	12144.	8151.3	11842.	11530.	11540.	11534.	201.25	0.	504.82	0.
XN2R	0.	11992.	11997.	12040.	8072.	11734.	11434.	11451.	11426.	199.88	0.	505.2	0.
PCN2R	0.	90.369	90.407	90.731	60.829	88.422	86.167	86.294	86.104	1.5063	0.	3.8071	0.
XN25	0.	15953.	15989.	15997.	13472.	15763.	15519.	15526.	15535.	104.24	0.	129.38	0.
XN25R	0.	12858.	12893.	12908.	12439.	12849.	12791.	12802.	12801.	101.2	0.	126.78	0.
PCN25R	0.	95.816	96.073	96.184	92.688	95.743	95.31	95.396	95.388	.75413	0.	.94468	0.
XN48	0.	1398.1	1398.1	1398.1	964.99	1398.2	1398.1	1398.1	1398.5	374.13	0.	103.14	0.
XN49	0.	1398.5	1399.1	1399.3	969.81	1398.9	1399.1	1399.1	1399.4	431.32	0.	116.27	0.
UT91R2	0.	849.79	849.73	851.19	586.83	850.77	851.38	851.91	850.76	228.19	0.	63.387	0.
UT92R2	0.	826.23	826.58	828.07	573.25	827.35	828.18	828.7	827.5	255.71	0.	69.454	0.
BTAN91	87.336	33.139	33.124	32.935	20.224	30.825	30.085	30.748	31.182	87.255	87.278	87.253	86.866
BTAN92	85.574	30.054	30.276	30.481	20.377	30.138	29.35	29.839	29.148	87.14	85.442	87.131	86.917
W13	-.5	14.817	14.697	14.646	51.451	14.115	13.783	13.517	13.244	-6.7529	-.5	-5.3	-.5
W15	0.	14.817	14.697	14.646	51.451	14.115	13.783	13.517	13.244	-6.7529	0.	-5.3	0.
WF36	162.3	6592.5	6523.7	6590.2	2429.	5853.4	5208.1	5176.7	5115.9	181.52	190.3	190.45	189.34
WF36R2	158.72	6723.6	6652.5	6735.8	2476.5	5977.	5323.	5295.5	5221.6	185.68	193.6	196.77	192.92
FNI1QA	1.5865	24344.	24309.	24524.	2993.1	23094.	21355.	21404.	21208.	-15.366	0.	0.	0.
SFC184	101.13	.2792	.27663	.27764	.8364	.26163	.25197	.25009	.24888	-12.215	.5	.5	.5
TAMB	533.89	528.93	529.47	528.67	528.82	528.56	527.69	527.57	527.47	525.5	522.01	518.15	529.97
T10	561.68	529.4	529.47	527.66	528.91	528.28	527.42	526.77	528.5	525.79	529.68	517.88	527.27
PAMB	14.235	14.24	14.241	14.242	14.242	14.242	14.242	14.242	14.242	14.244	14.249	14.25	14.271
P10M	14.237	14.238	14.242	14.24	14.243	14.24	14.241	14.244	14.241	14.245	14.25	14.252	14.273
HUMSER	49.69	59.717	54.082	60.142	56.723	62.711	62.285	60.208	61.896	60.495	63.104	56.639	65.236
RELHUM	38.462	54.559	48.57	55.454	52.07	58.003	59.348	57.635	59.436	62.225	73.304	75.581	57.574
WINVAV	3.4719	2.4118	2.2317	1.0139	3.0652	1.6798	2.0436	1.7738	2.4212	1.3143	1.2973	1.0878	6.5432
WINAAV	-163.45	-6.0663	14.235	-18.007	-109.41	-7.3376	1.7137	7.9257	25.487	.37115	-28.527	-24.851	-37.498
XM0	0.	0.	0.	0.	0.	0.	0.	0.	0.	0.	0.	0.	0.
P46Q2	9.99+10	3.32	3.3236	3.3546	0.	3.1072	2.8926	2.9014	2.8868	1.0013	9.99+10	1.0027	9.99+10
CT46	9.99+10	1925.9	1904.9	1897.1	2526.5	1852.	1804.8	1787.8	1780.9	930.45	9.99+10	929.7	9.99+10
T46X	601.82	1879.7	1863.5	1858.	1291.5	1805.1	1752.9	1745.5	1743.1	714.45	630.28	710.77	549.18
Comments:	Zero	DOWN POWER CAL., HIGH POWER →								Zero	Zero	Zero	Zero
		Pt.1a Max PLA	Pt.1b Max PLA	Max PLA+	BAD POINT Incomplete Reading	Pt.2a Possibly Incomplete	Pt.3a	Pt.3b	Pt.3c				

GE36/UDF1 Peebles Tests
082001-03
Test Log - Site IIID
Sheet 016 of 029

GE36/UDF-1 ENGINE 082001-('EST READINGS - SITE IIID
RDGS. 57 - 70 ON 06.29.86 RDGS. 71 - 77 ON 06.30.86
RDGS. 78 - 149 ON 07.01.86 RDGS. 150 - 197 ON 07.03.86
RDGS. 198 - 209 ON 07.04.86 RDGS. 210 - 251 ON 07.05.86

RDG.	200	201	202	203	204	205	206	207	208	209	210	211	212
XN2	471.61	0.	11594.	11645.	11626.	11683.	11700.	11546.	11575.	11056.	11514.	11484.	104.11
XN2R	465.86	0.	11457.	11517.	11500.	11564.	11568.	11417.	11458.	10942.	11405.	11407.	103.05
PCN2R	3.5106	0.	86.337	86.792	86.664	87.141	87.171	86.038	86.348	82.455	85.943	85.963	.77653
XN25	136.19	0.	15564.	15615.	15599.	15639.	15647.	15537.	15544.	15100.	15500.	15444.	152.95
XN25R	132.74	0.	12772.	12800.	12801.	12813.	12792.	12782.	12788.	12675.	12775.	12758.	147.06
PCN25R	.98915	0.	95.168	95.381	95.387	95.478	95.322	95.246	95.288	94.45	95.193	95.069	1.0958
XN48	616.04	0.	1397.6	1398.1	1397.9	1397.6	1397.6	1397.8	1397.6	1279.6	1397.6	1397.8	236.29
XN49	619.79	0.	1398.6	1399.	1398.3	1398.9	1398.7	1398.7	1398.9	1280.8	1398.5	1399.	281.3
UT91R2	373.7	0.	848.11	849.13	849.19	849.55	848.59	848.81	849.62	777.7	850.1	852.66	143.62
UT92R2	365.45	0.	824.93	825.91	825.66	826.48	825.47	825.61	826.55	756.64	826.77	829.51	166.19
BTAN91	86.895	79.922	30.898	31.368	31.116	31.046	31.62	31.212	30.567	30.088	30.209	30.874	87.113
BTAN92	86.857	79.841	28.992	29.731	29.847	30.212	30.359	29.296	29.536	28.865	29.371	29.471	87.129
W13	-5.7943	-.5	14.132	13.86	13.909	14.05	14.183	13.54	13.949	13.086	13.582	13.74	-7.1265
W15	-5.7943	0.	14.132	13.86	13.909	14.05	14.183	13.54	13.949	13.086	13.582	13.74	-7.1265
WF36	167.83	166.81	5303.9	5375.	5341.1	5473.8	5562.	5156.1	5228.1	4095.7	5124.	5165.6	179.37
WF36R2	170.14	168.46	5390.5	5468.6	5434.5	5574.5	5656.6	5244.	5323.6	4168.6	5221.6	5284.3	182.43
FN!1QA	0.	0.	21402.	21739.	21718.	22071.	22216.	21132.	21374.	17328.	21096.	21170.	0.
SFC184	.5	.5	.2546	.25429	.25295	.25532	.25739	.25086	.25178	.24319	.25021	.25233	.5
TAMB	532.73	533.57	531.67	530.45	529.82	530.1	530.95	530.17	529.72	529.28	528.81	526.64	528.13
T10	531.55	535.45	531.19	530.22	530.04	529.39	530.59	530.41	529.3	529.56	528.71	525.64	529.41
PAMB	14.264	14.247	14.25	14.253	14.253	14.254	14.251	14.254	14.256	14.257	14.256	14.259	14.258
P10M	14.266	14.249	14.251	14.254	14.257	14.256	14.253	14.255	14.259	14.258	14.259	14.261	14.26
HUMSER	64.593	75.625	74.366	79.608	74.766	75.027	74.892	73.585	74.568	73.056	73.966	77.018	74.503
RELHUM	51.911	58.862	61.74	68.822	66.117	65.71	63.701	64.318	66.171	65.839	67.718	75.933	69.894
WINVAV	6.028	1.2663	1.7037	2.8463	1.6761	2.3268	1.6221	2.2019	2.7516	2.2083	2.4046	3.0244	1.7111
WINAAV	8.1875	144.89	-22.761	-28.388	12.106	13.664	46.51	-42.139	29.641	23.411	12.249	-14.782	2.1186
XMO	0.	0.	0.	0.	0.	0.	0.	0.	0.	0.	0.	0.	0.
P46Q2	1.002	9.99+10	2.9092	2.9471	2.9344	2.9806	2.9827	2.8769	2.9077	2.5348	2.8722	2.8734	1.001
CT46	872.66	9.99+10	1829.2	1819.	1817.2	1825.5	1850.3	1802.8	1803.2	1682.6	1793.6	1802.5	948.35
T46X	724.75	547.95	1779.5	1776.2	1772.4	1780.1	1800.4	1758.1	1759.3	1653.8	1749.4	1754.9	719.65
Comments:	Zero	Zero	LCF CYCLES →										
			Pt.1	Pt.2	Pt.3	Pt.4	Pt.5	Pt.6	Pt.7	Full Back Pt. For Vibs.	Pt.8	Pt.9	Zero

GE36/UDF1 Peebles Tests
082001-03
Test Log - Site IIID
Sheet 017 of 029

GE36/UDF-1 ENGINE 082001- TEST READINGS - SITE IIID
RDGS. 57 - 70 ON 06.29.86 RDGS. 71 - 77 ON 06.30.86
RDGS. 78 - 149 ON 07.01.86 RDGS. 150 - 197 ON 07.03.86
RDGS. 198 - 209 ON 07.04.86 RDGS. 210 - 251 ON 07.05.86

RDG.	213	214	215	216	217	218	219	220	221	222	223	224	225
XN2	0.	11481.	11516.	11489.	11475.	11471.	11471.	11456.	282.14	0.	11439.	11473.	11476.
XN2R	0.	11357.	11396.	11396.	11395.	11401.	11408.	11392.	280.32	0.	11394.	11410.	11407.
PCN2R	0.	85.587	85.88	85.876	85.867	85.915	85.967	85.849	2.1124	0.	85.864	85.985	85.958
XN25	0.	15453.	15503.	15462.	15447.	15440.	15429.	15422.	122.57	0.	15369.	15434.	15432.
XN25R	0.	12732.	12771.	12767.	12770.	12770.	12763.	12764.	119.16	0.	12734.	12770.	12758.
PCN25R	0.	94.874	95.165	95.131	95.156	95.159	95.105	95.113	.88793	0.	94.887	95.159	95.064
XN48	0.	1397.8	1397.8	1397.8	1397.4	1397.8	1397.5	1397.5	431.32	0.	1397.4	1397.6	1397.6
XN49	0.	1398.7	1398.7	1399.	1399.	1398.6	1398.7	1398.6	470.7	0.	1398.6	1398.7	1398.6
UT91R2	0.	849.13	849.46	851.44	852.11	853.13	853.45	853.41	263.16	0.	854.72	853.59	853.07
UT92R2	0.	825.91	826.23	828.32	829.2	829.73	830.27	830.15	279.15	0.	831.51	830.33	829.74
BTAN91	87.033	30.729	30.546	30.756	30.694	31.07	31.161	31.107	87.138	87.08	30.49	30.855	30.85
BTAN92	87.127	29.552	29.813	29.318	29.546	29.568	29.407	29.253	87.179	87.125	29.403	29.333	29.564
W13	-.5	13.839	13.728	13.622	13.897	13.669	13.95	13.843	-6.3554	-.5	14.219	13.862	14.05
W15	0.	13.839	13.728	13.622	13.897	13.669	13.95	13.843	-6.3554	0.	14.219	13.862	14.05
WF36	178.62	5102.3	5114.5	5090.6	5093.7	5093.4	5128.8	5076.5	181.8	186.77	5157.4	5119.8	5155.4
WF36R2	180.98	5191.9	5206.8	5198.9	5209.3	5215.9	5256.2	5202.	185.89	189.71	5294.6	5243.4	5273.5
FN11QA	0.	20963.	21143.	21031.	21107.	21111.	21139.	21028.	0.	.11087	21205.	21204.	21203.
SFC184	.5	.25036	.24895	.24989	.24949	.24976	.25136	.25007	.5	1729.7	.2524	.24997	.25142
TAMB	528.38	530.99	527.69	527.7	526.33	525.72	525.5	525.45	525.39	523.49	523.17	525.04	525.83
T10	532.54	530.02	529.61	527.15	526.02	525.06	524.47	524.52	525.44	530.11	522.81	524.39	525.03
PAMB	14.254	14.253	14.254	14.255	14.255	14.256	14.255	14.256	14.256	14.264	14.263	14.266	14.272
P10M	14.255	14.255	14.256	14.257	14.258	14.257	14.258	14.258	14.258	14.265	14.264	14.268	14.274
HUMSER	75.293	73.494	75.927	74.906	76.225	75.769	76.541	76.658	75.077	77.036	76.729	78.684	78.832
RELHUM	69.917	62.476	72.21	71.234	75.955	77.134	78.508	78.764	77.331	84.786	85.407	82.021	79.964
WINVAV	1.6997	1.0864	2.3884	2.2434	1.4316	2.6265	2.52	2.5319	.67314	1.3366	2.9263	2.5411	1.5504
WINAAV	5.7865	29.185	74.409	-5.8209	6.9428	7.921	-8.0449	.32143	-4.4376	-52.011	-6.1593	50.804	-8.784
XMO	0.	0.	0.	- 0.	0.	0.	0.	0.	0.	0.	0.	0.	0.
P46Q2	9.99+10	2.8373	2.8668	2.8621	2.8643	2.8635	2.8727	2.8611	1.0021	9.99+10	2.8639	2.8715	2.8714
CT46	-9.99+10	1811.8	1795.9	1787.2	1785.8	1783.2	1790.8	1780.9	933.11	9.99+10	1801.9	1784.	1797.3
T46X	635.32	1767.7	1755.1	1747.2	1744.7	1743.3	1747.7	1740.5	718.53	612.55	1756.8	1743.5	1754.3
Comments:	Zero	LCF CYCLES →							Zero	Zero	LCF CYCLES →		
		Pt.10	Pt.11	Pt.12	Pt.13	Pt.14	Pt.15	Pt.16 Incomplete			Pt.16 Redone	Pt.17	Pt.18

GE36/UDF-1 ENGINE 082001-03 [illegible]ST READINGS - SITE IIID
RDGS. 57 - 70 ON 06.29.86 RDGS. 71 - 77 ON 06.30.86
RDGS. 78 - 149 ON 07.01.86 RDGS. 150 - 197 ON 07.03.86
RDGS. 198 - 209 ON 07.04.86 RDGS. 210 - 251 ON 07.05.86

RDG.	226	227	228	229	230	231	232	233	234	235	236	237	238
XN2	11468.	-999.	0.	11670.	11737.	11674.	11691.	11674.	11644.	11682.	11691.	11670.	11654.
XN2R	11395.	-999.	0.	11399.	11462.	11400.	11423.	11409.	11380.	11416.	11428.	11413.	11400.
PCN2R	85.874	-999.	0.	85.902	86.379	85.911	86.081	85.977	85.756	86.028	86.121	86.004	85.912
XN25	15431.	-999.	0.	15691.	15750.	15703.	15715.	15700.	15686.	15709.	15711.	15692.	15680.
XN25R	12761.	-999.	0.	12761.	12784.	12778.	12783.	12781.	12779.	12785.	12783.	12783.	12779.
PCN25R	95.087	-999.	0.	95.091	95.261	95.215	95.254	95.236	95.222	95.265	95.251	95.25	95.227
XN48	1397.6	-999.	0.	1397.6	1397.8	1397.6	1397.1	1398.1	1397.8	1397.5	1397.5	1397.8	1397.8
XN49	1402.1	-999.	0.	1399.	1398.3	1399.	1399.	1398.3	1398.9	1398.7	1398.9	1399.	1399.4
UT91R2	852.89	-999.	0.	838.38	838.29	838.17	838.25	839.05	838.86	838.63	838.91	839.46	839.67
UT92R2	831.63	-999.	0.	815.69	815.13	815.48	815.88	815.72	816.	815.86	816.2	816.66	817.1
BTAN91	30.72	-999.	77.575	31.012	31.215	30.895	30.942	31.132	30.741	31.121	30.475	30.599	30.474
BTAN92	29.471	-999.	82.452	29.332	29.504	29.535	29.738	29.312	29.595	29.654	29.593	29.83	29.594
W13	13.825	-999.	-.5	13.667	13.688	13.515	13.489	13.324	13.281	13.482	13.548	13.435	13.578
W15	13.825	-999.	0.	13.667	13.688	13.515	13.489	13.324	13.281	13.482	13.548	13.435	13.578
WF36	5124.7	-999.	130.74	5239.7	5329.7	5188.	5225.4	5194.7	5132.1	5208.1	5238.8	5197.5	5167.9
WF36R2	5240.	-999.	129.71	5230.1	5318.5	5176.7	5217.3	5188.	5125.8	5201.4	5234.4	5196.4	5169.2
FN11QA	21166.	-999.	0.	20795.	21166.	20771.	20922.	20820.	20696.	20886.	20967.	20879.	20800.
SFC184	.25025	-999.	.5	.25424	.254	.25193	.25208	.2519	.25037	.25174	.25236	.25158	.25122
TAMB	526.46	-999.	546.35	546.13	546.18	546.12	546.02	545.74	545.63	545.01	544.96	544.52	543.9
T10	525.26	-999.	547.19	543.6	543.82	543.87	543.35	543.04	543.08	543.16	542.81	542.3	542.03
PAMB	14.273	-999.	14.286	14.278	14.278	14.277	14.278	14.28	14.279	14.279	14.279	14.278	14.277
P10M	14.275	-999.	14.289	14.281	14.281	14.281	14.282	14.283	14.282	14.281	14.281	14.281	14.28
HUMSER	81.393	-999.	93.613	94.977	95.805	101.54	102.61	98.377	98.113	102.39	103.81	105.65	107.01
RELHUM	80.756	-999.	47.943	48.937	49.278	52.255	52.959	51.297	51.327	54.593	55.411	57.172	59.043
WINVAV	2.8332	-999.	4.6554	8.7407	6.9053	5.871	5.6385	5.2867	5.2784	5.5226	5.6124	4.6918	5.1901
WINAAV	-14.051	-999.	-42.05	-37.212	-19.554	-19.544	12.032	-31.585	-31.149	-24.903	-19.851	-12.571	-23.706
XHO	0.	-999.	0.	0.	0.	0.	0.	0.	0.	0.	0.	0.	0.
P46Q2	2.8674	-999.	9.99+10	2.8595	2.901	2.8596	2.8722	2.8676	2.8458	2.8676	2.8804	2.8648	2.8628
CT46	1789.9	-999.	9.99+10	1850.9	1847.4	1834.3	1834.3	1830.8	1823.6	1832.	1833.5	1828.	1822.9
T46X	1749.3	-999.	557.49	1806.1	1806.8	1791.8	1794.5	1790.7	1786.3	1791.8	1794.1	1789.2	1785.1
Comments:	LCF Cycle Pt.19	Zero	Zero	LCF CYCLES → Pt.20	Pt.21	Pt.22	Pt.23	Pt.24	Pt.25	Pt.26	Pt.27	Pt.28	Pt.29

GE36/UDF-1 ENGINE 082001-03 TEST READINGS - SITE IIID
RDGS. 252 - 304 ON 07.06.86 RDGS. 305 - 330 ON 07.07.86
RDGS. 331 - 358 ON 07.08.86

RDG.	252	253	254	255	256	257	258	259	260	261	262	263	264
XN2	0.	11532.	11551.	11536.	11512.	11520.	11547.	11465.	-999.	0.	11522.	11547.	11561.
XN2R	0.	11378.	11409.	11400.	11367.	11392.	11409.	11333.	-999.	0.	11397.	11418.	11428.
PCN2R	0.	85.743	85.977	85.906	85.659	85.851	85.974	85.402	-999.	0.	85.882	86.044	86.118
XN25	0.	15502.	15529.	15518.	15497.	15503.	15525.	15459.	-999.	0.	15486.	15524.	15534.
XN25R	0.	12740.	12770.	12767.	12755.	12770.	12768.	12752.	-999.	0.	12749.	12773.	12776.
PCN25R	0.	94.935	95.154	95.134	95.042	95.157	95.14	95.026	-999.	0.	94.998	95.18	95.2
XN48	0.	1397.8	1397.8	1397.6	1397.6	1397.6	1397.8	1397.6	-999.	0.	1397.6	1397.6	1397.6
XN49	0.	1398.7	1398.9	1399.	1398.7	1399.	1398.7	1398.7	-999.	0.	1398.7	1398.7	1398.7
UT91R2	0.	846.93	847.83	848.13	847.44	848.81	848.11	848.42	-999.	0.	848.94	848.71	848.42
UT92R2	0.	823.77	824.72	825.18	824.35	825.84	824.92	825.31	-999.	0.	825.81	825.58	825.3
BTAN91	87.022	31.032	30.946	30.336	30.915	30.995	31.151	30.607	-999.	87.004	30.85	31.008	31.148
BTAN92	87.068	28.943	29.245	29.42	28.912	29.441	29.782	29.144	-999.	87.129	29.169	29.553	29.202
W13	-.5	13.955	13.74	13.683	13.47	13.442	13.579	13.73	-999.	-.5	13.985	13.726	13.621
W15	0.	13.955	13.74	13.683	13.47	13.442	13.579	13.73	-999.	0.	13.985	13.726	13.621
WF36	166.76	5177.9	5151.8	5127.2	5044.1	5095.7	5138.6	4981.1	-999.	173.42	5156.6	5156.4	5175.8
WF36R2	167.17	5237.4	5217.5	5195.3	5104.7	5168.3	5205.5	5048.6	-999.	173.73	5229.1	5227.9	5243.9
FN11QA	0.	20860.	20955.	20925.	20638.	20846.	20974.	20505.	-999.	-1.3553	20944.	21056.	21047.
SFC184	.5	.2538	.2517	.25098	.25004	.25062	.25089	.24888	-999.	-129.58	.25239	.25098	.25186
TAMB	532.94	532.31	532.02	531.87	531.61	531.29	532.13	531.87	-999.	531.42	531.2	531.08	530.72
T10	538.89	532.78	531.65	531.17	532.04	530.32	531.3	530.8	-999.	538.78	530.15	530.44	530.8
PAMB	14.289	14.288	14.29	14.292	14.294	14.294	14.293	14.295	-999.	14.3	14.3	14.298	14.3
P10M	14.291	14.289	14.293	14.294	14.296	14.296	14.295	14.297	-999.	14.302	14.302	14.3	14.303
HUMSER	104.52	105.44	102.73	102.35	103.65	104.26	102.34	102.78	-999.	101.62	100.53	100.51	102.51
RELHUM	82.803	85.289	83.986	84.109	85.916	87.362	83.367	84.493	-999.	84.845	84.608	84.913	87.647
WINVAV	2.7125	3.5787	3.0577	3.8805	2.9405	3.4935	3.4693	2.9146	-999.	.84414	2.4213	2.6902	2.5535
WINAAV	-20.378	-32.196	-12.888	7.2764	-23.078	2.8457	3.1051	-5.08	-999.	-32.74	3.5376	22.477	-30.946
XM0	0.	0.	0.	0.	0.	0.	0.	0.	-999.	0.	0.	0.	0.
P46Q2	9.99+10	2.8475	2.8633	2.86	2.8339	2.8499	2.8583	2.8168	-999.	9.99+10	2.8541	2.8653	2.8726
CT46	-9.99+10	1825.9	1801.5	1796.9	1789.4	1792.4	1800.2	1782.6	-999.	9.99+10	1807.6	1800.	1800.9
T46X	625.94	1785.	1765.6	1761.1	1754.2	1756.7	1763.8	1748.	-999.	713.69	1771.3	1763.4	1764.
Comments:	Zero	LCF CYCLES →											
		Pt.37 Redone	Pt.38	Pt.39	Pt.40	Pt.41	Pt.42	Pt.43	Zero	Zero	Pt.44	Pt.45	Pt.46

GE36/UDF1 Peebles Tests
082001-03
Test Log - Site IIID
Sheet 021 of 029

GE36/UDF-1 ENGINE 082001-03 TEST READINGS - SITE IIID
RDGS. 252 - 304 ON 07.06.86 RDGS. 305 - 330 ON 07.07.86
RDGS. 331 - 358 ON 07.08.86

RDG.	265	266	267	268	269	270	271	272	273	274	275	276	277
XN2	11520.	11561.	11572.	11566.	11534.	11535.	11530.	360.	0.	11554.	11559.	11550.	11582.
XN2R	11393.	11439.	11455.	11452.	11414.	11425.	11423.	355.84	0.	11409.	11405.	11394.	11408.
PCN2R	85.858	86.201	86.326	86.303	86.011	86.096	86.083	2.6815	0.	85.977	85.948	85.862	85.971
XN25	15500.	15535.	15534.	15530.	15507.	15502.	15496.	139.33	0.	15531.	15563.	15559.	15613.
XN25R	12768.	12782.	12780.	12780.	12770.	12773.	12771.	134.74	0.	12753.	12779.	12778.	12791.
PCN25R	95.139	95.246	95.228	95.229	95.16	95.181	95.163	1.0041	0.	95.033	95.222	95.215	95.311
XN48	1397.6	1397.8	1398.1	1397.6	1397.8	1397.8	1397.6	498.84	0.	1397.5	1397.5	1397.2	1397.5
XN49	1398.9	1398.9	1398.7	1398.7	1398.7	1398.9	1398.9	539.15	0.	1398.9	1399.1	1399.	1399.
UT91R2	848.87	849.28	849.9	849.84	849.42	850.2	850.34	302.79	0.	847.41	846.79	846.43	845.36
UT92R2	825.82	826.14	826.51	826.68	826.2	827.03	827.25	318.1	0.	824.48	824.03	823.76	822.56
BTAN91	30.625	30.987	31.457	31.34	31.095	30.763	31.113	87.029	86.984	30.979	31.039	30.71	31.098
BTAN92	29.06	29.901	29.615	29.689	29.414	29.575	29.465	87.149	87.093	29.047	29.068	29.155	29.383
W13	13.773	13.676	13.655	13.715	13.659	13.705	13.735	-6.0613	-.5	14.043	13.752	13.691	13.387
W15	13.773	13.676	13.655	13.715	13.659	13.705	13.735	-6.0613	0.	14.043	13.752	13.691	13.387
WF36	5097.3	5191.7	5227.9	5218.7	5137.4	5153.4	5146.1	177.66	170.34	5247.8	5170.7	5140.8	5206.3
WF36R2	5167.3	5266.	5306.8	5298.7	5210.2	5232.3	5226.2	179.66	169.95	5299.3	5216.6	5184.9	5240.1
FN11QA	20863.	21211.	21246.	21223.	20991.	21069.	21038.	0.	0.	21056.	20915.	20850.	21004.
SFC184	.25037	.25096	.25249	.25238	.25091	.25104	.25111	.5	.5	.25441	.25213	.25137	.25219
TAMB	530.38	530.17	529.89	529.54	529.86	529.43	529.53	529.79	531.23	533.46	534.61	535.02	536.57
T10	530.24	529.83	529.26	529.03	529.65	528.69	528.41	530.87	540.78	531.97	532.75	532.99	534.55
PAMB	14.302	14.303	14.303	14.304	14.308	14.309	14.309	14.313	14.322	14.324	14.324	14.324	14.324
P10M	14.305	14.305	14.305	14.305	14.31	14.312	14.313	14.314	14.324	14.327	14.327	14.327	14.328
HUMSER	101.77	100.81	100.7	101.74	100.39	100.41	101.01	99.057	101.67	102.01	105.85	108.25	106.68
RELHUM	88.04	87.877	88.612	90.605	88.456	89.803	90.003	87.544	85.576	79.665	79.453	80.122	75.028
WINVAV	3.0664	2.1615	2.2359	2.3509	1.4518	2.4786	2.6833	.67881	1.0259	3.2599	3.2093	4.8278	5.1766
WINAAV	-48.952	22.963	16.972	-1.5047	-20.351	3.7005	-17.04	128.09	-46.081	-26.939	-12.201	-11.938	-12.834
XMO	0.	0.	0.	0.	0.	0.	0.	0.	0.	0.	0.	0.	0.
P46Q2	2.8518	2.8788	2.8892	2.8884	2.8643	2.8707	2.8665	1.0032	9.99+10	2.8697	2.8654	2.8605	2.8701
CT46	1791.1	1799.7	1803.	1801.6	1795.8	1793.5	1791.4	930.98	9.99+10	1824.3	1802.9	1799.1	1811.6
T46X	1756.2	1764.1	1766.1	1764.6	1759.3	1757.5	1757.3	729.08	681.74	1784.7	1767.7	1765.7	1776.1

Comments: LCF CYCLES →

Pt.47	Pt.48	Pt.49	Pt.50	Pt.51	Pt.52	Pt.53	Zero	Zero	Pt.54	Pt.55	Pt.56	Pt.57

GE36/UDF-1 ENGINE 082001-0. TEST READINGS - SITE IIID
RDGS. 252 - 304 ON 07.06.86 RDGS. 305 - 330 ON 07.07.86
RDGS. 331 - 358 ON 07.08.86

RDG.	278	279	280	281	282	283	284	285	286	287	288	289	290
XN2	11621.	11636.	11613.	11635.	11630.	11632.	90.893	0.	11666.	11640.	11669.	121.79	11663.
XN2R	11433.	11439.	11407.	11424.	11409.	11407.	88.947	0.	11406.	11379.	11399.	118.67	11393.
PCN2R	86.158	86.204	85.964	86.087	85.978	85.963	.67029	0.	85.953	85.753	85.898	.89424	85.858
XN25	15651.	15651.	15645.	15671.	15660.	15666.	97.952	0.	15705.	15689.	15720.	111.57	15670.
XN25R	12798.	12793.	12788.	12794.	12788.	12790.	94.35	0.	12775.	12782.	12785.	107.04	12750.
PCN25R	95.363	95.327	95.292	95.338	95.292	95.308	.70306	0.	95.197	95.246	95.271	.79762	95.005
XN48	1397.1	1397.6	1397.8	1397.8	1396.7	1396.	684.49	0.	1396.2	1394.	1396.8	104.08	1397.8
XN49	1398.6	1399.1	1398.5	1398.7	1399.	1398.9	688.24	0.	1398.7	1399.	1398.7	177.22	1399.
UT91R2	844.1	843.79	843.14	842.75	841.43	840.77	411.35	0.	838.28	836.92	837.91	62.277	838.56
UT92R2	821.34	821.03	819.93	819.71	819.21	818.88	402.02	0.	816.3	816.39	815.55	103.07	815.79
BTAN91	31.236	30.87	31.185	31.116	30.992	31.627	87.057	86.972	31.506	30.702	31.828	87.062	30.898
BTAN92	29.555	29.545	29.204	29.614	29.497	29.528	87.26	87.175	29.359	29.263	28.923	87.24	29.433
W13	13.567	13.655	13.473	13.446	13.539	13.199	-7.4642	-.5	13.721	13.357	13.31	-7.4284	13.631
W15	13.567	13.655	13.473	13.446	13.539	13.199	-7.4642	0.	13.721	13.357	13.31	-7.4284	13.631
WF36	5268.5	5259.5	5198.3	5243.7	5197.1	5183.6	160.98	137.39	5282.3	5152.9	5197.8	150.7	5217.6
WF36R2	5293.3	5278.9	5211.5	5253.5	5201.4	5185.7	160.38	135.59	5260.5	5131.4	5170.8	149.25	5191.3
FN11QA	21102.	21076.	20870.	21057.	20857.	20833.	0.	0.	20860.	20667.	20726.	0.	20758.
SFC184	.25357	.25319	.25243	.2522	.25209	.25163	.5	.5	.25492	.25099	.25219	.5	.25281
TAMB	538.03	538.62	539.67	540.52	541.18	541.62	542.42	544.66	545.75	545.85	546.58	546.93	547.13
T10	535.84	536.65	537.57	538.07	538.94	539.26	541.6	549.03	542.58	542.67	543.58	546.31	543.46
PAMB	14.326	14.327	14.326	14.325	14.325	14.325	14.327	14.329	14.329	14.329	14.327	14.327	14.326
P10M	14.329	14.329	14.328	14.329	14.328	14.328	14.33	14.332	14.332	14.331	14.33	14.33	14.329
HUMSER	104.96	108.85	110.29	100.13	100.99	108.23	112.58	108.25	108.72	103.61	104.19	101.94	104.07
RELHUM	70.365	71.504	69.981	61.936	61.123	64.483	65.298	58.485	56.732	53.953	52.989	51.298	52.025
WINVAV	5.2456	5.3941	3.7938	6.6219	4.1834	5.5384	6.3687	9.0881	6.4686	3.2953	2.7595	7.0233	3.5479
WINAAV	-24.319	11.592	-26.696	8.3128	41.399	-8.0851	-20.815	7.1789	-25.184	-20.565	21.69	40.733	36.176
XMO	0.	0.	0.	0.	0.	0.	0.	0.	0.	0.	0.	0.	0.
P46Q2	2.8838	2.8842	2.8641	2.8774	2.8615	2.8566	1.0011	9.99+10	2.8561	2.8413	2.8543	1.0024	2.8394
CT46	1821.4	1822.7	1817.8	1823.8	1822.8	1819.5	893.33	9.99+10	1853.7	1827.	1830.1	871.38	1849.1
T46X	1783.8	1784.6	1780.7	1786.7	1783.8	1783.3	738.09	650.84	1815.	1787.9	1794.6	741.01	1807.5
Comments: LCF CYCLES	Pt.58	Pt.59	Pt.60	Pt.61	Pt.62	Pt.63	Zero	Zero	Pt.64	Pt.65	Pt.66 Incomplete	Zero	Pt.66 Redone

GE36/UDF1 Peebles Tests
082001-03
Test Log - Site IIID
Sheet 023 of 029

GE36/UDF-1 ENGINE 082001-03 TEST READINGS - SITE IIID
RDGS. 252 - 304 ON 07.06.86 RDGS. 305 - 330 ON 07.07.86
RDGS. 331 - 358 ON 07.08.86

RDG.	291	292	293	294	295	296	297	298	299	300	301	302	303
XN2	11702.	11706.	11636.	586.96	0.	11688.	11715.	11673.	11642.	11631.	11683.	11646.	155.
XN2R	11428.	11431.	11348.	571.01	0.	11456.	11491.	11460.	11427.	11404.	11460.	11434.	151.51
PCN2R	86.118	86.141	85.517	4.303	0.	86.33	86.591	86.357	86.112	85.942	86.359	86.162	1.1417
XN25	15721.	15725.	15684.	89.571	0.	15709.	15730.	15688.	15664.	15659.	15702.	15664.	133.05
XN25R	12779.	12779.	12767.	85.633	0.	12803.	12816.	12803.	12799.	12786.	12804.	12796.	123.68
PCN25R	95.225	95.227	95.132	.6381	0.	95.404	95.502	95.4	95.369	95.288	95.41	95.348	.92158
XN48	1397.5	1397.6	1397.8	599.16	0.	1397.9	1397.8	1397.5	1397.8	1397.5	1397.5	1397.2	211.91
XN49	1398.7	1398.1	1398.9	624.48	0.	1398.9	1399.3	1399.	1399.	1399.	1399.	1399.1	299.11
UT91R2	838.12	838.13	837.12	357.95	0.	841.42	841.96	842.49	842.54	841.51	841.81	842.37	127.2
UT92R2	815.36	814.9	814.31	362.63	0.	818.42	819.25	819.76	819.66	818.82	819.1	819.88	174.52
BTAN91	30.764	31.096	30.084	87.033	77.596	31.305	31.687	31.664	31.227	31.093	31.425	31.096	86.971
BTAN92	29.687	29.149	29.416	87.316	77.313	30.055	29.977	29.75	30.005	29.916	29.976	29.791	87.18
W13	13.317	13.274	13.154	-5.3592	-.5	13.183	13.206	13.151	13.114	13.066	13.053	13.2	-6.9885
W15	13.317	13.274	13.154	-5.3592	0.	13.183	13.206	13.151	13.114	13.066	13.053	13.2	-6.9885
WF36	5228.2	5240.7	5065.5	148.49	147.58	5275.7	5319.2	5267.2	5194.4	5163.7	5265.5	5213.9	164.47
WF36R2	5199.8	5214.2	5032.3	146.84	146.79	5283.2	5332.	5285.	5209.9	5170.7	5274.9	5228.8	163.71
FN11QA	20936.	20825.	20374.	0.	0.	21151.	21259.	21104.	20984.	20844.	21105.	20931.	0.
SFC184	.25107	.25311	.24968	.5	.5	.2525	.25353	.25315	.25098	.25076	.25265	.25252	.5
TAMB	547.4	546.75	547.98	547.95	540.88	540.73	539.73	539.23	539.21	539.79	539.9	539.04	538.5
T10	543.83	543.92	545.34	548.05	544.08	539.87	539.08	538.21	538.34	539.45	539.07	538.15	542.86
PAMB	14.325	14.323	14.318	14.317	14.306	14.305	14.306	14.308	14.31	14.313	14.314	14.316	14.318
P10M	14.329	14.321	14.317	14.32	14.308	14.302	14.303	14.305	14.308	14.311	14.312	14.313	14.32
HUMSER	104.37	96.827	97.939	96.974	121.33	113.21	111.28	114.87	112.65	110.78	105.18	105.72	105.79
RELHUM	51.709	49.057	47.691	47.268	73.727	69.251	70.371	73.766	72.711	69.954	66.27	68.5	69.784
WINVAV	2.9323	6.138	4.9741	4.45	2.834	1.7139	2.6758	2.2137	2.4386	2.5759	3.4535	2.4244	.94296
WINAAV	-12.17	28.313	26.877	-17.783	2.6201	52.371	20.459	-37.067	41.334	43.604	26.024	15.795	-10.726
XMO	0.	0.	0.	0.	0.	0.	0.	0.	0.	0.	0.	0.	0.
P46Q2	2.8627	2.8656	2.8183	1.0037	9.99+10	2.8816	2.9034	2.8831	2.8589	2.8441	2.8825	2.8646	1.0018
CT46	1836.1	1841.	1825.6	860.18	9.99+10	1832.7	1830.1	1827.1	1820.1	1823.1	1829.1	1825.3	932.94
T46X	1798.9	1800.4	1788.3	738.52	580.67	1795.4	1795.2	1789.6	1783.6	1785.4	1791.4	1785.	722.39

Comments:	LCF CYCLES →												
	Pt.67	Pt.68	Pt.69	Zero	Zero	Pt.71	Pt.72	Pt.73	Pt.74	Pt.75	Pt.76	Pt.77	Zero

(NOTE: No DMS reading for point 70!)

GE36/UDF1 Peebles Tests
082001-03
Test Log - Site IIID
Sheet 024 of 029

GE36/UDF-1 ENGINE 082001- TEST READINGS - SITE IIID
RDGS. 252 - 304 ON 07.06.86 RDGS. 305 - 330 ON 07.07.86
RDGS. 331 - 358 ON 07.08.86

RDG.	304	305	306	307	308	309	310	311	312	313	314	315	316
XN2	155.	11566.	11597.	11598.	11583.	11545.	11692.	11586.	11582.	11586.	11561.	441.61	11558.
XN2R	151.24	11369.	11395.	11421.	11402.	11368.	11517.	11407.	11412.	11399.	11388.	434.42	11384.
PCN2R	1.1397	85.678	85.872	86.066	85.924	85.667	86.789	85.962	85.997	85.897	85.817	3.2737	85.786
XN25	133.05	15557.	15602.	15587.	15578.	15546.	15659.	15579.	15573.	15590.	15554.	166.05	15529.
XN25R	124.53	12750.	12770.	12774.	12773.	12764.	12793.	12773.	12775.	12775.	12765.	159.28	12737.
PCN25R	.92791	95.007	95.159	95.189	95.177	95.115	95.329	95.18	95.195	95.194	95.110	1.1869	94.911
XN48	211.91	1397.4	1397.6	1397.6	1397.2	1397.2	1397.8	1397.6	1397.8	1397.6	1397.5	534.47	1397.4
XN49	299.11	1399.	1398.9	1399.	1399.4	1399.3	1399.3	1399.	1399.1	1399.	1399.	556.03	1398.9
UT91R2	126.97	843.56	843.34	845.2	844.65	844.9	845.55	845.05	845.73	844.37	845.38	322.87	845.19
UT92R2	174.21	820.89	820.44	822.33	822.27	822.43	822.74	822.18	822.84	821.52	822.58	326.49	822.39
BTAN91	86.945	30.419	31.245	31.138	30.505	30.644	32.014	30.727	31.184	31.021	30.919	87.03	31.144
BTAN92	87.153	29.149	29.485	29.34	29.671	29.288	29.806	29.567	29.376	29.157	29.393	87.204	28.852
W13	-7.1299	13.663	13.132	13.235	13.38	13.02	13.188	13.193	13.446	13.47	13.43	-5.7376	13.769
W15	-7.1299	13.663	13.132	13.235	13.38	13.02	13.188	13.193	13.446	13.47	13.43	-5.7376	13.769
WF36	161.11	5132.8	5136.	5161.9	5127.1	5056.2	5368.9	5134.9	5130.1	5114.4	5086.3	171.91	5162.7
WF36R2	159.95	5156.	5156.2	5198.	5160.4	5091.2	5410.9	5172.6	5171.1	5144.	5124.8	172.7	5200.2
FN11QA	0.	20620.	20777.	20872.	20799.	20567.	21424.	20801.	20818.	20712.	20666.	0.	20726.
SFC184	.5	.25277	.25086	.25175	.2508	.25024	.2553	.25138	.2511	.25106	.25069	.5	.25363
TAMB	537.57	536.73	537.86	535.27	535.26	535.54	535.64	535.38	535.51	536.18	534.5	535.2	531.96
T10	544.8	536.73	537.22	534.85	535.24	534.93	534.52	535.04	534.29	535.91	534.53	535.98	534.67
PAMB	14.32	14.318	14.317	14.317	14.316	14.316	14.312	14.309	14.309	14.31	14.311	14.312	14.313
P10M	14.321	14.315	14.315	14.315	14.315	14.314	14.31	14.306	14.311	14.313	14.312	14.314	14.314
HUMSER	107.75	109.21	107.35	110.85	108.13	107.42	109.3	106.29	108.17	107.31	106.58	106.85	106.48
RELHUM	73.277	76.303	72.278	81.262	79.348	78.098	79.138	77.68	78.683	76.348	80.205	78.566	87.284
WINVAV	1.4407	2.1952	2.8558	3.3787	3.0981	3.5961	3.4321	2.2606	3.0785	2.2291	3.0035	1.1511	3.3196
WINAAV	7.6801	46.372	25.076	-37.059	21.133	11.003	7.7642	46.753	3.142	-15.26	13.773	-26.234	-27.476
XMO	0.	0.	0.	0.	0.	0.	0.	0.	0.	0.	0.	0.	0.
P46Q2	1.001	2.8292	2.839	2.8572	2.846	2.8217	2.9184	2.8465	2.8474	2.8399	2.8314	1.002	2.8314
CT46	903.42	1827.7	1816.8	1809.8	1808.7	1802.8	1827.8	1811.2	1804.6	1807.9	1804.	914.91	1829.5
T46X	696.74	1784.	1780.6	1774.5	1772.4	1765.3	1791.1	1772.9	1770.5	1772.8	1767.7	730.21	1788.5

Comments: LCP CYCLES →

Zero	Pt.78	Pt.79	Pt.80	Pt.81	Pt.82	Pt.84	Pt.85	Pt.86	Pt.87	Pt.88	Zero	Pt.89

(NOTE: No DMS reading for point 831)

GE36/UDF1 Peebles Tests
082001-03
Test Log - Site IIID
Sheet 025 of 029

GE36/UDF-1 ENGINE 082001-0. EST READINGS - SITE IIID
RDGS. 252 - 304 ON 07.06.86 RDGS. 305 - 330 ON 07.07.86
RDGS. 331 - 358 ON 07.08.86

RDG.	317	318	319	320	321	322	323	324	325	326	327	328	329
XN2	11592.	11588.	11595.	11604.	11585.	11604.	11558.	11522.	166.07	0.	11574.	11564.	11590.
XN2R	11429.	11424.	11425.	11443.	11416.	11434.	11413.	11371.	164.05	0.	11424.	11411.	11425.
PCN2R	86.129	86.092	86.1	86.228	86.029	86.165	86.006	85.691	1.2363	0.	86.087	85.992	86.096
XN25	15574.	15574.	15580.	15583.	15578.	15591.	15541.	15518.	99.523	0.	15541.	15557.	15590.
XN25R	12776.	12772.	12771.	12778.	12776.	12777.	12773.	12765.	96.313	0.	12756.	12778.	12787.
PCN25R	95.198	95.175	95.165	95.213	95.198	95.212	95.178	95.117	.71768	0.	95.049	95.219	95.285
XN48	1397.6	1397.1	1397.1	1397.8	1397.6	1397.5	1397.8	1397.6	262.54	0.	1397.4	1397.6	1397.5
XN49	1398.9	1398.9	1398.9	1399.1	1398.9	1398.7	1399.	1399.	309.43	0.	1398.9	1398.9	1398.9
UT91R2	846.21	845.84	845.38	846.43	845.74	845.66	847.57	847.07	159.27	0.	847.	846.94	845.97
UT92R2	823.23	823.18	822.74	823.52	822.77	822.7	824.55	824.15	182.45	0.	824.16	823.94	823.07
BIAN91	31.535	31.285	30.975	31.61	31.465	30.849	30.902	30.687	87.056	86.96	30.841	30.805	30.947
BIAN92	29.223	29.19	29.065	29.239	29.16	29.355	29.1	29.435	87.198	87.092	29.524	29.282	29.495
W13	13.556	13.528	13.312	13.309	13.375	13.513	13.452	13.303	-6.9756	-.5	14.027	13.594	13.584
W15	13.556	13.528	13.312	13.309	13.375	13.513	13.452	13.303	-6.9756	0.	14.027	13.594	13.584
WF36	5172.3	5163.1	5162.	5192.3	5142.9	5182.2	5127.5	5041.3	174.48	166.82	5243.9	5140.9	5167.7
WF36R2	5216.8	5207.	5202.7	5239.5	5184.7	5223.6	5182.3	5091.	176.23	166.55	5290.8	5134.2	5203.5
FN11QA	20917.	20862.	20817.	20924.	20818.	20951.	20835.	20622.	0.	0.	20993.	20820.	20900.
SFC184	.25211	.2523	.25264	.25313	.25176	.25203	.25144	.24956	.5	.5	.25476	.25171	.25168
TAMB	532.29	533.33	533.79	533.2	533.58	533.81	531.73	531.65	531.19	532.68	533.75	534.2	535.28
T10	533.58	533.64	534.22	533.41	534.18	534.17	531.98	532.5	531.52	539.84	532.38	532.66	533.79
PAMB	14.313	14.313	14.312	14.31	14.309	14.312	14.314	14.315	14.318	14.33	14.331	14.333	14.333
P10M	14.316	14.316	14.314	14.312	14.311	14.314	14.316	14.317	14.32	14.332	14.333	14.335	14.336
HUMSER	109.65	106.39	106.28	107.42	103.51	102.28	102.67	104.98	106.66	105.99	107.64	109.5	110.05
RELHUM	88.821	83.298	81.939	84.436	80.398	78.856	84.91	87.024	89.783	84.913	83.163	83.308	80.754
WINVAV	3.3948	2.6571	3.3841	4.5399	2.44	3.1757	1.8904	3.4553	1.5749	1.2339	3.2275	4.022	4.3768
WINAAV	-28.241	-13.556	-28.821	-39.569	-36.011	-51.621	-47.031	-43.399	-1.5978	-22.52	4.3432	-5.7813	-6.3353
XMO	0.	0.	0.	0.	0.	0.	0.	0.	0.	0.	0.	0.	0.
P46Q2	2.8586	2.857	2.8562	2.8618	2.8481	2.8623	2.8492	2.8179	1.0016	9.99+10	2.852	2.847	2.8565
CT46	1808.2	1808.2	1809.7	1811.2	1808.	1811.9	1801.6	1793.7	924.54	9.99+10	1833.3	1804.8	1808.4
T46X	1773.4	1773.	1773.8	1775.3	1773.7	1776.	1766.1	1761.9	727.31	632.74	1791.2	1770.3	1773.1
Comments: LCF CYCLES →	Pt.90	Pt.91	Pt.92	Pt.93	Pt.94	Pt.95	Pt.96	Pt.97	Zero	Zero	Pt.98	Pt.99	Pt.100

GE36/UDF-1 ENGINE 082001-03 TEST READINGS - SITE IIID
RDGS. 252 - 304 ON 07.06.86 RDGS. 305 - 330 ON 07.07.86
RDGS. 331 - 358 ON 07.08.86

RDC.	330	331	332	333	334	335	336	337	338	339	340	341	342
XN2	316.61	0.	11590.	96.428	11435.	11905.	691.25	10902.	11199.	10709.	10891.	11051.	11278.
XN2R	311.45	0.	11414.	95.004	11302.	11768.	682.42	10758.	11060.	10576.	10756.	10918.	11143.
PCN2R	2.347	0.	86.013	.71593	85.169	88.682	5.1426	81.068	83.347	79.697	81.058	82.277	83.968
XN25	113.67	0.	15571.	120.48	15428.	15815.	184.62	14904.	15177.	14743.	14947.	15085.	15280.
XN25R	109.79	0.	12757.	116.3	12747.	12859.	129.64	12569.	12671.	12543.	12617.	12655.	12712.
PCN25R	.81808	0.	95.063	.86664	94.985	95.819	.96603	93.659	94.42	93.467	94.017	94.301	94.725
XN48	402.26	0.	0.	0.	1300.	1300.	0.	1199.	1200.	1200.2	1299.6	1299.7	1299.2
XN49	442.57	0.	1399.	236.29	1399.3	1398.7	332.87	1100.9	1100.9	1100.8	1201.1	1200.3	1200.9
UT91R2	243.	0.	0.	0.	789.01	789.12	0.	726.56	727.81	727.88	788.23	788.56	788.28
UT92R2	259.87	0.	822.37	138.96	825.47	825.27	196.15	648.46	649.04	648.9	708.12	707.87	706.23
BTAN91	87.041	77.459	30.693	87.011	31.722	33.354	87.003	30.799	32.04	29.324	28.663	30.035	30.87
BTAN92	87.209	77.273	29.452	87.156	28.829	29.863	87.097	30.892	31.25	29.768	29.278	30.016	30.829
W13	-6.4015	-.5	13.655	-7.3441	13.464	14.194	-4.5868	13.247	14.031	12.356	12.406	12.932	13.639
W15	-6.4015	0.	13.655	-7.3441	13.464	14.194	-4.5868	13.247	14.031	12.356	12.406	12.932	13.639
WF36	167.02	286.99	5166.2	170.53	4836.2	5821.9	174.1	3776.1	4264.3	3389.8	3741.8	4029.9	4449.3
WF36R2	167.52	288.05	5212.1	171.99	4905.3	5907.1	176.16	3820.5	4319.9	3432.8	3790.	4083.6	4508.9
FN11QA	0.	0.	20899.	0.	19651.	21953.	16.518	15205.	16411.	14183.	15858.	16771.	17991.
SFC184	.5	.5	.2521	.5	.25233	.272	10.781	.254	.26609	.24466	.2416	.24613	.25334
TAMB	536.55	536.19	535.32	534.12	531.42	531.69	532.16	533.41	532.77	532.85	532.77	532.45	532.26
T10	536.	537.49	534.8	534.34	530.99	530.84	532.17	532.67	531.72	531.83	531.7	531.37	531.31
PAMB	14.334	14.299	14.287	14.287	14.282	14.281	14.281	14.283	14.284	14.284	14.285	14.285	14.286
P10M	14.336	14.299	14.289	14.288	14.283	14.283	14.282	14.284	14.285	14.286	14.287	14.287	14.288
HUMSER	110.12	111.52	110.33	108.58	108.66	108.91	109.22	106.31	106.89	106.81	107.09	107.28	107.26
RELHUM	77.484	79.196	80.593	82.577	90.477	89.869	88.702	82.835	85.081	84.8	85.262	86.318	86.872
WINVAV	2.7594	.01362	2 2952	2.7118	1.8074	1.8358	.48994	2.3319	1.618	3.1844	2.8655	3.9975	4.0501
WINAAV	-23.511	-3.6021	14.356	15.772	-17.945	11.204	2.2016	1[illegible].715	-1.6365	11.214	1.3371	-11.102	8.5497
XMO	0.	0.	0.	0.	0.	0.	0.	0.	0.	0.	0.	0.	0.
P46Q2	1.0026	9.99+10	2.8472	1.0018	2.7558	3.0845	1.0014	2.361	2.5422	2.2506	2.3807	2.4813	2.6226
CT46	899.04	9.99+10	1820.1	909.63	1769.6	1843.	904.43	1681.6	1709.4	1615.7	1658.3	1685.3	1724.9
T46X	727.15	555.93	1783.7	722.17	1737.7	1810.4	720.94	1658.6	1676.	1608.	1638.5	1661.7	1695.
Comments:	Zero	Zero	Part Power Bad XN48	Zero	Trim Balance → Mis-matched speeds		Zero	Trim Balance → Mis-matched speeds					

GE36/UDF-1 ENGINE 082001-03 TEST READINGS - SITE IIID
RDGS. 252 - 304 ON 07.06.86 RDGS. 305 - 330 ON 07.07.86
RDGS. 331 - 358 ON 07.08.86

RDG.	343	344	345	346	347	348	349	350	351	352	353	354	355
XN2	11537.	343.04	0.	12061.	192.14	192.14	192.14	192.14	192.14	192.14	192.14	192.14	192.14
XN2R	11391.	338.42	0.	11814.	187.27	187.06	186.87	186.82	186.73	186.62	186.63	186.39	186.35
PCN2R	85.842	2.5503	0.	89.025	1.4113	1.4097	1.4082	1.4078	1.4072	1.4063	1.4064	1.4046	1.4043
XN25	15500.	114.71	0.	16010.	108.95	108.95	108.95	108.95	108.95	108.95	108.95	108.95	108.95
XN25R	12771.	110.99	0.	12867.	103.8	103.58	103.48	103.65	103.84	103.94	104.2	104.21	104.55
PCN25R	95.167	.82703	0.	95.879	.7735	.77181	.77108	.77237	.77377	.77449	.77648	.77653	.77904
XN48	1299.6	103.14	0.	1397.4	97.517	96.579	96.579	98.454	97.517	97.517	97.517	97.517	97.517
XN49	1200.6	458.52	0.	1398.5	429.45	429.45	429.45	429.45	429.45	429.45	429.45	429.45	429.45
UT91R2	787.99	62.487	0.	840.49	58.367	57.74	57.68	58.784	58.198	58.164	58.167	58.093	58.078
UT92R2	707.58	270.01	0.	817.59	249.84	249.56	249.3	249.23	249.12	248.97	248.99	248.67	248.61
BTAN91	31.821	87.059	86.96	32.17	86.922	86.919	86.921	86.919	86.921	86.92	86.922	87.08	87.088
BTAN92	31.237	87.202	87.174	29.918	87.093	87.068	87.072	87.075	87.07	87.065	87.065	85.486	85.49
W13	14.002	-6.2052	-.5	14.273	-7.1532	-7.199	-7.2296	-7.284	-7.3102	-7.3098	-7.3433	-7.4088	-7.4429
W15	14.002	-6.2052	0.	14.273	-7.1532	-7.199	-7.2296	-7.284	-7.3102	-7.3098	-7.3433	-7.4088	-7.4429
WF36	4934.9	173.33	145.59	6103.8	145.8	141.92	138.87	137.15	136.53	136.11	135.38	129.89	129.81
WF36R2	4996.7	175.13	145.29	6110.4	144.81	140.73	137.5	135.76	135.05	134.53	134.83	128.22	128.12
FN11QA	19135.	0.	0.	22947.	0.	0.	0.	0.	0.	0.	0.	0.	0.
SFC184	.26396	.5	.5	.26918	.5	.5	.5	.5	.5	.5	.5	.5	.5
TAMB	532.91	532.57	540.15	543.69	544.31	544.76	545.28	545.14	544.99	545.22	545.56	546.24	546.06
T10	532.04	532.92	542.15	540.66	545.98	547.23	548.38	548.67	549.15	549.81	549.75	551.15	551.43
PAMB	14.287	14.288	14.295	14.291	14.293	14.293	14.293	14.293	14.293	14.292	14.291	14.288	14.286
P10M	14.289	14.289	14.296	14.295	14.295	14.295	14.296	14.295	14.296	14.295	14.292	14.29	14.287
HUMSER	106.98	107.05	117.4	114.12	113.57	114.57	116.92	115.1	114.22	115.38	116.87	114.85	113.54
RELHUM	84.784	85.798	73.056	63.358	61.832	61.472	61.662	61.	60.843	60.979	61.069	58.752	58.411
WINVAV	1.6926	2.6073	3.5739	7.9273	6.4991	6.3887	3.2672	3.5945	6.0797	6.0945	6.3706	6.9769	2.866
WINAAV	18.137	-1.1191	-52.506	-17.017	9.4036	-14.742	36.853	35.472	-18.244	10.382	27.22	23.613	-16.095
XMO	0.	0.	0.	0.	0.	0.	0.	0.	0.	0.	0.	0.	0.
P46Q2	2.7834	1.0021	9.99+10	3.134	1.0014	1.0013	1.0009	1.0008	1.0009	1.0008	1.001	1.001	1.0009
CT46	1769.5	907.86	9.99+10	1904.3	857.45	847.95	841.03	830.13	825.22	824.94	818.78	804.	797.89
T46X	1737.7	722.6	599.27	1870.3	653.85	661.43	663.39	666.83	667.7	659.1	661.06	646.5	637.11

Comments:	Trim Bal. Mis-matched Speeds	Zero	Zero	Part Power (Max Thrust?)	Zeros → Cool Down Period - time in minutes: → +0	+5	+10	+15	+20	+25	+30	+35	+40

GE36/UDF1 Peebles Tests
082001-03
Test Log - Site IIID
Sheet 028 of 029

```
G  /UDF-1 ENGINE 082001-0  EST READINGS    -    SITE III
RDGS. 252 - 304  ON 07.06.86    RDGS. 305 - 330 ON 07.07.86
                 RDGS. 331 - 358  ON 07.08.86

RDG.          356       357       358

XN2            0.    5348.6    94.464
XN2R           0.    5239.1     92.57
PCN2R          0.    39.481    .69759
XN25           0.    11678.    141.43
XN25R          0.    10976.    136.77
PCN25R         0.    81.786    1.0192
XN48           0.    700.03    124.71
XN49           0.    701.37    701.37

UT91R2         0.    421.08    75.048
UT92R2         0.    410.08    410.26
BTAN91     87.165    17.624    86.832
BTAN92     85.544     18.01    86.878

W13           -.5    5.3388   -7.5599
W15            0.    5.3388   -7.5599

WF36       125.42    826.12    152.07
WF36R2     123.88    830.97    153.06
FN11QA     3.8527    2175.7        0.
SFC184     32.503    .38609        .5

TAMB       549.31    541.55    540.52
T10        552.38    540.58    540.11
PAMB       14.257    14.213     14.21
P10M       14.259    14.215    14.211
HUMSER     108.41    114.37    114.33
RELHUM     50.297    67.668    69.933
WINVAV     4.9213    4.6068    5.2789
WINAAV     10.421   -12.914   -16.406
XMO            0.        0.        0.

P46Q2     9.99+10    1.1993    1.0017
CT46     -9.99+10    1340.2    853.09
T46X       590.38    1302.3    737.58
```

Comments: Zero   F.I.   Zero

ORIGINAL PAGE IS
OF POOR QUALITY

APPENDIX B

STRAIN DATA FOR THE STRUT

Figures B-1 and B-2 illustrate the locations of all the gages read except KD FAR1, KD FAR2, and KD FAR3. These three make up the vertical, diagonal, and axial axes, respectively, of a gage rosette located centrally on the inner surface of the mid-fairing.

The following graphs (Figures B-3 through B-40) contain maximum stress locations calculated from strains read on gages located as shown in Figures B-1 and B-2. These are shown versus engine frequencies and speeds as read from test diagrams. Each graph (with the exceptions of those combined because only one situation for each was recorded) displays the maximum stress versus speed or frequency for one gage only. Different situations are labeled for each point. Note that almost all are labeled with either an XN2, an XN25, or an XN48. These correspond to engine speeds as follows:

- XN2 refers to the intermediate pressure compressor
- XN25 refers to the high pressure compressor
- XN48 refers to the Stage 1 propulsor.

PRECEDING PAGE BLANK NOT FILMED

PAGE 278 INTENTIONALLY BLANK

ORIGINAL PAGE IS
OF POOR QUALITY

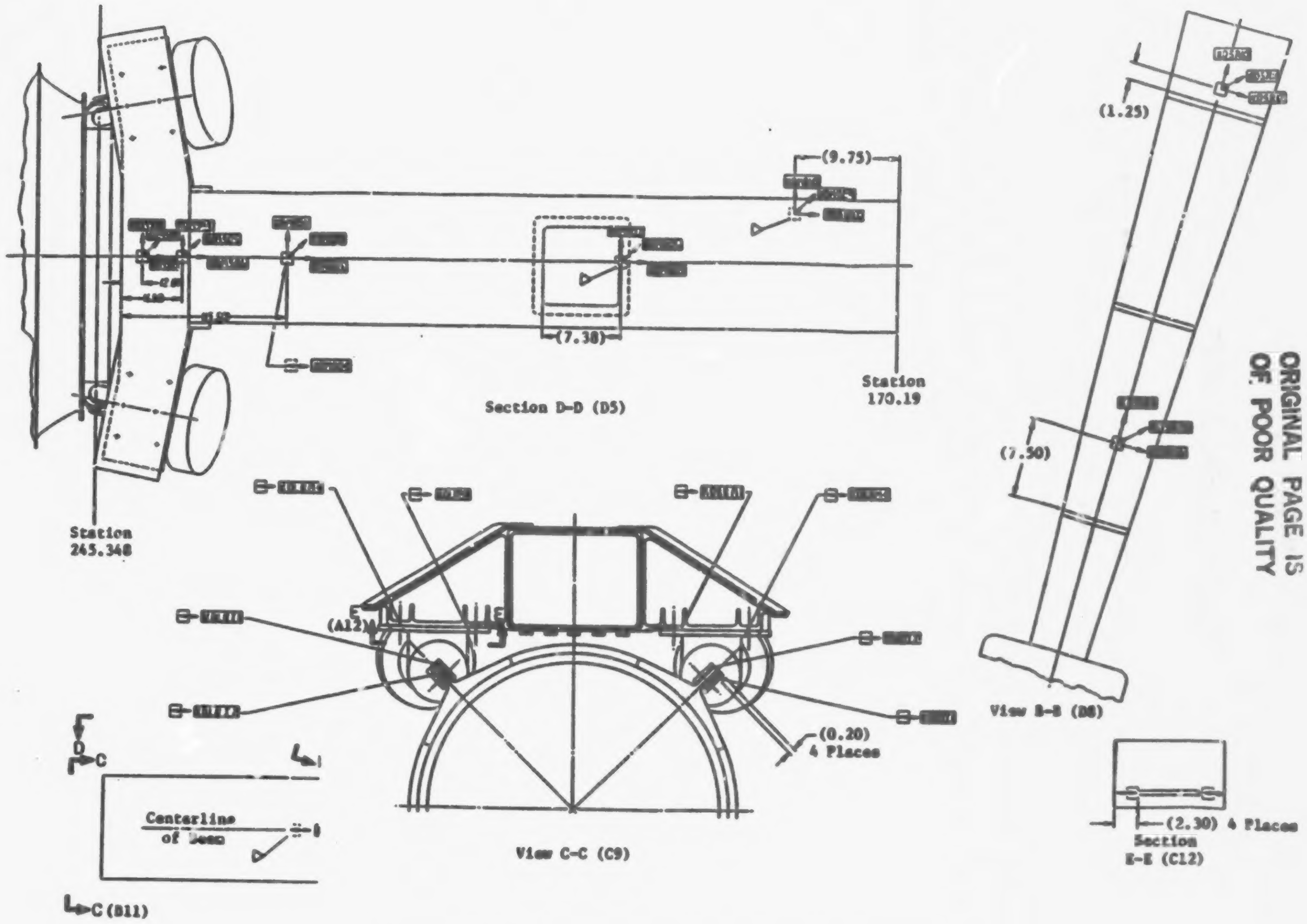
(9.75)
(7.38)
Station
170.19
Section D-D (D5)
Station
245.348
(1.25)
(7.50)
View B-B (B8)
(A12)
(0.20)
4 Places
View C-C (C9)
D
C
Centerline
of Beam
C (B11)
(2.30) 4 Places
Section
E-E (C12)

Figure B-1. Strain Gage Locations on Strut.

C-4

ORIGINAL PAGE IS
OF POOR QUALITY

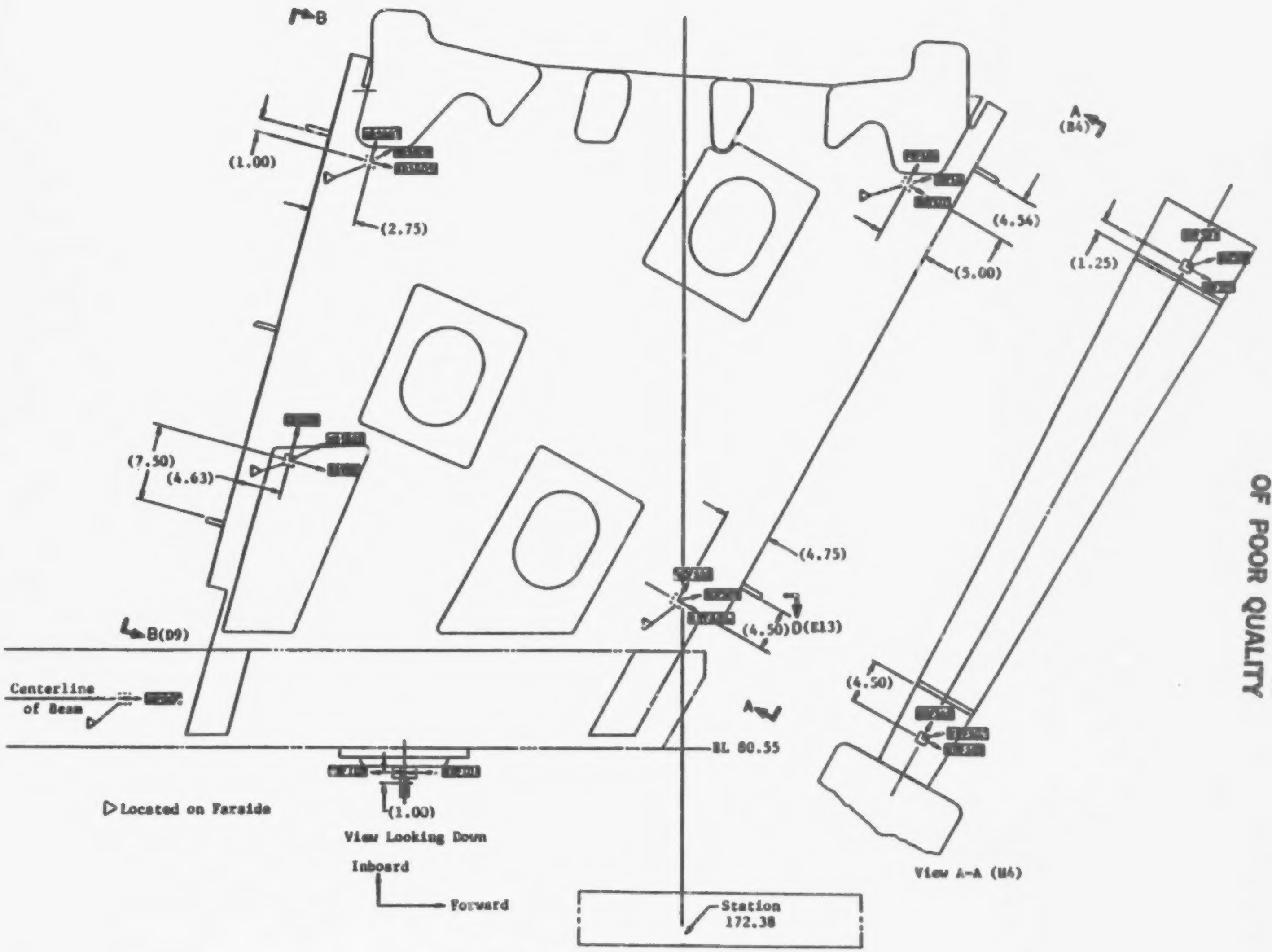
B
(1.00)
(2.75)
(7.50)
(4.63)
B(D9)
Centerline
of Beam
▷ Located on Farside
(1.00)
View Looking Down
Inboard
Forward
BL 80.55
Station
172.38
(4.75)
(4.50)
D(E13)
A
(4.54)
(5.00)
A
(H4)
(1.25)
(4.50)
View A-A (H4)

Figure B-2. Nacelle Instrumentation.

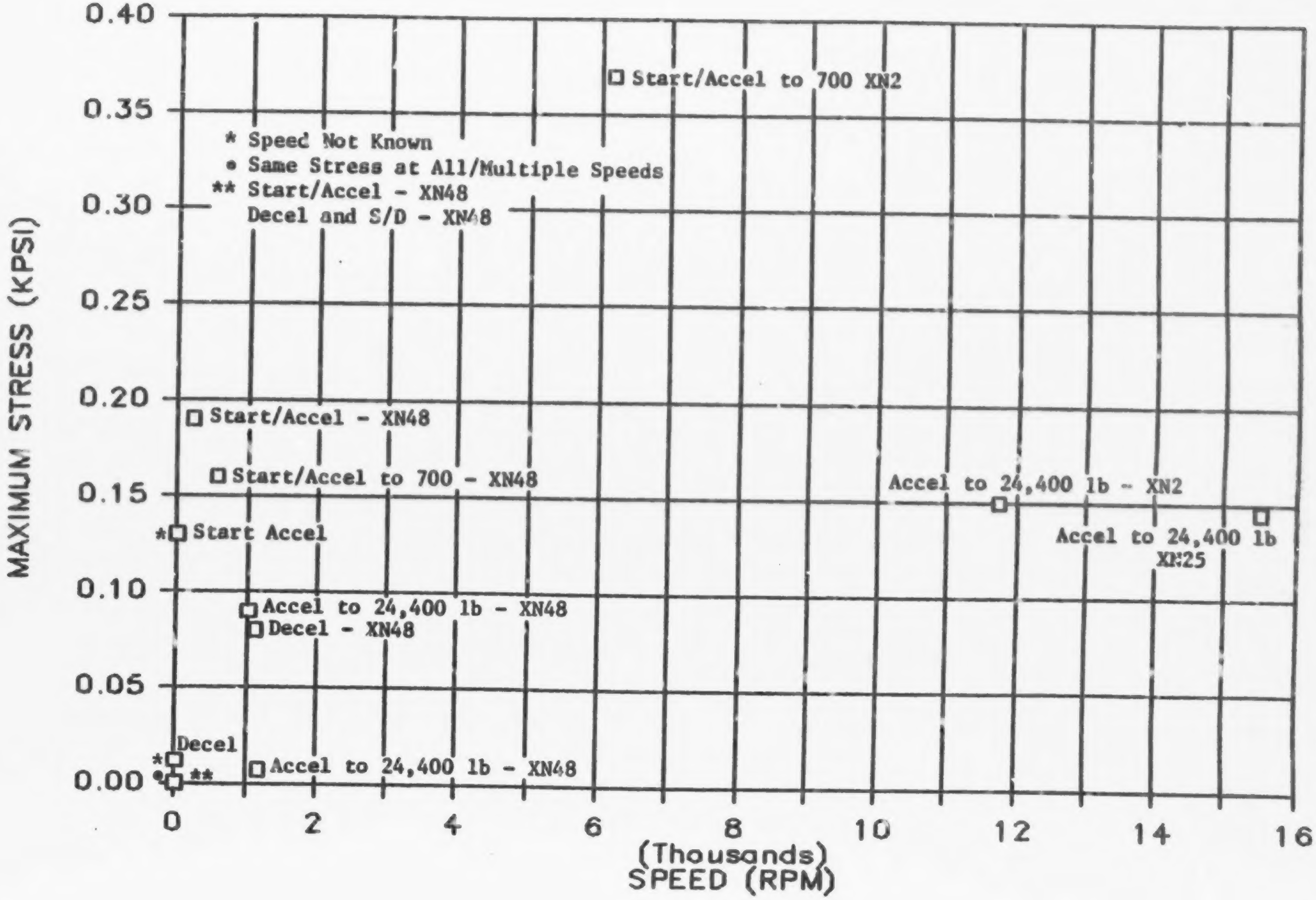

Figure B-3. Fairing Rosette No. 1 Vertical Axis (KD FAR1) Stress Versus Speed.

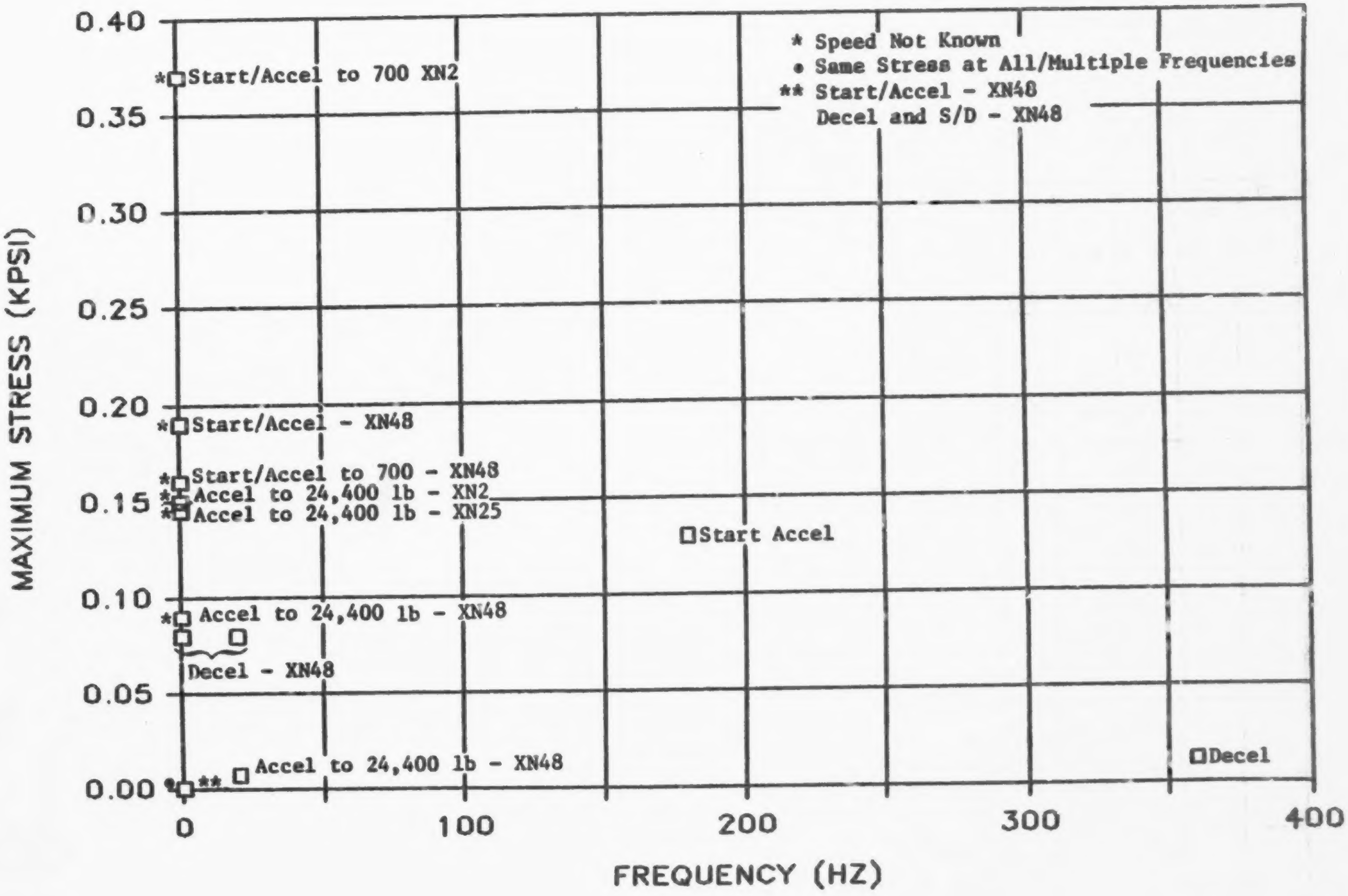

Figure B-4. Fairing Rosette No. 1 Vertical Axis (KD FAR1) Stress Versus Frequency.

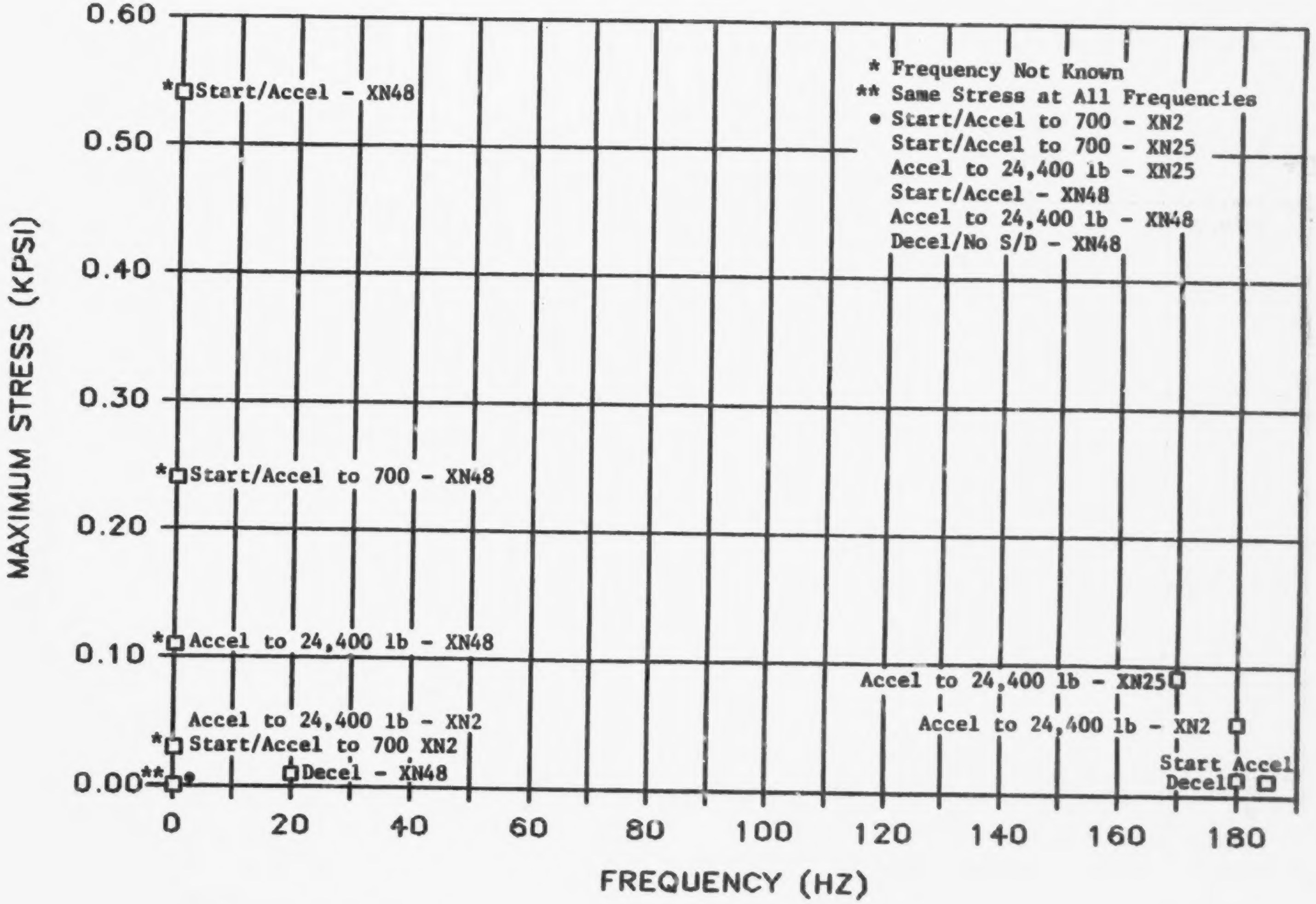

Figure B-5. Fairing Rosette No. 1 Diagonal Axis (KD FAR2) Stress Versus Frequency.

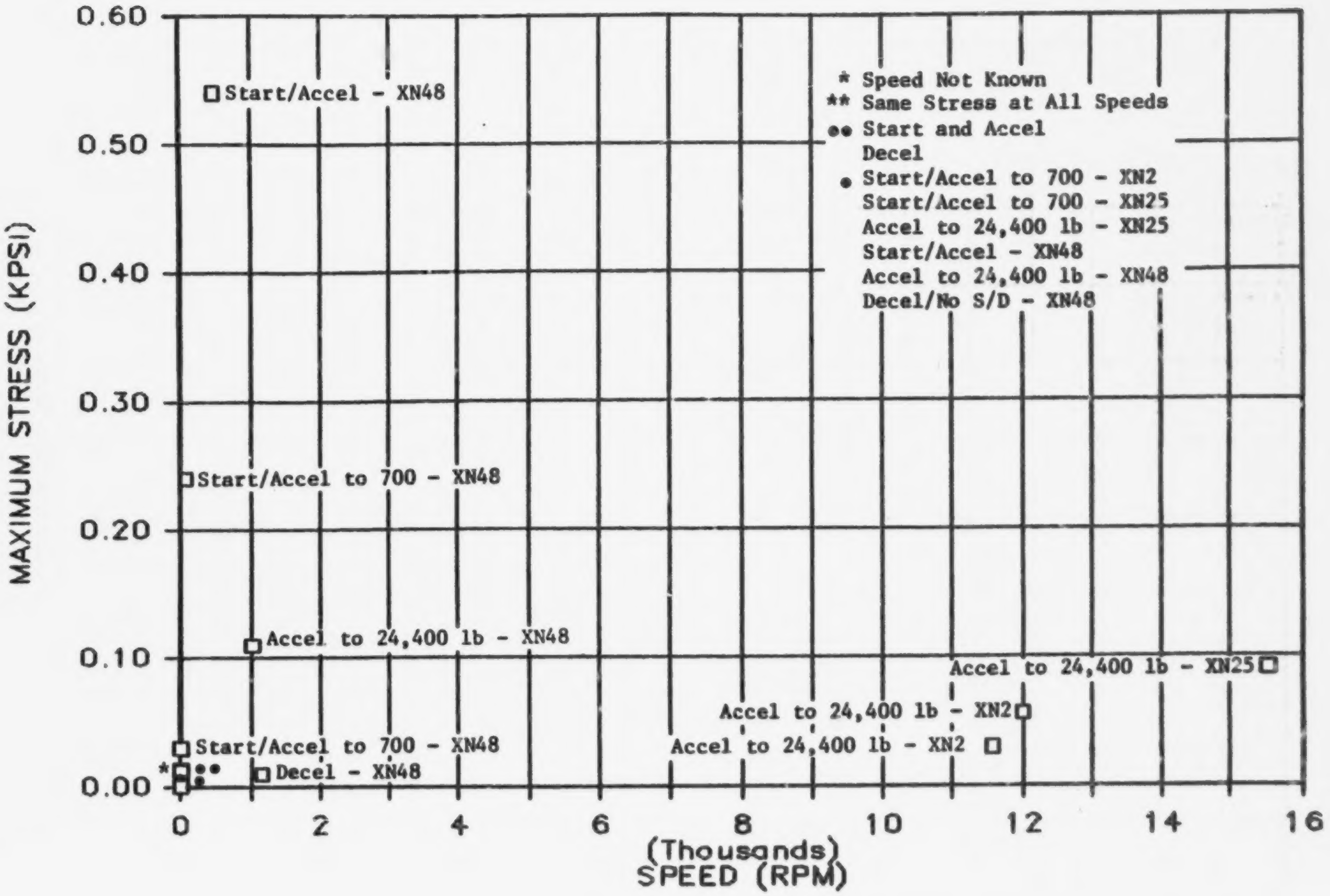

Figure B-6. Fairing Rosette No. 1 Diagonal Axis (KD FAK2), Stress Versus Speed.

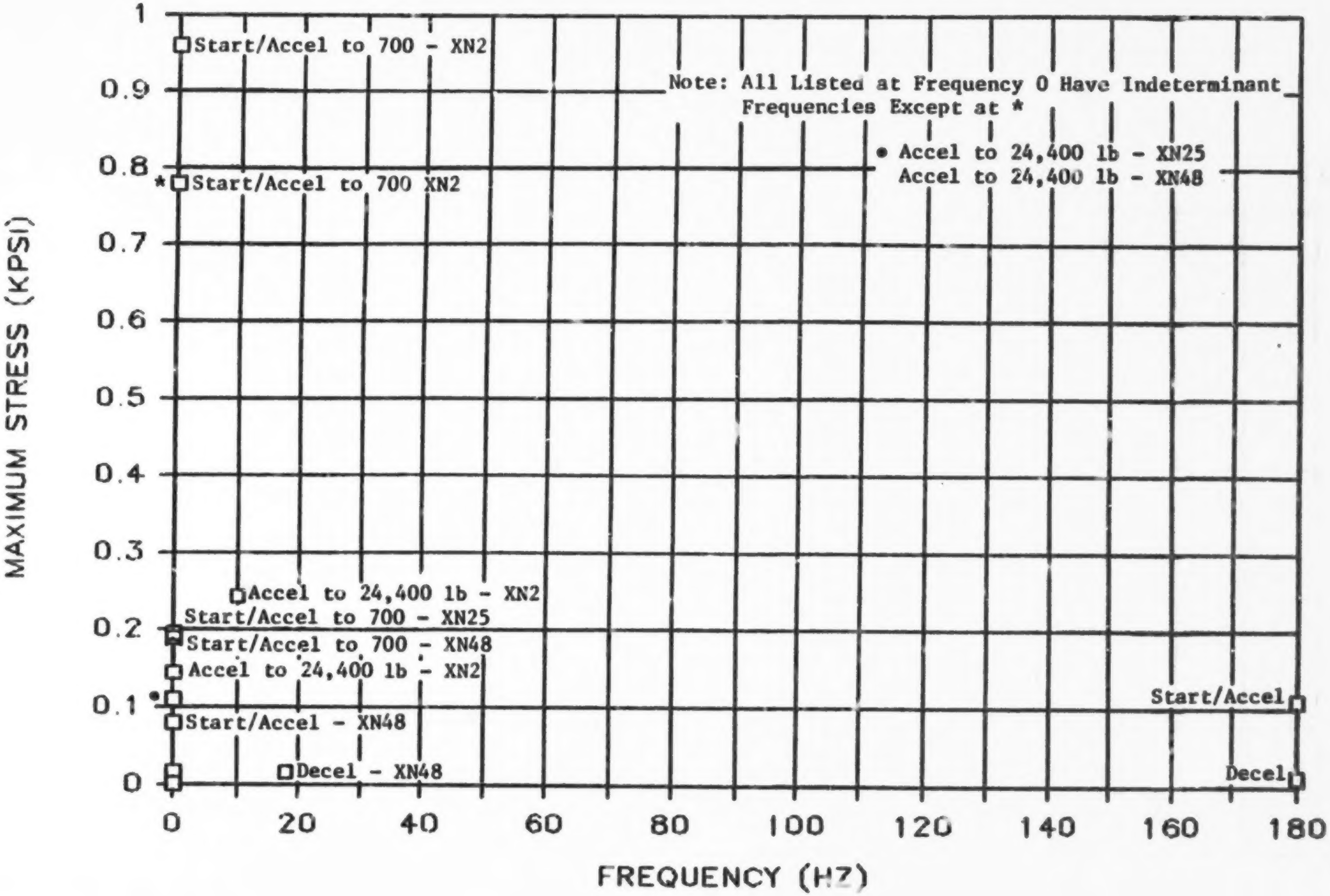

Note: All Listed at Frequency 0 Have Indeterminant Frequencies Except at *
- • Accel to 24,400 lb - XN25
- Accel to 24,400 lb - XN48

Figure B-7. Fairing Rosete No. 1 Axial Axis (KD FAR3), Stress Versus Frequency.

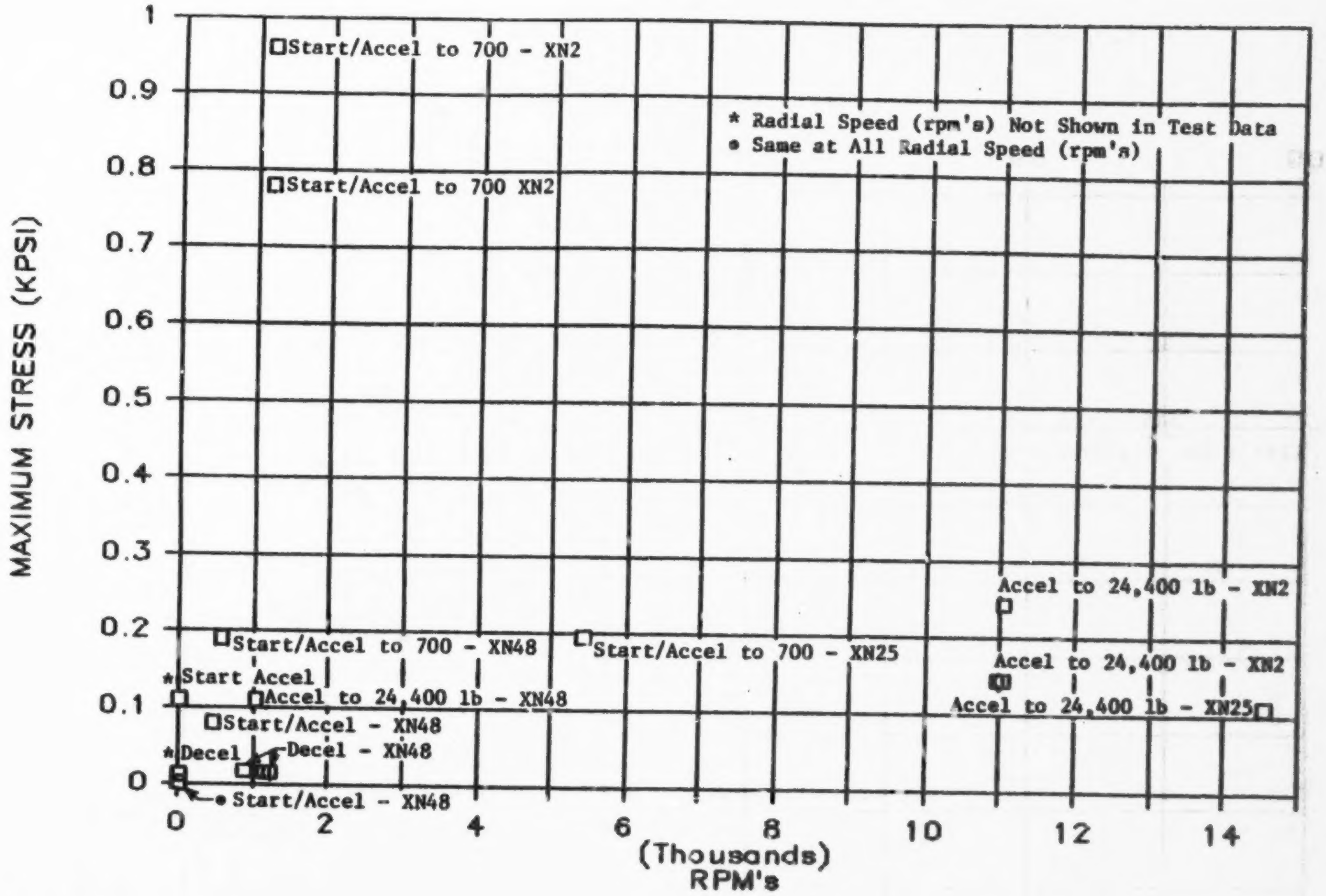

Figure B-8. Fairing Rosette No. 1 Axial Axis (KD FAR3), Stress Versus Speed.

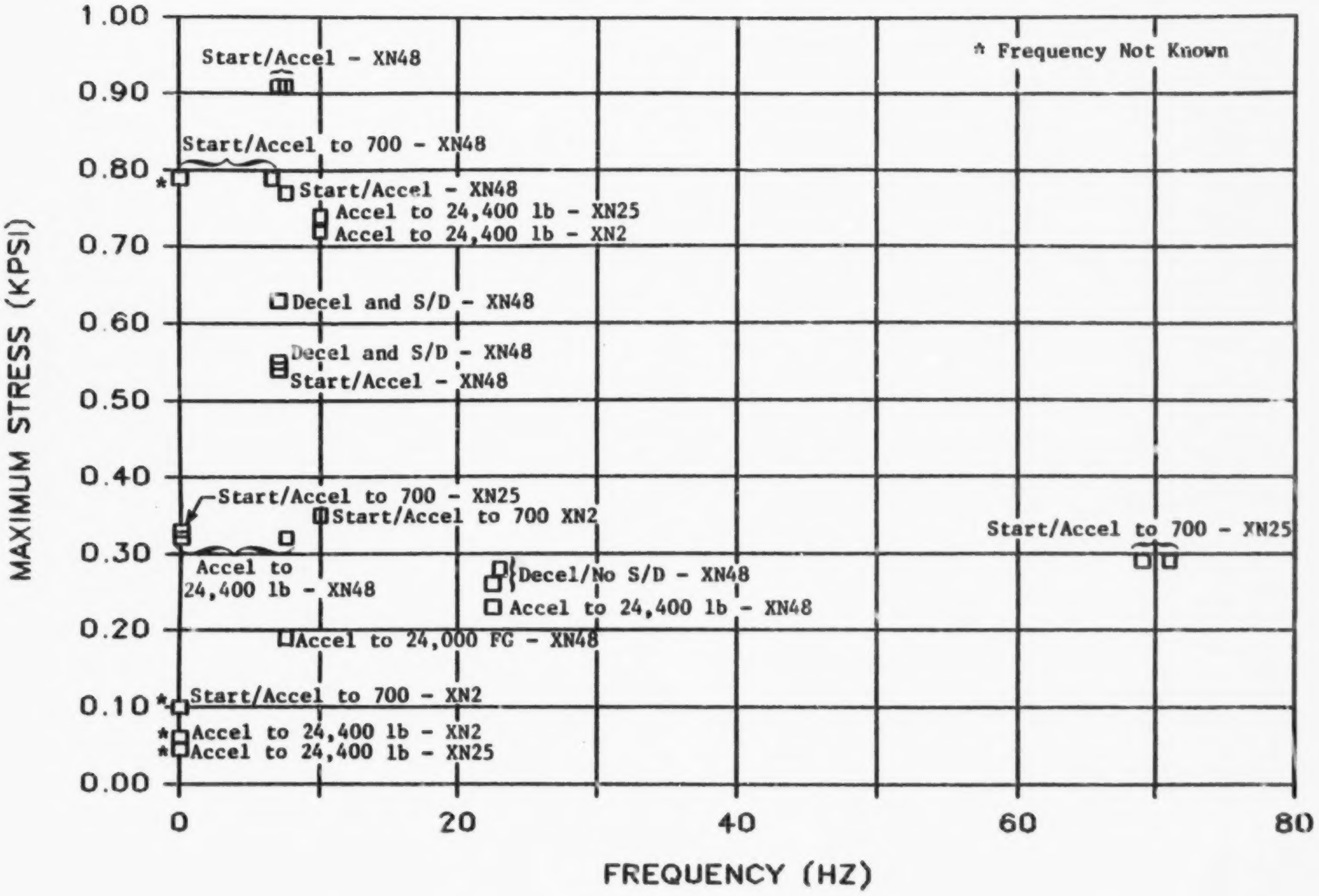

Figure B-9. Forward Isolator (KD F101), Stress Versus Frequency.

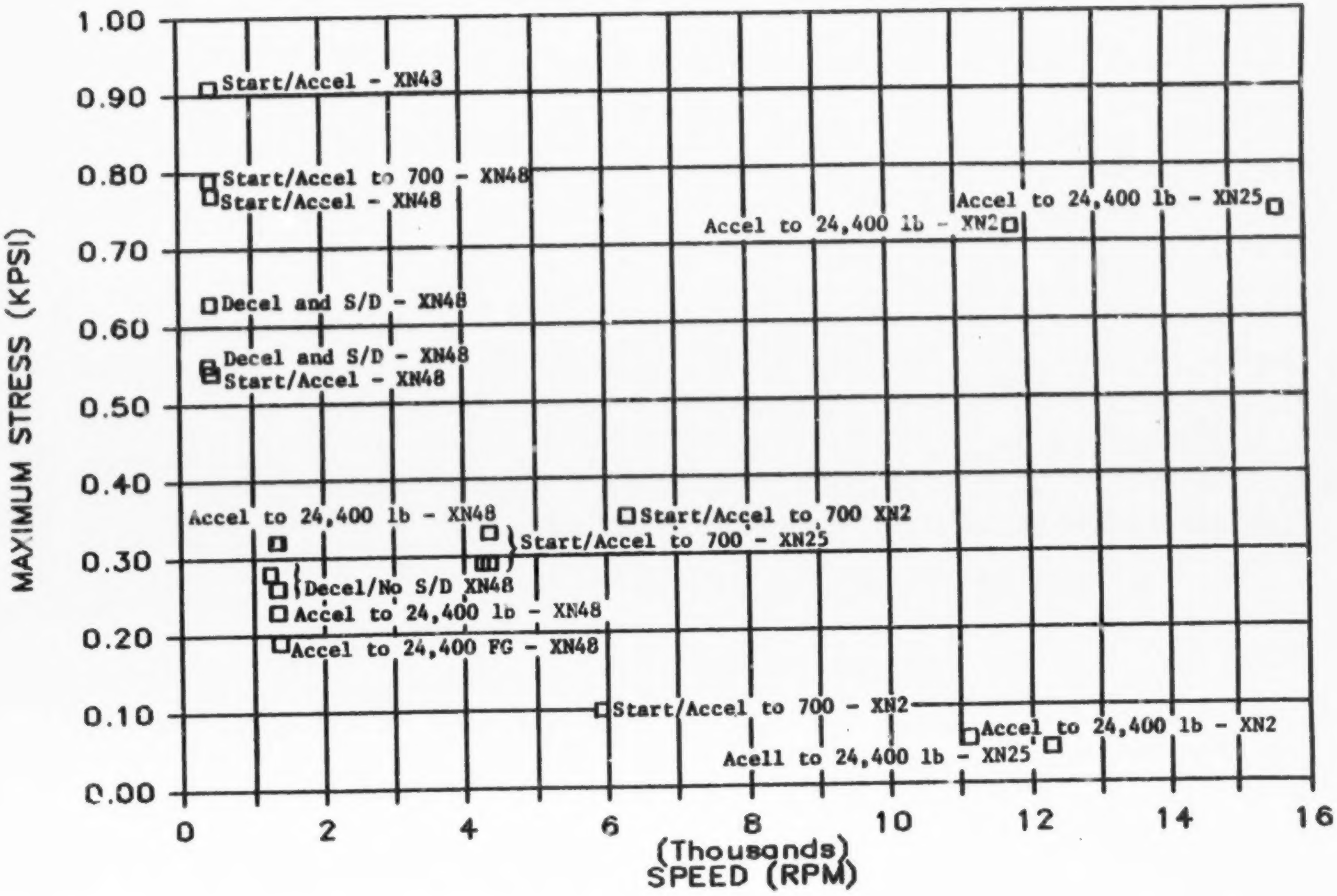

Figure B-10. Forward Isolator (KD F101), Stress Versus Speed.

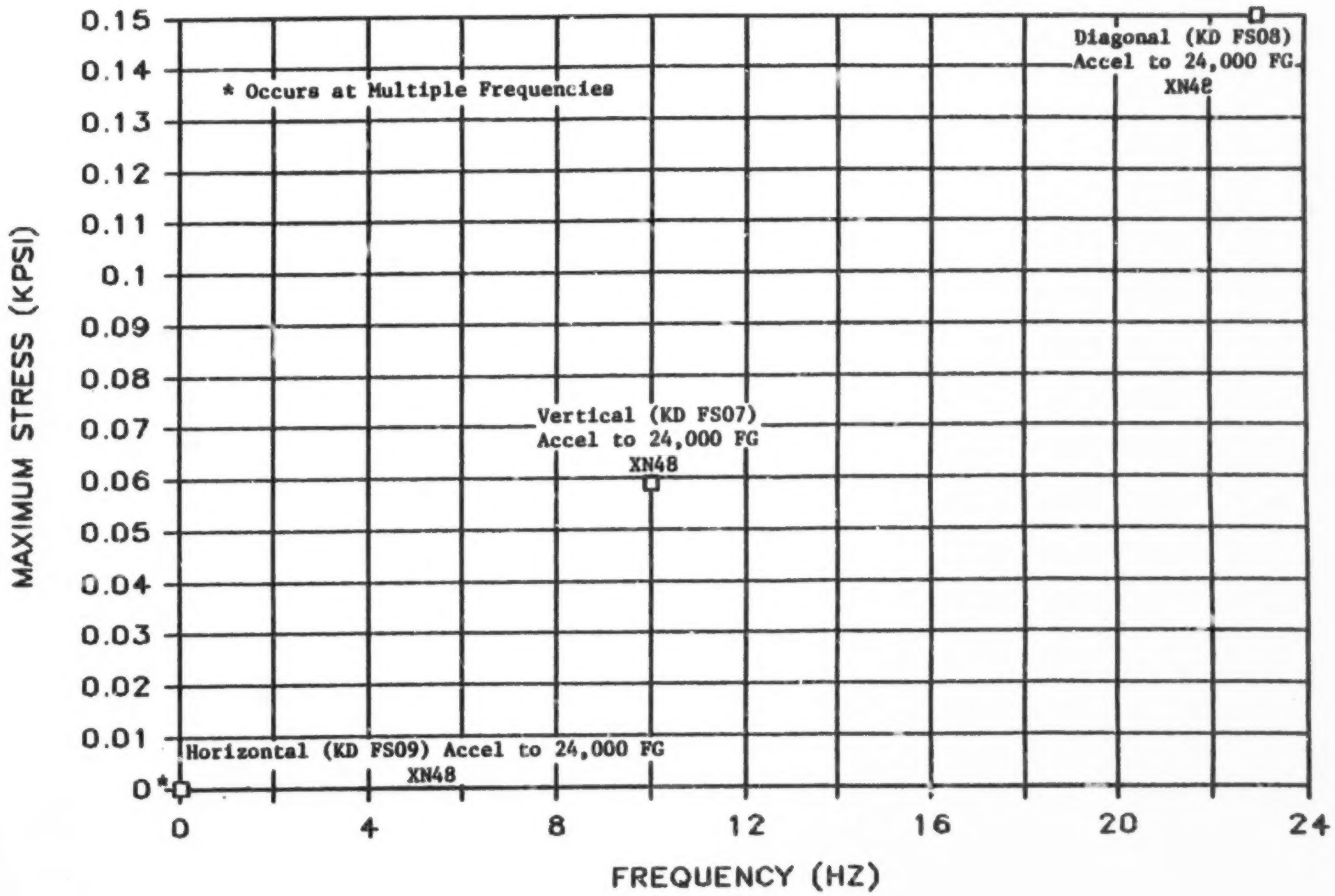

Figure B-11. Back of Spar - Upper Forward (KD FS07, KD FS08, and KD FS09), Stress Versus Frequency.

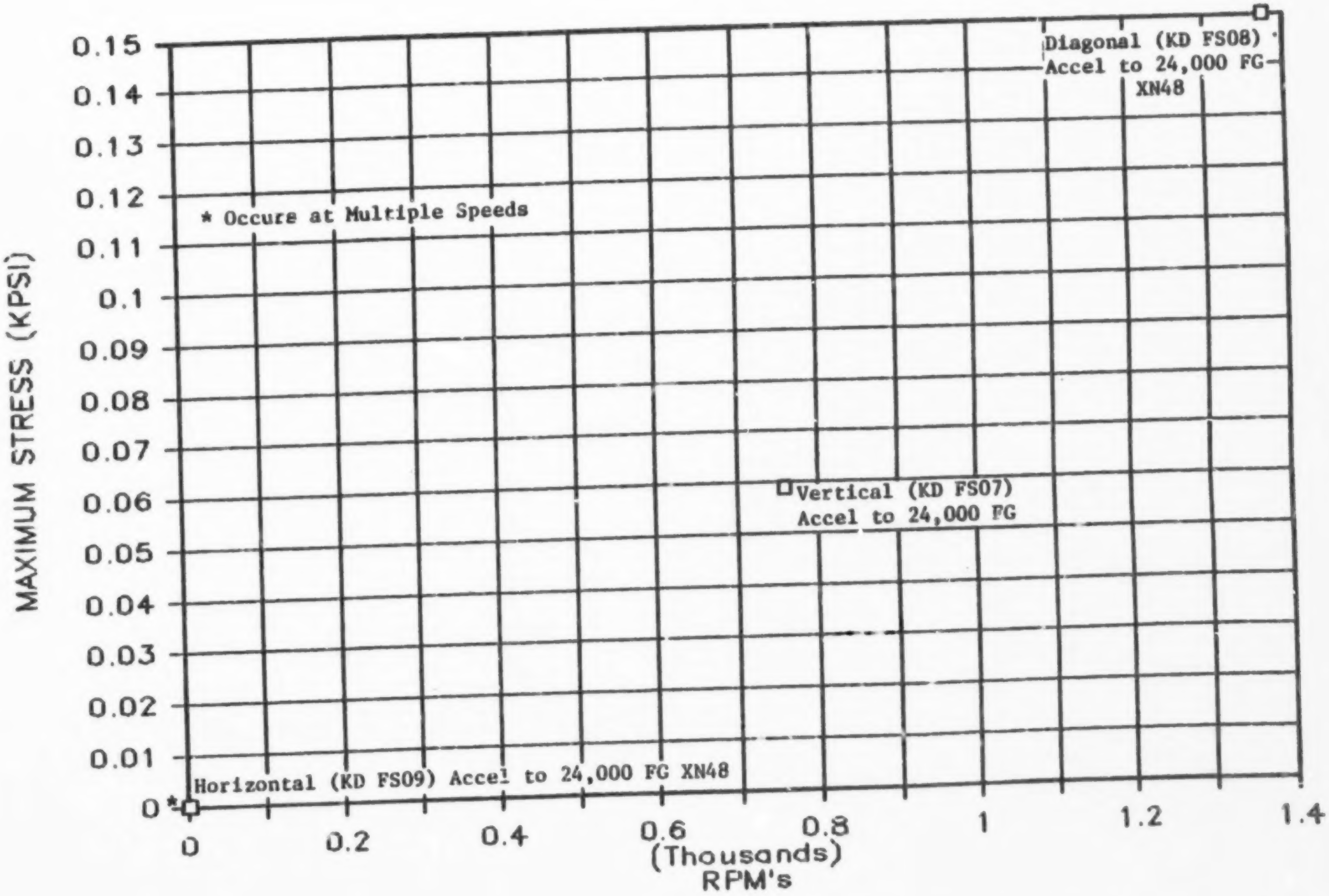

Figure B-12. Back of Spar - Upper Forward (KD FS07, KD FS08, and KD FS09), Stress Versus Speed.

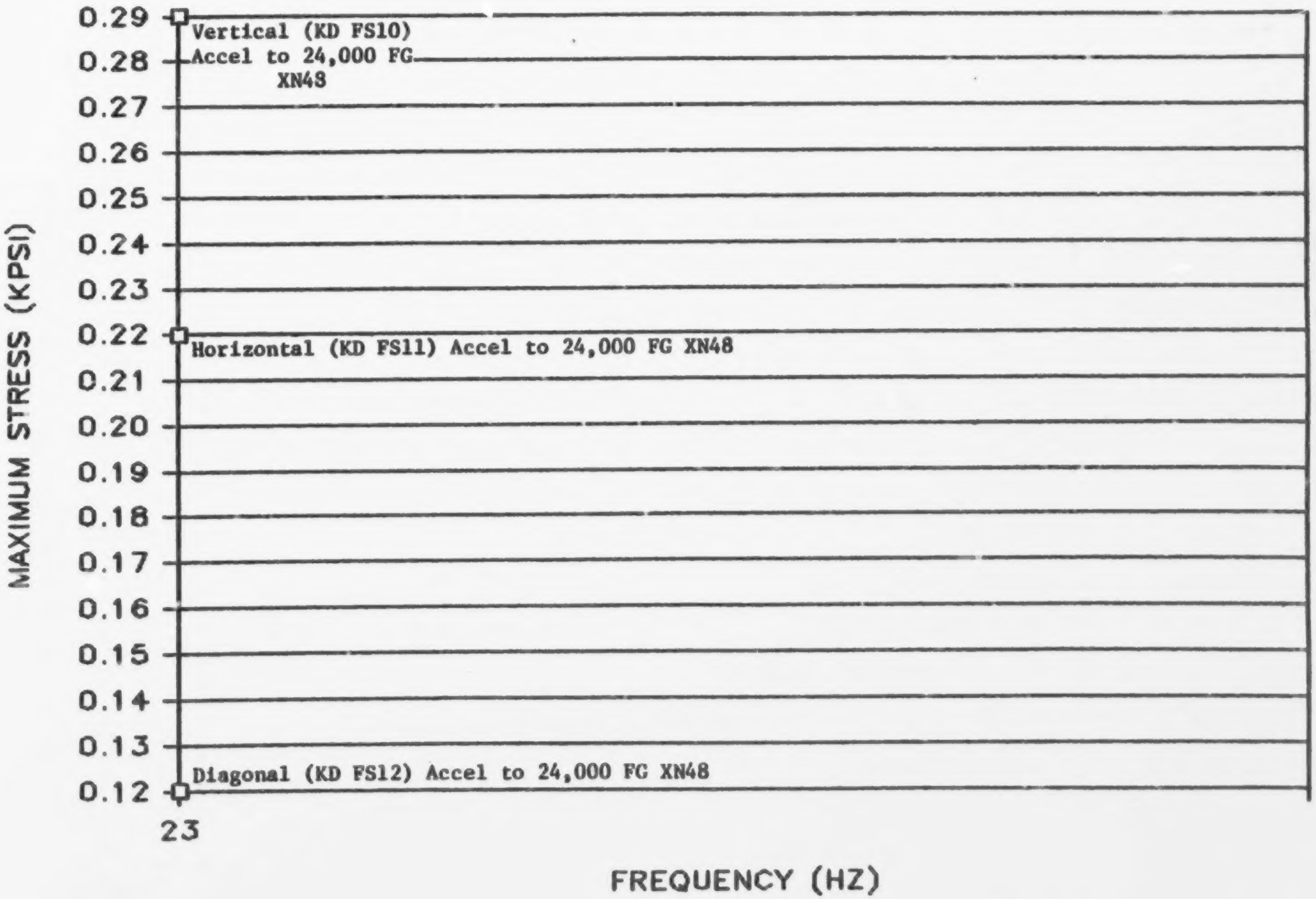

Figure B-13. Side of Spar - Upper Forward Vertical, Horizontal, and Axial (KD FS10, 11, and 12) Stress Versus Frequency.

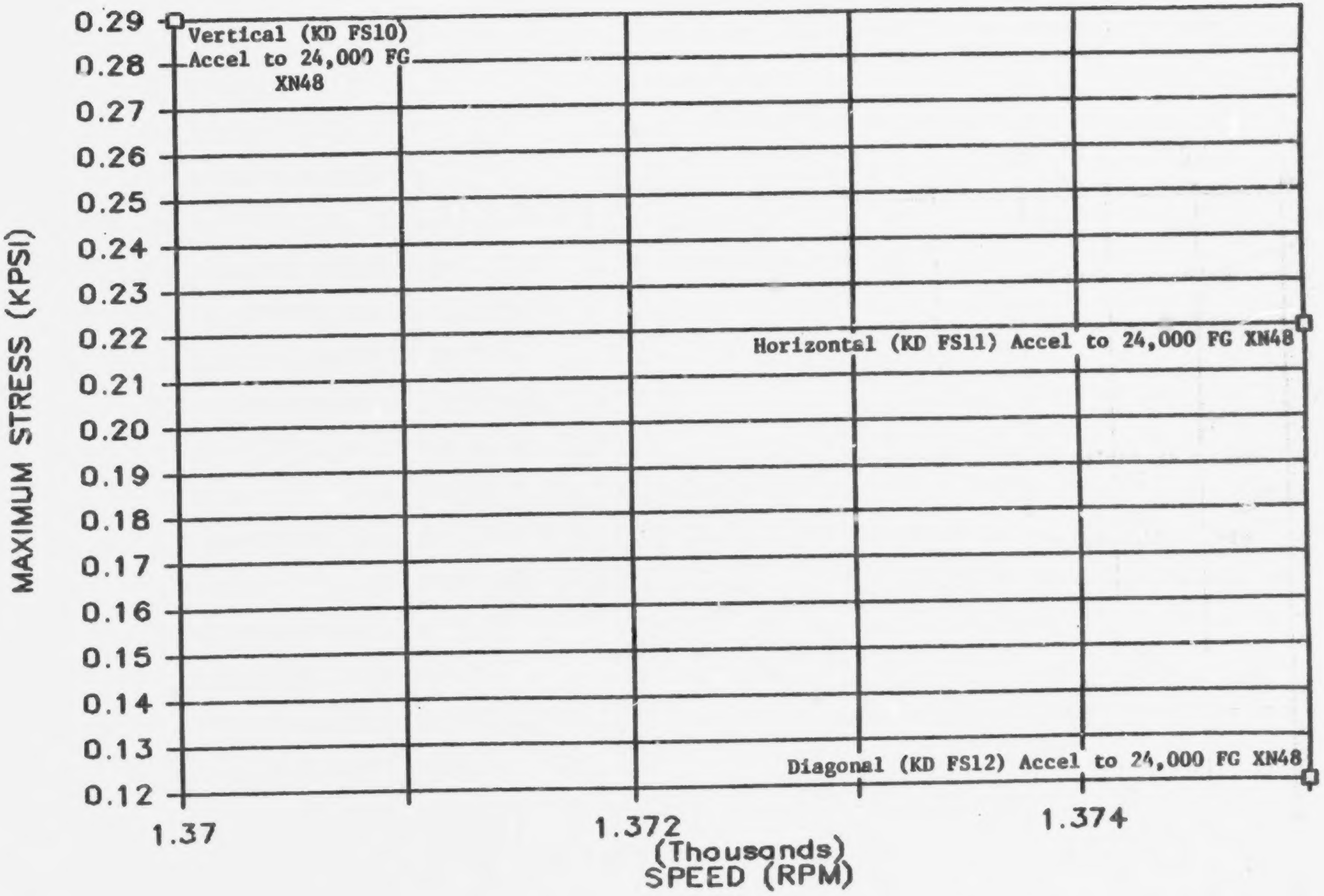

Figure B-14. Side of Spar - Upper Forward Vertical, Horizontal, and Axial (KD FS10, 11, and 12) Stress Versus Speed.

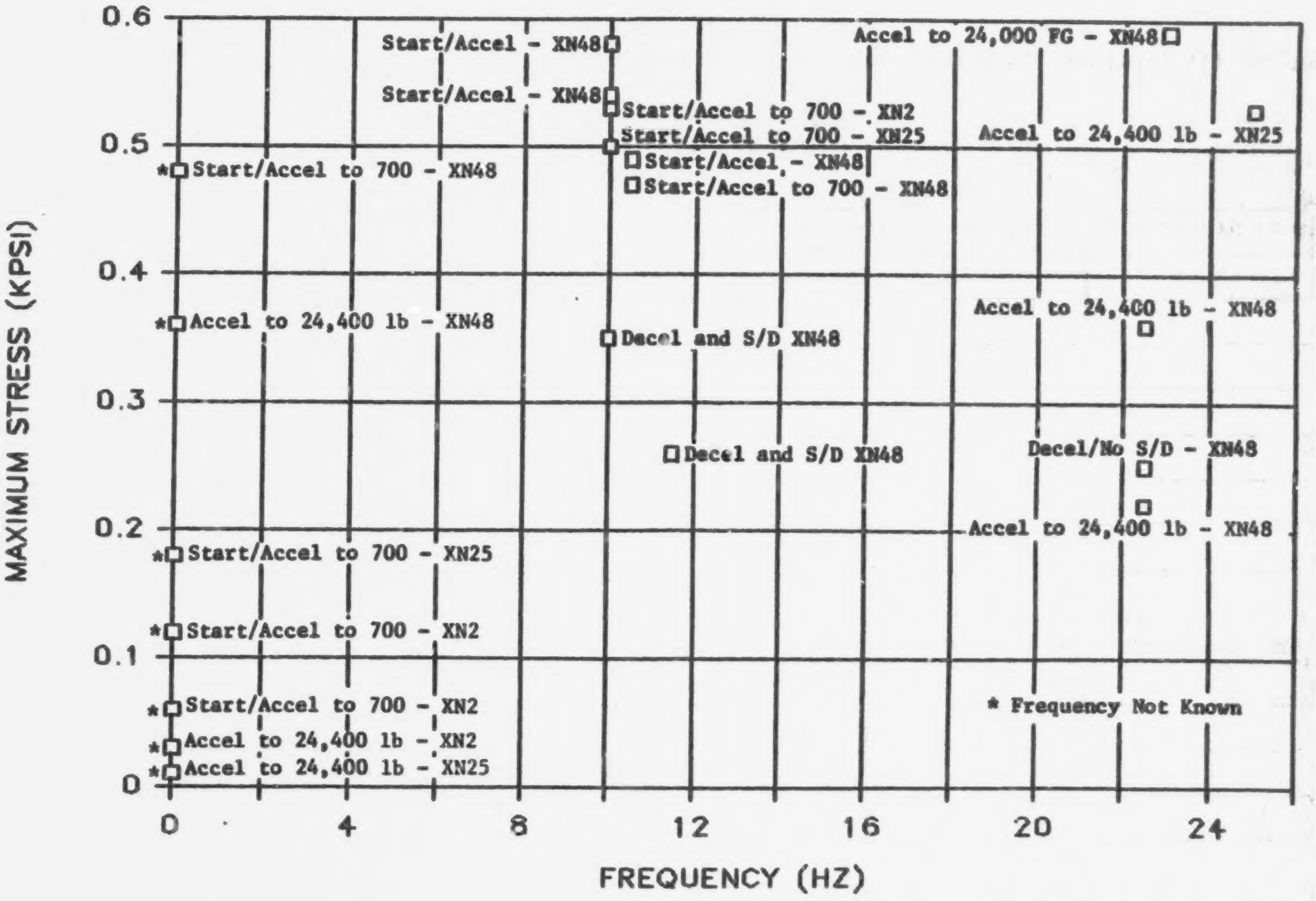

Figure B-15. Left Aft Isolator Clevis Axial (KD LRI1), Stress Versus Frequency.

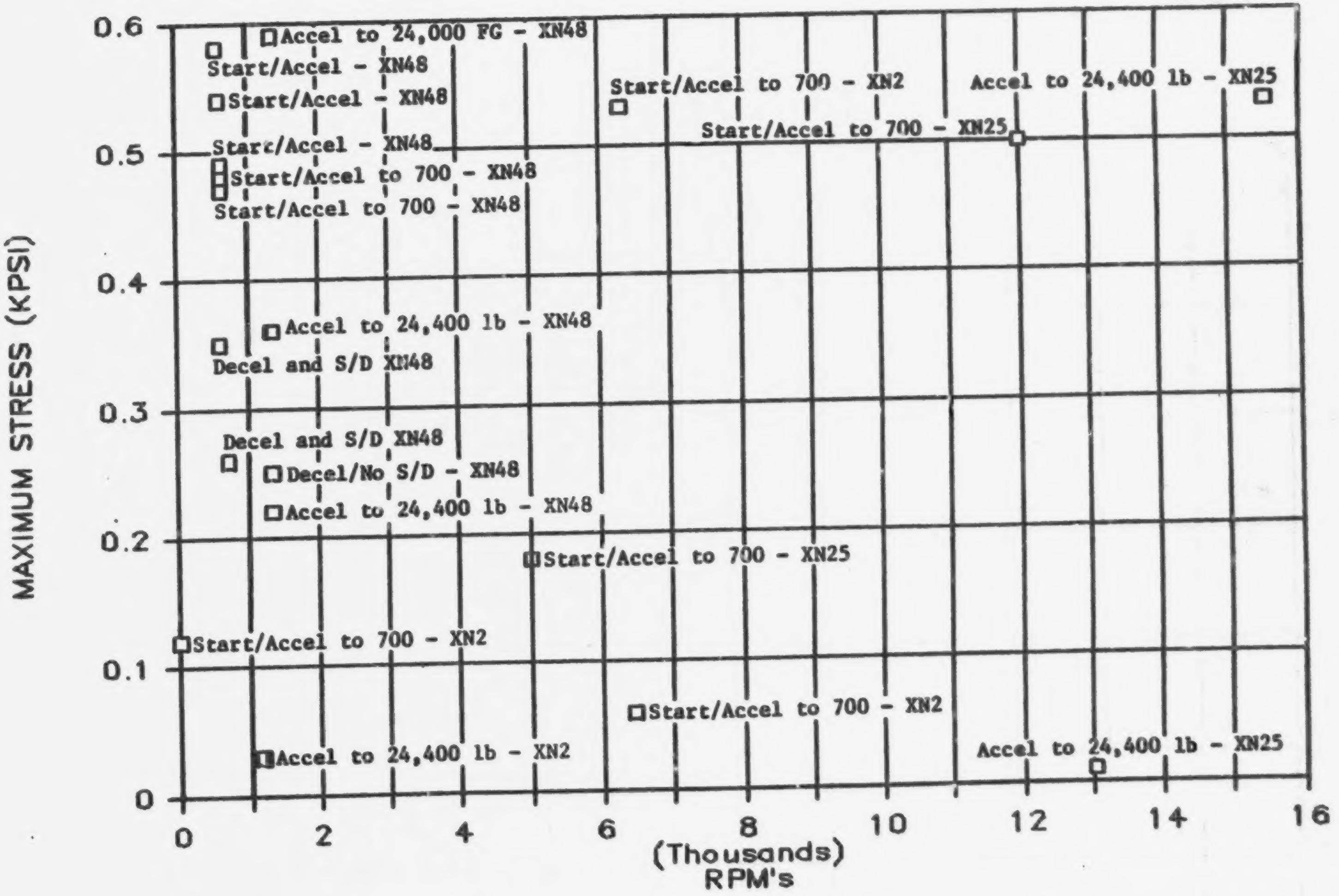

Figure B-16. Left Aft Isolator Clevis Axial (KD LRI1), Stress Versus Speed.

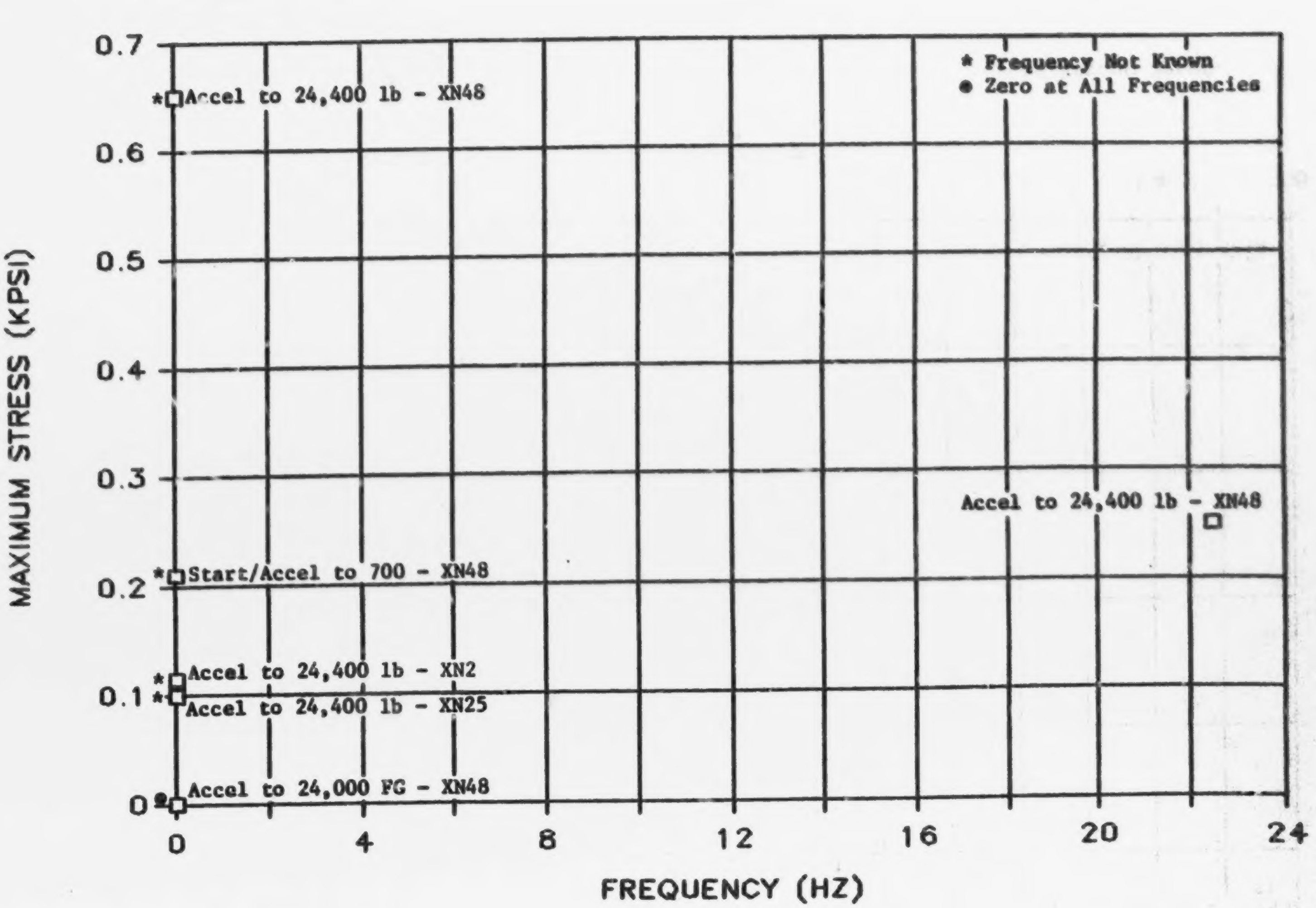

Figure B-17. Top of Mount Beam - Aft Vertical (KD MB01), Stress Versus Frequency.

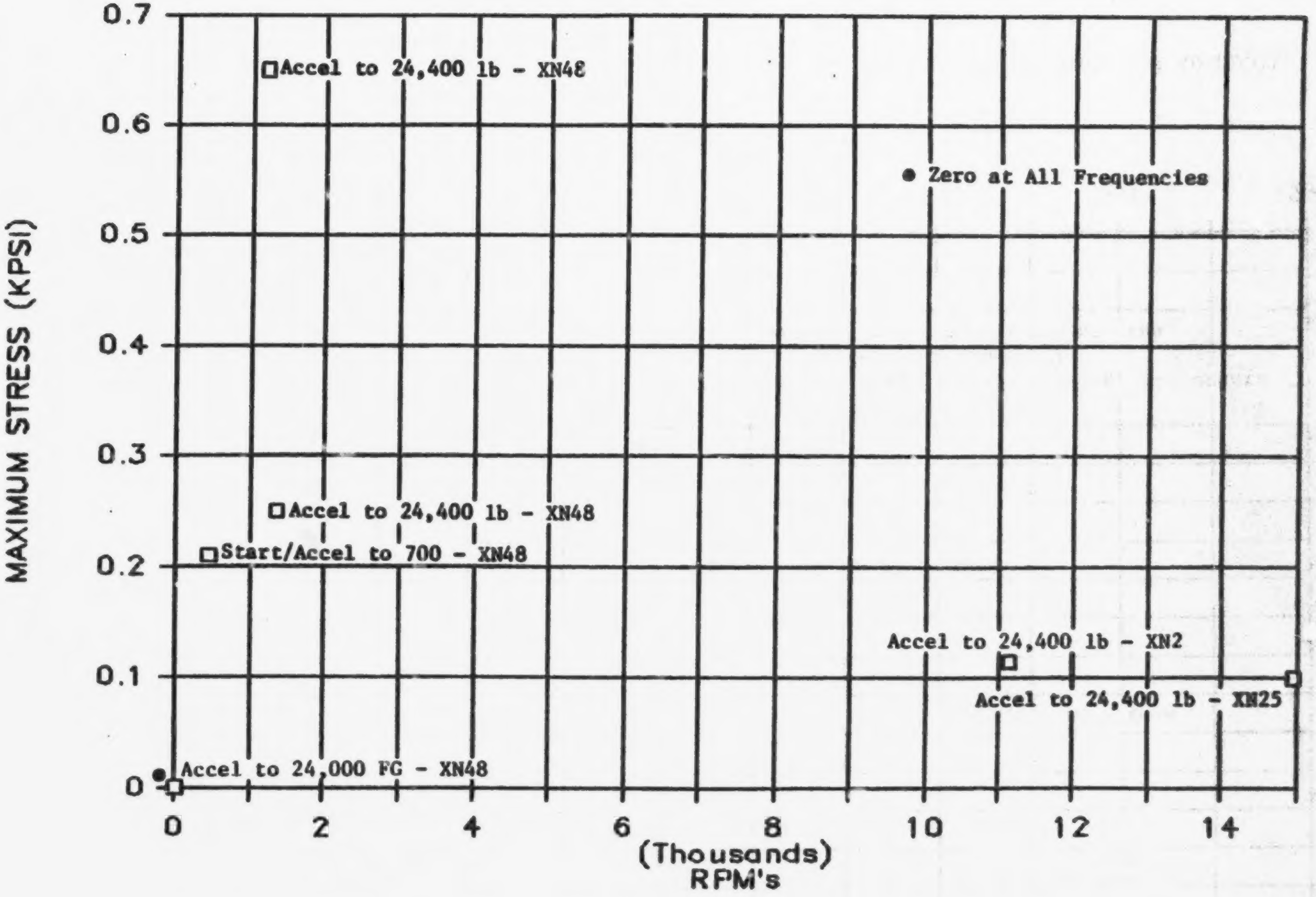

Figure B-18. Top of Mount Beam - Aft Vertical (KD MB01), Stress Versus Speed.

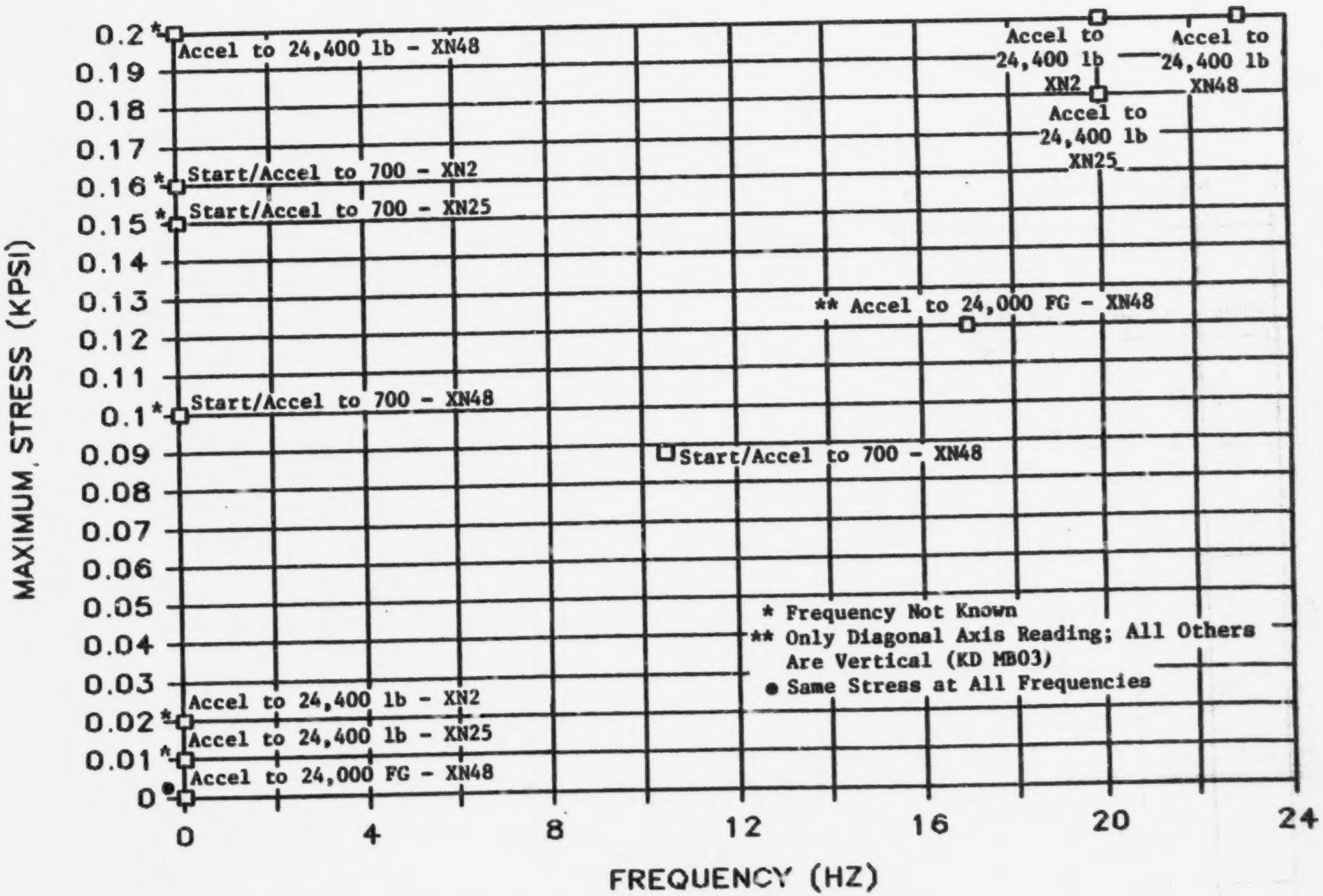

Figure B-19. Top of Mount Beam - Aft Diagonal and Horizontal (KD MB02 and KD MB03), Stress Versus Frequency.

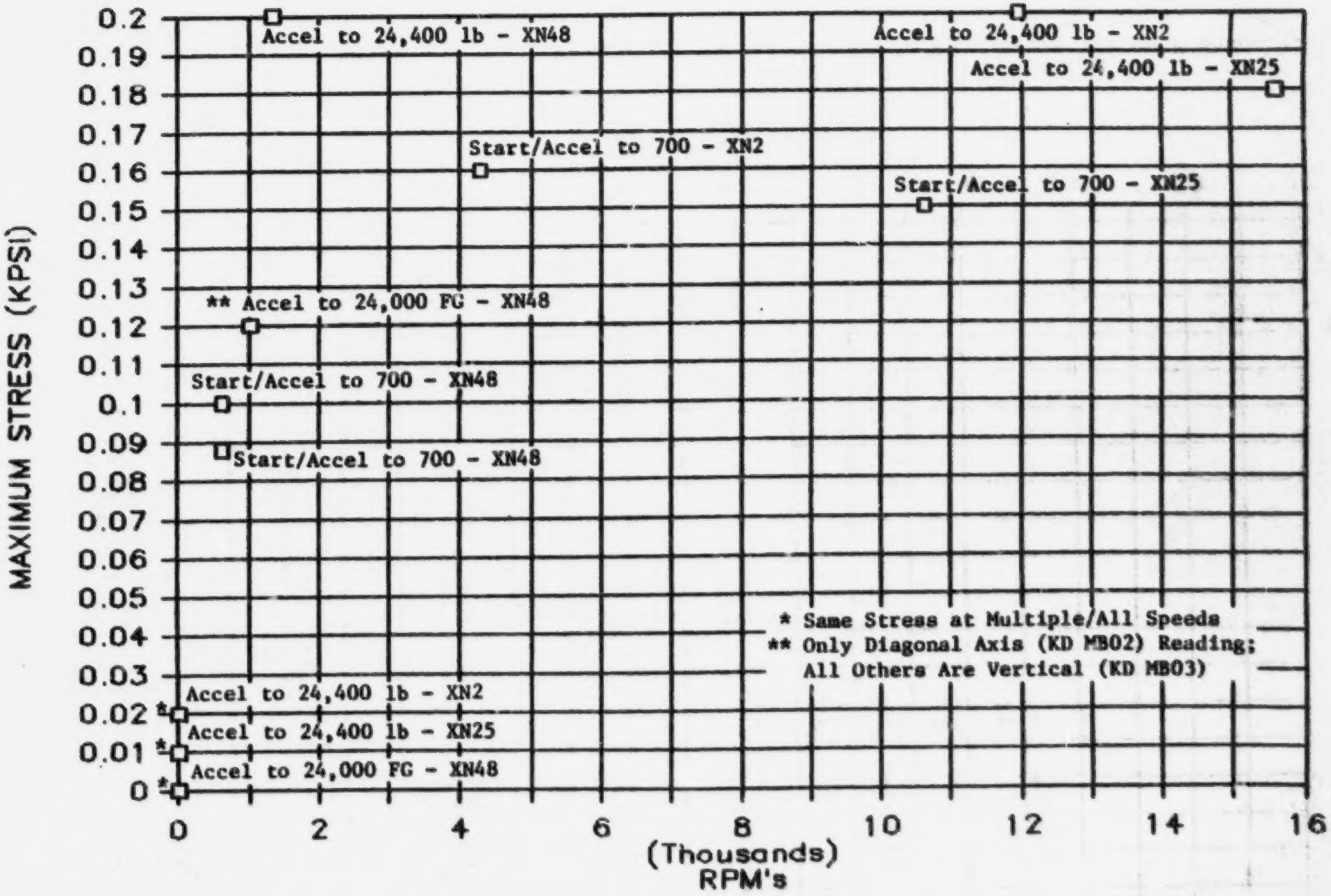

Figure B-20. Top of Mount Beam - Aft Diagonal and Horizontal (KD MB02 and KD MB03) Stress Versus Speed.

ORIGINAL PAGE IS
OF POOR QUALITY

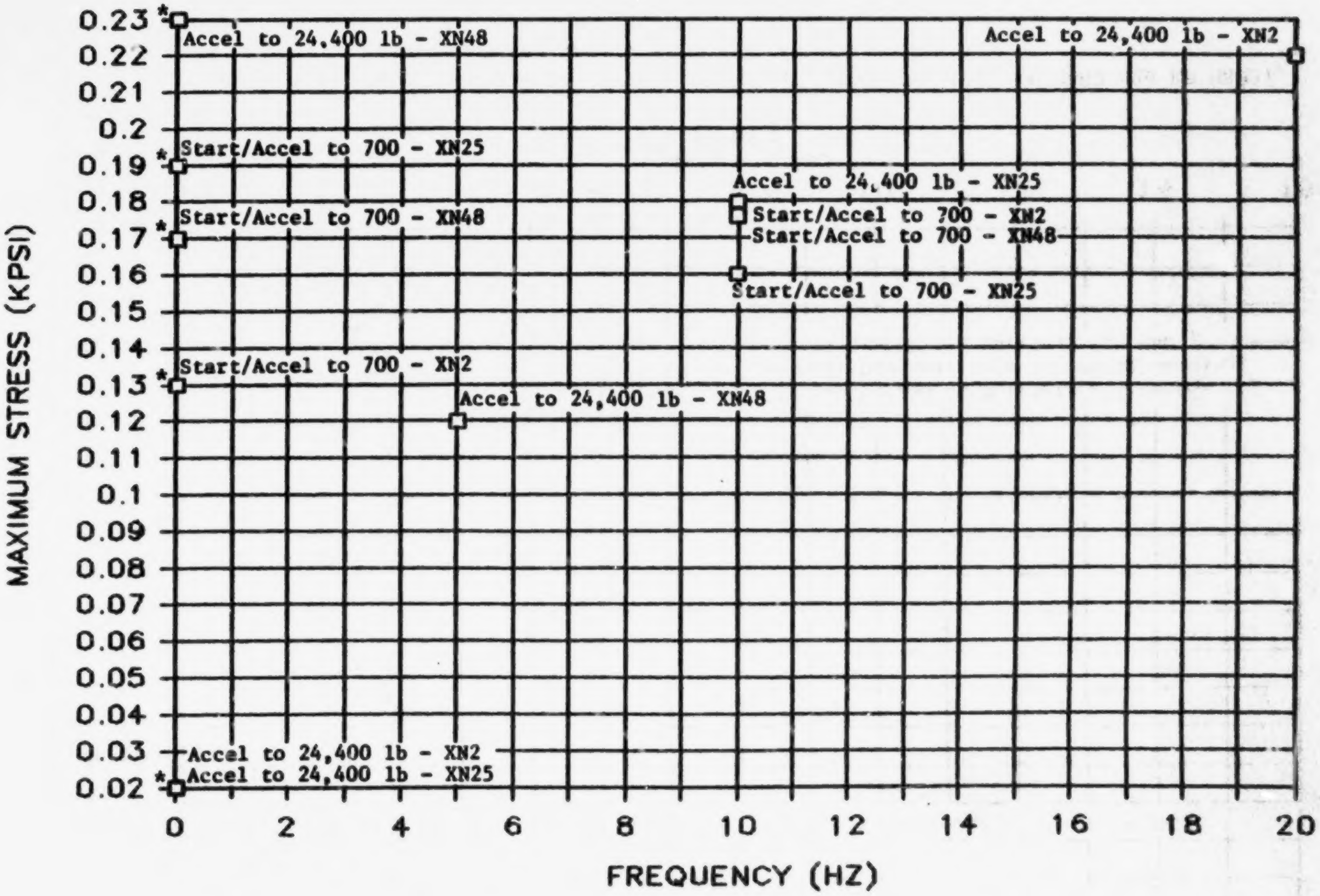

Figure B-21. Bottom of Mount Beam - Aft Horizontal (KD MB04), Stress Versus Frequency.

ORIGINAL PAGE IS
OF POOR QUALITY

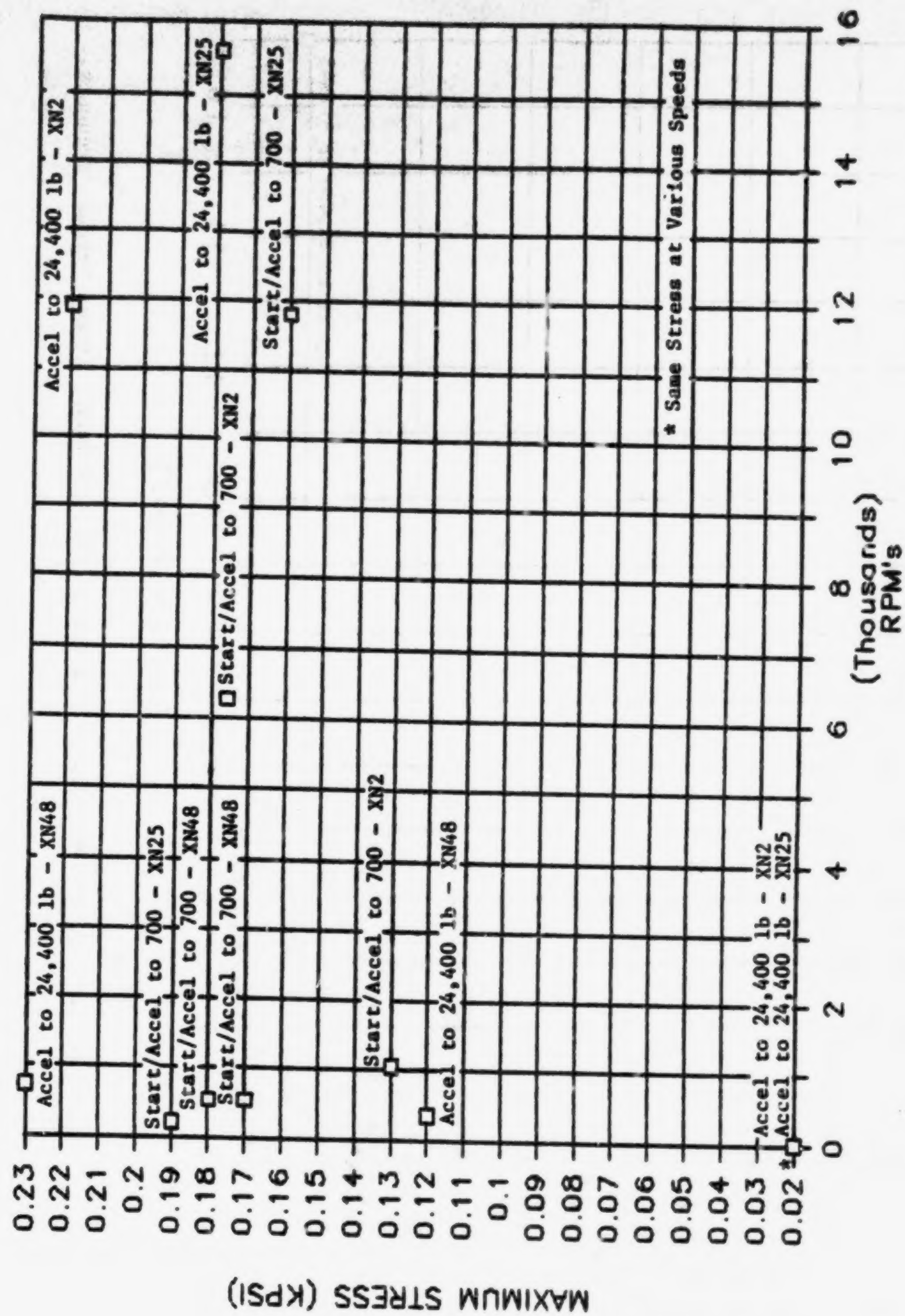

Figure B-22. Bottom of Mount Beam - Aft Horizontal (KD MB04), Stress Versus Speed.

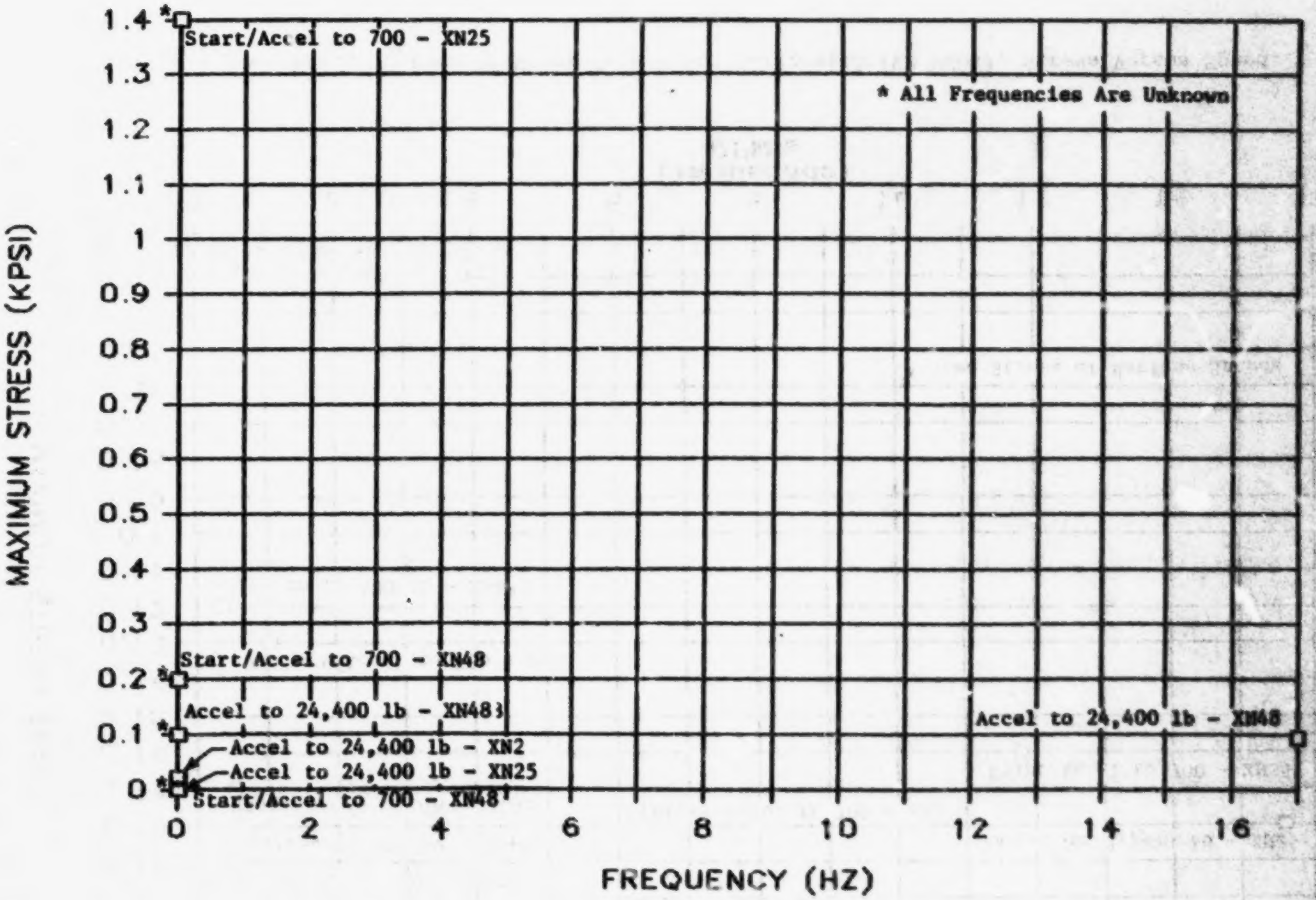

Figure B-23. Top of Mount Beam - Mid Horizontal (KD MB05), Stress Versus Frequency.

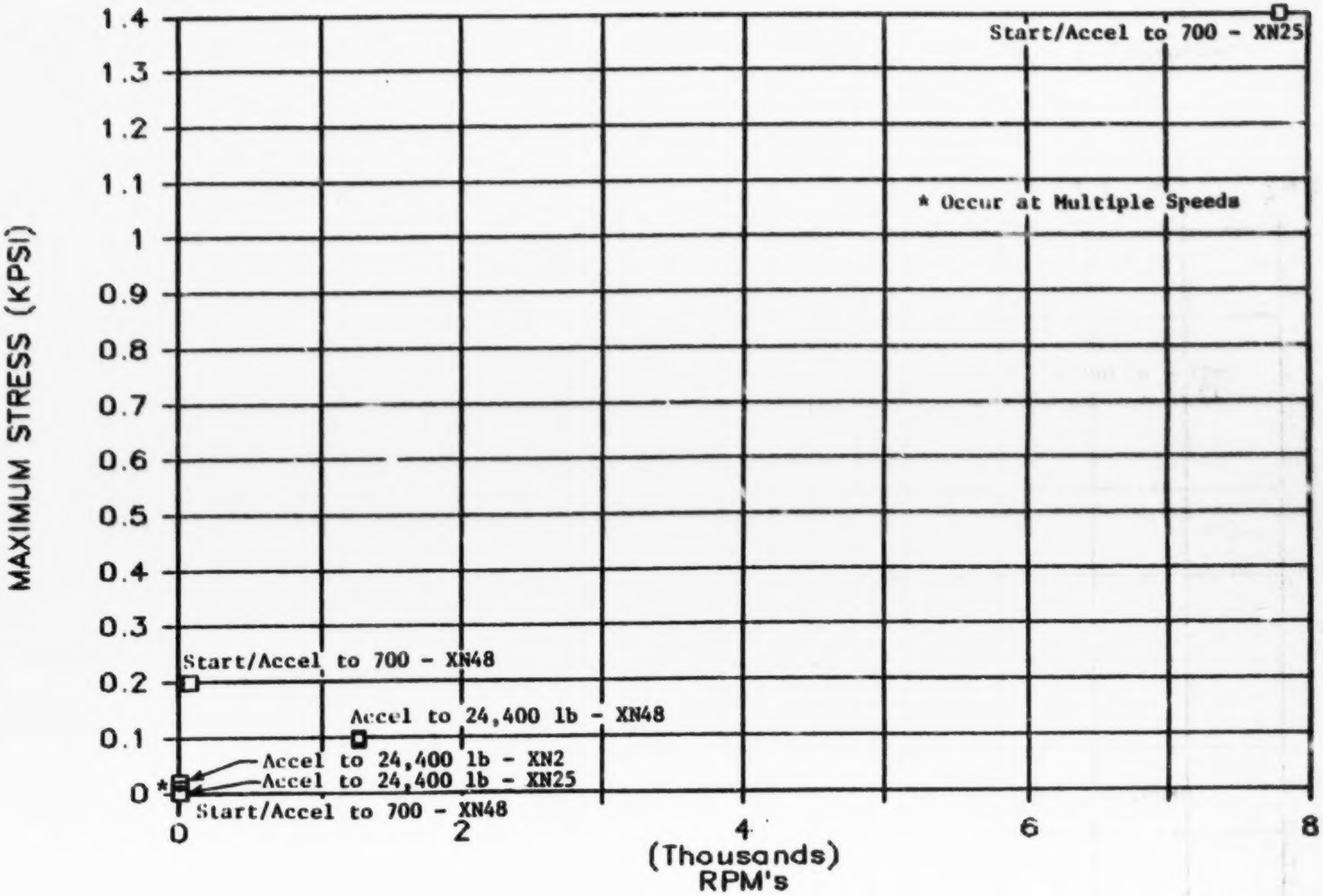

Figure B-24. Top of Mount Beam - Mid Horizontal (KD MB05), Stress Versus Speed.

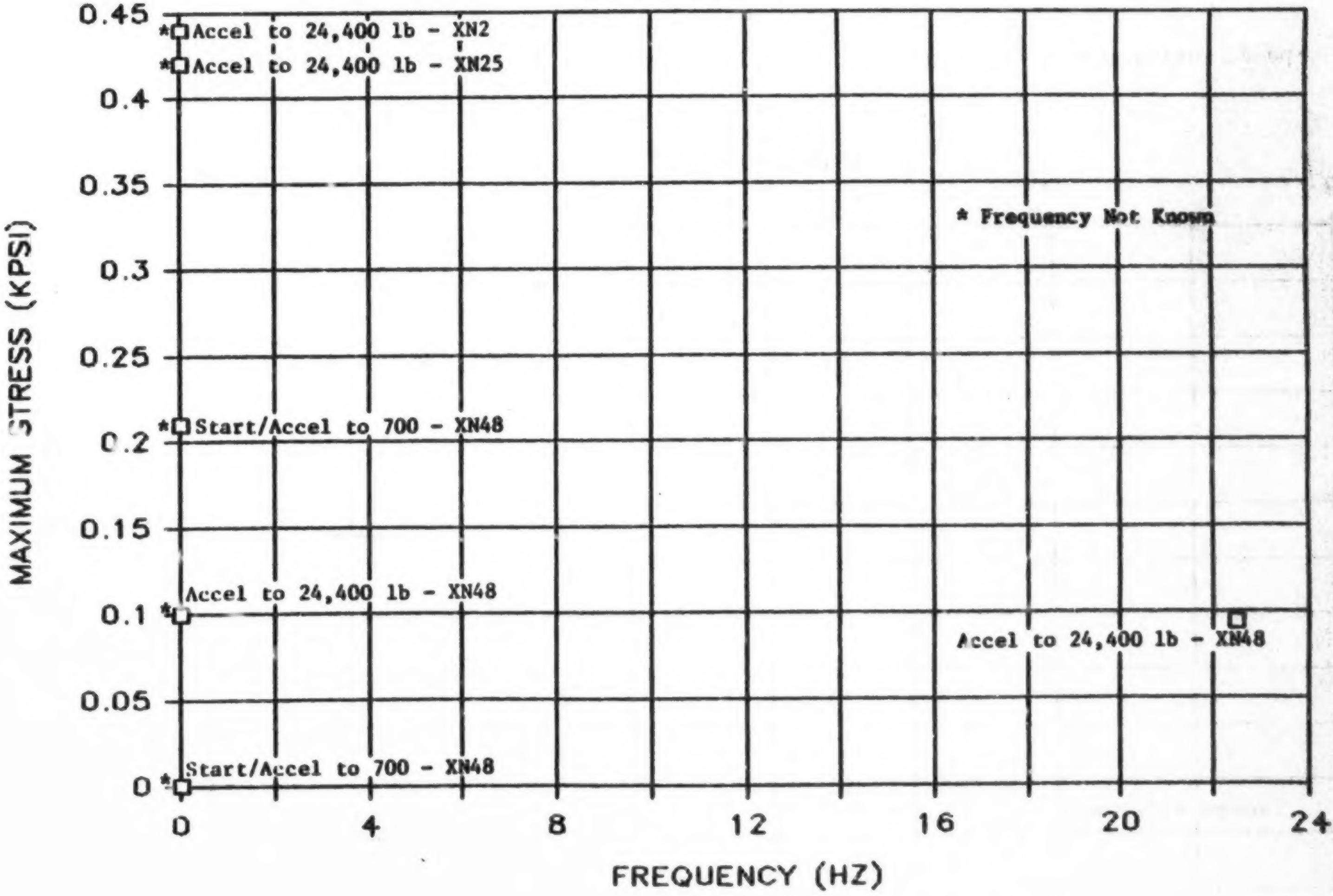

Figure B-25. Top of Mount Beam - Mid Vertical (KD MB07), Stress Versus Frequency.

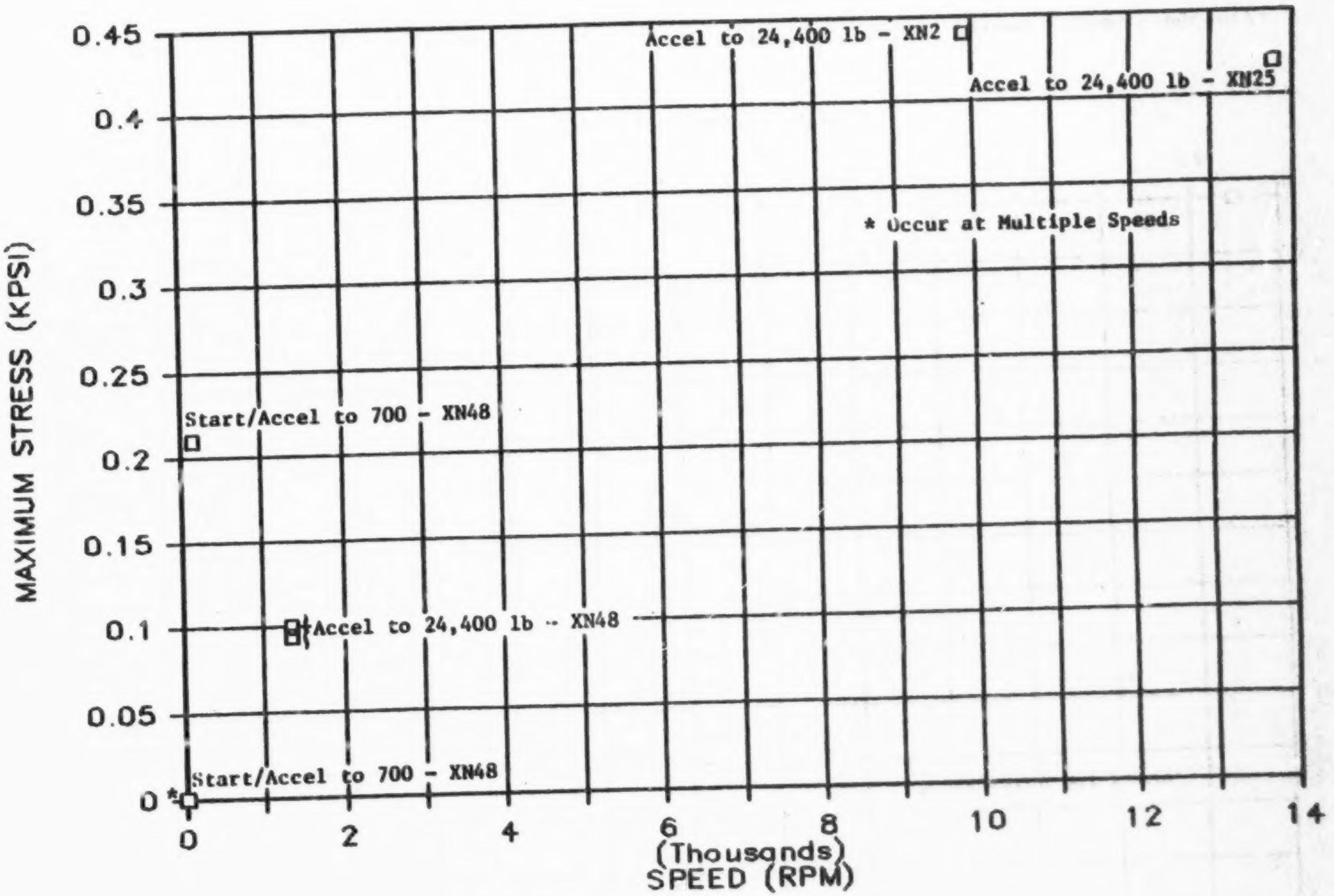

Figure B-26. Top of Mount Beam - Mid Vertical (KD MB07), Stress Versus Speed.

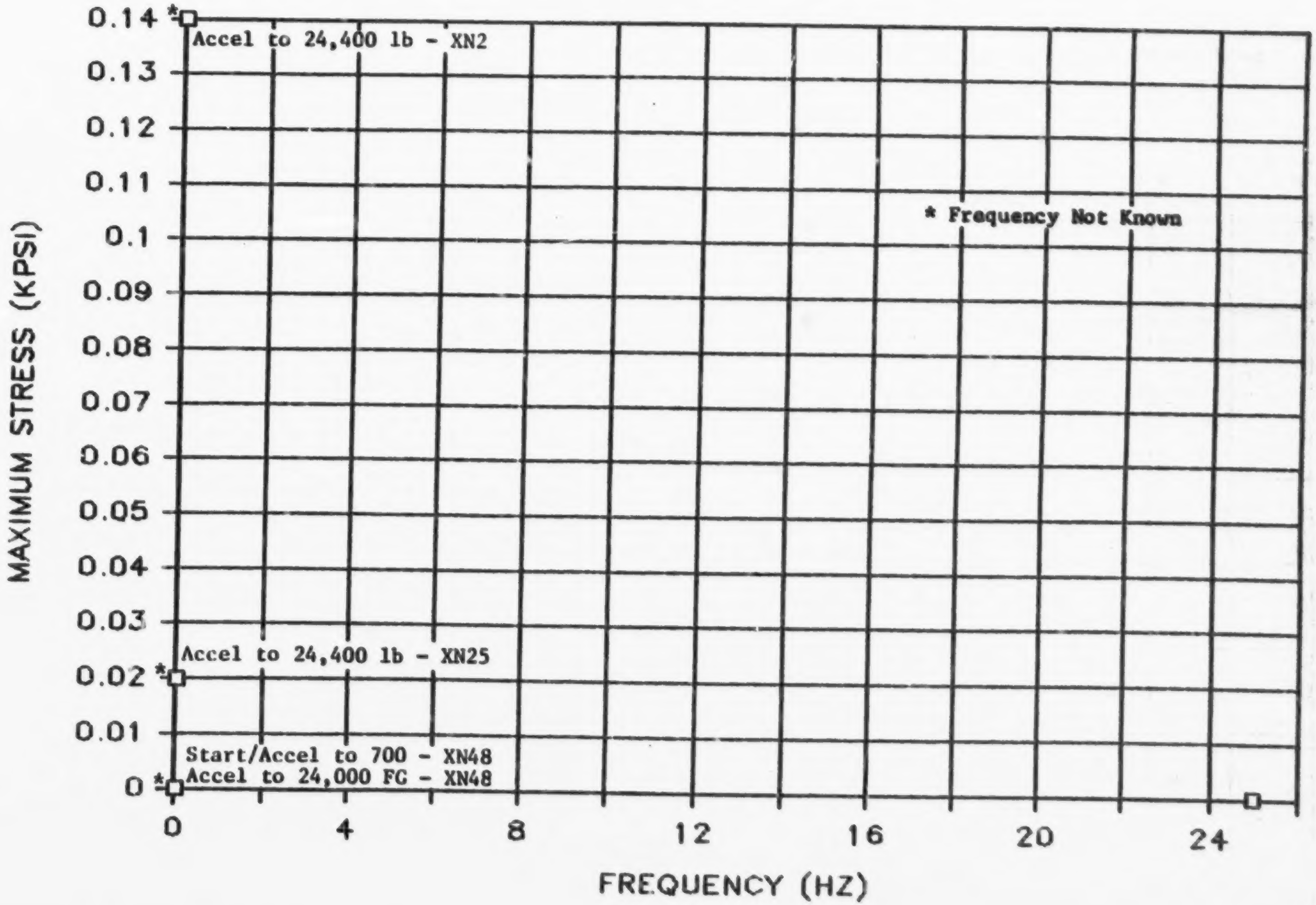

Figure B-27. Bottom of Mount Beam - Forward Vertical (KD MB10), Stress Versus Frequency.

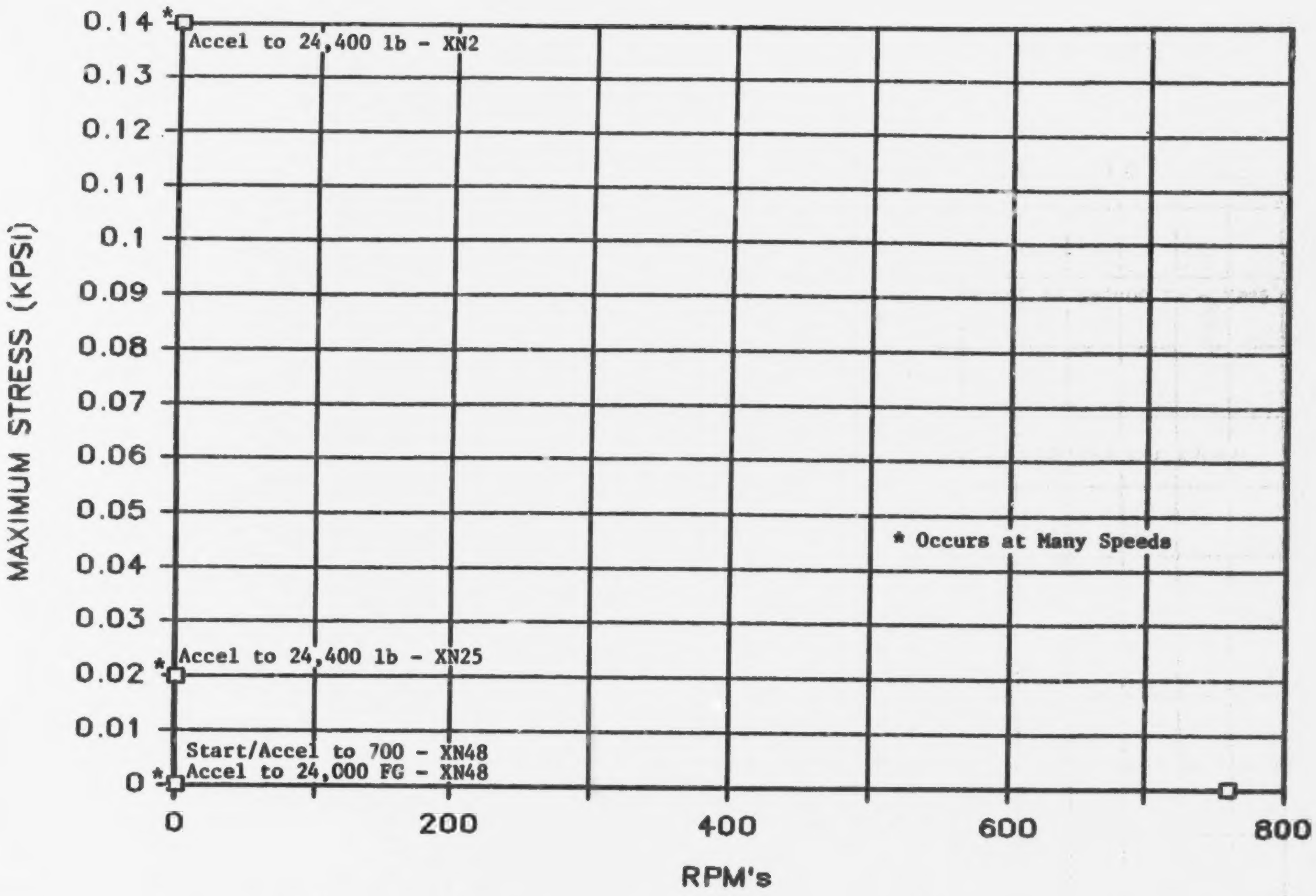

Figure B-28. Bottom of Mount Beam - Forward Vertical (KD MB10), Stress Versus Speed.

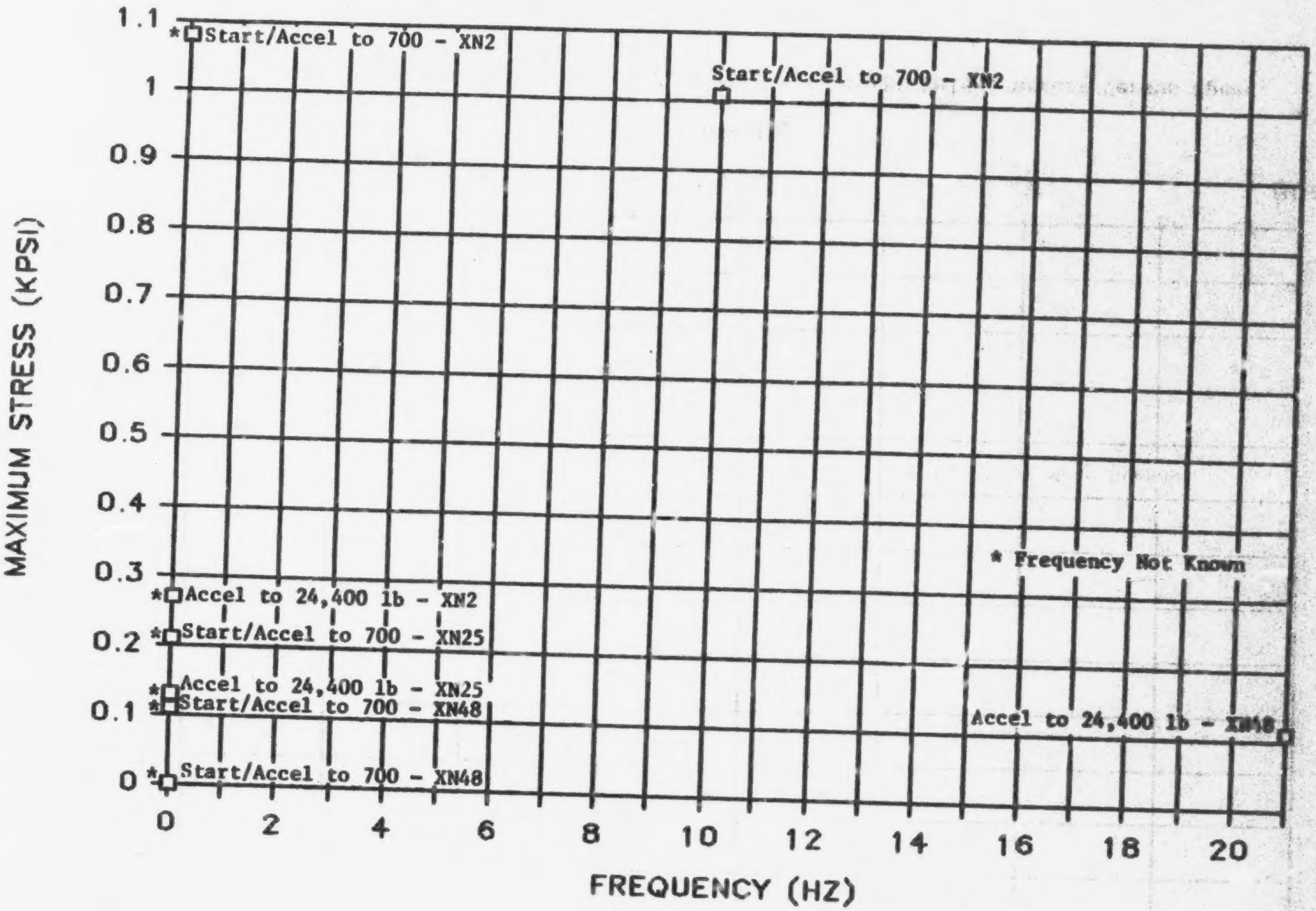

Figure B-29. Aft Mount Beam Support Fitting Horizontal (KD MS03), Stress Versus Frequency.

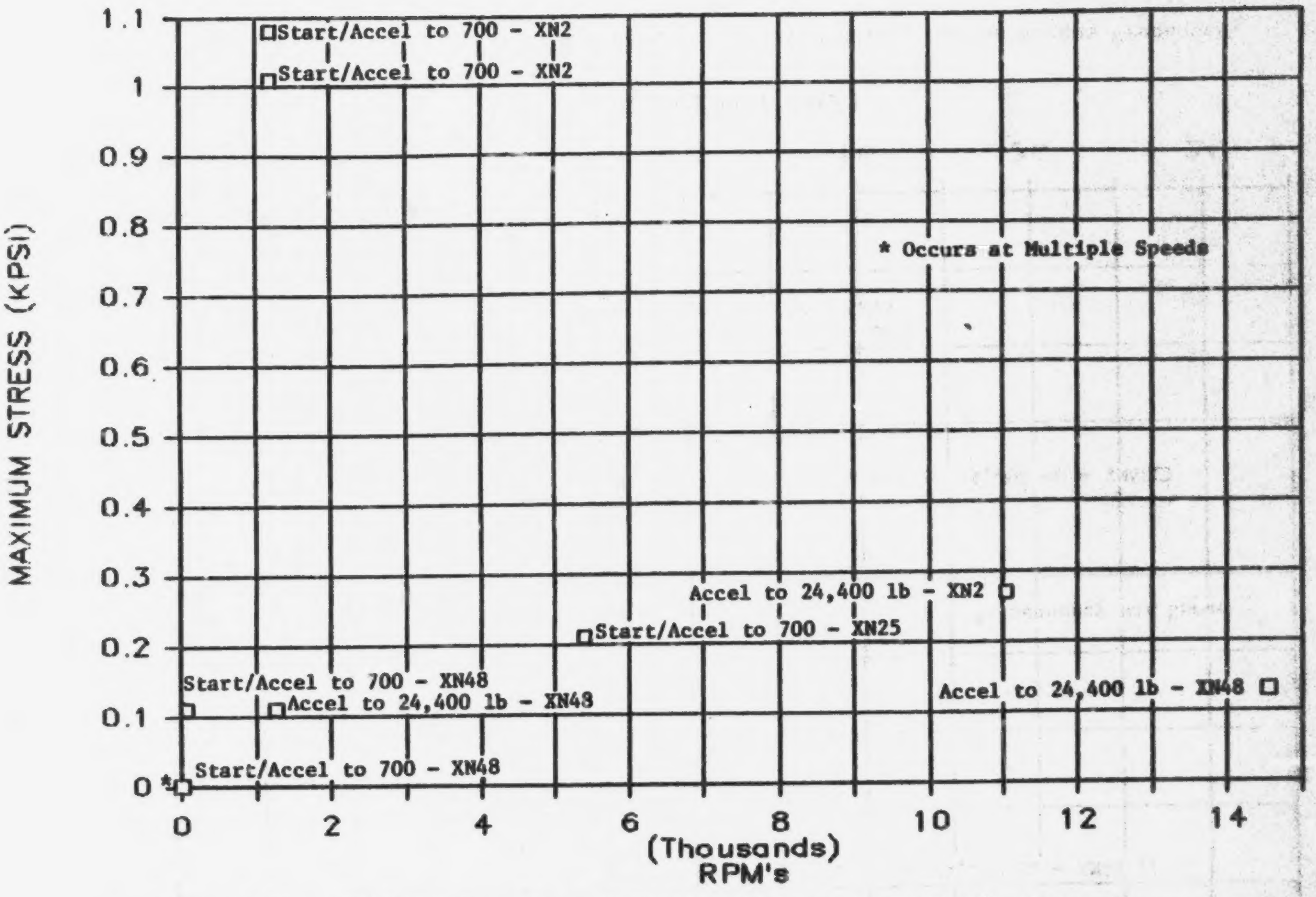

Figure B-30. Aft Mount Beam Support Fitting Horizontal (KD MS03), Stress Versus Speed.

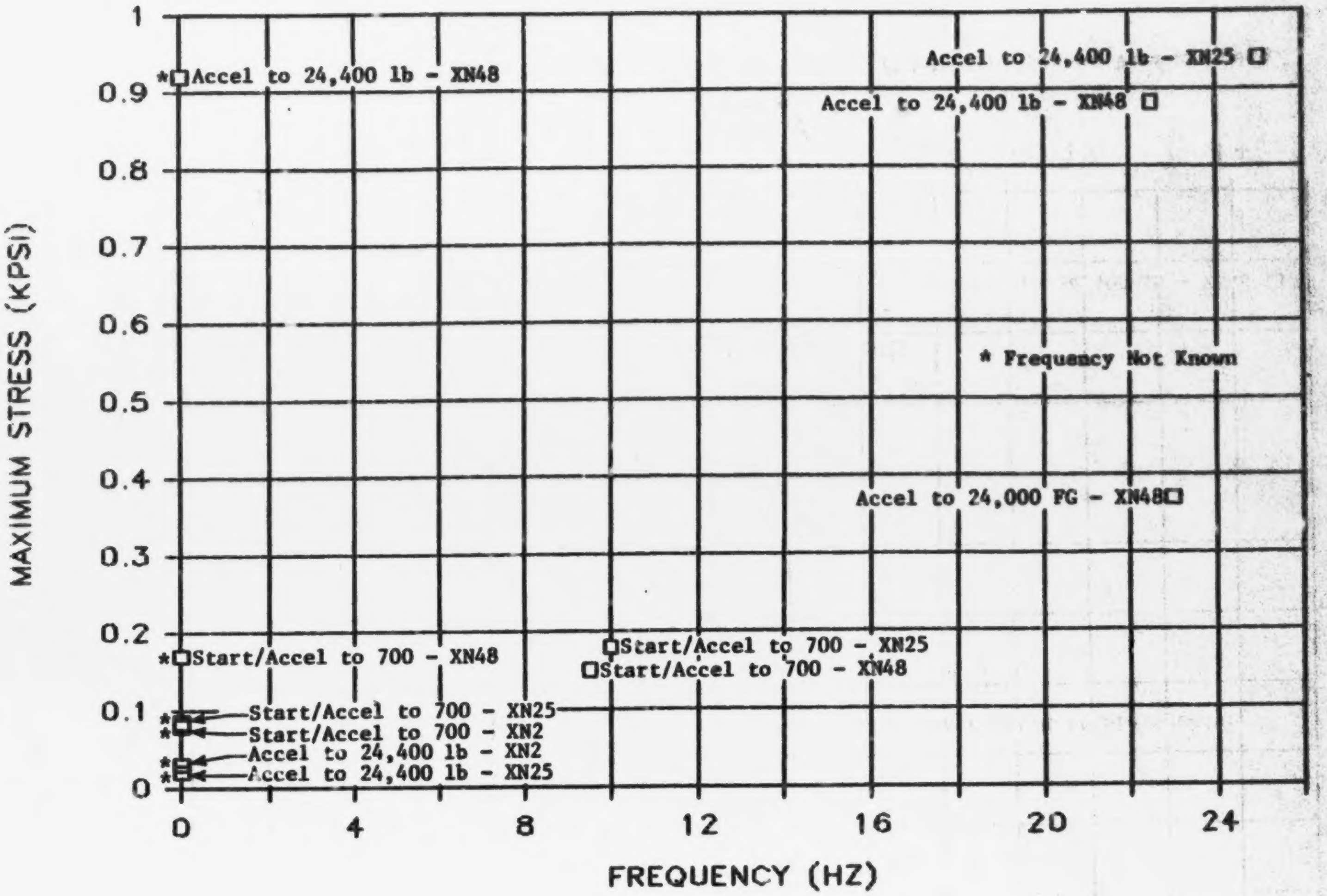

Figure B-31. Right Aft Isolator Clevis Axial (KD RRI1), Stress Versus Frequency.

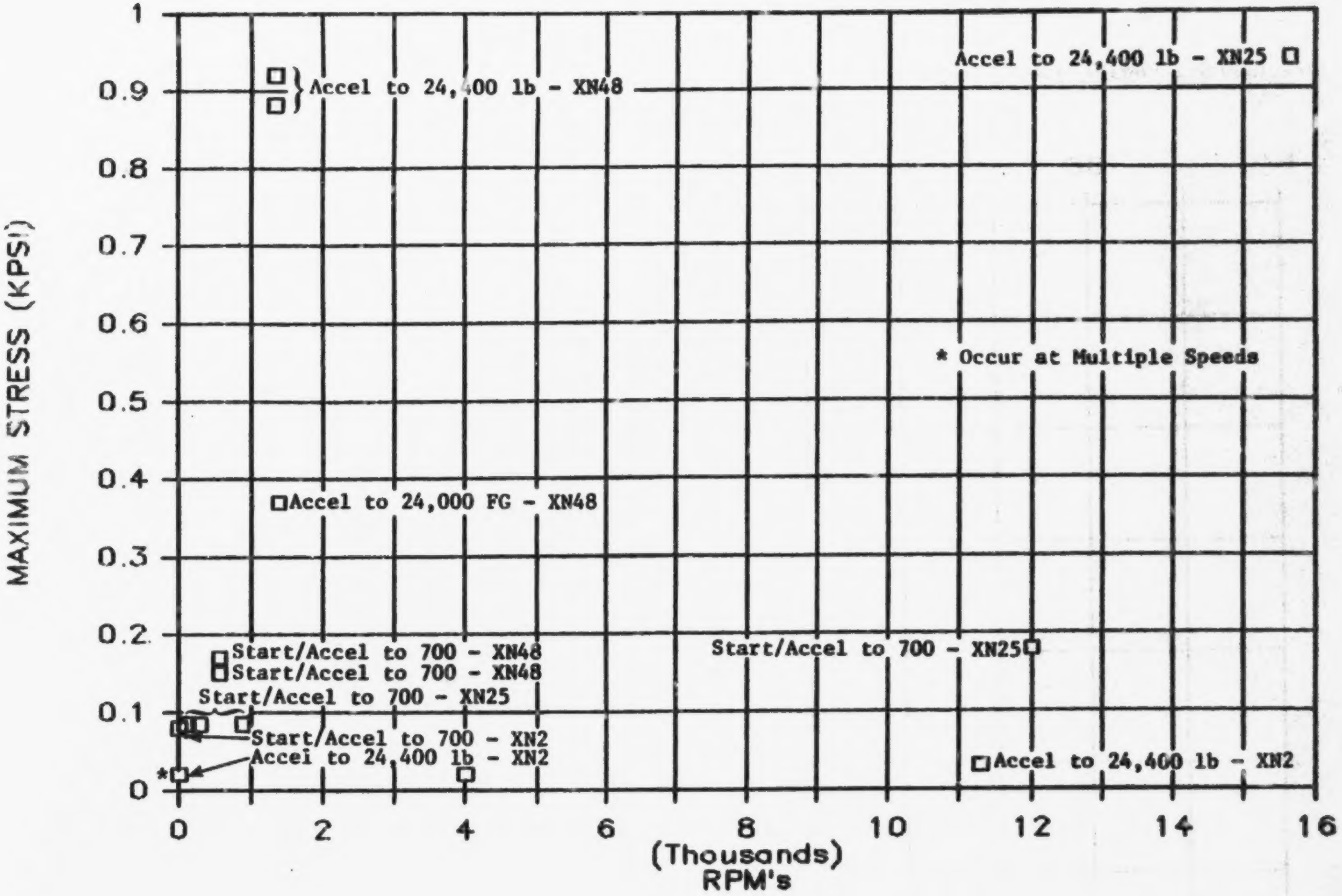

Figure B-32. Right Aft Isolator Clevis Axial (KD RRI1), Stress Versus Speed.

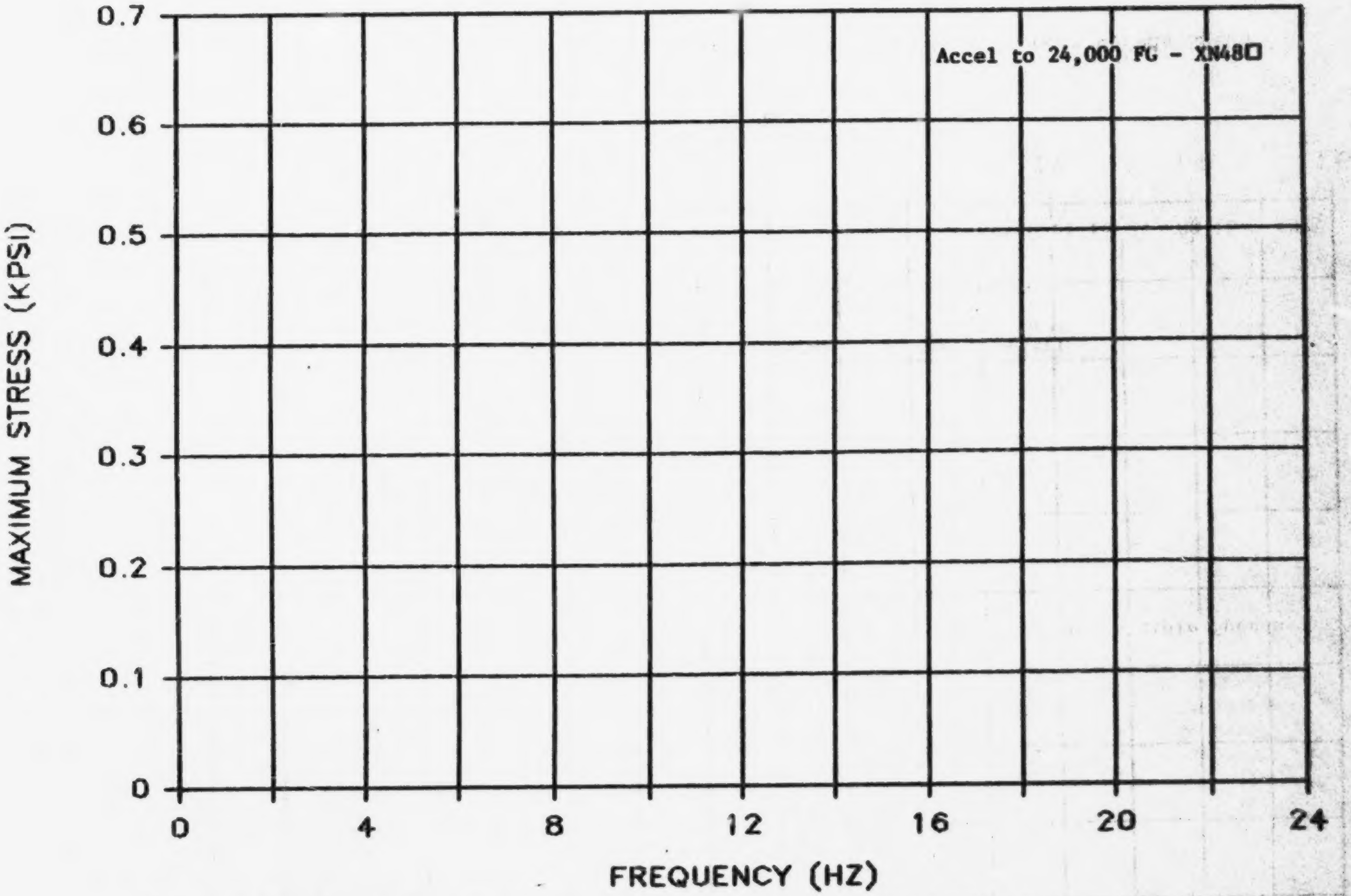

Figure B-33. Right Rear Mount Rosette No. 1 Tangential (KD RRM1), Stress Versus Frequency.

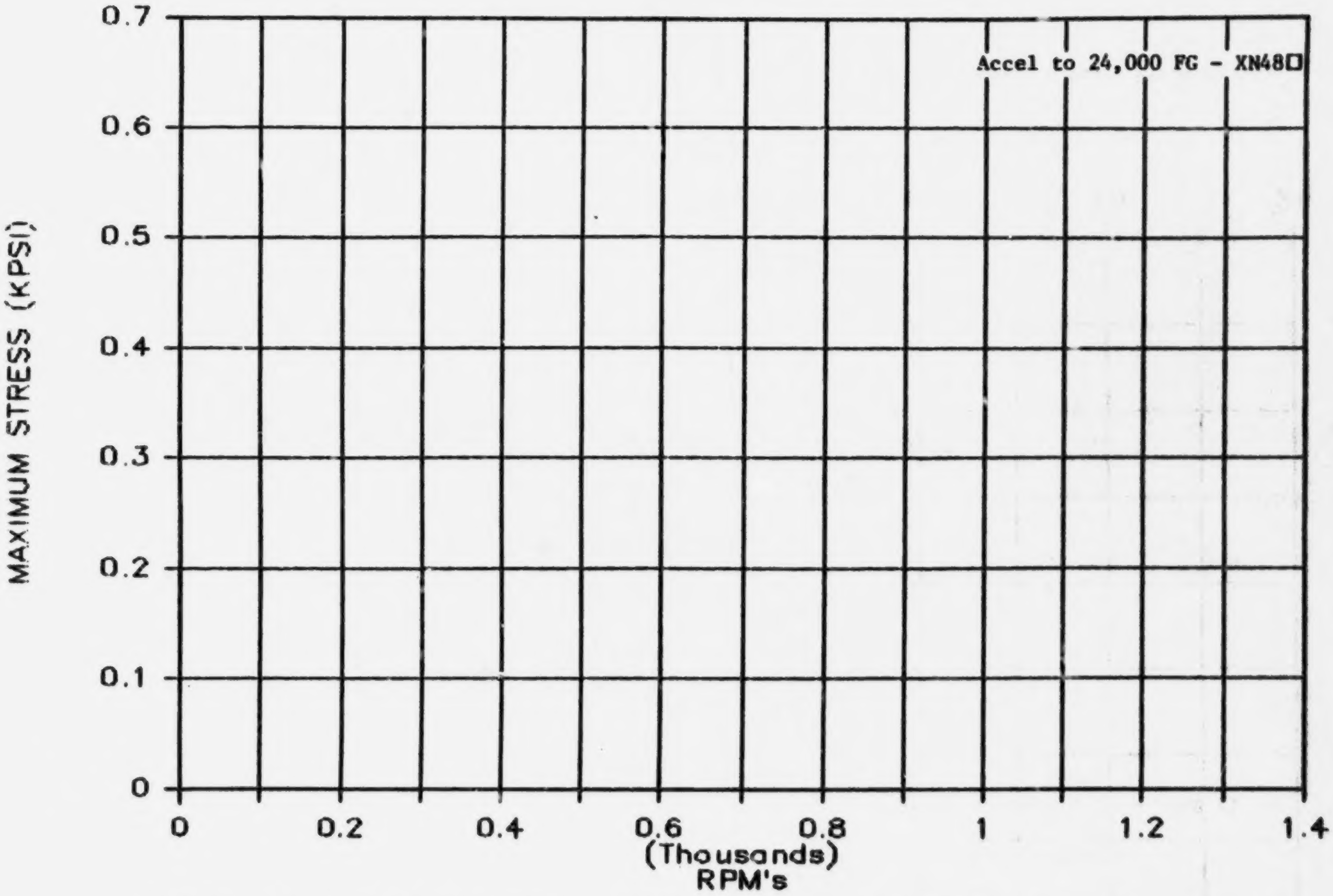

Figure B-34. Right Rear Mount Rosette No. 1 Tangential (KD RRM1), Stress Versus Speed.

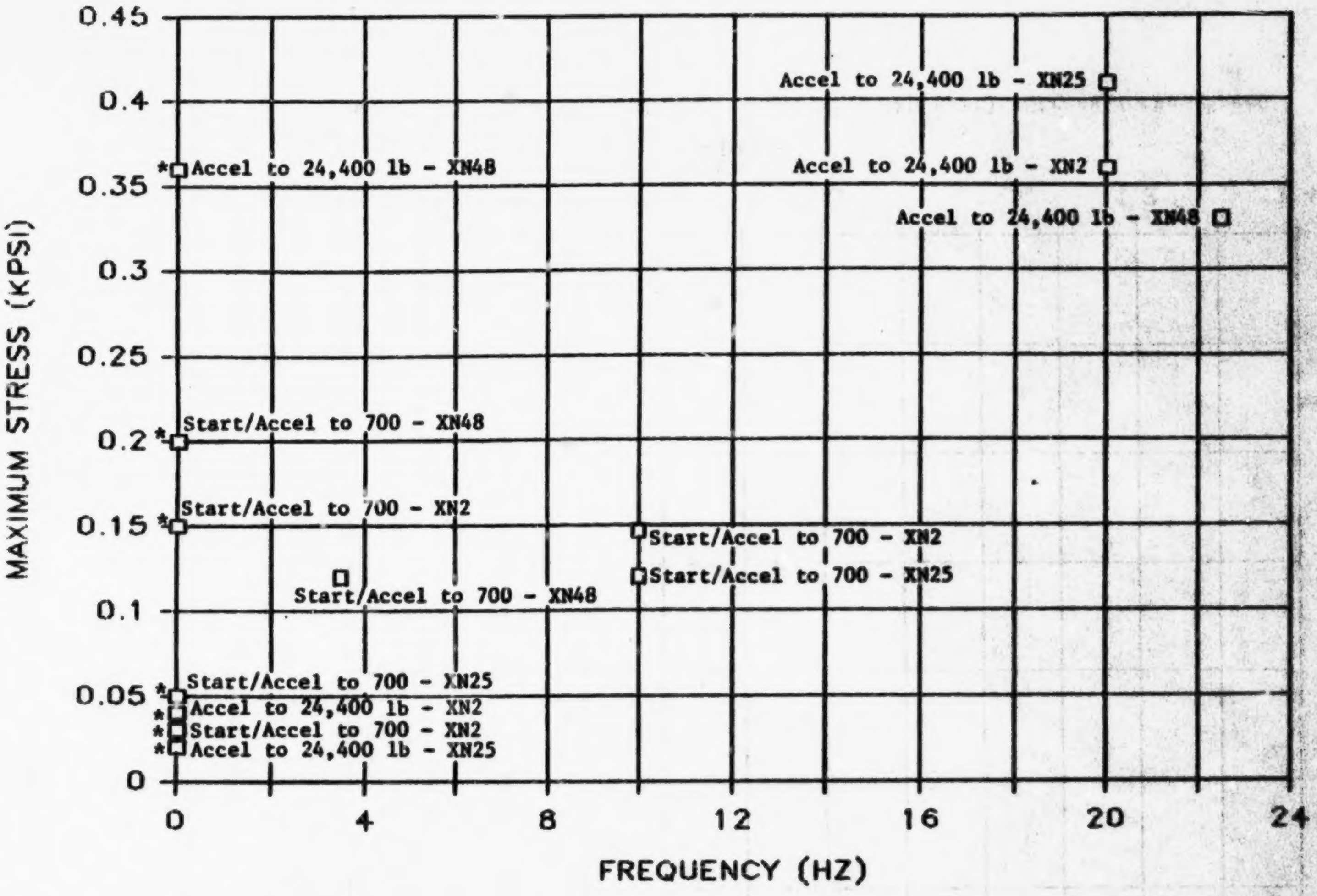

Figure B-35. Back of Spar - Lower Aft Vertical (KD SR04), Stress Versus Frequency.

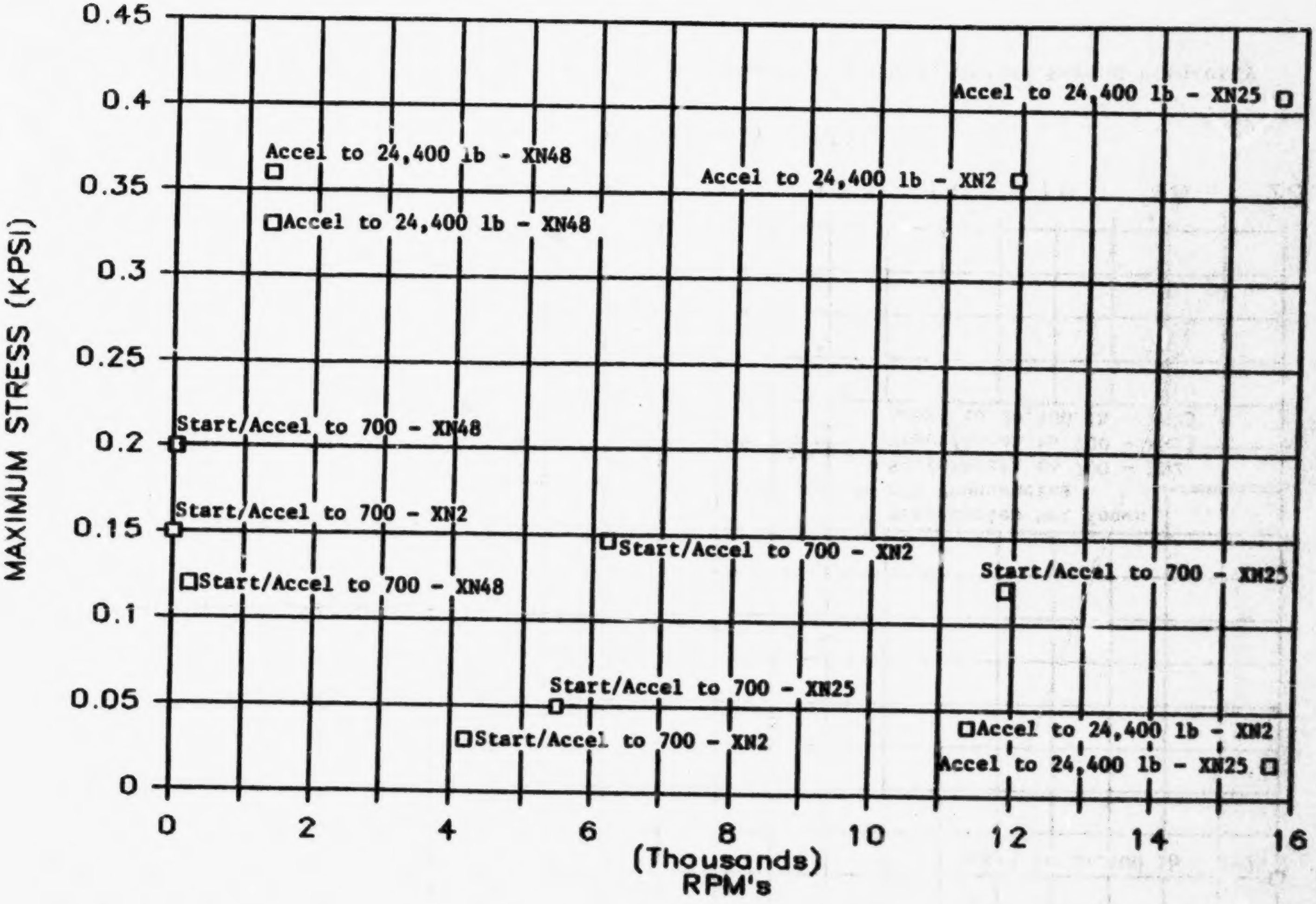

Figure B-36. Back of Spar - Lower Aft Vertical (KD SR04), Stress Versus Speed.

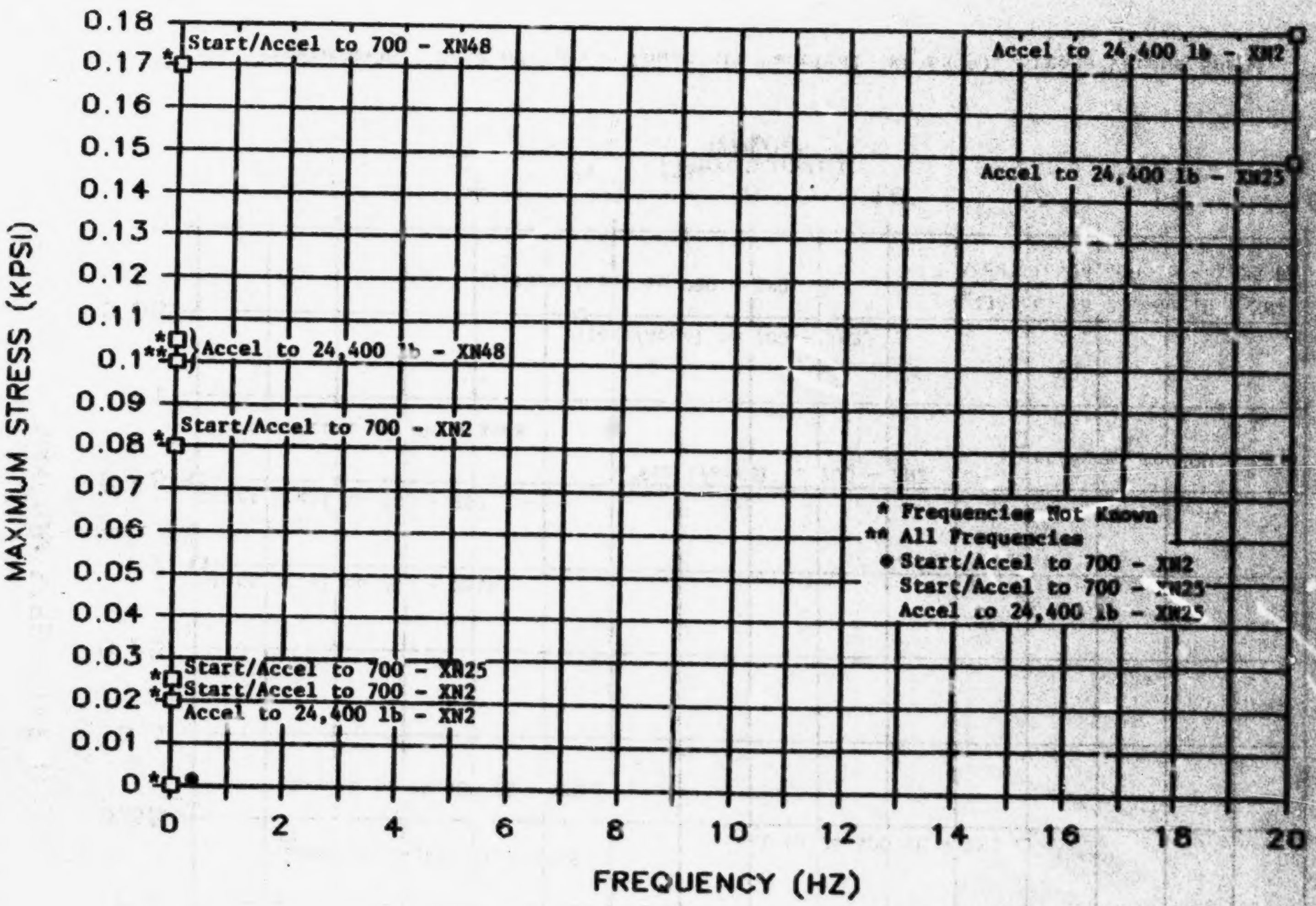

Figure B-37. Back of Spar - Lower Aft Horizontal (KD SR06), Stress Versus Frequency.

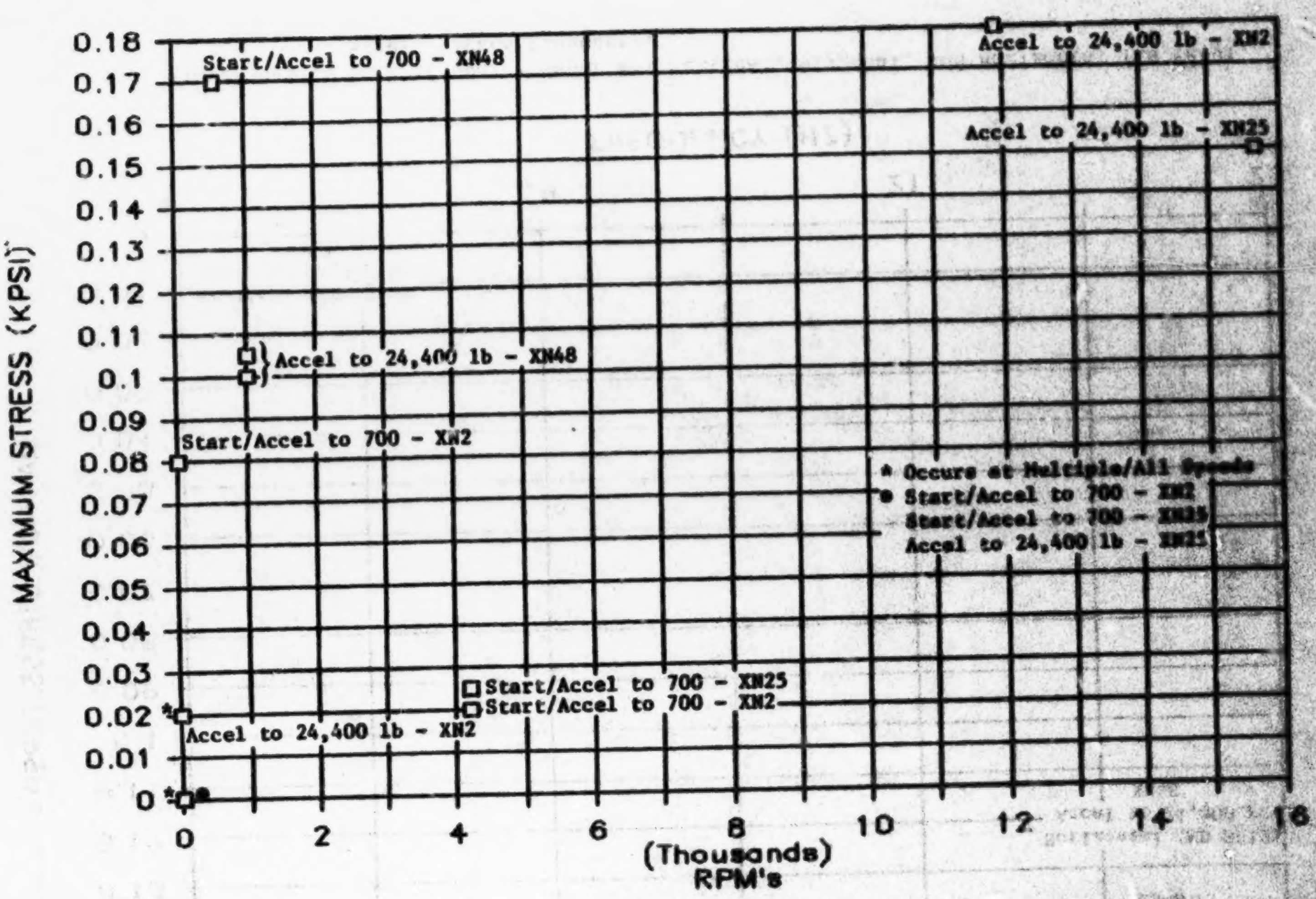

Figure B-38. Back of Spar - Lower Aft Horizontal (KD SR06), Stress Versus Speed.

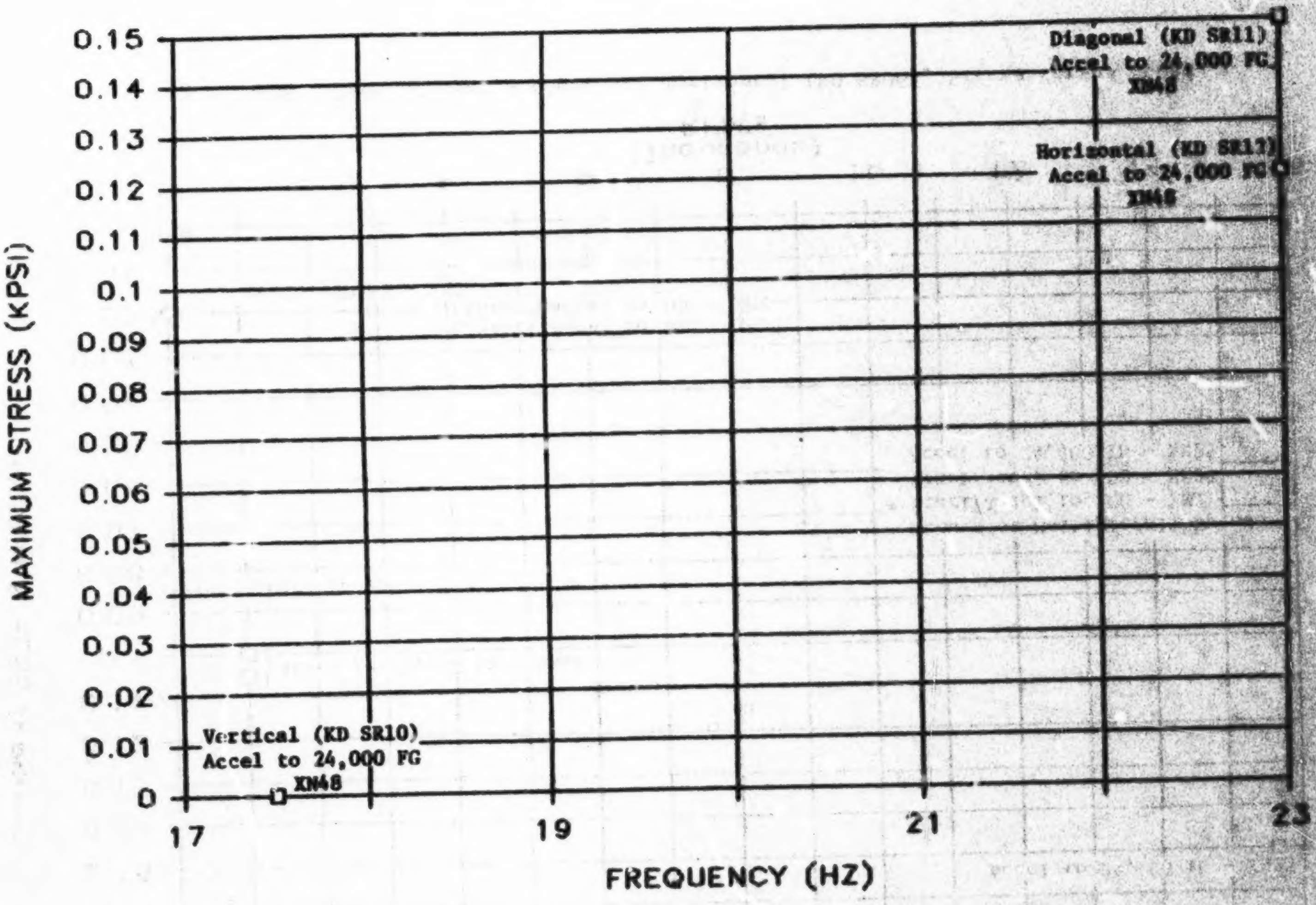

Figure B-39. Back of Spar - Upper Aft Vertical, Diagonal, and Horizontal (KD SR10), Stress Versus Frequency.

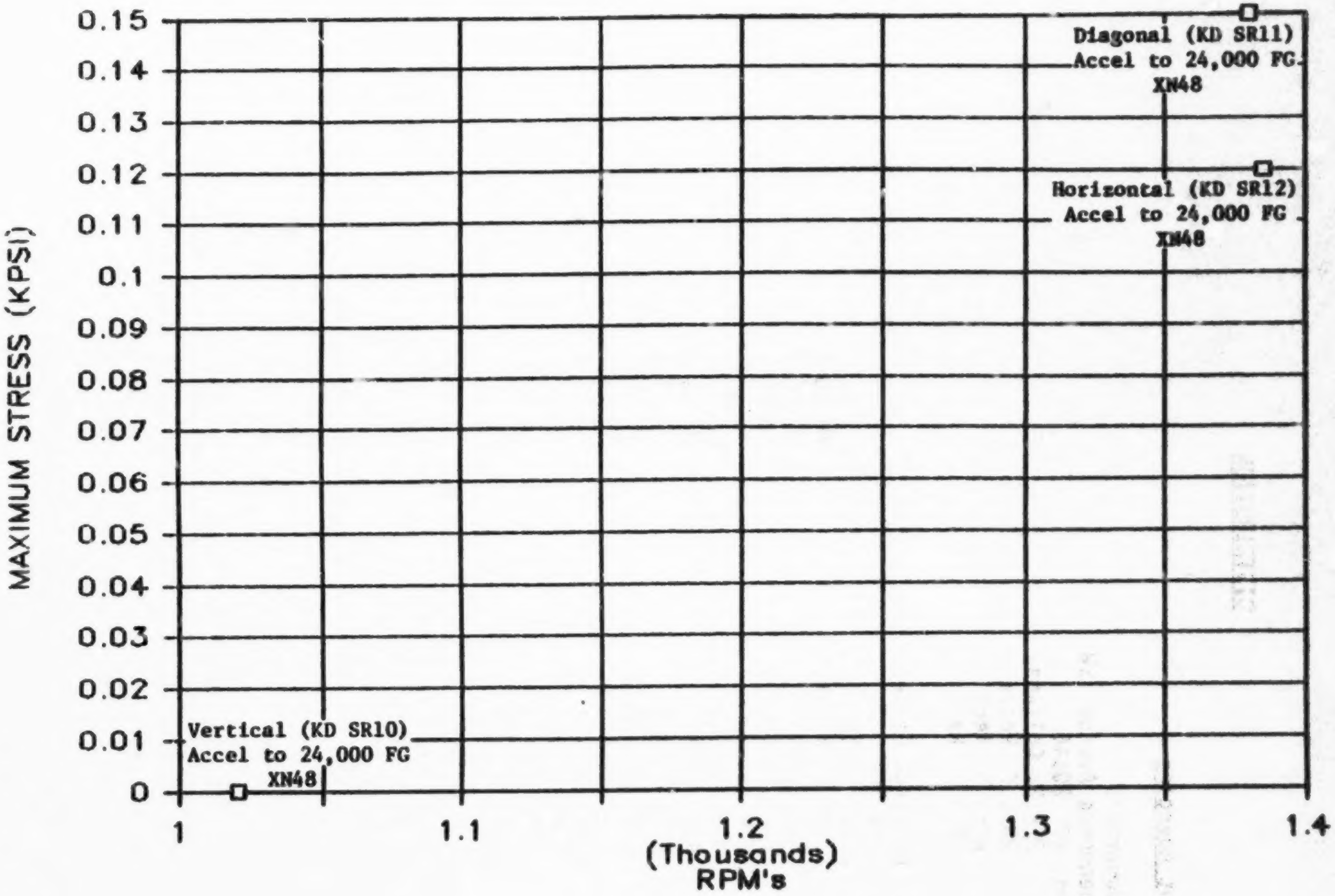

Figure B-40. Back of Spar - Upper Aft Vertical, Diagonal, and Horizontal (KD SR10, 11, and 12), Stress Versus Speed.

1. Report No.
CR-180869

2. Government Accession No.

3. Recipient's Catalog No.

4. Title and Subtitle
Full-Scale Technology Demonstration of a Modern Counterrotating Unducted Fan Engine Concept - Engine Test

5. Report Date
December 1987

6. Performing Organization Code
535-03-01

7. Author(s)
GE36 Design and Systems Engineering

8. Performing Organization Report No.

9. Performing Organization Name and Address
GE Aircraft Engines
One Neumann Way
Cincinnati, Ohio 45215

10. Work Unit No.

11. Contract or Grant No.
NAS3-24210

12. Sponsoring Agency Name and Address
NASA Lewis Research Center
21000 Brookpark Road
Cleveland, Ohio 44135

13. Type of Report and Period Covered
Topical

14. Sponsoring Agency Code

15. Supplementary Notes

16. Abstract

The UDF™ (unducted fan) engine is an innovative aircraft engine concept that is based on an ungeared, counterrotating, unducted, ultra-high-bypass turbofan configuration. This engine is being developed by GE Aircraft Engines to provide a high thrust-to-weight ratio power plant with exceptional fuel efficiency for subsonic aircraft application.

This report covers the successful ground testing of this engine. A test program exceeding 100-hours duration was completed, in which all of the major goals were achieved. The following accomplishments were successfully demonstrated: full thrust (25,000 lb); full counterrotating rotor speeds (1393+ rpm); low specific fuel consumption (< 0.24/lb/hr/lb); new composite fan blade design; counterrotation of structures, turbines, and fan blades; control system; actuation system; and reverse thrust.

17. Key Words (Suggested by Author(s))
Unducted Fan (UDF™); Counterrotation; Ultra-High-Bypass Fan; Propfan

18. Distribution Statement
[redacted]

19. Security Classif. (of this report)
Unclassified

20. Security Classif. (of this page)
Unclassified

21. No. of Pages
326

22. Price